

Bhela Central Library

PILANI (Rajasthan)

Class No : 621.384135

Book No : W53A -

Accession No : 44168

ANTENNA
THEORY AND DESIGN

VOLUME II



Front page

RADAR ANTENNA ON R.M.S. "QUEEN ELIZABETH"

The waveguide feed to the cheese antenna on the right hand side may be seen in the middle of the aperture.

(Courtesy of A. C. Cossor, Ltd.)

ANTENNA THEORY AND DESIGN

VOLUME TWO
THE ELECTRICAL DESIGN OF ANTENNAE

BY

H. PAUL WILLIAMS,

Ph.D., A.M.I.E.E., Sen.M.I.R.E.

*Head of Electronics Dept., The Fairey Aviation Co. Ltd., formerly Antenna
and Propagation Specialist with Standard Telephones and Cables, Ltd.,
New Southgate*



LONDON
SIR ISAAC PITMAN & SONS, LTD.

First published 1950

CIP SIR ISAAC PITMAN & SONS, LTD
PITMAN HOUSE, PARKER STREET, KINGSWAY, LONDON, W C.2
THE PITMAN PRESS, BATH
PITMAN HOUSE, LITTLE COLLINS STREET, MELBOURNE
27 BECKETTS BUILDINGS, PRESIDENT STREET, JOHANNESBURG

ASSOCIATED COMPANIES

PITMAN PUBLISHING CORPORATION
2 WEST 45TH STREET, NEW YORK
205 WEST MONROE STREET, CHICAGO

SIR ISAAC PITMAN & SONS (CANADA), LTD.
(INCORPORATING THE COMMERCIAL TEXT BOOK COMPANY)
PITMAN HOUSE, 381-383 CHURCH STREET, TORONTO

Preface

FOR practical reasons Volume II has been written so as to be as independent as possible of Volume I—even to the extent of a separate introductory chapter which discusses the basis of radiation in a non-mathematical manner. In addition considerable use has been made in the second volume of design curves based on a logarithmic scale, since in this way polar diagrams may be calculated without even the use of a slide rule. For example, the polar diagram and gain of a rhombic antenna may be determined very simply, using only a piece of tracing paper and a pencil, by means of the curves in Chapter VI. If one wishes to know the actual equations involved, these may be found in Chapter IV, Volume I, and their derivation may, in turn, be traced right back to the fundamental laws of electromagnetism.

The designing of antennae frequently involves a consideration of the propagation conditions; for this reason I have included a chapter on propagation which covers all the requirements which one might normally meet. A complete chapter on transmission lines has also been included.

Nevertheless I am conscious of several omissions in this book: for instance, the properties of waveguides receive only scant mention, there is no discussion of antenna systems as applied to navigational aids; furthermore the impedance concept has only been used to a limited degree.

Omissions of this nature have occurred because it was necessary to keep the book to a reasonable size, or because the subject was still in a state of flux. Also the book makes no special reference to measuring techniques. It is difficult to include a coherent account of such techniques, in spite of the fact that it is now possible to obtain commercial field strength and impedance measuring equipment over a wider range of frequencies.

Throughout the book I have used M.K.S. units and the metric system as far as possible. Perhaps no one is brought more face to face with the absurdities of our systems of units than the antenna engineer—he finds himself dealing with conductivities in c.s.u., powers in practical units, field strengths

in millivolts per metre at one mile, antenna dimensions in feet and, as a crowning stupidity, wire gauges and bolt sizes that conform to no simple or universally recognized standards at all.

I am indebted to Standard Telephones & Cables, Ltd., for permission to publish this work and in particular I should like to express my indebtedness to Mr. W. L. McPherson for his advice and encouragement. The manuscript has been examined by a number of people each of whom has reviewed two or three chapters and I should like to record my thanks to Mr. F. L. Brown, Mr. R. F. Cleaver, Dr. F. G. Hawkins and Dr. J. D. Weston for their comments and criticism.

For the appendix on mechanical design I am indebted to Mr. L. Linder for considerable assistance and advice.

Many of the illustrations are based on figures which have appeared in various technical journals and I am grateful to the publishers of these journals for permission to use them. In this respect I am especially indebted to the *Journal of the Institution of Electrical Engineers* and to the *Proceedings of the Institute of Radio Engineers*. The excellent articles which have appeared in these two journals virtually form the foundations of this volume and I owe much to the authors of these articles.

Other publications from which I have obtained figures are the *Journal of Applied Physics*, the *Philosophical Magazine*, and *Electric Waves and Electric Oscillations*, by G. W. Pierce (McGraw-Hill Book Co. Inc.). In every case the source has been indicated with the figure caption.

My thanks are also due to the companies and other bodies which have been kind enough to supply me with photographs. These are also acknowledged individually.

The task of proof reading has been greatly lightened by the efforts of my father and my wife. Most of the drawings have been prepared by Mrs. I. Coyston and Mr. J. Mitchell to whom I would like to express my thanks.

Finally I would like to thank my wife for her most valuable assistance and in particular for calculating practically all the original curves which appear in this book. Without her co-operation and encouragement this book would probably never have been written.

H. PAUL WILLIAMS

Contents

	PAGE
<i>Preface</i>	V
CHAPTER I	
GENERAL SURVEY OF ANTENNAE AND PROPAGATION	I
1.1. Conditions for radiation from a circuit.	
1.2. Grounded and ungrounded antennae.	
1.3. Influence of the ground.	
1.4. Influence of the ionosphere.	
CHAPTER II	
LONG- AND MEDIUM-WAVE ANTENNAE	30
2.1. Characteristics of a vertical radiator.	
2.2. Antenna reactance.	
2.3. Antenna resistance.	
2.4. Input impedance.	
2.5. Antenna losses.	
2.6. Polar diagrams.	
2.7. Figure of merit.	
2.8. Feeding circuits.	
CHAPTER III	
SHORT- AND ULTRA-SHORT-WAVE ANTENNAE	89
3.1. The half-wave dipole.	
3.2. Mutual impedance between dipoles.	
3.3. Dipole systems involving mutual impedance considerations.	
3.4. Variations of the half-wave dipole.	
3.5. Wide-band antennae for television.	
3.6. Feeding circuits.	
CHAPTER IV	
MICROWAVE ANTENNAE	135
4.1. The half-wave dipole and variations.	
4.2. Parabolic mirrors.	
4.3. Corner reflectors.	
4.4. Horn radiators.	
4.5. Slot antennae.	
4.6. Dielectric antennae.	

	PAGE
CHAPTER V	
RECEIVING ANTENNAE	195
5.1. Relations between transmission and reception.	
5.2. Sources of noise.	
5.3. Signal-to-noise ratio considerations.	
5.4. Non-directional receiving antennae.	
5.5. Directional receiving antennae.	
CHAPTER VI	
DIRECTIVE ANTENNAE AND ARRAYS	238
6.1. General principles.	
6.2. Gain of directive systems.	
6.3. Long wire antennae.	
6.4. Long wire arrays.	
6.5. Rhombic antennae.	
6.6. Arrays of horizontal elements.	
6.7. Arrays of vertical elements.	
CHAPTER VII	
D.F. ANTENNAE	315
7.1. The loop antenna.	
7.2. Performance of D.F. loops.	
7.3. Adcock antennae.	
CHAPTER VIII	
ANTENNAE FOR SHIPS, AIRCRAFT AND AUTOMOBILES	340
8.1. D.F. loops for ships.	
8.2. Communication antennae on ships.	
8.3. Aircraft antennae for D.F. and landing systems.	
8.4. Aircraft antennae for communication channels.	
8.5. Automobile antennae.	
CHAPTER IX	
PROPAGATION OF RADIO WAVES	366
9.1. Surface, space and sky waves.	
9.2. Long waves.	
9.3. Medium waves.	
9.4. Short waves.	
9.5. Ultra-short waves.	
9.6. Microwaves.	

Contents

ix

CHAPTER X

PAGE

TRANSMISSION LINES	433
10.1. Basic transmission-line equations.	
10.2. Transmission-line constants.	
10.3. Reflection, voltage and current equations.	
10.4. Impedance diagrams.	
10.5. Practical considerations.	
10.6. Use of stub to increase antenna bandwidth.	

APPENDIX I

DIELECTRIC CONSTANT AND CONDUCTIVITY TABLES	475
---	-----

APPENDIX II

THE M.K.S. SYSTEM	477
-----------------------------	-----

APPENDIX III

NOTES ON THE MECHANICAL DESIGN OF ANTENNA STRUCTURES	479
--	-----

APPENDIX IV

LIST OF SYMBOLS	492
---------------------------	-----

<i>Bibliography</i>	495
<i>Author Index</i>	517
<i>Subject Index</i>	519

List of Plates

	Radar Antennae on R.M.S. "Queen Elizabeth"	<i>Frontispiece</i>
PLATE		<i>Facing page</i>
I.	The Top-capacitor Antenna of WXXX, near New York	44
II.	An Outrigger-type Vertical Radiator at San Paulo, Brazil	56
III.	The Base of a Shunt-excited Antenna at Pretoria, showing the Radial-wire Earth System	68
IV.	The Sectionalized Antenna at Brookman's Park, London	76
V.	The Base of the Vertical Radiator at Melnik, Czechoslovakia	80
VI.	Yagi Arrays with Wire-netting Reflectors, for Searchlight Control	116
VII.	Cartwheel Type of Unipole Antenna as used for Railway Communications on Ultra-short Waves	120
VIII.	Television Mast at Alexandra Palace, showing the Two Groups of Eight Vertical Wire-cage Dipoles	126
IX.	Parabolic Mirrors with Hemispherical Reflectors at the Focus—used for Cross-Channel Communication on a Wavelength of 17 cm in 1931	160
X.	An Array of Inverted-V Antennae at Ballygomartin	284
XI.	Curtain of Two Type HR _{4/4/1} Kooman Arrays at Daventry	302
XII.	Array of Franklin Antennae at Bodmin, Cornwall	312
XIII.	The Crossed-loop D.F. Antenna on S.S. "Orion"	342
XIV.	A Lockheed "Electra" showing the Mounting of the D.F. Loop and the V-type Communication Antenna	346
XV.	A B.O.A.C. "Speedbird" York Aircraft, showing Communication and Navigational Antennae	352
XVI.	The Erection of a 95 ft Tubular Mast by means of the "Falling Derrick" Method	484
<i>Inset.</i>	Fig. 10.16. Circle Diagram of Impedance	456

General Survey of Antennae and Propagation

THE aim of the following sections is to give the reader a simple overall picture of radio antennae and to state the basic principles of radiation in a manner that is mainly descriptive. At the same time the general aspects of radio-wave propagation are also discussed, for they are inseparable from the design of antenna systems. All design details have been omitted; they will be found in the subsequent chapters to which the present account is in the nature of an introduction.

It is not essential to have studied any of the contents of Volume I before reading this chapter (or, for that matter, before reading any of the chapters in this volume). However, references to Volume I are given wherever they might prove useful for further study.

Since a general discussion involves frequent reference to the order of the wavelength under consideration, it is appropriate to state beforehand what classification of the frequency spectrum is employed in the text. The classification is as follows—

	<i>Wavelength</i>	<i>Frequency</i>
Long waves	above 1 000 m	below 300 kc/s
Medium waves	100 m to 1 000 m	3 000 kc/s to 300 kc/s
Short waves	10 m to 100 m	30 Mc/s to 3 Mc/s
Ultra-short waves	1 m to 10 m	300 Mc/s to 30 Mc/s
Microwaves	below 1 m	above 300 Mc/s

It is true that the use of names indicating the order of the frequency would be more scientific, but the use of a wavelength terminology can be defended when dealing with antennae on the grounds that it results in an immediate comprehension of the order of the dimensions involved. It has been the author's experience that the majority of engineers think in terms of wavelengths despite the fact that the frequency is more fundamental. Whenever the wavelength is referred to without

qualification we understand it to mean the wavelength in free space or air; this is given by

$$\lambda_{\text{metres}} = \frac{3 \times 10^8}{f_{\text{c/s}}}$$

I.1. CONDITIONS FOR RADIATION FROM A CIRCUIT

Radiation from Current Elements

In discussing the electric or magnetic fields associated with a radiator it is convenient to start by considering the field from a doublet. A mathematical definition of a doublet is given in Vol. I, but from a physical point of view we may think of a doublet as a short piece of wire excited by a uniform current. (By a "short" piece we mean one whose length is short in comparison with the wavelength.) Any practical antenna may be subdivided into a series of doublets and the total field found by integration.

An analysis of the field due to a doublet (*see* Vol. I, § 4.2) shows that the electric component consists of—

- (a) An electrostatic field which depends on the instantaneous charge distribution,
- (b) An induction field which is determined by the velocity of the charges (i.e. by the current) in the system,
- (c) A radiation field which depends on the acceleration of the charges (i.e. on the *frequency* as well as on the strength of the current).

The radiation field varies inversely as the first power of the distance while the induction and static fields vary inversely as the second and third powers respectively; as a result the radiation component soon predominates over the others, except along the axis, where the radiation field is zero. For example, in the equatorial plane of the doublet at a distance of only one wavelength the radiation field already accounts for over 95 per cent of the total electric intensity. Consequently the word "field" may be taken as being synonymous with "radiation field" except in the immediate vicinity of the radiator and along the axis.

With these provisos in mind we may say that the field due to a doublet depends on the current strength, direction of field point and frequency in the manner shown in Fig. 1.1.

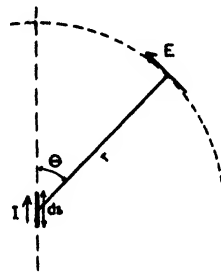
The radiation field arises through an outward flow of power from the wire travelling at the velocity of light and, unless there are some nearby reflectors, the whole of the out-going power is eventually dissipated. Thus an antenna is a dissipator of power and as such will have some apparent value of resistance at the input terminals. The effect of reflecting surfaces or wires is merely to change the total power dissipated and hence the input resistance.

This apparent resistance of the antenna is termed the "radiation resistance" and gives the total power radiated when multiplied by the square of the current. The value of the current is, of course, dependent on the point at which it is measured so that the radiation resistance refers to this point also. Usually the reference point is either at the input terminals or at a current antinode.

To illustrate the influence of frequency on the properties of an antenna, we may consider a short length of wire which is supplied in case (a) by a generator of frequency f_1 and in case (b) by a generator of frequency f_2 where $f_2 > f_1$.

In order to obtain the same radiated field strength at a distant point in the two cases, we must have a far greater current at the lower frequency f_1 than at f_2 —for the field strength is proportional to (current) \times (frequency). Assuming equal powers are supplied in both cases and that there are no heat losses, it follows that generator (a) is feeding into a circuit whose effective resistance is $(f_1/f_2)^2$ times lower than in case (b), i.e. the radiation resistance of a short antenna varies as the square of the frequency.

It would appear, therefore, to be just as easy to obtain a given field strength at the lower frequency f_1 as at f_2 provided that the generator in the first case is capable of delivering the power into such a low load resistance. In practice this proviso is a serious obstacle to the use of frequencies in cases where the length of the antenna is very short in comparison with a wavelength. Furthermore the heat losses are also serious under such conditions, particularly when the ground is part of the antenna circuit. Yet another difficulty with relatively short antennae is that they have a higher reactive impedance which must be



$$E = \frac{\pi}{5} \cdot \frac{I ds \sin \theta}{r} \cdot f_{Mc/s}$$

E is directed along a line of longitude

FIG. 1.1. FIELD DUE TO AN ELEMENT OF CURRENT

tuned out by an inductance, thereby introducing further heat losses in the antenna circuit.

Practical Forms of Radiators

So far we have only considered an antenna consisting of a "short" piece of conductor. In more general cases, the field strength of a system depends on the phasing of the current elements as viewed from the point under examination.

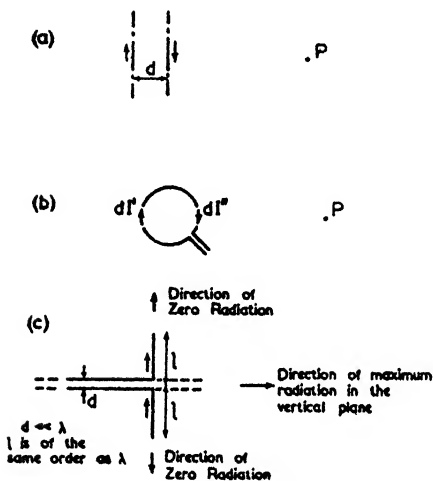


FIG. 1.2. DIAGRAMS FOR RADIATION FROM VARIOUS TYPES OF SOURCES

- (a) A portion of a parallel-wire transmission line, (b) A small loop, (c) A dipole.

Thus in Fig. 1.2 (a) the field strength at a distant point P is very low when $d < \lambda$. This represents the case of a normal transmission line in which the separation between the lines is relatively small. Increasing the spacing increases the field until a maximum is reached when

$$d = \frac{\lambda}{2};$$

further increases would cause the field to diminish and when $d = \lambda$ there would be complete

cancellation at P (although in certain other directions the field components would be augmenting each other).

In Fig. 1.2 (b) the loop of wire would have negligible radiation at a distant point if $d < \lambda$ since for every element of current dI' there is an equal and opposite element dI'' . Hence the radiation from ordinary radio-frequency coils, in which the dimensions are small in comparison with a wavelength, is negligible.

Fig. 1.2 (c) represents the case of a transmission line the ends of which have been bent outwards until they are collinear. The radiations from these two portions therefore augment each other in the direction shown.

Since the end of the transmission line is now a good radiator it will have greater power losses than in the unbent case (shown dotted in Fig. 1.2 (c)). The same losses could be introduced

into the latter by assuming the line to have an appropriate value of uniformly distributed series resistance. In this way we arrive at an "equivalent transmission line" whose input impedance equals that of the antenna for both real and

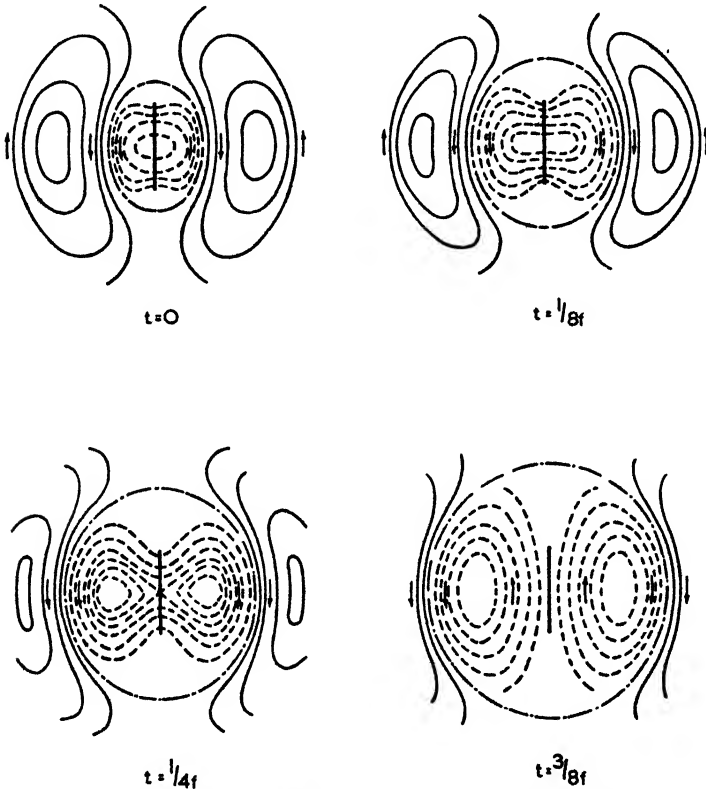


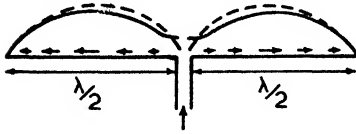
FIG. 1.3. ELECTRIC LINES OF A LINEAR RADIATOR AT DIFFERENT PHASES OF A CYCLE

imaginary terms. This conception of an equivalent transmission line may be used in antenna calculations in the manner described in Vol. I, § 5.3.

The previous discussions indicate that in order to obtain good radiation from the alternating current circulating in some system, this system should be "opened out" to provide a path of current whose length is comparable to a wavelength *without at the same time introducing a return path in which the currents are*

in antiphase as viewed from the field point. Here then we have a generalized statement of the problem of creating an antenna.

One solution is that shown in Fig. 1.2 (c) and repeated again in Fig. 1.3 with the generator directly across the terminals of the antenna. In the latter figure a succession of pictures illustrating the electric lines of force at varying times of a complete cycle is shown.

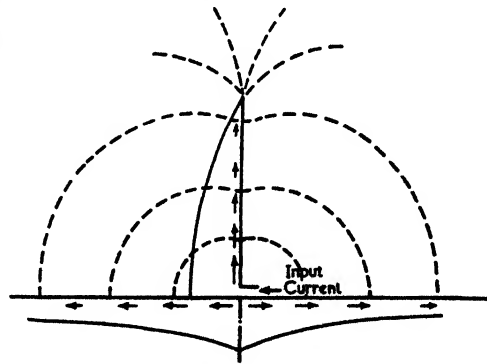


Full line = actual current distribution
Dotted line = sinusoidal current distribution as assumed for most theoretical calculations

FIG. 1.4. MODIFICATION TO A SINUSOIDAL CURRENT DISTRIBUTION DUE TO RADIATION

These pictures indicate how one may regard the radiated energy as "snapping off" from the antenna due to the rapid variations in current taking place along the wire. The current distribution along the antenna is in the form of a standing wave for complete reflection takes place at the end of the wire. This standing wave is not quite sinusoidal as would be the case in a lossless portion of open-circuited transmission line, but has the slightly modified distribution appertaining to a line of equivalent total losses (see Fig. 1.4).

Another solution is illustrated in Fig. 1.5, in which the lower half of the previous antenna has been replaced by a good conductor which, as in the case of medium and long waves, is usually the earth. Again a standing wave is set up, but this time the current in the lower member surges radially to and fro from the base of the antenna. When the lower conductor is the ground, considerable heat losses may take place, and to minimize such losses it is necessary to bury extra radial conductors in

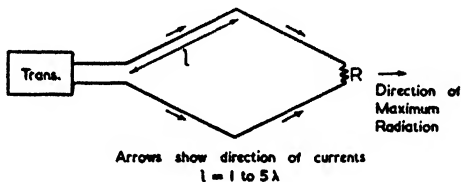


Full lines = relative current amplitudes shown graphically
Dotted lines = electric lines of force in air

FIG. 1.5. CURRENT DISTRIBUTION WITH A GROUNDED ANTENNA

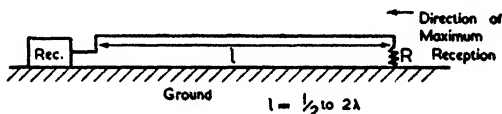
the earth—alternatively an artificial or “counterpoise” earth system may be used.

It will be noticed that both the solutions given make use of standing waves, i.e. we overcome the difficulty of a nearby return current by omitting altogether a conducting return path, but by leaving the ends open-circuited we cause the current to surge up and down the unterminated conductors. The process may therefore be viewed as the rapid charging and discharging of a capacitor whose lines of force fill the neighbouring medium and which consists of the capacitance between the two conductors on either side of the generator.



(a) Rhombic Antenna

However, it is not essential that a standing-wave method should be used. If a correctly terminated section of a transmission line were sufficiently opened out the radiation from the two sides would



(b) Beverage Antenna

FIG. 1.6. TRAVELLING-WAVE TYPE ANTENNAE

no longer cancel but would result in appreciable radiation in certain directions. The directions in which such radiation takes place depends on the time and space phasing of the current elements into which the system may be analysed. A typical antenna of this type is the well-known rhombic antenna illustrated in Fig. 1.6 (a).

Another form of travelling-wave antenna is the wave or Beverage antenna (Fig. 1.6 (b)) in which the earth forms one of the conductors. This is used mainly as a receiving antenna, for it relies on the earth losses to produce the necessary wave tilt. Nevertheless its inefficiency from a transmitting point of view is compensated for to some extent by its directivity and great effective height, so that transmitting wave antennae are not unknown.

It will have been noticed that apart from the classification of antennae into standing- or travelling-wave radiators, it is possible to group them into grounded and ungrounded

radiators. Such a grouping has certain advantages for a general discussion and permits convenient mention of the historical background to antennae.

1.2. GROUNDED AND UNGROUNDED RADIATORS

The Ungrounded or Hertz Antenna

When Hertz made his classical experiments in 1888 he used antennae consisting of loops of wire, the ends of which terminated in a spark gap. For transmission the loop was energized by a Leyden jar in series while a similar loop (but without a Leyden jar) formed the receiver. The damped oscillations obtained in this way had a wavelength of about eight times the diameter of the loop. It might also be added that Hertz employed parabolic reflecting sheets which focused the radiation from his spark-gap oscillators, thereby originating a form of directive antenna which has become more common again with the advent of good generators for microwaves. Thus these early experiments used ungrounded radiators at ultra-short wavelengths.

Provided an ungrounded radiator is situated a wavelength or more above the earth, the earth plays a negligible part in the determination of the characteristics of the radiator. It is therefore easy to avoid losses in such a radiating system and to obtain a high ratio of radiated to dissipated power. This favourable situation is, of course, greatly helped by the fact that the wavelengths concerned are short enough to make it possible to use radiators whose dimensions are of the same order as a wavelength (this follows from the initial assumption that it is physically possible to raise the radiator at least one wavelength above the ground).

We have been using the word "radiator" so far as synonymous with "transmitting antenna," but the same remarks hold true of receiving antennae. Indeed, a receiving antenna is merely a radiator in which excitation is in the form of a distributed e.m.f. in contrast with the transmitting case where the excitation is due to a concentrated e.m.f. In this chapter we shall therefore use the word "radiator" to imply an activated antenna whether in the receiving or transmitting condition. (In antenna design a distinction arises between the transmitting and receiving design because in the first case one is interested in radiating the maximum amount of power,

whereas in the second case it is the signal-to-noise ratio which is the main consideration.)

Practical examples of ungrounded radiators are television antennae, short-wave arrays, parabolic antenna systems and horn radiators. A characteristic feature of this class of radiator is that ordinary geometrical optics may be used in the study of the propagation from such antennae. That is to say, the radiator may be regarded as a source of spherical waves whose behaviour can be analysed without making any allowances for the effect of neighbouring bodies (such as the earth) on the radiator itself.

In spite of the high efficiency of ungrounded radiators they were soon abandoned in the early history of radio. This was due mainly to the lack of satisfactory methods of generating the higher radio frequencies, but also to the fact that it was soon found that great distances could be covered by the use of long wavelengths. Before passing on to grounded radiators, however, it should be mentioned that in 1897 Marconi succeeded in transmitting over a distance of eight miles across the Bristol Channel using a wavelength of 1.25 m. In the course of these experiments the importance of elevating the antennae as much as possible was clearly demonstrated. This is a feature of ultra-short-wave propagation and is seen nowadays, for example, in television transmissions in which both transmitting and receiving antennae are raised as high as practicable.

The Grounded, or Marconi, Antenna

It was the use of the long wavelengths together with a *grounded* radiator that first made long-distance radio communication possible. For his famous experiment of 1901, in which radio signals were first received across the Atlantic, Marconi used grounded transmitting and receiving antennae and a wavelength of 1 300 m. At the transmitting site in Cornwall the antenna consisted of a fanlike structure suspended between masts 52 m high, while at the receiving end in Newfoundland a wire 150 m long suspended from a kite was employed.

The success of these experiments was, of course, due to the existence of reflecting layers in the upper atmosphere and the use of a frequency that was not high enough to penetrate these layers. For the present, however, we shall confine our attention to the antenna aspect of the story. The fact is that Marconi had devised an antenna system in which the earth formed

part of the oscillatory circuit. In this way the linear dimensions of the radiator were halved whilst maintaining the same current distribution along what was the upper half of the ungrounded radiator.

A vertical transmitting antenna which is grounded in this way is capable of giving considerable field strengths along the surface of the earth provided medium or long waves are used. The first two decades of this century therefore saw the establishment of a number of long-wave stations employing tall grounded radiators which were energized by means of arc or high-frequency alternator machines. One might almost say that this period in the history of radio reached its culminating point in 1927 with the establishment of the G.P.O. station at Rugby which used an antenna system supported by twelve masts each 250 m high and operated on a wavelength as long as 18 000 m (it should be added that by that time valves were being used instead of arcs or alternators). At such a great wavelength the earth and the ionosphere together form what is virtually a transmission line, and in the space between them waves are able to propagate with relatively little attenuation. In fact, with the high power used at Rugby it became possible to have a 24 hr telegraph service to most parts of the globe.

In the meantime the ungrounded radiator had taken on a new lease of life for it was discovered that great distances could be spanned with remarkably little power by the use of short waves. These discoveries were made largely by amateurs who worked on wavelengths that had been assigned to them because they had been considered virtually useless from a commercial point of view. By 1926 the Marconi Wireless Telegraph Co. had established a regular service between Bodmin and Canada using wavelengths of 16 and 32 m. The antenna used at Bodmin was the first example of a commercial beam array and was named after its inventor, C. S. Franklin.

From that time on, more and more short-wave beam systems came into use for their cost is only a fraction of the equivalent long-wave station. But simultaneously with this development, a large number of broadcasting stations were set up using medium waves and grounded radiators—a combination which gives an efficient local service over a radius of 150 km or so.

The present situation may be summarized by saying that *grounded radiators* are used at very long wavelengths for long-distance commercial services, and at medium wavelengths for local broadcast services. On the other hand *ungrounded radiators*

are employed at short wavelengths for commercial, broadcast and amateur services over medium and long distances, at ultra-short wavelengths for various local services, and with microwaves for a great variety of purposes such as radar, radio altimeters, navigational aids and radio-telephone links.

The Tuning of a Radiator

It is well known that in order to obtain the maximum circulating current in a circuit the series reactance should be zero. Since the radiation from an antenna system is proportional to the current, it follows that the same need for tuning out the reactance arises in the case of antennae.

The typical form of an ungrounded radiator is the half-wave dipole which, when actually half a wavelength long, has an impedance of 73 ohms in series with 42 ohms inductive reactance. A much simpler way of tuning out this reactance than by adding a series capacitor is to shorten the length by about 5 per cent, whereupon the reactance may be reduced to zero (at the same time the radiation resistance is reduced to between 60 and 70 ohms). A half-wave dipole tuned in this manner forms an excellent radiator for, with any conductor of reasonable conductivity, the loss resistance is but a fraction of an ohm.

We may define the Q of an antenna in a similar manner to that of a tuned circuit, i.e. as the frequency on tune divided by the bandwidth measured between points at which the admittance is $\sqrt{2}$ times that on tune. A thin half-wave dipole, whose length-to-diameter ratio is of the order of 10 000, will have a Q of about 10, but a thick dipole, whose length-to-diameter ratio is only of the order of 10, has a Q of about 2 or 3. The precise figures depend on the shape and, except in the case of a spheroidally shaped or very thin antenna, are still not computable to any high degree of accuracy.

Most grounded radiators have an electrical height which is shorter than a quarter of a wavelength. As a result it is necessary to resort to tuning out the capacitive reactance of such antennae by means of a so-called "loading coil" at the base of the antenna. The situation is aggravated at really long wavelengths by the fact that the inductance must be large and yet have a very low resistance—for the radiation resistance of a long-wave antenna may be but a fraction of an ohm. In such cases the coil may consist of Litz wire having as many as 6 000 strands and a Q of 2 000.

Figures of Merit

In many cases, particularly where grounded vertical radiators are concerned, it is convenient to specify the performance of an antenna in terms of a "figure of merit." This figure is usually taken to mean the field strength in some specified direction at 1 km distance for 1 kW input to the terminals of the antenna. When the direction is not specified it is assumed to be either along the ground or, in the case of a free-space dipole, in the equatorial plane of the dipole.

Assuming the radiation resistance of a half-wave dipole to be 73.2 ohms we find (the calculation is given in Vol. I, § 4.4) that the field strength in the equatorial plane at a distance of 1 km for 1 kW is given by

$$E = 222 \text{ mV/m}$$

The field strength varies directly as the square root of the power and inversely as the distance, so that the above expression may be modified to

$$\frac{E_{mV}D}{\sqrt{P}} = 222 \quad . \quad . \quad . \quad (1.1)$$

where E_{mV} = field strength in millivolts/metre,
 D = distance in kilometres,
 P = radiated power in kilowatts.

Unfortunately the above units, which follow the conventional method of presentation, do not conform to the M.K.S. system. In the latter system the expression is given to an accuracy of $\frac{1}{2}$ per cent by

$$\frac{Er}{\sqrt{W}} = 7 \quad . \quad . \quad . \quad (1.2)$$

where E = field strength in volts/metre,
 r = distance in metres,
 W = radiated power in watts.

The corresponding case in a grounded antenna to a half-wave free space dipole is the quarter-wave vertical radiator shown in Fig. 1.7 (b). Such an antenna has exactly half the impedance of the corresponding free-space antenna, so that a quarter-wave antenna has an impedance of 36.6 ohms (the value 36 ohms—or 72 ohms for the half-wave dipole—is often used since the precise value is open to dispute). For a given input power, therefore, the antenna (b) has $\sqrt{2}$ times the

current of antenna (a). Moreover when considered together with the image in the ground, it has effectively the same total length as antenna (a). Consequently, the field strength from the grounded quarter-wave antenna is $\sqrt{2}$ times greater, so that for such an antenna

$$\frac{E_{mv}D}{\sqrt{P}} = 314 \quad \dots \quad (1.3)$$

The extra field strength of the grounded radiator is simply due to the fact that the energy is being radiated only through a hemisphere.

In M.K.S. units the above figure of merit becomes (to an accuracy of 1 per cent)

$$\frac{Er}{\sqrt{W}} = 10 \quad (1.4)$$

It will be noticed that in both cases the M.K.S. version gives particularly simple values, each having an accuracy which is perfectly satisfactory, taking into consideration the lack of precision in radiation resistance figures. On the whole, equation (1.3), or the short antenna variation of it given below, will be found suitable for long- and medium-wave calculations, whereas (1.2) forms a convenient basis for calculations on shorter wavelengths. The short antenna variation of (1.3) (i.e. for heights below 0.1λ) is particularly convenient and forms the basis of most field strength charts; it is given by

$$\frac{E_{mv}D}{\sqrt{P}} = 300 \quad \dots \quad (1.5)$$

For vertical antennae whose heights exceed 0.1λ the proportionality factor given by Fig. 2.28 may be used.

In the case of grounded radiators, it must be remembered that the figure of merit would only give the field strength at any distance *if the earth were a perfect conductor*. At distances of a few kilometres and more there will be definite ground losses

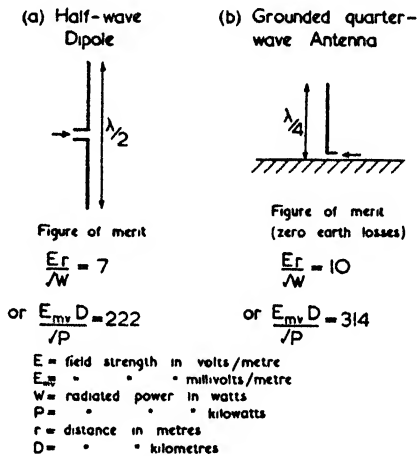


FIG. 1.7. FIGURES OF MERIT FOR FREE-SPACE HALF-WAVE DIPOLE AND GROUNDED QUARTER-WAVE ANTENNAE

which will reduce the field strength obtained in practice, even if the antenna has a perfect earth return system. On medium and long waves it is fairly reasonable to take a field strength measurement at a distance of 1 km and call the result the figure of merit, but on short waves the strength at even 1 km may be well below the theoretical value. Thus it will be realized that the figure of merit is essentially an index of the degree of horizontal radiation from an antenna and that in estimating field strengths the attenuation of the earth

must also be taken into account.

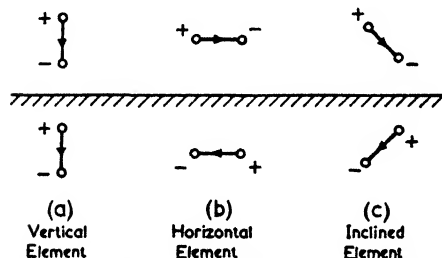


FIG. 1.8. EXAMPLES OF IMAGES IN A PERFECTLY CONDUCTING GROUND

1.3. INFLUENCE OF THE GROUND

In discussing the effect of the ground on antennae and radio propagation, it is convenient to consider first of all the hypothetical case of a perfectly conducting ground.

For long waves the ground does approximate fairly well to the case of a perfect conductor, but at microwaves the correct approximation is to consider the ground as a perfect dielectric. At intermediate wavelengths it is usually necessary to take both the dielectric constant and the finite conductivity of the ground into account.

For a perfectly conducting earth we may suppose the antenna to have an image in the ground as depicted in Fig. 1.8 (a) and (b) for vertical and horizontal antennae respectively; then the radiation field above the ground is the sum of the fields due to the antenna and its image. The radiation in a horizontal plane is augmented by the image in the case of a vertical antenna but complete cancellation takes place in the case of a horizontal antenna. The latter type of antenna is therefore unsuitable for obtaining radiation along the ground. Even when the finite conductivity of the ground is taken into account, the radiation along the ground is relatively weak whatever the wavelength may be.

We therefore turn to the case of a vertical radiator with its positive image if good transmission along the surface of the ground is required. A study of this case, including the effect of finite conductivity, is particularly important since it represents

the conditions under which long- and medium-wave radio transmissions take place.

The classical paper on this subject appeared as long ago as 1909 when Sommerfeld⁽²⁸⁵⁾ made a theoretical analysis of this subject, assuming a plane earth. Ten years later Weyl⁽²⁸⁹⁾ indicated even more clearly how the total field strength at a point could be regarded as consisting of two distinct components. These components are—

(1) A “space wave” which is the resultant of a direct ray and a ray reflected off the ground according to the laws of optical reflection.

(2) A “surface” wave which is characterized by the fact that the planes of constant amplitude do not coincide with the equiphase planes (such a wave can travel in a tilted manner along the surface of a medium without reflection from that medium).

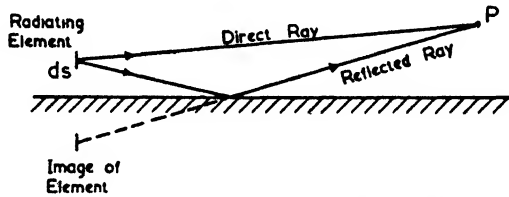


FIG. 1.9. GEOMETRY OF A SPACE WAVE

The solution by Weyl contains a surface-wave term which is not identical with the one obtained by Sommerfeld. This discrepancy is not appreciable except when the dielectric constant of the ground is high compared with the product of the conductivity and the wavelength. In order to put the matter to a practical test, Burrows⁽²⁹⁰⁾ carried out experiments over a fresh-water lake at a frequency of 150 Mc/s. His experimental results were entirely in agreement with the Weyl solution.

Space Waves

The space wave consists of two components as shown in Fig. 1.9, the total field strength being the sum of all such fields due to all the elements of current along the antenna. In each case the coefficient of reflection for the indirect ray is given in phase and amplitude by a reflection coefficient R_r , which depends on the angle of incidence, the wavelength and the ground constants (dielectric constant and conductivity). The formula for R_r is given in Vol. I by equation (3.52).

Over an earth of finite conductivity the space wave becomes

zero along the ground owing to the fact that $R_v = -1$ for grazing incidence so that the direct and indirect rays cancel. A typical polar diagram showing this effect is given in Fig. 1.10. In the same diagram the corresponding pattern for infinite conductivity is also shown and this, it will be noticed, shows a maximum field strength at the surface of the ground. The

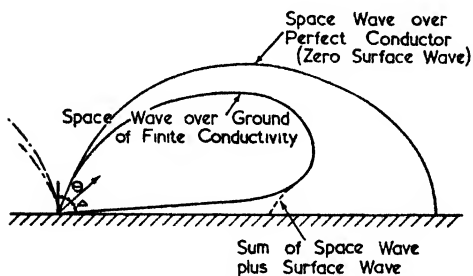


FIG. 1.10. POLAR DIAGRAMS OF A VERTICAL RADIATOR OVER GROUNDS OF FINITE AND INFINITE CONDUCTIVITY

reason for this maximum is that the reflection coefficient, R_v , has now become $+1$. With infinite conductivity the surface wave is zero (i.e. the space-wave polar diagram represents the complete solution), but with a finite conductivity it has some particular value which partially "fills in" the slot in the polar diagram of the space wave (see Fig. 1.10). The surface wave is attenuated exponentially in the upward direction from the ground and reaches a negligible value in the matter of a degree or so on the polar diagram.

The analysis of the surface-wave component is complicated and, in order to effect a certain simplification, Sommerfeld introduced the use of a "numerical distance" which is a function of the distance from the antenna, the wavelength and the ground constants. For a given distance, the use of a long wavelength gives a low numerical distance, whilst at short wavelengths the same parameter increases to large values.

Having determined the numerical distance, we may then obtain the value of an attenuation constant, A_1 , which, on being multiplied by the field strength under perfect earth conditions, gives the actual field strength at the surface of the ground. This attenuation constant is a function of an important parameter which is proportional to the product of the wavelength and the conductivity, for it is numerically equal to $60\lambda g$ where λ is in metres and g is in mhos per metre.

Whether the ground should be considered primarily as a conductor or as a dielectric depends on the magnitude of this parameter in comparison with the relative dielectric constant

ϵ_r . If $60\lambda g > \epsilon_r$, the ground behaves as a conductor, whereas if $60\lambda g < \epsilon_r$, the ground acts like a dielectric.

Provided $60\lambda g$ is at least 12 times ($\epsilon_r + 1$), we may use Van der Pol's approximation for the attenuation constant which is then given by

$$A_1 = \frac{2 + 0.3\rho}{2 + \rho + 0.6\rho^2} \quad (1.6)$$

where $\rho =$ the numerical distance

$$= \frac{\pi}{60\lambda g} \cdot \frac{r}{\lambda}$$

Although the surface wave has been discussed with regard to vertical antennae only, a horizontal antenna has a radiation field which also contains a surface-wave component, but in this case the component is so weak that it can nearly always be neglected in practice.

Long and Medium Wavelengths

The discussion on the surface wave showed that the effectiveness of the conductivity of the ground depends on the product of the conductivity and the wavelength, i.e. on the parameter $60\lambda g$. For long wavelengths this product is high enough to show only small variations in the field strength over different types of earth; but at medium wavelengths the value of the product decreases to such an extent that the differences in earth conductivities cause appreciable variations in the field strength at a distance. Some specimen figures are given in the following table.

Wavelength in Metres	Frequency in kc/s	Field Strength in mV/m at 100 km for 1 kW Radiated		
		Sea Water ($g = 5$ mhos/m)	Earth of Good Conductivity ($g = 0.01$ mho/m)	Earth of Bad Conductivity ($g = 0.001$ mho/m)
200	1 500	3	0.2	0.03
500	600	3	1.6	0.3
1 500	200	3	2.8	1.8

The above figures illustrate the superior propagation characteristics of long waves. Unfortunately the utility of the longer

waves is limited by the fact that very high antennae are required to obtain good efficiency and also by the fact that the number of available channels is very few.

However, the more limited range of the medium waves is an advantage when only local broadcasting is required, but this advantage is nullified at night time when reflections from the ionosphere can cause a great increase in range.

It is interesting to note that although the ground causes greater horizontal figures of merit, because it restricts the radiation to a hemisphere only, the subsequent attenuation in propagation at medium waves results in a decrease in field strength relative to the corresponding free space case. Indeed it is only with short-wave beam systems operating on sky waves that the presence of the ground has any beneficial effect.

Short Wavelengths

In the short-wave region, namely between 10 and 100 m, the propagation of the wave which travels along the surface of the ground becomes progressively poorer as the wavelength is decreased. The surface range of such waves is therefore distinctly limited, the only method of overcoming this deficiency being to elevate both transmitting and receiving antennae as far as possible above the ground. Since the elevation is measured in terms of wavelengths, such a procedure is only practical on ultra-short waves.

Whenever a vertical antenna is situated a wavelength or more above the ground (or a horizontal antenna but a fraction of a wavelength) the surface wave is negligible so that a complete analysis may be made on ray theory only. Indeed in the case of horizontal radiating elements it is usually sufficiently accurate to base the analysis simply on an out-of-phase image.

On short waves the resultant polar diagram conveniently gives a beam which is directed upwards at an angle depending on the height of the antenna. Such a beam is suitable for long-distance propagation by means of reflections from the ionosphere—a feature which is considered more fully in the next section. Figs. 3.10, 3.11 and 3.12 show the polar patterns obtained with a vertical dipole and a horizontal dipole whose centres are at various heights above the ground.

In the case of transatlantic traffic, the required beam should make an angle of about 10° with the horizontal if the wavelength is 20 m. A beam whose maximum is at this angle is

readily obtained by setting up some form of antenna system whose centre is about 1.5 wavelengths above the ground. The image in the ground from such an arrangement virtually doubles the field strength in the desired direction, so here we have a case in which the presence of the earth is used to definite advantage. The polarization of the antenna system is preferably horizontal, for this form results in more reliable polar patterns and greater freedom from variations in ground constants.

The field strength of a wave transmitted via the ionosphere will vary widely according to the reflection coefficient. At the best, this coefficient may approach unity, in which case a horizontal dipole, whose height is at least $\lambda/2$ above the ground, would give nearly twice the field strength indicated by equation (1.2) in the direction of maximum radiation. The distance in this case is, of course, that travelled by the sky wave (which in long-distance cases will differ but little from the ground distance).

As an example, the field strength at 1 000 km distance due to an elevated horizontal dipole (in this case the height should be about $\frac{1}{2}\lambda$) has a maximum value given approximately by

$$\frac{E}{\sqrt{W}} = 14\mu\text{V/m}$$

Thus a radiated power of only 100 W is capable of giving, under favourable circumstances, a field strength of $140\ \mu\text{V/m}$ at 1 000 km. In practice the maximum field strength is likely to be more like half this value.

Sky waves therefore have the great advantage of a law of attenuation with distance which is not much inferior to the simple inverse distance law for free space. This fact accounts for the long-distance transmissions which are possible on short waves using only moderate power.

Ultra-short Wavelengths

For wavelengths below 10 m reflections from the ionosphere cannot be relied upon, a fact which prohibits their use for regular long-distance communication. In addition the wave along the surface of the earth is negligible, whether a vertical grounded antenna is used or not.

Thus the only way in which a useful service can be obtained at such wavelengths is by the use of elevated antennae, i.e.

by producing a beam which is so near to the horizontal that appreciable field strengths can be obtained even at a fraction of a degree off the ground.

As an example, one may cite the television service from Alexandra Palace which uses a wavelength of 7.2 m. In this case the transmitting antennae are about 12 wavelengths above the ground and therefore produce a beam which is only 1° off the ground (assuming this were level). At a distance of 10 km it would be necessary to elevate the receiving antennae 170 m above the ground to obtain the maximum field strength from this beam. This method of propagation is obviously exceedingly wasteful; so much so, in fact, that experiments have been carried out recently in the United States to investigate the possibility of carrying television transmitters in high-flying aircraft. These experiments seem to have demonstrated the feasibility, both technically and economically, of such a procedure.

It will be appreciated that the need for elevated antennae on ultra-short waves is easily satisfied on aircraft. Hence wavelengths of a few metres are suitable for communication between aircraft, or aircraft and ground stations. In the case of radio signals passing between two nearby aircraft the ground reflections are obviously of no importance, so that free-space conditions prevail.

For communication between ground stations using antennae elevated at least one wavelength, the following simple field strength formula often applies for half-wave dipoles (the circumstances under which it is valid are discussed in § 9.5)—

$$E = 88\sqrt{W} \frac{h_T h_R}{r^2} \quad (1.7)$$

where E = field strength in volts/metre,

W = power in watts,

h_T, h_R = height of transmitting and receiving antennae in metres,

λ = wavelength in metres,

r = distance between transmitter and receiver in metres.

The units used in the above formula may be remembered more easily if one bears in mind that they conform to the M.K.S. system. The formula applies to vertical dipoles and also to horizontal dipoles provided that in the latter case the receiving and transmitting antennae are broadside on.

More precise calculations, and in particular ones involving rays which make an angle with the ground of more than 1° , require the use of the complex reflection coefficient. This coefficient is a function of the "complex dielectric constant" ($\epsilon_r - j60\lambda g$). The real part is the relative dielectric constant of the ground and the imaginary part is the parameter mentioned before in connexion with the surface wave.

In the range 1 to 10 m the conductivity parameter for all types of soil is smaller than the dielectric constant but not by so much that it can be neglected. The calculation of the field strength under conditions for which equation (1.7) does not apply may therefore be quite a complicated matter.

Microwaves

When microwaves are employed the antenna system is normally highly directive and in many cases an attempt is made to avoid the ground altogether.

An early example of such a microwave system was the two-way telephony system established across the English Channel in 1931 by Standard Telephones and Cables, Ltd. and Le Matériel Téléphonique. This used a wavelength of 18 cm and parabolic mirrors 3 m in diameter. Even so the beams were not sufficiently directive to be completely independent of the ground conditions—as was demonstrated by variations in signal strength with the tides.

In radar systems the beam is often projected at greater angles of elevation, so that complete freedom from ground conditions becomes possible.

In cases where ground reflections cannot be avoided the ground may be regarded as a dielectric whose relative dielectric constant varies between 3 (very dry soil) and 20 (damp soil). This is because at these wavelengths the product of the conductivity and the wavelength is so small that the complex dielectric constant reduces to the dielectric constant itself. An exception must be made in the case of sea water, for which the real and imaginary parts of the complex dielectric constant are equal at 25 cm wavelength, i.e. the wavelength must be distinctly less than 25 cm for the "ground" to be considered as a dielectric.

The field strength on microwaves may be calculated in a manner similar to that outlined for ultra-short waves, but care must be taken to allow for possible differences in the direct

and indirect rays due to the sharpness of the polar pattern of the antenna system.

Under certain atmospheric conditions (usually associated with fine weather) the rate of change with height of the density of the air and also the relative humidity of the air are such that very-long-distance propagation becomes possible. This phenomenon is known as super-refraction and the portion of the atmosphere in which this takes place forms what is called a "radio duct" which is virtually a dielectric waveguide. When ducts of this nature are formed they rarely extend for more than 100 m above the surface of the earth; consequently their waveguide properties are mostly effective at centimetre wavelengths only. In order to guide wavelengths of a few metres efficiently much bigger ducts are needed; as a result the phenomenon of super-refraction occurs far less frequently at ultra-short wavelengths and is virtually absent at wavelengths above 10 m.

1.4. INFLUENCE OF THE IONOSPHERE

The Discovery of the Ionosphere

After Marconi, in 1901, succeeded in transmitting from Cornwall to Newfoundland, there was much speculation as to the manner in which the radio waves had propagated round so large a portion of the earth's curved surface. The first attempts at an explanation evoked the theory of diffraction but without success, for calculations showed that the bending which could be accounted for in this way was insufficient.

In the following year Kennelly in America and Heaviside in England both put forward the hypothesis of a reflecting layer in the upper atmosphere. It was further suggested that this reflecting layer might be due to the ionizing action of the sun.

Not until 1925 was any direct evidence obtained as to the existence of such a layer though the known features of short-wave propagation had provided very strong confirmation of the theory. In that year Appleton and Barnett⁽²²²⁾ published the results of experiments which gave the first direct demonstration by a method which measured the frequency of beats obtained between the direct and indirect rays when the transmitter frequency was modulated in a known manner. Before long the existence of a reflecting layer was not only confirmed

but considerable information was obtained both about this layer (the E or Kennelly-Heaviside layer) and yet another layer (the F or Appleton layer). The whole region in which these layers are situated was appropriately named the "ionosphere."

An important contribution to the technique of ionosphere measurements was made by Breit and Tuve⁽²²⁹⁾ in 1926. They employed pulses of radio energy whose duration was short enough to measure the time interval between the arrival of

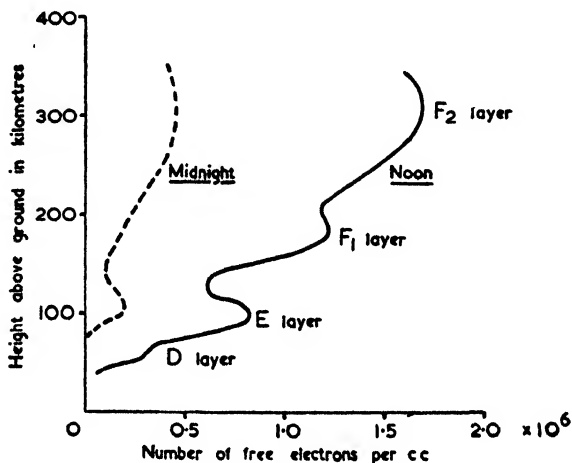


FIG. 1.11. TYPICAL DISTRIBUTION OF IONIZATION IN THE IONOSPHERE

the direct ground ray and the indirect ray which had been reflected from the ionosphere.

The investigations on the ionosphere showed that the E region is at a height of about 100 km, but the F region is very broad, being often in the form of a double layer, the lower one, or F₁ region, being at about 200 km and the upper one, the F₂ region, at about 300 km. Of these the F₂ layer is the most variable in height and also has the greatest reflecting power. Curves showing a typical distribution of ionization for temperate zones are given in Fig. 1.11.

At the heights at which these layers exist the atmospheric pressure is very low (less than one-millionth of the pressure on the ground) which permits ionization by solar radiation without too rapid a recombination of the freed charges. Observations taken during eclipses show that whereas the E and F₁ regions appear to be due almost wholly to ultra-violet radiation, the F₂ region is only partly due to this cause.

The influence of the sun on these ionized regions is most marked; their diurnal and seasonal variations are all functions of the intensity of the solar radiation—the greater this intensity the stronger is the ionization and therefore the reflecting power of the layer. There is one notable exception to this rule, for the summer noon ionization of the F_2 layer is actually *less* than the corresponding winter value. This anomaly is attributed to expansion caused by the existence of very high temperatures in the F_2 region during the summer day.

A further correlation with solar activity is the increase of ionization in all the layers during periods of sun-spot maxima. These periods occur every eleven years, a maximum being due during the period 1949–50. For example, at a latitude of 40° during the sun-spot maximum conditions the F_2 layer will reflect at vertical incidence frequencies as high as 12 Mc/s but during the periods of minimum activity the critical frequency will drop to about 6 Mc/s.

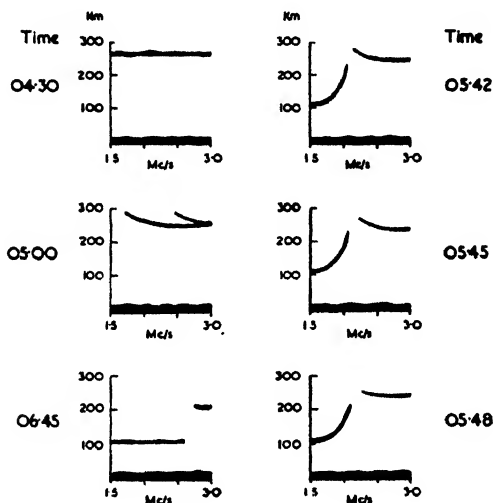
The earth's magnetic field was also found to play a prominent part in the behaviour of the ionosphere. It happens that the natural frequency of vibration of an electron in the earth's magnetic field over England is about 1.3 Mc/s, a frequency which is within the radio-frequency spectrum. This particular frequency is known as the "gyro frequency" and must be taken into account in a thorough explanation of the properties of the ionosphere. The theory arising from the complete problem is known as the "magneto-ionic" theory and is quite complicated, although the basic equations are simply Maxwell's equations and the force equation of the charge in the presence of a magnetic field.

Critical and Maximum Usable Frequencies

When making measurements on the ionosphere, the transmitter and receiver are normally situated within a few kilometres of each other; thus the indirect ray strikes the ionized layers at practically vertical incidence (*see* Fig. 1.13). If the frequency of the transmission is increased there comes a time when the reflecting powers of the ionized layer are insufficient to give a return signal. The frequency at which this occurs is known as the *critical frequency* and refers essentially to the case of vertical incidence.

Both the pulse and frequency-change methods of determining the height of a layer depend on the time interval between the

direct and indirect rays. Therefore the height obtained in this way would only be accurate if reflection took place at a sharp boundary—in actual fact the wave penetrates for some distance into the ionized region, travelling with continually decreasing group velocity. For this reason the heights measured by ionosphere experiments are known as “equivalent heights,”



(Sept 3rd 1937- Cambridge, England)

FIG. 1.12. EXAMPLES OF h' - f IONOSPHERE RECORDS

and are denoted by h' so that a curve of equivalent height versus frequency is known as an h' - f curve.

Examples of such curves are given in Fig. 1.12 which also illustrates the transition of echoes from a lower to an upper layer as the frequency is increased.

It will be noticed that there is a sharp increase in the value of h' as the critical frequency of the lower layer is approached. This is known as the group retardation effect and is due simply to appreciable decreases in the signal velocity in the neighbourhood of the critical frequency. A study of the shape of this part of the curve can be made to give a value for the thickness of the layer (based on the assumption of a parabolic distribution) and this in turn will determine the maximum usable frequency for any distance at that time.

The *maximum usable frequency* (abbreviated to M.U.F.) gives the value of the highest frequency which can be employed

for communication between two points at a given distance apart. A frequency higher than the M.U.F., if it can be reflected at all, will have to strike the ionized layer at a greater angle of incidence to suffer reflection and will therefore return to the ground at a greater distance than the required one. This point is expressed pictorially in Fig. 1.13, in which account is also taken of the fact that the rays may travel some distance in the ionosphere before finally bending back to earth.

A lower frequency than the M.U.F. will follow almost the

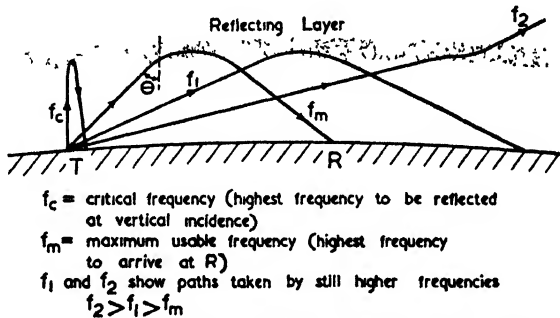


FIG. 1.13. EXAMPLES OF PATHS TAKEN BY SKY WAVES

same path but will suffer more attenuation in its passage through the ionosphere.

Consequently it is usual in practice to employ frequencies which lie between 85 per cent and 50 per cent of the M.U.F. The use of an 85 per cent value may result in occasional failure to secure reflections at the required angle (since published M.U.F. figures are merely statistical averages which are used for predicting the future conditions); on the other hand a 50 per cent value will occasionally be completely attenuated.

If a reflecting layer had a sharp boundary, the relation between the critical frequency, f_c , and the maximum usable frequency, f_m , for a given angle of incidence, θ , would be given by Snell's law, namely

$$f_m = f_c \sec \theta \quad . \quad . \quad . \quad (1.8)$$

In actual fact the layers are not sharp, but this does not make any radical difference. A point of greater importance is that owing to the curvature of the earth and the surrounding ionosphere there is a maximum angle of incidence which can be made with the layers by a ray leaving the earth tangentially. In the case of the E layer this angle is about 80° and for the

F_2 layer it is about 73° . The corresponding great circle distances covered by reflections at such angles are 2 200 km and 3 600 km and the values of f_m are $5.8f_c$ and $3.4f_c$ respectively.

Appleton and Beynon⁽²²³⁾ have calculated the f_m/f_c ratios more accurately making use of the assumption of a parabolic layer. Their calculations show that in a typical long-distance single-hop transmission the passage through the ionosphere represents about one-third of the total path distance between

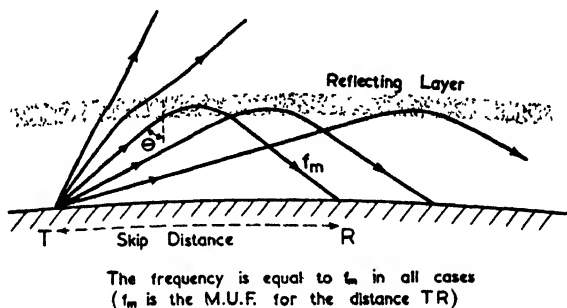


FIG. 1.14. PATHS TAKEN BY SKY WAVES FOR VARIOUS ANGLES OF INCIDENCE WHEN THE FREQUENCY IS KEPT CONSTANT

transmitter and receiver. In spite of this fact, their curve of the f_m/f_c ratio against distance (which is reproduced in Fig. 9.26) shows no great departure from the simple theory—though in general the ratios given by the more exact theory are about 25 per cent lower.

Skip Distance

There is a maximum usable frequency for any distance and this distance is also the *minimum* distance at which this particular frequency can be received (this does not, of course, take into account reception very close to the transmitter due to the surface wave). This distance is therefore known as the skip distance for the frequency in question—it is illustrated in Fig. 1.14.

From the remarks made previously about the variability of the ionosphere, it is obvious that the skip distance for any one frequency will vary both diurnally and seasonally. Fig. 1.14 shows only one reflecting layer, although in practice both the E and F regions have to be taken into account. In the majority of cases the skip distance depends on the F_2 layer, but for

periods round about a summer noon the E layer is likely to be the determining factor.

Long and Medium Wavelengths

At long wavelengths the simple ray theory is inapplicable since the distance between the earth and the ionosphere is only a small multiple of a wavelength. It is therefore more correct to look upon the ionosphere as the boundary of a transmission line (for both the earth and the ionosphere are quite good conductors at such low frequencies), the other boundary being the earth itself. For this reason long waves are propagated remarkably well round the curvature of the earth.

It may seem unfortunate that the theory of the effect of the ionosphere on radio waves should be split into two, i.e. into transmission line and ray theory, for it is obvious on physical grounds that the two theories should merge into one another. A method of calculation applicable throughout the whole of the radio spectrum is Eckersley's⁽²³⁸⁾ phase integral method which is based on image theory. At medium wavelengths, however, the ray method of treatment is already quite satisfactory and covers practically all normal requirements.

Except for wavelengths below about 200 m, medium waves are reflected from the ionosphere all the year round even at vertical incidence. In spite of this they do not necessarily give a good sky-wave service for in the daytime they suffer considerable attenuation. This attenuation is due to their passage through the D region which exists at about 60 km height. The ionization in the D region is insufficient to cause reflection (although some cases of reflection have been reported from India) but it does cause considerable attenuation at wavelengths of the order of 200 m, i.e. at frequencies of the same order as the gyro-frequency.

At night time the D region is rapidly de-ionized because of the relatively high atmospheric pressure so that medium-wave stations may be received at a considerable distance by means of the sky wave. In regions where the sky and ground waves are of comparable strength the two components combine; fading is then experienced owing to the variability of the sky wave.

Short Wavelengths

At short wavelengths the attenuation will not be great unless the frequency is half or less of the maximum usable frequency.

Therefore under normal conditions there is always some wavelength at which good sky-wave propagation can be obtained. The determination of this wavelength depends on the critical frequency in the manner indicated previously in this section; as full design data are given in Chapter IX we shall merely indicate the method of choosing the wavelength in this account.

Let us suppose, for instance, that we wish to communicate between London and New York. The most probable transmission consists of two hops each 3 000 km long. By taking a figure between those published for Washington, D.C., and London we can estimate the probable critical frequency for a given time of the day, year, and sunspot cycle. There will be two such figures, one for the apex of each hop. Of the two the lower frequency must obviously be chosen. Suppose this proves to be 6 Mc/s, then the curves of Fig. 9.26 show that a frequency three times this value is the M.U.F. for 3 000 km. To achieve greater certainty of communication we take 80 per cent of the M.U.F., i.e. a frequency of 14.4 Mc/s.

In passing through the ionosphere, the plane of polarization of the waves is rotated to such an extent that the polarization on arrival at the receiving end bears no predictable relationship to the initial state of polarization. Moreover the received polarization varies readily with changes in the ionosphere, thereby causing fading in the reception.

Reception by means of waves reflected from the ionosphere is therefore only of relatively poor quality unless special systems are used and even then it is not comparable with reception from nearby medium-wave transmitters. Consequently the main application for short-wave transmissions is for long distance transmissions on moderate powers.

Ultra-short Wavelengths and Microwaves

Although many cases have been reported of the reflection of waves whose frequencies were as high as 50 Mc/s or so, the reflection of waves whose frequency exceeds 30 Mc/s is not to be relied upon. The ionosphere is therefore not taken into account in the design of systems employing wavelengths below 10 m.

Long- and Medium-wave Antennae

WHEN using long or medium wavelengths the main object is to transmit as much of the radiated energy as possible along the surface of the earth; this may be achieved by using a vertical radiator whose height is of the order of half a wavelength. Such heights are not feasible for long wavelengths because of structural difficulties, neither are they suitable for low-power installations because of economic considerations, so that in both these circumstances we are forced to use radiators whose heights are only a fraction of a wavelength. To increase the current in such cases it is usual to add some form of capacitance loading at the top of the radiator; this may be a conducting disk, a horizontal wire, or a collection of horizontal wires in the shape of a cage or flat multi-wire top. In this manner the "effective height" of an antenna may be increased from 0.5 to as much as 0.75 times the actual height, with a corresponding increase in field strength.

During the hours of daylight the range of a medium-wave station does not depend greatly on the radiated power or the type of antenna. This is due to the fact that the ground losses cause considerable attenuation at distances of more than about 50 km. For example, using a wavelength of 300 m over ground of moderate conductivity, it requires a hundred times more power to produce a given field strength at 200 km than it does at 100 km. These daytime limitations in range are not altogether undesirable since they reduce the interference between stations in different parts of the world.

A complication arises at night time because of reflections from the ionosphere. These reflections are sufficiently strong at distances of 100 to 200 km to be comparable in strength with the direct radiation along the ground and, since they are never consistent in amplitude and polarization, the combined

signal is subject to fluctuations in strength. It is important, therefore, to obtain as high a ratio as possible of ground signal to sky-wave signal in the design of broadcast antennae. This ratio is determined by the polar pattern in a vertical plane through the antenna, from which it can be deduced that the ratio is particularly favourable for antennae whose heights lie between 0.5 and 0.6 of a wavelength.

2.1. CHARACTERISTICS OF A VERTICAL RADIATOR

Assuming that the wavelength to be used has been stipulated, the design of an antenna depends on the following main considerations—

(a) The horizontal “figure of merit.” This figure of merit is a measure of the field strength at any given zenith angle at 1 km for 1 kW input (*not* 1 kW radiated). It therefore takes into account the losses in the antenna system. The losses due to propagation over an imperfect ground are normally neglected (they may make about 2 per cent difference at 1 km).

(b) The input impedance. The antenna impedance at the driving point must be known in order to design the feeders and the transmitter output circuit.

(c) The vertical polar diagram. From this the relative strengths of the sky and ground waves can be calculated and hence an estimate of the probable fade-free radius obtained.

None of the above characteristics can be determined without a knowledge of the current distribution along the radiator. By analogy with an open-circuited transmission line we can assume a sinusoidal distribution of current. This assumed current distribution enables us to calculate the radiation resistance whereupon, if greater accuracy is required, a closer approximation to the current distribution can be obtained by assuming a dissipative transmission line whose losses just account for the radiation losses. A further refinement is to include some estimated value of the dead-loss resistance (i.e. earth losses, etc.) in the evaluation of the equivalent dissipative transmission line.

A more accurate form of equivalent transmission-line technique has been devised by Schelkunoff,⁽⁷⁹⁾ who uses the biconical horn as his basic shape and regards an antenna of uniform cross-section as a line of slowly varying impedance. In this way we can define an average characteristic impedance for the radiator. Curves based on this method are given later

in Figs. 2.15 and 2.16. They give values which check up far better with practical measurements, particularly in the case of relatively thick masts (i.e. masts whose characteristic impedance is less than 400 ohms) and antennae whose heights are in the region of $\lambda/4$. The curves of Figs. 2.15 and 2.16 should therefore be used whenever possible, i.e. for all simple cylindrical, or approximately cylindrical, radiators.

For inverted-L, T-type and reactance-loaded antennae in general, the equivalent transmission-line method is still used. Fortunately for T and L antennae of moderate dimensions the transmission-line method is more accurate than for anti-fade antennae.

In practice, differences between theory and experiment may arise because of the effect of supporting guys, base capacitance to ground, wrong estimate of earth losses, etc. Furthermore it has been found⁽¹⁰⁴⁾ that antenna characteristics may show small variations with the weather. In the face of such inevitable discrepancies, the above-mentioned methods are distinctly useful, whatever criticisms may be levelled against them on purely theoretical grounds.

2.2. ANTENNA REACTANCE

When the total length of an antenna is less than $\lambda/20$, the input impedance is that of a capacitor whose value is equal to the electrostatic capacitance of the system.

For longer antennae it becomes necessary to consider the wires as part of a non-dissipative transmission line whose input impedance can be found from the angular length and the characteristic impedance of the system. The characteristic impedance may be obtained from the static capacitance per unit length, i.e. the determination of the static capacitance is again involved.

If the antenna consists of a vertical radiator together with some form of top-capacitance loading (such as a horizontal wire or wires) then the calculation must be made in two steps—though in cases where the vertical and horizontal portions are of similar cross-section the error made by not doing so seldom exceeds 5 per cent. When the height of the antenna exceeds 0.3λ for a mast or 0.4λ for a wire it becomes necessary to allow for the dissipation in the circuit (the dissipation will be mainly radiation resistance provided the antenna has a good earth system). With a T or inverted-L antenna the

total length may exceed these values since the top of the antenna is relatively non-dissipative. After making an estimate of the total losses, the full dissipative transmission line formula is used. The effect of dissipation on the input reactance is shown by a comparison of the full and dotted curves of Fig. 2.1.

In the case of a simple vertical radiator of approximately cylindrical cross-section and length greater than 0.2λ , the

$$Z_0 = 500 \text{ Ohms}$$

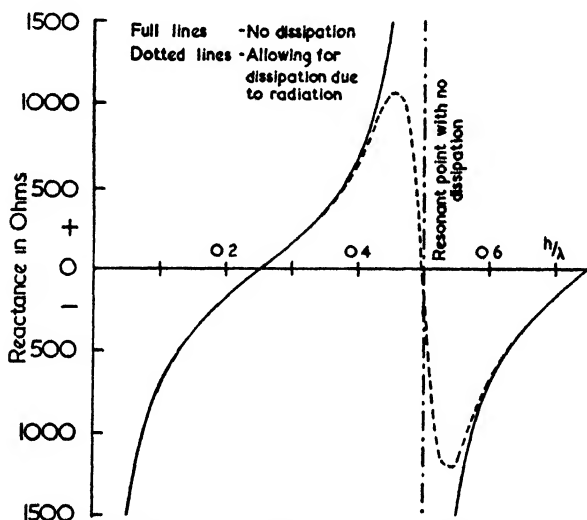


FIG. 2.1. REACTANCE OF A VERTICAL WIRE ABOVE THE GROUND

reactance may be obtained directly from the curves of Figs. 2.15 and 2.16. These curves are more accurate than those in Fig. 2.14 which are based on the normal transmission-line method.

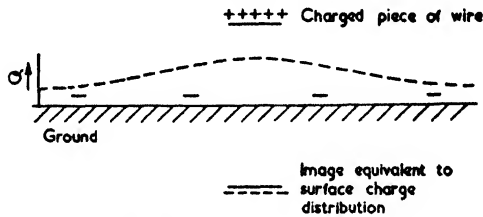
(a) *Determination of Static Capacitance*

(Applicable to very short antennae.)

In electrostatics the capacitance of a conductor is defined as the ratio of the charge to the potential, i.e. $C = Q/V$; furthermore, the potential energy of the conductor is proportional to QV . Thus if a certain increase in charge is given to two capacitors the one with the greater capacitance will experience the least increase in total energy. We can think, therefore, of the capacitance of a conductor as being a measure of the ease (from a work point of view) with which a unit charge can be

brought up from infinity against the repulsion caused by like charges already on the conductor.

Such elementary considerations help in visualizing the



The dotted line shows graphically the distribution of the surface charge density (denoted by σ)

FIG. 2.2. DIAGRAM FOR ILLUSTRATING THE CHANGE IN THE CAPACITANCE OF A PIECE OF WIRE DUE TO THE PRESENCE OF THE GROUND

effect on the capacitance of a system of conductors whose geometry is varied. For instance, it follows that the capacitance of a T antenna is less than that of an inverted-L antenna whose

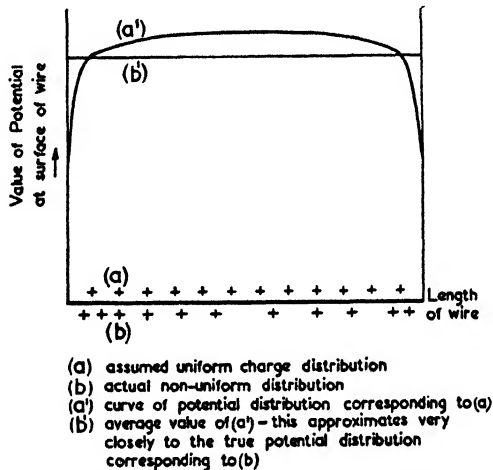


FIG. 2.3. APPROXIMATION ASSUMED BY HOWE FOR THE CALCULATION OF CAPACITANCE

vertical and horizontal lengths are respectively equal to those of the former type. If we imagine both to be equally charged it is apparent that the charges are more concentrated in the case of the T antenna, so that on the average the conductor would be harder to approach by further charges of like sign.

On similar grounds it can be inferred that the capacitance of a piece of wire is increased on bringing it nearer to the ground; the induced charges at the surface are of opposite sign and their presence reduces the work required to increase the charge on the conductor. By adopting the theory of images (see Fig. 2.2) the situation can be even more clearly visualized.

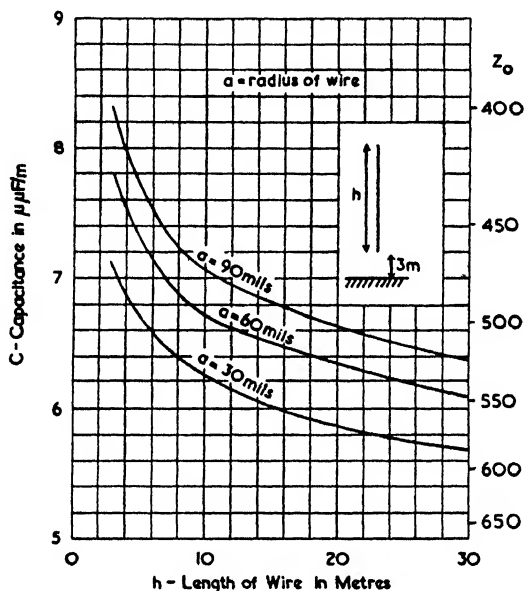


FIG. 2.4. CAPACITANCE OF VERTICAL WIRES
(Grover, Bureau of Standards Paper No. 568)

In quantitative calculations a difficulty arises owing to the fact that the charge distribution on a conductor is not uniform. Only in cases such as an infinitely long pair of parallel wires do we have uniformity. The problem was approached by Howe⁽⁵¹⁾ in the following manner. We assume a uniform charge distribution and from this calculate the potential distribution (in actual fact the surface of the conductor must be at a uniform potential), then the capacitance is given as the total charge divided by the *mean* potential. For a discussion of the conditions under which this method is valid the reader may refer to Appendix 3 of a paper by Grover,⁽³⁵⁶⁾ though from the point of view of antenna calculations the method may be assumed to be adequate for all practical cases.

Howe's approximation is shown diagrammatically in Fig. 2.3

in which (a) represents the assumed and (b) the actual charge distribution. Then curves (a') and (b') are the corresponding potential curves—the assumption being that (b') is the arithmetic mean of (a').

There is yet another assumption which has to be made, and that is that the charge distribution is along the axis of

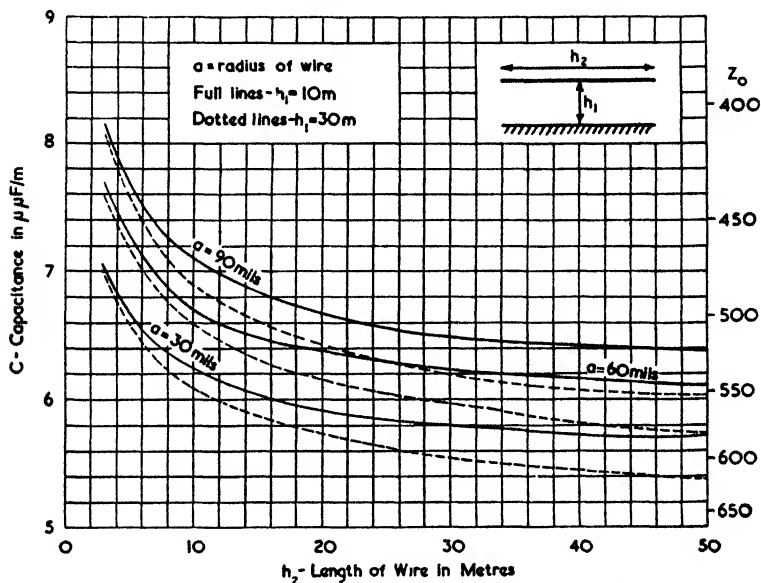


FIG. 2.5. CAPACITANCE OF HORIZONTAL WIRES
(Grover, Bureau of Standards Paper No. 568)

the wire, i.e. we neglect the variations of surface charge density in the cross-section of the wire when in the presence of other conductors. The errors introduced by this simplification are usually less than one part in a million and are therefore quite negligible.

Curves based on tables given by Grover⁽³⁵⁶⁾ are shown in Figs. 2.4 and 2.5, while those of Figs. 2.6 and 2.7 are from Howe's original article.⁽⁶¹⁾ In the interests of uniformity, as much use as possible has been made of the metre as the standard of length. Unfortunately, wire tables give the diameters in thousandths of an inch, or "mils," so that this unit has been adhered to. Even more unfortunate is the fact that there are several systems of wire gauges and that none of them conveys even the most elementary facts by the gauge number.

Fig. 2.4 shows the capacitance of a vertical wire whose lower end is 3 m off the ground. In view of the previous remarks it

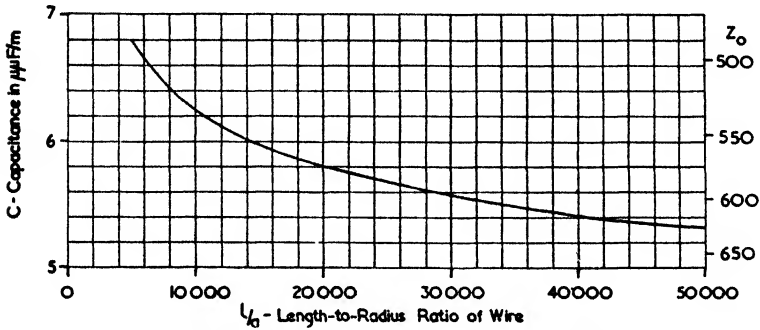


FIG. 2.6. CAPACITANCE OF A SINGLE WIRE IN FREE SPACE
(Howe, *Electrician*, Aug., 1914)

is obvious that the capacitance will vary with the height of the antenna above the ground. However these variations are not

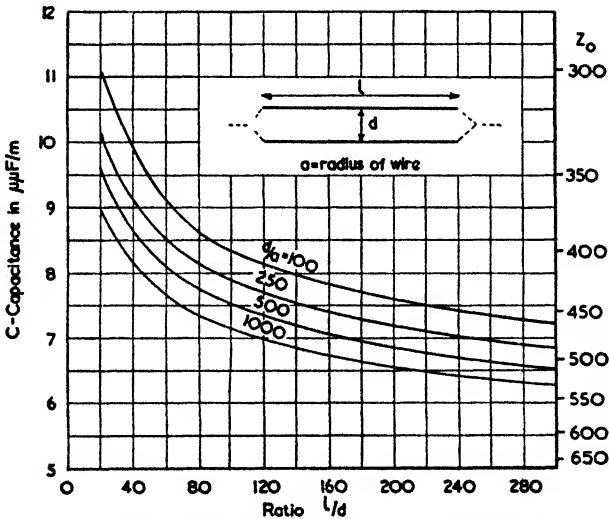


FIG. 2.7 (a). CAPACITANCE OF TWO PARALLEL WIRES IN FREE SPACE
(Howe, *Electrician*, Aug., 1914)

large; for example, a change of height from 1 to 10 m will produce less than 5 per cent change in capacitance in all practical cases.

In Fig. 2.5 the variations in capacitance with height have

been indicated by showing the values for $h_1 = 10$ m and $h_1 = 30$ m. An additional factor is the presence of the down-lead and this tends to *decrease* the capacitance. For an inverted-L antenna whose horizontal portion is between 30 and 50 m

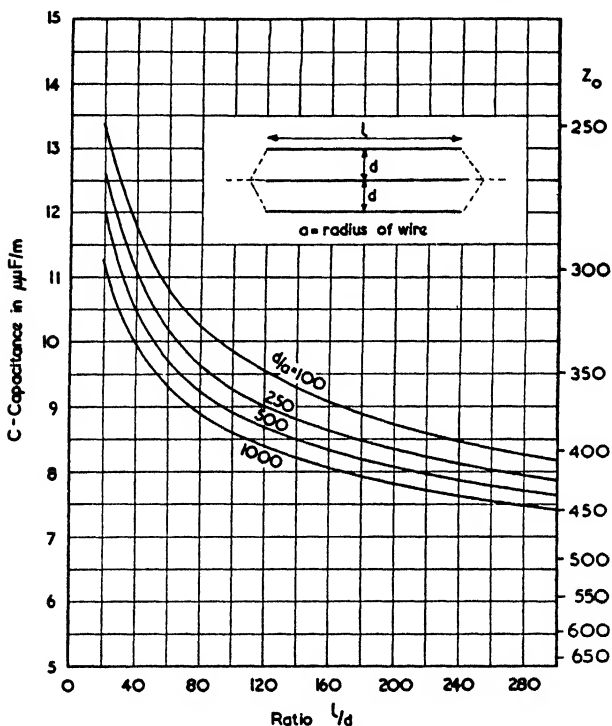


FIG. 2.7 (b). CAPACITANCE OF THREE PARALLEL WIRES IN FREE SPACE
(Howe, *Electrician*, Aug., 1914)

long, the capacitance is decreased by some 2 to 3 per cent if $h_1 = h_2$, and by about 5 per cent if $h_1 = \frac{1}{2}h_2$.

It happens that this percentage decrease is of the same order as the percentage *increase* due to the proximity of the ground. Consequently the two effects have a compensating action; hence a calculation based on the sum of the capacitances of the vertical and horizontal portions (each considered separately and in free space) gives quite a reasonable estimate of the total capacitance when arranged as an inverted-L antenna. The capacitance of a single wire in free space is given by Fig. 2.6.

If the antenna is of the T type the percentage decrease in

capacitance is nearly twice as great. One consequence of this is that the "compensating effect" mentioned above is not so good.

The free-space capacitance values of horizontal tops are shown in Fig. 2.7 for 2-, 3- and 4-wire antennae. In this case

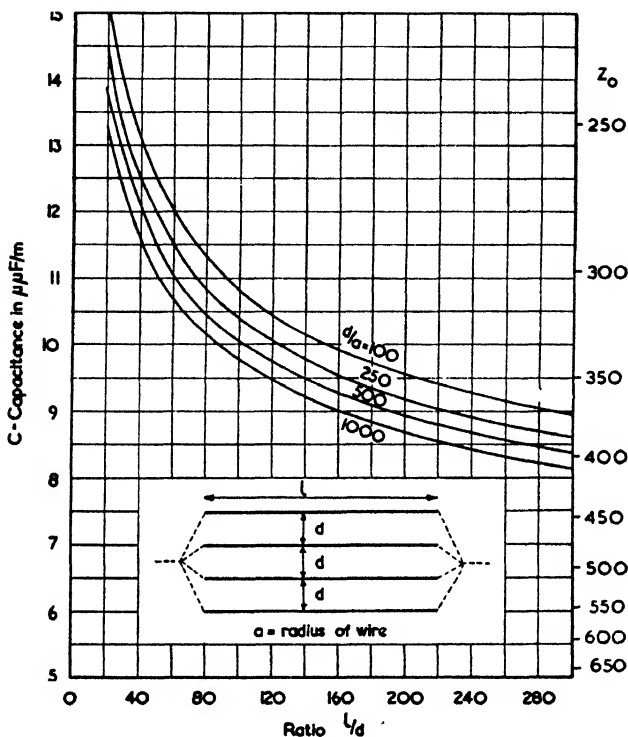


FIG. 2.7 (c). CAPACITANCE OF FOUR PARALLEL WIRES IN FREE SPACE
(Howe, *Electrician*, Aug., 1914)

the proximity of the ground causes a greater increase in capacitance than with the single-wire case, while the reduction in capacitance due to the down-lead is relatively less. Hence with inverted-L antennae with multi-wire tops the "compensating effect" is no longer as good as with the single-wire case, but with T-type antennae there is an improvement in this respect, i.e. reasonable estimates can be made by simply adding the free-space values of the down-lead (as given by Fig. 2.6) to those of the multi-wire top (as given by Fig. 2.7).

From the foregoing remarks it is apparent that the precise calculation of the static capacitance of an antenna is no simple

matter. For a thorough account of such calculations the reader may consult the Bureau of Standards' paper by Grover.⁽³⁵⁶⁾ In addition there are further papers by Howe which illustrate the application of his methods to umbrella antennae⁽⁵²⁾ and

to the effect of supporting masts.⁽⁵³⁾

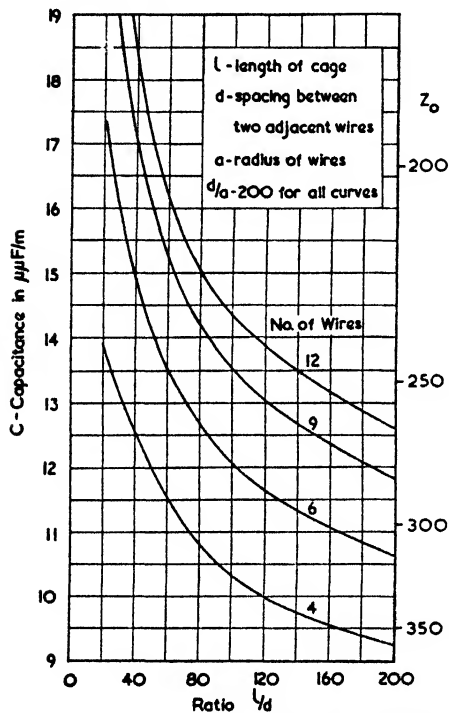


FIG. 2.8. CAPACITANCE OF WIRE CAGES
(McPherson, *Elec. Comm.*, April, 1938)

that as many vertical leads as is practicable should be used and that these wires should be well spaced out. Some formulae for such configurations are given by Grover but, where such facilities are available, it is easier to make measurements on a small model at high frequencies.

(b) *Non-dissipative Transmission-line Formulae*
(Applicable to antennae of medium length.)

As the total length of an antenna is increased so the effective capacitance exceeds the static capacitance by increasingly greater amounts until eventually the quarter-wave resonance point is reached and the reactance becomes zero; increasing

When dealing with antennae for long waves it is necessary to obtain as large a capacitance as possible to avoid excessive losses in large tuning coils. In such cases it is an advantage to use a cage for the vertical lead in addition to making the top capacitance as large as possible (either by the use of cages or flat multi-wire tops). A set of curves showing the capacitance of cages whose wire spacing is 200 times the radius of the wire is given by Fig. 2.8. These curves are based on a table given by McPherson.⁽¹⁰¹⁾

Other arrangements such as a fan or cone of wires may also be used—the guiding principle is

the length still further causes the base impedance to become inductive. The reactance over the range $\lambda/20$ to $\lambda/4$ (and even longer antennae in the case of L and T types) is conveniently obtained by the non-dissipative transmission-line formula.

There is some difficulty in defining the effective characteristic impedance of an antenna since, except for a conical antenna, the capacitance per unit length is not uniform. We therefore use an *average* characteristic impedance; this can be done by finding the mean capacitance per unit length from the static formula or by assuming the antenna to be a modified conical antenna. The former method, which is given below, is particularly suitable for T and inverted-L antennae, whereas the latter is to be preferred for unloaded antennae whose lengths are of the order of $\lambda/4$ or $\lambda/2$. If the characteristic impedance is Z_0 , then the reactance at the base of a simple vertical radiator is given by

$$X_b = - Z_0 \cot \beta h \quad . \quad . \quad . \quad (2.1)$$

where $\beta = 2\pi/\lambda$,

and $h =$ height of antenna in the same units as λ .

The characteristic impedance of a non-dissipative line is equal to $\sqrt{L/C}$ where L and C are the inductance and capacitance per unit length. Since the product of L and C is fixed by the surrounding medium, a knowledge of either will determine Z_0 ; in fact, with air as a dielectric we have

$$Z_0 = \frac{3\,333}{C} \text{ ohms} \quad . \quad . \quad . \quad (2.2)$$

where $C =$ capacitance per unit length in $\mu\mu\text{F}/\text{metre}$.

Using the above equation, an extra scale has been added to Figs. 2.4 to 2.8 which gives the values of Z_0 for the different cases. Thus the values of Z_0 are given directly by these figures. It is noteworthy that a long single wire has a characteristic impedance of about 600 ohms; this figure is often used in rough calculations.

For a straight vertical radiator we may use the following formula (due to Howe) which gives Z_0 directly—

$$Z_0 = 60 \left(\log_e \frac{h}{a} - 1 \right) \quad . \quad . \quad (2.3)$$

where $a =$ radius of antenna in the same units as h .

Another formula for the same case is one based on Schelkunoff's method and is

$$\zeta_0 = 60 \left(\log_e \frac{2h}{a} - 1 \right) \quad (2.4)$$

Both the above formulae are shown plotted in Fig. 2.9

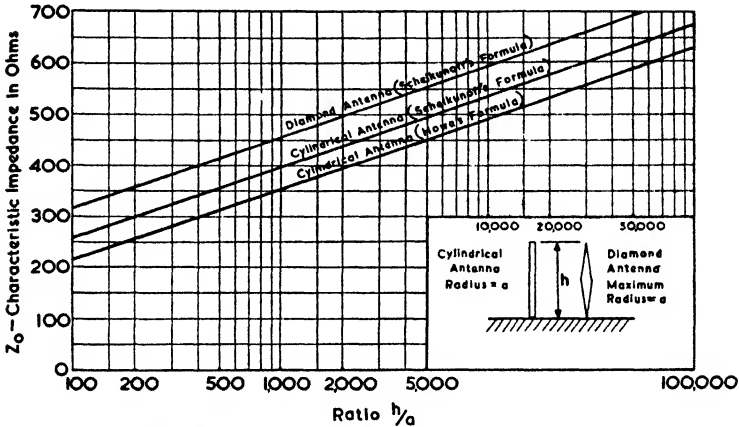


FIG. 2.9. CHARACTERISTIC IMPEDANCE OF UNIFORM AND DIAMOND-SHAPED VERTICAL RADIATORS

together with Schelkunoff's formula for a diamond-shaped antenna (also called a cigar-shaped antenna) which is

$$\zeta_0 = 60 \log_e \frac{2h}{a} \quad (2.5)$$

It is obvious that the precise value of ζ_0 is an open question; it should, in fact, be a function of the angular length of the antenna. Assuming a value of $\zeta_0 = 500$ ohms, then equation (2.1) gives the full curves of Fig. 2.1. On the same graph are shown curves which allow for the radiation resistance; from these it can be seen that appreciable error arises beyond the quarter-wave resonance point if the dissipation is neglected.

It should be noticed that when dealing with centre-fed free-space antennae (see Fig. 2.10) of total length $2h$, the value of ζ_0 is doubled, for C is halved and L is doubled. Therefore the input impedance of a free-space antenna is exactly double that of the corresponding antenna above a perfectly conducting earth.

The following analysis of loaded antennae is of practical value but not strictly correct. Its limitations are apparent

when we compare a T and an inverted-L antenna of corresponding dimensions—at very low frequencies the formulae quoted would give the same capacitance for both, whereas it is known that the static capacitance of the T is lower owing to the increased proximity between the various portions of the wire in the system.

Antenna with Non-radiating Top

The physical height of an antenna which is about half a wavelength high may be reduced without impairing the

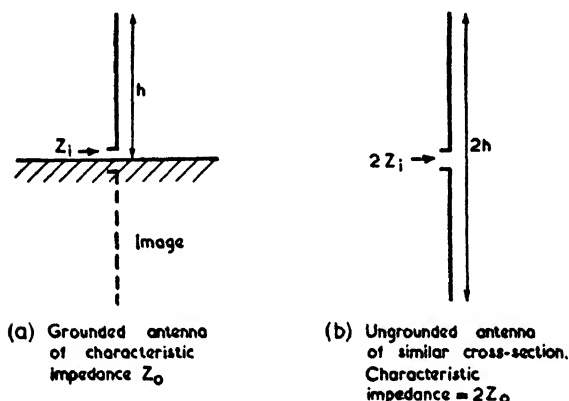


FIG. 2.10. CORRESPONDENCE BETWEEN GROUNDED AND UNGROUNDED ANTENNAE

performance appreciably by substituting a capacitor at the top for the last thirty or so degrees of the angular length. Such a capacitor will be essentially non-radiating if it is in the form of a horizontal disk or an equivalent conducting network (an example of a radiator of this type is shown in Plate I). The capacitance of a thin, solid, circular disk elevated some distance above the ground is given by

$$C_2 = 70.8a \mu\mu F \quad . \quad . \quad . \quad (2.6)$$

where a = radius of disk in metres.

For computing purposes the reactance is often required and this is given by

$$X_2 = -7.5 \lambda/a \text{ ohms} \quad . \quad . \quad . \quad (2.7)$$

To find the reactance of the antenna according to equation (2.1) we must add to the vertical height a fictitious length of

line whose characteristic impedance is the same as that of the vertical portion and whose length, h_2' , is such that the reactance of this imaginary length is equal to that of the top capacitor. This length is given by

$$h_2' = (1/\beta) \cot^{-1} (-X_2/Z_0) \quad (2.8)$$

The input reactance is then given by (2.1) on substituting $(h_1 + h_2')$ for h .

In most cases a non-radiating top of this type is used for antennae whose total angular heights are in the region of half a wavelength; under such conditions it becomes necessary to allow for dissipation in the manner given in § 2.4.

T-type Antenna

In principle we should first find the characteristic impedance of each half of the horizontal portion of the antenna and then regard the two halves as two transmission lines coupled in parallel to the top of the antenna. Actually such a calculation would give too high a value for the capacitance since the proximity effect between the two halves is thereby neglected. It is more accurate, therefore, to assume a characteristic impedance which is based on the capacitance per unit length of the *whole* of the top. With this assumption the reactance is given by

$$X_2 = \frac{Z_{02}}{2} \cot \beta h_2/2 \quad (2.9)$$

where Z_{02} = characteristic impedance of the top portion *as a whole*,

h_2 = total length of top portion.

The total reactance X_2 which the top presents is then expressed in terms of the equivalent length of transmission line, h_2' , as given by equation (2.8), in which it should be remembered that Z_0 refers to the vertical portion of the antenna. By way of an example the reader may refer to the problem at the end of this chapter which includes the calculation of the impedance of a T-type antenna with a 3-wire top.

Inverted-L Type Antenna

To find the input impedance of the above type of antenna the same methods as used for the T type are employed. If Z_{02}

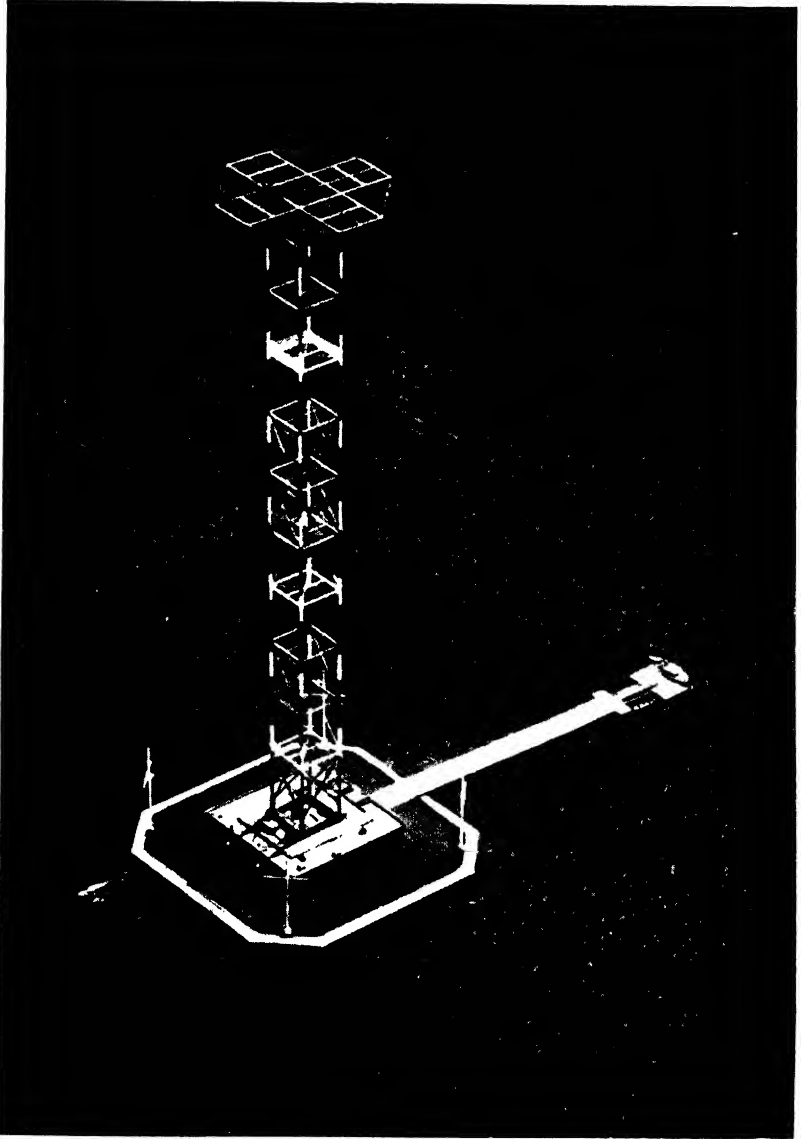


PLATE I. THE TOP-CAPACITOR ANTENNA OF WXXX, NEAR NEW YORK
(Courtesy of Federal Telegraph & Telephone Co. Inc.)

represents the characteristic impedance of the whole of the top portion, then the value of X_2 is given by

$$X_2 = -Z_{02} \cot \beta h_2 \quad . \quad . \quad (2.10)$$

Whenever the vertical and horizontal portions are of similar cross-section it will be found that the equivalent length of the horizontal portion, h_2' , is nearly the same as the actual length, h_2 . In such cases it is convenient (and sufficiently accurate) to write

$$X_b = -Z_0 \cot \beta (h_1 + h_2) \quad . \quad . \quad (2.11)$$

2.3. ANTENNA RESISTANCE

The total losses in an antenna system may be expressed in terms of a resistance at the driving point which is in series with the antenna reactance. If the current at that point is I amps and the power dissipated is W watts, then the resistance is given by

$$R = \frac{W}{I^2}$$

This loss resistance can be split into two components—one due to the energy lost in the form of radiation, the other due to joulean losses in the ground and other parts of the antenna system. The first component is R_r , the radiation resistance, the second is R_d , the dead-loss resistance. It is the *ratio* of these two resistances which determines the efficiency of an antenna system. Were it possible to reduce R_d to negligible values, even a minute vertical antenna (giving a correspondingly small value of R_r) would give almost the same field strength at a distance as a quarter-wave antenna. (In practice a further difficulty would arise owing to the losses in the output circuit whose resistance should also be negligible.)

R_r and R_d need not necessarily be measured at the driving point of the antenna. For some cases it is convenient to refer these values to the current antinode when they are known as the "loop radiation resistance," R_{lr} , and the "loop dead-loss resistance," R_{ld} , respectively. They may also be referred to the current at the base of the antenna, which in most cases is also the driving point.

It is usual to assume in the first case that the current distribution along the radiator is sinusoidal. This enables us to work out the loop radiation resistance, after which the input

impedance may be determined by the normal dissipative transmission-line formula as described in the next section. The assumption of a sinusoidal current distribution means that

$$R_{\text{loop}} = R_{\text{base}} \sin^2 \beta h \quad . \quad . \quad (2.12)$$

If the total effective length of the antenna is less than 0.3λ , then the above formula immediately gives R_b in terms of R_l ;

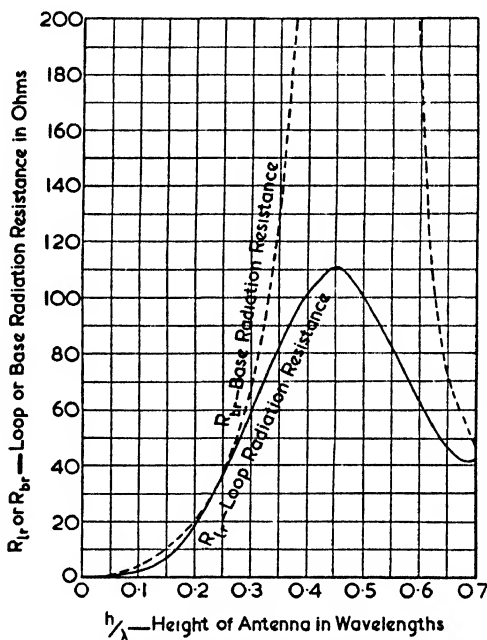


FIG. 2.11. LOOP AND BASE RADIATION RESISTANCE OF AN INFINITELY THIN VERTICAL WIRE

for in such cases there is no need to obtain a second approximation by means of the dissipative transmission-line formula.

The value of the loop radiation resistance of a vertical radiator is given in Vol. I by equation (5.9), while a graph of R_l , for different lengths of antenna is given in Fig. 2.11, together with the base radiation resistance.

For an antenna with a non-radiating top, the loop radiation resistance is given in Vol. I by equation (5.10). Graphs of this formula are shown in Fig. 2.12; they are based on a table of figures given by McPherson⁽¹⁰¹⁾ and in conjunction with equation (2.12) will give the base resistances. The same set

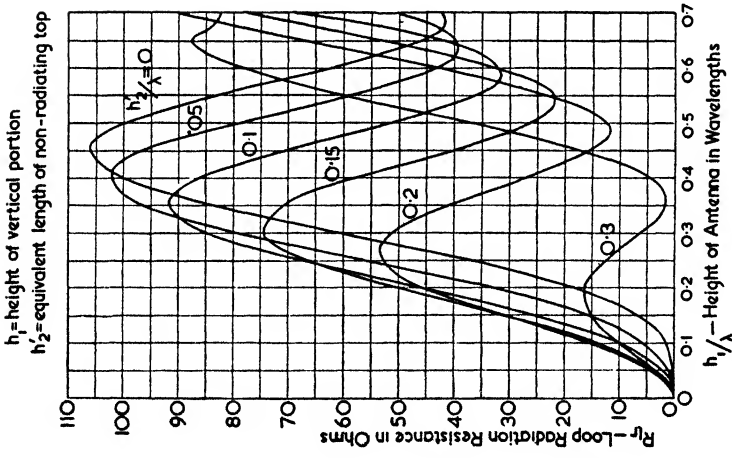


FIG. 2.12 (a). LOOP RADIATION RESISTANCE OF AN ANTENNA WITH A NON-RADIATING TOP (McPherson, *Elec. Comm.*, April, 1938)

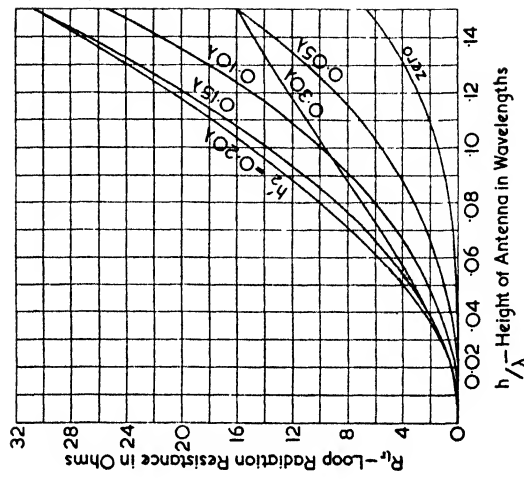


FIG. 2.12 (b). LOOP RADIATION RESISTANCE OF AN ANTENNA WITH A NON-RADIATING TOP (Enlarged portion of Fig. 2.12 (a))

of curves may also be used for a T antenna and, with less accuracy, for an inverted-L antenna. The base radiation resistance of the latter may be determined directly from the

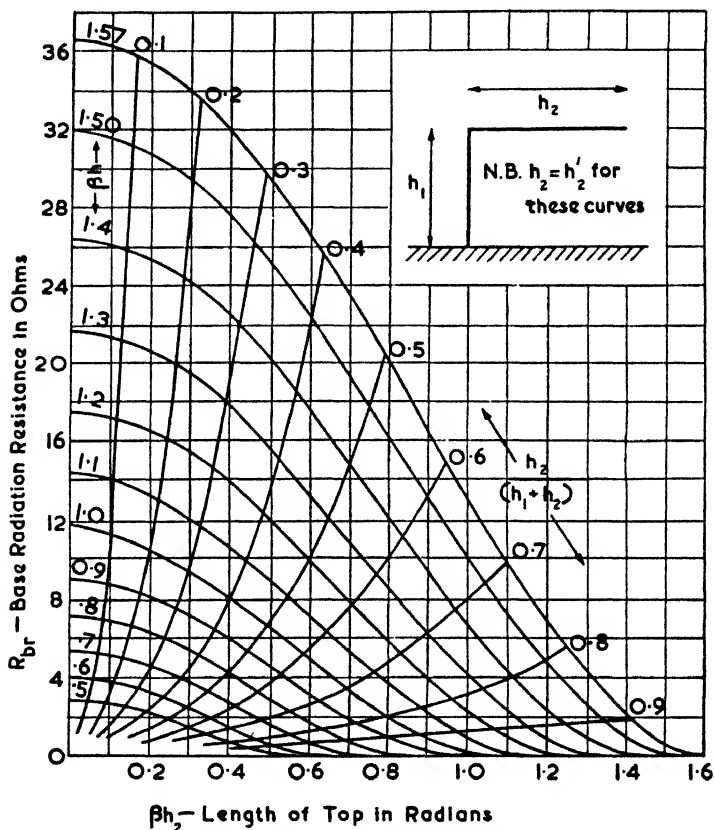


FIG. 2.13 (a). BASE RADIATION RESISTANCE OF AN INVERTED-L ANTENNA (Pierce, *Electric Oscillations and Electric Waves*, McGraw-Hill, 1920)

formula given by Pierce⁽¹⁷⁾ who first published the curves shown in Fig. 2.13.

2.4. INPUT IMPEDANCE

Uniform Vertical Antenna

Combining the results of the previous two sections leads to formulae giving the input impedance of a vertical radiator on the assumption that the antenna is equivalent to a uniform

dissipative transmission line. Such an equivalent transmission line will have a propagation constant $P = \alpha + j\beta$, where α is the attenuation constant and β is the phase constant—they are given in Vol. I by equations (5.32) and (5.29) respectively.

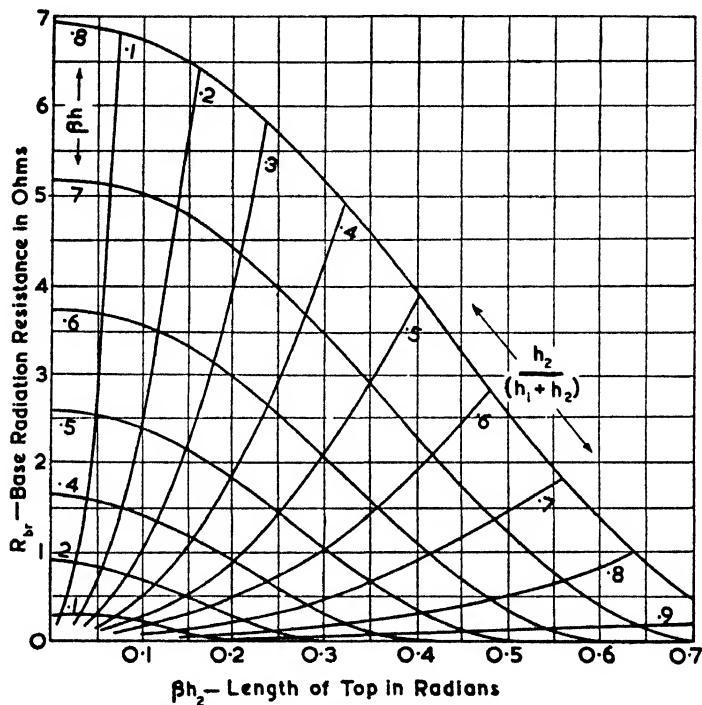


FIG. 2.13 (b). BASE RADIATION RESISTANCE OF AN INVERTED-L ANTENNA
(Enlarged portion of Fig. 2.13 (a))

We shall not discuss the details of the present calculation, since the end results are given by the curves of Fig. 2.14. It should be noted, however, that these curves apply only if the earth losses are negligible (which is more or less true if the antenna is provided with an extensive earth system whose radius is at least 0.3λ). When the earth losses are not small, we must include the value of R_{1d} , the loop dead-loss resistance, in the figure for R_i in equation (5.32) given in Vol. I. This increases the value of α but in many cases R_b may be obtained straight away from equation (2.12) while X_b is often given with sufficient accuracy by equation (2.1). The method of estimating R_{1d} is given in the next section.

Knowing α and β , the values of the series base resistance R_b and the series base reactance X_b can be found from equations (5.36) and (5.37) in Vol. I. Fig. 2.14 gives graphs of R_b and

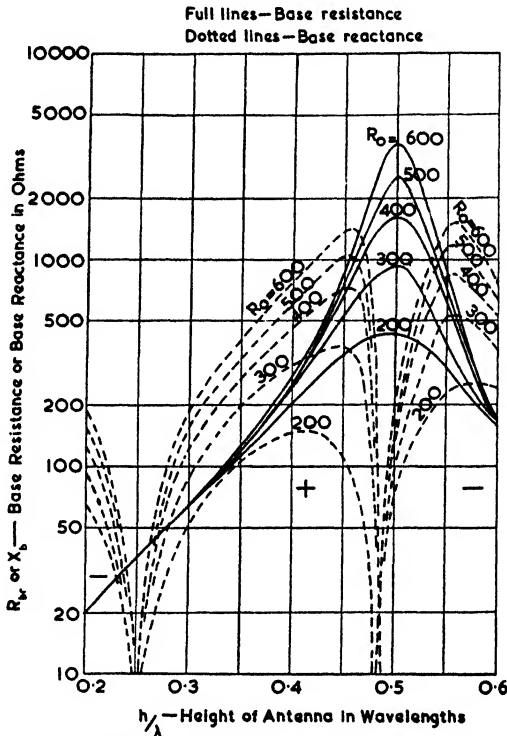


FIG. 2.14. BASE RESISTANCE AND REACTANCE OF A UNIFORM VERTICAL RADIATOR AS CALCULATED BY THE EQUIVALENT TRANSMISSION-LINE METHOD

X_b for various values of R_0 . It should be noted that R_0 is the real part of the characteristic impedance of the line and is

therefore equal to $\sqrt{\frac{L}{C}}$.

A study of the graphs for R_b and X_b shows that the reactance is zero for values of h very slightly above 0.25λ and a little below 0.5λ . The conditions in the vicinity of 0.25λ are certainly not correct, for the resonant length should be a few per cent short of a quarter of a wavelength. In the region of the second resonance, however, the results are qualitatively correct though

not quantitatively (the shortening effect is actually distinctly greater). It is apparent, therefore, that the equivalent transmission-line formulae are inaccurate as far as the reactance is concerned in the immediate neighbourhood of the resonant lengths; moreover they are inaccurate for relatively thick antennae (R_0 less than 400 ohms).

The curves of R_b and X_b given in Figs. 2.15 and 2.16 respectively are based on the biconical antenna method, and give

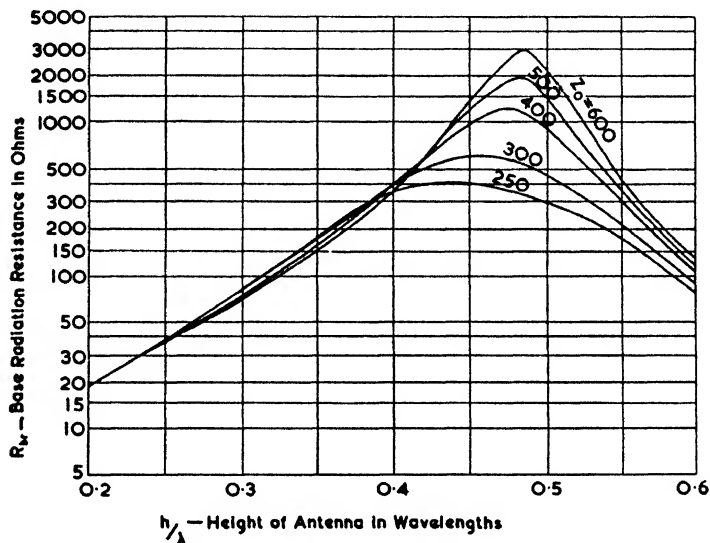


FIG. 2.15. BASE RESISTANCE OF A UNIFORM VERTICAL RADIATOR AS CALCULATED BY SCHELKUNOFF'S BICONICAL ANTENNA METHOD

distinctly better agreement with practical measurements than those of Fig. 2.14. In fact, the equivalent transmission-line method gives results which are so far out that it has become customary to assume that the base of a mast antenna has some 200 $\mu\mu\text{F}$ in shunt with the input impedance (Morrison and Smith⁽¹⁰²⁾ also assumed a series inductance of 6.8 μH to obtain agreement with experimental figures). This extra capacitance was attributed to the capacitance to ground of the bottom portion of the antenna—an idea which really allows for the capacitance twice over, since it should be allowed for already in the characteristic impedance of the antenna. Use of the curves of Figs. 2.15 and 2.16 makes the addition of such arbitrary shunt capacitances unnecessary. It should not be forgotten, however, that the addition of mast lighting, static

leaks and the probable proximity of a copper-clad building containing the coupling circuits will all tend to add some capacitance in the final layout.

Broadcast Antennae

The calculations discussed in the previous paragraphs apply to cylindrical antennae, and in order to apply them to self-

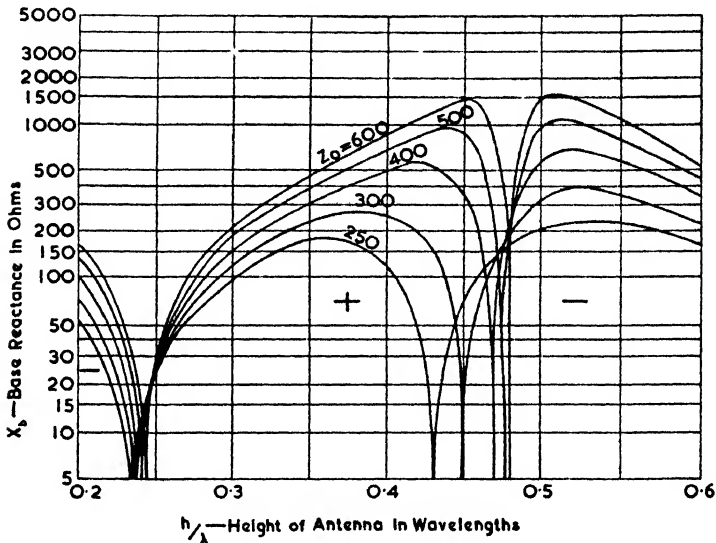


FIG. 2.16. BASE REACTANCE OF A UNIFORM VERTICAL RADIATOR AS CALCULATED BY SCHELKUNOFF'S BICONICAL ANTENNA METHOD

radiating masts of triangular or square cross-section some equivalent radius must be assumed. This "equivalent radius" can only be based on experimental evidence. A study of known experimental results suggests a value which is roughly mid-way between that of a circle of the same cross-sectional area and that given by the distance between the mid-point and one of the corners of the antenna. Reasonable values are $a = 0.50b$ for the triangular cross-section and $a = 0.63b$ for the square cross-section (in each case " a " is the equivalent radius and " b " the width of one side).

An application of the above rule is shown in Fig. 2.17, which gives the experimental curves of Morrison and Smith⁽¹⁰²⁾ together with calculated curves obtained from Figs. 2.15 and 2.16. It will be seen that even with the biconical method the

accuracy of the theoretical curves leaves something to be desired, though the results are distinctly superior to those obtained using the equivalent transmission-line method.

Truly cylindrical antennae are obtained if boiler tubing is used (in Germany antennae over 150 m high have been erected which were made out of sections of thin boiler tubing

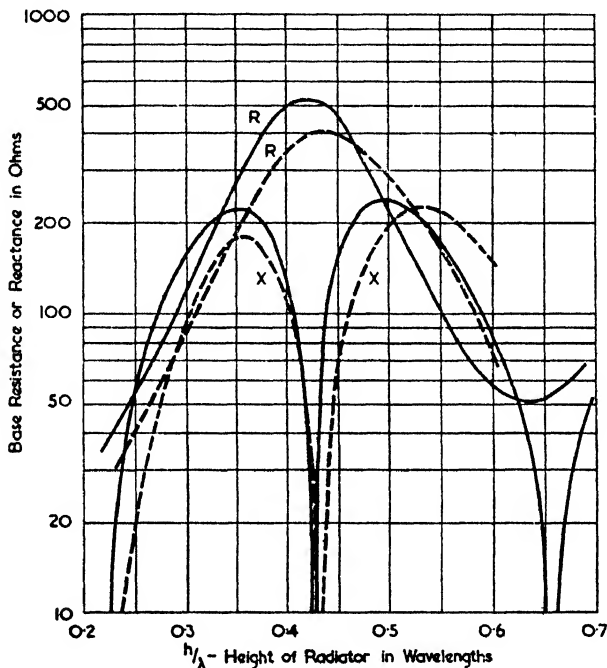


FIG. 2.17. A COMPARISON OF EXPERIMENTAL AND THEORETICAL VALUES FOR THE IMPEDANCE OF THE UNIFORM MAST RADIATOR SHOWN IN FIG. 2.34

whose diameter was only about 1 m) or if a vertical wire is suspended from a wooden tower (for example, the antennae at Copenhagen and Mühlacker). Unfortunately there appears to be no information available on the impedance of the boiler tubing antennae while the wire types have end capacitances; as a result the only direct checks on the curves of Figs. 2.15 and 2.16 are ones which have been made at much shorter wavelengths.

The biconical antenna method could be used for diamond-type antennae and Schelkunoff⁽⁷⁹⁾ has given the necessary formulae for this purpose (again an equivalent radius would

have to be assumed). When the transmission-line method is used it is customary to assume a value of characteristic impedance lying between 200 and 250 ohms (see, for instance, an article by McPherson⁽¹⁰¹⁾). Some experimental values have

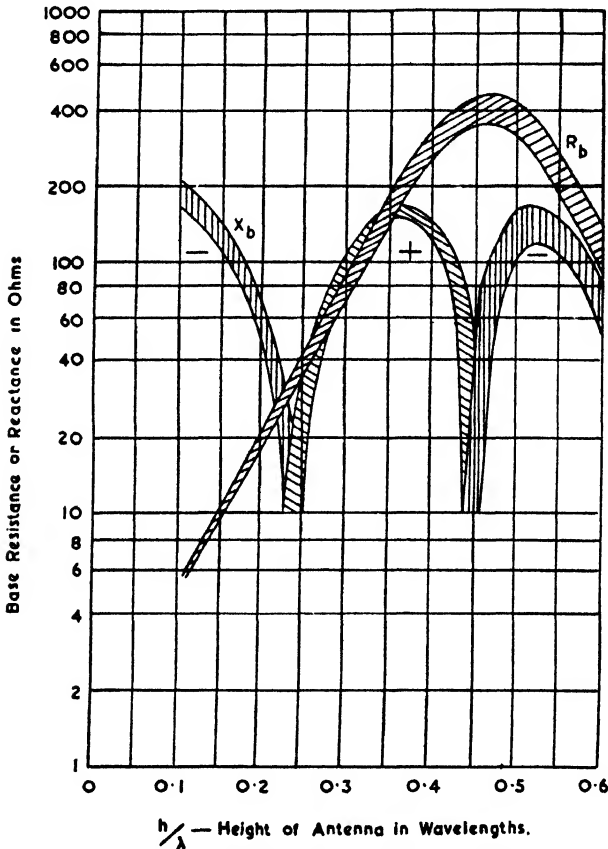


FIG. 2.18. AVERAGE CHARACTERISTICS OF FIVE EXISTING DIAMOND-TYPE ANTENNAE

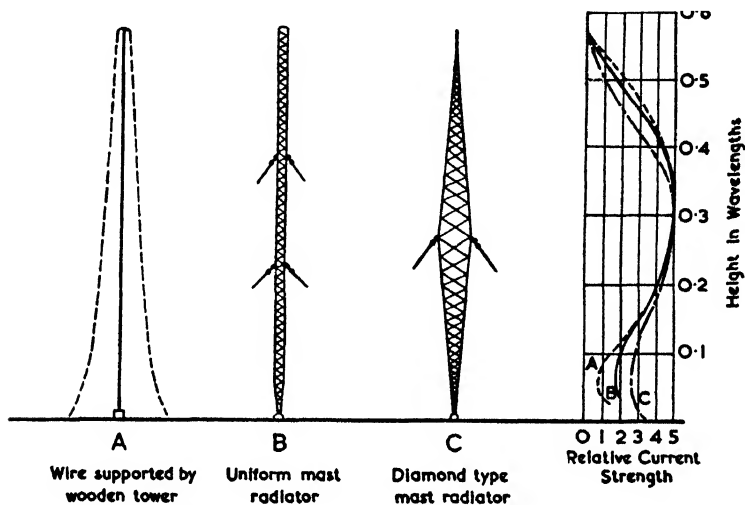
(Chamberlain and Lodge, *Proc. I.R.E.*, Jan., 1936)

been given by Chamberlain and Lodge,⁽⁹⁵⁾ who published the curves shown in Fig. 2.18.

At the present time diamond-type masts are falling into disfavour, since the current distribution they give has a poor minimum, with the result that their anti-fade properties are not quite so good as those of uniform masts. The current

distribution is shown in curve *C* of Fig. 2.19 where it is contrasted with that due to a thin-wire antenna (curve *A*) and that due to a mast of uniform cross-section (curve *B*). The poor minimum of curve *C* is a result of the decreasing cross-section of the top half of the mast; this causes a greater proportion of the current to be in the lower half.

A third general type of broadcast antenna is the self-supporting mast. This also suffers from a downward displace-



All antennae are series fed at the base

FIG. 2.19. THREE TYPES OF BROADCAST ANTENNAE WITH CORRESPONDING CURRENT DISTRIBUTIONS

ment of the current due to the tapering cross-section towards the top, though in recent times the cross-sections in the lower portions have been made remarkably small, with a corresponding reduction in the amount of taper. The effect of the tapering on the input impedance is to make the second resonance occur for heights as low as 0.35λ . Fig. 2.20 shows the measured average impedance of three self-supporting towers.

Top-loaded Antennae

When the antenna is loaded with a top reactance (this may be due to a capacitor with or without an inductor in series) then it is customary to fall back on the transmission-line method. In particular the full transmission-line formula as

given in Vol. I by equation (5.34) must be employed if the antenna is of the tall anti-fade type.

If X_t is the top reactance as determined by the methods

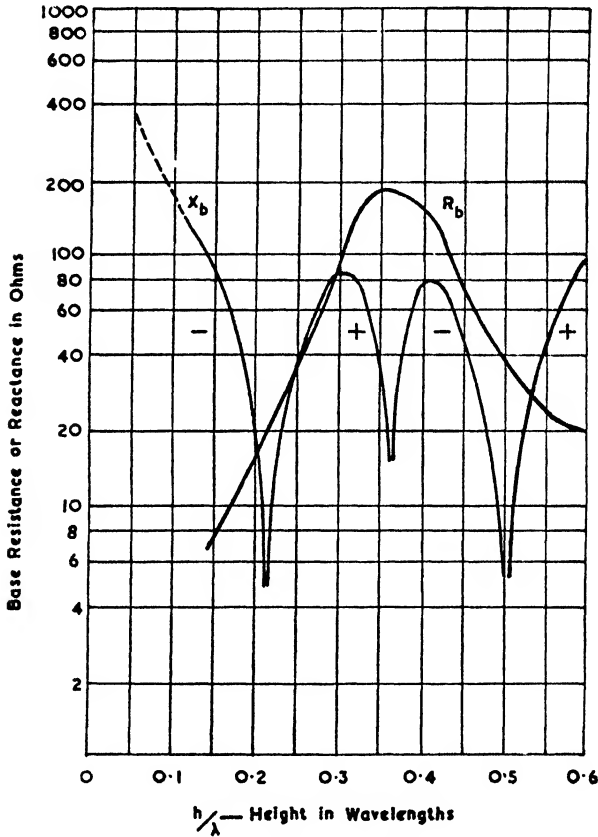


FIG. 2.20. AVERAGE CHARACTERISTICS OF THREE EXISTING SELF-SUPPORTING RADIATORS

(Chamberlain and Lodge, *Proc. I.R.E.*, Jan., 1936)

given in § 2.2 then the base impedance is given by equation (5.38), (Vol. I).

Provided that the dead-loss resistance is small (i.e. if the antenna has an extensive ground system) then $R_t \doteq R_{t,r}$ and is therefore given by the curves of Fig. 2.12. The value of R_0 may be taken to be given by equation (2.3) which is the lower curve in Fig. 2.9.

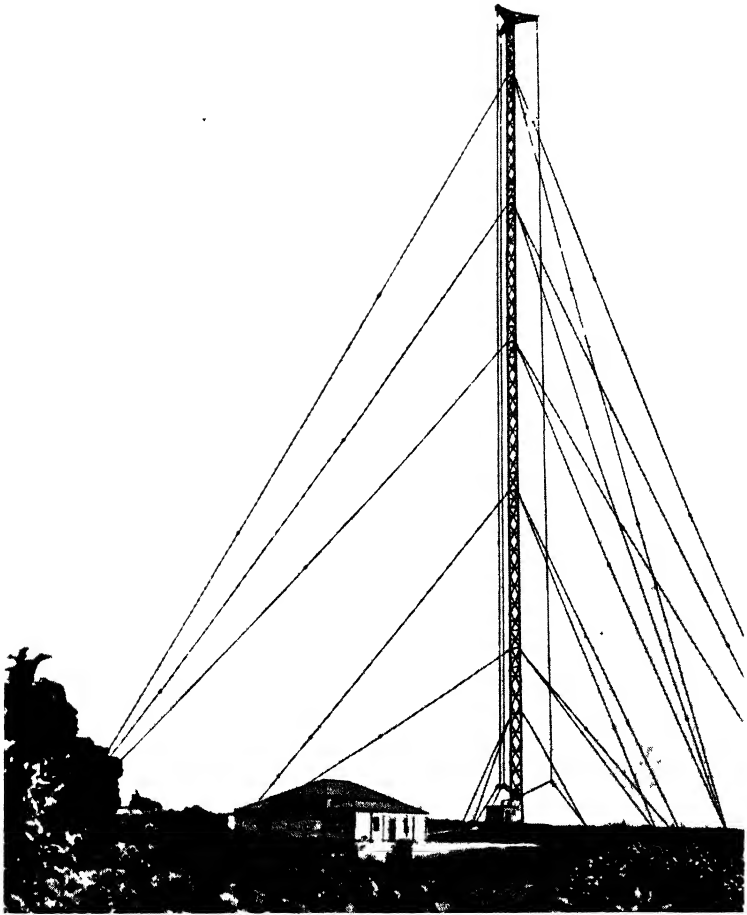


PLATE II. AN OUTRIGGER-TYPE VERTICAL RADIATOR AT SAN PAULO, BRAZIL.
(Courtesy of Marconi Wireless Telegraph Co. Ltd.)

Fortunately equations (5.33) and (5.38) given in Vol. I need not be used for normal small T and inverted-L antennae since the reactance and resistance may then be calculated separately according to the methods given in § 2.2 and § 2.3. This remark applies to wire antennae whose total effective lengths do not exceed 0.4λ and to thick radiators whose lengths are less than 0.3λ . An example of a wire type of antenna is given at the end of this chapter.

2.5. ANTENNA LOSSES

Conductor Losses

With metals of good conductivity the conductor losses are quite negligible except for very short radiators whose radiation resistance is only a few ohms. Mast radiators should be galvanized to prevent rusting at the joints which would cause a large increase in losses. In some cases copper strips are run along the length of the mast but it will be realized that, unless there are many such strips, they cannot carry the major part of the current.

To estimate the losses in a conductor we make use of the "skin depth" which is the depth below the surface of a conductor at which the current is reduced to $\frac{1}{e}$ (i.e. 0.368) of its surface value. This depth is given by $\frac{1}{\alpha}$, where α is the attenuation constant of the metal as given in Vol. I by equation (3.40). From the latter equation we have

$$\frac{1}{\alpha} = \frac{1}{\sqrt{\pi\mu fg}} \quad . \quad . \quad . \quad (2.13)$$

For cylindrical conductors whose radius "a" is many times the skin depth (a stipulation which is obeyed in all practical cases) the resistance per unit length is given by

$$\begin{aligned} R &= \frac{\alpha}{2\pi ag} \\ &= \frac{1}{2a} \sqrt{\frac{\mu f}{\pi g}} \text{ or } \frac{1}{2\pi a} R_m \quad . \quad . \quad . \quad (2.14) \end{aligned}$$

where R_m is the real part of the intrinsic impedance of the metal as given in Vol. I, in equation (3.42).

The effective loss resistance, R_a , at the terminals of the antenna depends on the current distribution. Assuming this to be sinusoidal, we have $I_z = I_l \sin \beta h$, where I_l is the loop current, so that

$$R_a = \frac{I}{I_b^2} \int_0^h I_z^2 R dz$$

$$= Rh \frac{1 - \frac{I}{2\beta h} (\sin 2\beta h)}{1 - \cos 2\beta h} \quad (2.15)$$

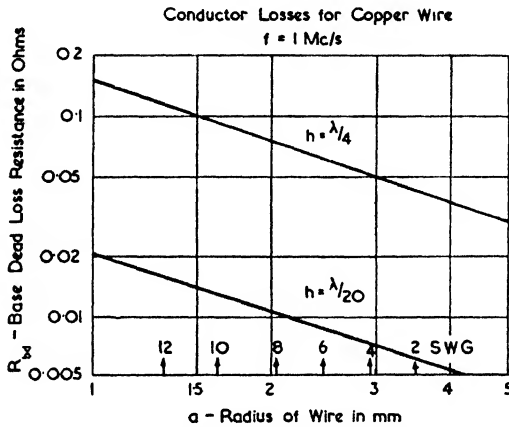


FIG. 2.21. CONDUCTOR LOSSES FOR WIRE ANTENNAE OF HEIGHTS 0.05λ AND 0.25λ

For short radiators (i.e. $h \leq \lambda/20$) the above equation simplifies to

$$R_a = \frac{Rh}{3} \quad (2.16)$$

Some typical values are illustrated by the graphs in Fig. 2.21. These values of R_a may be compared with the corresponding radiation resistances which are 36.6 ohms for $h = \lambda/4$ and 1 ohm for $h = \lambda/20$.

Dielectric Losses

The losses due to heating of the insulators form quite a small part of the total power dissipated, especially where mast antennae are concerned. Consequently we find that porcelain has a power factor low enough to make the use of low-loss

ceramics unnecessary in long- and medium-wave technique. A comparison of the different dielectrics is given in Appendix I. As a typical figure for porcelain we may take a power factor (i.e. reactance/parallel resistance) of 0.007.

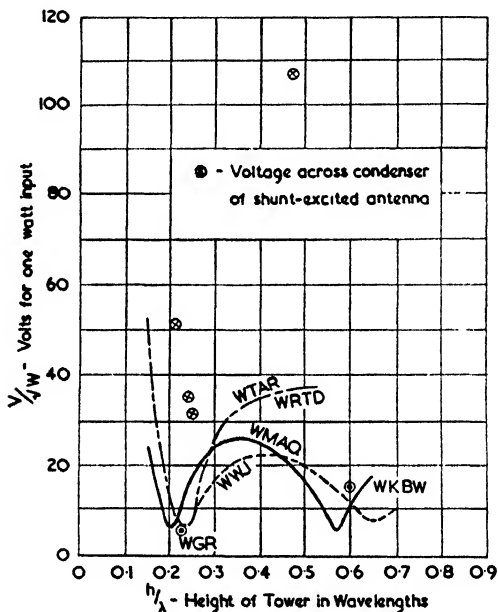


FIG. 2.22. VOLTAGE ACROSS BASE INSULATORS OF TOWERS OF UNIFORM CROSS-SECTION
(Brown, *Proc. I.R.E.*, Sept., 1939)

In the case of the base insulator the voltage is given by

$$V = \sqrt{\frac{W}{R_b}} \sqrt{R_b^2 + X_b^2} \quad (2.17)$$

where V = r.m.s. volts across insulator,
 W = power input in watts.

It is convenient to express the voltage in terms of one watt input when comparing different antennae. This is equivalent to taking V/\sqrt{W} as the variable and we find that for almost any type of mast radiator whose height exceeds 0.2λ , the value of V/\sqrt{W} lies between 10 and 25. For lower heights, and in particular for thin wires, the values of V/\sqrt{W} will greatly exceed these figures owing to the high reactive impedance. Fig. 2.22 shows the voltage at the base of self-radiating masts of uniform cross-section.

On the same figure are included values referring to the shunt-excited antenna of Morrison and Smith.⁽¹⁰²⁾ The voltages in this case are those appearing across the series tuning capacitance when the input resistance has been adjusted to 70 ohms. The voltages are obviously very great if the height of the mast is in the region of 0.5λ .

The base insulator of a tower antenna is not likely to have a greater capacitance than $30 \mu\mu\text{F}$, and as a result the modification to the base impedance is quite small. Taking the particular case of an antenna 0.55λ high whose base impedance is $210 - j320$, we find that a capacitance of $30 \mu\mu\text{F}$ only changes the impedance to $203 - j309$ when the frequency is 620 kc/s.

With the above values $V/\sqrt{W} = 24.8$ so that the r.m.s. voltage for 100 kW input would be 7 840 V. To find the peak voltage when the carrier is modulated by 100 per cent we multiply by $2\sqrt{2}$, which gives 22 200 V peak.

The power dissipated in the insulator is given by

$$W' = V^2 \times \frac{\text{Power factor}}{X_c} \quad . \quad . \quad (2.18)$$

where $X_c =$ impedance of insulator.

The above equation is pessimistic, since not all the lines of force are threading the material of the insulator. The *effective* voltage across the insulator is, in fact, somewhere between 0.5 and 1.0 times the base voltage V .

Continuing the previous example we find that the power dissipated in the absence of modulation is

$$\begin{aligned} W' &= (7\,840)^2 \times \frac{0.007}{8\,500} \\ &= 50.6 \text{ W} \end{aligned}$$

This is obviously a negligible loss. It has been found, however, that unless an earth mat is underneath or very close to the insulator the capacitance current travels through sufficient soil to cause a small but noticeable loss.

The losses in the guy insulators are negligible in the case of tower antennae. A detailed investigation into this problem has been made by Brown.⁽⁹²⁾ He showed that for an antifade antenna whose guys were fixed somewhere between one-third and two-thirds of the way up the mast (and broken into 2 or 3 sections according to height) the maximum r.m.s. voltage

across any insulator was only slightly above 1 000 V with an input as high as 500 kW. His figures correspond to about 1.6 V/W for insulators next to the mast and 0.8 V/W for insulators near the ground.

We may use these figures to find the power dissipated by assuming a value of 10 $\mu\mu\text{F}$ for the capacitance of the insulators (medium- and large-size egg insulators have capacitances ranging between 5 and 10 $\mu\mu\text{F}$). The result of such a calculation on the same antenna as was used in the base insulator example showed that the losses for 100 kW input were only 1.5 W.

With wire T or inverted-L antennae the extreme ends need supporting by means of insulators and since at these points the voltages can be very high, it is an advantage to use more than one insulator for the ends of the antenna. The voltage at the ends is related to that at the base as follows—

$$V_t = V_b \sec^2 \beta(h_1 + h_2') \quad . \quad . \quad (2.19)$$

This is a simplification of equation (10.39), in which we have put $x = l$ and $\alpha = 0$, the value of l being equal to $(h_1 + h_2')$. If the antenna is operating very near to quarter-wave resonance (say $\beta(h_1 + h_2') = 90^\circ \pm 5^\circ$) the value of α cannot be neglected; and if, in addition, the antenna has capacitance top loading we must put $Z_R = X_2$, $l = h_1$ and work out αh_1 according to Vol. I, equation (5.33).

At the end of this chapter the insulator losses for a T antenna are calculated. In this particular case the antenna is just far enough above quarter-wave resonance for α to be neglected (it will be realized that the determination of insulator losses and voltages is, in any case, only a fairly rough calculation).

The safe working and the breakdown voltages for egg insulators are shown in Appendix III.

Ground Losses

Of the various losses in a grounded antenna, those due to the inferior conductivity of the earth are by far the most serious. This is a result of making the earth a part of the oscillatory system, a fact which is illustrated in the sketch of Fig. 1.5. The problem is attacked in practice either by burying a large number of radial wires in the ground or by using a "counter-poise" earth which virtually forms an artificial earth for the system. The latter method requires fewer wires, but they

should be at least a metre or two above the ground to render the system relatively free from earth currents. This elevation of the wires causes complications in erection as well as decreasing the effective height of the antenna.

To calculate the ground losses we may first derive the ground current distribution on the assumption of a perfectly conducting ground, and then assume that the case of finite conductivity does not vary this distribution sensibly. Knowing the current distribution and the conductivity of the soil, we

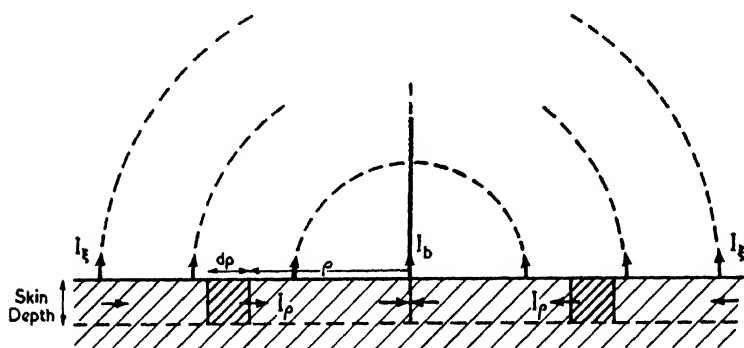


FIG. 2.23. DIAGRAM FOR EARTH LOSS CALCULATIONS

may then estimate the ground losses and therefore the effective loss resistance. Such a process is, by its very nature, only an approximation, but it is a very good approximation for long and medium wavelengths and normal soil conductivities.

The current distribution is entirely along the surface for a perfect conductor but will penetrate for some distance into the ground in practice. In either case, we may surround the antenna with a coaxial cylinder as shown in Fig. 2.23, whereupon, on equating the total radial current, I_ρ , to the sum of the current, I_b , at the base of the antenna and the displacement current I_ϵ , we have

$$I_\rho = I_b + I_\epsilon \quad . \quad . \quad . \quad (2.20)$$

Using Ampère's law that the line integral of the magnetic intensity equals the current threading the circuit (by Maxwell's extension this applies also to displacement currents) we have

$$2\pi\rho H_\phi = I_\rho = I_b + I_\epsilon \quad . \quad . \quad . \quad (2.21)$$

The value of H_ϕ may be obtained from Vol. I, equation (5.14), on putting $r_o = \rho$ and $\xi = 0$ and doubling to allow for the

image in the ground (at this point we are assuming that the ground is a perfect conductor so that the system is symmetrical about the surface). This results in

$$H_\phi = j \frac{I_b}{2\pi\rho \sin \beta h} [e^{-j\beta r_1} - e^{-j\beta\rho} \cos \beta h]$$

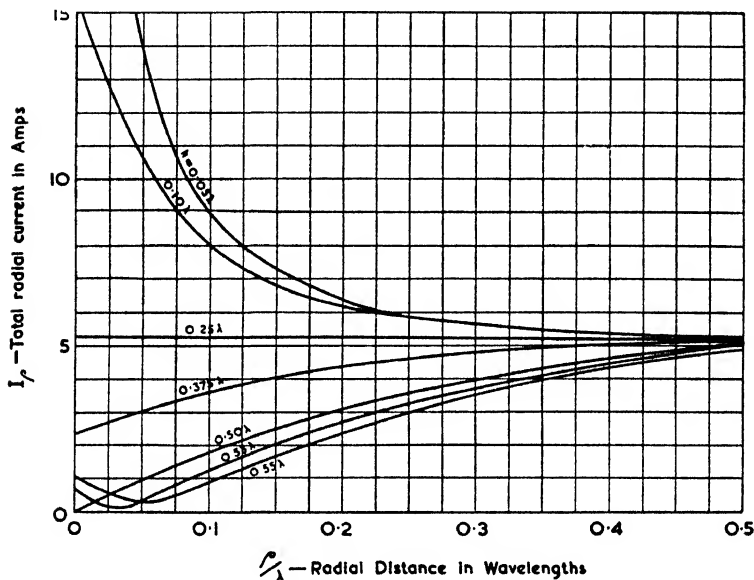


FIG. 2.24. TOTAL RADIAL EARTH CURRENTS FOR DIFFERENT ANTENNA HEIGHTS

The time phase $\sin \omega t$ has been dropped, and the relation $I_b = I_i \sin \beta h$ has been used. The radial current is therefore given by

$$I_\rho = j \frac{I_b}{\sin \beta h} [e^{-j\beta r_1} - e^{-j\beta\rho} \cos \beta h] \quad (2.22)$$

Some curves of $|I_w|$, based on the above formula, are given in Fig. 2.24. It will be noticed that the distribution for $\beta h = \lambda/4$ is particularly simple, $|I_w|$ being constant for all values of ρ . The total radial current is obviously appreciable for all large values of ρ , but it should be remembered that beyond the region of the induction field (say $\rho > \lambda/2$) the earth losses should be classified as propagation losses, since they do not influence the efficiency of the antenna system.

With short antennae the earth currents are particularly

high near the base, so that such antennae require a good earth system in this region, the more so on account of their inherently low radiation resistance. Steps are often taken to improve the horizontal radiation from short antennae by adding some form of non-radiating top. In such cases the previous analysis applies, provided the change in current distribution is allowed

$$\text{Skin depth, } s = \frac{1}{\alpha} = \frac{1}{\sqrt{\pi \mu f \rho}}$$

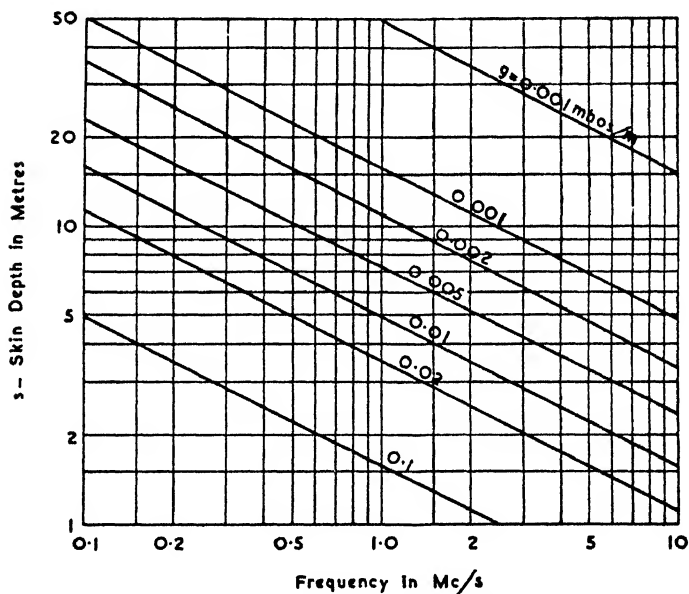


FIG. 2.25. VARIATION OF SKIN DEPTH WITH FREQUENCY

for. If h_1 is the height of the vertical portion and h_2' the equivalent length of the top capacitance, giving a total electrical length h , we have

$$I_p = j \frac{I_b}{\sin \beta h} \left[e^{-\beta r_1} \left(\cos \beta h_2' - j \frac{h_1}{r_1} \sin \beta h_2' \right) - e^{-\beta \rho} \cos \beta h \right] \quad (2.23)$$

The above formula will also apply to T (and, to a first approximation, even to inverted-L) antennae, for it is apparent that the currents in the horizontal portions of such an antenna will not influence the ground distribution appreciably. This fact has been verified quantitatively by Brown⁽⁹⁸⁾ in an

appendix to a general article on earth currents which also includes an experimental check for the case $\beta h_1 = 75^\circ$, $\beta h_2 = 0$.

The earth currents have two components in phase quadrature; one of these is due to the induction field and decreases (for $h < 0.25\lambda$) from a maximum value at $\rho = 0$ to a fraction of this value at $\rho = 0.5\lambda$; the other is associated with the radiation field and increases with distance to a limiting value, a limit which is almost attained by the time $\rho = 0.5\lambda$.

In order to determine the resistance losses due to these currents, we adopt the well-known technique of assuming that the currents are relatively unaffected by the losses and that the current is concentrated in a region whose lower boundary is given by the skin depth. Some curves showing the skin depth for typical conductivities are given in Fig. 2.25. Proceeding on exactly the same lines as were used for obtaining the conductor losses, we find that the resistance of a volume of unit surface area and depth equal to the skin depth is given by $R_m = \alpha/g = \sqrt{(\pi\mu f/g)}$. Since the skin depth is equal to $1/\alpha$ the value of R_m is readily obtained from the curves of Fig. 2.25 on dividing $1/g$ by the skin depth in metres. Hence the resistance to radial currents of an element of annular ring as shown in Fig. 2.23 is equal to $(R_m/2\pi\rho)d\rho$, and therefore the watts dissipated are given by

$$dW = I_\rho^2 = \frac{R_m}{2\pi\rho} d\rho \quad . \quad . \quad (2.24)$$

The total dissipation between any two radii is given by

$$\begin{aligned} \int_{\rho_1}^{\rho_2} dW &= \int_{\rho_1}^{\rho_2} I_\rho^2 \frac{R_m}{2\pi\rho} d\rho \\ &= I_\rho^2 \frac{R_m}{2\pi} \log_e \frac{\rho_2}{\rho_1} \quad . \quad . \quad (2.25) \end{aligned}$$

The evaluation of (2.25) is best performed graphically using the curves of Fig. 2.24 for I_ρ . It will be noticed that when I_ρ is constant ($h = 0.25\lambda$) then equal contributions are made by rings of soil whose ratio of outer to inner radius is constant. Thus as we come towards the centre of the antenna the losses continually increase since an unlimited number of rings of given ρ_2/ρ_1 may be constructed. The total power dissipated is therefore very sensitive to the radius of the earthing pin which determines ρ_1 .

In the table given below we assume that the minimum $\rho_1 = 5$ cm; this means that a metal rod 10 cm in diameter

and some 5 m deep would have to be sunk into the ground for the results shown in the table to hold. In practice one would be far more likely to construct an earth system out of a set of radial wires (the table on p. 67 compares the earth rod with radial-wire systems). A method of finding the earth resistance in such cases was devised by Brown⁽³⁸⁾ and will be described later on.

The upper limit of the integration is determined by the fact that outside the induction field the losses should be classed as propagation losses. A convenient limit is therefore $\rho_2 = 0.5\lambda$. In the following table we have taken steps of $\rho_2/\rho_1 = \sqrt{2}$.

Example:

$h = 0.05\lambda$ $\lambda = 300$ m $g = 0.01$ mhos/m
 ρ_1 minimum = 5 cm $R_m = 20$ ohms
 ρ_2 maximum = 145 m I_p given by 18° curve in Fig. 2.24
 Assumed radiated power = 1 W
 Base radiation resistance = 1 ohm
 Base current = 1 ampere

From equation (2.24)

$$W = 1.093 I_p^2 \text{ watts/zone}$$

Zone	1	2	3	4	5	6	7	8
ρ_1	0.05		0.10		0.20		0.40	
W	1.093	1.090	1.080	1.071	1.064	1.050	1.030	1.000
Zone	9	10	11	12	13	14	15	16
ρ_1	0.80		1.6		3.2		6.4	
W	0.972	0.925	0.853	0.762	0.660	0.536	0.420	0.300
Zone	17	18	19	20	21	22	23	
ρ_1	12.8		25.6		51.2		102.4	
W	0.207	0.134	0.086	0.058	0.044	0.035	0.032	

Total watts dissipated = 14.5
 Efficiency of antenna, $\eta = 6.5$ per cent
 Base loss resistance, $R_{ba} = 14.5$ ohms

A similar calculation has been performed for a quarter- and a half-wave antenna with the results shown below. It is interesting to note that the maximum losses in the case of a

$\lambda/2$ antenna occur at a distance of 0.35λ from the base—a fact first pointed out by Brown.⁽³⁸⁾ In calculating the $\lambda/2$ case we use the loop current since the assumption of a sinusoidal current distribution makes $I_b = 0$ if $h = \lambda/2$.

TABLE OF EARTH LOSSES
($\lambda = 300$ m; $g = 0.01$ mhos/m)

Height of Simple Vertical Antenna	$\lambda/20$ (15 m)		$\lambda/4$ (75 m)		$\lambda/2$ (150 m)	
Base (or Loop) Radiation Resistance	1		36.6		99.5 (loop)	
Ground Loss Resistance and Efficiency	R_{bd}	η	R_{bd}	η	R_{ld}	η
(a) With 10 cm diameter earth rod	14.5	6.5%	25.2	63.3%	6.4	94.0%
(b) With 15 radial wires each 25 m long	0.96	51.0%	8.7	80.7%	6.3	94.1%
(c) With 120 radial wires each 150 m long	0.072	93.3%	2.13	94.4%	3.5	96.7%

(All resistance values are in ohms)

From the above table we see that a $\lambda/2$ antenna is inherently more efficient but the assumption of a sinusoidal current distribution has exaggerated this property—more practical values are 80 per cent and 90 per cent for cases (a) and (b) respectively. When, however, a short antenna is fitted with a highly efficient earth system its performance becomes comparable with that of a $\lambda/2$ antenna.

Minimizing of Earth Losses

From the foregoing descriptions it will be realized that an ideal earth system should consist of a concentric cylinder of metal sunk for a depth equal to the skin depth and connected to the input terminal by many radial wires. Such an earth system would remove all ground losses other than those outside the cylinder. In practice, if the radial wires are long enough, say over $\lambda/3$, then there would be little gained by sinking such an elaborate cylinder (or by taking the equivalent step of sinking deep conducting poles at the ends of the wires).

The efficiency of a radial-wire system has been carefully

investigated by Brown, Lewis and Epstein.⁽⁸⁴⁾ Their experiments verified the fact that, with an efficient earth system, the radiation from an antenna whose height is only $\lambda/20$ is very little inferior to that from a $\lambda/4$ antenna. Additional

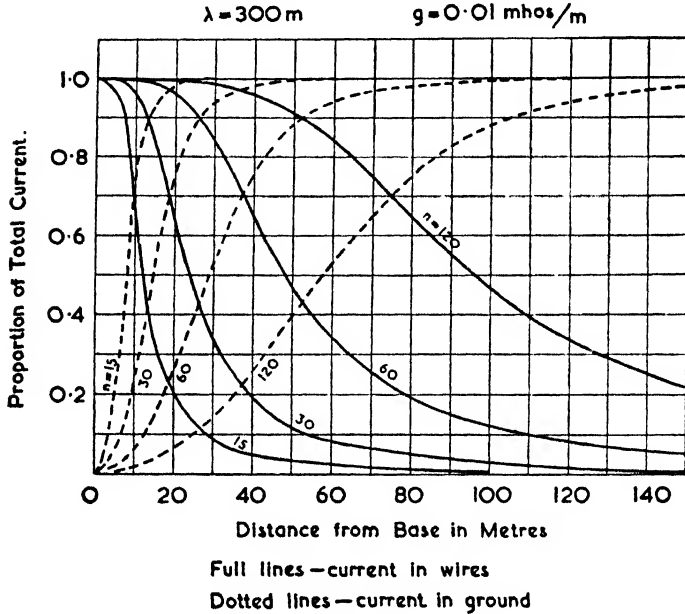


FIG. 2.26. DISTRIBUTION OF CURRENTS IN AN EARTH SYSTEM OF n RADIAL WIRES UNIFORMLY SPACED (GOOD CONDUCTIVITY SOIL)

experiments indicated that a system of wires lying loose on the ground but terminated by ground rods was equally efficient.

When radial wires are used the radial current I_p will consist of a component I_w flowing in the wires and I_e flowing through the earth.

Thus
$$I_p = I_w + I_e$$

The ratio of I_e to I_w has been given by Brown⁽⁸⁸⁾ in the following simple form—

$$\frac{I_e}{I_w} = j \left(\frac{\pi \rho}{sn} \right)^2 \left[\log_e \left(\frac{\pi \rho}{an} \right) - 0.5 \right]. \quad (2.26)$$

where $s = \text{skin depth} = 1/\alpha,$
 $a = \text{radius of earth wire},$
 $n = \text{number of earth wires}.$

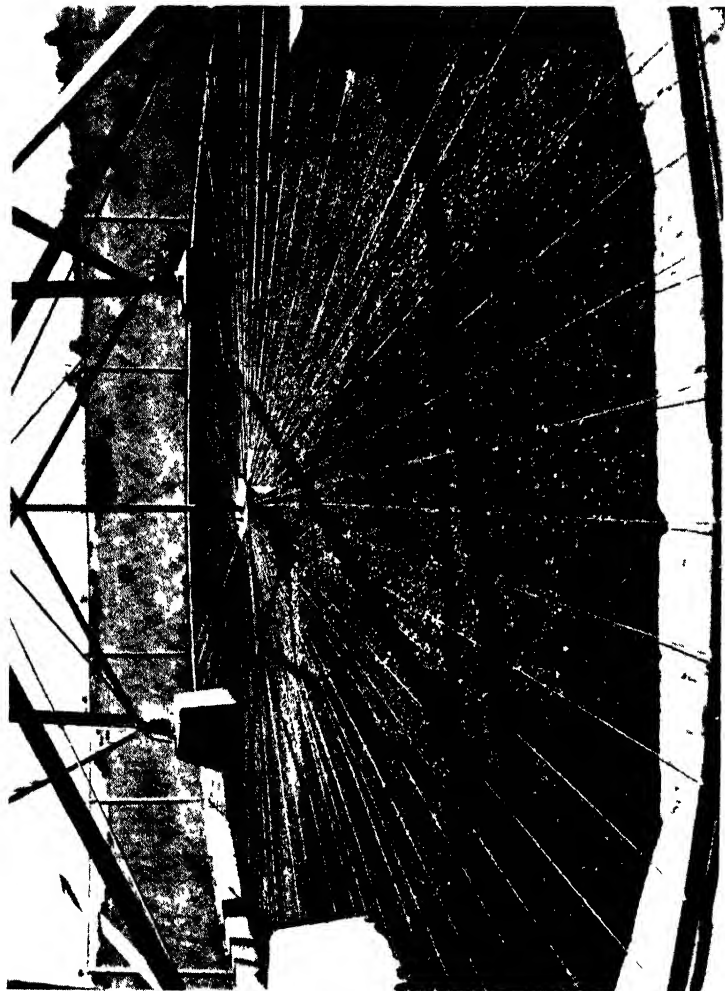


PLATE III THE BASE OF A SHUNT-EXCITED ANTENNA AT PRETORIA
(Courtesy of Standard Telephones & Cables Ltd.)

Figs. 2.26 and 2.27 show some curves based on this formula using the typical conductivity values employed in the rest of this book. The wire gauge for these curves is No. 10 S.W.G.—the wire diameter has little effect within quite wide limits.

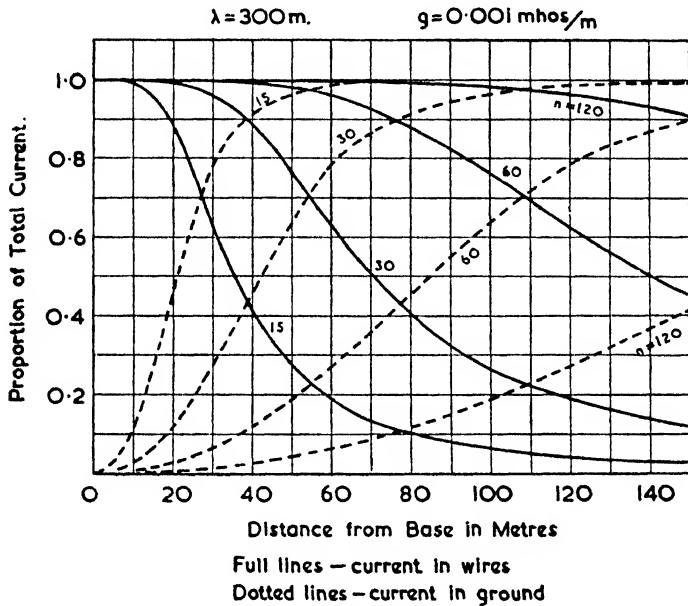


FIG. 2.27. DISTRIBUTION OF CURRENTS IN AN EARTH SYSTEM OF n RADIAL WIRES UNIFORMLY SPACED (POOR CONDUCTIVITY SOIL)

It should be remembered that I_e and I_w are in phase quadrature so that the sum of their magnitudes does not equal unity unless one of them is zero.

Equation (2.24), giving the power loss in the soil (the losses in the wires are negligible in comparison), now becomes

$$dW = I_e^2 \frac{R_m}{2\pi\rho} d\rho \quad . \quad . \quad . \quad (2.27)$$

The improvement obtained with an earth system can be observed from the figures in the last two rows of the previous table which are for 15 radials each 25 m long and 120 radials each 150 m long respectively. These figures were obtained with the aid of Fig. 2.26 and equation (2.27). It is apparent from the curves of Figs. 2.26 and 2.27 that when only 15 radials are employed there is nothing to be gained by extending them

beyond a distance of 30 m in the case of good conductivity soil, or about 70 m when the soil conductivity is low.

Very satisfactory agreement with these theoretical methods has been obtained both by Brown and his colleagues⁽⁹⁴⁾ and by Brückmann.⁽⁷⁾ It appears, therefore, that the theory is

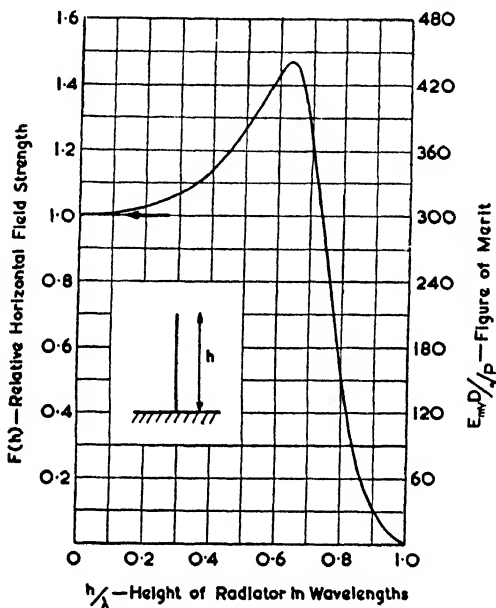


FIG. 2.28. HORIZONTAL FIGURE OF MERIT FOR A SIMPLE VERTICAL RADIATOR

sufficiently accurate to give a useful estimate of the antenna efficiency with different ground systems.

Plate III shows the above-ground centre portion of a radial-wire earth system for a shunt-excited antenna.

2.6. POLAR DIAGRAMS

Horizontal Polar Diagrams

For straight vertical radiators, with or without a top capacitor, the conditions are obviously equal at all horizontal angles so that the polar diagram in the equatorial plane is a circle. The actual field strength contours may show considerable departure from a circular pattern, because such contours depend on ground attenuation. For example, at 150 km radius

from the transmitter, one quite often finds differences in field strength of over 2 to 1 for different bearings. Hilly country, in particular, will show great increases in attenuation.

A T-type antenna also has a circular horizontal polar diagram and so too has an inverted-L antenna, provided the

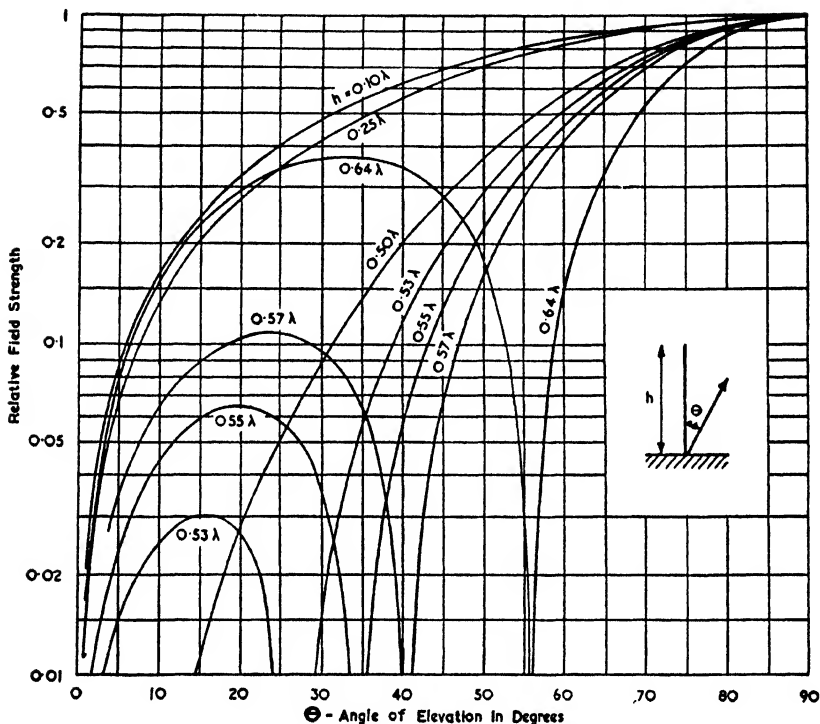


FIG. 2.29. POLAR DIAGRAMS FOR A VERTICAL RADIATOR BASED ON AN ASSUMED SINUSOIDAL CURRENT DISTRIBUTION

top portion is relatively short. With long top portions an inverted-L antenna gives greater radiation in the direction opposite to that in which the end is pointing.

Vertical Polar Diagrams

(a) Simple Vertical Radiator

The object in medium- and long-wave transmissions is to provide as great a field strength as possible in a horizontal plane. This problem was studied by Ballantine⁽⁸⁰⁾ who showed

that the optimum height of a vertical radiator is 0.64λ . A curve giving the relative field strengths for different antenna heights is shown in Fig. 2.28 and the corresponding vertical polar characteristics for certain h/λ values are given in Figs. 2.29 and 2.30.

In spite of the optimum existing at 0.64λ the usual height of this class of broadcast antennae is between 0.52λ and 0.55λ .

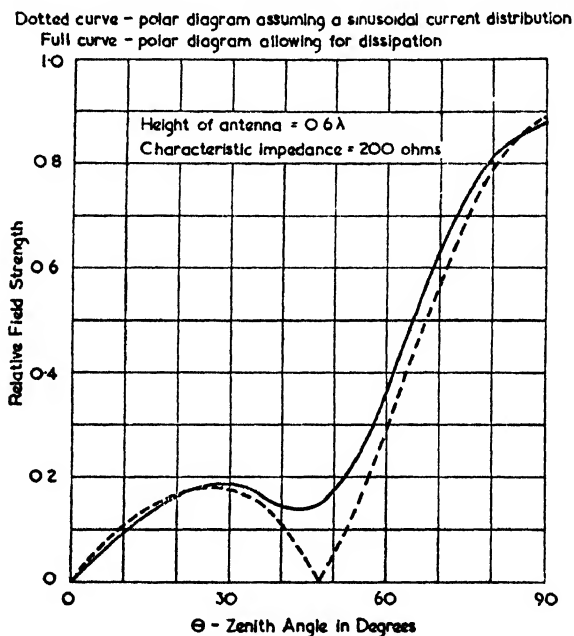


FIG. 2.30. VERTICAL POLAR DIAGRAM TAKING DISSIPATION INTO ACCOUNT
 (McPherson, *Elec. Comm.*, July, 1938)

The reason for this is that the need for as high as possible a ratio of ground wave to sky wave overrides the small increase in ground wave obtained by increasing the height to 0.64λ .

The calculated optimum anti-fading height varies according to the initial assumptions made as to the probable reflecting power of the ionosphere, the ground conductivity, and the minimum tolerable ratio of ground to sky waves. Whatever set of assumptions may be taken the optimum anti-fading height decreases slightly with increase in frequency. The method of calculating this height is given in § 9.3 of the chapter on propagation.

All the above figures are based on the assumption of a perfectly conducting earth and a sinusoidal distribution of current. With these assumptions, the loop radiation resistance is given in Vol. I by equation (5.9) and the polar coefficient $P(\theta)$ by equation (5.5) which is

$$P(\theta) = \frac{\cos(\beta h \cos \theta) - \cos \beta h}{\sin \theta} \quad (2.28)$$

It will be noticed that the function $P(\theta)$ varies in magnitude for different values of βh , even for the value of $\theta = 90^\circ$. This is due to the fact that the field strength in equation (5.6), Vol. I, has been expressed as the product of the loop current and the polar coefficient. If we wish to standardize the polar coefficient (i.e. to make it unity at $\theta = 90^\circ$ for all antenna heights) it should be divided by $(1 - \cos \beta h)$. Therefore the field strength may be expressed either as

$$E_\theta = \frac{60I_1}{r} P(\theta) \quad (2.29)$$

where $P(\theta)$ is as given in (2.28), or else as

$$E_\theta = \frac{60I_1}{r} KF(\theta) \quad (2.30)$$

where $K = 1 - \cos \beta h$
 = "form factor" as referred to the loop current

and $F(\theta) = \frac{\cos(\beta h \cos \theta) - \cos \beta h}{\sin \theta(1 - \cos \beta h)}$

In both formulae

E_θ = field strength in volts/metre,

I_1 = loop current in amperes

= $\frac{I_b}{\sin \beta h}$ where I_b is the base current,

r = distance from radiator in metres.

A more accurate calculation of the polar pattern may be made by treating the antenna as a dissipative transmission line in the manner described in Vol. I, § 5.3. The principle consists of calculating the radiation resistance according to equation (5.9), Vol. I, assuming a uniformly dissipative line whose attenuation constant, α , just accounts for the radiated losses, calculating the current distribution according to equation (5.39), Vol. I, and finally performing a graphical integration from the current

distribution. Such a procedure yielded the dotted curve shown in Fig. 2.30, which is taken from a comprehensive paper by McPherson⁽¹⁰¹⁾ dealing with the electrical properties of broadcast antennae.

Examination of Fig. 2.30 shows that the more correct current distribution produces a minimum, instead of a zero, at 47° . This filling-in of the minimum is a characteristic feature of the more accurate polar diagrams of antennae whose heights exceed half a wavelength and, in general, the thicker the antenna the more the minimum is filled in.

(b) *Top-loaded Antennae*

In the case of anti-fade antennae the purpose of loading the top with a capacitor is to enable a 10 to 20 per cent reduction

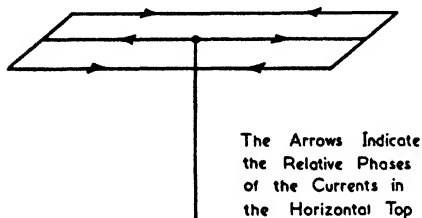


FIG. 2.31. FOLDED-TOP ANTENNA

in height to be made without at the same time causing any significant change in the vertical polar diagram. If, however, we are dealing with short antennae (i.e. radiators less than 0.2λ high), then the polar diagram remains independent of height whether the antenna is loaded or not.

The object in top loading in such cases is an entirely different one—it is to increase the base radiation resistance so that a higher overall efficiency may be obtained.

By way of illustration, let us consider the antenna given in the example at the end of this chapter. The efficiency of this antenna with its three-wire top is 75 per cent, but if the top were to be removed the radiation resistance would drop to 4 ohms, and hence the efficiency would be only 45 per cent. (In this particular case the antenna is fitted with quite a big earth system; had the earth system been indifferent the ratio of the two efficiencies would have been even greater.)

The top capacitor may take the form of a radial set of wires, or the horizontal portion of a T antenna. Both types are shown in Fig. 2.32. The horizontal portion of an inverted-L antenna may also be treated as a non-radiating top capacitor, provided the total length is less than about 0.25λ . Yet another type of loaded antenna is the "folded-top" type, one form of which is shown in Fig. 2.31. The object of this folding is to

decrease the unwanted radiation from the horizontal top and to effect some reduction in the size of the top portion for a given performance.

In all cases the non-radiating top may be considered to have an equivalent electrical length h_2' in which case the polar coefficient is given by

$$P(\theta) = \frac{1}{\sin \theta} [\cos \beta h_2' \cos (\beta h_1 \cos \theta) - \sin \beta h_2' \cos \theta \sin (\beta h_1 \cos \theta) - \cos \beta (h_1 + h_2')] \quad (2.31)$$

The methods by which h_2' may be calculated are given in § 2.2 and § 2.4. The following rule is useful in making a rough estimate of the performance of a T-type antenna (it is assumed that the antenna has a single vertical wire of the same gauge as the horizontal wire or wires)—

$$h_2' \doteq h_2 \text{ if } \begin{array}{l} h_2 < \lambda/20 \quad (\text{single-wire top}) \\ \lambda/20 < h_2 < \lambda/10 \quad (\text{double-wire top}) \\ \lambda/10 < h_2 < \lambda/5 \quad (\text{treble-wire top}) \end{array} \quad (2.32)$$

For instance, in the example at the end of this chapter the three-wire top has an actual length of 60° (i.e. $\lambda/6$) and an effective length of 62.9° . Had the top been just a single wire the effective length would have been 49° .

The top loading in the case of anti-fade antennae takes the form of a horizontal disk of circular, square or possibly triangular shape. The result of such loading is that the vertical polar diagram of an antenna only 0.4λ high can be made to simulate closely that which would be obtained by a simple radiator of height 0.53λ .

The problem was studied in detail by Brown,⁽³⁹⁾ who showed that whilst in theory such simulation could be obtained by antennae whose heights were as low as 0.25λ , in practice the efficiency fell off badly below about 0.4λ . The reason for this lies in the fact that, for antennae below about 0.4λ , the required capacitance is so great that it must be obtained by the use of a series inductance, whereupon coil losses are introduced. A further shortcoming of the tuned capacitor top method (shown in Fig. 2.32 (d)) is that high insulation is required on account of the high voltages across the coil. Even so this method has been used on a number of occasions. It is interesting to note that the principle of a tuned top was suggested as long ago as 1919 by van der Pol.⁽⁷³⁾

Examination of equation (2.8) shows that it is easier to obtain a given effective electrical length from the top loading

if the characteristic impedance of the vertical portion is high. A high characteristic impedance means a thin radiator such as may be obtained by running a wire down a wooden tower. An example of such a radiator was the one used at Wroclaw (formerly Breslau)⁽⁷⁾ which had a top of only 30 ft diameter (without coil tuning) but which nevertheless gave good anti-fade characteristics with a height of 0.42λ .

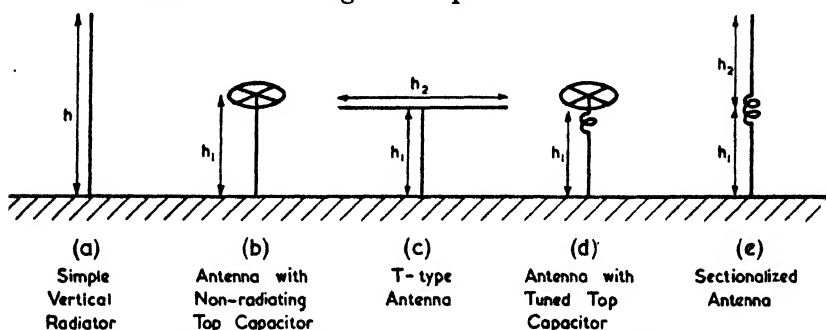


FIG. 2.32. BASIC TYPES OF VERTICAL RADIATORS

Sectionalized Antennae

Yet another method of obtaining a high field strength along the ground with a correspondingly reduced sky wave is to load the radiator with a coil about one-third of the distance from the top (Fig. 2.32 (e)). Here again the method is most suitable for an antenna whose total height is 0.4λ and much less so as the height is reduced below this value.

Sectionalizing has the advantage that the insulators do not have to stand up to such high voltages as in the case of a tuned top capacitor antenna. A view of a sectionalized antenna system is given in Plate IV, which shows the 500 ft antenna at Brookman's Park, London. This antenna also has a triangular top capacitor.

The polar coefficient of a sectionalized antenna as shown in Fig. 2.32 (e) is given by⁽³⁰⁾

$$\begin{aligned}
 P(\theta) = & \left[\cos \beta h_2 \cos (\beta h_1 \cos \theta) - \cos \theta \sin \beta h_2 \sin (\beta h_1 \cos \theta) \right. \\
 & - \cos \beta (h_1 + h_2) + \frac{\sin \beta h_2}{\sin \beta (h - h_1)} \{ \cos (\beta h \cos \theta) \\
 & - \cos (\beta h - \beta h_1) \cos (\beta h_1 \cos \theta) \\
 & \left. + \cos \theta \sin \beta (h - h_1) \sin (\beta h_1 \cos \theta) \right] / \sin \theta \quad (2.33)
 \end{aligned}$$

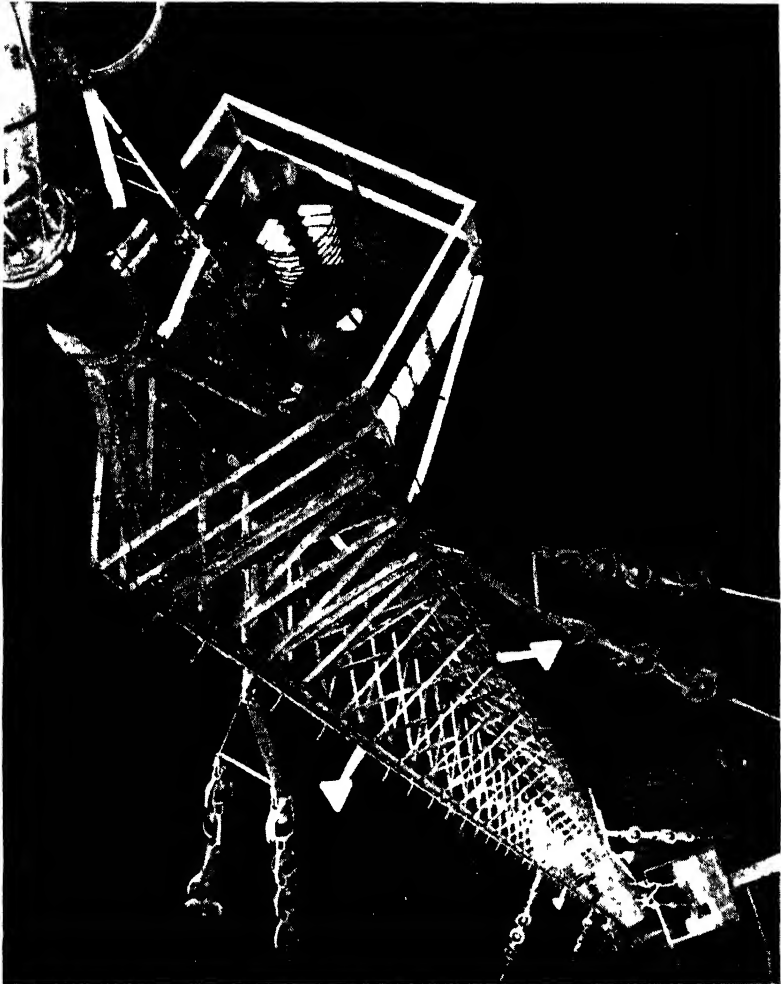


PLATE IV. THE SECTIONALIZED ANTENNA AT BROOKMAN'S PARK, LONDON

This view shows the sectionalizing insulator and the platform with the loading coil

(Courtesy of B.I. Callenders Cables, Ltd)

The form factor is given by

$$K = \cos \beta h_2 - \cos \beta(h_1 + h_2) + \frac{\sin \beta h_2}{\sin \beta(h_1 + h_2)} [1 - \cos \beta(h - h_1)] \quad (2.34)$$

Best Form of Anti-fade Antenna

From time to time various forms of radiators have been suggested to fulfil the function of an anti-fade antenna with the least possible cost and height. These include top-loaded, sectionalized, elevated and uniformly loaded ("low-velocity") antennae as well as antennae grouped in rings.

Among the investigations as to their relative merits was a notable one by Brown⁽³⁹⁾ who came to the conclusion that there was remarkably little advantage in any one of these forms over the simple vertical antenna. In addition he studied the case of a uniform current distribution (not a practical form, of course) and of a single-wire Franklin antenna. The former gave almost the identical height for optimum design as a simple vertical radiator and the latter showed a moderate improvement only at the expense of almost doubling the height.

These conclusions are not surprising when one considers that the polar pattern is merely due to space phasing between the radiation from various current elements whose spacings are not more than about half a wavelength at the most. It is apparent, therefore, that with such systems there is no prospect of cancellation over an appreciable range of angles of elevation.

Bouwkamp and de Bruign⁽³⁵⁾ have shown that, from a purely theoretical point of view, the anti-fade radius can be increased without limit, but unfortunately the current distribution involved rapidly becomes quite impractical as the ratio of ground to sky wave is increased. The principle concerned is discussed on p. 265.

Of the various forms quoted, the top-loaded and the sectionalized antennae are the most practical, for they give a moderate reduction in height without undue complications. The elevated antenna (basically a half-wave dipole) has some points of interest, for when fed at the centre of the radiator the current distribution is very nearly sinusoidal so that a lower minimum radiation is possible for some predetermined angle. Another point is that the radiator need not be half a wavelength long but could be shortened (keeping the centre at the same height

above the ground) and still give virtually the same polar diagram. As, however, the shortening is limited in practice by a reduction in efficiency this virtue cannot be exploited to any appreciable extent. Some practical forms of elevated dipoles are quoted by Brückmann,⁽⁷⁾ while a discussion of the relative merits of all the above-mentioned types is given in an article by Williams.⁽¹⁰⁵⁾

The value of an anti-fade antenna was demonstrated very clearly by Guy⁽⁹⁹⁾ by means of continuous recordings of the field strength at various distances.

2.7. FIGURE OF MERIT

The figure of merit for an antenna was defined in § 2.1 as the field strength at any given zenith angle at 1 km for 1 kW input—a definition which gives the value of 314 mV/m at ground level for the case of a lossless vertical quarter-wave antenna. To conform to the M.K.S. system this definition should be in terms of “one watt input at one metre distance,” then the previously quoted figure for a $\lambda/4$ antenna becomes 10 V/m. This is a remarkably convenient number to have as a standard though it must be admitted that the impression might be gained that the field strength should be measured at 1 m, an idea which would, of course, be entirely wrong. For long- and medium-wave antennae we shall therefore use the old definition which also has the merit of giving the round figure of 300 mV/m for very short lossless antennae.

The field strength from a vertical radiator is given in Vol. I by equation (5.6) which, on omitting the phase term, substituting $\sqrt{(W/R)}$ for I and rearranging, gives

$$\frac{Er}{\sqrt{W}} = \frac{60}{\sqrt{R_t}} P(\theta) \quad . \quad . \quad . \quad (2.35)$$

where E = field strength in volts/metre,
 W = power dissipated in watts,
 r = radial distance to field point in metres,
 R_t = total loss resistance in ohms (loop value)
 $= (R_{lr} + R_{ld})$,
 $P(\theta)$ = polar coefficient
 $= K F(\theta)$.

The appropriate values for $P(\theta)$ (or K and $F(\theta)$) may be obtained from equations (2.28), (2.30), (2.31), (2.33) and (2.34).

The term E_r/\sqrt{W} is the *figure of merit* for it is the field strength standardized in terms of unit power and unit distance. This field strength is directed along the lines of longitude, i.e. in the direction of θ increasing or decreasing, a fact which is indicated in Vol. I, equation (5.6), by the retention of the suffix θ .

R_i is the resistance representing the total losses in terms of the current at some specified point. This point must be the current antinode in view of the fact that all the equations as given for $P(\theta)$ or K are in terms of the loop current. Therefore R_i is equal to the sum of the loop radiation resistance, R_{lr} , and the loop dead-loss resistance, R_{ld} .

In most cases the horizontal figure of merit (for which $\theta = 90^\circ$) is of prime interest whereupon the formulae for $P(\theta)$ simplify somewhat so that we have—

$$\frac{E_r}{\sqrt{W}} = \frac{60}{\sqrt{(R_{lr} + R_{ld})}} [1 - \cos \beta h] \quad (2.36)$$

for a simple vertical radiator, and

$$\frac{E_r}{\sqrt{W}} = \frac{60}{\sqrt{(R_{lr} + R_{ld})}} [\cos \beta h_2' - \cos \beta (h_1 + h_2')] \quad (2.37)$$

for an antenna with a non-radiating top whose electrical length is h_2' .

Both the above expressions are more commonly given in terms of millivolts per metre, kilometres and kilowatts, in which form they become

$$\frac{E_m D}{\sqrt{P}} = \frac{1\ 900}{\sqrt{(R_{lr} + R_{ld})}} [1 - \cos \beta h] \quad (2.38)$$

and
$$\frac{E_m D}{\sqrt{P}} = \frac{1\ 900}{\sqrt{(R_{lr} + R_{ld})}} [\cos \beta h_2' - \cos \beta (h_1 + h_2')] \quad (2.39)$$

where E_m = field strength in millivolts/metre,

D = distance in kilometres,

P = power in kilowatts,

h = height of simple vertical antenna,

h_1 = height of vertical portion of top-loaded antenna,

h_2' = electrical length of non-radiating top.

If the dead-loss resistance R_{ld} were zero, then for a short antenna (i.e. one for which $\sin \beta h = \beta h$) equation (2.38) becomes

$$\frac{E_m D}{\sqrt{P}} = 300 \quad (2.40)$$

i.e. $E_{mV} = 300$ mV/m for one kilowatt at one kilometre.

2.8. ANTENNA COUPLING CIRCUITS

In general the input impedance of an antenna is unsuitable for direct coupling to a transmission line in which case a coupling circuit is needed between the two impedances. The simplest matching section is the well-known "reactance transformer" (complicated sections are to be avoided since they usually entail further losses).

An alternative method of exciting the antenna is to shunt feed it by means of a sloping wire which is fastened about one-seventh of the way up the mast. This method is only suitable for antennae whose heights exceed 0.2λ , for with shorter antennae the tapping point is too far up the mast.

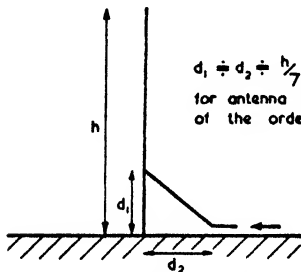


FIG. 2.33. DIAGRAM OF A SHUNT-EXCITED ANTENNA

disadvantages are (a) that the current at the base of the antenna is increased (this is detrimental to the vertical polar characteristics of anti-fade antennae), and (b) that the voltage across the series capacitor is very great if the mast is of the order of half a wavelength high. These features can be observed in the curves of Figs. 2.34 and 2.22 respectively.

In view of the above considerations shunt excitation is mainly of use for masts which are about a quarter of a wavelength high.

Fig. 2.33 shows a shunt-excited mast, and it will be noticed that the arrangement is virtually one-half of a delta matched dipole circuit. Normally d_1 and d_2 are both approximately equal to one-seventh of the mast height. For instance if $h = 0.25\lambda$ and $d_1 = d_2 = 0.03\lambda$, then the impedance at the input end is about $70 + j300$ ohms. Such a value permits direct matching to a 70-ohm line on balancing out the positive reactance by means of a series capacitor.

shorter antennae the tapping point is too far up the mast. The reactance transformer, on the other hand, can be applied to any size of antenna.

Shunt-fed Antenna

Shunt feeding has the merit of allowing the base of a self-radiating mast to be connected directly to earth. Its

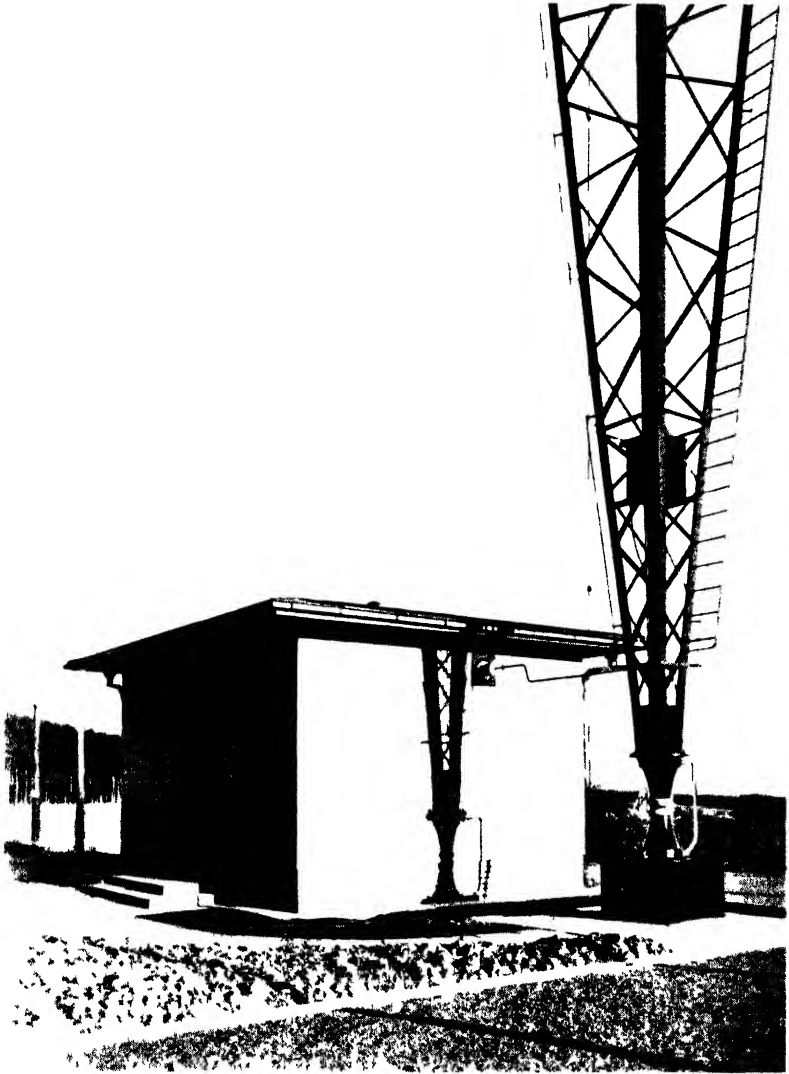


PLATE V THE BASE OF THE VERTICAL RADIATOR AT MELNIK, CZECHOSLOVAKIA

This view shows the copper wires which run up the edges of the mast the spark gap for lightning protection and the box housing for the mast lighting system

(courtesy of Standard Telephones & Cables Ltd)

The variations of input impedance with d_1 and d_2 may be summarized as follows—

for d_1 increasing:

- Positive reactance increases,
- Resistance increases,

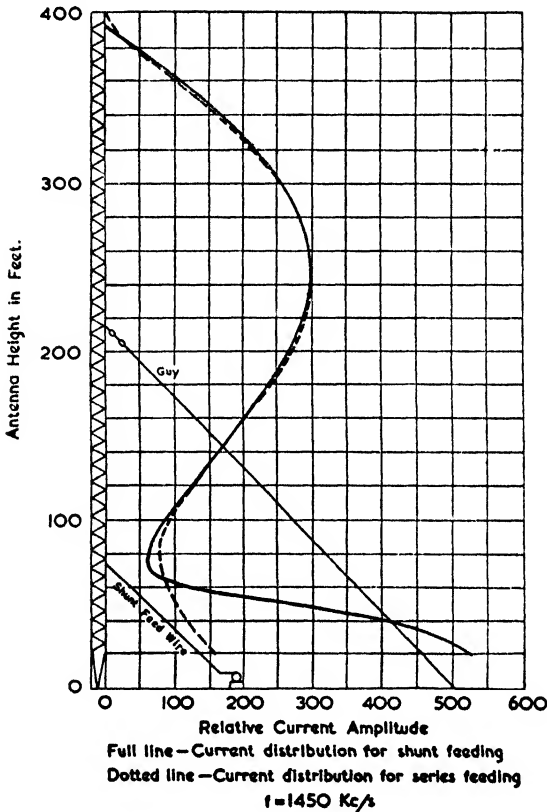


FIG. 2.34. EXPERIMENTALLY DETERMINED CURRENT DISTRIBUTION ALONG A SHUNT-FED ANTENNA

(Morrison and Smith, *Proc. I.R.E.*, June, 1937)

for d_2 increasing:

- Positive reactance decreases,
- Resistance decreases.

The exact values of d_1 and d_2 can only be determined by trial and error methods. We may either measure the input

impedance by means of an h.f. bridge, or the current at both ends of the wire may be noted when the series capacitor is tuned for maximum feed current (the adjustment is correct when the two currents are equal—for further details the reader may consult an article by Bauer⁽⁸¹⁾).

The Reactance Transformer

The principle of this transformer is illustrated in Fig. 2.35, in which R_1 and R_2 are the two resistances which require matching.

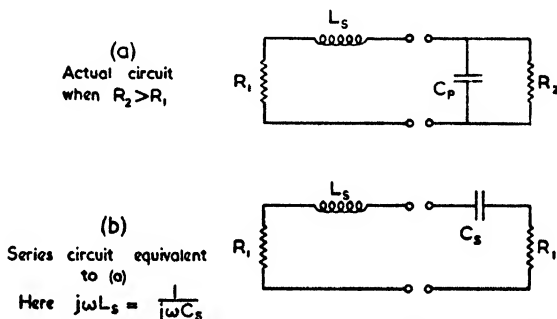


FIG. 2.35. THE PRINCIPLE OF THE REACTANCE TRANSFORMER

By connecting a suitable capacitor C_p across R_2 , the equivalent series circuit can be made to be equal to R_1 plus C_s in series (it will be noted that this is only possible if $R_2 > R_1$). For maximum energy transfer between generator and load the two impedances must be conjugate, i.e. the reactive impedance of L_s must be equal and opposite to C_s . When the necessary relationships are obeyed we have

$$R_1 R_2 = L_s / C_s = \zeta_0^2, \text{ say.}$$

There is an obvious resemblance between the above equation and that for the matching of two unequal resistances by means of a quarter-wave section of transmission line of inductance L_s per unit length and capacitance C_s per unit length.

If either or both the resistances R_1 and R_2 have associated reactances, these reactances can be incorporated in the values chosen for L_s and C_p . It should be noticed that, although Fig. 2.35 shows a parallel capacitance and a series inductance, the two types of reactors could equally well have been reversed and matching could still be obtained. Whichever combination one chooses, the impedance of the parallel reactor will exceed

that of the series reactor; for this reason the inductor is usually chosen to be the series element since it is then of a more reasonable size. In addition the combination of series inductor and parallel capacitor will reduce the output of the second and higher harmonics.

Another consideration that comes into play is the response of the network off tune. With normal broadcast bandwidths this causes no difficulty since the sideband losses will only be a fraction of a decibel, but with relatively wide bandwidths the losses may need watching.

The calculation of the reactive elements is quite straightforward, the most convenient forms for the equations being those which are expressed in the ratio of R_2/R_1 . The values of the elements may also be found by simple graphical constructions.

If in Fig. 2.36 $R_2 > R_1$ and $R_2/R_1 = n$, then X_1 and X_2 are given by

$$X_1 = R_1(n - 1)^{\frac{1}{2}} \quad (2.41)$$

$$X_2 = nR_1(n - 1)^{-\frac{1}{2}}$$

For the reasons previously given X_1 and X_2 must be of opposite sign.

The application of the above formulae is illustrated by the following example.

Example :

(This goes through the calculations from the beginning and therefore also serves as an example for some of the previous sections.)

A T antenna whose height $h_1 = 30$ m and whose length of top $h_2 = 50$ m is operated at a frequency of 1 Mc/s. The top portion consists of 3 parallel wires spaced 1 m apart. All wires are No. 10 S.W.G. (radius 1.625 mm). The antenna is to be fed via a coaxial cable whose characteristic impedance is 70 ohms.

(a) Calculation of Base Reactance

From the curves of Fig. 2.7 we find that the static capacitance of the top is $9.9 \mu\text{F}/\text{metre}$, i.e. the characteristic impedance Z_{02} as given by equation (2.2) is

$$Z_{02} = \frac{333}{9.9} = 337 \text{ ohms}$$

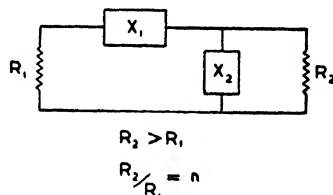


FIG. 2.36. DIAGRAM FOR REACTANCE TRANSFORMER FORMULAE

Using equation (2.9) gives the impedance of the non-radiating top as

$$\begin{aligned} X_2 &= -\frac{337}{2} \cot \frac{h_2}{2} \\ &= -168.5 \cot 30^\circ \\ &= -292 \text{ ohms} \end{aligned}$$

The characteristic impedance, Z_{01} , of the vertical portion can be found from Fig. 2.6. The result is, of course, the free-space value but—as has been pointed out in § 2.2—a compensating effect arises if free-space values are used for *both* the horizontal and the vertical portions. Hence the reason for preferring the curves of Fig. 2.6 to those of Fig. 2.9. We find

$$Z_{01} = 570 \text{ ohms}$$

The equivalent length of the top portion (equation (2.8)) is therefore

$$\begin{aligned} \beta h_2' &= \cot^{-1} \frac{292}{570} \\ &= 1.10 \text{ radians or } 62.9^\circ \end{aligned}$$

The total length of the antenna is therefore given by

$$\beta(h_1 + h_2') = 98.9^\circ$$

Hence the base reactance (as given by equation (2.1)) is

$$\begin{aligned} X_b &= -570 \cot 98.9^\circ \\ &= \underline{\underline{+89.3 \text{ ohms}}} \end{aligned}$$

(b) *Calculation of Base Radiation Resistance*

The base radiation resistance may be found by interpolation from the curves of Fig. 2.12, using the fact that $h_1 = 0.1\lambda$ and $h_2' = 0.175\lambda$.

The result is

$$R_{br} = \underline{\underline{15 \text{ ohms}}}$$

Before the actual base resistance can be found, an estimate of the total losses must be made. These will be predominantly earth and insulator losses, the former depending on the earth system employed and the ground conductivity.

(c) *Estimation of Earth Losses*

We will suppose that a large earth system consisting of 60 radial wires each 50 m long is used. The diameter of the

wire will have no noticeable effect on the antenna efficiency if the wires are of reasonable thickness—say No. 10 S.W.G.

The distribution of the currents in the ground is given by equation (2.23) and is shown in the full curve of Fig. 2.37 (an input current of 1 amp is assumed).

If the ground conductivity is about 0.01 mhos/m, then the curves of Fig. 2.26 apply. In the present case $n = 60$ and

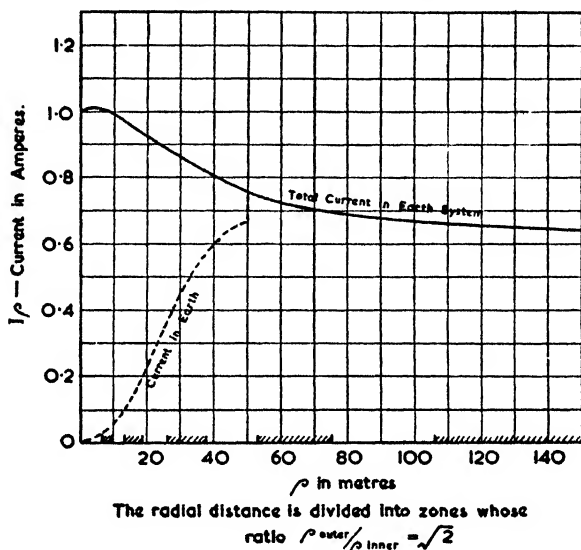


FIG. 2.37. DISTRIBUTION OF EARTH CURRENTS IN THE EXAMPLE

hence the radial current distribution in the earth itself takes the form shown by the dotted line in Fig. 2.37. The dotted line will be seen to return abruptly to the full line when $\rho = 50$ m, for this distance marks the boundary of the earth system.

The earth losses per zone are determined by equation (2.25) where ρ_2 and ρ_1 are the inner and outer limits respectively of a zone whose total radial current is I_ρ . Fig. 2.37 is marked out in zones for which $\rho_2/\rho_1 = \sqrt{2}$. Therefore the watts dissipated per zone are

$$W = 1.093 I_\rho^2$$

since

$$R_m = 20 \text{ ohms}$$

$$= 1/gs$$

where $g = 0.01$ mhos/m (ground conductivity),
 $s = 5$ m (skin depth as given by Fig. 2.25).

The total earth losses are given by the sum of the losses for each zone taken between the limits of $\rho = 0$ and $\rho = 0.5\lambda$. This sum may be found with ample accuracy from the curves of Fig. 2.37 on taking an average value of I_ρ for each zone. The result is

$$W_{\text{earth losses}} = 2.27 \text{ W}$$

(d) *Estimation of Insulator Losses*

The total joulean losses will include conductor and insulator losses, of which only the latter are significant. In particular we need only consider the insulators which support the top since this is where the high voltages occur.

The base voltage is given by equation (2.17) and is obviously more dependent on the base reactance than on the base resistance in the present case. We shall assume provisionally therefore that $R_b = 20$ ohms. This makes the total input impedance $Z_b = \sqrt{(20^2 + 89.3^2)} = 91.5$ ohms and hence $V_b = 91.5$ V.

From equation (2.19) we find that V_t , the voltage at the ends of the horizontal portion, is equal to 3 820.

If the top is suspended with four egg insulators in series at each end, then the capacitance to the earthed mast will be about $2 \mu\mu\text{F}$ at each end. In practice there would also be three egg insulators joining the ends of the wires to the triatics (the wires themselves being connected by jumpers), but since these are in parallel the increased insulation they afford may be neglected for the purposes of this calculation.

Using equation (2.18) to find the total watts dissipated in the eight insulators, we find

$$\begin{aligned} W_{\text{insulators}} &= 2 \times (3\ 820)^2 \times \frac{0.007}{79\ 500} \\ &= 2.57 \text{ W} \end{aligned}$$

(e) *Total Base Impedance*

Since the radiation resistance is 15 ohms and the input current 1 amp the power radiated is

$$W_{\text{radiated}} = 15 \text{ W}$$

The sum of the radiated power and that dissipated in the earth and insulators is therefore 19.84 W. Since we have assumed $I_b = 1$ amp, the base impedance is

$$\begin{aligned} R_b &= R_{br} + R_{ba} \\ &= 15 + 4.84 \\ &\doteq 20 \text{ ohms} \end{aligned}$$

Therefore the total base impedance is

$$Z_b = \underline{\underline{20 + j89.3 \text{ ohms}}}$$

(f) *Efficiency and Figure of Merit*

The antenna efficiency is given by

$$\begin{aligned} \eta &= \frac{15}{20} \times 100 \\ &= \underline{\underline{75 \text{ per cent}}} \end{aligned}$$

The horizontal figure of merit is given by using either equation (2.37) or equation (2.39) in conjunction with (2.12). The two methods of expression give

$$\frac{Er}{\sqrt{W}} = 8.3$$

or

$$\frac{E_{mv}D}{\sqrt{P}} = 263$$

A quicker, but slightly rougher, estimate of the figure of merit could be obtained by simply assuming that the vertical polar diagram follows a cosine law whereupon

$$\begin{aligned} \frac{E_{mv}D}{\sqrt{P}} &= 300 \times \sqrt{0.75} \\ &= \underline{\underline{260}} \end{aligned}$$

(g) *Design of Coupling Unit*

From the above results we see that the matching problem is such that in Fig. 2.36 we have $R_1 = 20$ ohms and $R_2 = 70$ ohms. The ratio R_2/R_1 is therefore equal to 3.5, so that equations (2.41) give

$$\begin{aligned} |X_1| &= 31.6 \text{ ohms} \\ |X_2| &= 44.3 \text{ ohms} \end{aligned}$$

Since we have already a series inductance in the low impedance side, an obvious choice is to make X_1 positive and X_2 negative. This has the additional advantage of using a capacitor for the high-impedance arm so that losses are kept to a minimum as well as giving some suppression of harmonics. The value of this capacitor is given by

$$\begin{aligned} C_2 &= \frac{1}{2\pi \times 10^6 \times 44.3} = 0.00358 \times 10^{-6} \\ &= \underline{\underline{0.0036 \mu\text{F}}} \end{aligned}$$

The series inductance due to the antenna exceeds that required for X_1 , hence a series capacitor must be used. This must have an impedance of $-(89.3 - 31.6)$ ohms and is therefore given by

$$C_1 = \frac{1}{2\pi \times 10^8 \times 57.7} = 0.00276 \times 10^{-8}$$

$$= \underline{\underline{0.0028 \mu\text{F}}}$$

The coupling circuit therefore takes the form shown in Fig. 2.38. In practical forms of coupling units the series

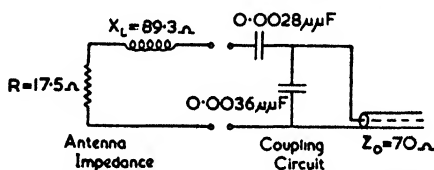


FIG. 2.38. COUPLING CIRCUIT IN THE EXAMPLE

capacitor is given a convenient nominal value and the final adjustments made by means of an extra series inductor—this is simply because it is easier to make an adjustable coil than to provide a large selection of capacitors.

Short- and Ultra-short-wave Antennae

At short wavelengths there is no difficulty in having an antenna whose length is an appreciable part of a wavelength, with the result that a high radiation resistance (with a correspondingly high efficiency) is readily attainable.

For wavelengths between 10 and 100 m, i.e. in the short-wave band, the normal aim is to produce a strong sky wave at some predetermined angle. This aim can be achieved by mounting the antenna at heights varying between a quarter of a wavelength and one or two wavelengths. For ultra-short waves (1 to 10 m) line-of-sight propagation is relied upon, so that both transmitting and receiving antennae should be elevated as far as possible.

Consequently both short- and ultra-short-wave antennae are normally operated at such heights above the ground that the ground losses may be neglected.

The half-wave dipole is by far the most common type of antenna in use at the wavelengths mentioned above. Most of the present chapter will therefore be concerned with such dipoles or with variations of the simple dipole.

Grounded vertical radiators are rarely used in short-wave transmission. Where, however, a special case may call for such a radiator, the design methods would follow the same lines as those which were given for medium-wave antennae.

3.1. THE HALF-WAVE DIPOLE

The half-wave dipole owes its usefulness to the fact that it is the longest uniform linear radiator which will support a standing wave for which all the elements of current are in phase. In practice, the actual length of the dipole is usually about 5 per cent less than half a wavelength—a fact which

reduces the radiation resistance at the centre from about 73 ohms to some value between 60 and 70 ohms but at the same time reduces the reactance from $+j42$ ohms to zero. A shortened half-wave dipole is therefore admirably suited to being fed directly via a concentric line, since such a line can readily be made to have a characteristic impedance equal to the input impedance at the centre of the dipole.

There is nothing to be gained electrically by using still shorter dipoles—the polar pattern remains virtually the same but the radiation resistance is reduced to less practical values. On the other hand, increasing the length to more than half a wavelength results in a less omnidirectional radiation (a feature which may, of course, be desired in some cases).

It will be seen, therefore, that the half-wave dipole represents a fundamental and highly convenient form of antenna. For this reason it is appropriate to use it as a standard by which other antennae may be judged. In particular the gain of directive antenna systems may be specified in terms of the half-wave dipole. Such a specification is given in terms of the field strength in the equatorial plane of the dipole, i.e. in a direction of maximum radiation. In this direction the half-wave dipole (in free space) has a field strength which is given by

$$E = 7 \frac{\sqrt{W}}{r} \quad . \quad . \quad . \quad (3.1)$$

where E = field strength in volts/metre,

W = input power in watts,

r = distance to field point in metres.

The above formula is based on the assumption that the radiation resistance at the centre is 73.2 ohms so that it represents the field from a true half-wave dipole, but this does not differ from the field due to a half-wave dipole shortened to give zero reactance by more than a fraction of one per cent.

In the following pages the properties of a half-wave dipole are discussed at greater length under specific headings.

Input Impedance

The self-impedance, Z_{11} , of a half-wave dipole as calculated by the induced e.m.f. method is stated in Vol. I, equation (5.19). Evaluation of this equation gives the result

$$Z_{11} = 73.2 + j42.5 \text{ ohms} \quad . \quad . \quad (3.2)$$

This is the impedance at the centre of an infinitely thin dipole which is exactly half a wavelength long and is situated in free space. (The double suffix to Z has been introduced because of the convenient distinction which can thereby be obtained between self and mutual impedances.)

The variation of this impedance with the thickness and length of the dipole is shown in Figs. 3.1 and 3.2. These

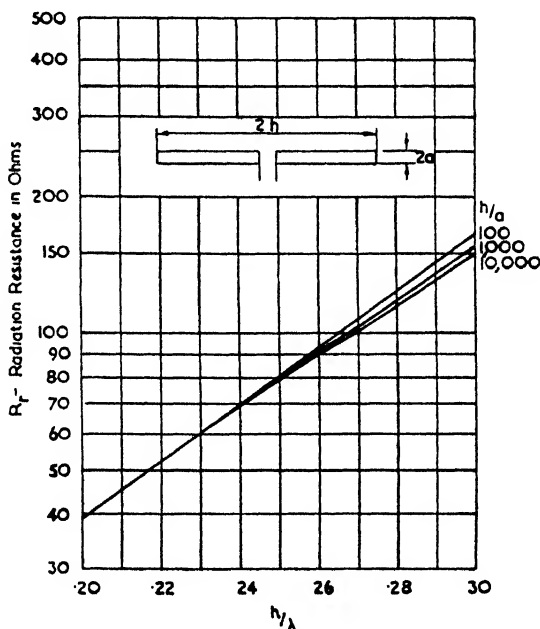


FIG. 3.1. RADIATION RESISTANCE OF A CYLINDRICAL DIPOLE
(Calculated by Schelkunoff's biconical antenna method)

curves are based on Schelkunoff's biconical antenna method and have been calculated by means of equations (5.52), (5.55) and (5.56), Vol. I. In addition, Fig. 3.3 shows the percentage shortening required to bring a half-wave dipole to resonance.

The problem of the cylindrical dipole has also been studied by King and Harrison⁽⁵⁹⁾ who based their work on the methods of Hallén.⁽⁴⁸⁾ Their results indicate changes in impedance due to changes in antenna thickness which differ from those shown in Figs. 3.1 and 3.2, but their values are not so well supported by the experimental evidence of Brown and Woodward.⁽⁴¹⁾ Only by assuming a spheroidally shaped antenna is it possible to obtain a rigorous solution. Solutions of this

nature have been obtained by Stratton and Chu,⁽⁸⁷⁾ whose results for lengths about the half-wave resonance are given in Figs. 4.4 and 4.5. The low values of reactance (indicating

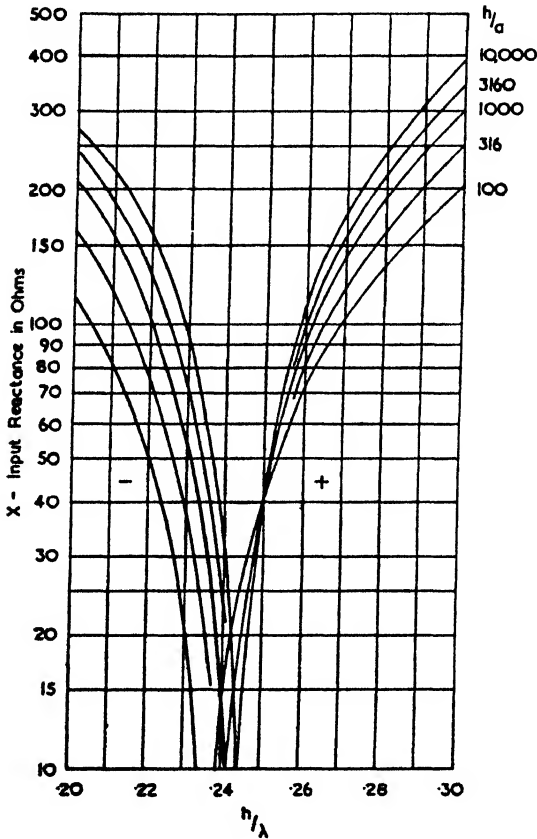


FIG. 3.2. INPUT REACTANCE OF A CYLINDRICAL DIPOLE
(Calculated by Schelkunoff's biconical antenna method)

a wide bandwidth) of the thicker prolate spheroids are particularly worthy of note.

The experiments of Brown and Woodward⁽⁴¹⁾ on cylindrical antennae confirmed the value of 73 ohms for the input resistance of a thin centre-fed half-wave dipole. This value remained unchanged until the ratio of h/a was less than 200. For thicker dipoles the resistance increased until a value of 110 ohms was reached for $h/a = 20$, after which the value decreased. (The values for the very thick antennae were affected

by the appreciable shunt capacitance which the relatively big ends presented at the input terminals.)

A notable feature of these experiments was that no measurable difference was found whether the ends of the antennae were hollow or solid. The experiments also gave the percentage shortening curve shown by the dotted line in Fig. 3.3.

Full curve—Theoretical (Schelkunoff, Proc. I.R.E. Sept 1941)
Dotted curve—Experimental (Brown and Woodward, Proc. I.R.E. Apr 1945)

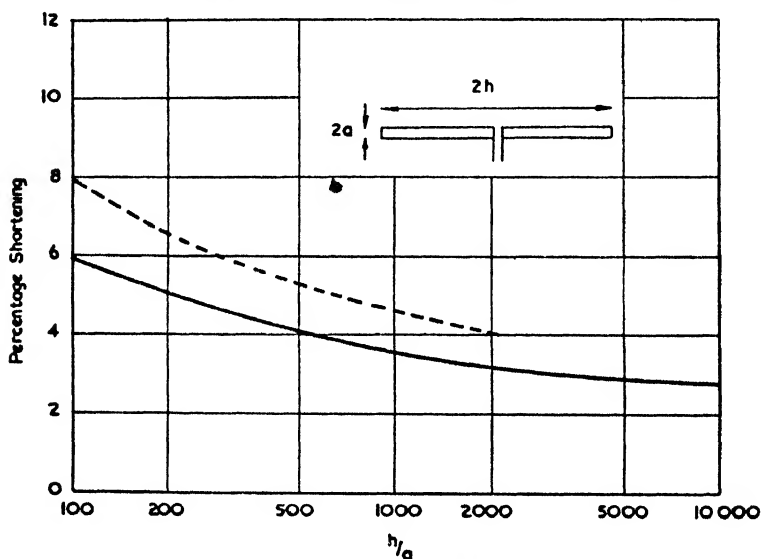


FIG. 3.3. PERCENTAGE SHORTENING TO BRING A HALF-WAVE DIPOLE TO RESONANCE

The effect of the ground on the input resistance is demonstrated by the curves of Fig. 3.14, which show both the theoretical values and those obtained experimentally by Friis, Feldman and Sharpless.⁽²⁵⁰⁾

At the extreme end of a dipole there is no current and therefore the radiation resistance would appear to be infinite when referred to the end. However, in the practical case of an end-fed half-wave dipole there certainly is a current at the feed point for the assumption of a sinusoidal current distribution (on which equation (3.2) is based) is not quite correct. The impedance under these conditions is given in Fig. 3.4, the curves for which have been calculated by using the

equivalent transmission-line method and giving the dipole a characteristic impedance based on the capacitance per unit length in free space. The method of feeding illustrated in Fig. 3.4 is well known as the "Zepp feed" among amateurs.

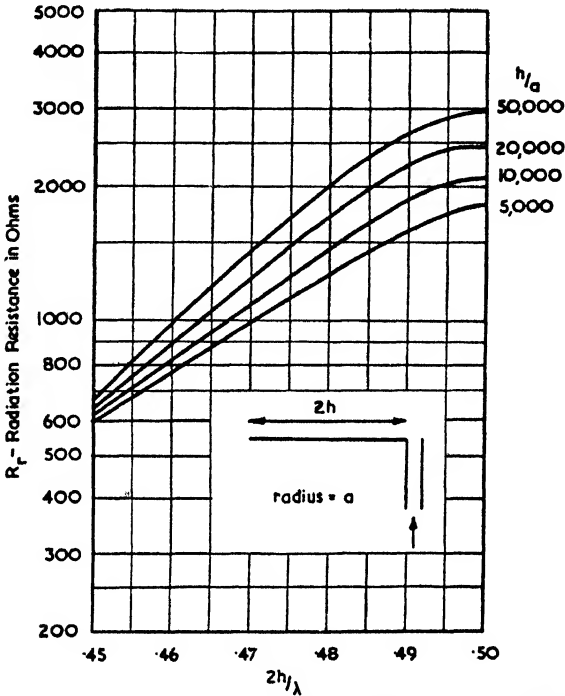


FIG. 3.4. RADIATION RESISTANCE OF AN END-FED HALF-WAVE DIPOLE

Free-space Polar Diagram

It is obvious from the symmetry of the conditions that a polar diagram in the equatorial plane of a dipole, or in any parallel plane, is simply a circle.

By making the usual assumption of a sinusoidal current distribution, it was shown in Vol. I, § 4.4, that the polar diagram in a plane containing the dipole (see Fig. 3.5) is the following function of θ —

$$F(\theta) = \frac{\cos\left(\frac{\pi}{2} \cos \theta\right)}{\sin \theta} \quad (3.3)$$

A graph of this function for values of θ between 0° and 90° is given in Fig. 3.6, together with a sine curve for comparison.

Equation (3.3) would appear to indicate that there is no field in a line with the dipole. Actually this is only true for distances greater than a few wavelengths from the antenna. In the immediate neighbourhood, there is a radial field whose strength in the case of a doublet is given by equation (4.38), Vol. I. Because of this local field, there is a definite mutual coupling between collinear dipoles of moderate separation.

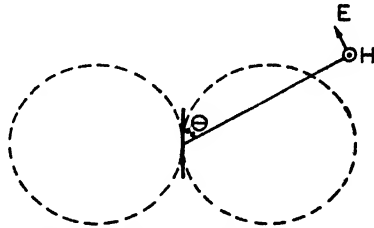


FIG. 3.5. DIAGRAM SHOWING THE RADIATION PATTERN IN THE MERIDIAN PLANE OF A HALF-WAVE DIPOLE

The polar diagram represents the radiation field and is therefore only valid at a wavelength or more from the antenna. In the radiation field the electric intensity is directed along a

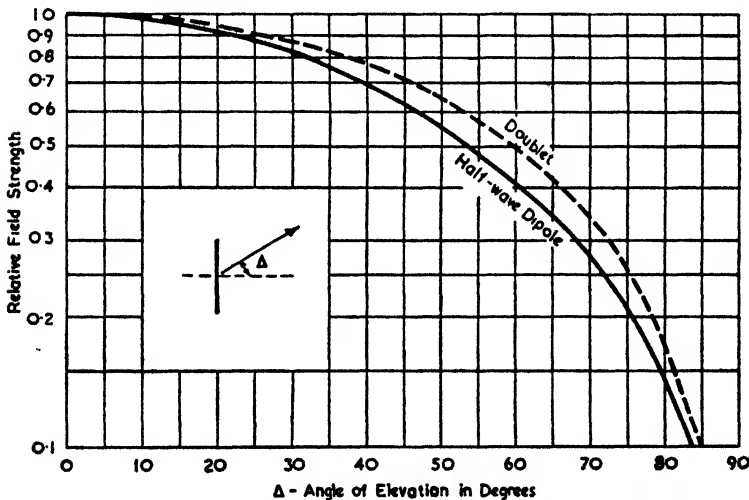


FIG. 3.6. POLAR DIAGRAMS OF A HALF-WAVE DIPOLE AND A DOUBLET

line of longitude as shown in Fig. 3.5. Hence the polarization of a vertical dipole is only strictly vertical in the equatorial plane. Indeed, in directions approximating to the line of the dipole the polarization is practically horizontal, though the field strength is relatively low.

Polar Diagram above the Ground

In determining the polar patterns of a dipole above the ground it is convenient to assume initially that the ground is a perfect conductor. The modifications caused by imperfect ground conductivity are not great in the case of horizontal dipoles,

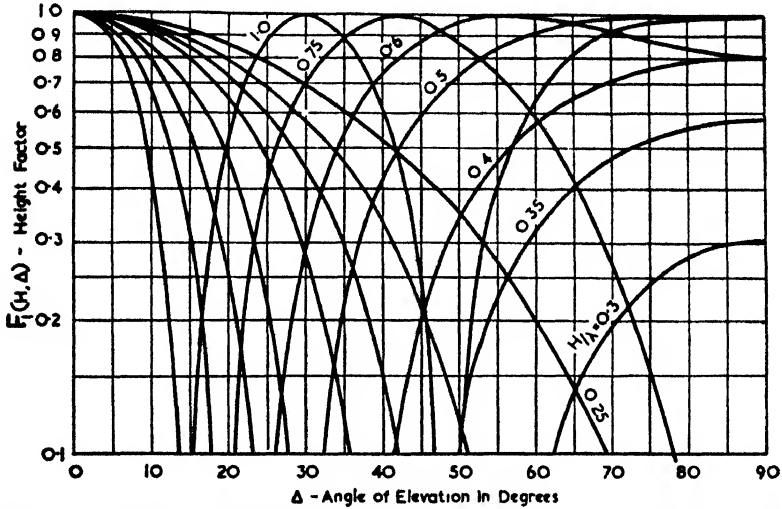


FIG. 3.7. HEIGHT FACTOR FOR POSITIVE IMAGES: RANGE $H = 0.25\lambda$ TO 1.0λ

but for vertical dipoles the differences from the idealized case may be quite appreciable, especially at low angles to the ground.

The perfect ground case can be dealt with quite simply by using image theory, with the result that a vertical element of current has an image for which the current is in phase (Fig. 1.8 (a)), whereas a horizontal current element has an out-of-phase image (Fig. 1.8 (b)).

Applying these principles to vertical and horizontal half-wave dipoles we see that the former has an in-phase image and the latter an out-of-phase image. In both cases the resultant polar pattern may be found by multiplying the pattern of a dipole in free space by that due to two point sources (situated at the centre of the dipole and at the centre of the image respectively) which are either in phase or out of phase according to whether the dipole is vertical or horizontal.

The polar pattern due to the dipole only is given in Fig. 3.6, whilst that due to the two point sources may be called the "ground reflection factor," or "height factor," and is given

in Figs. 3.7 and 3.8 for positive and negative images respectively up to a height of one wavelength. The derivation of these ground reflection factors is discussed in Chapter VI along with the general principles of obtaining polar patterns. Chapter VI also contains additional height factor curves (Figs. 6.4 to 6.7) which cater for heights between 1λ and 3λ .

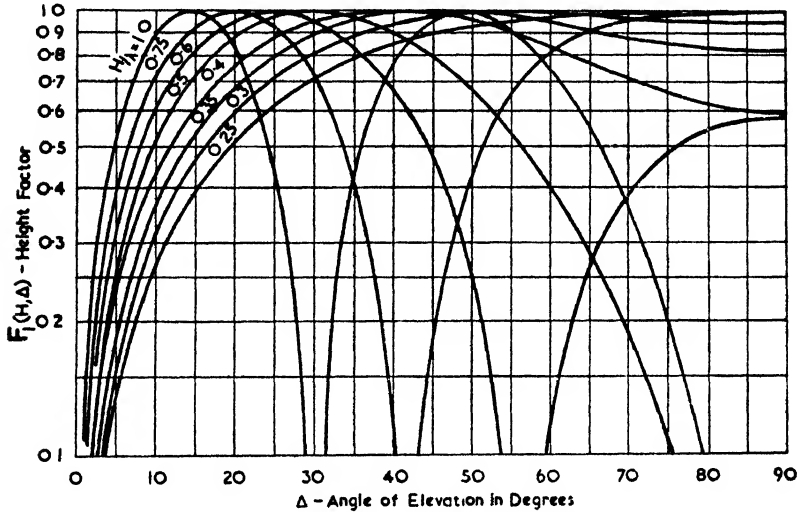


FIG. 3.8. HEIGHT FACTOR FOR NEGATIVE IMAGES: RANGE $H = 0.25\lambda$ TO 1.0λ

In all cases the curves have been drawn with a logarithmic scale for the ordinates. The reason for doing this is that it then becomes a very simple matter to multiply the curves together using transparent paper. One merely traces out one of the required curves and (on making due allowances for any possible differences in the horizontal scales) one then superimposes this tracing over the graph by which the first curve must be multiplied, whereupon the multiplication may be performed by simple addition of the ordinates. The method is illustrated in Fig. 3.9. Thus the vertical scale is used in the same manner as a slide rule but with the advantage that no figures need be noted. Moreover, the trend of the whole curve is easily observed even before the multiplication is undertaken; consequently inappropriate curves can soon be rejected.

Any number of curves may be multiplied together in this way, though the accuracy naturally decreases with the number. For all practical purposes the accuracy obtained is ample and

furthermore the technique is very labour-saving, especially when dealing with the polar patterns of arrays or rhombic

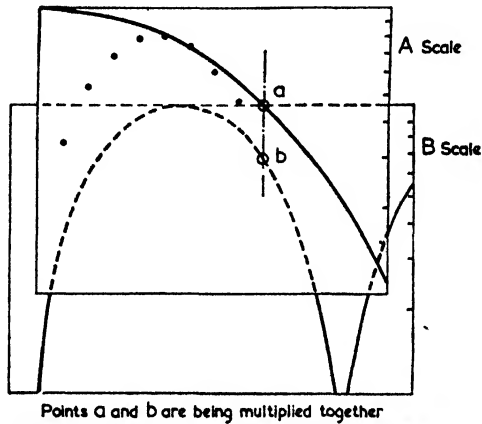


FIG. 3.9. DIAGRAM ILLUSTRATING THE METHOD OF MULTIPLYING CURVES DRAWN ON A LOGARITHMIC SCALE

antennae. The actual polar form of the radiation pattern is instructive but for most practical purposes it is sufficient to leave the curve in the form obtained on the logarithmic paper.

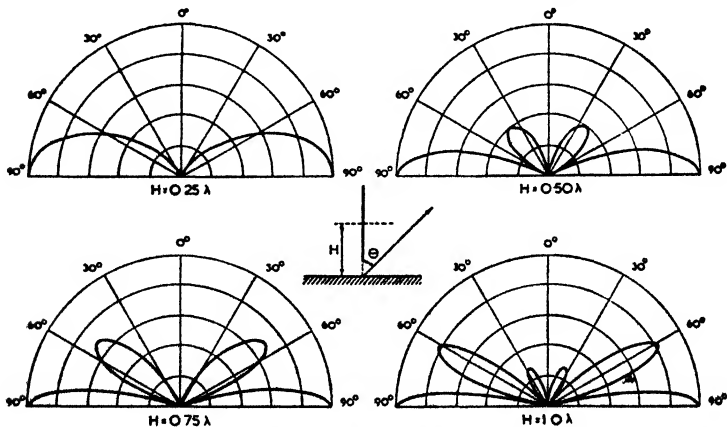


FIG. 3.10. POLAR DIAGRAMS OF A VERTICAL HALF-WAVE DIPOLE ABOVE A PERFECTLY CONDUCTING EARTH

Figs. 3.10, 3.11 and 3.12 show the polar diagrams for vertical and horizontal dipoles whose centres are at heights of $\lambda/4$,

$\lambda/2$, $3\lambda/4$ and λ . In the case of a horizontal dipole, it is necessary to give separate diagrams for the plane at right angles

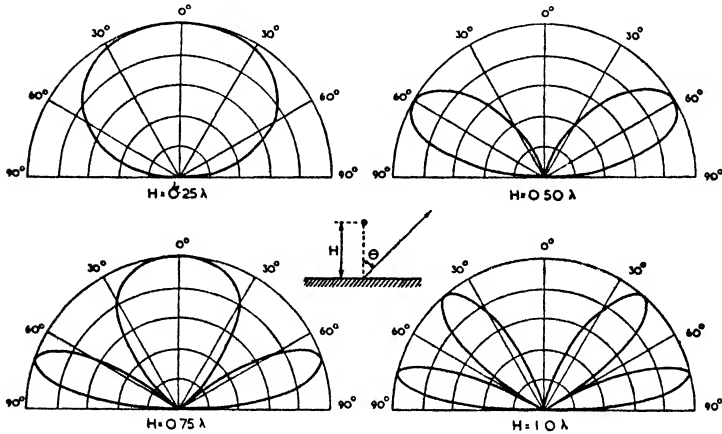


FIG. 3.11. POLAR DIAGRAMS (IN THE EQUATORIAL PLANE) OF A HORIZONTAL HALF-WAVE DIPOLE ABOVE A PERFECTLY CONDUCTING EARTH

and the plane in line with the dipole since these two cases differ appreciably.

It would appear from these diagrams that excellent radiation in a horizontal direction may be obtained by using a vertical

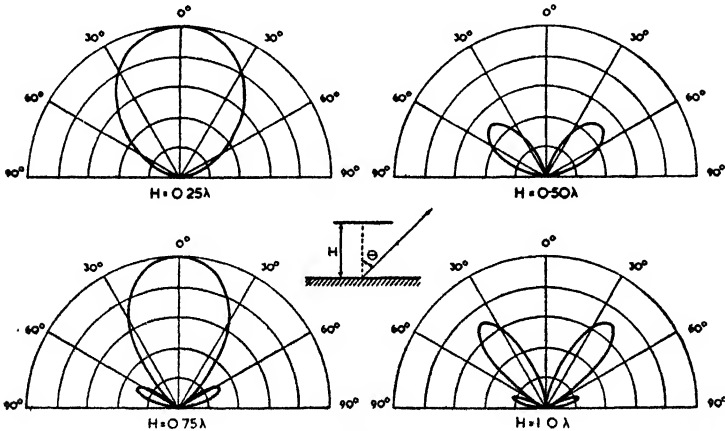


FIG. 3.12. POLAR DIAGRAMS (IN A MERIDIAN PLANE) OF A HORIZONTAL HALF-WAVE DIPOLE ABOVE A PERFECTLY CONDUCTING EARTH

dipole. Actually this is quite wrong, for the imperfect ground conductivity causes very high attenuation at large angles of

incidence when the wavelengths are in the short- or ultra-short-wave region. The horizontal dipole patterns, which in any case show little radiation at large angles of incidence, are much less affected by the conductivity of the ground.

A much better assessment of the true polar diagram can be obtained by calculating the relative field strength at the different angles on the basis of a ray treatment, i.e. for each angle we use the reflection coefficient R_v or R_h (for vertically

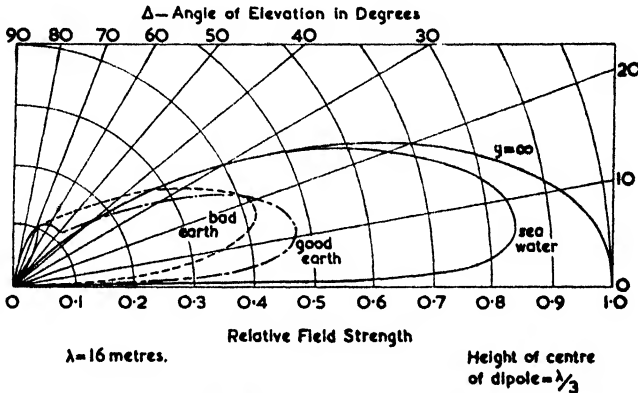


FIG. 3.13. POLAR DIAGRAMS OF A VERTICAL HALF-WAVE DIPOLE ABOVE A GROUND OF FINITE CONDUCTIVITY
(Feldman, *Proc. I.R.E.*, June, 1933)

or horizontally polarized waves respectively). R_v and R_h are given in Vol. I by equations (3.52) and (3.53) and are shown plotted in Figs. 9.33, 9.34 and 9.35 of the present volume for representative ground conditions and wavelengths of 0.3, 3, 30 and 300 m. These reflection coefficients modify the ground reflection pattern but this modified pattern is multiplied by the polar pattern of the dipole itself in the same way as before. Fig. 3.13 shows the corrected form of polar diagram for a dipole raised $\lambda/3$ above the ground and working on a wavelength of 16 m—the figure is derived from curves given by Feldman.⁽²⁴⁸⁾

From the above figure we see that the radiation from a vertical dipole is zero when the angle of incidence equals 90° and not a maximum as was shown in Fig. 3.10. The true state of affairs lies between these extremes for the ray treatment does not take into account a surface wave which causes a small but definite radiation along the ground. This surface wave is quite negligible for horizontal polarization and soon becomes so even for vertical polarization if the antenna is raised to

a height of a few wavelengths above the ground. At the wavelengths under consideration we are not normally interested in propagation along the ground; consequently the ray treatment represents a good method of approaching the problem.

In view of the high dependence of the polar pattern from a vertical dipole on the earth conductivity, it is preferable for most transmission systems to use horizontal polarization. With horizontal polarization it becomes quite a reasonable proposition to regard the earth as a perfect reflector, especially for large angles of incidence (i.e. small angles of elevation).

Figure of Merit

The term "figure of merit" is more commonly used for medium- and long-wave antennae when it is expressed in the form

$$\frac{E_r}{\sqrt{W}} = \frac{60}{\sqrt{R_t}} P(\theta)$$

where R_t is the total loop resistance. For a quarter-wavelength antenna above the ground $P(\theta) = 1$ in the horizontal plane.

In the case of a free-space half-wave dipole this loop resistance is almost entirely radiation resistance; also the value of this resistance is exactly double that of the quarter-wave grounded antenna. Hence the figure of merit in the equatorial plane is

$$\frac{E_r}{\sqrt{W}} = 7 \quad . \quad . \quad . \quad (3.4)$$

This is simply a rearranged version of equation (3.1) in which it is given as a field strength formula. The same formula is frequently expressed in the form given in equation (1.1), which is

$$\frac{E_{mv}D}{\sqrt{P}} = 222 \quad . \quad . \quad . \quad (3.4A)$$

It is important to note that when the dipole is at a moderate distance above the ground the impedance at the centre may be either increased or decreased according to the height and orientation of the dipole. This will modify the figure of merit so that it becomes

$$\frac{E_r}{\sqrt{W}} = 7 \sqrt{\frac{73.2}{R_t}} \quad . \quad . \quad . \quad (3.5)$$

where R_t is the new radiation resistance.

The value of R_i may be obtained from the curves in Fig. 3.14. These curves are based on the mutual impedance between the dipole and its image in the ground as obtained by the induced e.m.f. method (see, for instance, Carter⁽⁴³⁾).

On Fig. 3.14 are also shown experimental points obtained by Friis, Feldman and Sharpless⁽²⁵⁰⁾ using wavelengths between

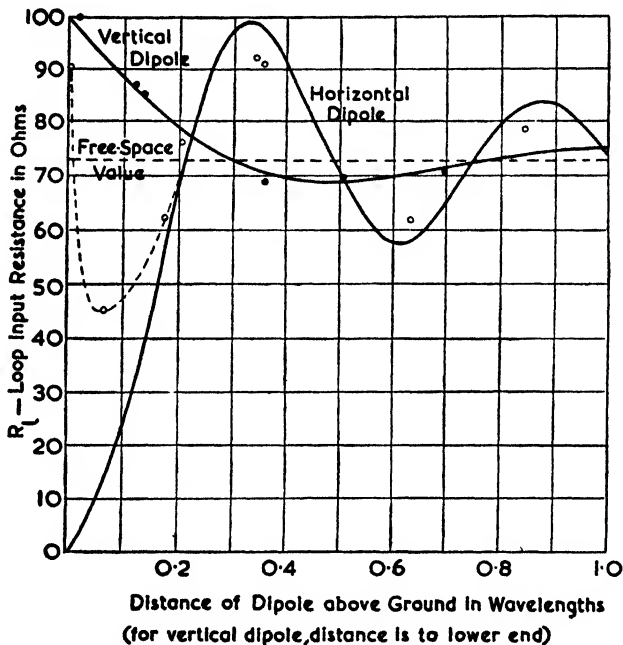


FIG. 3.14. VARIATION OF THE INPUT RESISTANCE OF A HALF-WAVE DIPOLE WITH HEIGHT ABOVE THE EARTH (Friis, Feldman and Sharpless, *Proc. I.R.E.*, Jan., 1934)

8 and 27 m over ground of good conductivity. It will be seen that below a height of 0.2λ the theoretically low input resistances for the horizontal dipole do not materialize. This can be attributed to the large increase in ground losses which must occur when the induction field of the dipole is partially in the ground. Theoretical investigations of the effect of finite ground conductivity have been made by Barrow⁽⁸¹⁾ and also by Hansen and Beckerley.⁽⁴⁹⁾

Equation (3.5) introduces a scale factor which should be applied to all the polar diagrams which have been given of half-wave dipoles above the ground in the previous figures.

In many cases the correction is small and may be neglected in making a rough estimate. The reason for having to apply this factor is that in these polar diagrams the current at the

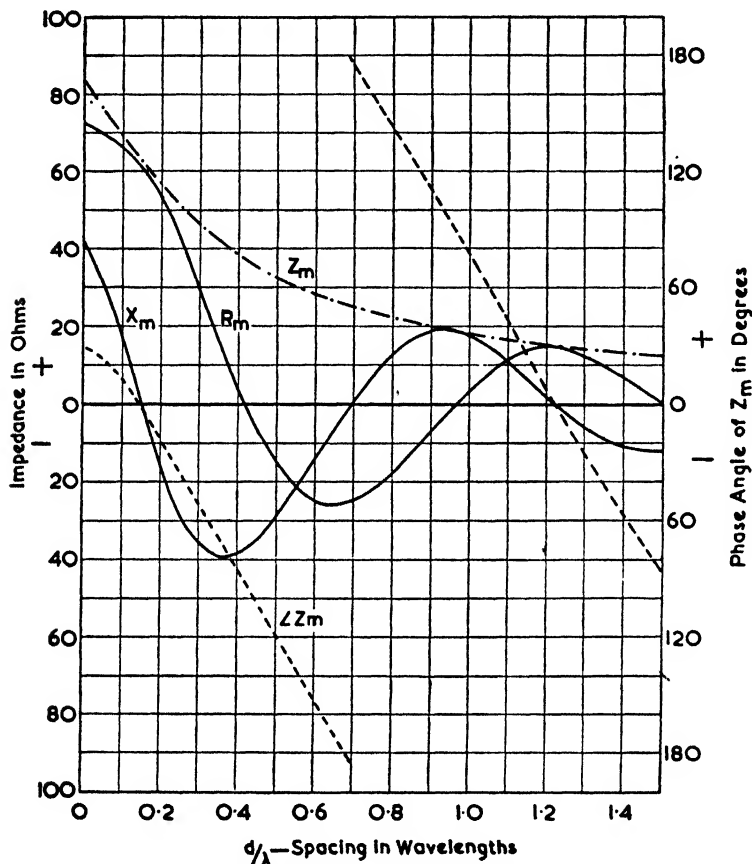


FIG. 3.15. MUTUAL IMPEDANCE CURVES FOR PARALLEL NON-STAGGERED HALF-WAVE DIPOLES

centre of the dipole has been assumed to remain unchanged whether the ground is present or not. This assumption is only true at certain distances above the ground, when the real part of the mutual impedance is zero, or at heights exceeding a few wavelengths, when the mutual impedance is negligible.

3.2. MUTUAL IMPEDANCE BETWEEN DIPOLES

A knowledge of the mutual impedance between half-wave dipoles is required when we have more than one dipole (including any images due to reflecting surfaces).

The method of calculation may be based on the induced e.m.f. method discussed in Vol. I, § 5.2. This method is not strictly true for antennae of finite thickness and lengths other

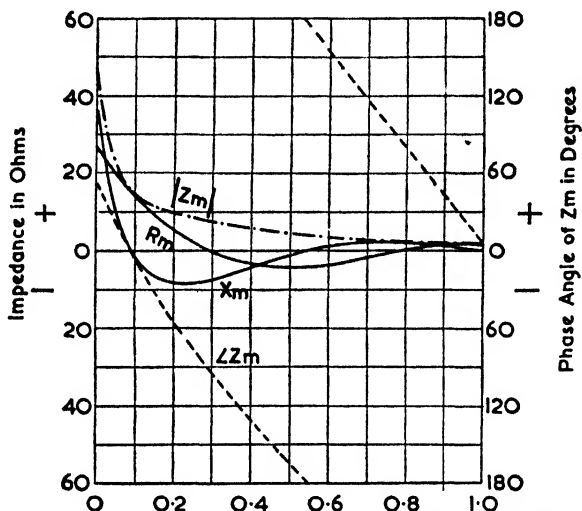


FIG. 3.16. MUTUAL IMPEDANCE CURVES FOR COLLINEAR HALF-WAVE DIPOLES
The abscissa gives the distance in wavelengths between the ends of the dipoles

than multiples of $\lambda/2$, but more rigorous methods are necessarily complicated. In Vol. I, § 5.2, the application to mutual impedances was shown and equation (5.21) gave the formula for the mutual impedance between parallel non-staggered dipoles. More general formulae are quite complicated, the simplest being that for parallel radiators whose lengths are multiples of $\lambda/2$; this formula is given below (for the others the reader may refer to the articles by Pistolkors⁽⁷²⁾ and Carter⁽⁴⁸⁾).

(a) Parallel Non-staggered Wires of Length $l = n\lambda/2$

The formula for this case is

$$\begin{aligned} Z_{21} = 30[2Ei(-j\beta d) - Ei\{-j\beta(\sqrt{d^2 + l^2} + l)\} \\ - Ei\{-j\beta(\sqrt{d^2 + l^2} - l)\}] \quad (3.6) \end{aligned}$$

When $n = 1$, the above formula gives the half-wave dipole case, for which Fig. 3.15 shows the real and imaginary parts of the mutual impedance.

(b) *Collinear Half-wave Dipoles*

Curves showing the mutual impedance for collinear dipoles are given in Fig. 3.16.

(c) *Staggered Half-wave Dipoles*

It would require many curves to show the mutual impedance between dipoles whose relative positions are as shown in Fig. 3.17. For most problems, however, a knowledge of the resistive component is sufficient and this is given in the table below for spacings which are multiples of $\lambda/2$.

The mutual impedance between antennae has a similar definition to that used in networks—i.e. it is the ratio of the induced e.m.f. in the second antenna to the current in the first—but in the antenna case the points of reference must be specified. For half-wave dipoles the point of reference is always the centre and in the general case the reference point is also a current loop unless otherwise stated.

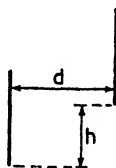


FIG. 3.17. DIAGRAM OF PARALLEL STAGGERED DIPOLES

d/λ	h/λ						
	0	0.5	1.0	1.5	2.0	2.5	3.0
0	+ 73.29	+ 26.40	- 4.06	+ 1.78	- 0.96	+ 0.58	- 0.43
0.5	- 12.36	- 11.80	- 0.78	+ 0.80	- 1.00	+ 0.45	- 0.30
1.0	+ 4.08	+ 8.83	+ 3.56	- 2.92	+ 1.13	- 0.42	+ 0.13
1.5	- 1.77	- 5.75	- 6.26	+ 1.96	+ 0.56	- 0.96	+ 0.85
2.0	+ 1.18	+ 3.76	+ 6.05	+ 0.16	- 2.55	+ 1.59	- 0.45
2.5	- 0.75	- 2.79	- 5.67	- 2.40	+ 2.74	- 0.28	- 0.10
3.0	+ 0.42	+ 1.86	+ 4.51	+ 3.24	- 2.07	- 1.59	+ 1.74

When all the antennae in a system are fed by transmission lines, the relative current phases and amplitudes are known, so that the mutual impedances may be determined by multiplying the mutual impedance vector, as given in the graphs, by the complex ratio of the antenna currents.

In general all the dipoles will not be forcibly fed, so that a set of simultaneous equations as given by Kirchhoff's laws has to be solved. The simplest case, which also is an important one in practice, is that of a transmitting dipole plus a reflector as shown in Fig. 3.18. The equations in this case are—

$$\begin{aligned} V_1 &= I_1 Z_{11} + I_2 Z_{21} \\ 0 &= I_1 Z_{12} + I_2 Z_{22} \end{aligned}$$

On solving them it is found that the input impedance of the driven antenna is modified from the self impedance Z_{11} to a value given by

$$Z_1 = Z_{11} - \frac{Z_{21}^2}{Z_{22}} \quad . \quad . \quad . \quad (3.7)$$

Both this equation and the initial equations are identical with those used in normal network theory.

3.3. DIPOLE SYSTEMS INVOLVING MUTUAL IMPEDANCE CONSIDERATIONS

Dipole with Parasitic Antenna

The polar pattern of the two antennae can be established once the complex ratio of I_2 to I_1 has been calculated, but the actual *scale* of this pattern depends on the driving impedance. Thus if the input impedance is low, the antenna current for a given input power will be high, so that the scale factor expressed in terms of I_1 will also be high. This means that the intensity in the direction of the maximum is high compared with that in other polar patterns for the same spacing; such a result can only be due to the radiation being restricted into a relatively narrow solid angle, for the total radiated powers must be equal. We should therefore expect the scale factors to be highest when the lobes in the polar diagrams are at their narrowest. A simple illustration of this effect is afforded by a two-antenna case, on varying either the spacing or the current phases, the antennae being fed with equal currents.

A set of correctly scaled polar diagrams for the single-reflector case is shown in Fig. 3.18. They are obtained from the well-known article by Brown,⁽⁴⁰⁾ which gives a comprehensive treatment of mutual effects between antennae. Figs. 3.19 and 3.20 are also from the same article and show the

conditions for maximum forward or backward radiation, and also the variation of the input resistance under these conditions.

Examination of these curves shows that there is no special virtue attached to a spacing of $\lambda/4$; indeed the optimum spacings for both reflector and director operation are in the region of 0.1 to 0.15λ . Practical measurements have confirmed

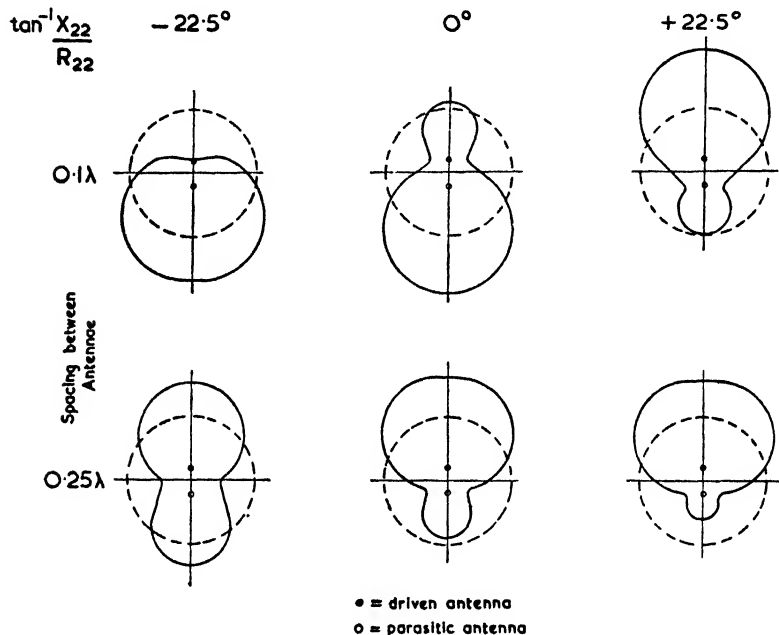


FIG. 3.18. POLAR DIAGRAM OF A HALF-WAVE DIPOLE WITH A SINGLE PARASITIC REFLECTOR

(Brown, *Proc. I.R.E.*, Jan., 1937)

these conclusions—an example of such measurements is shown in Fig. 3.21.

The close spacings have the disadvantage that the input resistance is only of the order of 20 ohms, therefore greater spacings are employed where simpler matching conditions are more important than the greatest possible gain. Moreover at spacings of 0.20 to 0.25λ the tuning conditions are less critical.

It should be noted that for the theoretical curves the tuning of the reflector is meant to be done by means of a lumped reactance in the middle, thereby permitting the length of the antenna to remain constant. In practice it is more convenient

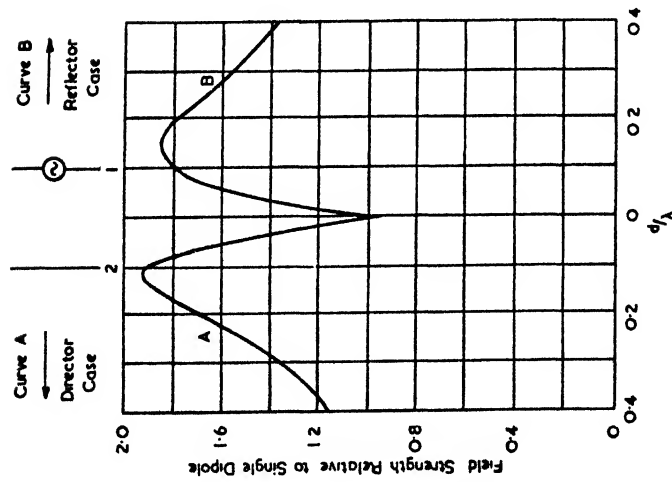


FIG. 3.19. EFFECT OF SPACING ON THE GAIN OBTAINABLE WITH ONE PARASITICALLY EXCITED DIPOLE (Brown, *Proc. I.R.E.*, Jan., 1937)

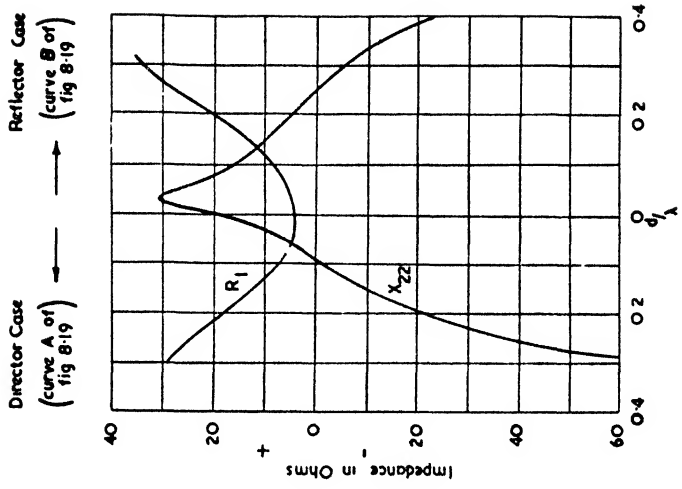


FIG. 3.20. TUNING OF PARASITIC DIPOLE (X_{zz}) AND RESISTANCE OF DRIVEN DIPOLE (R_1) FOR CONDITIONS SHOWN IN FIG. 3.19 (Brown, *Proc. I.R.E.*, Jan., 1937)

to vary the tuning by alterations to the length of the reflector, in which case the curves still apply but with diminished accuracy.

At spacings greater than about 2λ it is permissible to regard the parasitic antenna as being in a uniform field the value of which is given in Vol. I by equation (4.49), or to include the phase relationship with the current, by equation (4.47).

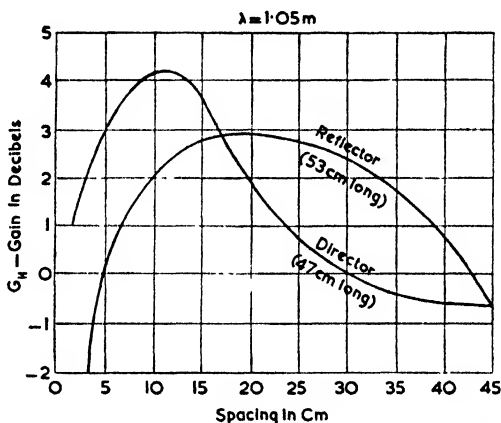


FIG. 3.21. EXPERIMENTAL GAIN CURVES FOR A DIPOLE PLUS A PARASITIC DIPOLE (McPetrie and Saxton, *Wir. Eng.*, April, 1946)

These formulae show that the field intensity in the equatorial plane is

$$E = 60 \frac{I}{r} e^{\left(\frac{\pi}{2} - \beta r\right)}$$

The induced voltage V_i equals the product of the effective height of the dipole and the field intensity, so that the mutual impedance is

$$\begin{aligned} Z_{21} &= \frac{V_i}{I} = \frac{\left(\frac{2}{\pi} \cdot \frac{\lambda}{2}\right) E}{I} \\ &= \frac{19.1}{r/\lambda} \angle (90^\circ - 360^\circ r/\lambda) \quad . \quad . \quad (3.8) \end{aligned}$$

where r/λ is greater than 2.

Modification of Dipole Impedance due to the Ground

To find the impedance of a half-wave dipole near the ground we calculate its mutual impedance with the image in the

ground. Assuming a perfectly conducting ground we have images for a vertical and a horizontal dipole as shown in Figs. 1.8 (a) and 1.8 (b) respectively.

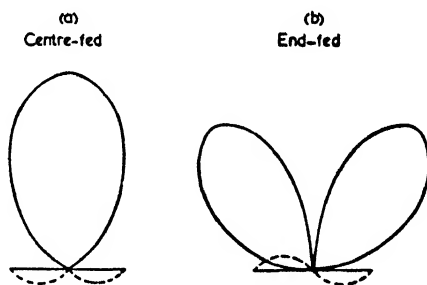
The vertical case is that of collinear dipoles carrying equal cophasal currents so that the driving impedance is

$$\mathcal{Z}_1 = \mathcal{Z}_{11} + \mathcal{Z}_{21} \quad . \quad . \quad . \quad (3.9)$$

With horizontal antennae we have parallel dipoles with out-of-phase currents; hence

$$\mathcal{Z}_1 = \mathcal{Z}_{11} - \mathcal{Z}_{21} \quad . \quad . \quad . \quad (3.10)$$

For dipoles whose centres are one-quarter of a wavelength above the ground the formulae give the values $\mathcal{Z}_1 = 99 + j80$



Dotted lines indicate current distribution.

FIG. 3.22. TWO WAYS OF EXCITING A FULL-WAVE DIPOLE TOGETHER WITH THE CORRESPONDING POLAR DIAGRAMS

(vertical antenna) and $\mathcal{Z}_1 = 88 + j70$ (horizontal antenna). The resistive component of the input impedance is shown plotted in Fig. 3.14. The theoretical curves assume a perfectly conducting earth but the error due to the conductivity of the soil is quite small at wavelengths above 10 m unless the soil is exceptionally dry or the centre of the antenna is less than 0.2λ off the ground.

Impedance of a Full-wave Dipole

Two ways of feeding a full-wave dipole together with the corresponding polar diagrams are shown in Figs. 3.22 (a) and (b).

Application of the mutual impedance figures for collinear dipoles shows that the loop radiation resistances *per arm* are—

- (a) 99.6 ohms
- (b) 46.8 ohms

Hence the loop currents are in the proportion of 1 : 1.46 for equal powers and from this proportion the scale factor to which the two patterns should be drawn can be derived. This does not mean that the lobe maxima are in this proportion, for the maxima in case (b) are reduced by space-phasing. The total field may be taken to be due to two point sources situated at the current antinodes each of which has the same polar pattern as a half-wave dipole; in fact the polar diagrams can be obtained by multiplying the dipole curve in Fig. 3.6 by the curve for $F_1(H, \theta) = 0.25\lambda$ in Figs. 3.7 and 3.8 for cases (a) and (b) respectively.

The maxima in (b) occur at $\theta = \pm 54^\circ$. In this direction the field of a dipole is 0.75 times the maximum while the space-phasing as given by $F_1(H, \theta)$ introduces a further factor of 0.8, so that taking into account the relative loop currents we have—

$$\frac{\text{Lobe maximum of case (a)}}{\text{Lobe maxima of case (b)}} = \frac{1}{1.46 \times 0.75 \times 0.8} = 1.14$$

A centre-fed full-wave dipole produces case (a) and the input impedance is given by the curves of Figs. 2.15 and 2.16 on doubling the indicated values for Z_0 and the ordinates. The abscissae refer to the half-length of the full-wave dipole, while the characteristic impedance of the dipole (*see* p. 42) is

$$Z_0 = 120(\log_e 2h/a - 1) \quad (3.11)$$

For example, a full-wave dipole of 10 S.W.G. wire, working on $\lambda = 30$ m, will have $h/a = 10\,000$; $Z_0 = 1\,100$; $R = 2\,400$ and $X = 0$ (with 4 per cent shortening).

Dipole in Front of Reflecting Sheet

This case is analogous to the case of a horizontal dipole above the ground, but with a metallic sheet the conductivity is far better so that a perfect anti-phase image may be assumed with greater justification. The polar diagram in the equatorial plane is simply proportional to $\sin \beta d$, where d is the distance between the dipole and the sheet, and the field strength in this plane is

$$E'' = \frac{60}{r} \sqrt{\frac{W}{R_{11} - R_{21}}} (2 \sin \beta d)$$

where R_{21} is given by Fig. 3.15.

The gain over the field, E' , without the reflecting sheet is therefore

$$\left| \frac{E''}{E'} \right| = \frac{2 \sin \beta d}{(1 - R_{21}/R_{11})} \quad (3.12)$$

This gain is shown plotted in Fig. 3.23 and leads to the striking conclusion that the dipole is virtually touching the

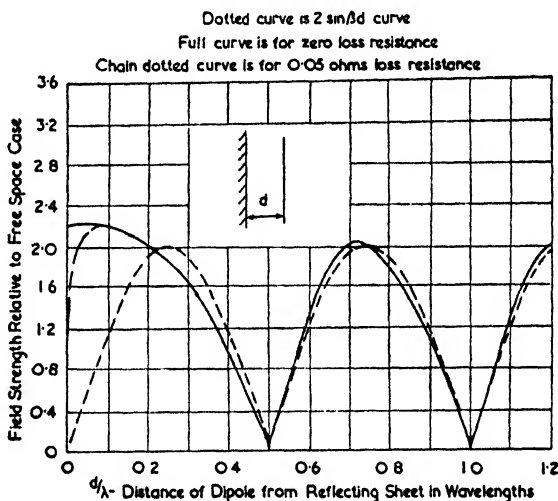


FIG. 3.23. VARIATION OF THE GAIN OF A TRANSMITTING DIPOLE WITH DISTANCE FROM A REFLECTING SHEET

(Brown, *Proc. I.R.E.*, Jan., 1937)

sheet for the greatest forward field strength. In practice a slight resistive loss will cause the gain curve to dip sharply just before the zero distance point is reached. Furthermore, the input resistance falls rapidly as the spacing is decreased below 0.25λ .

The "Flat-top" Array

Two horizontal dipoles fed in anti-phase and separated by only a short distance (usually about 0.15λ) form what is known as a flat-top or 8JK array. The latter name is used among radio amateurs for whom this type of antenna is particularly convenient since the short spacing permits easy mounting of rotatory beam antennae.

The disadvantage of close spacing is that the radiation resistance is lowered to such an extent that the losses may no longer be negligible. To find the radiation resistance for

each dipole we use the curves of Fig. 3.15 and subtract the mutual resistance term as in equation (3.10).

If the spacing is less than 0.2λ the polar diagram in a vertical plane simply follows a cosine law, while that in a horizontal plane is given by the product of a cosine law and the polar diagram of a single dipole.

The maximum field strength relative to a single dipole fed with the same total power can be determined from the curves of Fig. 3.23 on doubling the x scale and dividing the z scale by $\sqrt{2}$ (i.e. the distance between the dipole and the sheet

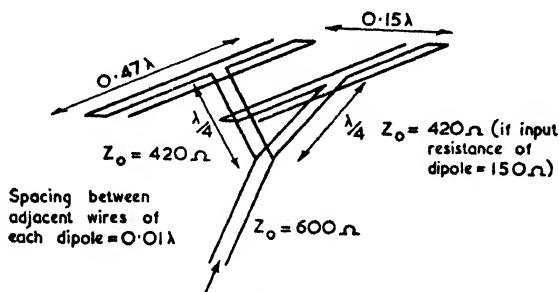


FIG. 3.24. A "FLAT-TOP" ARRAY OF THREE-WIRE FOLDED DIPOLES

corresponds to half the spacing between the anti-phase dipoles, while the fact that the "image" in this case is supplied with power decreases the field strengths in the ratio of $\sqrt{2} : 1$. These curves show that even if the loss resistance is as low as 0.5 ohm per dipole the spacing should not be less than 0.1λ . A practical value for the spacing is 0.15λ in which case the radiation resistance of each dipole is about 13 ohms; hence a reasonable estimate for the total input resistance is 15 ohms.

The above input resistance is on the low side for efficient matching (especially if open wire lines are used) so that it is preferable to make each dipole of the "folded" type described in the next section. By using a three-wire folded dipole the input resistance may be increased by a factor of 9 (according to the *Amateur Radio Handbook* the input resistance is 180 ohms—this is presumably a measured value in which case both the losses and the differences in the spacing would be taken into account). Whatever the exact value may prove to be, the system may now be matched to a 600 ohm open wire line by means of lines whose characteristic impedance has some value lying between 400 and 450 ohms. A system of this nature is shown in Fig. 3.24 together with probable impedance values.

The Yagi Array

A dipole with several coplanar parasitic dipoles is commonly called a "Yagi"⁽¹⁸⁰⁾ array. A typical array of this nature is

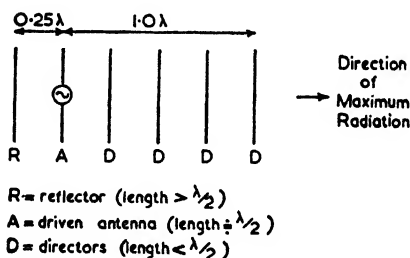


FIG. 3.25. A TYPICAL YAGI ARRAY

shown in Fig. 3.25, which shows a single reflector and four directors—for obvious reasons there is little to be gained by using more than one reflector. It is usual to set up such an

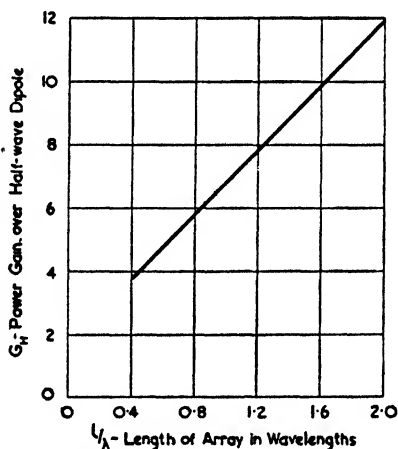


FIG. 3.26. MAXIMUM GAIN OF IDEALIZED YAGI ARRAY
(Reid, *Jour. I.E.E.*, Pt. IIIA, No. 3, March-May, 1946)

array by "cut and try" methods, i.e. the reflector and the directors are added one by one and each time the dipoles already there are retuned. Actually this operation is quite simple to perform for the retuning required on the previously set-up elements becomes progressively less. A good clear site

should be chosen and if ground reflections cannot be avoided care must be taken to see that the direct and reflected rays do not vary their relative intensities appreciably as the polar diagram is sharpened by the addition of further elements.

In view of the large number of variables, theoretical calculations on Yagi arrays are necessarily involved. For this reason some calculations on an idealized array of a sheet of elements were made by Reid.⁽¹⁷⁵⁾ His curves show that the maximum possible gain may be summarized as shown in Fig. 3.26. (To determine the "length" of the array we may take the distance between the outer dipoles and add 0.2λ .)

A detailed analysis of a number of cases has been made by

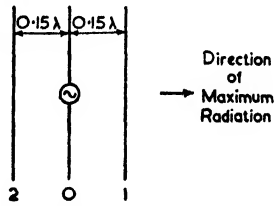
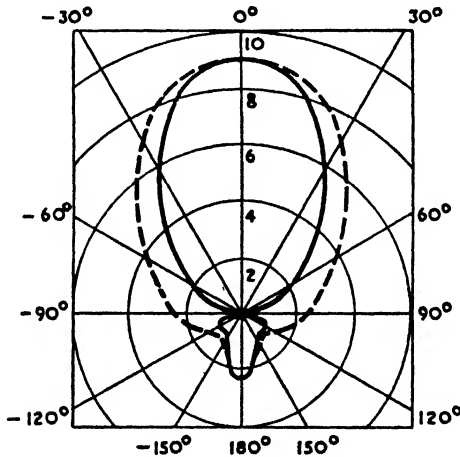


FIG. 3.27. CLOSELY-SPACED THREE-ELEMENT ARRAY



Full Curve — Horizontal Polar Diagram.

Dotted Curve — Vertical Polar Diagram.

FIG. 3.28. POLAR DIAGRAMS OF THREE-ELEMENT ARRAY SHOWN IN FIG. 3.27
(Walkinshaw, *Jour. I.E.E.*, Pt. IIIA, No. 3, March-May, 1946)

Walkinshaw.⁽¹⁷⁸⁾ His results show that whenever the system is tuned for maximum forward gain the input resistance is low, say 20 to 40 ohms. A case of considerable practical interest, since it can be used for a short-wave rotatory beam, is shown in Fig. 3.27. For this array Walkinshaw shows that the maximum

power gain is just over 5, but since the corresponding input impedance is only about 4 ohms, a better practical combination is given by

Power Gain	$G_H = 5$
Reflector Self-reactance	$X_{22} = + 40 \text{ ohms}$
Director Self-reactance	$X_{11} = - 10 \text{ ohms}$
Resistance of Driven Antenna	$R_0 = 7 \text{ ohms}$

The corresponding polar diagrams are shown in Fig. 3.28. The approximate lengths of the reflector and director may be found from Fig. 3.2—the driven antenna being exactly half a wavelength long.

If the reflector in a Yagi array is replaced by a reflecting screen, the polar diagram is less sensitive to movements of personnel or objects behind the antenna. In Plate VI we have a number of such Yagi arrays serving as the radar antennae for searchlight control. It will be noticed that some of the driven antennae are of the folded dipole type; in this way the bandwidth of the combination is slightly widened and also the input impedance is increased to a value which permits direct matching to a coaxial line.

3.4. VARIATIONS OF THE HALF-WAVE DIPOLE

A number of antennae have been devised whose polar patterns are substantially similar to that of a half-wave dipole. They may therefore be classified as variations of the half-wave dipole. In some cases the polarization of the radiated energy is opposite to that of a dipole and this must be taken into account when the polar diagram in the presence of the ground is being calculated. The presence of the ground will also modify the radiation resistance, but unless the antenna is only a fraction of a wavelength over the ground this modification will merely be of minor importance.

The Folded Dipole

An ordinary half-wave dipole may be considered as an open-circuited transmission line which has been "opened out" so that the radiations from the two sides of the last $\lambda/4$ section will augment each other. If we started with a short-circuited piece of line we should again have a standing-wave system, and this time the last $\lambda/2$ section could be used by folding the wire

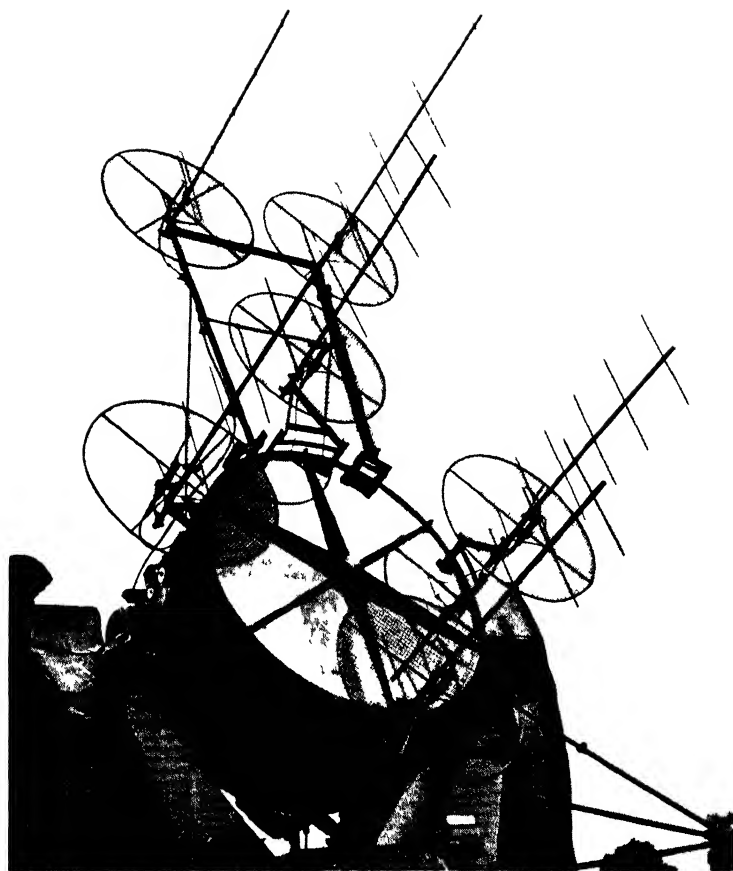


PLATE VI. YAGI ARRAYS WITH WIRE-NETTING REFLECTORS
FOR SEARCHLIGHT CONTROL
(*Courtesy of Fox Photos, Ltd*)

as shown in Fig. 3.29 (a). An alternative way of viewing this folded dipole antenna is to consider it as an ordinary half-wave dipole the ends of which voltage feed a near-by half-wave dipole.

The separation between the two radiators should be small compared with a wavelength (typical transmitting values are 30 cm separation for $\lambda = 40$ m and 20 cm for $\lambda = 20$ m), then the radiation from the two is sensibly in phase for all directions so that the polar pattern is identical with that due to a single half-wave radiator. It follows that for a given input power the loop current must be twice as great in the single dipole

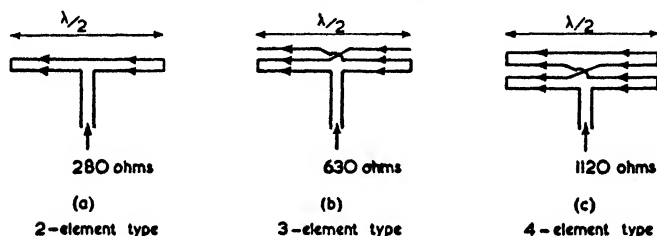


FIG. 3.29. EXAMPLES OF FOLDED DIPOLES

as in each limb of the folded dipole. This in turn means that the input resistance of the folded dipole must be four times that of the single dipole, i.e. of the order of 300 ohms.

The virtues of a folded dipole are—

- (a) it can be fed via a 300 ohm open line,
- (b) it has a slightly greater bandwidth than that of a single dipole.

Folded dipoles using three or four elements can be devised by arranging the elements as shown in Fig. 3.29 (b) and (c). The input resistance can be reasoned out on the same lines as before and proves to be n^2 times that of a single radiator where n is the number of elements.

Intermediate multiplying factors may be obtained by using conductors of unequal thicknesses. If in a two-element type, the fed dipole is the thicker conductor then the resistance will be less than four times that of an unfolded dipole and vice versa. The actual ratio obtained depends on the spacing of the conductors as well as their relative thicknesses. Experiments by the author gave multiplying factors of 5.5 and 3.3 for diameter ratios of 3 to 5 when the separation between the centres of the conductors was equal to the sum of their diameters.

A theory for the unequal diameter case has recently been developed by Roberts⁽¹²¹⁾ who gives a formula for the input resistance of the two-element type in terms of the resistance of the two elements connected in parallel to form a single dipole. Calling the latter value R'' , the formula is

$$R = R'' \left(1 + \frac{Z_1}{Z_2} \right)^2$$

where Z_1 = characteristic impedance of a transmission line consisting of two conductors of the same diameter as the driven element and whose centre-to-centre spacing is the same as that of the actual element.

Z_2 = as for Z_1 , but the two conductors have diameters equal to that of the folded element.

The formula presupposes that the elements are "well spaced." Applying it to the above-mentioned experimental cases, we find that the theoretical R/R'' ratios are 5.9 and 2.9. The length-to-diameter ratios of the elements employed were fairly large, so that the difference between R'' and the resistance of a single element as a dipole (which was the criterion in the experimental case) would be quite small. We must therefore conclude that the differences between the experimental and theoretical values are due to the spacing in the present case being too close for high accuracy.

Considered as a receiving antenna, the folded dipole has an effective height which is n times that of a simple dipole of equal length. Although this means that the induced e.m.f. is n times greater, it must not be forgotten that the resistance of the folded version is increased by a factor of n^2 , i.e. the folded and the simple dipoles both abstract the same power from the incident field.

The Terminated Dipole or "Squashed Rhombic"

A further variation of the folded dipole which is akin to the rhombic antenna is shown in Fig. 3.30. In this form a terminating resistance equal to the characteristic impedance of the feeder line is employed so that the radiators carry travelling and not standing waves. The polar pattern is identical with that of a standing wave radiator of the same length (this point is discussed in connection with the series phase array). A far

wider bandwidth is obtainable in this way (nearly a 3 : 1 frequency range can be covered) but at the usual expense inherent in such an aperiodic system, i.e. between one-third and one-half of the power is dissipated in the resistance. This type of antenna was described in an unpublished memorandum

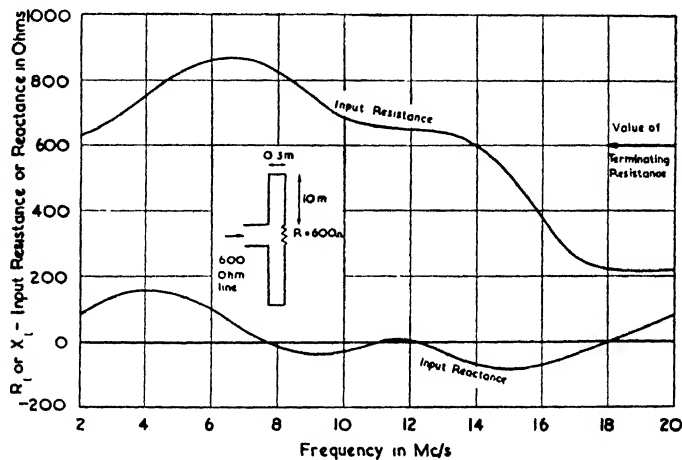


FIG. 3.30. INPUT IMPEDANCE OF A TERMINATED DIPOLE

by W. L. McPherson, from which the experimental curves shown in Fig. 3.30 were taken.

The Ground-plane Antenna

Half-wave dipoles of the J-type or of the coaxial type have the advantage that the coaxial feeder can act as a support for the antenna, but unless a detuning sleeve is used the outside of the feeder is excited to some extent so that if the feeder is long the resultant polar diagram will be appreciably distorted. In order to overcome the latter disadvantage, Brown and Epstein⁽¹⁰⁸⁾ devised the antenna illustrated in Fig. 3.31. The four horizontal rods form a virtual ground below the vertical quarter-wave rod and restrict the excitation of the feeder below.

According to Hasenbeck⁽¹¹²⁾ an antenna which is some 12 per cent shorter than 0.25λ will have an impedance equal to $25 - j35$ ohms when the radials are exactly 0.25λ long, but experimental results quoted by G. H. Brown in a letter to *Electronics* (Dec. 1943, p. 338) show values whose resistance component is distinctly lower than 25 ohms. In fact, for a

shortening of only 6 per cent Brown obtained a value of 20 ohms. Experiments by the author gave good agreement with the latter figures since they showed that a 5 per cent shortening corresponded with resistance values of between 20 and 21 ohms. Agreement was also obtained for the frequency at which the reactance is zero—this frequency is such that the counterpoise rods are then one per cent short of 0.25λ .

In order to convert the input impedance to a more suitable value for transmission lines the vertical portion may be folded, or a quarter-wave transformer may be added, or else a matching

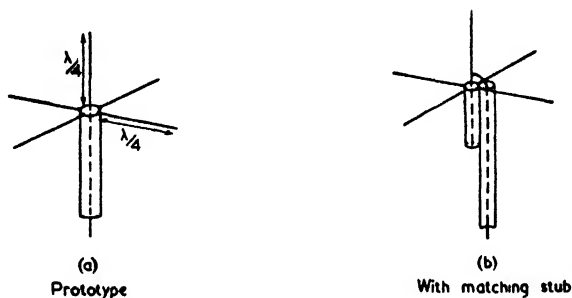


FIG. 3.31. GROUND-PLANE ANTENNA

stub may be used. An example of a “folded unipole” antenna is shown in Fig. 5.13, while the corresponding impedance curves are given in Fig. 5.14. If a stub is used (Fig. 3.31 (b)) the correct length of stub will be about 0.1λ . Since this stub is short-circuited at the end the whole antenna, including the centre conductor, can be grounded; in this way a static drain is provided as well as some protection against damage by lightning.

Whichever method one uses, the bandwidth will prove to be only 3 to 4 per cent for a standing wave ratio limit of 1.5 : 1. This bandwidth is actually some 3 times less than would be obtained by a vertical quarter-wave rod of the same thickness above a large conducting sheet.

If a parasitic reflector is added this takes the form of a quarter-wave rod grounded to the stub and spaced about 0.1λ away from the vertical rod. In this way a forward gain of about 3 db may be obtained.⁽¹⁰⁸⁾

A further variation of the ground-plane antenna is the “cartwheel antenna.” In this form the number of radial rods is increased to about eight while their outer ends are joined

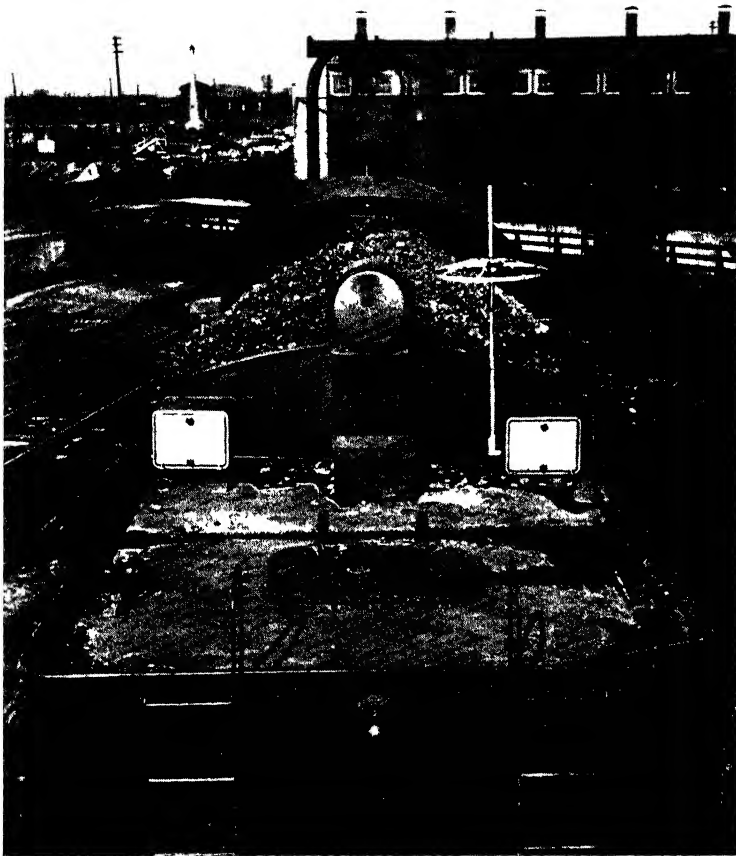


PLATE VII CARTWHEEL TYPE OF UNIPOLE ANTENNA AS USED FOR
RAILWAY COMMUNICATIONS ON ULTRA-SHORT WAVES
(courtesy of "E. M. and Television")

by a circular conductor. The cartwheel antenna has the advantage of being more robust—a photograph of one is given in Plate VII (facing p. 120), which shows the antenna mounted on the tender of a locomotive.

The Alford Loop Antenna

A loop antenna devised by Alford⁽¹⁰⁶⁾ consists of four radiating elements folded in the manner shown in Fig. 3.32. Each

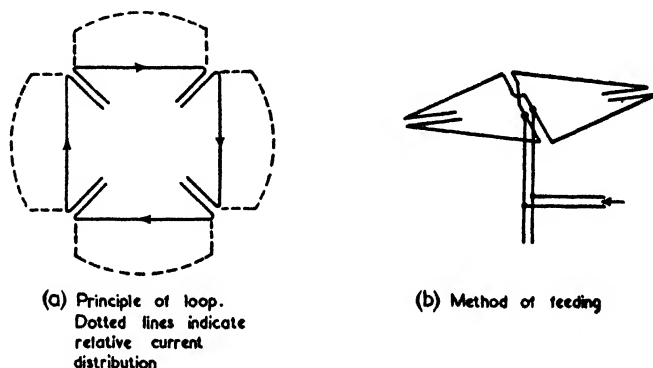


FIG. 3.32. THE ALFORD LOOP ANTENNA

element has a length of $\lambda/2$, although shorter lengths may be used to give a more uniform polar pattern at the expense of overall efficiency. The ends of the four elements are folded together in such a way that the radiation from them is neutralized by the adjacent end. In this manner a loop of almost uniform in-phase current is obtained and when the loop is mounted in a horizontal plane the polar pattern is almost identical with that of a vertical half-wave dipole, but the polarization is horizontal. Unlike the half-wave dipole, however, the polarization remains constant for all positions in space. Because of these properties, the Alford loop antenna forms a convenient radiator for aircraft beacons and other systems where reliable polar patterns employing ground reflections are required.

On account of the similarity mentioned above of the polar pattern with that of a half-wave dipole, the field strength for a given input power may be taken to be the same as that due to a dipole whose position is along the axis of the loop.

The radiation resistance of such a loop (referred to the current at the centre of one of the sides) is given by

$$R = 20(\beta l)^4 \text{ ohms}$$

This formula gives values which are too high if l/λ is greater

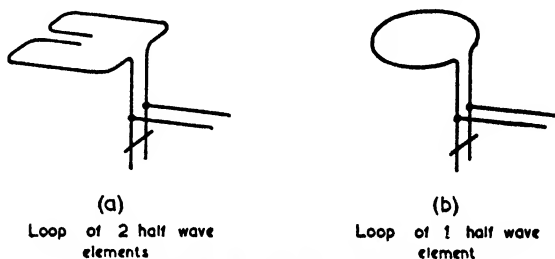


FIG. 3.33. SIMPLER FORMS OF ALFORD LOOPS

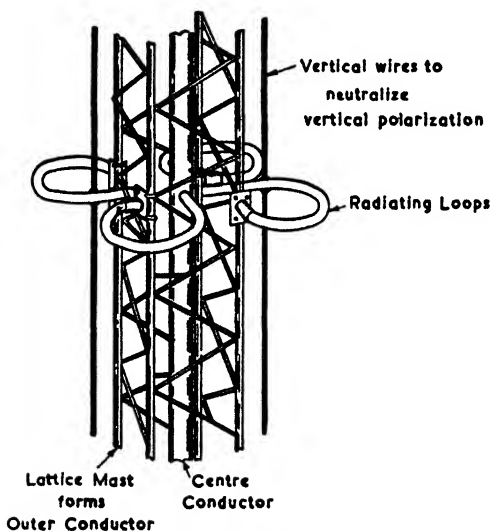


FIG. 3.34. THE CLOVER-LEAF ANTENNA

than about $1/6$. A better approximation is given by the semi-empirical formula

$$R = 320 \left(\sin \frac{\beta l}{2} \right)^4 \dots \dots \dots (3.13)$$

In practice the loop is end-fed in the manner shown in Fig. 3.32 (b) where a resonant piece of transmission line is employed to cancel the large reactive component of the field.

A simpler version of this loop antenna is shown in Fig. 3.33 (a) and a still simpler one in Fig. 3.33 (b). As the forms become simpler so the antennae become less efficient for a given degree of symmetry in the polar patterns.

An Alford loop should be constructed of strip metal to keep the characteristic impedance, and therefore the losses, as low as possible. Consequently the whole structure becomes very bulky at wavelengths greater than about 6 or 7 m, so that they find their chief application at the lower end of the ultra-short waveband.

The Clover-leaf Antenna

A recent type of magnetic dipole which is particularly suited to stacking on a mast is the "clover-leaf" antenna shown in Fig. 3.34. For an operating wavelength of 3 m the mast is about 30 cm square, and forms the outer conductor. In view of the narrow cross-section of the mast a further supporting mast of greater dimensions is required if the antennae are to be mounted at an appreciable height.

The inner conductor is a tube of 7.5 cm diameter and the curved elements are fed directly from this tube, the return circuit being via the mast.

At the corners of the mast are vertical wires to nullify the effect of induced currents which would otherwise produce vertically polarized waves.

The power gain over a half-wave dipole is about $0.6n$, where n is the number of stacked elements spaced at intervals of 0.5λ .

The Slotted Cylinder Antenna

The loading of a transmission line with loops as shown in Fig. 3.35 will increase the phase velocity along the line to an extent which depends on the diameter of the loops and their spacing. In the figure the ratio of the wavelength along the

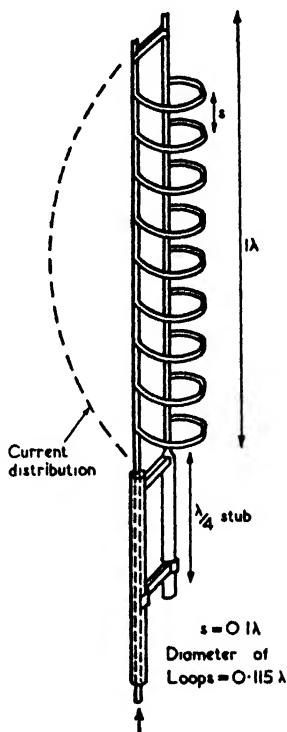


FIG. 3.35. OPEN FORM OF SLOTTED CYLINDER ANTENNA

line to that in free space is 2 : 1 (i.e. $\lambda/\lambda_0 = 2$) so that the radiation from the loops is in phase over a distance of one free-space wavelength. The polar diagram of such a system is therefore that of a magnetic dipole except for the fact that the increased space phasing due to the physical length being doubled will sharpen the pattern in a vertical plane.

This form of antenna is the "skeleton" version of the slotted cylinder type shown in Fig. 3.37. It will be seen therefore

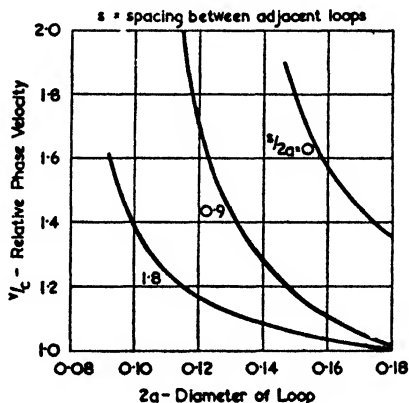


Fig. 3.36. VARIATION OF WAVELENGTH ALONG A PARALLEL-WIRE LINE WITH SIZE AND SPACING OF SHUNT LOOPS (Alford, U.S.A. Pat. No. 641 692)

that the loops may all be fixed to a metal mast, a suitable position for this purpose being the mid-points of each loop. In order to feed the antenna via a coaxial line the input circuit is fitted with a quarter-wave stub at the junction of the balanced and unbalanced lines. For tuning purposes we may vary the position of the shorting bar at the upper end of the balanced line.

The above descriptions are given by Alford (U.S.A. Patents 641 692 and 644 519) who also gives some experimental curves of the values of λ/λ_0 to be expected. These curves are shown in Fig. 3.36; they include the case of a slotted cylinder which corresponds to $s/a = 0$.

The simplest form of slotted cylinder antenna is shown in Fig. 3.37 (a) in which the antenna is fed at the open end via a coaxial line which is brought up the inside of the cylinder. At the fed point the impedance is about 160 ohms in series with a negative reactance. Alford recommends a diameter of

between 0.12 and $0.14\lambda_0$, an overall length of about 1.1λ and a slot width equal to one-sixth of the diameter. With these dimensions an average power gain of 1.6 over a half-wave dipole is obtained in the equatorial plane.

If two of these antennae are placed end to end they may be fed in the middle and both ends can be closed with metal disks.

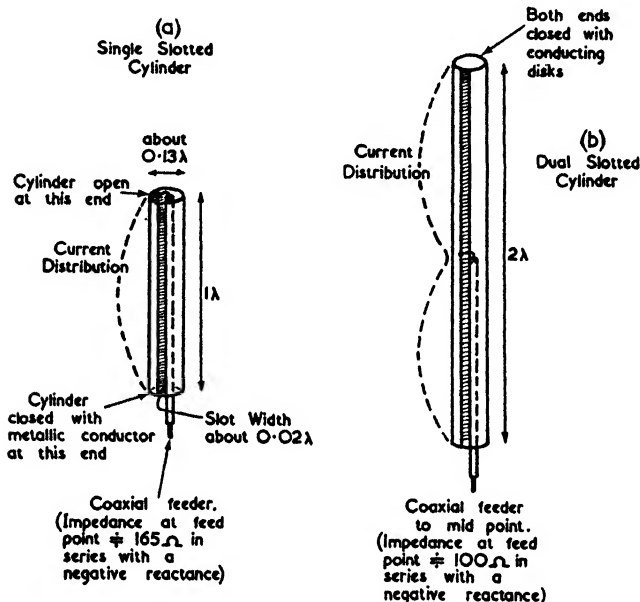


FIG. 3.37. TWO FORMS OF SLOTTED CYLINDER ANTENNA

Such an arrangement is shown in Fig. 3.37 (b) and results in an average power gain of 2.5 . The corresponding polar diagrams are shown in Fig. 3.38.

Finally it might be mentioned that the slotted cylinder type of antenna has also been called a "rocket" or a "pylon" antenna (the one in Fig. 3.38 is known as a "dual-rocket" antenna).

3.5. WIDE-BAND ANTENNAE FOR TELEVISION

In the case of a television service the total bandwidth of the transmission is several hundred times as wide as that of a normal communication channel. As a result it is no longer possible to neglect the variation of the antenna impedance

with side-band frequency. For present-day transmissions using both side-bands this means that a substantially flat characteristic over a range of fully ± 5 per cent of the carrier frequency is required.

The necessary degree of flatness of the antenna characteristic depends on whether it is being used for transmission or reception.

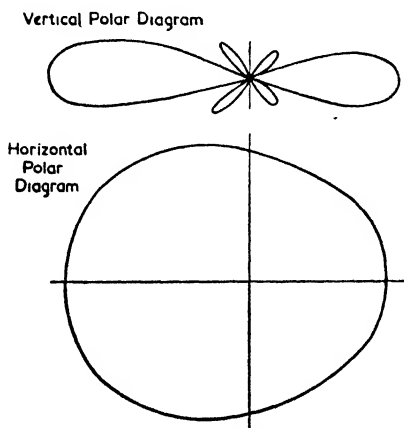


FIG. 3.38. POLAR DIAGRAMS OF A DUAL SLOTTED CYLINDER ANTENNA
(Alford, U.S.A. Pat. No. 644 519)

This difference (in what is otherwise a reciprocal relationship) occurs on account of the following considerations—

- (a) the maximum possible efficiency is required under transmitting conditions;
- (b) in the transmitting case the transmission line is likely to be very long.

The first of these factors means that the bandwidth cannot be improved by a resistance in series (or the equivalent coupling circuit) when the antenna is used for transmitting. The second point results in the need for accurate matching of the antenna to the feeder line to avoid ghost images and this in turn demands a flatter impedance characteristic.

As an example of the care needed to secure good matching in the transmitting case, we may take the case of the London Television transmitter⁽³⁵⁹⁾. A view of the aerial system is given in Plate No. VIII which shows the two rings of eight full-wave dipoles round the mast. Each dipole consists of a three-wire

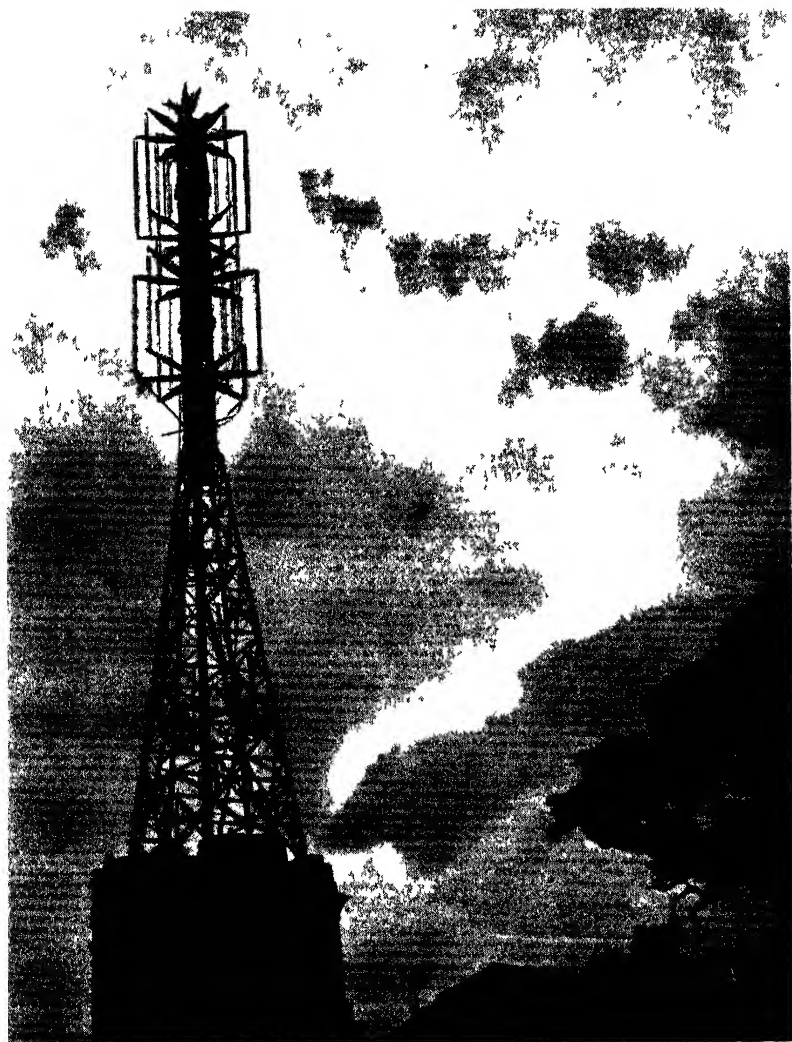


PLATE VIII TELEVISION MAST AT ALEXANDRA PALACE, SHOWING THE
TWO GROUPS OF EIGHT VERTICAL WIRE-CAGE DIPOLES
(*Courtesy of the B.B.C.*)

cage (15 in. spacing) together with an energized reflector between the dipole and the mast.

Cage-type aerials have been described by Lutkin, Cary, and Harding⁽¹¹⁶⁾ together with the design of appropriate wide-band transmission lines. Their requirements necessitated even

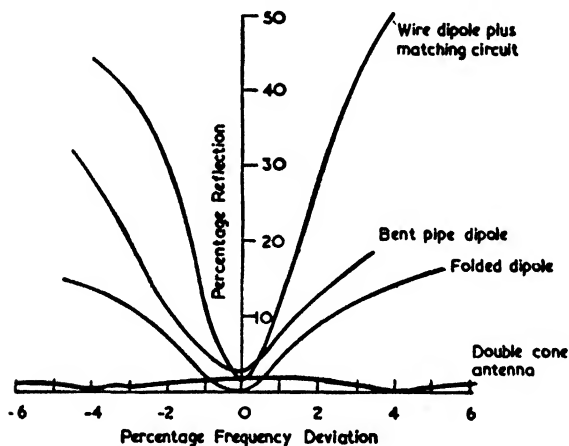


FIG. 3.39. COMPARISON OF BANDWIDTHS OF DIFFERENT TYPES OF DIPOLES
(Carter, *R.C.A. Rev.*, Oct., 1939)

broader bandwidths than are required for present-day television purposes, but the principles involved are the same.

Fig. 3.39 shows the reflection coefficients obtained experimentally for a number of different types of antennae. Antennae for which the reflection coefficient is less than 5 per cent over a frequency range of ± 5 per cent are suitable for transmitting purposes, while for reception reflection coefficients not exceeding 30 per cent are adequate for all types of coupling.

An interesting form of transmitting antenna is the one which radiates the vision frequencies from the top of the Empire State Building. The antenna, which is described in an article by Lindenblad,⁽¹¹⁵⁾ consists of four quarter-wave elements in the form of a turnstile. Each element has a bandwidth which is not much inferior to that given by the double cone antenna shown in Fig. 3.39. When four such elements are arranged in the manner shown in Fig. 3.40 (a) the combined impedance characteristic is even smoother; the same holds true of a turnstile of folded dipoles (Fig. 3.40 (b)).

For simple dipoles whose length-to-diameter ratio exceeds

50, the following formula gives a useful approximation for the Q -factor—

$$Q = \frac{\pi}{4} \cdot \frac{Z_0}{R_{lr}} \quad (3.14)$$

where Q = frequency divided by total bandwidth,
 Z_0 = average characteristic impedance of dipole,
 R_{lr} = loop radiation resistance (at resonance, to be precise).

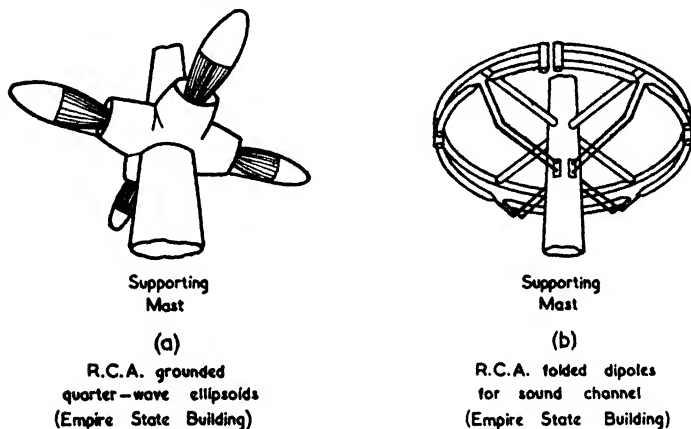


FIG. 3.40. TWO TYPES OF TURNSTILE ANTENNA

The above formula is based on the fact that the reactance variations of the dipole about the first resonance point are only slightly affected by the radiation resistance. Assuming a lossless open-circuited line, then the reactance is given by $X = -Z_0 \cot \beta l$ which, in the neighbourhood of $\beta l = \pi/2$, may be written $X = -Z_0 \beta l$.

The problem is shown in the form of a transmission line impedance diagram in Fig. 3.41 in which βl_1 and βl_2 mark the extremes of the bandwidth (defined in the usual network way as the point for which $|X| = R$). From this diagram it is obvious that

$$\begin{aligned} Q &= \pi/2 \cdot (\beta l_1 - \beta l_2) \\ &= \pi/4 \cdot \frac{Z_0}{R_{lr}} \end{aligned}$$

since

$$\cot R_{lr}/Z_0 \doteq R_{lr}/Z_0$$

To take a particular example, let us suppose that we have a cylindrical antenna whose length-to-diameter ratio is 200, i.e. $h/a = 200$. Then $Z_0 = 600$ ohms (Schelkunoff's method) or 516 ohms (Howe's method)—the values may be obtained from the curves in Fig. 2.9. Taking a round figure of 70 ohms for R_{1r} , we therefore find that $Q = 6.7$ or 5.8 according to the way in which we define Z_0 . Using the curves of Fig. 3.2 we find that $Q = 6.0$ for $h/a = 200$.

Taking the latter figure and keeping to the biconical antenna method of defining characteristic impedance, we have the easily remembered trio of figures $h/a = 200$ gives $Z_0 = 600$ ohms and $Q = 6$. For other ratios of semi-length to radius we may use the middle line of Fig. 2.9 and divide the value of Z_0 by *one hundred* to obtain the value of Q .

It happens that a Q of 6 is also an appropriate value for a television receiving antenna. The case of a receiving antenna is considered in detail in Chapter V.

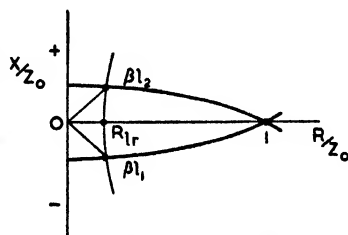


FIG. 3.41. USE OF TRANSMISSION-LINE IMPEDANCE DIAGRAMS FOR FINDING THE Q OF AN ANTENNA

3.6. FEEDING AND COUPLING CIRCUITS

In many cases the same fundamental form of antenna has come to be known by different names which are really descriptive of the method of feeding and not of the antenna itself. Thus the "Zeppelin," the "Windom," the "Western Electric" and the "J-type" antenna are all essentially half-wave dipoles—the only differences lie in the methods employed to energize them.

The positions of the antenna and transmitter output circuit are rarely such that direct coupling is possible. Some form of transmission line is therefore necessary to connect the two. Such lines may be either matched or unmatched (the two cases are also referred to as untuned or tuned respectively). The first mode of operation gives less radiation from the line itself and is to be preferred whenever possible; the unmatched method is sometimes more convenient for small installations, particularly when these use a long wire for multi-band working.

Half-wave Dipole Feeders

(a) Matched Feeders

If a half-wave dipole is open-circuited at the centre, it may be fed at this point via a transmission line of about 70 ohms characteristic impedance. In this way a perfect match may be obtained and at the same time discrimination against all

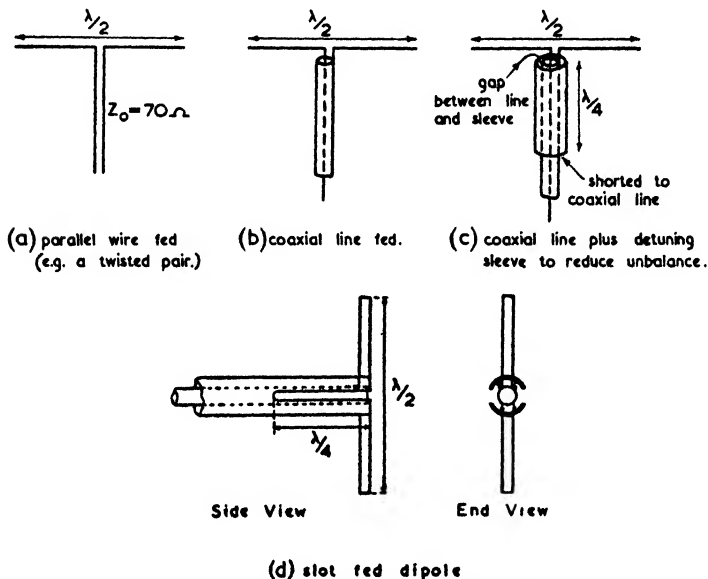


FIG. 3.42. METHODS OF FEEDING A HALF-WAVE DIPOLE

odd harmonics will be given. The transmission line may consist either of a twisted pair (suitable only for low-power installations) or a concentric line.

The concentric line method is particularly convenient at very short wavelengths when the outer conductor may be used as a means of support. This method of feeding causes a slight unbalance so that a certain amount of radiation takes place from the outside of the transmission line. The unbalance may be reduced to negligible proportions by adding a quarter-wave sleeving as shown in Fig. 3.42 (c), which introduces a high impedance to any currents flowing on the outer surface of the line. This refinement is usually only used on microwaves when the unbalance is liable to be greater (owing to the relative increase in size of the line as compared with the

antenna) and when it is mechanically easy to add such a sleeve.

An alternative method of balancing is by means of a "slot feed" as illustrated in Fig. 3.42 (d). The principle on which this works is that the dipole is excited by a TE_{11} wave which can exist at the end of the line by virtue of the slotted sides. This wave is set up since, together with the original TEM wave, it satisfies the imposed boundary condition of zero radial

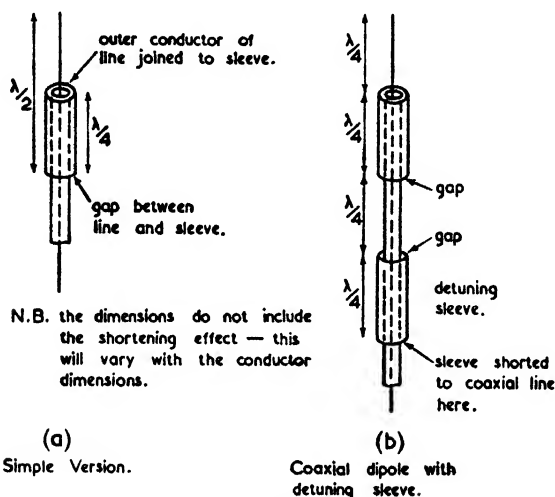


FIG. 3.43. COAXIAL DIPOLES OR "SLEEVE" ANTENNAE

e.m.f. along the plug. In the plan view of the feeder the contributions to the radial e.m.f.'s in the vertical direction are shown by dotted arrows for the TE_{11} wave and by full arrows for the TEM wave.

A neat way of feeding a half-wave dipole in which the coaxial feeder actually enters the inside of one limb of the antenna is illustrated in Fig. 3.43. This form of antenna is known as a "coaxial" or "sleeve" antenna. The field pattern produced in this way is more symmetrical than usual, especially if radiation from the feeder is reduced by adding a quarter-wave sleeving as shown in Fig. 3.43 (b). (The high-impedance end of this sleeving should be at a current antinode, i.e. at an odd number of quarter wavelengths from the bottom of the dipole.) This type of antenna is mainly useful for ultra-short waves and microwaves on account of mechanical considerations.

A common method of matching which is suitable for all powers is the delta match shown in Fig. 3.44. With this system

the dipole is continuous and is matched to a parallel transmission line by fanning out the end of the line. This process

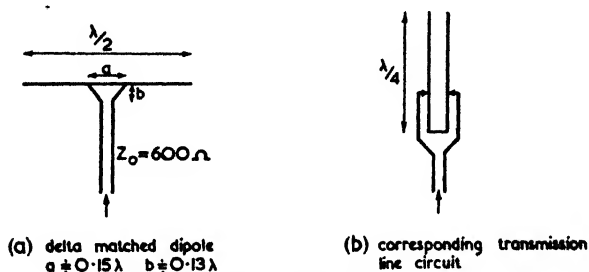
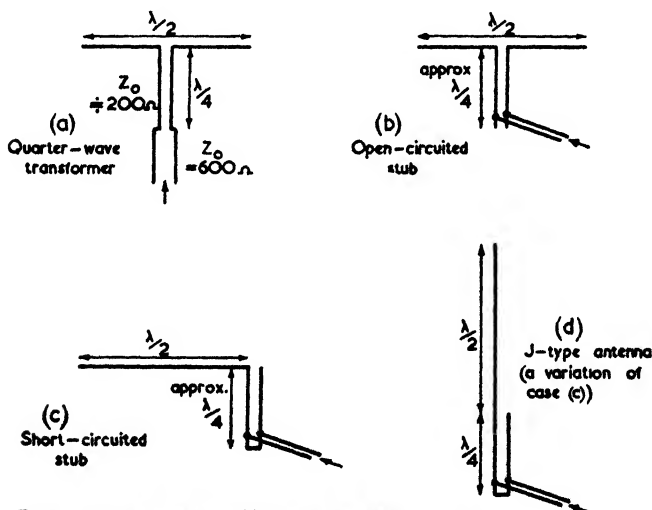


FIG. 3.44. DELTA-MATCHED DIPOLE

is equivalent to tapping along the line of a dissipative transmission line (Fig. 3.44 (b)). For a 600-ohm transmission line



The stubs in figs (b)(c) and (d) may have any characteristic impedance between 300 and 600 ohms.

FIG. 3.45. FOUR METHODS OF MATCHING A DIPOLE TO A PARALLEL-WIRE LINE

the dimensions of the delta portion of Fig. 3.44 (a) are approximately

$$a = 0.15\lambda, \quad b = 0.13\lambda$$

The correctness of the match depends on the thickness of the wire and on the height above the ground, so that in practice

it is usual to check this by measuring the standing wave ratio of the line current.

Instead of fanning out the ends of the line a quarter-wave matching section may be used (Fig. 3.45 (a)), an open-circuited stub for centre feeding (Fig. 3.45 (b)), or a short-circuited stub for end feeding (Fig. 3.45 (c)). The correct matching conditions can be found quite easily with the aid of impedance diagrams as described in § 10.4. The method of Fig. 3.45 (c) is sometimes used for vertical radiators when the configuration

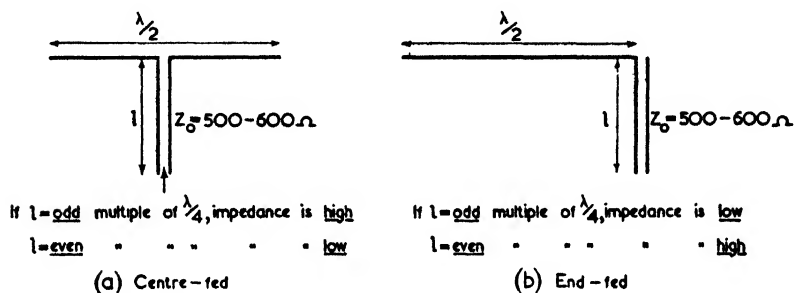


FIG. 3.46. UNMATCHED FEEDER SYSTEMS

appears as shown in Fig. 3.45 (d) and is known as a "J" antenna.

(b) Unmatched Feeders

It is sometimes convenient to use unmatched feeders (e.g. in multiband working when the radiation resistance is not constant) provided the power used is low and the transmission line is not too long. The line should approximate to some multiple of $\lambda/4$ to avoid an unduly great reactive component to the input impedance to the line. This assumes that the impedance at the input terminals of the antenna is also mainly resistive—which is true at the centre and ends of a resonant half-wave dipole. Therefore an unmatched line may be attached to a half-wave dipole as shown in Figs. 3.46 (a) and (b).

The centre-fed case has the virtue of giving less radiation from the wire should the antenna not be correctly tuned. This is due to the fact that the currents in the two sides of the transmission line remain balanced under all conditions, whereas with end-feed the free end of the line is necessarily a current node.

(c) *Single-wire Feeder*

Another form of matched feeder is the single-wire feed illustrated in Fig. 3.47. The return circuit in this case is via the ground so that good ground conductivity is essential for reasonable efficiencies—in fact, the antenna resembles a T-type antenna with an unsymmetrical top. The difference lies in the fact that when the system is correctly matched standing waves exist only along the horizontal portion. Even so the

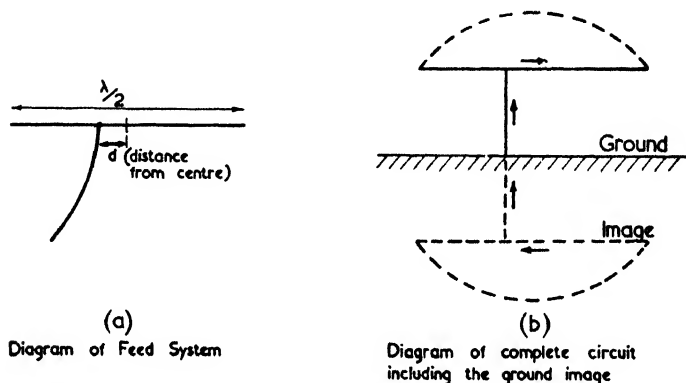


FIG. 3.47. SINGLE-WIRE FEED TO A HALF-WAVE DIPOLE

vertical portion will radiate for it carries a travelling wave the field from which is not neutralized by a nearby parallel return circuit. When used with a half-wave dipole the antenna is sometimes called a “Windom” and the distance of the tap from the centre is approximately one-sixth of the length of the dipole. The feeder wire shown leaves the antenna at right angles for at least a quarter of a wavelength to avoid coupling and should have no sharp bends.

Coupling to the Transmitter Tank Circuit

The coupling of the transmitting end of a feeder line to the transmitter output circuit is essentially a network problem and therefore will not be dealt with in the present volume. A wide range of such coupling circuits is given in the *Amateur Radio Handbook* and in the *A.R.R.L. Antenna Book*.⁽⁸⁾ The theoretical aspects of coupling circuit design are dealt with in various books such as Everitt's *Communication Engineering* and Terman's *Radio Engineers' Handbook*.⁽²³⁾

Microwave Antennae

FOR wavelengths below 1 m the number of different types of antennae is particularly great. Many of these are only small variations of more general types. Nevertheless there are quite a number of essentially different types—thus at these wavelengths solid conducting surfaces may be used either as reflectors or as guiding surfaces; the radiation may emerge from a slot in a conductor; rods of dielectric can be used to produce a certain radiation pattern; finally all the types commonly employed at greater wavelengths can also be used. Only the grounded radiator is unknown at these high frequencies, but the equivalent form, in which a conducting sheet is used as an artificial earth, is quite practicable.

Many of the antennae described below are highly directive and could therefore have been included in Chapter VI, but the present arrangement was considered more convenient. It will be assumed, however, that the reader is acquainted with the basic principles concerning the formation of directive patterns as given in § 6.1. In this section the directive properties considered are those for radiation originating from discrete sources, whereas in microwave technique we are more often concerned with radiation from a continuous distribution of virtual sources.

4.1. THE HALF-WAVE DIPOLE AND VARIATIONS

The ordinary half-wave dipole was considered at some length in the previous chapter, where the induced e.m.f. method was employed for mutual impedance and the biconical antenna method for the variations of the self-impedance about the point of resonance. All these results are equally applicable to microwave antennae.

In the present section some additional information is given to aid in the design of very thick antennae. The difficulties of

the problem have already been stressed in Chapter V, Vol. I, where it was mentioned that only the spheroidal shape was capable of virtually exact analysis.

Under the heading of "variations" we shall include all antennae whose polar diagrams approximate to that of a half-wave dipole.

Thick Half-wave Dipoles

It is instructive to consider first of all the limiting case of a dipole which is so thick that its width is equal to its length.

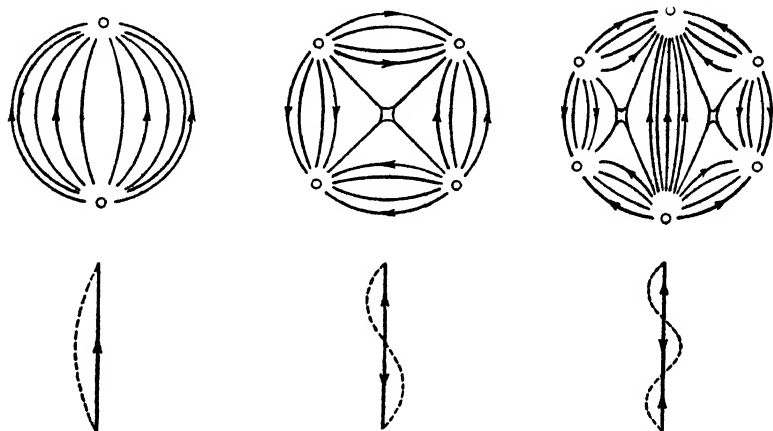


FIG. 4.1. THREE MODES OF OSCILLATION FOR A SPHERE AND FOR A LINEAR RADIATOR

A sphere which is excited across a gap through the equator would form such a dipole; this shape is, indeed, the only one amenable to calculation.

In Fig. 4.1 are shown the electric lines due to the first three modes of vibration of a metallic sphere. These are on a spherical surface surrounding the sphere, for on the sphere itself the tangential electric intensity must be zero. A comparison with the modes of vibration of a linear radiator (shown in the same figure) demonstrates that in the case of the sphere the successive modes are more closely grouped on a frequency scale than they are for the linear radiation. It is to this fact that the spheres (and thick antennae in general) owe their wide-band frequency characteristics.

The problem of forced oscillations of a sphere has been studied by Stratton and Chu⁽⁸⁷⁾ and they obtained the curves

shown in Figs. 4.2 (a) and (b) for a sphere excited across the equator. From these two figures we can obtain a curve giving

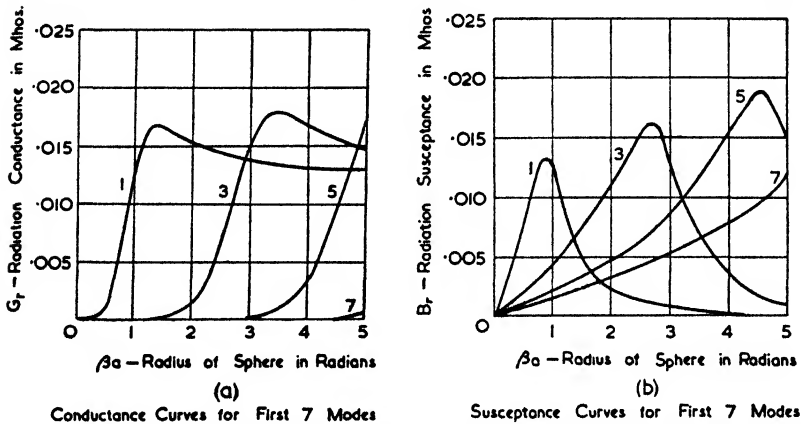


FIG. 4.2. CONDUCTANCE AND SUSCEPTANCE CURVES FOR A SPHERE EXCITED ACROSS THE EQUATOR

(Stratton and Chu, *Jour. Appl. Phys.*, March, 1941)

the series resistance and series reactance and this has been done in Fig. 4.3. The latter curves show the interesting feature

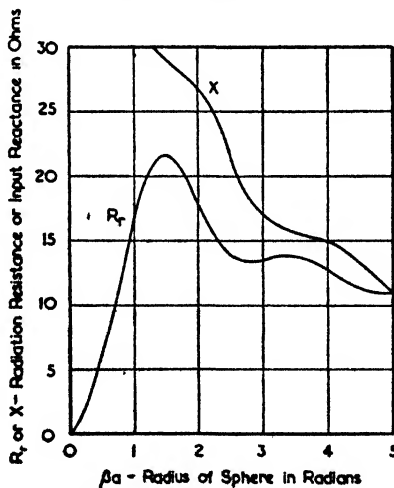


FIG. 4.3. INPUT IMPEDANCE OF A SPHERE EXCITED ACROSS THE EQUATOR

(Stratton and Chu, *Jour. Appl. Phys.*, March, 1941)

that the input impedance remains capacitive for all frequencies—a fact which is also apparent from the susceptance

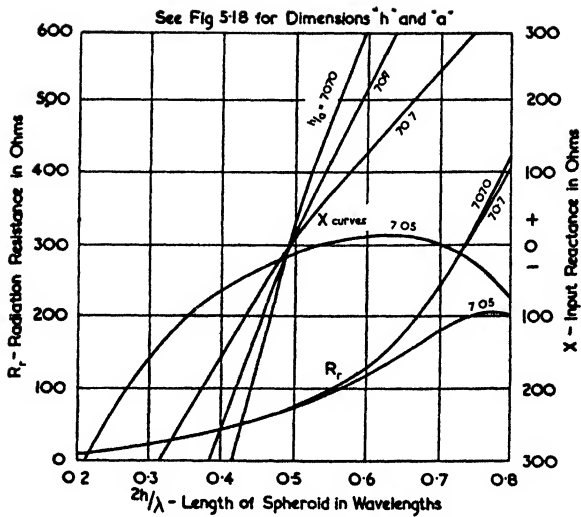


FIG. 4.4. CONDUCTANCE AND SUSCEPTANCE CURVES FOR A PROLATE SPHEROID
(Stratton and Chu, *Jour. Appl. Phys.*, March, 1941)

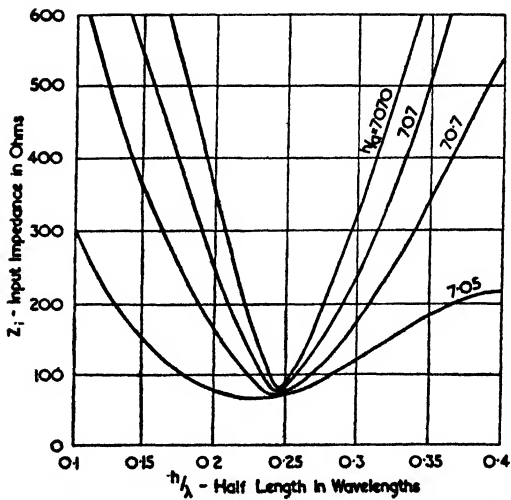


FIG. 4.5. INPUT ADMITTANCE OF A PROLATE SPHEROID
(Stratton and Chu, *Jour. Appl. Phys.*, March, 1941)

curves of Fig. 4.2 (b). It should be noticed that in dealing with forced oscillations across the equator only the odd modes can be excited.

Stratton and Chu also extended their work to deal with prolate spheroids for which they obtained the results shown in Figs. 4.4 and 4.5. In these figures the semi-minor axis has been called "a" (to conform with our use of this symbol for radii) and the semi-major axis "h" (to conform with our

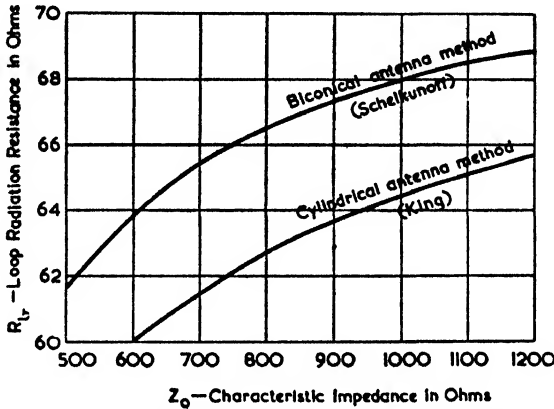


FIG. 4.6. RADIATION RESISTANCE OF A CYLINDRICAL HALF-WAVE DIPOLE AT RESONANCE

symbol for the half-length of a dipole). It will be noticed that the thickest spheroid, whose total length is seven times the maximum diameter, is very nearly capacitive throughout the frequency range.

The problem of the spheroidal antenna has also been studied by Page and Adams⁽⁶⁸⁾ and by Ryder.⁽⁷⁶⁾ Their deductions in the case of relatively thin antennae are as follows—

$$Q = \frac{\Omega}{1.55} \quad \dots \quad (4.1)$$

$$R_{lr} = 73.08 \left(1 - \frac{0.04}{\Omega^2} \right) \quad \dots \quad (4.2)$$

where $\Omega = 2 \log_e \frac{2h}{a} \quad \dots \quad (4.3)$

R_{lr} = loop radiation resistance of a half-wave dipole.

The parameter Ω was first used by Abraham⁽⁸⁸⁾ and is also employed by Hallén⁽⁴⁸⁾ and King⁽¹²⁾ in their work on cylindrical

antennae. In a book⁽¹²⁾ of which he is part author, King has a résumé of his work on cylindrical antennae which includes the calculation of mutual impedances allowing for the finite thickness of the antennae. Fig. 4.6 gives one of his curves and shows the input resistance at resonance for a half-wave dipole of varying thickness. On the same graph the corresponding values given by Schelkunoff are also shown—it will be seen that the values obtained by King are distinctly lower.

Sometimes the results obtained for spheroidal antennae are adopted for cylindrical antennae by assuming an “equivalent” cylindrical antenna whose length slightly exceeds that of the spheroid and whose diameter is slightly less. There is, however, no theoretical justification for such an equivalence. Brillouin⁽³⁷⁾ is of the opinion that sharper edges lead to narrow bandwidths, in which case the spheroidal antenna would have the wider bandwidth for a given length-to-diameter ratio.

The problem of the thick antenna is by no means settled, though the results quoted here will give the engineer an indication of its properties. The reader who wishes to delve further into the problem will find the references mentioned above a useful starting point.

Experimental Verifications with Dipoles

Although it is quite simple to perform rough experiments with dipoles—for example one can easily measure the standing waves on the feeders to a moderate degree of accuracy—it becomes quite a difficult matter to do the experiment accurately enough to decide between two theories. For one thing an allowance must be made for the capacitance across the gap where the antenna is being fed in the case of relatively thick antennae. This has been done in some experiments by Essen and Oliver.⁽¹³⁷⁾ The general shape of these curves is in excellent agreement with theory, so we shall merely quote the more critical points of the curves.

The experiments were performed at a frequency of 432 Mc/s and employed No. 12 S.W.G. copper wire which was cut to different lengths. Consequently as a half-wave dipole the characteristic impedance Z_0 as given by equation (3.11) was 550 ohms, while as a full-wave dipole Z_0 was 630 ohms. The corresponding Ω values as defined by equation (4.3) are 11.1 and 12.5 respectively. From the curves by Schelkunoff⁽⁷⁹⁾ and King⁽¹³⁾ we can deduce the following figures. The table also

includes the corresponding experimental results obtained by Brown and Woodward⁽⁴¹⁾ using a frequency of 60 Mc/s.

CONSTANTS FOR ANTENNA WHOSE DIAMETER = $\frac{1}{283}$ OF A WAVELENGTH
(i.e. $a \doteq 0.002\lambda$)

Measurement	Experimental Results		Theoretical Results	
	(Essen and Oliver)	(Brown and Woodward)	Biconical Antenna Method (Schelkunoff)	Cylindrical Antenna Method (King)
Total length for zero reactance at first resonance (half-wave dipole)	0.465λ	0.47λ	0.465λ	0.48λ
Maximum resistance near second resonance (full-wave dipole)	1 400 ohms at 0.89λ	1 800 ohms at 0.91λ	1 500 ohms at 0.92λ	2 000 ohms at 0.95λ
Maximum reactance before second resonance	520 ohms at 0.81λ	600 ohms at 0.78λ	550 ohms at 0.79λ	800 ohms at 0.87λ
Total length at second resonance	0.89λ	0.90λ	0.91λ	0.95λ

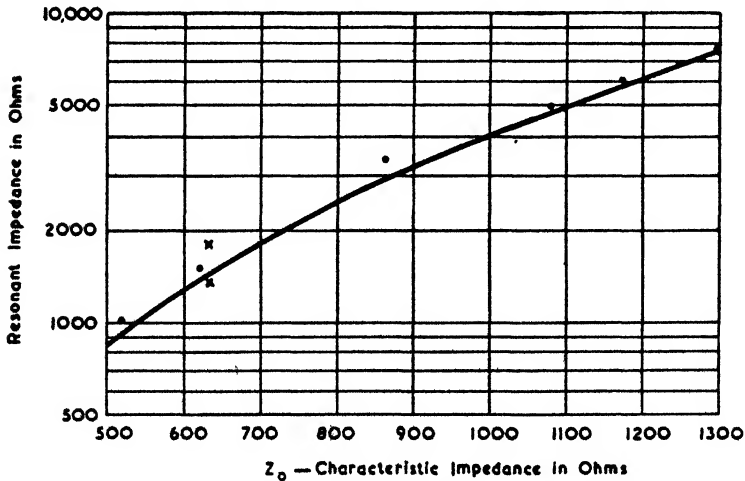


FIG. 4.7. RADIATION RESISTANCE AT FULL-WAVE RESONANCE ACCORDING TO THE BICONICAL ANTENNA METHOD, WITH POINTS SHOWING EXPERIMENTAL VALUES

(Schelkunoff, Proc. I.R.E., Sept., 1941)

In the table on p. 141 the "biconical horn method" gives better agreement with experimental values. It has been noticed before⁽⁷⁹⁾ that the "cylindrical antenna" method gives high impedance values in the region of the second resonance. This does not mean to say that the former method is essentially more correct. Neither method is exact, and it is possibly more a matter of good fortune that certain assumptions should prove to give better agreement with experiment than others.

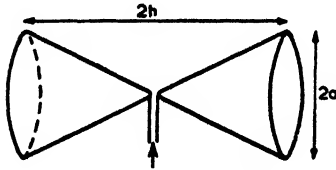


FIG. 4.8. A THICK BICONICAL ANTENNA

As a further example of correlation with experiment, a curve given by Schelkunoff⁽⁷⁹⁾ is shown in Fig. 4.7. This shows the variation of the resonant impedance

of a cylindrical antenna with the thickness of the antenna when operating as a full-wave dipole (the dots indicate experimental values). The experimental values from the above tables have also been added and are shown as crosses. Owing to reading and reproducing inaccuracies there is a slight difference between the theoretical value as mentioned in the

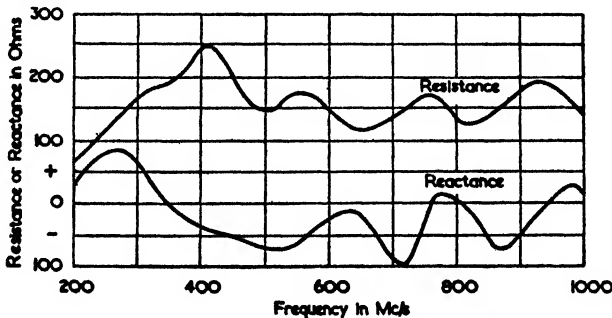


FIG. 4.9. INPUT IMPEDANCE CURVES OF A THICK BICONICAL ANTENNA
($h = 2a = 26.7$ cm, see Fig. 4.8)

table (taken from the curves of Figs. 2.15 and 2.16) and the one indicated for $Z_0 = 630$ ohms in Fig. 4.7.

Thick Biconical Antenna

The biconical antenna method of calculation breaks down if the antennae are too thick, i.e. if the length-to-maximum diameter ratio is less than about 50. Consequently the antenna

shown in Fig. 4.8 is not capable of calculation. Such an antenna has been measured by Essen and Oliver⁽¹³⁷⁾ with the results shown in Fig. 4.9 while Fig. 4.10 gives curves for the same antenna when operating with a single cone protruding from a reflecting sheet. The relatively small impedance

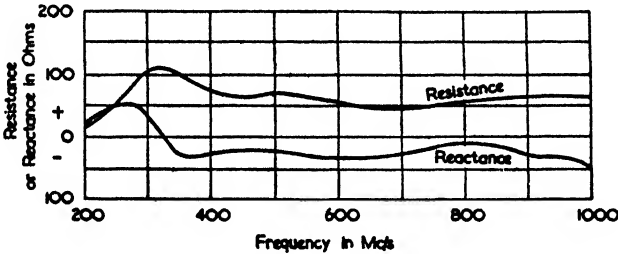


FIG. 4.10. INPUT IMPEDANCE CURVES OF AN ANTENNA CONSISTING OF A CONE AND A FLAT CONDUCTING SHEET

variations over a very wide frequency range are a striking feature of these curves.

The polar diagram from such an arrangement must obviously become more directive at the higher frequencies. Indeed the

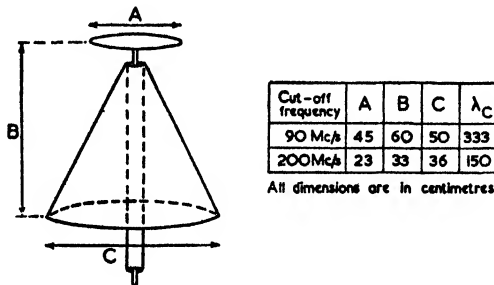


FIG. 4.11. THE "DISCONE" ANTENNA
(Kandoian, *Proc. I.R.E.*, Feb., 1946)

antenna borders on being a biconical horn when the overall length exceeds half a wavelength.

The Discone Antenna

An antenna whose lower half resembles a thick biconical antenna but whose upper half is a disk has been described by Kandoian⁽¹³⁹⁾ under the name of "discone antenna." A sketch

of the antenna is shown in Fig. 4.11 together with the principal dimensions for cut-off frequencies of 90 Mc/s and 200 Mc/s.

Fig. 4.12 shows the standing wave ratio versus frequency for an antenna whose cut-off is at 200 Mc/s. The notable features of the curve are the extremely wide-band characteristics of the antenna and the very sharp cut-off. In round figures a standing wave ratio of less than 2 is obtainable over

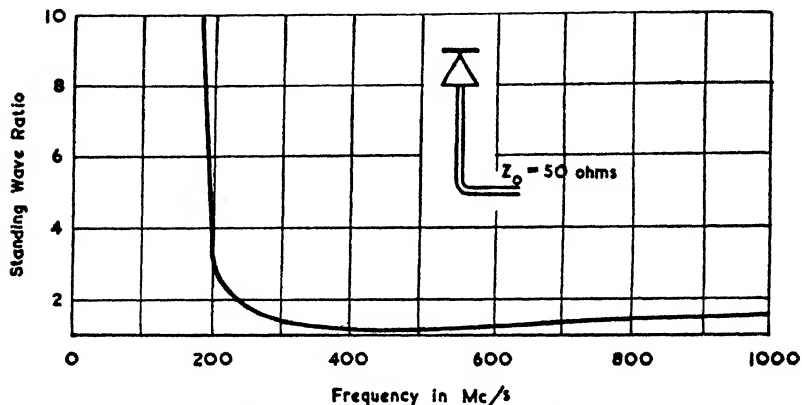


FIG. 4.12. STANDING WAVE RATIO OF A DISCONE ANTENNA
(Kandoian, *Proc. I.R.E.*, Feb., 1946)

a 5 : 1 frequency range and of less than $1\frac{1}{2}$ over a 4 : 1 frequency range. The characteristic impedance of the coaxial feeder line for these figures is 50 ohms.

Over most of the frequency range the polar diagram of a disccone antenna resembles that of a half-wave dipole, but at frequencies above three times the cut-off frequency, the lobes of the vertical polar diagram are directed at about 30° above the horizontal plane.

Magnetic Dipole Antenna

Any radiator whose polar diagram resembles that of a half-wave dipole but whose polarization is reversed (i.e. the polarization in the equatorial plane is horizontal instead of vertical) may be called a magnetic dipole. Since more than one form of antenna will give this result it is safer to give each form a separate name. We shall, however, refer to a dipole which consists of a rod of material of high permeability, together with a coupling loop round the centre, as a "magnetic dipole."

The following antennae are all of the above-mentioned class—

(a) *The Alford Loop Antenna*

This was described in the previous chapter in § 3.4, since its original applications were in the ultra-short waveband. It is, however, equally suitable for microwave operation.

(b) *The Coaxial Loop Antenna*

Kandoian⁽¹³⁹⁾ has described a form of loop antenna which is a variation of the Alford loop. Three variations of the coaxial loop are shown in Fig. 4.13.

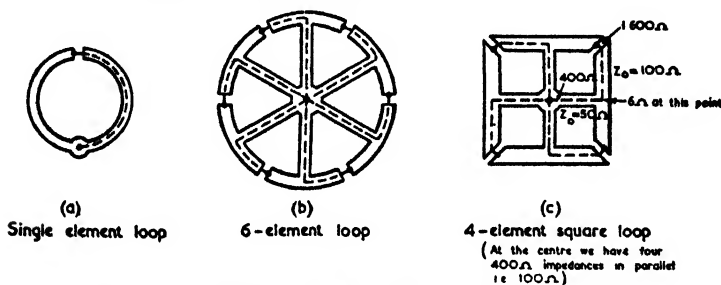


FIG. 4.13. THREE FORMS OF COAXIAL LOOP ANTENNA

By varying the characteristic impedance of the supporting input sections, the input impedance of the antenna may be given any value between 50 and 100 ohms. The bandwidths obtained are quite moderate, being only about 3 per cent of the operating frequency for a standing wave ratio of $1\frac{1}{2}$ with a 4-element loop. If the system were matched at the operating frequency, the Q of the antenna would be given by the limits for a standing wave ratio of less than 2.6. On this basis the curve published by Kandoian shows that a 4-element loop has a Q of 20.

For many purposes the loop is more conveniently made in the shape of a square—this can be done without any significant change in the radiation characteristics. Fig. 4.13 (c) shows such a loop and also indicates the approximate impedance at different points in the feeder system. It will be seen that the loop consists essentially of four thick end-fed dipoles.

Square loops of the above type may conveniently be mounted on steel towers and stacked one above the other with spacings of about one wavelength between adjacent loops (antennae of this type are described in publications issued by the Federal

Telephone and Radio Corporation). The power gain of such stacked loops is approximately equal to the number of loops.

(c) *The Slotted Cylinder Antenna*

A description of the slotted cylinder or "rocket" type of antenna is given in § 3.4. Although the first designs were for ultra-short-wave working, it is obviously quite a practical type of antenna for microwave operation.

(d) *The Magnetic Dipole*

What might truly be called a "magnetic dipole" has been studied theoretically by Page⁽⁶⁷⁾ in a recently published article.

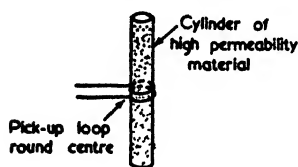


FIG. 4.14. A MAGNETIC DIPOLE

He arrives at the conclusion that a dipole of magnetic material as shown in Fig. 4.14 should have an effective height which is several times that of an electric dipole of equal length. It should be noted, however, that if the polar diagrams are the same (which they must be if the antennae are short enough) this increase in effective height is accompanied by a corresponding increase in radiation resistance.

Page's analysis shows an effective height h_e' whose ratio to that given by the equivalent electric dipole is expressed by

$$\frac{h_e'}{h_e} = \frac{1}{2} \mu_r \beta a \left(\frac{|N|}{\mu \pi a^2} \right)^2 \quad (4.4)$$

where N = flux of induction through a cross-section of the cylindrical antenna.

The curves given by Page of the bracketed term show that if $\epsilon_r = 9$, then the term has a maximum value of between 3 and 4. For example, if $\mu_r = 25$, then the term has a maximum of 3.4 when $\lambda/a = 50$, and if $\mu_r = 100$ the maximum value is 3.7 with $\lambda/a = 110$. In general the higher the value of μ_r , the thinner the antenna must be for optimum performance.

If $\epsilon_r = 25$, the maximum values of the bracketed term lie between 6 and 7. Taking the optimistic values of $\epsilon_r = 25$ and $\mu_r = 100$, then

$$h_e'/h_e = 15$$

The diameter of such an antenna would have to be 4 cm for a wavelength of 3 m. No experimental results appear to have been published yet on such antennae.

(e) The "Electromagnetic" Dipole

By adding a vertical conductor about $\lambda/4$ long to the coaxial loop antenna, a radiator may be obtained which is, in effect, a combination of an "electric" and a "magnetic" dipole. With such a transmitting antenna the pick-up on a receiving dipole would be independent of the orientation of the receiving

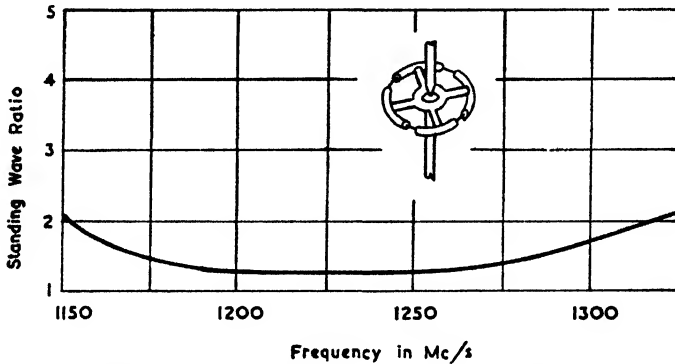


FIG. 4.15. STANDING WAVE RATIO OF AN "ELECTROMAGNETIC" DIPOLE (Kandoian, *Proc. I.R.E.*, Feb., 1946)

antenna (provided, of course, it is kept in the plane of the wavefront).

Kandoian⁽¹³⁹⁾ has described such an antenna and gives the curve of Fig. 4.15 as an example of its performance. It has a moderately wide bandwidth of about 10 per cent for a standing wave ratio of 1.5.

4.2. PARABOLIC ANTENNAE

General Features

By placing a curved sheet of metal behind an antenna (Fig. 4.16) and making the curvature follow a parabolic law, the field strength in the forward direction can be greatly augmented. The simplest version is shown in Fig. 4.17 (a) and is sometimes known as a cylindrical-parabolic mirror to distinguish it from a full-parabolic shown in Fig. 4.17 (b), which is a paraboloid of revolution. We shall use the terms semi- and full-parabolic mirror whenever the distinction is needed.

From the well-known properties of a parabola we know that rays (i) and (ii) in Fig. 4.16 may be considered to be

coming from sources at P_1 and P_2 where these points are situated on the directrix. It is therefore permissible to consider an "equivalent plane" of sources on the plane of the directrix.

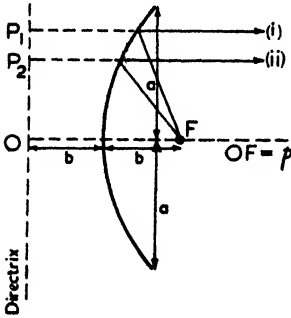


FIG. 4.16. DIAGRAM OF A PARABOLIC REFLECTOR

This assumption will be in error if the angle ϕ between the direction of the field point and the main axis of the mirror is great (greater than about $\pm 30^\circ$); it will also be in error for a semi-parabolic mirror if the angle θ is appreciable (Fig. 4.17 (a)). A further inaccuracy arises if the antenna is close to the mirror, say less than half a wavelength, when the mutual impedance with the metallic surface modifies the optimum shape. It is apparent, therefore, that accurate theoretical calculations are out of the question for small mirrors, but for

relatively large ones the theoretical estimates are quite satisfactory. This is not a serious limitation since for small systems (i.e. for apertures of less than 1 to 2 wavelengths) a corner reflector will function just as well and is easier to construct.

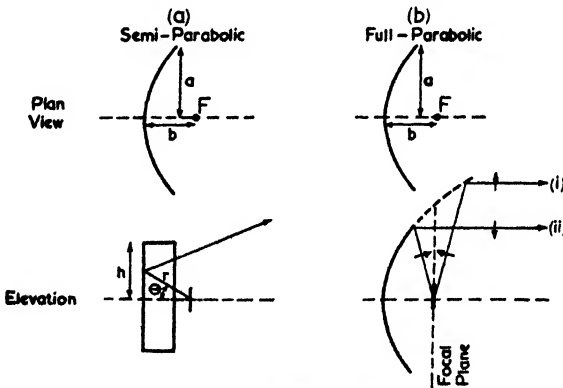


FIG. 4.17. FULL- AND SEMI-PARABOLIC MIRRORS

The plan view of Fig. 4.17 shows that, for a fixed focal distance b , more and more of the radiated energy is directed forwards as the value of a is increased. However, the solid angle included by the reflector increases but slowly as the sides are extended beyond the focus.

Referring to the elevation views of Fig. 4.17, we see that in the case of a semi-parabolic mirror there is a zone from which the reflected rays interfere with those directly along the axis. This zone occurs when $r > (b + \lambda/2)$. In the case of a full-parabolic mirror we see that the extension of the sides eventually leads to a reversal in polarization—i.e. a part of the surface of the mirror will have currents which tend to reduce the forward field strength. There is therefore hardly anything to be gained by extending the sides of a full-parabolic mirror beyond the focal plane.

The simplest way of increasing the gain of a parabolic mirror is to place a reflecting antenna about a quarter of a wavelength in front of the driven antenna. A more elaborate method giving slightly more gain is to place a hemispherical reflector in front of the dipole as shown in Fig.

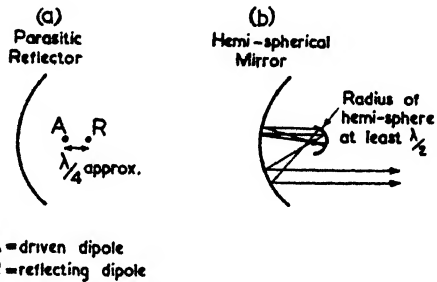


FIG. 4.18. REFLECTOR SYSTEMS FOR INCREASING THE ENERGY REFLECTED FROM THE SURFACE OF A PARABOLIC MIRROR

4.18. If such a reflector is too small, the impedance of the dipole will be seriously decreased; if it is too large it will obscure some of the forward radiation from the parabolic mirror. When the backward directivity of the antenna system at the focus is appreciable the optimum position for the focus is outside the opening of the mirror.

Since the advent of horn radiators the question of how they compare with parabolic mirrors often arises. Restricting ourselves to full parabolics of several wavelengths aperture, the answer is that for a given aperture area the parabolic mirror has the slightly sharper beam but somewhat greater side-lobes. Mechanically, the parabolic mirror is more difficult to construct but possesses the distinct advantage of having less depth and therefore occupying less space.

Semi-parabolic Mirrors

For reasons mentioned above, semi-parabolic mirrors are restricted to sizes of about two wavelengths aperture, and furthermore their polar patterns are not calculable with

accuracy. A theoretical study of such mirrors has been made by Brendel⁽¹³¹⁾ who gives the following approximate power gain

$$G_H = 16(\tan^{-1} 2a/b)^2 \quad (4.5)$$

This assumes a height of $2h$ (Fig. 4.17) which just avoids the destructive zones. The formula is optimistic judging by practical results.

An interesting set of experimental results was obtained by Gresky⁽¹³⁸⁾ using a wavelength of 3 m. His mirror, whose dimensions are given in Fig. 4.19, consisted of vertical wires, spaced at distances d apart. When d was equal to $\lambda/30$ the lengths of the wires were relatively uncritical provided they were at least $\lambda/2$ long. With $d = \lambda/7.5$ an optimum forward gain was obtained when the wires were 0.43λ long—the resultant polar diagram being much the same as with the closely spaced untuned elements. His curves of gain versus length of wire are shown in Fig. 4.20. In both cases the energy radiated backwards was about 2 per cent of the forward radiation and the main lobes had a width at the half-power points of approximately 44°

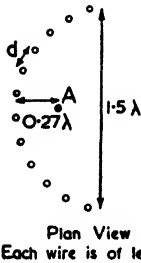


FIG. 4.19. EXAMPLE OF A GRID-TYPE SEMI-PARABOLIC MIRROR (GAIN CURVES GIVEN IN FIG. 4.20)

(the tuned-wire case was only slightly inferior on both accounts). There is no doubt that equivalent results would be obtained in the microwave region and, since these experiments concern parabolic mirrors, it is convenient to mention them in the present chapter.

Somewhat similar experiments were performed by Nagy⁽¹²⁰⁾ who also tried various configurations employing from 1 to 4 parasitic elements.

Full-parabolic Mirrors

The first theoretical investigation into parabolic mirrors appears to have been made by Darbord.⁽¹³⁵⁾ He showed that if an incident wave of intensity E' falls on an element da of the conducting surface (see Fig. 4.21), then the reflected intensity at P is given by

$$E = \frac{E' da}{\lambda D} \cos \theta \quad (4.6)$$

In deriving this formula the assumption is made that most of the reflected energy is concentrated in a relatively narrow

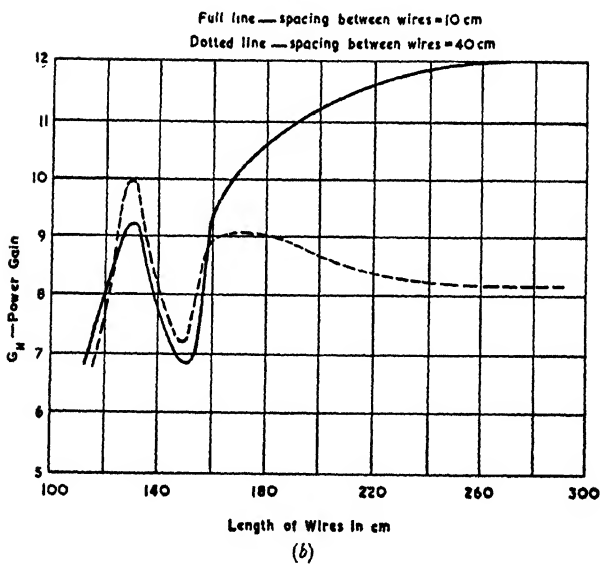
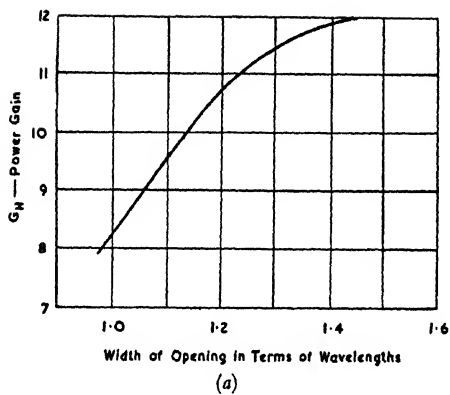


FIG. 4.20. GAIN CURVES OF SEMI-PARABOLIC MIRROR ILLUSTRATED IN FIG. 4.19
(Grenky, *Zeit für Hoch*, Nov., 1928)

region around P and that all the incident energy is reflected. By means of this formula we can obtain an equivalent distribution of radiation which is assumed to be in the plane of the directrix. When the source at the focus is a doublet the equivalent distribution is as shown in Fig. 4.22 in which the

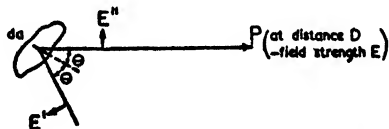
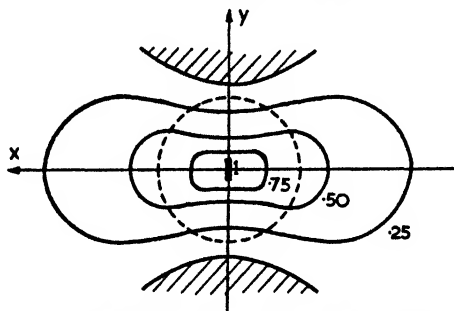


FIG. 4.21. DIAGRAM OF REFLECTION FROM AN ELEMENT OF SURFACE

contour lines join portions of the surface from which the intensities of the radiation per unit area are equal. The numbers indicate the relative field strengths from each contour; in particular the shaded areas are the destructive zones whose origin was discussed at the beginning of this section. The



The contours indicate the energy density of the illumination relative to that at the centre

FIG. 4.22. EQUIVALENT ENERGY DISTRIBUTION IN THE PLANE OF THE DIRECTRIX FOR A PARABOLIC MIRROR EXCITED BY A DOUBLET AT THE FOCUS

corresponding plot of the lines of equal efficiency if we have a half-wave dipole at the focus is very similar to that shown in Fig. 4.22.

By integration, Darbord found that the voltage gain of a parabolic mirror with a doublet at the focus is given by $\beta pa^2/(p^2 + a^2)$. Hence the power gain over an omnidirectional radiator is

$$G_0 = 1.5 \beta^2 \left[\frac{pa^2}{p^2 + a^2} \right]^2 \quad \dots \quad (4.7)$$

where p = distance from focus to directrix
 = twice focal distance, b ,
 a = radius of aperture of mirror.

The effect of replacing the doublet by a half-wave dipole is to increase the illumination in the central regions, thus broadening the major lobe a little but reducing the side lobes. The total forward gain with the half-wave dipole is therefore also given by equation (4.7) for all practical purposes (the formula is only moderately accurate in any case). If the focus is in the plane of the aperture we have $a = 2b = p$, and therefore

$$G_0 = 0.375\beta^2 a^2 \\ = 1.5 \left(\frac{\pi a}{\lambda}\right)^2 \quad . \quad . \quad . \quad (4.8)$$

In § 5.1 it is shown how the gain of an antenna may also be expressed in terms of the effective area of cross-section, A_e , and the corresponding effective area, A_0 , of an omnidirectional radiator.

Equation (5.4) shows that

$$G_0 = \frac{A_e}{A_0} = \frac{4\pi A_e}{\lambda^2} = \frac{\beta^2 A_e}{\pi}$$

Using the previous equation we therefore obtain

$$A_e = 0.375 \pi a^2 \quad . \quad . \quad . \quad (4.9)$$

i.e. the effective area is equal to $\frac{3}{8}$ of the actual area.

Equations (4.7), (4.8) and (4.9) all apply to the case of a single doublet at the focus. However, we may also apply them to the case of a half-wave dipole at the centre without an appreciable loss in accuracy.

In the majority of practical cases the direct forward radiation is reflected back on to the mirror by means of a parasitic antenna or a hemispherical bowl.⁽²⁶²⁾ This results in a gain of 2.5 db in a well-designed mirror, which means that

$$A_e = 0.667 \pi a^2 \quad . \quad . \quad . \quad (4.10)$$

i.e. the effective area with a reflector is equal to $\frac{5}{8}$ of the actual area.

The corresponding gain formula is then

$$G_0 = 2.67 \left(\frac{\pi a}{\lambda}\right)^2 \quad . \quad . \quad . \quad (4.11)$$

A convenient way of remembering the above equation is to note that G_0 is equal to $\frac{3}{8}$ times the square of the circumference in wavelengths. Fig. 4.25 shows the above relationship together with some experimental points. The majority of these were obtained from Report 54-11 by the Massachusetts Institute of Technology, one is from a paper by Brewitt-Taylor⁽¹³⁸⁾ and two are due to the author. The M.I.T. Report also gave experimental values which showed the gain decreasing with respect to the theoretical value as the aperture of the antenna was increased—for apertures greater than 20 wavelengths the experimental gain was only some 50 per cent of the theoretical value. There appears to be no obvious explanation for these anomalous results.

Polar Diagram of Full-parabolic Mirror

The contoured diagram of Fig. 4.22 also determines the polar pattern from the parabolic mirror, since it is a diagram of an equivalent current distribution of which all the elements are in phase and which is situated in the plane of the directrix. Therefore the vertical polar pattern may be found by dividing the equivalent surface into horizontal strips (the field intensity contributed by each strip being proportional to the total value of all the elements in that strip), while the horizontal pattern is given by considering the corresponding set of vertical strips. Obviously in each case the contribution from the strips reaches zero as we approach the boundary of the projection of the parabolic surface on the directrix.

If we take the vertical strips, the resultant curve for the relative strengths for the equivalent distribution of sources along the x -axis has the form shown in curve (a) of Fig. 4.23; for horizontal strips we have curve (b). These curves give "equivalent line" distributions with a vertical doublet at the focus.

The shape of such curves has been calculated by Staal⁽¹⁴⁷⁾ assuming a doublet at the focus, but even so the subsequent integral is unmanageable except by assuming an *approximately* correct law. At this point we therefore proceed to assume some simple laws for the equivalent line distribution. These laws must show a reasonable fit with calculated curves whose derivation is based on a graphical integration of the contours of Fig. 4.22, which in turn are obtained from equation (4.6). The simplest approximation to curve (a) in Fig. 4.23 is a square law distribution $E_x = k_1(1 - x^2/a^2)$, while a useful

approximation to curve (b) can be obtained by simply assuming the linear distribution $E_y = k_2(1 - y/a)$.

Whatever law is assumed, the polar diagram in either plane is obtained by taking pairs of elements on each side of the centre as shown in Fig. 4.24 and the total intensity at any

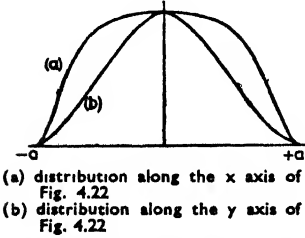


FIG. 4.23. EQUIVALENT LINE DISTRIBUTIONS FOR A PARABOLIC MIRROR

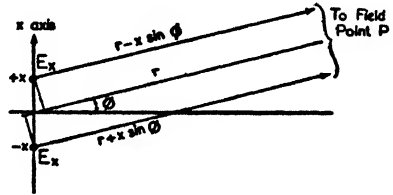


FIG. 4.24. RESOLUTION OF AN EQUIVALENT LINE DISTRIBUTION INTO PAIRS OF SOURCES

point is the sum of the resultants of all such pairs. In this way the following formulae are obtained—

Horizontal Polar Pattern

$$E_\phi = \int_0^a 2E_x \cos(x \sin \phi) dx$$

Vertical Polar Pattern

$$E_\theta = \int_0^a 2E_y \cos(y \sin \theta) dy$$

In the above formulae, we put E_x and E_y as functions of x and y respectively. It is instructive to compare the linear and square law distributions with a uniform distribution and with one in which all the energy is equally divided between two cophasal sources whose separation corresponds to the diameter of the parabolic mirror. These distribution laws give the following formulae—

Distribution Law

Formula for E_ϕ or E_θ

Linear

$$E_\theta \propto \frac{\sin^2(a\theta/2)}{(a\theta/2)^2}$$

Square

$$E_\theta \propto \frac{\sin(a\theta) - a\theta \cos(a\theta)}{a^3\theta^3/3}$$

Constant

$$E_\theta \propto \frac{\sin(a\theta)}{a\theta}$$

Point Sources at $\pm a$

$$E_\theta \propto \cos(a\theta)$$

Although the above formulae are in terms of θ , they are just the same if ϕ is the variable. It has been assumed that θ is small enough for $\sin \theta$ to be approximately equal to θ , i.e. a range of about $\pm 25^\circ$ from the lobe maximum is catered for. Thus all the formulae are valid for the main lobe if $a > 2.5\lambda$, and most of them are valid for appreciably smaller parabolae.

From the above formulae we can find the beam widths which are given in the table below (the width between the half-power points can be obtained by integration).

Distribution Law	Width of Main Lobe (Radians)		Ratio (a)/(b)	Specimen Case
	(a) Between Null Points	(b) Between Half-power Points		Width between Half-power Points if $a = 5\lambda$
Linear	$2.0 \lambda/a$	$0.637 \lambda/a$	3.14	7.3°
Square law	$1.43 \lambda/a$	$0.573 \lambda/a$	2.50	6.54°
Constant	$1.0 \lambda/a$	$0.445 \lambda/a$	2.25	5.1°
Two point sources	$0.5 \lambda/a$	$0.25 \lambda/a$	2.00	2.86°

The above figures are very instructive for they show how the beam widths compare with the one due to two cophasal sources situated at the extremities of a diameter, i.e. separated by a distance equal to $2a$. The two-source case (which would produce a great many lobes of equal strength distributed over 360°) actually gives a beam which, between the null points, is twice as sharp as that given by the constant distribution law and four times as sharp as for the linear law.

A constant distribution cannot be obtained in practice since E_x is necessarily zero at distances of $\pm a$. A graphical analysis shows that the E_x distribution when $a = b$ is slightly more uniform than that given by the square law, while the E_y distribution is a fair approximation to the linear law. From these facts we can derive the following rules for full paraboloids whose radii are approximately twice the focal distance.

Beam Width between Half-power Points

In the plane of the dipole

$$\text{beam width} = 37\lambda/a \text{ degrees} \quad . \quad . \quad (4.12A)$$

In the equatorial plane of the dipole

$$\text{beam width} = 33\lambda/a \text{ degrees} \quad . \quad . \quad (4.12B)$$

The above beam width formulae may be regarded as giving the minimum values likely to be obtained. In particular, when a reflector is used the beam widths obtained in practice

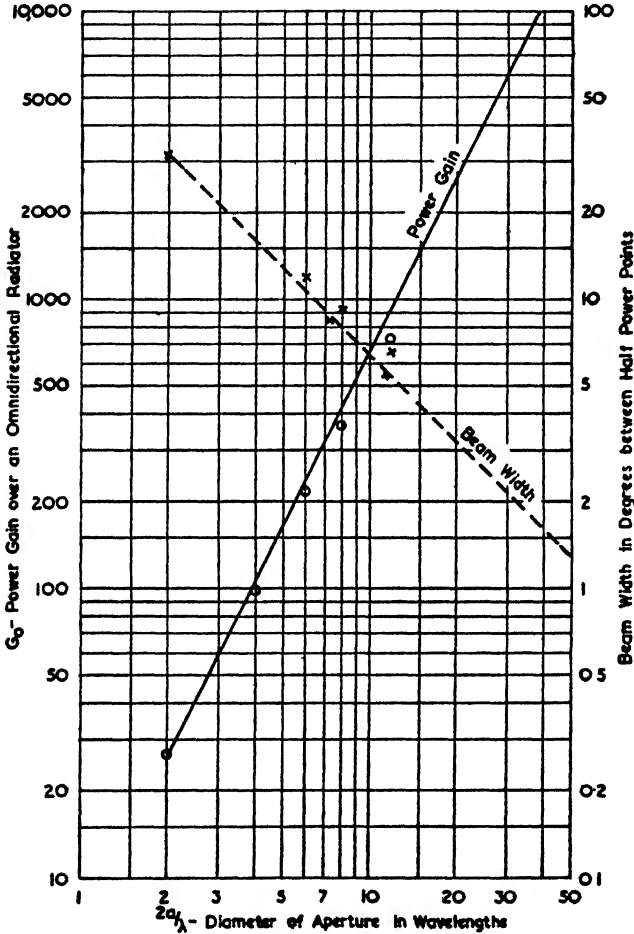


FIG. 4.25. POWER GAIN AND BEAM WIDTH OF A PARABOLIC MIRROR

may be as much as 15 per cent greater. The dotted curve in Fig. 4.25 shows the beam width as given by equation (4.12B), while the crosses indicate experimental values.

The nulls are more highly dependent on the precise current distribution than the half-power points, hence better correlation

between theory and practice is obtained by referring to the half-power points. The latter are usually more significant in problem applications and have the additional advantage over the null points of never being ill-defined.

The full lines in Fig. 4.26 show the theoretical polar diagrams obtained assuming linear and square law distributions; the dotted lines show experimental polar diagrams obtained with

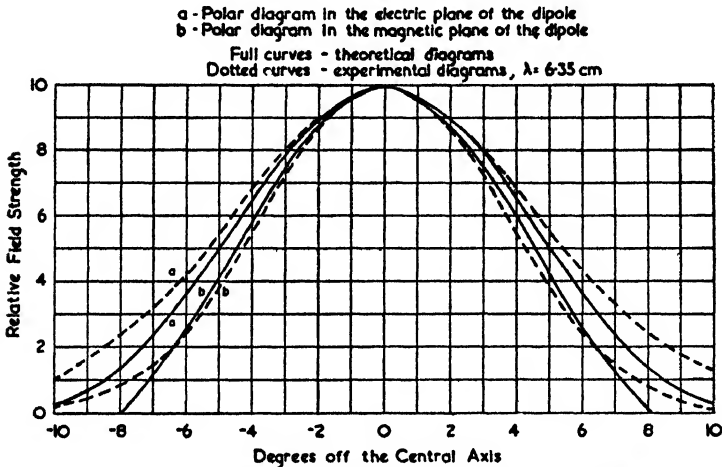


FIG. 4.26. THEORETICAL AND EXPERIMENTAL POLAR DIAGRAMS OF A PARABOLIC MIRROR OF TEN WAVELENGTHS APERTURE

a mirror whose radius was 5 wavelengths and whose aperture was 4 times the focal length (the operating wavelength was 6.35 cm).

Tilting the Beam from a Parabolic Mirror

If the dipole is displaced sideways from the focus as shown in Fig. 4.27 (a) the equivalent sources on the directrix are no longer in phase but have a phase relationship as shown in Fig. 4.27 (b). As a result the beam from the mirror is slewed in the opposite sense to that in which the dipole has been moved. Such tilting of the beam has important radar applications, although the principle was probably first used for producing overlapping patterns for aircraft guidance.

The calculation of the tilt produced is formidable if an attempt at any exactness is made. As a rough guide we may assume a linear phase shift with distance along the directrix (shown by the dotted line in Fig. 4.27 (b)). For a typical

distribution law the field at a distant point along the axis would have components as shown in Fig. 4.27 (c).

On moving away from the axis, the field vectors begin to spin at a rate which is proportional to their distances along the x -axis from the centre. Since their relative phases are proportional to this distance, this rate of spin is also proportional to their initial phase displacement. If we therefore explore the field on the side of the axis on which the beam maximum is situated, the field vectors in Fig. 4.27 (c) "fold

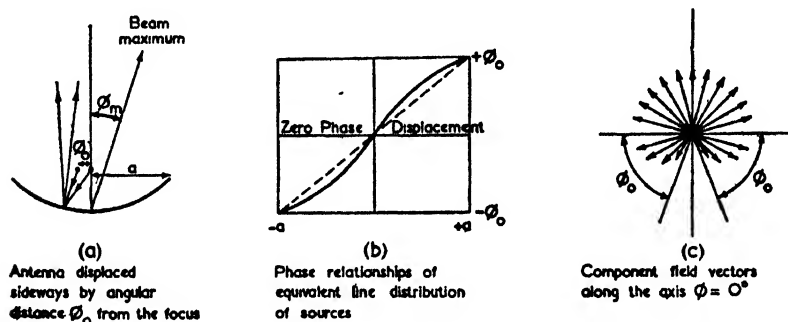


FIG. 4.27. DIAGRAMS ILLUSTRATING THE SLEWING OF THE BEAM FROM A PARABOLIC MIRROR

up" until they are all in phase along the perpendicular, for some exploring angle ϕ_m . This is the angle at which the lobe maximum occurs.

In "folding up" the outermost vectors have travelled through an angle ϕ_0 , where ϕ_0 is the angular displacement of the dipole. This phase movement of the outermost field vectors is equal to $\beta a \sin \phi_m$ radians which, since we are dealing with small exploring angles only, is equal to $\beta a \phi_m$. Hence the lobe maximum is reached when

$$\phi_0 = \beta a \phi_m$$

i.e.

$$\phi_m = \frac{\phi_0}{\beta a}$$

For example, if the displacement were $\phi_0 = \lambda/4$ (0.5π radians) and $a = 5\lambda$ ($\beta a = 10\pi$ radians) then $\phi_m = 0.05$ radians, or 2.86° .

It can be seen from Fig. 4.27 (c) that a change in the law for $|E_\theta|$ will not affect the result, provided only that the distribution is symmetrical about the centre. But the departure of the phase law from the simple linear case assumed above

does not affect the value of ϕ_m . For mirrors whose radius is twice the focal distance ($a = 2b$), rough calculations show that the departure from the linear phase relationship is such as to increase the tilt to about 1.4 of the value calculated above,

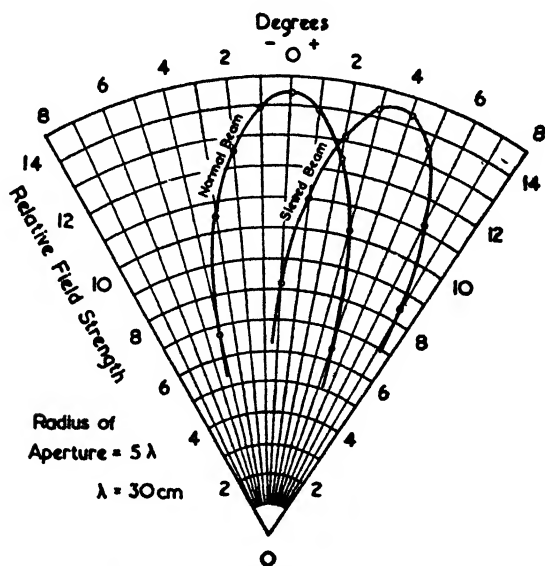


FIG. 4.28. EXAMPLE OF SLEWED BEAM OBTAINED BY A SIDEWAYS DISPLACEMENT OF 0.25λ OF THE DIPOLE IN A PARABOLIC MIRROR

e.g. if $\phi_0 = \lambda/4$ and $a = 5\lambda$ as before, then $\phi_m = 1.4 \times 2.86 = 4.0^\circ$.

Fig. 4.28 shows an experimental result in which a slew of 3.6° was obtained; this corresponds to a multiplying factor of 1.26. The parabolic mirror had a radius of 1.5 m, the focal length was 1 m and the operating wavelength was 0.3 m. The mirror in question was one of those used on the cross-channel link and is shown in Plate IX. The results of Brewitt-Taylor⁽¹³²⁾ also show a similar law for the tilt angle. In his case the factor proved to be 1.3. We may therefore give the following formula for the tilt ϕ_m produced by displacing the source sideways by ϕ_0 radians—

$$\phi_m = 1.3 \frac{\phi_0}{\beta a} \text{ radians or } 75 \frac{x}{a} \text{ degrees} \quad (4.13)$$

where x = displacement in the same units as "a."



PLATE IX. PARABOLIC MIRRORS WITH HEMISPHERICAL REFLECTORS AT THE FOCUS—USED FOR CROSS-CHANNEL COMMUNICATION ON A WAVELENGTH OF 17 CM IN 1931

(Courtesy of Standard Telephones & Cables, Ltd.)

Cheese Antennae

If a fan-shaped beam is required this may be produced by a section of a parabolic cylinder bounded by two flat surfaces. This type of radiator is known as a "cheese antenna" and is particularly suitable for radar on ships, since it gives a narrow beam in the horizontal plane together with a moderately wide one in the vertical plane. The frontispiece shows a cheese antenna for radar on board the R.M.S. "Queen Elizabeth."

Between the two flat surfaces the wave is transmitted as in a waveguide; consequently (assuming the surfaces to be horizontal) the vertical polar pattern will depend on the mode of propagation as well as on the height of the "cheese." In order to reduce the variations with frequency a specific mode should be chosen at the source. Apart from the TEM mode the two simplest modes of excitation are as shown in Fig. 4.39, in which the distribution between the sides of the waveguide corresponds to the distribution between the flat surfaces. The TE_{10} mode in Fig. 4.39 (a) would then produce horizontal polarization while the TM_{10} mode in Fig. 4.39 (b) would result in vertical polarization.

To calculate the horizontal polar pattern we start by taking an equivalent line distribution on the directrix, the said distribution being given by a horizontal section through a diagram of the type shown in Fig. 4.22. The vertical polar diagram will be similar to that produced by the radiation from the open end of a waveguide excited in the corresponding mode and considered in the corresponding plane.

A cheese antenna is usually fed via a "hohorn" which consists of a waveguide flared out in the vertical plane to a cylindrical parabolic reflector which then reflects the energy into the main antenna. The back of this small parabolic reflector may be seen in the middle of the aperture of the "cheese" shown in the frontispiece.

4.3. CORNER REFLECTORS

General Features

Antennae of the type shown in Fig. 4.29 were termed "corner reflectors" by Kraus,⁽¹⁴²⁾ who published curves for reflectors with corner angles of 60° and 90° . This type of antenna is also known as a "V reflector" type, but since this terminology

is liable to cause confusion with V-type wire antennae, the former name seems more serviceable. A corner reflector provides a highly convenient method of obtaining gains of 10 to 12 db over the half-wave dipole.

The work of Kraus showed that, provided the sides were at least one wavelength long, very satisfactory agreement could

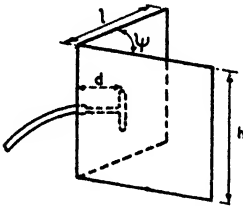


FIG. 4.29. DIAGRAM OF A CORNER REFLECTOR

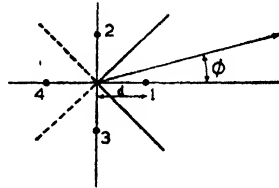


FIG. 4.30. IMAGE DIAGRAM FOR A 90° CORNER REFLECTOR

be obtained between experimental polar diagrams and those calculated on the assumption of simple image theory with sides of infinite extent. Actually the experimental curve may be either slightly narrower or slightly wider than the "ideal" curve obtained by calculation using the above assumptions—

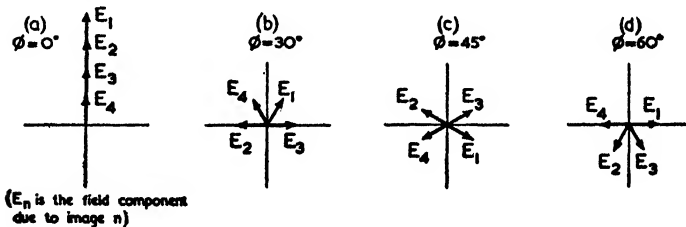


FIG. 4.31. FIELD COMPONENTS IN FIG. 4.30 WITH $d = 0.5\lambda$

examples showing such deviations from the ideal are given in an article by Moullin.⁽¹⁴⁴⁾

The theoretical curve is easily obtained if the corner angle, ψ , is equal to $180^\circ/n$ where n is an integer. When $n = 2$ we have the plan view shown in Fig. 4.30 in which the driven antenna is denoted by 1 and the three images by 2, 3 and 4. If O is the reference point from which the space phasing of the four sources is to be calculated, and if the reference phase at O is equal to the time phase of the driven antenna, then vector diagrams of the field components at a distant point take the form shown in Fig. 4.31. In these diagrams the

particular case of $d = \lambda/2$ has been taken, both for simplicity and because such a spacing gives a very practical solution.

When $\phi = 0^\circ$ all the field components are in phase; for $\phi = 30^\circ$ they are as shown in Fig. 4.31 (b) and their resultant is less than half the maximum value; for $\phi = 60^\circ$ the resultant has changed sign (which indicates that a new lobe has started)

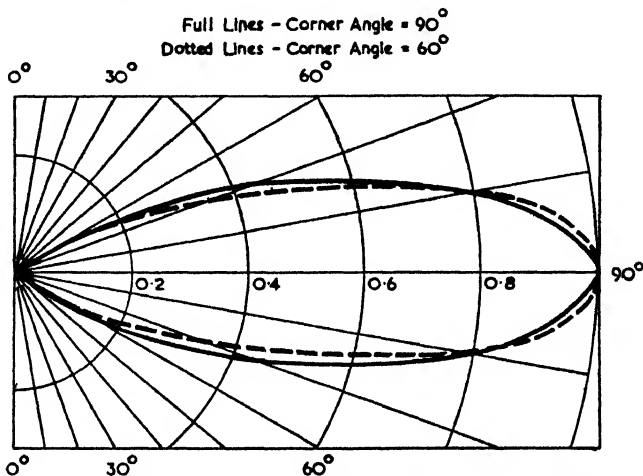


FIG. 4.32. THEORETICAL POLAR DIAGRAMS FOR CORNER REFLECTORS WITH ANGLES OF 60° AND 90°

but this value does not appear in practice since the reflector limits the radiation to $\phi = \pm 45^\circ$.

It is obvious from Fig. 4.31 that we may simply take the algebraic sum of the two pairs of field components; hence the total field is given by

$$E_{(\psi = 90^\circ)} = 2E_1[\cos(\beta d \cos \phi) - \cos(\beta d \sin \phi)] \quad (4.14)$$

The polar diagram given by the above equation is shown in Fig. 4.32, together with the corresponding pattern for $\psi = 60^\circ$. The latter is given by

$$E_{(\psi = 60^\circ)} = 4E_1 \sin\left(\frac{\beta d}{2} \cos \theta\right) \left[\cos\left(\frac{\beta d}{2} \cos \theta\right) - \cos\left(\frac{\sqrt{3}\beta d}{2} \sin \theta\right) \right] \quad (4.15)$$

It will be noticed that in both equations (4.14) and (4.15) the trigonometrical expressions involved are of the type $\cos(x \cos \theta)$. These correspond to the formulae for the height

factor curves of Figs. 3.7 and 3.8 (they also cover the forms $\cos(x \sin \theta)$ and $\sin(x \sin \theta)$ by simply reversing the angle scale). Multiplication of these curves can be performed directly on tracing paper in the manner outlined in § 3.1, but the additions must be performed separately.

Calculation of Gain

The value of E_1 is not, in general, that given by the field from an isolated dipole, since the induced currents on the reflecting

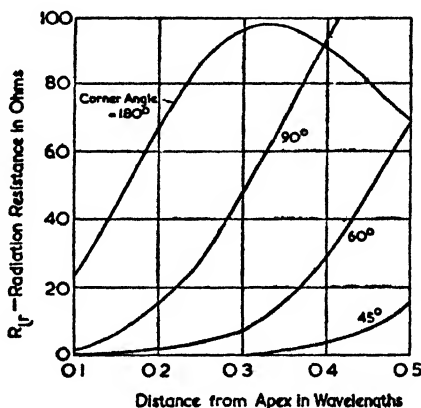


FIG. 4.33. INPUT RESISTANCE OF THE DIPOLE IN A CORNER REFLECTOR FOR DIFFERENT SPACINGS AND CORNER ANGLES
(Kraus, *Proc. I.R.E.*, Nov., 1940)

surfaces will modify the input resistance of the dipole. These modifications can be taken into account by allowing for the mutual impedance between the images and the driven dipole. If the field due to an isolated dipole is denoted by E_0 , then

$$\frac{E_1}{E_0} = \sqrt{\left(\frac{R_{11}}{R_{11} + R_{14} - 2R_{12}} \right)} \quad (4.16)$$

where R_{nm} = mutual impedance between antennae n and m (obtainable from Fig. 3.15). Curves showing the input resistance of the dipole, $(R_{11} + R_{14} - 2R_{12})$, are given in Fig. 4.33 for $\psi = 180^\circ, 90^\circ, 60^\circ$ and 45° . Combining equations (4.16) and (4.14) gives

$$G_H = \frac{E}{E_0} \sqrt{\left(\frac{R_{11}}{R_{11} + R_{14} - 2R_{12}} \right)} [\cos(\beta d \cos \phi) - \cos(\beta b \sin \phi)] \quad (4.17)$$

The expression for E_0 is given by equation (1.3) if the actual field strength is required. Kraus⁽¹⁴²⁾ has calculated the above expression with the result shown in Fig. 4.34 in which the corresponding curves for $\psi = 45^\circ$ and 60° are also shown. Furthermore he also took into account the effect of some dead loss resistance at the dipole terminals and this has the effect shown by the dotted lines in Fig. 4.34.

The conclusion which is to be drawn from these curves is that there is a definite optimum range of values for d . Below this range the effect of loss resistance becomes serious, above

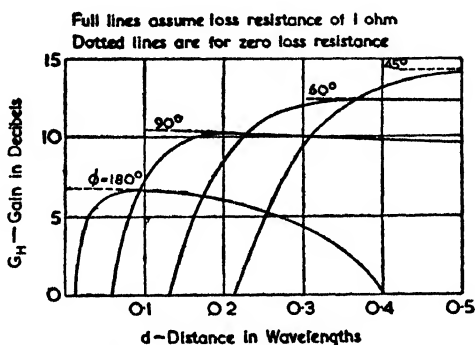


FIG. 4.34. VARIATION OF GAIN WITH SPACING OF DIPOLE IN A CORNER REFLECTOR (Kraus, Proc. I.R.E., Nov., 1940)

this range the beam will be split into two lobes, one on either side of the centre line. The following ranges are suggested by Kraus—

Angle	Distance d
180°	$0.1 - 0.3\lambda$
90°	$0.25 - 0.7\lambda$
60°	$0.35 - 0.75\lambda$
45°	$0.5 - 1.0\lambda$

Suitable dimensions for the sides are $h = d + \lambda/2$ and $l = d + \lambda$.

The theory of the corner reflector has received further treatment by Moullin,⁽¹⁴⁴⁾ who uses the method of expanding terms such as $\cos(\beta d \cos \phi)$ into a Fourier series whose coefficients are Bessel functions of the first kind. One of the results of this method of analysis is to show that the polar diagram is indistinguishable from a sine curve (when the angles are plotted on a linear scale) if the circumferential width at the

dipole does not exceed $\lambda/2$; even if this circumferential width is as great as $3\lambda/2$ the departure from a sine curve is not appreciable.

Some Experimental Results

In addition to the experimental results of Kraus and Moullin an interesting set was obtained by McPetrie, Ford and

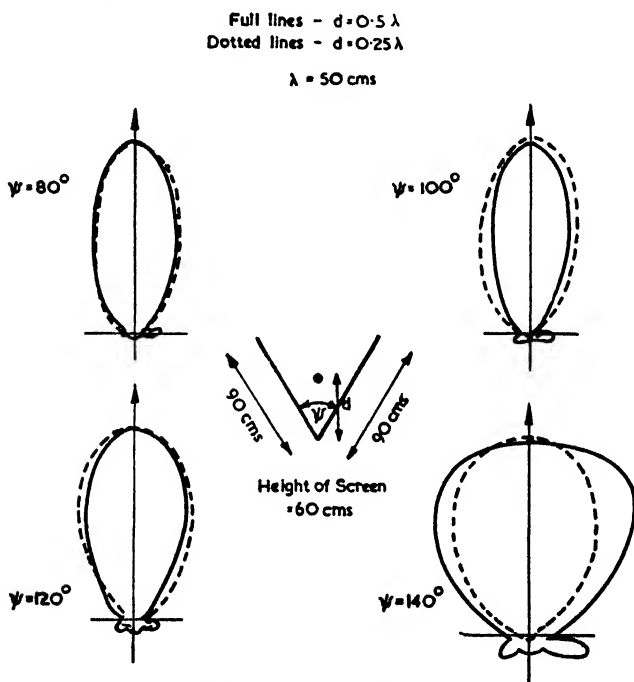


FIG. 4.35. EXPERIMENTAL POLAR DIAGRAMS OF CORNER REFLECTORS
(McPetrie, Ford and Saxton, *Wir. Eng.*, June, 1945)

Saxton.⁽¹¹⁸⁾ The polar diagrams of Fig. 4.35 have been selected from their results, while Fig. 4.36 shows the gain characteristics of their reflectors.

A convenient and easily remembered set of dimensions is $\psi = 90^\circ$, $d = \lambda/2$, $h = \lambda$ and $l = 1.5\lambda$ (the dimensions for h and l are not at all critical, while those for ψ and d are moderately uncritical).

Both Kraus and Moullin found that the sides could be made of wire netting or else of parallel rods whose spacing was about 0.1λ and whose total lengths were in excess of 0.5λ . One of

the results of some similar experiments is shown in Fig. 4.37. It was found that the spacing of the rods for a grid-type corner

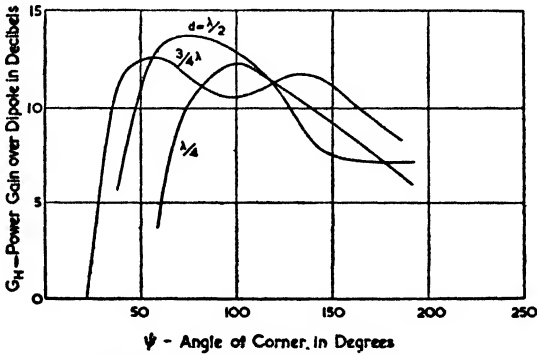


FIG. 4.36. EXPERIMENTAL CURVES SHOWING POWER GAIN OF CORNER REFLECTORS
(McPetrie, Ford and Saxton, *Wir. Eng.*, June, 1945)

reflector could be reduced to $\lambda/4$ before the forward gain was reduced by as much as 3 db, while with a spacing of $\lambda/8$ the

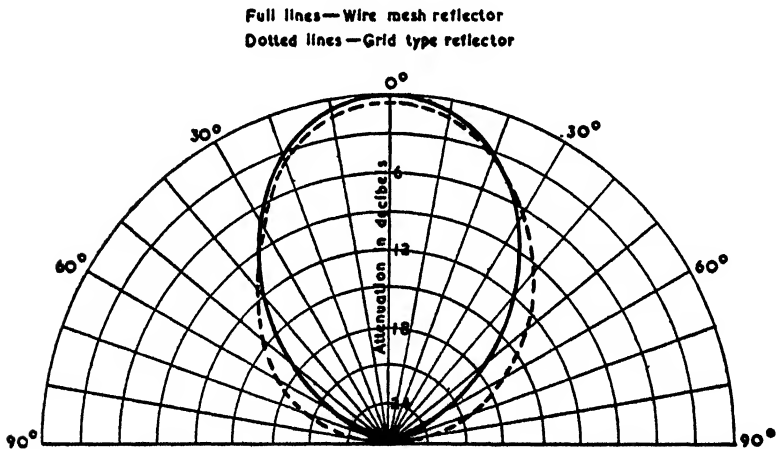


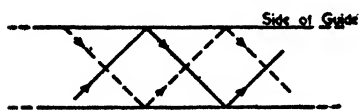
FIG. 4.37. EXPERIMENTAL POLAR DIAGRAMS OF A GRID-TYPE CORNER REFLECTOR

gain was within 1 db of that given by a solid sheet. The effect of varying the lengths of the parasitically excited rods was similar in principle to that observed by Köhler⁽¹⁴¹⁾ for semi-parabolic mirrors, i.e. with the wider spacing the tuning was

in the region of $l = \lambda/2$ but for the $\lambda/8$ spacing a maximum was obtained with greater lengths, the adjustment of the lengths being quite uncritical. It is obvious that, when relatively widely spaced tuned parasitic elements are used, the most favourable disposition is given by a Yagi type of array since the end elements of a grid-type corner reflector are not very effective.

4.4. HORN RADIATORS

Since an electromagnetic horn is essentially a flared-out waveguide, a discussion of such horns involves reference to waveguide properties and terminology. The subject of waveguides has been dealt with quite extensively in recent literature (see,



The full and dotted lines represent the direction of propagation of two distinct plane waves

for example, references (14), (18), (20), (21) and (24)), but we shall commence with a very brief outline of their properties.

Waveguides

FIG. 4.38. WAVEGUIDE PROPAGATION VIEWED AS SUCCESSIVE REFLECTIONS BY TWO INTERSECTING PLANE WAVES

An instructive way of viewing the action of a waveguide is to consider the case of a rectangular guide in which two waves are being propagated in the manner shown in Fig. 4.38. The two sets of waves make equal angles with the line of the guide and are reflected from the walls at equal angles.

The wavelength must be such as to give the correct boundary conditions, i.e. there must be no tangential electric intensity at the conducting surfaces of the guide. Conversely if the wavelength is fixed the angle of intersection of the two sets of waves must be such as to give this boundary condition. The phase velocity of the resultant wave is directly related to the angle at which the two sets intersect, and becomes infinite at the cut-off frequency. As this condition is approached the two component sets of waves suffer a greater and greater number of reflections for a given distance along the guide until at the cut-off frequency they are striking the walls at right angles.

The structure of the resultant wave down the guide is such that it either has a longitudinal component of electric intensity (when it is called an E wave) or else it has a longitudinal component of magnetic intensity (an H wave). The first case

would arise if the polarization of the component waves in Fig. 4.38 were in the plane of the paper, and the second case if the polarization were at right angles to the paper. Fig. 4.39 shows the simplest configuration of lines of electric intensity and magnetic intensity which can result in the two cases—examples of two higher modes are given in Fig. 4.40. It will be noticed that the method of classification is such that an

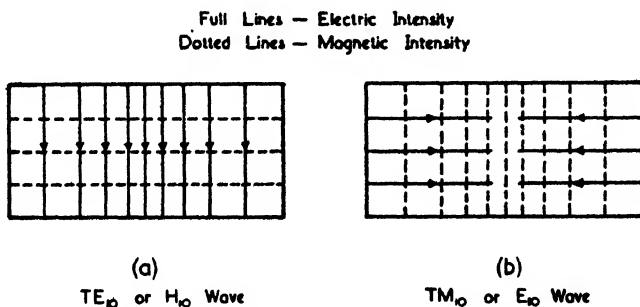


FIG. 4.39. SIMPLEST FIELD PATTERNS FOR E AND H WAVES IN A GUIDE OF RECTANGULAR CROSS-SECTION

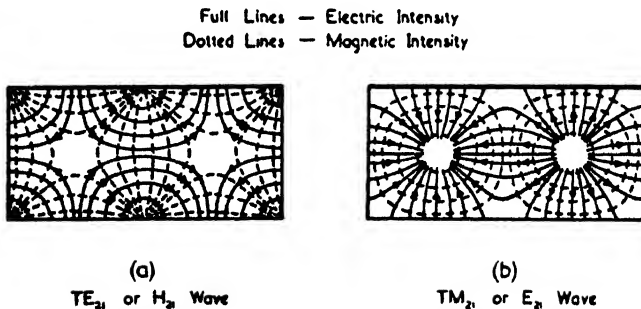


FIG. 4.40. EXAMPLES OF HIGHER MODES IN A RECTANGULAR WAVEGUIDE

H_{mn} wave has m half-sinusoids in the distribution of electric field intensity along the side a , and n half-sinusoids along the side b . It is usual for m to refer to the longer side, though sometimes the opposite convention is used. When $n = 0$ the length of the short side is immaterial.

An alternative designation for E and H waves is to call them transverse magnetic, or TM, waves, and transverse electric, or TE, waves respectively. This form of classification is also shown on Figs. 4.39 and 4.40. It has the advantage that the suffixes then refer to the half-sinusoids of the same

type of field as the symbols to which they are attached, i.e. a TE_{10} wave has one half-sinusoid of *electric* field distribution. A TEM wave, that is a transverse electromagnetic wave, has no longitudinal components of either form and therefore represents the case of a normal wave propagation in space.

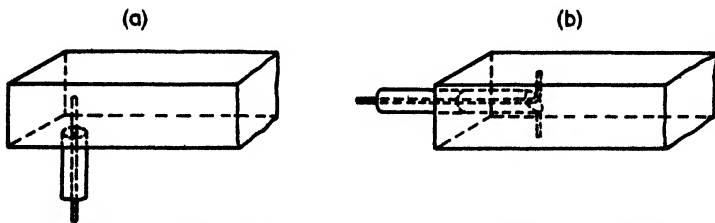


FIG. 4.41. TWO METHODS OF EXCITING TE_{10} WAVES IN A RECTANGULAR WAVEGUIDE

Excitation of Waveguides

Fig. 4.41 shows two methods of producing a transverse electric wave in a rectangular waveguide when the energy is fed via a coaxial line. The guide may also be excited directly by the

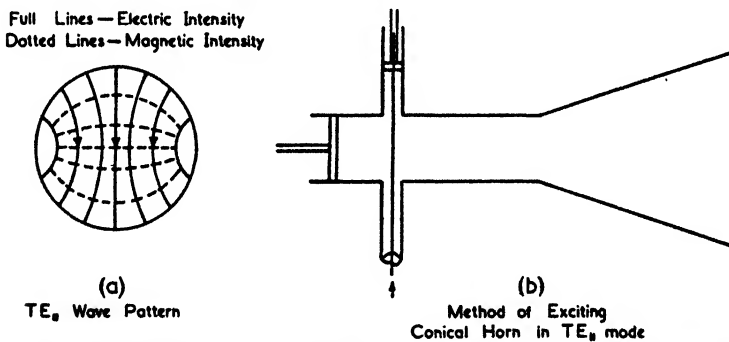


FIG. 4.42. EXCITATION OF TE_{11} WAVE IN A GUIDE OF CIRCULAR CROSS-SECTION

electron stream of the generating valve in which case the generator and the guide are built as one unit.

The matching conditions with the coaxial feed are complicated and must, in the main, be determined experimentally. For this purpose one can employ either two tuning stubs or else one tuning stub with a variable piston at the back of the guide. A tuning arrangement on the latter lines is shown in Fig. 4.42, in which the application is the excitation of TE_{11}

waves in a guide of circular cross-section. The field distribution of this particular mode is also shown and it will be noticed that it resembles that of a TE_{10} mode for a rectangular guide.

The difference in the suffixes is due to the fact that the solutions in the case of the circular guide are expressed in cylindrical co-ordinates. TE_{01} and TM_{01} modes are possible in circular guides, the corresponding field distributions of E and H being concentric circles; these modes therefore have the useful property of circular symmetry. Of the two forms the TM_{01} is more convenient since the critical wavelength is $1.31d$, whereas for the TE_{01} mode it is only $0.82d$ (d being the diameter of the tube).

Radiation from Waveguides

The simplest theoretical approach is to apply Huygens' principle to the wavefront at the mouth of the guide. This involves considering each portion of the wavefront as a secondary source of radiation whose amplitude and phase are given by the general pattern of the wave as it exists in the waveguide, i.e. the pattern is assumed to be substantially unaltered in the region of discontinuity where the wave is being launched into free space. As is well known in optics, the secondary source must be assumed to have a polar characteristic which is zero in the reverse direction to that in which the wave is travelling—in this way we can account for the fact that the radiation is not also propagated backwards from the secondary sources. This polar characteristic is called the "obliquity factor" and is given by

$$F(\phi) = 1 + \cos \phi \quad (4.18)$$

where ϕ = angle with the normal to the wavefront at the secondary source.

There are a number of difficulties associated with the formulation of the correct boundary conditions (for a discussion of this problem the reader may consult Baker and Copson⁽⁴⁾) but from an engineering point of view this fact may be overlooked. Indeed even the obliquity factor may be neglected to a first approximation in considering the main forward lobe.

The radiation from the open end of a waveguide is fairly directive because the guide is at least half a wavelength wide in one of its dimensions. If the sides of the waveguide are several wavelengths long the polar diagram will be quite sharp.

We shall consider first the forward gain of a *uniform* sheet of current or secondary sources: this can be shown to be⁽²¹⁾

$$G_o = \frac{A}{\pi(\lambda/2\pi)^2} \quad . \quad . \quad . \quad (4.19)$$

where A = surface area of sheet.

This result is true for both rectangular and circular surfaces but their area should be at least half a square wavelength. The denominator has been left in the form which indicates that it equals the area of a circle whose circumference is equal to one

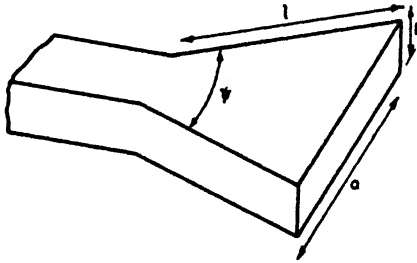


FIG. 4.43. DIAGRAM OF A SECTORAL HORN

wavelength. This is also the cross-sectional area of absorption of an isotropic radiator as is shown by equation (5.3).

Schelkunoff⁽⁷⁷⁾ has shown that for a rectangular waveguide excited in its dominant mode, the gain of the radiation pattern from an open end is given by

$$G_o = \frac{32}{\pi} \frac{ab}{\lambda^2} \quad . \quad . \quad . \quad (4.20)$$

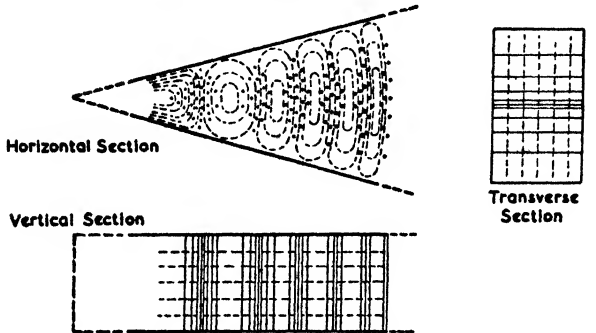
Comparing this with equation (4.19) shows that the opening has an *effective area* of as much as $8/\pi^2$ times the actual area. As a numerical example, we may consider the radiation from a guide whose sides are $a = 3\lambda$ and $b = 0.5\lambda$; then the forward gain is $G_o = 15.3$ (i.e. 24 db).

Using the open end of a large waveguide as a radiator has two disadvantages. One is that the actual size of such a guide is undesirably large; the other is that if the guide is large it will also have higher transmission modes and these will cause irregularities in the polar diagram. Both these objections can be overcome by the use of a flared waveguide, or horn radiator as it is more commonly called. Such radiators may be subdivided into sectoral, pyramidal, conical and biconical horns.

The Sectoral Horn

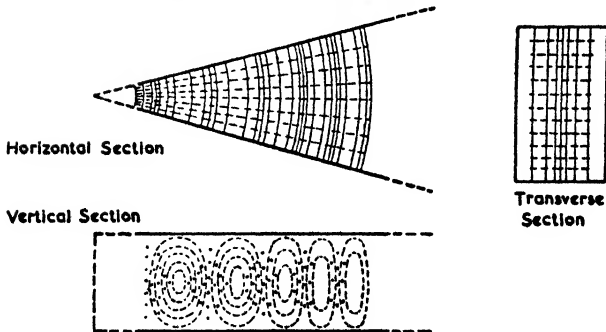
The sectoral horn is flared out in one dimension only and therefore has a beam which is sharp in the plane of the flaring

Full line — electric field
Dotted line — magnetic field



(a) TE_{10} mode of excitation

Full line — electric field
Dotted line — magnetic field



(b) TE_{01} mode of excitation

FIG. 4.44. FIELD DISTRIBUTION IN A SECTORAL HORN

but relatively broad in the other plane. To keep the size as small as possible the horn is normally excited in the TE_{10} or TE_{01} modes, as illustrated in Fig. 4.44.

The dimensions of the horn will be specified in the manner shown in Fig. 4.43. An important difference arises in

comparison with the case of a uniform waveguide, and that is that the attenuation of the wave in the guide is no longer uniform but decreases as the wave travels towards the opening. It was shown by Barrow and Chu⁽¹²⁵⁾ that the attenuation of the higher modes persisted over a greater radial distance than that of the simplest mode. Hence the horn acts as its own filter by producing extra attenuation on the higher modes.

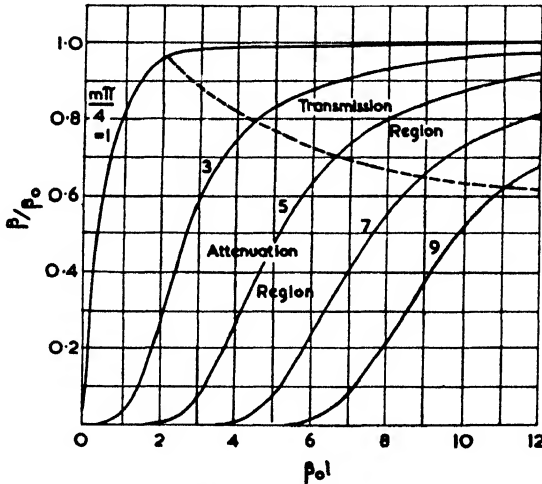


FIG. 4.45. VARIATION OF PHASE VELOCITY WITH DISTANCE ALONG HORN
(Barrow and Chu, *Proc. I.R.E.*, Jan., 1939)

In the attenuating region the phase velocity β is less than the corresponding free-space value β_0 (in most other parts of the book the distinction is not needed and β_0 has been written without the suffix). The variation of β with radial distance along the horn is shown in Fig. 4.45 for various flare angles and transmission modes of the type TE_{m0} . The border line between the attenuating and transmission regions is indicated by the dotted curve (the transition does not, of course, occur at a sharply defined radius). Suppression of higher modes of the type TE_{0n} may be obtained by choosing a value for b which is intermediate between the values $\lambda/2$ and $3\lambda/2$. The TE_{03} wave is then strongly attenuated, while to discriminate between the TE_{03} and other even modes a symmetrical exciting system should be used.

Fig. 4.46 shows some of the experimental polar diagrams obtained by Barrow and Lewis⁽¹²⁷⁾ using a sectoral horn whose

flare angle could be altered. A curve of the power gain (Fig. 4.47) shows that this reaches a maximum value of 16 when

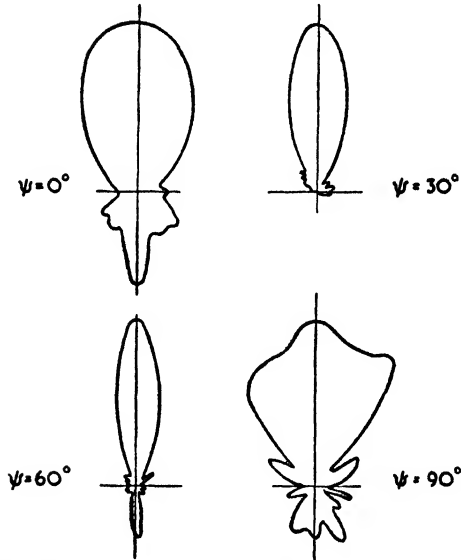


FIG. 4.46. EXPERIMENTAL POLAR DIAGRAMS FOR VARIOUS ANGLES OF FLARE (Barrow and Lewis, *Proc. I.R.E.*, Jan., 1939)

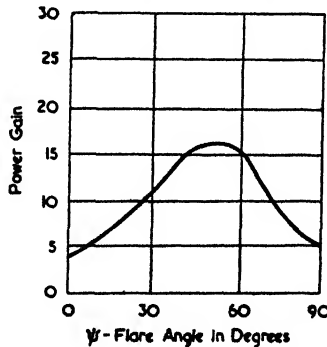


FIG. 4.47. POWER GAIN OF SECTORAL HORN (Barrow and Lewis, *Proc. I.R.E.*, Jan., 1939)

$\psi \doteq 50^\circ$. (The gain figure is approximately that referred to a half-wave dipole, i.e. it is roughly equal to G_H .)

The reason for this optimum value of flare angle is easy to see; for small angles the gain is low, due to the smallness of

the width a , while for angles approaching 90° the wavefront at the mouth of the horn has become so nearly spherical that the radiation components from the secondary sources on this wavefront are not in phase at field points along the axis. This latter state of affairs is illustrated in Fig. 4.48. A convenient

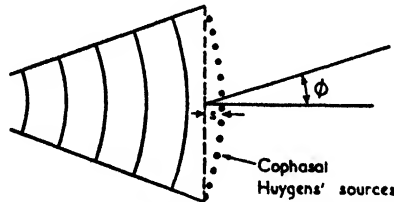


FIG. 4.48. DIAGRAM SHOWING PHASE SLIP IN HORNS

rule of thumb giving the greatest permissible "phase slip" without noticeable loss of gain is that the distance s in Fig. 4.48 should not exceed $\lambda/4$.

Barrow and Lewis also measured the field distribution across the mouth and found that as ψ approached 90° the distribution

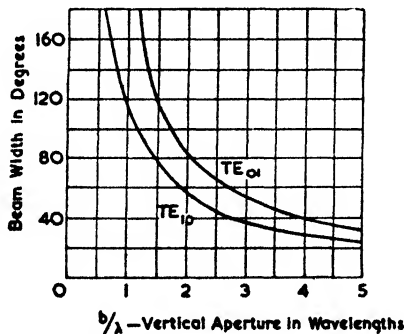


FIG. 4.49. DEPENDENCE OF VERTICAL BEAM WIDTH ON HEIGHT OF SECTORAL HORN

(Chu and Barrow, *Trans. A.I.E.E.*, July, 1939)

became very uneven and that this had its counterpart in the jaggedness of the corresponding polar diagram. These distribution diagrams corresponded to the "equivalent current distributions" in the plane of the directrix as discussed in the section on parabolic antennae. If the intensity distribution is reasonably cophasal the resultant polar diagram may be arrived at in exactly the same manner as described for parabolic

mirrors, i.e. we base our calculations on a reasonably well fitting distribution law, the equation for which may readily

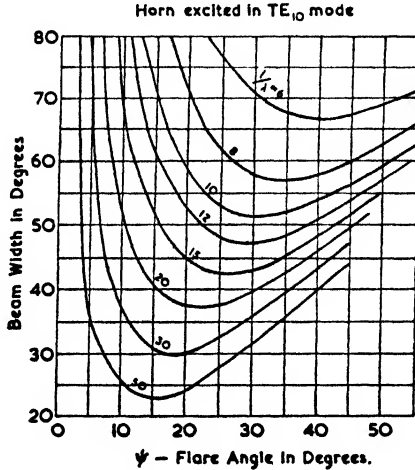


FIG. 4.50. VARIATION OF THE HORIZONTAL BEAM WIDTH WITH THE FLARE ANGLE OF A SECTORAL HORN (Chu and Barrow, *Trans. A.I.E.E.*, July, 1939)

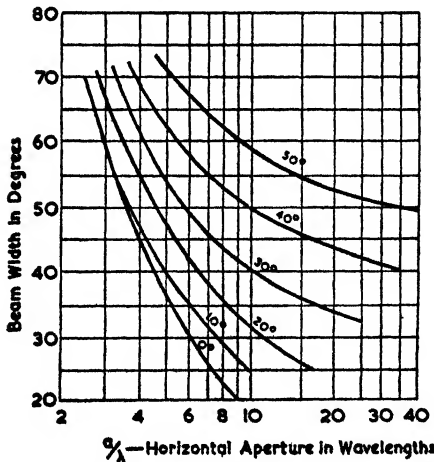


FIG. 4.51. VARIATION OF THE HORIZONTAL BEAM WIDTH WITH THE APERTURE OF A SECTORAL HORN (Chu and Barrow, *Trans. A.I.E.E.*, July, 1939)

be integrated. Barrow and Lewis obtained reasonable agreement with experimental results for flare angles up to 50° by

simply assuming a sinusoidal distribution of cophasal sources across the mouth of the horn.

Chu and Barrow⁽¹⁸⁸⁾ have given a detailed set of design curves for the sectoral horn, some of which are reproduced in Figs. 4.49 to 4.52. The beam width referred to is defined as the angle between the direction for which the field is 10 per

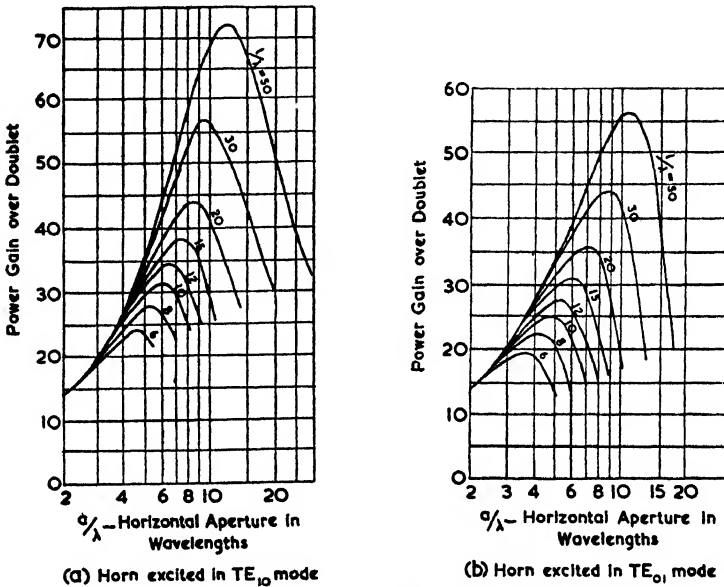


FIG. 4.52. VARIATION OF POWER GAIN WITH THE APERTURE OF A SECTORAL HORN

(Chu and Barrow, *Trans. A.I.E.E.*, July, 1939)

cent of its maximum value. Also side “ a ” is the horizontal side for these figures, i.e. the horn is flared in a horizontal plane. The figures are self-explanatory but one or two observations are of interest.

Fig. 4.50 shows that sharper beams are obtainable with the smaller flare angles, but it should not be overlooked that the horns become excessively long at small angles. It is to be expected that the vertical polar diagram would be sharper for the TE_{10} mode than for the TE_{01} mode (Fig. 4.49), since in the former case the field distribution in the direction of b is uniform whilst in the latter case it has a sinusoidal variation of amplitude. This extra concentration in the vertical plane accounts for the higher gains obtainable with the TE_{10} mode.

The Pyramid Horn

A pyramid horn is one which is flared in both planes. The design features of such horns are largely covered by the previous discussion on sectoral horns. This follows from the fact that a flare in the vertical plane for a TE_{10} mode corresponds to a flare in the horizontal plane for a TE_{01} mode and vice versa.

The same maximum permissible phase slip may be assumed as was given for sectoral horns, i.e. the middle of the spherical wave at the mouth should not be more than one-quarter of a wavelength in front of the plane of the mouth. By inserting

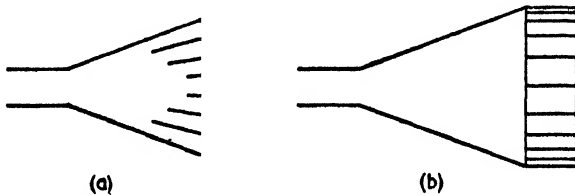


FIG. 4.53. BAFFLES FOR CORRECTING PHASE SLIP IN HORNS

correcting plates in the horn as shown in Fig. 4.53 this phase slip can be corrected since the phase velocity is increased at the ends by their presence. In this way the forward gain of large horns can be appreciably increased (the alternative would be to make the horn exceedingly long—which is not practicable in most cases). Correcting baffles of this nature have been described by Rust⁽¹⁴⁵⁾ and are essentially for very large horns whose apertures are large enough to permit such subdivisions.

The Conical Horn

Conical horns are flared-out waveguides of circular cross-section; hence the most suitable mode of excitation is the TE_{11} mode shown in Fig. 4.42. A detailed experimental study of such horns was made by Southworth and King.⁽¹⁴⁶⁾ Their results showed that for a conical horn whose sides have a length of about 3λ the optimum flare angle is about 50° . Another set of experiments demonstrated that if the flare angle was kept fixed at 40° , then the forward gain was not increased appreciably for side lengths exceeding 4λ —up to such a length the power gain increases directly as the area of the aperture.

Fig. 4.54 shows the effect of varying the flare angle when the length of the sides is kept approximately constant, while Fig. 4.55 shows the polar diagrams for the opposite change in the variables.

The Biconical Horn

The biconical horn of Fig. 4.56 may be considered either as a particularly thick biconical antenna (in which form it is

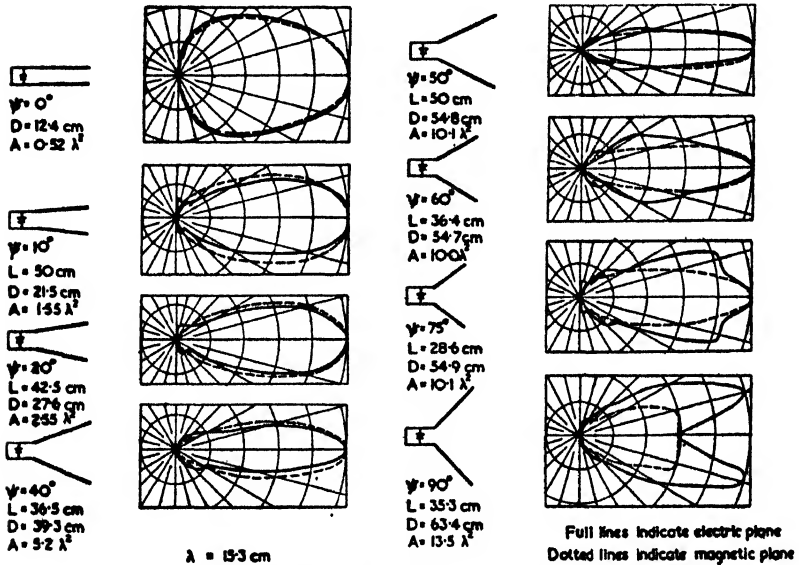


FIG. 4.54. POLAR DIAGRAMS OF CONICAL HORNS WITH VARIOUS ANGLES OF FLARE

(Southworth and King, *Proc. I.R.E.*, Feb., 1939)

mentioned in § 4.1) or as a horn of revolution about the central axis.

There are two main modes in which such an antenna may be excited. The first is the TEM mode which gives vertical polarization and is equivalent to an electric dipole and the second is the TE_{01} mode which gives horizontal polarization and therefore is related to the magnetic dipole—in both cases the vertical polar diagrams may be considerably sharper than those obtained with the related form of dipole.

A theoretical analysis of the two cases has been given by Barrow, Chu and Jansen⁽¹²⁶⁾ who obtained the curves shown in Fig. 4.57. The TEM mode may be excited by feeding the

antenna as shown in Fig. 4.56 (i.e. by treating the horn as a simple centre-fed antenna), while the TE_{01} mode is obtained by placing a small "magnetic dipole" between the two apices

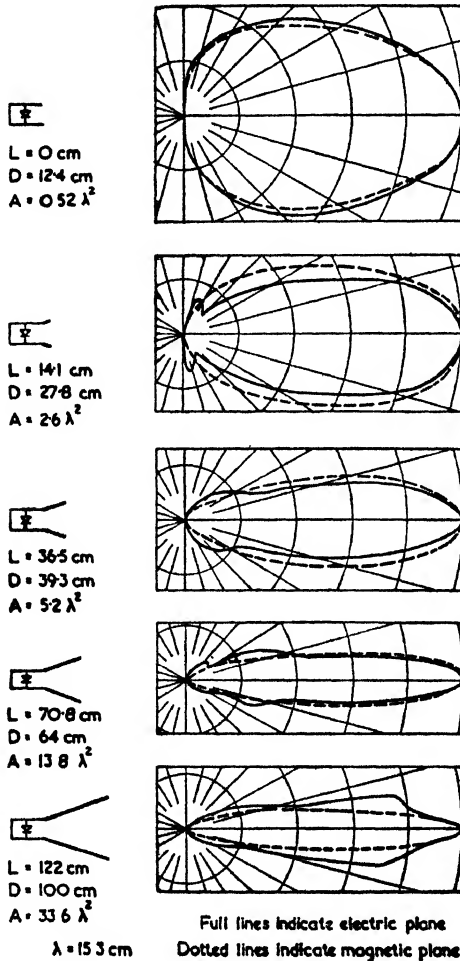


FIG. 4.55. POLAR DIAGRAMS OF CONICAL HORNS OF DIFFERENT LENGTHS (Southworth and King, *Proc. I.R.E.*, Feb., 1939)

of the cones which then act as unconnected guides. The magnetic dipole may take the form of any of the loops of the Alford type or of a coaxial-loop type of antenna.

The sharpness of the radiation pattern in a vertical plane may be determined from the sectoral horn of corresponding

flare angle and mode of excitation. Provided the phase slip is less than 90° (which is true if the length does not exceed the optimum for the flare angle in question) the polar diagram can also be calculated by the methods described for parabolic mirrors and the sectoral horn. We assume an equivalent source distribution across the aperture of the horn and interpolate from the calculated distributions

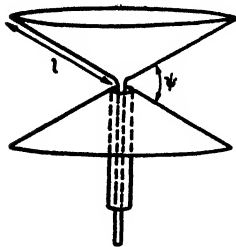


FIG. 4.56. BICONICAL HORN EXCITED IN TEM MODE

given on page 156. The assumed distribution will depend on the mode of excitation—for the TEM mode it will be a constant, and for the TE_{01} mode it will be sinusoidal.

In order to discourage the generation of higher unwanted modes, the spacing between the apexes should be kept to a small fraction of a wavelength; also for the TE_{01} mode the exciting antenna should be as symmetrical as possible. Barrow, Chu and Jansen found in their experiments that a spacing of about $\lambda/12$ gave best results for the TEM mode.

4.5. SLOT ANTENNAE

General Principles

The current distribution around a slot may be obtained by first considering the radial distribution of electric intensity along a metallic antenna of similar dimensions. Such an antenna is a half-wave dipole in the form of a strip which would just fill the slot. The distribution of electric intensity in the immediate neighbourhood of this dipole varies throughout a cycle in a manner similar to that shown in Fig. 1.3, for a thin dipole. If we consider the conditions during the part of the cycle shown in Fig. 1.3 by $1/8f$, then the electric field has the direction corresponding to the dotted lines in Fig. 4.58 (a). In the latter figure, however, they represent the magnetic lines round a slot, i.e. we have interchanged magnetic and electric lines on going from the case of a half-wave strip to a half-wave slot. Now the currents around the slot are everywhere at right angles to, and proportional to, the magnetic intensity at the surface and hence they have the distribution shown by the arrows in Fig. 4.58.

The above parallel which we have drawn between dipoles

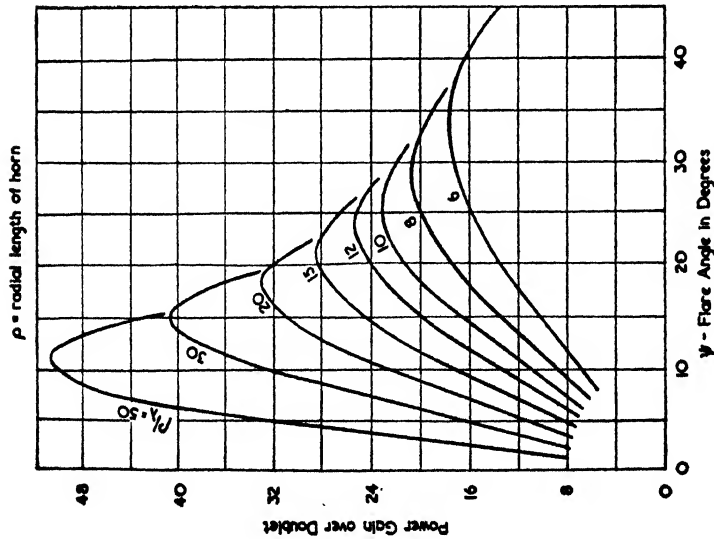


FIG. 4-57 (a). VARIATION OF THE POWER GAIN OF A BICONICAL HORN EXCITED IN THE TEM MODE WITH LENGTH AND ANGLE OF FLARE (Barrow, Chu and Jansen, *Proc. I.R.E.*, Dec., 1939)

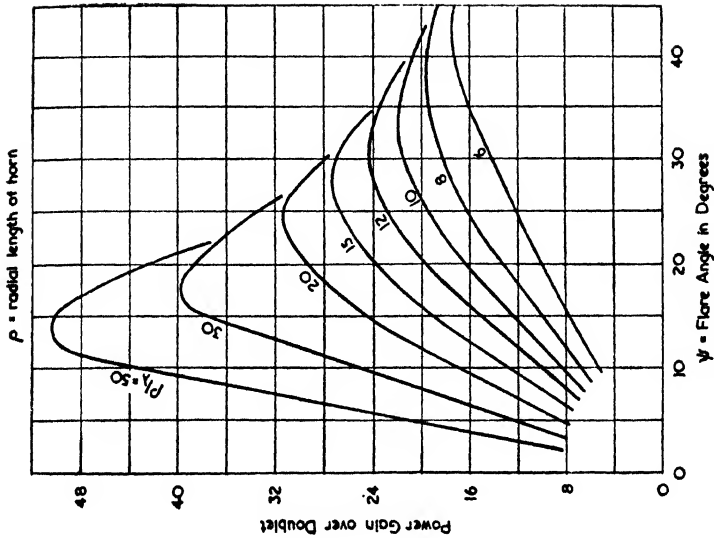


FIG. 4-57 (b). VARIATION OF THE POWER GAIN OF A BICONICAL HORN EXCITED IN THE TE₀₁ MODE WITH LENGTH AND ANGLE OF FLARE (Barrow, Chu and Jansen, *Proc. I.R.E.*, Dec., 1939)

and slots serves, amongst other things, to give an estimate of the size of the conducting surface that we must have around the slot—the surface must be of such a size as to embrace most of the static and induction fields that would exist around the complementary dipole. This criterion indicates a wide conductor of at least one-fifth of a wavelength around the edges of the slot.

A complete statement of the complementary nature of slots and strip dipoles can be obtained with the aid of Babinet's principle. For a discussion of this principle as applied to radio frequencies the reader may refer to the article by Booker.⁽¹³⁰⁾

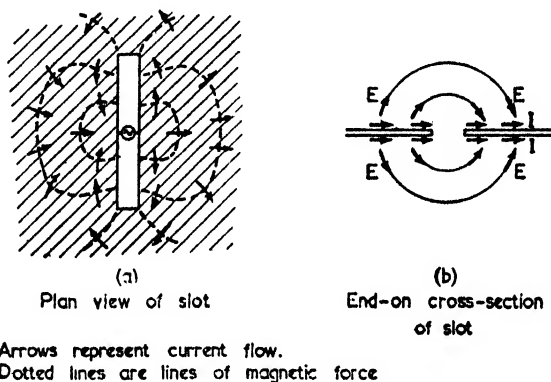


FIG. 4.5B. A SLOT ANTENNA

The principle may be stated by considering a source of electromagnetic waves (or a distribution of sources) and a plane thin sheet of metal which is pierced by any arbitrary configuration of holes. The field in the vicinity of the metal screen will be modified by its presence.

If we now replace this conducting sheet by a complementary screen (one which has obstructions where the other had holes and vice versa) then the new field distribution will be such that if added to the former field the resultant will exactly equal the field distribution obtained in the absence of any screens.

An important point is that the complementary screen must either be a perfect conductor of magnetism (a purely hypothetical case) or else the system of sources must be replaced by a conjugate system of sources which consists of elementary magnetic dipoles in place of the former elementary electric dipoles. In either case the object is to interchange the electric and magnetic fields beyond the screen.

A direct application of the above principle is shown in Fig. 4.59. Figure (a) represents an array of half-wave dipoles, while (b) is the complementary screen in which the slots have been rotated through 90° to interchange electric and magnetic quantities. In the first case the "screen" acts as a band-stop filter to the incident wave, while in the second case the screen behaves as a band-pass filter.

Input Impedance of Slot Antennae

The application of the above principle to slot antennae is shown in Fig. 4.60, in which (a) represents the case of an

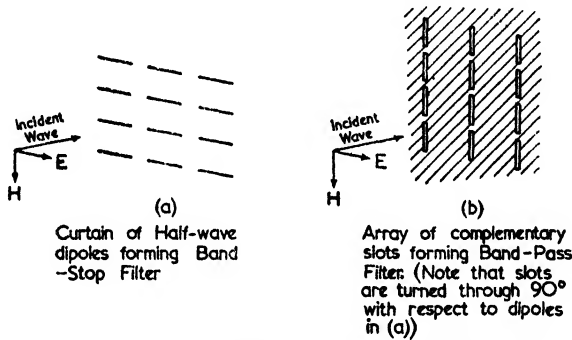


FIG. 4.59. AN APPLICATION OF BABINET'S PRINCIPLE

electric dipole and (b) that of a magnetic dipole. In the electric case E is normal to the strip and the generator is inserted between two points the impedance between which is zero; in the magnetic case H is normal to the strip and the generator is a loop of current inserted along a path of infinite impedance.

We now place a perfectly conducting screen of infinite extent around the magnetic dipole of Fig. 4.60 (b) and this state of affairs is illustrated in Fig. 4.60 (c). It will be noticed that the fields are unaltered by this addition since the condition that E should be normal to the sheet is already fulfilled.

On reversing the direction of one of the generators the field obtained becomes as shown in Fig. 4.60 (c). We may now remove the perfect conductor of magnetism, which simply leaves a slot in the conducting sheet across which are a pair of current generators connected in parallel. This change does not affect the field since there was no discontinuity in H at the strip of magnetic conductor.

The field of figure (d) is therefore identical with that of figure (a) except that

(i) the electric and magnetic components are interchanged,

(ii) the sense is changed as we cross the boundary made by the conducting sheet.

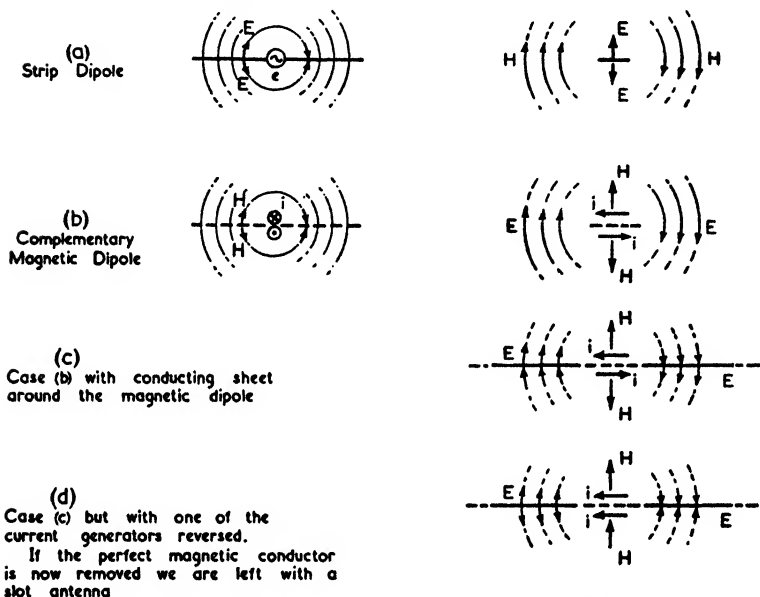


FIG. 4.60. DERIVATION OF A SLOT ANTENNA FROM THE COMPLEMENTARY DIPOLE

All the above arguments assume a sheet of infinite extent. With the practical case of a finite sheet, the reversal in sense causes the field in the plane of the sheet to be zero (Fig. 4.61 (a)). If, however, one side of the sheet is enclosed (Fig. 4.61 (b)), then the field in the plane of the sheet is approximately half that obtained with the corresponding dipole—the precise polar diagram involves taking into account the effects of diffraction and of currents round the edges.

The input impedance of the slot may be determined as follows—

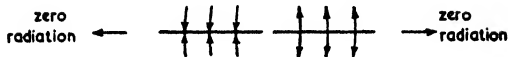
Fig. 4.62 may represent either

- (1) a strip-shaped dipole, or
- (2) a slot in a large metallic sheet.

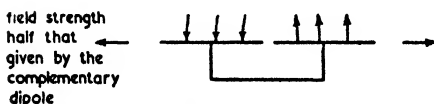
In case (1) we have

$$V_1 = \int_{XYZ} \mathbf{E}_1 ds = \int_{XY'Z} \mathbf{E}_1 ds \quad . \quad . \quad . \quad (i)$$

$$I_1 = \int_{ABCB'A} \mathbf{H}_1 ds = 2 \int_{ABC} \mathbf{H}_1 ds \quad . \quad . \quad . \quad (ii)$$



(a) Sheet open both sides (end-on view)



(b) One side of slot boxed in

FIG. 4.61. SLOT ANTENNAE WITH CONDUCTING SHEETS OF FINITE DIMENSIONS

In case (2) we have

$$V_2 = \int_{ABC} \mathbf{E}_2 ds = \int_{AB'C} \mathbf{E}_2 ds \quad . \quad . \quad . \quad (iii)$$

$$I_2 = \int_{XYZZY'X} \mathbf{H}_2 ds = 2 \int_{XYZ} \mathbf{H}_2 ds \quad . \quad . \quad . \quad (iv)$$

From the conjugate properties discussed previously it follows that

$$\int_{XYZ} \mathbf{E}_1 ds = z_{00} \int_{XYZ} \mathbf{H}_2 ds \quad . \quad . \quad . \quad (v)$$

$$\int_{ABC} \mathbf{E}_2 ds = z_{00} \int_{ABC} \mathbf{H}_1 ds \quad . \quad . \quad . \quad (vi)$$

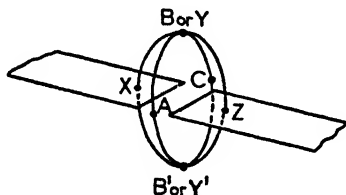


FIG. 4.62. DIAGRAM FOR CALCULATION OF SLOT IMPEDANCE

Using equations (i) and (iv) in (v) we find that

$$V_1 = \frac{1}{2} z_{00} I_2 \quad . \quad . \quad . \quad (vii)$$

Also from (ii), (iii) and (vi) we have

$$V_2 = \frac{1}{2} z_{00} I_1 \quad . \quad . \quad . \quad (viii)$$

Equations (vii) and (viii) give

$$\frac{V_1 V_2}{I_1 I_2} = \frac{1}{4} z_{00}^2$$

Hence

$$Z_1 Z_2 = \frac{1}{4} z_{00}^2 \quad . \quad . \quad . \quad (4.21)$$

The geometric mean of the input impedance of a slot and its complementary dipole is therefore equal to half the intrinsic impedance of free space (i.e. to $377/2$ ohms). Assuming a resonant impedance of 70 ohms for the dipole, we therefore have

$$\begin{aligned} Z_2 &= 503 \\ &\doteq 500 \text{ ohms} \end{aligned}$$

Practical Versions of Slot Antennae

It is normally desirable to box up one side of the slot so as to radiate over a hemisphere only. The effect of this on the

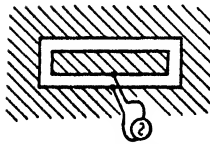
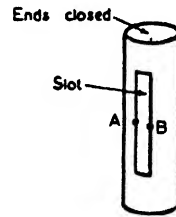


FIG. 4.63. A FOLDED SLOT ANTENNA



(a)

Position of slot
in mirror



(b)

Slot in cylinder excited
across points A B

FIG. 4.64. EXAMPLE OF SLOT ANTENNA AT THE FOCUS OF A PARABOLIC MIRROR

input impedance is to double the resistive component making it approximately 1 000 ohms.

This rather high input resistance can be reduced by using the equivalent of a folded dipole which, in its slot form, is illustrated in Fig. 4.63. Whereas a folded dipole has an input impedance which is four times that of a simple dipole, the folded slot has an input impedance which is one-quarter that of the simple slot. Hence a folded slot which is boxed up on one side will have an input resistance of about 250 ohms.

An interesting application of slot antennae has been mentioned by Ratcliffe⁽³⁶²⁾ and is shown in Fig. 4.64. In this case the slot is cut into the side of the cylinder which is mounted at the focus of a semi-parabolic mirror designed to give a sharp beam in the horizontal plane. As a result good illumination of the reflecting surface of the mirror is obtained with horizontal polarization. Under the same conditions a horizontal dipole would fail to give adequate illumination of the edges of the mirror.

An array of slots can be obtained by making a series of slots along a waveguide; if these slots interrupt the lateral currents in the guide they will effectively be in parallel. This mode of operation may be obtained as shown in Fig. 4.65 (a) which shows "shunt-displaced" slots, or else the "shunt-inclined" method of Fig. 4.65 (b) may be used. The former method has the advantage of negligible mutual coupling between the slots, while the latter is more easily constructed if the operating wavelength is less than 3 cm.

In order to minimize secondary lobes the cophasal sources should be as close together as possible. This means in practice

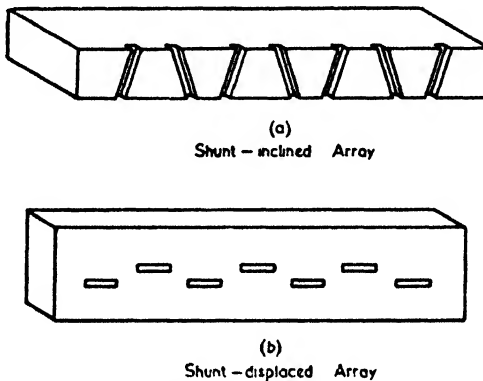


FIG. 4.65. TWO TYPES OF SLOT ARRAYS

that the slots are spaced every half-wavelength along the guide and adjacent slots are excited in the opposite sense. For this reason adjacent shunt-displaced slots are spaced on opposite sides of the centre line, while adjacent shunt-inclined slots are inclined in the opposite sense. For details on the design of slot arrays the reader is referred to a recent book by Watson.⁽²⁴⁾

4.6. DIELECTRIC ANTENNAE

As the wavelength of the shortest radio waves generated has decreased, so the techniques employed have come nearer to those used in optics. One of these steps has been the use of dielectric material to obtain a lens action or its equivalent. Two examples of the use of dielectrics are shown in Fig. 4.66, both of which have the object of matching the wave impedance in the interior of the horn to that in free space, thereby simplifying the tuning adjustments. Antennae of this type were

investigated by Mallach whose work is described in *Evaluation Report No. 273* of the British Ministry of Supply.

A more direct use of the dielectric is to make it in the form of a rod (Fig. 4.67) one end of which is excited by a small

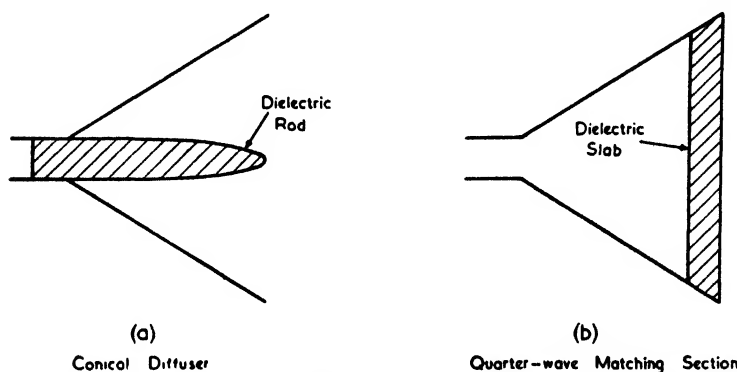


FIG. 4.66. USE OF DIELECTRIC MATERIAL IN HORNS TO IMPROVE MATCHING

antenna. This form of dielectric antenna is commonly called a "polyrod" antenna, since the dielectric material is often polystyrol. The rod in this case may be considered as a leaky waveguide which results in a continuous endfire array. The

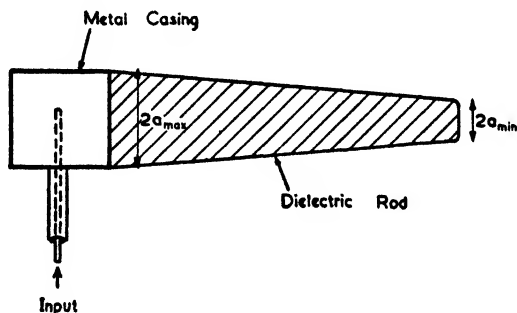


FIG. 4.67. A POLYROD ANTENNA

beam width of a polyrod varies with the length of the rod in the manner shown in Fig. 4.68. This figure suggests that a length of three wavelengths is a useful compromise between good directivity and reasonable size.

The effect of tapering the rod is shown in Fig. 4.69, from which it can be seen that tapering reduces the secondary lobes, but the beam width of the main lobe is slightly increased at

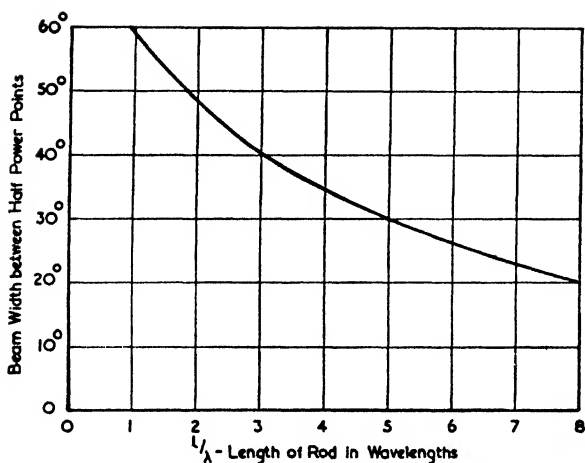


FIG. 4.68. VARIATION OF BEAM WIDTH WITH LENGTH FOR A TYPICAL UNIFORM POLYROD ANTENNA

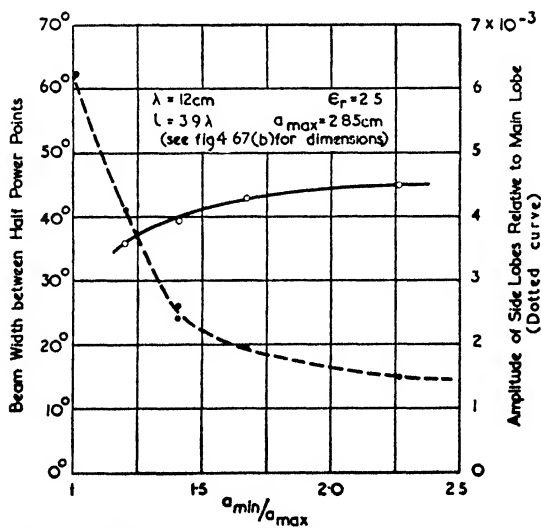


FIG. 4.69. BEAM WIDTH AND SIDE LOBES OF A POLYROD ANTENNA FOR VARIOUS DEGREES OF TAPER (Mallach and Zinke, *L'Onde El.*, Oct., 1946)

the same time. Overall bandwidths of 30 per cent of the mid-frequency are obtainable for changes in input resistance of 2 : 1 while the input impedance may have any value between

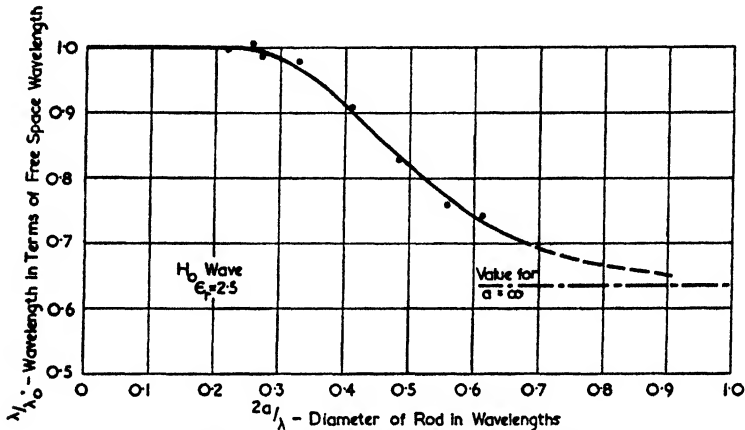


FIG. 4.70. VARIATION OF WAVELENGTH ALONG A DIELECTRIC ROD WITH DIAMETER OF ROD

(Mallach and Zinke, *L'Onde El.*, Oct., 1946)

10 and 300 ohms according to the dimensions of the input circuit.

If we measure the wavelength along a dielectric rod in terms of the free-space wavelength we obtain a curve of the type

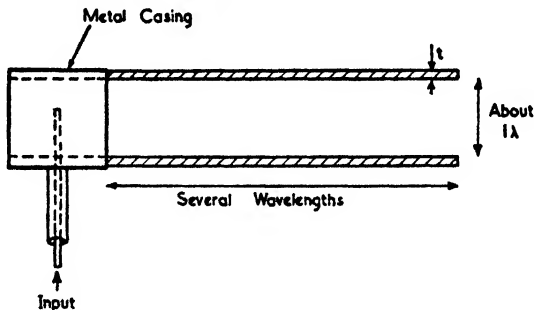


FIG. 4.71. SKETCH OF A HOLLOW POLYROD ANTENNA

shown in Fig. 4.70 in which the diameter of the rod is the independent variable. From this curve we see that when the diameter is less than about one-third of the free-space wavelength then $\lambda \cong \lambda_0$. Mallach and Zinke⁽¹⁴⁸⁾ have obtained

the following empirical formulae for determining the cross-sectional areas of a polyrod (the cross-section may be either circular, square or rectangular).

$$\begin{aligned} \text{Initial cross-section } A_1 &= \frac{\lambda_0^2}{4(\epsilon_r - 1)} \\ \text{Final cross-section } A_2 &= \frac{\lambda_0^2}{10(\epsilon_r - 1)} \end{aligned} \quad (4.22)$$

To avoid appreciable dielectric losses the power factor of the material should not exceed 50×10^{-4} .

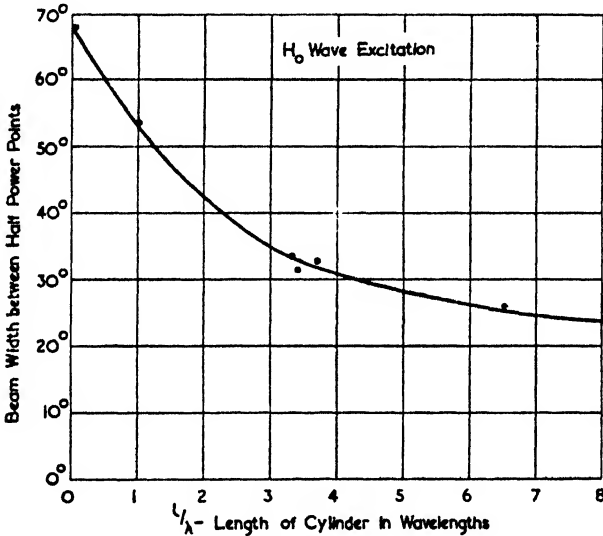


FIG. 4.72. VARIATION OF BEAM WIDTH WITH LENGTH OF A HOLLOW POLYROD (Mallach and Zinke, *L'Onde El.*, Oct., 1946)

Hollow tubes may also be used for dielectric antennae (Fig. 4.71). For example, Mallach made an antenna consisting of a hollow cardboard tube ($\epsilon_r \doteq 4$) some 12λ long and this gave a beam whose width at the half-power points was 20° . Fig. 4.72 shows the variation of the beam width with the length of the tube.

Hollow polyrods should be about a wavelength in diameter and have a thickness which is given by

$$t = \frac{\lambda_0}{10\sqrt{\epsilon_r - 1}} \quad (4.23)$$

where λ_0 = wavelength in free space.

The bandwidth of a hollow tube is rather wider than that of the solid polyrod—a total band of 40 per cent can be covered for a standing wave ratio limit of 2 : 1. Since with the hollow rod a smaller proportion of the total energy travels in the dielectric, a greater power factor can be tolerated so that materials with a power factor of as much as 200×10^{-4} may be used.

Receiving Antennae

IN the previous chapters the discussion on antennae has been confined almost entirely to their properties as transmitters of energy. For this purpose an antenna is excited at a pair of terminals situated in most cases at the base or at a current antinode. On the other hand, if an antenna is functioning as a receiver of energy the applied e.m.f. is distributed throughout its entire length, though in all other respects the system is essentially the same. We should therefore expect a close similarity in the properties of an antenna whether used as a transmitter or as a receiver of electromagnetic energy. The theoretical reasons for these similarities are given in Vol. I, § 4.6, while the following section contains a summary of the physical results.

Since the ultimate performance of a receiving system depends on the signal-to-noise ratio, an appreciable proportion of this chapter is devoted to noise considerations. When noise limitations are taken into account, the efficiency of an antenna rarely proves to be of any importance and hence receiving antennae may be designed without paying special attention to joulean losses. In the case of long- and medium-wave reception the losses in the input coupling circuits are also immaterial—provided that the transmission loss is not excessive and that the first valve is not unduly noisy.

There are two other respects in which the design of a receiving antenna may differ from that of a transmitting antenna—one is that strict economy must often be practised, and the other that the reception is usually desired over a very wide range of frequencies.

It is only in the case of direction finding, where the position of the loop antenna for minimum pick-up is utilized, that the joulean losses become important. This case is discussed in detail and illustrated by examples on pages 326–34.

5.1. GENERAL PROPERTIES

Relations between Transmission and Reception

In Vol. I, § 4.6, it was shown that the following characteristics of an antenna are identical for both transmission and reception—

- (a) the impedance,
- (b) the polar diagram,
- (c) the effective height.

In applying these results it must be remembered that the impedance is measured between the same pair of terminals in both cases. Furthermore the equality of the polar diagrams assumes that the generator impedance of the transmitting case is replaced by an equal load when the antenna is acting as a receiver. The equality of the effective heights depends only on a uniform field for reception and is independent of ground constants or height above the ground.

Owing to the fact that in reception the applied e.m.f. is distributed over the conductor, the current distribution is not necessarily the same as in the transmitting case. This fact was first pointed out by Korshenewsky⁽⁶¹⁾ and has been elaborated by Colebrook.⁽¹⁵⁸⁾

Equivalent Circuit

Since the impedance of a receiving antenna is independent of the field distribution we may replace the antenna by the equivalent circuit shown on the left-hand side of the dotted line in Fig. 5.1. In the case of a plane wavefront parallel to a straight antenna and polarized in the same direction, the equivalent series e.m.f. is given by

$$e = Eh_e \quad . \quad . \quad . \quad (5.1)$$

where E = field in volts/metre,

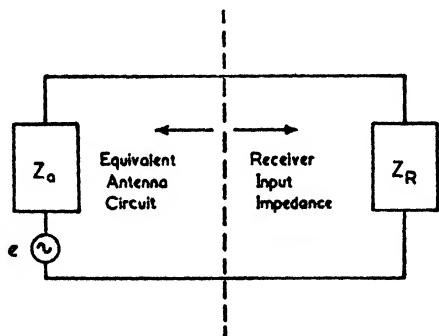
h_e = effective height of antenna in metres.

If E is the r.m.s. value of the field, then e will also be the r.m.s. value. In the more general case in which the electric vector in the wavefront makes an angle θ with the antenna, the induced e.m.f. will be equal to $Eh_e \cos \theta$.

The concept of effective height was discussed in Vol. I, § 4.3, where it was shown that for a simple vertical antenna

whose height h is less than $\lambda/10$ the effective height is 0.5 times the actual height. By providing some form of capacitance loading at the top, this value may be increased in practical cases to about 0.7 or 0.8 times the actual height. For a half-wave dipole the effective height is λ/π .

It will be noticed that the only difference between the equivalent circuit in Fig. 5.1 and the corresponding circuit for transmission is that the series e.m.f. is on the left-hand side,



Z_0 = impedance of antenna (determined in the same way as in the transmitting case)

e = induced e.m.f. (given by equation 10.1)

FIG. 5.1. EQUIVALENT CIRCUIT OF A RECEIVING ANTENNA

whereas for the transmission case it would be on the right-hand side (and Z_R would represent the generator impedance).

Noise Considerations

In the transmitting case the main requirement is to radiate as much of the available energy as possible, whereas in the receiving case the chief consideration is a good signal-to-noise ratio. These requirements lead to the same design if the conditions are such that even in the receiving case the joulean losses have to be kept low.

However, if the atmospheric noise together with the noise associated with the radiation resistance is high in comparison with the thermal noise generated by the dead-loss resistance, then the efficiency of the receiving antenna is quite unimportant. This condition applies to all antennae operating on wavelengths above about 1 m, and hence it would appear

that it is only with microwave receiving antennae that any care need be taken with regard to joulean losses. With the present valves, however, the noise due to the first valve is relatively high at wavelengths below 1 m so that even at these wavelengths the noise due to joulean losses in the antenna will be negligible (but in this case long transmission lines or other "lossy" input circuits must be avoided).

On the other hand it is always an advantage to use a directive antenna for reception. For a given radiation and loss resistance the received noise power will be the same (assuming both thermal and atmospheric noise to be uniformly distributed) but the directive properties of the antenna cause a greater power to be abstracted from the wanted signal and hence the signal-to-noise ratio is improved. A similar reasoning applies to cases in which valve noise is appreciable.

A detailed consideration of the various factors which arise is given in the next two sections—the situation is summarized to some extent by the curves in Fig. 5.6.

Effective Area of Absorption

A convention which is often useful, particularly with microwaves, is the definition of the receptive properties of an antenna in terms of an effective area of absorption. This area is equal to the area of the wavefront over which complete absorption of the radiated energy must take place in order to abstract a power equal to the available power obtained at the antenna terminals. When applied to the case of a doublet we have the following results—

Maximum available power from a doublet is given by

$$W = \frac{e^2}{4R_r}$$

where e = equivalent series e.m.f.,
 R_r = radiation resistance.

The factor 4 arises out of the fact that for maximum power absorption the load is equal to R_r , so that the voltage across the load is half the induced e.m.f. The power lost in the generator impedance takes the form of re-radiation and is not therefore a part of the absorbed power.

If the doublet is of length l and the incident field strength E , then in the direction of maximum pick-up we have $e = El$.

The radiation resistance is given by equation (4.44), Vol. I; hence

$$W = E^2 l^2 / \left(\frac{8l^2}{3\lambda^2} \pi z_{00} \right)$$

The energy in the wavefront is given by Poynting's vector which is

$$\mathbf{S} = \mathbf{E} \times \mathbf{H} \text{ watts/square metre}$$

i.e. $S = E^2 / z_{00}$

(*N.B.* In the present case we are keeping to r.m.s. values throughout; hence the use of the complex form of Poynting's vector is unnecessary.)

If A_D is the effective cross-sectional area in the direction of maximum pick-up, then

$$\begin{aligned} W &= A_D S \\ &= A_D \frac{E^2}{z_{00}} \end{aligned}$$

On equating this with the previous equation we obtain

$$A_D = \frac{3\lambda^2}{8\pi} \quad . \quad . \quad . \quad (5.2)$$

The maximum gain of a doublet over an isotropic radiator is 1.5; therefore an isotropic radiator has an effective cross-sectional area given by

$$A_0 = \frac{\lambda^2}{4\pi} \quad . \quad . \quad . \quad (5.3)$$

Consequently if the gain of an antenna system over an isotropic radiator is G_0 , it will have an effective cross-sectional area of A_e , where

$$\begin{aligned} A_e &= G_0 A_0 \\ &= \frac{G_0 \lambda^2}{4\pi} \quad . \quad . \quad . \quad (5.4) \end{aligned}$$

In the case of a half-wave dipole the gain in the equatorial plane is 1.64 and hence the effective area is

$$A_H = 0.13\lambda^2 \quad . \quad . \quad . \quad (5.5)$$

The above formula shows that the effective cross-section is approximately equal to a rectangle whose length equals that of the dipole and whose width is equal to half the length of the dipole. This result may seem strange—it would appear more logical to suppose that Poynting's vector should be integrated over the cross-sectional area which the dipole presents to the wavefront. But it will be noticed that, if the above simple idea were true, then a very thin dipole would absorb far less energy than a relatively thick dipole of the same length! There are, in fact, difficulties in interpreting Poynting's vector under all circumstances. These difficulties are also commented on by King⁽¹²⁾ and by Stratton.⁽²²⁾

5.2. SOURCES OF NOISE

The noise output from a receiver will be due partly to external and partly to internal sources. Under these headings we may list the following specific causes—

External Sources

Atmospheric noise, cosmic noise, precipitation static, man-made static, noise associated with radiation resistance.

Internal Sources

Ohmic resistance of the antenna, resistance of input circuits, shot noise in the first amplifier or mixer.

The above division is not, however, the most suitable for discussion: for this purpose it is better to consider noise under the following headings—

- (a) thermal noise,
- (b) cosmic noise,
- (c) atmospheric noise,
- (d) man-made static,
- (e) valve noise.

(a) *Thermal Noise*

Owing to the thermal agitation of the charges in a conductor, there is a certain amount of high-frequency energy present which may be regarded as being uniformly spread over the whole of the radio-frequency spectrum. The formula giving the e.m.f. resulting from this energy was obtained by Nyquist⁽²¹⁴⁾

and verified experimentally by Johnson.⁽³⁰⁹⁾ Nyquist's formula is as follows—

$$e^2 = 4kRTB \quad . \quad . \quad . \quad (5.6)$$

where e = r.m.s. value of noise voltage,

k = Boltzmann's constant

= 1.37×10^{-23} joules/degree,

R = resistance of conductor in ohms,

T = temperature in degrees Kelvin,

B = bandwidth in cycles/second.

This noise e.m.f. is to be regarded as acting in series with the resistance R of the conductor producing it. We therefore have a noise generator of internal resistance R , so that the maximum available power from this generator is equal to $e^2/4R$ watts. If we denote the available noise power by W_n , then equation (5.6) may be rewritten as

$$W_n = kTB \quad . \quad . \quad . \quad (5.7)$$

It will be noticed that in the above form the actual value of the resistance is not present; *for this reason the definition of noise parameters is preferably made in terms of "available power" rather than in terms of e.m.f.'s.* A convenient figure to remember in microwave calculations is that if $T = 290^\circ\text{K}$ (i.e. 17°C) then

$$W_n = 4 \cdot 10^{-15} \text{ watts/megacycle bandwidth}$$

The bandwidth in question is the total "energy bandwidth" of the amplifier following the resistance and this is given by

$$B = \frac{\int G df}{G_f} \quad . \quad . \quad . \quad (5.8)$$

where G_f = available power gain at mid-frequency f_0 ,

G = available power gain at frequency f .

For most purposes B is given sufficiently accurately by the bandwidth between the half-power points of the amplifier response.

The noise power discussed above is present in all the resistive components of the input circuit (see, for instance, the example in § 7.2, which includes a calculation allowing for the effects of a slightly dissipative line). It is also present in the radiation resistance of the antenna, but in this case the effective noise temperature is not necessarily equal to the ambient temperature.

The reason for this is perhaps best appreciated by invoking the theorem of reciprocity, i.e. by first considering the antenna as a transmitter. When transmitting, the radiated energy will be absorbed in various regions of the surrounding space, the amount absorbed in any region being dependent on the distance from the source and the electrical properties of the region as well as those of the intervening space. For many frequencies this energy will be absorbed in the surrounding countryside and in the ionosphere, but for very high frequencies a fair proportion of the energy will travel much farther into space. The degree to which the various portions of the space surrounding the antenna absorb energy from it is also a measure of the radiated noise energy which these portions will deliver towards the antenna when considered as a receiver. This radiated noise from the surrounding space is the radio-frequency component of the thermal radiation and therefore is a function of the absolute temperature of the surrounding medium. Consequently the effective temperature which is to be associated with the radiation resistance depends very much on the frequency and the polar diagram of the antenna; for example, with a microwave antenna pointing skywards the effective temperature may be only a few degrees absolute, whereas for a directive 10 m array pointing towards the Milky Way it would be about 120 000°K.

Burgess⁽²⁹⁷⁾ has shown that this thermal noise from the absorbing region surrounding the antenna may be derived from the Rayleigh-Jeans law which leads to the result that the mean-square e.m.f. induced in the antenna is given by

$$e^2 = 4kR_r T_r B$$

where R_r = radiation resistance of the antenna,

T_r = absolute temperature of the sources of thermal radiation.

This is identical in form with (5.6) and therefore justifies the inclusion of the radiation resistance in the value for R —assuming that the appropriate absolute temperature is taken for that fraction of R which is due to the radiation resistance.

The value of T_r may be conveniently expressed in terms of T_0 , where T_0 is the ambient temperature of the antenna and is assumed to be 290°K (in America the “standard” value is often taken as 300°K).

Typical values for T_r are as follows—

The surface of the earth	$T_r = T_0$
E region of the ionosphere	$T_r = 1.2 T_0$
F region of the ionosphere	$T_r = 3 \text{ to } 4 T_0$
Parts of the Milky Way	$T_r = 400 T_0$
Outer space in general	$T_r = (\lambda^3/15) T_0$ ($\lambda = 2 \text{ to } 16 \text{ m}$)

The last value is based on a report on cosmic noise by Scott quoted by Norton and Allen.⁽²⁷²⁾ More accurate values are given by Moxon.⁽³¹²⁾

Cosmic noise is discussed separately in the next paragraphs, though it is possibly only another form of thermal noise.

(b) Cosmic Noise

In 1932 Jansky⁽³⁰⁶⁾ published an account of some studies on the reception of noise at a frequency of 20.5 Mc/s which indicated clearly that a certain portion of the noise was arriving from some region outside the earth's atmosphere. Subsequent experiments⁽³⁰⁷⁾ showed that the direction of arrival coincided with a sidereal day and not a solar day—that is, the direction showed a period of rotation which was 4 minutes less than a solar day—and furthermore that the origin was in the direction of the Milky Way. A number of other investigators have confirmed these results using still higher frequencies (the lowest frequency on which cosmic noise is observable is about 15 Mc/s).

The origin of the cosmic noise may well be due to thermal agitation in which case such noise is a special case of thermal noise and can therefore be treated on the lines indicated in the previous paragraphs. Thomas and Burgess⁽³¹⁷⁾ have done this and arrived at the conclusion that the maximum value of T_r is equal to 400 times T_0 , i.e. that the source of noise in interstellar space may have a temperature of 120 000°K. Judging by the known experimental results this applies only with frequencies between 18 and 30 Mc/s, for at higher frequencies the effective value of T_r appears to drop until at 160 Mc/s it is only of the order of 5 T_0 . It is considered that this drop may be due to absorption of the higher frequencies in interstellar matter.

It should be remembered that these cosmic noise fields apply only to highly directive antenna systems which are pointing towards the Milky Way (the centre of which has a Right Ascension of 17 hr 30 min and a Declination of -30°). Only under such conditions will the temperature of the source of the noise radiation average as high as 400 T_0 over the whole

of the polar diagram of reception. In other cases the value of T_r will be much lower, being an average of the "hot" and "cold" sources of noise.

An idea of the directiveness of this noise can be obtained from Fig. 5.2, which shows a curve obtained by Fränz⁽³⁰²⁾ in which the ordinates are in terms of T_r/T_0 .

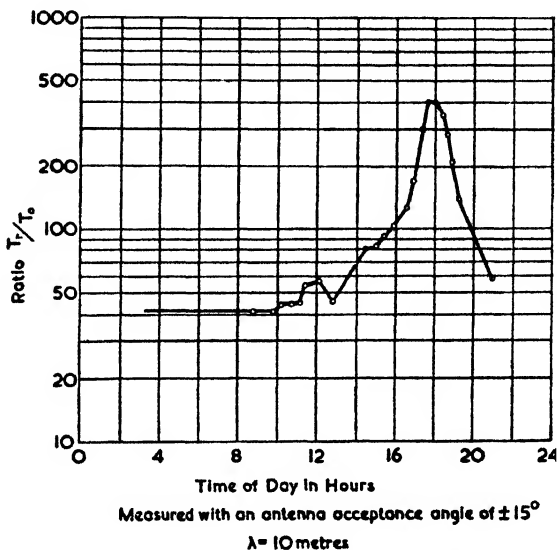


FIG. 5.2. THE EFFECT OF THE MILKY WAY ON THE TEMPERATURE OF THE RADIATION RESISTANCE

The average value over the range $\lambda = 2$ to 16 m has been shown to be approximately as follows—

$$T_r = (\lambda^3/15)T_0 \quad . \quad . \quad . \quad (5.9)$$

This expression shows that T_r decreases rapidly as we approach the microwave region; for example, if $\lambda = 1$ m, then $T_r = 0.067 T_0 \doteq 20^\circ\text{K}$. Measurements made on microwave radar sets beamed on to the sky do, in fact, indicate very low temperatures of only a few degrees Kelvin.

(c) Atmospheric Noise

The currents caused by flashes of lightning are of such intensity and short duration that they produce a continuous spectrum of energy throughout the range of radio frequencies. When these flashes are intermittent they give rise to impulse

noise in a receiver, but the combined field of many flashes in a short space of time will show as fluctuation noise. (It has been estimated that about two thousand thunderstorms are taking place over the globe at any one moment.)

Analysis of the pulse, or rather pulses, of current due to a lightning discharge shows that the lower radio frequencies will contain the greater energy for a given bandwidth. On the other hand the higher frequency components propagate over longer distances so that on short-wave bands the atmospheric noise is the sum of the noise due to a large number of storm centres. Even so the noise on short waves is lower than on medium and long waves, and in particular the atmospheric noise at wavelengths of less than 10 m is usually negligible.

Thunderstorm activity is known to vary with the sunspot cycle, but since this variation is less than 20 per cent it may be neglected for ordinary estimates in radio communication. An indication of the order of magnitude of atmospheric noise is provided by Fig. 5.6, in which the curves for such noise are based on the summary made by Thomas and Burgess.⁽³¹⁷⁾

Another form of atmospheric noise is that due to discharges taking place in the immediate vicinity of the receiving antenna. This form of noise is known as "precipitation" static for it is due to charges being built up in the first place by electrically charged particles which may be raindrops, hailstones, snow, or dust clouds.

The conditions most favourable to their accumulation occur in aircraft, when the effect can be serious—for the noise field may reach values as high as 10 mV/m on medium wavelengths. For a description of tests made on aircraft the reader may refer to an article by Huckle⁽³⁰⁵⁾ and also to the U.S.A. Army-Navy investigations.⁽²⁹⁵⁾ The measures taken to minimize the effect consist of screening all loop antennae and using an insulated trailing wire joined by a high resistance to the fuselage. From the end of this trailing wire a relatively smooth corona discharge can take place.

(d) *Man-made Static*

Under the heading of man-made static we include all noise sources due to electrical machinery and appliances. The obvious cure is to mount the receiving antenna as far away as possible from such noise sources and to use a screened lead-in. This is quite feasible in point-to-point communication systems

but it is not so easy in normal broadcast reception (for instance, in tropical towns much interference is caused by electric fans during the summer months).

Electrical machinery such as generators, rotary converters and also neon signs or contact breakers have an interference zone of about 100 m radius. Overhead lines such as trolley bus wires or high-voltage lines have a greater range of interference—something of the order of 1 to 2 km. Noise due to ignition systems has a value which is intermediate between the two values given above. These values, which are based on data collected by Thomas and Burgess⁽³¹⁷⁾ all apply to un-suppressed systems—if efficient measures are taken to suppress the unwanted radiation the range of interference can be greatly reduced.

A study of the noise fields due to motor-car ignition systems has been made by George.⁽³⁰⁰⁾ In particular he studied the noise field due to motor vehicles 30 m away from a receiving antenna 10 m high. This represents the order of height and distance involved in the majority of television receiving conditions. Under these conditions it was found that the average noise field (for a 10 kc/s bandwidth) due to a single motor vehicle was about $50 \mu\text{V/m}$ at 40 Mc/s and that this value varied by less than 2 : 1 throughout the range of 40 to 450 Mc/s. These figures may be taken to apply to either vertical or horizontal polarization. Maximum noise fields were about ten times the average and minimum fields about one fifth of the average.

By fitting interference suppressors to the ignition system, improvements of the order of 30 db are obtainable.

(e) *Valve Noise*

Owing to slight irregularities in the current streams in a valve, the valve itself acts as a source of noise. The noise generated in this way is often known as "shot noise," and has been the subject of many investigations (those by Harris⁽³⁰⁴⁾ and Moxon⁽³¹²⁾ are suggested as convenient starting points to the literature on the subject).

At frequencies below about 10 Mc/s the contribution to the total noise made by the valve is usually quite small and estimates of this contribution may be conveniently made by the use of a fictitious equivalent resistance in series with the grid. This equivalent resistance is one which, at the normal ambient temperature, would give the same noise output as the valve

does. For ordinary triodes the following formula⁽⁸⁰⁴⁾ gives a rough approximation to the value of this resistance—

$$R_{eq} = \frac{2.5}{g_m} \quad (5.10)$$

where g_m = transconductance of valve in mhos.

If, for example, g_m were equal to 2 500 micromhos, then R_{eq} would be equal to 1 000 ohms and hence, by equation (5.6), the series noise e.m.f. for a bandwidth of 10 kc/s would be $0.4 \mu\text{V}$.

The equivalent noise resistance of an ordinary pentode is some 3 to 5 times greater so that, for a given transconductance, the noise from a pentode is distinctly greater.

If the valve is a frequency changer, then the low conversion transconductance leads to correspondingly higher equivalent noise resistance, but in addition a factor of anything between 2 and 10 must be included. Consequently the equivalent noise resistance of a mixer valve may be as high as 250 000 ohms (it should be noted that the equivalent resistance should be compared with the *dynamic impedance* of the input circuit when assessing the relative noise contributions from the input circuit and the valve).

Above frequencies of about 10 Mc/s the noise contributed by the valve varies with frequency, so that no single value of equivalent noise resistance can be stated. The overall noise contribution is then expressed in terms of a "noise figure" which is a function of the frequency of operation. The use of "noise figures" is discussed in the next section.

5.3. SIGNAL-TO-NOISE RATIO CONSIDERATIONS

Limitations Imposed by Signal-to-noise Ratios

Provided the receiver is capable of a sufficiently high degree of amplification, the ultimate performance of a receiving system depends entirely on the signal-to-noise ratio obtained at the output terminals. In order to put different types of receivers on a comparative basis, it is customary to measure this ratio immediately before the detector stage using an unmodulated carrier. Thus the final signal-to-noise ratio will depend on the depth and type of modulation. For example, with frequency modulation an improvement over amplitude modulation of $\sqrt{2}$ times the deviation ratio is obtainable.

Additional improvements are possible by the use of pre-emphasis and more favourable methods of transmitter modulation, so that existing F.M. systems, which use a deviation ratio of 5, can show as much as 25 db improvement over A.M. systems using the same output power for the unmodulated carrier.

There is naturally some difficulty in defining the minimum signal-to-noise ratio required for any type of reception, but the column of figures quoted below will provide a rough guide—the figures are based on a number of experimenters' results and are quoted by Thomas and Burgess.⁽⁸¹⁷⁾ The values given for radar are merely typical since they depend both on the pulse width and on the repetition frequency.

<i>Type of Transmission</i> (Full amplitude modulation assumed)	<i>Minimum Signal-to-noise Ratio</i>
Telegraphy (recorder)	— 6 db
Telegraphy (aural)	0 db
Telephony	+ 20 db
Television (high quality)	+ 30 db
Broadcasting (high quality)	+ 40 db
Radar (A-scope presentation)	0 db
Radar (PPI presentation)	+ 20 db

In taking practical measurements the results are highly dependent on the time constants of the circuits involved and also on the type of noise. A satisfactory meter circuit has been described by Burrill⁽²⁹⁹⁾ who also correlated its readings with listening tests using three types of noise. His results are shown in the graph of Fig. 5.3, together with the appropriate circuit constants.

The actual effect of noise on reception depends both psychologically and analytically on the average rate of repetition and on the waveform. When the noise pulses occur at long intervals they are known as impulse noise, but when they occur at intervals distinctly shorter than the inverse of the receiver bandwidth they are referred to as fluctuation noise.

It has been shown both theoretically and experimentally that fluctuation noise has a peak value between 3.5 and 4.5 times the r.m.s. value; also both peak and r.m.s. values are proportional to the square root of the bandwidth. On the other hand, a unit impulse has a peak value which is directly

proportional to the bandwidth, though the r.m.s. value still remains proportional to the square root of the bandwidth.

Because of this variation in the total noise energy with bandwidth, it must be understood that in all general remarks on noise it is assumed that the bandwidth is constant. In

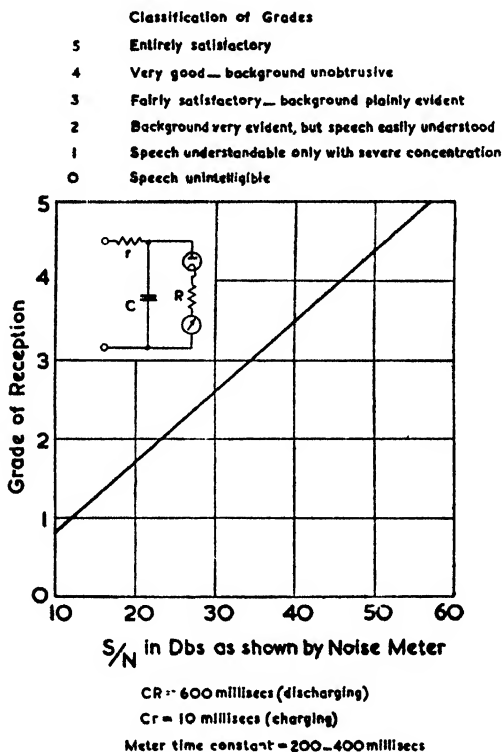


FIG. 5.3. A NOISE METER CIRCUIT AND ITS CALIBRATION CURVE
 (Burrill, *Proc. I.R.E.*, Aug., 1941)

practice this means that receivers for the higher frequencies are more subject to noise than they would otherwise be, for in most cases such receivers have appreciably wider bandwidths than are employed at, say, broadcast frequencies.

Noise Figures

The deterioration in the signal-to-noise ratio caused by inserting an amplifier (or any 4-terminal network for that matter)

between a source and its output terminals may be expressed in terms of a "noise figure." This figure may be defined as follows—

$$\mathcal{N} = \frac{\text{Available output noise power with actual receiver}}{\text{Available output noise power with ideal receiver}}$$

In both cases the source is a dummy antenna whose impedance equals that of the actual antenna and whose temperature is equal to the ambient temperature (standardized at 290°K). By stipulating a dummy antenna we cut out any external sources of noise, neither is the effective noise tempera-

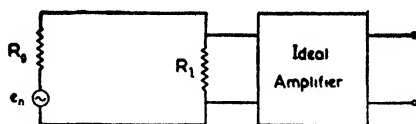


FIG. 5.4. DIAGRAM FOR DISCUSSION OF THE EFFECT OF MATCHING ON THE OVERALL NOISE FIGURE

ture of the radiation resistance involved. For calculation purposes the definition may be rearranged as follows—

$$\mathcal{N} = \frac{W_{si}}{W_{ni}} \times \frac{W_{no}}{W_{so}} \quad (5.11)$$

where W_{si} = available signal power at input,
 W_{ni} = available noise power at input,
 W_{so} = available signal power at output,
 W_{no} = available noise power at output.

On account of the definition being in terms of *available* powers the noise figure is independent of the output load impedance of the amplifier. It is not independent of the matching conditions between the generator and the input impedance of the amplifier; hence the need for simulating the actual antenna by a dummy antenna of similar impedance. If, however, the input impedance of the amplifier is high in comparison with the generator impedance, then the noise figure is virtually independent of the generator impedance.

Let us suppose that we connect a simple resistance R_l to a generator of internal resistance R_g as shown in Fig. 5.4. The generator has signal and noise e.m.f.'s equal to e_s and e_n respectively. Then

$$W_{si} = \frac{e_s^2}{4R_g} \quad W_{ni} = \frac{e_n^2}{4R_g}$$

In the particular case $R_i = R_o$

$$W_{so} = \left(\frac{e_s}{2}\right)^2 / 4 \left(\frac{R_o}{2}\right) = \frac{e_s^2}{8R_o}$$

$$W_{no} = \frac{e_n^2}{2} / 4 \left(\frac{R_o}{2}\right) = \frac{e_n^2}{4R_o}$$

Using equation (5.11) we have

$$N = 2 \text{ (for } R_i = R_o\text{)}$$

The matched load has therefore caused a 2:1 deterioration in the signal-to-noise available power ratio. If we followed this network by an ideal noise-free amplifier we should still have an overall noise figure of 2 due to the presence of R_i .

In the above example $e_n = 4kTR_oB$, but the available noise power is given directly by equation (5.7) and is obviously independent of the resistance. Consequently in Fig. 5.4 we have $W_{ni} = W_{no} = kTB$ for all values of R_i and R_o . In general if $R_i = nR_o$ then $N = (n + 1)/n$.

The addition of an ideal amplifier produces an overall noise figure which depends on the ratio of R_o to R_i and only if $R_i \geq R_o$ is the combination "noise free." With practical amplifiers the best matching conditions will depend on the input impedance and the effective noise temperature of the source—in general these optimum conditions will not coincide with those for simple power matching.

The power gain of an amplifier as expressed in equation (5.8) is given by

$$G = \frac{W_{so}}{W_{si}}$$

Using equation (5.11) we may therefore express the available noise output power as

$$\begin{aligned} W_{no} &= N G W_{ni} \\ &= N G k T_o B \end{aligned} \quad (5.12)$$

Of the above amount the signal generator contributes $GkTB$ watts so that the contribution by the amplifier is given by

$$(W_{no} - GW_{ni}) = (N - 1) GkT_oB$$

If the source were not at the standard temperature T_o but

at an effective noise temperature of T_r , then the total noise output power would be modified to

$$\begin{aligned} W_{no}' &= W_{no} - GW_{ni} + \frac{T_r}{T_o} GW_{ni} \\ &= \left(N - 1 + \frac{T_r}{T_o} \right) GkT_oB \quad . \quad . \quad . \quad (5.13) \end{aligned}$$

Comparison with equation (5.12) shows that the effective noise figure is now

$$N' = N - 1 + \frac{T_r}{T_o} \quad . \quad . \quad . \quad (5.14)$$

The change in the noise figure when $T_r \neq T_o$ is due to the fact that this figure is based on a standardized temperature so that in all cases $W_{ni} = kT_oB$. For this reason it would seem preferable to use the expression "noise figure" rather than "noise factor" (an expression which is also often used). The use of the word "factor" is inclined to give one the idea that the total noise output power is obtained by simply multiplying the noise power at the source by this factor and the power gain of the amplifier. Equation (5.13) shows that this is true only if $T_r = T_o$.

In cases where the gain of a stage is low, the subsequent stages may also add an appreciable amount of noise power to the output. If, as is mostly the case, the overall bandwidths as measured at the various stages in the chain are virtually equal, then the overall noise figure is given by

$$N = N_1 + \frac{N_2 - 1}{G_1} + \frac{N_3 - 1}{G_1 G_2} + \dots \quad . \quad (5.15)$$

where N_n = noise figure of stage n ,

G_n = power gain of stage n .

It should be noted that the noise figure of any stage depends on the output impedance of the preceding stage for the reasons previously mentioned with regard to a single network.

An example of considerable practical importance arises in the case of a chain of relay stations whose overall signal-to-noise ratio must be kept high. In such cases the power gain per "stage" is generally of the order of unity.

The diode mixer provides an example which involves both the stage gain (in this case the "gain" is actually a loss) and

an effective source temperature. These two factors together give the overall noise figure as

$$N = \frac{N_{if} - 1 + T_m/T_0}{G_m} \quad (5.16)$$

where N_{if} = noise figure of intermediate frequency amplifier,
 T_m = effective temperature of diode,
 G_m = conversion gain of diode.

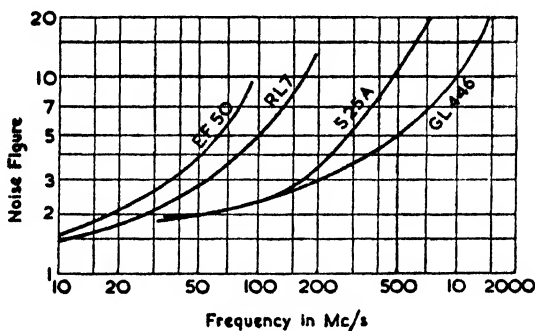


FIG. 5.5. NOISE FIGURE CURVES OF SOME TYPICAL VALVES
 (Moxon, *Jour. I.E.E.*, Pt. IIIA, No. 6, Mar.-May, 1946)

With crystal mixers the values for T_m range between 1.2 and $4 T_0$, while for G_m the range of likely values is 0.1 to 0.3.

Noise Figure of Valves

The noise figure of a valve does not vary appreciably from the optimum with variations in matching conditions, particularly if we let the input impedance give the necessary damping and bandwidth. Therefore it is possible to associate a noise figure with the valve for any operating frequency.

Fig. 5.5 shows the noise figure versus frequency curves for four commonly used valves—the values are based on those given by Moxon⁽³¹²⁾ and also Norton and Allen.⁽²⁷²⁾ The following example will serve to show the application of such data.

Example

A television receiving system consists of a half-wave dipole followed by an amplifier whose first valve is an EF 50.

If $\lambda = 7$ m, what is the minimum field strength needed for reasonable reception?

The criterion for high-quality reception is given in the table on p. 208 as a signal-to-noise ratio of 30 db, but quite reasonable reception is obtainable with a ratio of only 20 db. As a matter of fact the television camera itself may not have a better signal-to-noise ratio than 20 db, for the signal-to-noise ratios of such cameras vary in value between 20 and 40 db.

For the purpose of this example, we will assume a camera with a ratio of 30 db while the final signal-to-noise ratio is to be 20 db.

According to equation (5.9) the average effective noise temperature of the radiation resistance is given by

$$T_r = 22.8 T_0$$

From Fig. 5.5 the noise figure for an EF 50 is equal to 3.4 when $\lambda = 7$ m. The effective noise figure of the receiver is given by equation (5.14) and is

$$\begin{aligned} \mathcal{N}' &= 3.4 - 1 + 22.8 \\ &= 25.2 \end{aligned}$$

For present-day television we may assume a bandwidth of 3 Mc/s, and since $k T_0 B = 4 \times 10^{-16}$ watts per megacycle bandwidth, we find that equation (5.12) gives

$$W_{no}' = 25.2 \times G \times 12 \times 10^{-16} \text{ watts}$$

To this we must add the camera noise output, W_{no}'' , which is equal to $0.00316 W_{si} \times G$, where W_{si} is the available signal input power. Therefore the total noise output power is

$$W_{no} = G(25.2 \times 12 \times 10^{-16} + 0.00316 W_{si})$$

The output signal power, W_{so} , must be 100 times as great and, since it is equal to GW_{si} , we have

$$W_{si} = 25.2 \times 12 \times 10^{-13} + 0.316 W_{si}$$

Therefore

$$W_{si} = 44.2 \times 10^{-12} \text{ watts.}$$

This power is to be absorbed by an antenna whose effective cross-sectional area is given by equation (5.5) and is

$$A_H = 0.13 \times 7^2 = 6.37 \text{ m}^2$$

The power absorbed is equal to the product of this area and Poynting's vector, that is

$$W_{si} = A_H S = A_H \frac{E^2}{377}$$

The required field strength is therefore

$$E = \sqrt{\left(\frac{44.2 \times 377}{6.37}\right)} \times 10^{-6} \text{ V/m}$$

$$= \underline{\underline{51 \mu\text{V/m}}}$$

The above calculation takes no account of ignition noise or other man-made interference. From the results quoted on

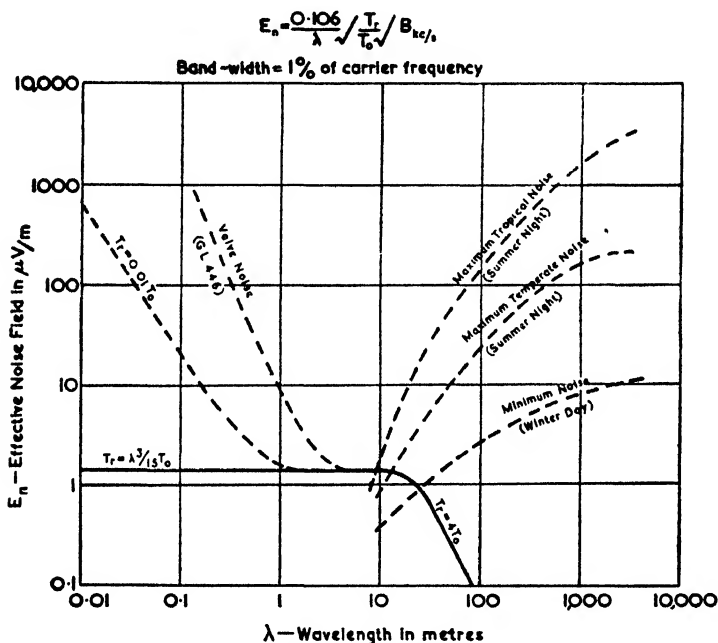


FIG. 5.6. THE DISTRIBUTION OF NOISE OVER THE RADIO SPECTRUM

p. 206 we can deduce that with a 3 Mc/s bandwidth the noise due to an unsuppressed car passing at 30 m from an antenna 10 m high will be of the order of 1 mV/m. It is clear, therefore, that the universal fitting of suppressors would considerably increase the area over which satisfactory television reception could be obtained.

Typical Noise Fields over the Radio Spectrum

The chart in Fig. 5.6 gives some indication of the noise fields which may be expected at different wavelengths. In all cases

the bandwidth has been assumed to be 1 per cent of the operating frequency; for example, if $\lambda = 300$ m, $B = 10$ kc/s; if $\lambda = 3$ m, $B = 1$ Mc/s.

The effective noise field due to radiation resistance has been calculated on the assumption that the receiving antenna is a half-wave dipole; the result is therefore approximately correct for any antenna whose effective height is of the order of half the actual height.

The thermal field is given by

$$E_n = \frac{e_n}{h_e} = \frac{\sqrt{(4kR_r T_r B)}}{h_e}$$

For a half-wave dipole, $h_e = \lambda/\pi$ and $R_r = 73$ ohms, hence

$$E_n = \frac{3.37}{\lambda} \sqrt{\frac{T_r}{T_0}} \sqrt{B_{\text{Mc/s}}} \mu\text{V/m} \quad (5.17)$$

The horizontal line in Fig. 5.6 is based on the assumption that $T_r = (\lambda^3/15)T_0$, while in the short-wave region it is assumed that $T_r = 4 T_0$ (a smooth join has been made between the lines given by these two laws). It will be noticed that below $\lambda = 10$ the value of E_n is constant—this is simply due to a compensating effect arising from the fact that we have stipulated a constant percentage bandwidth.

As the wavelength decreases below 1 m the value of T_r becomes an increasingly small fraction of T_0 until only quite a small amount of loss resistance (which is essentially at ambient temperature) will produce an even greater noise power than that due to the radiation resistance. Also the antenna may not be beamed entirely skywards, in which case a small percentage of the incident thermal energy will be associated with the temperature of the ground. In order to show the effect of such factors the dotted curve marked $T_r = 0.01 T_0$ has been added. It is obvious from this curve that only a small percentage of the total thermal noise field need be at a temperature of T_0 in order to cause quite big increases in the effective noise field at the shortest wavelengths.

Nevertheless we are spared the trouble of taking any elaborate measures to reduce the inherent noise due to dead-loss resistance in the antenna because the noise due to the valve predominates in microwave systems. This is shown by the chain dotted line which assumes the noise figure curve given for the GL 446 valve in Fig. 5.5.

At wavelengths for which valve noise is negligible, we find either that the noise due to radiation resistance is far greater than that due to loss resistance (cases for which $T_r > T_o$ and $R_r > R_a$), or else that the atmospheric noise predominates (in these cases $T_r \doteq T_o$, $R_r < R_a$ but $\sqrt{B/\lambda}$ is small). The net result is that a receiving antenna need not be designed

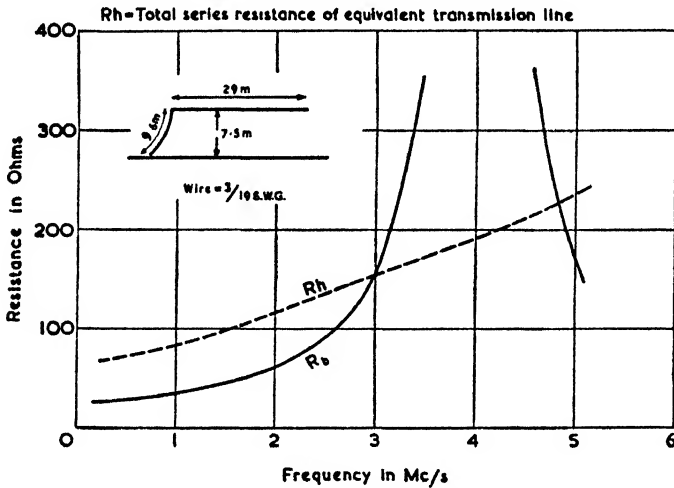


FIG. 5.7. EXPERIMENTALLY DETERMINED RESISTANCE VALUES OF AN INVERTED-L ANTENNA
(Colebrook, *Jour. I.E.E.*, July, 1932)

with any particular attention to efficiency whatever the operating frequency may be. This deduction is mainly of interest with long- and medium-wave receiving antennae, for in such cases quite elaborate measures would be needed to obtain a reasonable efficiency.

5.4. NON-DIRECTIONAL RECEIVING ANTENNAE

Long-wave and Medium-wave Antennae

The antennae used for non-directional reception on long and medium waves are mostly of the T or inverted-L type and the same methods as were described in Chapter II may be used to determine their characteristics. In the majority of cases the antenna will be quite short in comparison with a wavelength, consequently the capacitance of the antenna is equal

to the static capacitance, while the radiation resistance is negligible. The input resistance is therefore due almost entirely to earth losses, etc., and since no special measures are normally taken against such losses, their magnitude cannot be predicted with any accuracy.

An extensive analytical investigation on the grounded receiving antenna was carried out by Colebrook.⁽¹⁵³⁾ He employed the equivalent transmission-line method and obtained typical values for the attenuation constant, α , and the effective total distributed resistance, Rh , experimentally. Fig. 5.7 is a reproduction of one of his curves (the corresponding reactance curve is of the form shown by the dotted line in Fig. 2.1).

The base resistance was found to vary according to wire gauge and earth system in the following manner—

$$\begin{aligned} \text{Frequency} &= 842 \text{ kc/s } (\lambda = 9.4 h) \\ \text{Radiation Resistance} &= 0.5 \text{ ohm} \end{aligned}$$

Earth System	Antenna Wire	Base Resistance R_b
(a) Buried copper plate . . .	No. 47 S.W.G.	138.5
(b) " " " " . . .	No. 34 S.W.G.	33.8
(c) " " " " . . .	$\frac{1}{8}$ S.W.G.	30
(d) Parallel wire 1 m high . . .	" "	9
(e) Wire lowered on ground . . .	" "	108
(f) Small earthing pin . . .	" "	150

The parallel-wire earth referred to above was run underneath the horizontal portion of the antenna—in the one case at a height of 1 m and in the other on the surface of the ground. The effectiveness of a counterpoise earth is clearly demonstrated, while the lowered-wire case shows the great increase in losses due to the field round the earth wire being in the immediate neighbourhood of a lossy medium. Wire losses are obviously small except for extremely thin wires.

Let us consider the thermal noise introduced by the loss resistance, taking as examples cases (d) and (f) since the first represents a highly efficient earth system and the second a typical simple earth. A reasonable assumption to make is that in equation (5.6) $R = R_b$ and $T = 290^\circ$, then on putting the overall bandwidth B equal to 10 kc/s we have

$$(d) \quad e_n = 0.038 \mu\text{V}$$

$$(f) \quad e_n = 0.155 \mu\text{V}$$

From the curves of Fig. 5.6 it can be inferred that the minimum atmospheric noise field at 84.2 kc/s would be about $5 \mu\text{V}/\text{m}$, whilst the worst case is about $100 \mu\text{V}/\text{m}$. The effective height of the antenna is approximately 5 m, consequently the induced atmospheric noise e.m.f.'s would have minimum and maximum values of

$$e_n' = 25 \mu\text{V} \text{ (winter day)}$$

$$e_n' = 500 \mu\text{V} \text{ (summer night)}$$

It will be seen that even the lowest value of atmospheric noise is many times the noise e.m.f. and this for a case which represents an indifferent earthing system. Hence on medium wavelengths atmospheric noise will predominate over antenna circuit noise even when the earthing system is poor. A good earth system is, however, of assistance in reducing noise which comes in via the power cords—this type of noise is considered below.

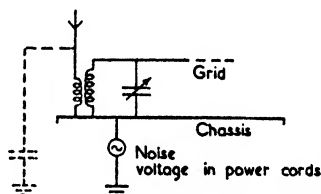


FIG. 5.8. INJECTION OF NOISE VIA THE POWER CORDS WITH A SIMPLE INPUT CIRCUIT

Noise Reducing Antennae

In practice an appreciable amount of noise can enter the receiver as a result of noise e.m.f.'s which are induced between the chassis and the earth by the power cords. The normal antenna input circuit is shown in Fig. 5.8, from which it can be seen that the noise of this nature is applied to the grid of the first valve. The cure lies in adopting some form of balanced injection for the wanted signals. This can be done by using a balanced transmission line as shown in Fig. 5.9 (a). Such a system also permits the antenna to be located in some position which is relatively noise free.

The circuits of Fig. 5.9 (b) and (c) are described by Landon and Reid⁽¹⁵⁶⁾ and are based on the bridge circuit of Fig. 5.10. In this bridge circuit the balancing condenser C_2 is adjusted to give minimum power-line noise in the primary coil. To keep the adjustment relatively insensitive to frequency, the top-end capacitance of the input transformer must be kept low.

Fig. 5.9 (b) shows the applications of this principle to an inverted-L or T antenna—practical dimensions are 25 m total antenna length and a counterpoise of half this length spaced 15 cm away. An all-wave version is shown in Fig. 5.9 (c).

All-wave Antennae

The general-principle of all-wave antennae is to use some form of balanced antenna for the short-wave bands, and let the

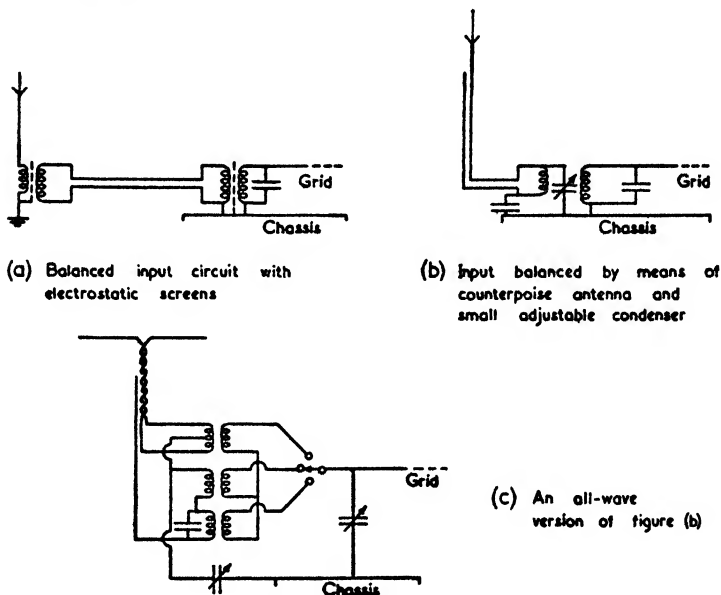
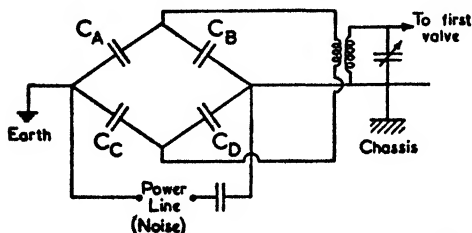


FIG. 5.9. INPUT CIRCUITS FOR THE REDUCTION OF POWER-CORD NOISE



C_A = Antenna capacitance
 C_B = Balancing capacitance

C_C = Counterpoise capacitance
 C_D = Capacitance between lower end of primary winding and chassis

FIG. 5.10. PRINCIPLE ON WHICH POWER-LINE NOISE IS BALANCED OUT

downloads form an unbalanced antenna for the broadcast bands (when the top portion acts as a loading capacitance). An antenna designed on these lines to cover the range 0.54 to

18 Mc/s has been described by Wheeler and Whitman⁽¹⁸⁰⁾ and is shown in Fig. 5.11.

The top portion is a double-V antenna which covers the

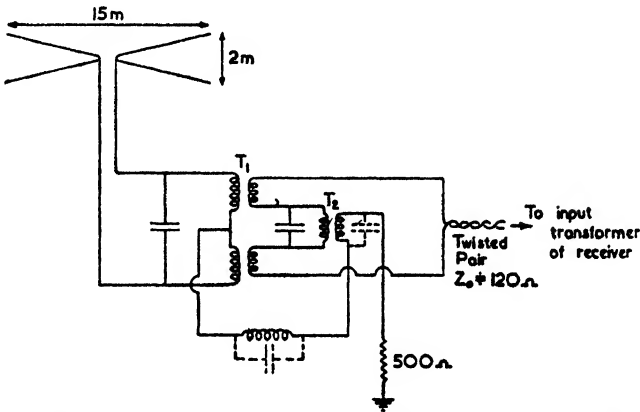


FIG. 5.11. AN ALL-WAVE RECEIVING ANTENNA SYSTEM
(0.54-18 Mc/s)

(Wheeler and Whitman, *Proc. I.R.E.*, Oct., 1936)

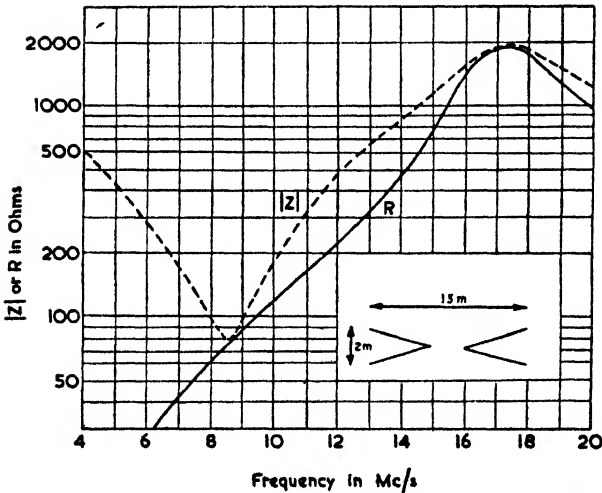


FIG. 5.12. IMPEDANCE CURVE FOR THE SHORT WAVE RANGE OF THE ANTENNA SHOWN IN FIG. 5.11

(Wheeler and Whitman, *Proc. I.R.E.*, Oct., 1936)

range 6 to 18 Mc/s. On account of the diverging wires the impedance characteristic is relatively flat (see Fig. 5.12); in particular at the full-wave resonance point the impedance is

about one-half that of a single dipole. At 5 Mc/s the arrangement acts as a mixed balanced and unbalanced antenna, while at still lower frequencies the mode of operation is entirely unbalanced (the transformer for this case, marked T_2 , has an iron-dust core). The presence of the 500 ohm resistance to ground is to damp out resonances.

An overall loss of only 1 to 5 db is claimed for this all-wave circuit (this figure is exclusive of transmission-line losses).

At all frequencies the transmission line to the receiver will be balanced; hence all the noise-reducing advantages of the circuit shown in Fig. 5.9 (*a*) can be obtained on employing an input transformer with an electrostatic shield.

Short-wave Antennae

The simplest type of short-wave receiving antenna is a vertical rod or wire about one-quarter of a wavelength high. When reception is required over the whole of the short-wave band the antenna should avoid the half-wave resonance condition at the high-frequency end of the range, i.e. it should not be more than 4 to 5 m high.

The disadvantage of the vertical wire is that it has a poor pick-up for sky waves originating from transmitters within, say, 100 to 200 km radius (the distance varies according to whether E or F layer reflections are occurring). For any particular transmission this shortcoming can be mitigated by inclining the wire away from the direction of the transmitter. A further disadvantage of a vertical antenna is that it is more susceptible to locally generated noise—a feature which is largely due to the propagation differences between vertically and horizontally polarized waves over short distances.

An elevated horizontal dipole is therefore to be preferred and to obtain broad-band characteristics it may be used with a resistance termination as described on p. 118. Such a dipole is more omnidirectional than one might at first suppose since, except for very distant sky waves, the angle of the down-coming wave is such that not more than about 10 db are lost for reception in line with the dipole (the polar characteristics of an elevated horizontal dipole are shown in Figs. 3.11 and 3.12). The omnidirectional qualities may be improved by employing two dipoles at right angles. An arrangement of this type in which a transmission line end-feeds the two dipoles is described by Wells.⁽¹²³⁾

It is sometimes an advantage to place a horizontal dipole to point in the East-West direction since the amount of atmospheric noise received from the tropics may thereby be reduced. This may seem strange at first, but the fact is that often more noise is picked up in the end-on position for, with signals coming in nearly at grazing incidence, the vertically polarized signals from the sky strike the antenna in phase with those reflected from the ground; consequently their sum may actually exceed that of the horizontally polarized noise signals which are picked up in antiphase in the broadside-on position.

Assuming that the polar diagram of the dipole alone follows a cosine law, it is a simple matter to show that for antenna heights of less than $\lambda/6$ the end-on pick-up will exceed the broadside-on pick-up for low-angle noise. Ground constants also affect the result to some extent, but in general one may say that the East-West orientation is preferable for dipoles suspended less than a sixth of a wavelength above the ground.

Ultra-short-wave Antennae

At wavelengths below 10 m there is no great mechanical difficulty in erecting half-wave dipoles whether vertical or horizontal. Since sky waves cannot be relied upon at these wavelengths, a horizontal dipole is no longer sensibly omnidirectional as on short waves; it must therefore be roughly broadside on to the direction of the transmitting antenna.

If truly omnidirectional reception is required with horizontally polarized waves either a pair of crossed dipoles or some form of folded-loop antenna (such as the Alford loop or coaxial loop) is required.

Perhaps the most common form of ultra-short-wave antenna is the television antenna. For this reason the following example is given as an illustration of the calculation of the thickness required to give a sufficiently wide bandwidth.

Example

If we set ourselves the limits suggested on p. 127 of not more than 30 per cent reflection at ± 5 per cent off tune, what is the necessary diameter of a half-wave dipole working on a wavelength of 7 m?

From equation (10.43) we see that a 30 per cent reflection corresponds to a standing wave ratio, ρ , of 1.86 (since $|B||A| = 0.3$). As a first approximation we may assume

that the resistance of the antenna remains constant at 70 ohms, then from Fig. 10.15 we find that the reactance may vary by approximately $\pm 0.6 Z_0$ before the $\rho = 1.86$ circle is reached. With Z_0 equal to 70 ohms this means a reactance variation of ± 42 ohms.

This variation must take place over a frequency range of ± 5 per cent. From Fig. 3.2 we find that $+j42$ corresponds to $h = 0.25\lambda$ for all curves. The lower limit will be about 10 per cent less, i.e. 0.225λ , and at this length we require a reactance of $-j42$ ohms.

Interpolating from the curves of Fig. 3.2 gives $-j42$ ohms at 0.225λ for an h/a ratio of about 200. This is the ratio of half the length of the dipole to the radius and is therefore the same as the length divided by the diameter.

Since $\lambda/2 = 3.5$ m we have—

$$\underline{\text{Diameter of antenna} = 1.75 \text{ cm}}$$

Actually the bandwidth of a dipole varies only slowly with the diameter of the conductor. From equation (3.14) we see that the bandwidth of the dipole is inversely proportional to Z_0 , the characteristic impedance of the dipole.

We may determine the characteristic impedance by doubling the value given by equation (2.4) to allow for the fact that the present case is a centre-fed conductor in free space. In this way we find that

$$Z_0 = 120 \log_e \left(\frac{2h}{a} - 1 \right)$$

If, therefore, the diameter of the dipole were decreased to 1.2 cm the bandwidth would be decreased by only 7 per cent.

Limiting the maximum reflection coefficient has a twofold purpose: it ensures a wide-band response and also it reduces the possibility of "ghost-images" due to reflections at both ends of the line. Actually the likelihood of ghost images from this cause is quite small. If the input impedance of the receiver is matched to the characteristic impedance of the line no such images will be formed, and even where mismatching exists the length of feeder line would have to be more than 10 m for the images to be visible.

In the majority of cases we can therefore consider the frequency response only, and this is conveniently expressed in terms of the 3 db points. With this criterion it can be shown

that the diameter of the dipole is quite immaterial if the line is correctly terminated. To illustrate this, let us assume as before that the radiation resistance of the dipole remains constant at 70 ohms and also that the induced e.m.f. is constant. The characteristic impedance of the line and the input impedance will also be taken to be 70 ohms.

At any given frequency the voltage across the input resistance will be independent of the length of line (this follows at once from power considerations). Hence the input voltage versus frequency characteristic is the same as that for zero length of line and taking this simple case we see at once that the response will be 3 db down when the antenna reactance is ± 140 ohms. From the curves of Fig. 3.2 it is clear that the necessary bandwidth can be obtained even with a thin wire. The corresponding standing wave ratio can be found from Fig. 10.16 which shows that impedances of $Z_0(1 + j2)$ give a standing wave ratio of 6.

Going to the other extreme and assuming either a very high or a very low input impedance, we find that the voltage will vary as the square root of the resistive component of the generator impedance as viewed through the line. Consequently the response will be confined within the limits ± 3 db if the standing-wave ratio does not exceed 2, i.e. if the antenna reactance is within the range $\pm 0.7Z_0$. These limits are much the same as those obtained with the 30 per cent reflection coefficient stipulation, which means that a diameter of nearly 2 cm would be required under these conditions.

The above observations make it clear that considerable liberties can be taken with the length-to-diameter ratio of the dipole if the resonant impedance of the antenna, the characteristic impedance of the feeder line and the input impedance of the receiver are all matched.

The situation is considerably more complicated if a director or reflector is used, for in such cases not only is the impedance versus frequency characteristic dependent on the initial choice of spacings and antenna lengths, but the polar diagrams will also vary with frequency. The former may be regarded as changes in the internal impedance of a generator, while the polar diagram variation corresponds to the generator e.m.f. varying with frequency.

Because of the above complications it is usual to place the parasitic element about 0.25λ away from the dipole for, although slightly greater gains can be obtained with say 0.15λ

spacing, it requires more careful design work to obtain a good performance from more closely spaced arrays.

Fig. 5.13 (a) shows the dimensions of a typical dipole plus

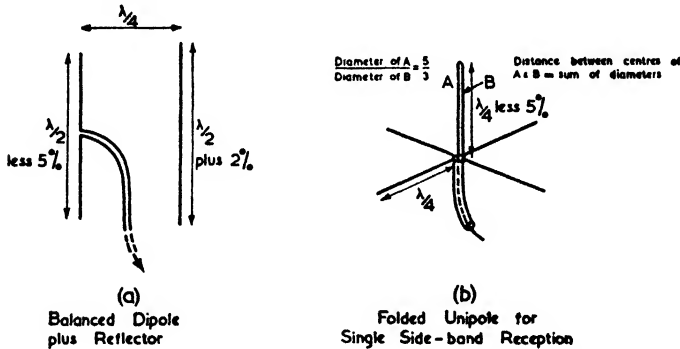


FIG. 5.13. TWO EXAMPLES OF TELEVISION ANTENNAE

reflector array with 0.25λ spacing, while Fig. 5.13 (b) shows a folded unipole antenna which is suitable for mounting in an attic. The latter antenna is designed for single-side-band

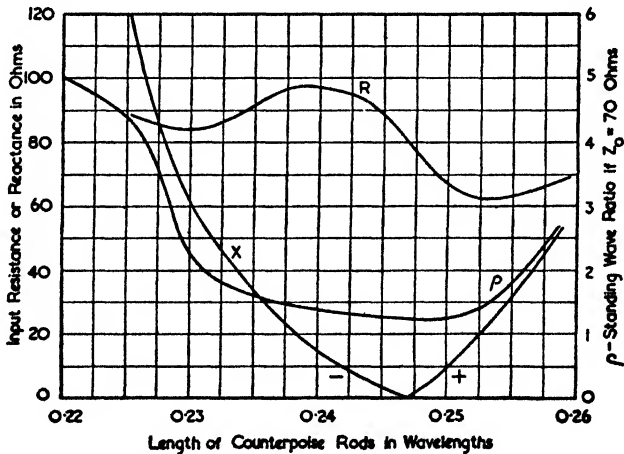


FIG. 5.14. IMPEDANCE CURVES OF ANTENNA SHOWN IN FIG. 5.13 (b)

working and owing to the folding of the quarter-wave element it actually has substantially the same pick-up as a full half-wave dipole. Impedance curves of the folded unipole are given in Fig. 5.14.

Built-in television antennae have been described by Carlson⁽¹⁰⁹⁾ who tried a loaded dipole and also a small loop antenna. Unfortunately it will be found that whenever the antenna is actually in the room, the movement of people in the room will cause the picture to fade and even to come out of synchronization. For this reason it is far more practicable to have the antenna at some distance from the set—either above the roof or, if in the attic, with a counterpoise earth system.

Microwave Antennae

Practically all microwave receiving antennae are directional since reception is normally required from one direction only. For this reason the single half-wave dipole or the corresponding loop antenna are not used for reception at these wavelengths.

Among the least directional of microwave antennae is the receiving antenna for a radio altimeter. This usually consists of a dipole mounted a quarter of a wavelength below the metal body or wing of the aeroplane. In this way a polar diagram approximating to half a figure 8 is obtained—the objection to higher directivity is that on banking the aeroplane would lose the ground reflected signal.

The “Capacity Antenna”

A form of antenna known as a “capacity antenna” (or sometimes as an “all-wave antenna”) can often be found for sale in radio shops. Such antennae make use of the pick-up on the earth lead, and contain nothing more than a capacitor of $0.001 \mu\text{F}$ or thereabouts. A diagram of such an “antenna” is shown in Fig. 5.15 (*a*) in which *A* and *E* are the antenna and earth terminals of the set respectively—it will be seen that the antenna terminals of the set are connected to earth via a $0.001 \mu\text{F}$ condenser. A third lead is usually provided for insertion in the earth terminal, in which case the lead will be found to make no electrical connection at all in the antenna box.

Only in the case of a long earth lead will such an arrangement have any pick-up. Fig. 5.15 (*b*) illustrates the action which, it will be seen, is tantamount to placing the receiver input terminals at the top end of a capacitance-loaded antenna (the capacitor being the receiver chassis and the antenna the long earth lead). This arrangement will therefore give some

results when the receiver is in a room above the ground floor, but near the ground the pick-up is so poor that an antenna consisting of 1 m of vertical wire would give far better results. It should be remembered that Fig. 5.15 (b) represents an idealized case, in practice the "antenna" formed by the earth lead will be very poor indeed owing to the lead running alongside walls, etc. If it were thought that such a system

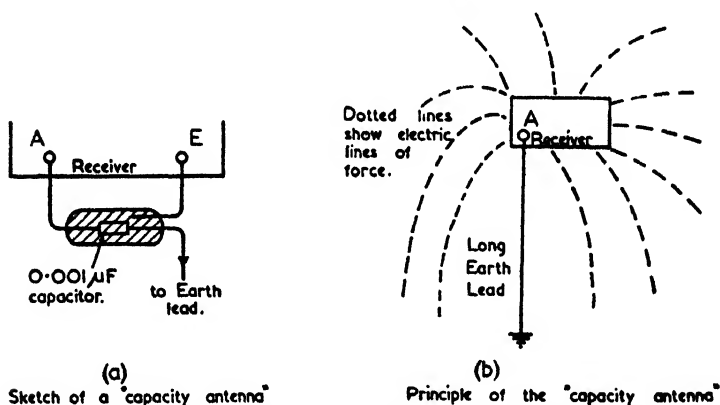


FIG. 5.15. THE SO-CALLED "CAPACITY ANTENNA"

might serve for the stations whose reception was required, it would be simpler (and cheaper) to insert the earth lead into the antenna socket directly.

5.5. DIRECTIONAL RECEIVING ANTENNAE

The Wave or Beverage Antenna

In 1923 there appeared an important article by Beverage, Rice and Kellogg⁽¹⁵⁰⁾ which described a novel form of directive antenna for long-wave reception. The type of antenna they described consists in its fundamental form of a single horizontal wire, several kilometres long, supported on wooden poles at a height of some 5 to 8 m above the ground. Fig. 5.16 (a) shows such an antenna diagrammatically and indicates that one end of the wire is terminated by a resistance (equal to the characteristic impedance of the line) while the other end goes to the receiver input terminals.

Reception takes place owing to the fact that the wavefront of a surface wave has a forward tilt and hence a horizontal

component of electric intensity. This component causes an induced current in the wire and, since the velocity of propagation along the wire is approximately equal to that in air, this current is continually augmented as the incident wave sweeps over the wire. The action is illustrated in Fig. 5.16 (b), which shows a wave travelling towards the receiver end of the wire. A similar build-up of current takes place in the reverse direction

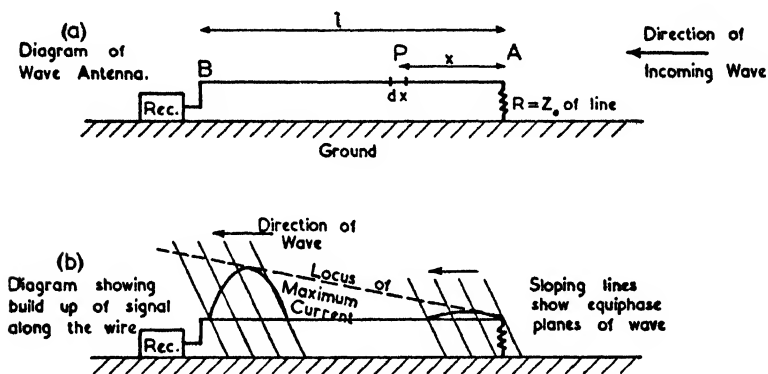


FIG. 5.16. THE WAVE, OR BEVERAGE, ANTENNA

but it is dissipated in the terminating resistance—without this resistance the antenna would be bidirectional.

The currents induced by a wave travelling from A to B (Fig. 5.16 (a)) may be calculated in the following manner—

Let E' be the horizontal component of the incident wave (E' will be equal to $E \tan \theta$, where E is the total field strength and θ is the tilt of the wave as given by the curves in Fig. 9.2). Then the instantaneous induced e.m.f. in an element of length dx is given by

$$e_A = E' dx \sin \omega t$$

where E' is the peak value of the horizontal field.

The time taken for the wave to travel from A to P is equal to x/c seconds. Multiplying this time by the angular frequency gives the phase lag of the induced voltage at P which is therefore given by

$$e_P = E' dx \sin \omega(t - x/c)$$

The induced e.m.f., e_P , in this element of length acts as a generator which causes currents flowing towards both A and B . If both ends of the wire are terminated by its characteristic

impedance Z_0 then the induced e.m.f. is feeding into a load impedance of $2Z_0$, and hence the current set up by this e.m.f. is

$$\begin{aligned} di_P &= \frac{e_P}{2Z_0} \\ &= \frac{E' dx}{2Z_0} \sin \omega(t - x/c) \end{aligned}$$

Assuming the attenuation of the line is negligible, then the resulting currents at A and B are given by

$$\begin{aligned} di_{AP} &= \frac{E' dx}{2Z_0} \sin \omega(t - x/c - x/v) \\ di_{BP} &= \frac{E' dx}{2Z_0} \sin \omega\left(t - x/c - \frac{l-x}{v}\right) \end{aligned}$$

where v = velocity of propagation along the wire.

By integration over the entire length, l , of the wire we obtain the following values for the total instantaneous currents at A and B —

$$I_A = \frac{E'}{Z_0 \beta (1 + v/c)} \sin \frac{\beta l}{2} (1 + v/c) \quad . \quad (5.18)$$

$$I_B = \frac{E'}{Z_0 \beta (1 - v/c)} \sin \frac{\beta l}{2} (1 - v/c) \quad . \quad (5.19)$$

where β = phase constant of the line

$$= 2\pi/\lambda,$$

λ = wavelength along the line

$$= v/f,$$

and λ_0 = wavelength in air

$$= c/f.$$

In the idealized case of $v = c$, we find that $I_B = E'l/2Z_0$, i.e. the current at B is proportional to the length of the wire. The value of I_A oscillates with the length of wire as shown in Fig. 5.17, which illustrates the currents for the case $v = c$, $\lambda_0 = 12$ km, $E' = 10 \mu\text{V/m}$ and $Z_0 = 500$ ohms.

In practice v is approximately equal to $0.8c$ which changes the I_B curve to the one shown by the dotted line. This dotted line attains a maximum value at $l = 2\lambda_0$, owing to the fact that if $v < c$, then the induced e.m.f. becomes out of phase with the propagated currents for wires whose lengths are several wavelengths. There is therefore a practical limit to

the length of wire which may be employed—practical forms of wave antennae have lengths varying between $0.5\lambda_0$ and $2\lambda_0$.

A further modification which occurs in practice is that the curve for I_B oscillates very slightly due to the effect of attenuation in the line.

When the direction of the incident wave makes an angle ϕ

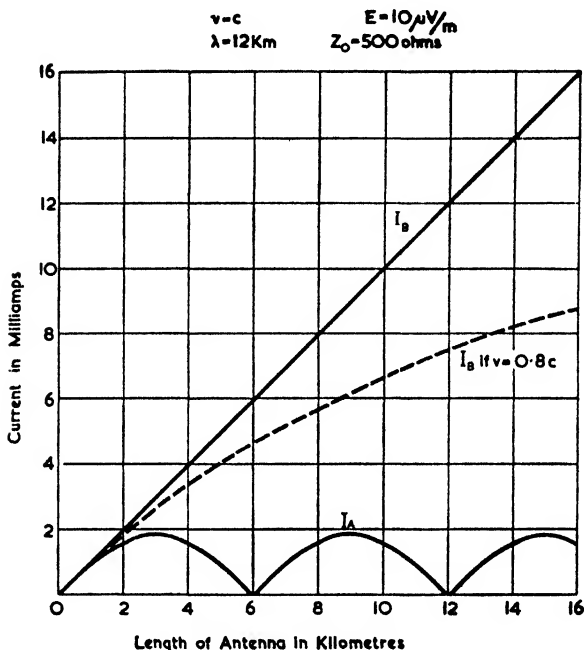


FIG. 5.17. DEPENDENCE OF THE CURRENT AT THE ENDS OF A WAVE ANTENNA ON THE LENGTH OF THE ANTENNA

with the wire, the value of E' must be replaced by $E' \cos \theta$, and the ratio v/c by $(v/c) \cos \theta$. The equation for I_B is then

$$I_B = \frac{E' \cos \theta}{Z_0 \beta (1 - (v/c) \cos \theta)} \sin \frac{\beta l}{2} (1 - (v/c) \cos \theta) \quad (5.20)$$

If in addition we allow for the attenuation constant, α , of the wire the equation becomes⁽¹⁵⁰⁾

$$I_B = \frac{E' \cos \theta e^{-j\beta l \cos \theta} (1 - e^{-\alpha l - j\beta l (1 - (v/c) \cos \theta)})}{2 Z_0 (\alpha + j\beta (1 - (v/c) \cos \theta))} \quad (5.21)$$

Beverage, Rice and Kellogg found that a typical value for the attenuation constant using wires of some 2.6 mm diameter

and lengths of 7 to 25 km was 0.4 db per km. Fig. 5.18 shows the polar diagrams in rectangular co-ordinates of three different lengths of wire using typical attenuation and phase constants. It is apparent from these curves that a wave antenna, in

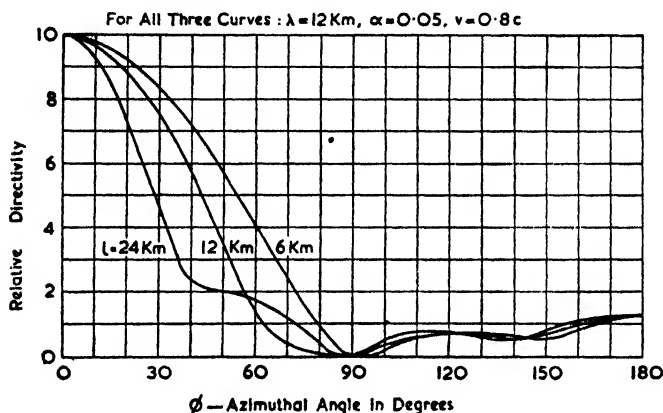


FIG. 5.18. THEORETICAL POLAR DIAGRAMS OF WAVE ANTENNAE OF THREE DIFFERENT LENGTHS
(Beverage, Rice and Kellogg, *Trans. A.I.E.E.*, Feb., 1933)

common with other long-wire travelling-wave systems, can be used over quite a wide range of frequencies.

The effective height of a wave antenna depends on the ratio of E' to E , i.e. on the tilt of the surface wave. For moderate

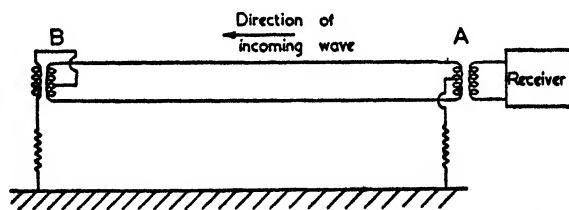


FIG. 5.19. TWIN-WIRE WAVE ANTENNA WITH REFLECTION TRANSFORMER

ground conductivity ($g = 0.005 \text{ mhos/m}$), the effective height would be 2 per cent of the length if $\lambda = 5000 \text{ m}$ or 8 per cent of the length if $\lambda = 500 \text{ m}$.

A useful feature of the wave antenna is that it is possible to produce a null in the polar diagram in any desired direction in the rear (i.e. for angles lying between $\phi = 90^\circ$ and 270°). The necessary adjustments consist of tuning the terminating

impedance and balancing some of the current through this with a portion of the current at the input terminals. The tuning operations can be more efficiently carried out if the receiver input is at the same end of the wire as the terminating resistance. Such an arrangement can be obtained by the circuit shown in Fig. 5.19 and was described by Beverage, Rice and Kellogg.⁽¹⁵⁰⁾

In Fig. 5.19 the single wire is replaced by a twin wire along which the induced currents flow in parallel. The "reflection" transformer at the end *B* returns the signal to the wire in push-pull, and the returned signal is applied to the receiver input terminals via a transformer at *A*. This arrangement therefore brings the receiver input and terminating impedance together so that it becomes a simple matter to fit a balancing circuit between them.

Medium-wave Loop Antennae

In spite of their low effective height, small loops can make quite good receiving antennae. When used in the position of maximum pick-up, the received atmospheric noise will still exceed the noise due to loss resistance—hence the extreme inefficiency of the loop antenna is not a serious matter when the loop is used for reception. Loops have a polar diagram which is a figure 8, and this directional quality can be useful in discriminating between wanted and unwanted signals.

Loop antennae are discussed in some detail in Chapter VII and will therefore not be enlarged upon here. There is one point of interest, however, which it is appropriate to mention in the present chapter—it is that the fading on loops is greater than on vertical antennae.

The distinction between the two cases is due to the fact that on medium wavelengths the ground acts as an almost perfect reflector to the sky waves. Hence the effective sky-wave field to a vertical wire is $2E \sin \theta$ (where θ is the angle between the downcoming sky wave and the vertical) whereas for the loop it is simply $2E$. The interfering sky-wave signal on a vertical antenna is therefore smaller by a factor of $\sin \theta$ than that on a loop antenna of the same effective height. The extent to which this difference is noticeable depends, of course, on the relative strengths of the ground and sky waves. This difference between the behaviour of loop antennae and vertical wires was used by Appleton and Barnett⁽²²²⁾ to determine the height of the Heaviside layer.

Diversity Reception

Except in tropical countries, reception on short waves is not seriously handicapped by noise. A more vital problem is that of fading due to variations in polarization of the sky wave and variations in its intensity. To reduce these variations some form of diversity reception is often used, the principle being to combine the rectified output from two or more receiving antennae on the assumption that severe fading rarely occurs simultaneously in all antennae. By having some form of automatic gain control operated by the strongest signal, the combined signal can show a distinct improvement over that due to a single antenna only. The various forms of diversity reception are as given below.

(a) *Polarization Diversity*

The receiving antenna system may consist of a vertical and a horizontal antenna or two horizontal antennae at right angles. The choice depends on the site conditions and the probable angle of the downcoming rays. Polarization diversity has the advantage of a compact antenna system but is less effective than space diversity.

(b) *Space Diversity*

In space diversity reception the antennae are separated by a distance of up to ten wavelengths (the greater the separation the better). As might be expected, the improvement obtained by increasing the number of antennae from one to two is greater than that obtained by making an increase from two to three. Consequently dual diversity is usually used for telegraphy, whilst treble diversity is employed for telephony where the extra expense is more justified. A diversity system is useful with any type of antenna, but since a large amount of ground is involved it is mostly used with large directional antennae of the rhombic or fishbone variety.

(c) *Musa System*

The Musa system⁽¹⁵⁴⁾ (Multiple Unit Steerable Antenna) is an extension of the diversity principle in which all the signals from a line of six antennae are combined so that the antennae have a joint directivity which is in the direction of the strongest sky wave. This overall directivity is obtained by phasing circuits and, since several such circuits may be put

in parallel, the system can be made to have more than one directivity. The other circuits are used for monitoring or for picking out the direction of the second best reception. The system would obviously not be practicable if there were not certain preferred angles to the vertical for reception and if these angles were not relatively stable.

There are other methods of reducing the effects of fading such as frequency diversity, single-side-band working, carrier shift keying, special telegraphy codes, etc., but these are outside the scope of this book. References to such systems will be found in Terman's *Radio Engineers' Handbook*.⁽²³⁾

The Rhombic Antenna

The calculation of the polar pattern and gain of a receiving rhombic may be carried out by assuming that it is transmitting energy, and therefore all the equations and methods described in § 6.5 will apply to the receiving case as well. The polar diagram of the antenna should not be too sharp since the angle of the downcoming sky waves may vary between fairly wide limits—an example of such variations is given in Fig. 9.23.

It will be noticed that since the overall length of a rhombic antenna is of the order of a few wavelengths, an antenna of this type has inherently some "space diversity" effect. Nevertheless in important installations it is desirable to use two or three spaced rhombics and to combine the outputs from them.

In reception the accuracy of the matching between the antenna and its transmission line is of minor importance, so that for this reason a rhombic with single-wire sides is adequate. On the other hand, tests have shown that a multiple-wire rhombic can have certain advantages for reception. In the results quoted by Harper⁽⁸⁾ a signal gain of about 1 db was obtained with a three-wire rhombic; also during periods of precipitation static the noise level was some 9 db lower (the latter feature is more significant than the small increase in gain).

To reduce the pick-up of local noise a buried coaxial line should be used for coupling the antenna to the receiver. The necessary impedance conversion—and the transition from balanced to unbalanced working—can be readily obtained by means of a shielded transformer with a toroidal iron dust core. A well-designed transformer of this nature will have a response which is level to within ± 1 db over a frequency range of

3 to 20 Mc/s. The centre of the balanced side of the transformer should be provided with a d.c. path to ground so that there is no accumulation of charge on the wires of the rhombic.

Both the input transformer and the terminating resistance should be mounted as near to the ends of the antenna as possible. They are therefore housed in small weatherproof boxes at the tops of the two masts supporting the extreme ends of the rhombic.

The Fishbone Antenna

The fishbone antenna consists of a series of non-resonant antennae which are loosely coupled to a transmission line

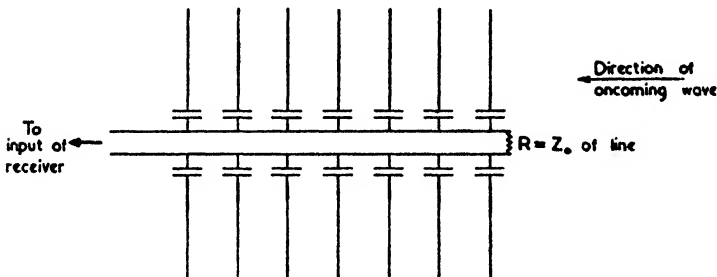


FIG. 5.20. DIAGRAM OF A FISHBONE ANTENNA

some three or more wavelengths long, the end of which is terminated by a resistance equal to its characteristic impedance. A wave approaching in the direction shown in Fig. 5.20 will induce voltages along the line which are in the correct phase to cause a travelling wave to be set up in the same direction as the incident wave. This could only be so if the coupling between the side collectors and the line were weak, since it presupposes that the phase constant of the line would be substantially unaltered by the presence of these side elements. In practice a reduction in the phase constant of as much as 10 per cent can be tolerated. The system is therefore inefficient from the transmitting point of view (the array is sometimes known as a high-frequency Beverage antenna—a name which suggests its equivalence to the long-wave Beverage antenna).

A fishbone antenna is essentially an end-fire type of array and therefore is highly directional in a vertical plane but not in a horizontal plane. For this reason two units are often arranged in parallel. In this form two arrays each five wavelengths long will have a gain of some 30 db over a single

dipole, i.e. the signal-to-noise ratio will be improved by this amount if the noise is uniformly distributed. Even a single antenna, one wavelength long, will provide a useful degree of discrimination against noise or unwanted signals from the reverse direction.

At the optimum working wavelength the collectors have a length of about 0.3λ and are spaced at intervals of about $\lambda/12$. The coupling capacitances have a value of approximately $3 \mu\mu\text{F}$ if $\lambda = 30 \text{ m}$ and may be simple insulators with metal foil added to give the right capacitance.

The frequency range is limited at the higher frequencies by the fact that the collectors become resonant and at the lower frequencies by the fact that they become relatively short. A frequency range of 0.5 to 1.2 times the optimum frequency is the accepted working range (a frequency range of 1 : 2.5 is typical of non-resonant long antennae).

Directional Antennae and Arrays

THE various types of antennae described in the present chapter are used mostly in short-wave transmission. Directional antennae of the type peculiar to microwave transmission are described separately in Chapter IV. These divisions are merely ones of convenience for the same fundamental principles apply in each case. The account given below on general principles therefore applies to all types of directive antennae.

Formulae have been derived (see, for example, refs. (20) and (176)) for determining the polar diagram of any symmetrical array of radiating elements. In practice, however, it is advisable to approach the problem from a synthetic point of view by acquiring a geometrical picture of the contribution of the various elements to the polar pattern. Such a line of approach is particularly useful in investigating problems in which the actual antenna system is initially unspecified since it gives an insight into the problem which is unobtainable by purely algebraic analysis.

6.1. GENERAL PRINCIPLES

Derivation of Polar Diagrams

To obtain a directive polar pattern the radiating elements must occupy an area of which at least one side is an appreciable fraction of a wavelength. This results in "space phasing" between the radiation from the various elements, i.e. the electric intensities from each element have relative time phases which depend on the differences in the path lengths from the elements to the field-point.

The elements to which we have referred may be half-wave dipoles, subdivisions of a long-wire system, parasitically-excited

portions of a metallic screen, or even the various portions of a wavefront such as exist at the mouth of an electromagnetic horn. In all cases the space-phasing principle applies.

Suppose we have three antennae, A_1, A_2 and A_3 , with currents I_1, I_2 and I_3 whose relative magnitudes and phasings are as shown in Fig. 6.1. Then at a distant point P they cause fields E_1, E_2 and E_3 , whose magnitudes are proportional to their

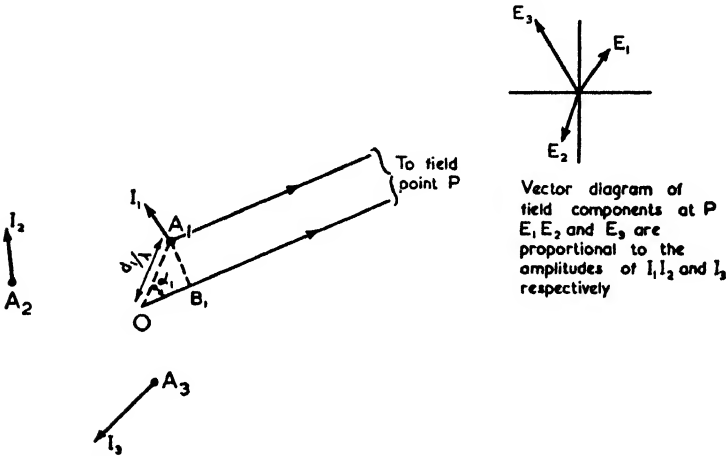


FIG. 6.1. DIAGRAM FOR CALCULATION OF POLAR PATTERNS

respective currents and whose phases depend on the current phases together with the path differences between A_1, A_2 and A_3 to the point P . Taking some reference point O in the antenna system, then all the space-phase differences may be referred to this origin by considering a radiation from O to P as having no phase shift. It is obvious from Fig. 6.1 that antenna A_1 , for instance, has a phase advance equal to OB_1 (in addition to whatever phase difference the current I_1 may have with regard to the arbitrary standard phase at O).

The distance of P from O is such that A_1P and OP are approximately parallel so that $OB_1 = \beta d_1 \cos \alpha_1$ radians. If we rotate P about O , the space-phasing OB_1 goes through the values $+\beta d_1, 0, -\beta d_1, 0$ and back to $+\beta d_1$ as the angle $(\phi + \alpha_1)$ takes on the values $0^\circ, 90^\circ, 180^\circ, 270^\circ$ and 360° respectively. Let us suppose that $d_1 = 0.375\lambda$, then $\beta d_1 = 3\pi/4$ radians or 135° . Consequently the vector E_1 will rotate as shown in Fig. 6.2 as $(\phi + \alpha_1)$ varies from 0° to 360° . In this figure the phase change in E_1 is shown for every 10° change in

$(\phi + \alpha_1)$. It is apparent that the phase of E_1 varies slowly at 0° and 180° (when P is in line with OA_1) but rapidly at 90° and 270° (when P is at right angles to the line OA_1). At 90° and 270° the space-phasing between O and A_1 is zero so that the angle β_1 shown in Fig. 6.2 represents the initial phase of E_1 with respect to the standard phase from O .

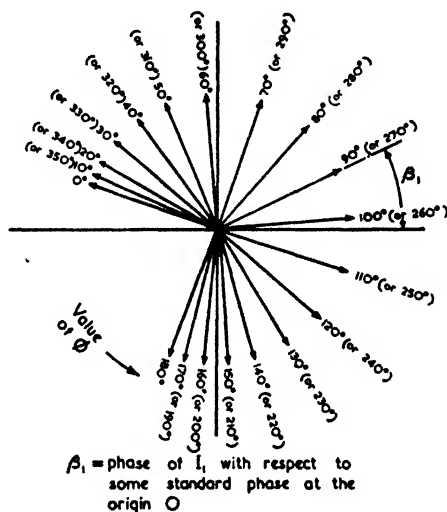


FIG. 6.2. VARIATION OF THE TIME PHASE OF E_1 (FIG. 6.1) WITH EXPLORING ANGLE ϕ

The above considerations show that in the general case the resultant field E at P due to n coplanar elements is given by

$$\begin{aligned}
 E &= \sum_1^n E_n \text{ (vector sum)} \\
 &= k \sum_1^n I_n \angle [360^\circ (d_n/\lambda) \cos(\phi + \alpha_n) + \beta_n] \quad (6.1)
 \end{aligned}$$

where k = a constant depending on the distance to the field point and the frequency of the radiation,

I_n = current in antenna n ,

d_n = distance of antenna n from the origin,

α_n = angular position of antenna,

β_n = relative phase of antenna current,

ϕ = exploring angle of polar diagram.

The symbols α_n and β_n should not be confused with α and β , the attenuation and phase constants of a medium or a transmission line.

A machine described by Williams⁽³⁶⁶⁾ performs the summation given by equation (6.1) for values of n up to 5, d_n up to 2λ , and any values of I_n , α_n or β_n . The principle of the machine, which employs "Selsyn motors," is such that it permits extension to greater values of n and d_n —the sole limitation being one of accuracy in manufacture. Recently a purely electronic machine has been described by Brown and Morrison⁽³⁵⁰⁾ in which the polar diagram is shown on a cathode-ray tube.

In the foregoing account it has been assumed that the radiation from each element is omnidirectional (i.e. the polar diagram of a single element is a circle) in the plane of exploration. When this is not so, but all the elements have the same individual polar diagram, then the combined diagram may be obtained by first assuming omnidirectional antennae and then multiplying the resultant pattern by the particular pattern of a single element.

Height Factors for Positive and Negative Images

An important form of equation (6.1) arises in the case of an antenna (or antenna system) which is situated above the ground and for which a positive or negative image may be assumed. The assumption of a positive image applies to the case of vertical radiating elements and that of a negative image to horizontal elements. Both forms are shown in Fig. 1.8. The validity of these assumptions is discussed in § 3.1 where it is pointed out that only in the case of horizontal polarization is the image as stated. With vertical polarization on short waves and with small angles of elevation from the ground, it is actually more correct to assume a *negative* image as is done for horizontal polarization. The border line depends on the Brewster angle and this is discussed in § 9.5 (and § 3.5, Vol. I).

Although it is inaccurate to assume a positive image for low-angle short-wave radiation, curves based on the assumption of a positive image are of value, since they serve to determine the radiation pattern of pairs of cophasal elements in an array. In fact these "height factor" curves apply to any case in which we have a pair of identical antenna systems that are either cophasal (the positive image case) or in antiphase (the negative image case).

In Fig. 6.3 the following special cases of equation (6.1) are obtained, putting $\alpha_1 = \beta_1 = 0$

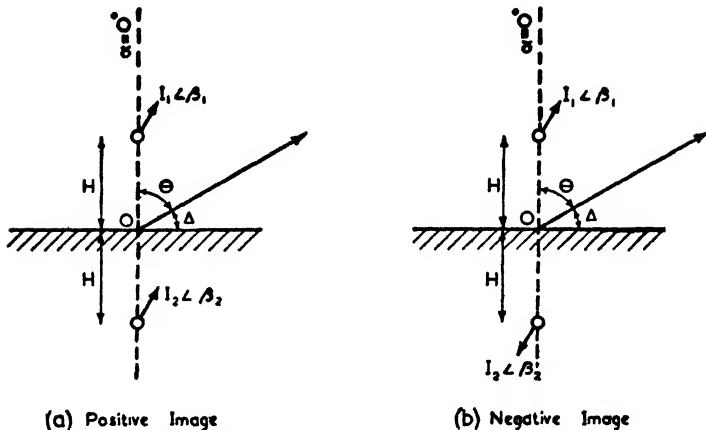
Positive Image

$$\alpha_1 = 0 \qquad \beta_1 = 0$$

$$\alpha_2 = \pi \qquad \beta_2 = 0$$

Using radians instead of degrees, i.e. using $\beta = 2\pi/\lambda$ to turn lengths into radian measure, we have

$$\begin{aligned} E &= k[I_1 \angle (\beta H \cos \theta) + I_2 \angle \{\beta H \cos (\theta + \pi)\}] \\ &= 2kI_1 \cos (\beta H \cos \theta) \end{aligned}$$



(a) Positive Image

(b) Negative Image

FIG. 6.3. DIAGRAMS FOR CALCULATION OF HEIGHT FACTORS

It is convenient to define a height function $F_1(H, \theta)$ whose value gives the relative amplitude of the polar diagram in a vertical plane. This may be done by putting $2kI_1$ equal to unity in the above equation, which gives

$$F_1(H, \theta) = \cos (\beta H \cos \theta) \quad (\text{positive image}) \quad (6.2)$$

or $F_1(H, \Delta) = \cos (\beta H \sin \Delta)$

where $\Delta =$ angle of elevation.

Negative Image

$$\alpha_1 = 0 \qquad \beta_1 = 0$$

$$\alpha_2 = \pi \qquad \beta_2 = \pi$$

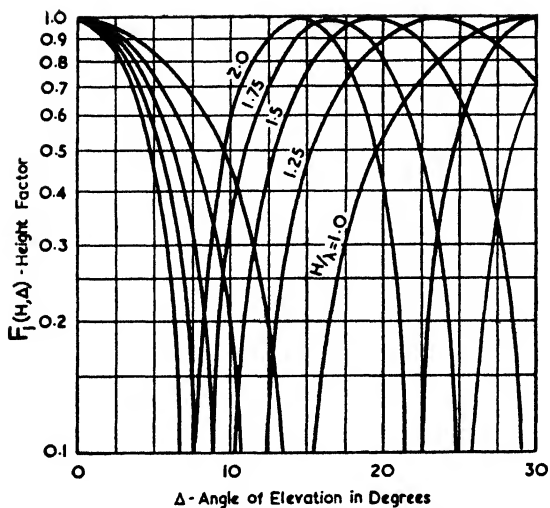


FIG. 6.4 (a). HEIGHT FACTOR CURVES FOR POSITIVE IMAGES, RANGE $H = 1\lambda$ TO 2λ AND $\Delta = 0^\circ$ TO 30°

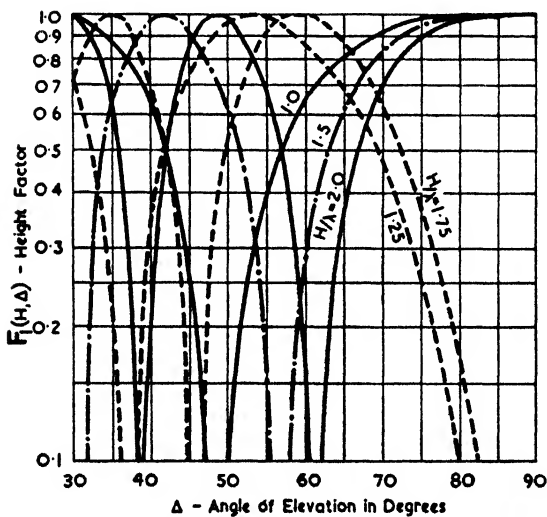


FIG. 6.4 (b). HEIGHT FACTOR CURVES FOR POSITIVE IMAGES, RANGE $H = 1\lambda$ TO 2λ AND $\Delta = 30^\circ$ TO 90°

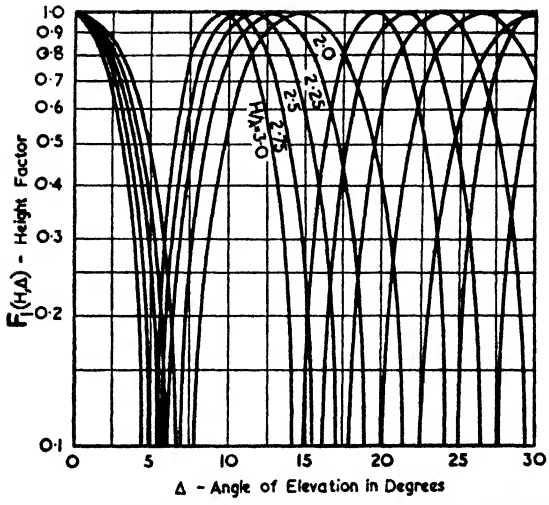


FIG. 6.5 (a). HEIGHT FACTOR CURVES FOR POSITIVE IMAGES, RANGE $H = 2\lambda$ TO 3λ AND $\Delta = 0^\circ$ TO 30°

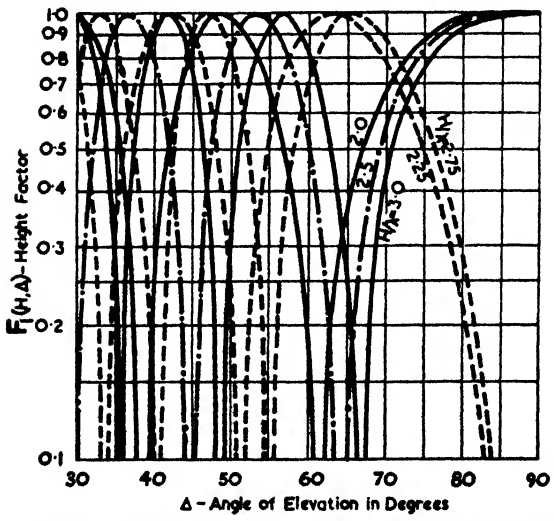


FIG. 6.5 (b). HEIGHT FACTOR CURVES FOR POSITIVE IMAGES, RANGE $H = 2\lambda$ TO 3λ AND $\Delta = 30^\circ$ TO 90°

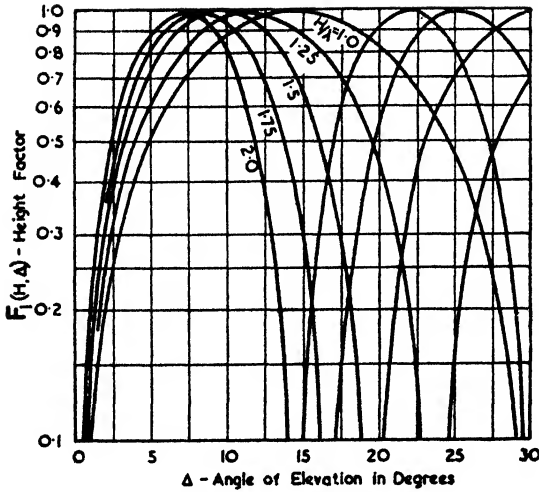


FIG. 6.6 (a). HEIGHT FACTOR CURVES FOR NEGATIVE IMAGES, RANGE $H = 1\lambda$ TO 2λ AND $\Delta = 0^\circ$ TO 30°

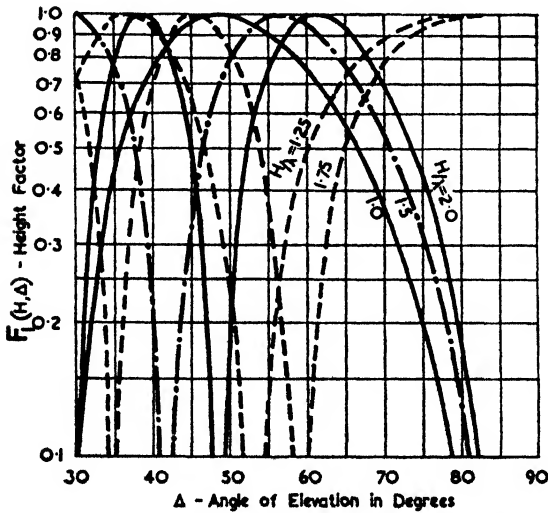


FIG. 6.6 (b). HEIGHT FACTOR CURVES FOR NEGATIVE IMAGES, RANGE $H = 1\lambda$ TO 2λ AND $\Delta = 30^\circ$ TO 90°

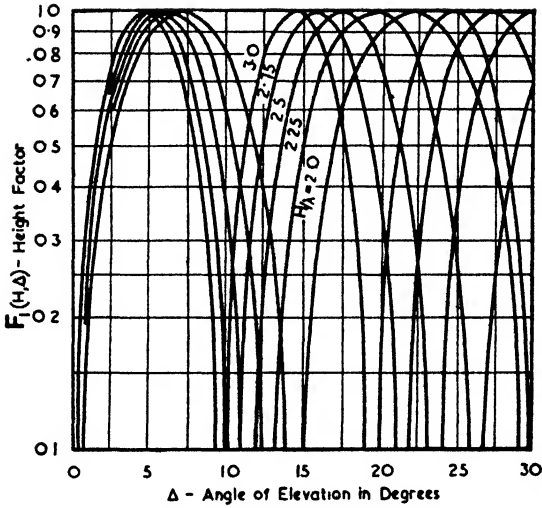


FIG. 6.7 (a). HEIGHT FACTOR CURVES FOR NEGATIVE IMAGES, RANGE $H = 2\lambda$ TO 3λ AND $\Delta = 0^\circ$ TO 30°

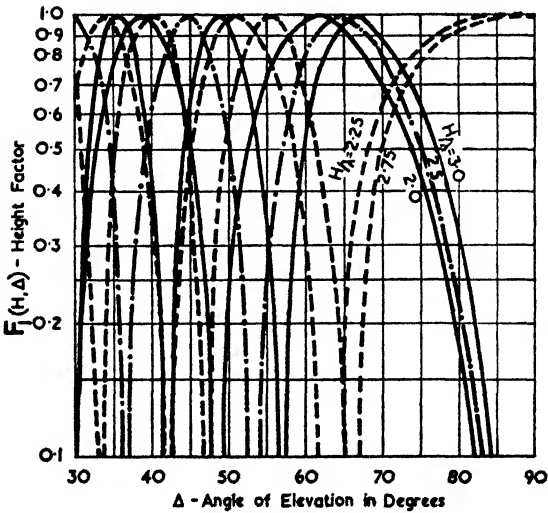


FIG. 6.7 (b). HEIGHT FACTOR CURVES FOR NEGATIVE IMAGES, RANGE $H = 2\lambda$ TO 3λ AND $\Delta = 30^\circ$ TO 90°

Proceeding on the same lines as before we find

$$F_1(H, \theta) = \sin(\beta H \cos \theta) \quad (\text{negative image}) \quad (6.3)$$

or $F_1(H, \Delta) = \sin(\beta H \sin \Delta)$

where $\Delta =$ angle of elevation.

The curves given by equations (6.2) and (6.3) find a great number of applications. They have therefore been given in Figs. 6.4 to 6.7 for various values of H ranging between 1λ and 3λ , while the curves of Figs. 3.7 and 3.8 cover the range of 0.25λ to 1λ .

Analysis of Polar Diagrams by Vector Diagrams

The analysis of two typical polar diagrams is considered below to illustrate the geometrical method which views the time phases of the field components as rotating vectors. Such a viewpoint will be found superior in most cases to the more usual method of constructing a polygon of the vector components. For example, problems involving the course width of aircraft beam-approach systems can be solved very easily by a consideration of rotating vectors.

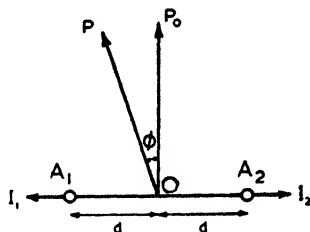


FIG. 6.8. DIAGRAM OF TWO ANTENNAE FED WITH EQUAL BUT ANTI-PHASE CURRENTS

(a) Two Antennae in Anti-phase

Fig. 6.8 represents a plan view of two vertical dipoles A_1 and A_2 fed 180° out of phase, or the side elements of a vertical loop as considered in a horizontal plane. It is always easier to choose symmetrical conditions for the reference point and the line of zero angular direction; in this case, therefore, the reference point O is taken midway between A_1 and A_2 and $\phi = 0$ is along OP_0 which is the right bisector of A_1A_2 .

Along the path OP_0 the electric field vectors E_1 and E_2 , due to A_1 and A_2 respectively, are in anti-phase as shown in Fig. 6.9 (a). As ϕ increases positively in an anti-clockwise direction, the phase of E_1 is gaining with respect to a standard reference phase at O , while that of E_2 is losing; consequently the vectors begin to spin as shown.

The rate of spin for equal increments in θ is at first quite uniform since the path difference is $\beta d \sin \phi$, which for small

values of ϕ equals $\beta d \phi$. In fact, the resultant increases linearly with ϕ . Thus a plot of field strength versus angle would commence as an Archimedean spiral, and this has the same

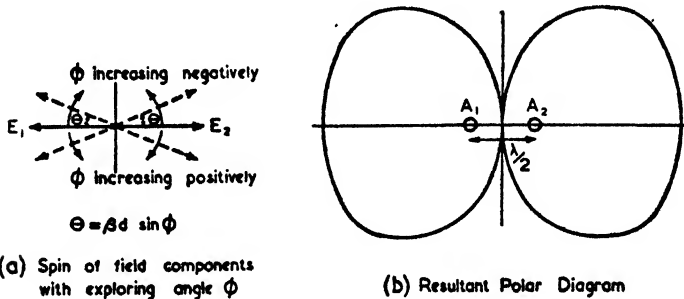


FIG. 6.9. POLAR DIAGRAM OF ANTI-PHASE SOURCES SHOWN IN FIG. 6.8 WHEN $d = 0.25\lambda$

shape as a square law curve over a small range of angles near the origin.

If $d = 0.25\lambda$, the total angular spin by the vectors as ϕ progresses from 0 to 90° will also be 90° although the *rate of*

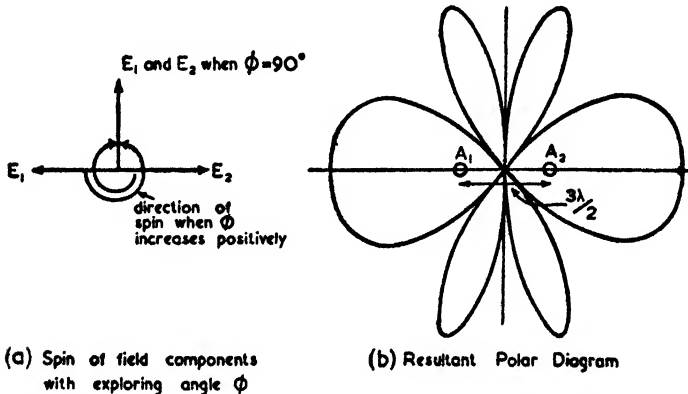


FIG. 6.10. POLAR DIAGRAM OF ANTI-PHASE SOURCES SHOWN IN FIG. 6.8 WHEN $d = 0.75\lambda$

spinning decreases as ϕ approaches the value 90° . Because the rate of spinning varies with $\sin \phi$, this decrease as ϕ approaches 90° takes place whatever the value of d may be. Thus all beams are sharper if produced broadside than if produced end-on to an array. In the present case the effect is to give solely a broad end-on beam as shown in Fig. 6.9 (b).

If the antenna separation were increased to, say, $d = 0.75\lambda$, the rate of spin of the E vectors would be trebled for given increments in ϕ and their total spin becomes equal to 270° as shown in Fig. 6.10 (a). The resultant of E_1 and E_2 reaches a maximum when $\beta d \sin \phi = \pi/2$ and $3\pi/2$ and a minimum when $\beta d \sin \phi = \pi$. Since the speed of rotation is greatest for small values of ϕ , the angular distance between adjacent maxima and minima is less in the region $\phi = 0^\circ$ than in the neighbourhood of $\phi = \pm 90^\circ$. Furthermore it is obvious that

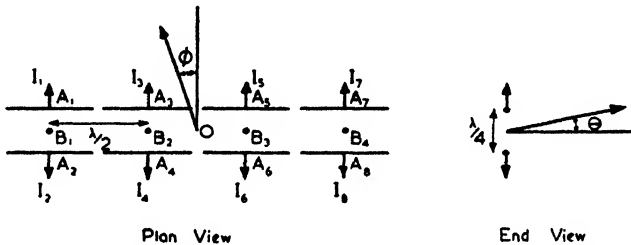


FIG. 6.11. ARRAY OF EIGHT DIPOLES FOR EXAMPLE IN THE SYNTHESIS OF POLAR DIAGRAMS

the polar pattern will be symmetrical in all four quadrants. The complete polar diagram is shown in Fig. 6.10 (b).

(b) Eight Horizontal Dipoles

In Fig. 6.11 is shown an array of eight half-wave dipoles which are fed with equal current having the phase relationships shown diagrammatically by the current vectors. For the purpose of this example, the array will be considered to be in free space. The effect of the ground can easily be taken into account by the method of images.

The polar diagram in a vertical plane is obviously given by the previous example on putting the half-distance equal to 0.125λ . In considering the vertical polar diagram it might appear that greater forward radiation could be obtained by increasing the separation between the rows to $\lambda/2$; for then the electric field vectors due to the two rows would be completely in phase when $\theta = 90^\circ$, whereas in the present arrangement they are still 90° out of phase at this vertical angle. Actually the difference in the two cases is quite small for in the more closely spaced case the mutual impedance is such as to decrease the radiation resistance and thereby increase the current values for a given input power.

To evaluate the horizontal polar diagram it is easiest to consider the antennae in four pairs and to calculate the pattern

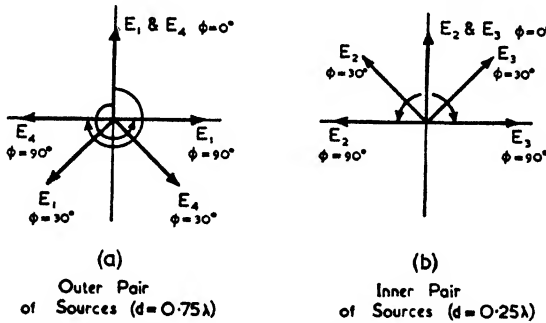


FIG. 6.12. FIELD VECTORS FOR PROBLEM SHOWN IN FIG. 6.11

of point sources at B_1, B_2, B_3 and B_4 , each of which represents the centre of a pair of dipoles. Then the polar diagram of these point sources is simply multiplied by the polar diagram

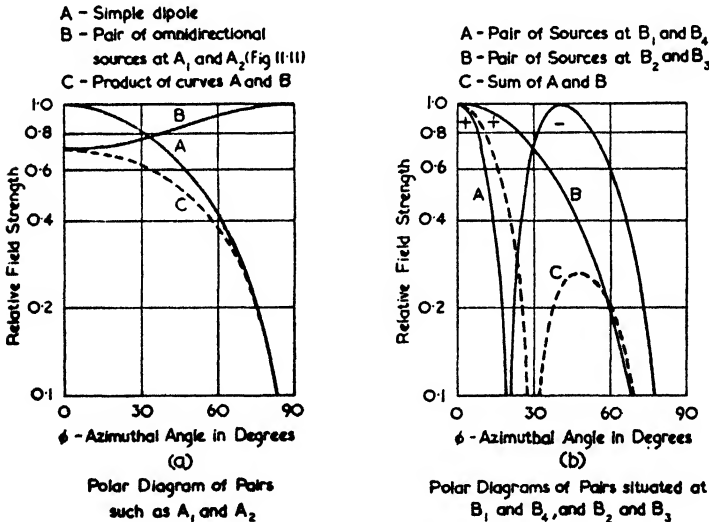


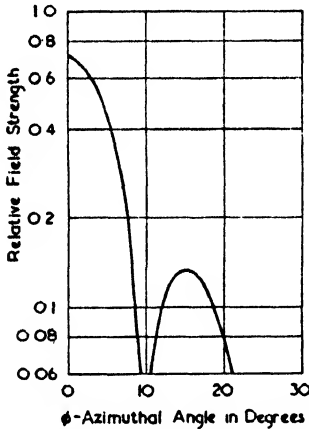
FIG. 6.13. POLAR DIAGRAMS OF CERTAIN PAIRS OF SOURCES IN FIG. 6.11

of a single pair. The justification for this procedure lies in the fact that the resultants for each pair have exactly the same phase.

The polar diagram of a single pair is obtained by regarding the centres of the dipoles as point sources and by multiplying

the result by the polar pattern of a single half-wave dipole. For both this and the previously mentioned multiplication, the simplest method is to perform the multiplications by means of logarithmic paper as described on page 97. Thus the pattern of a single pair can be obtained as shown in Fig. 6.13(a).

In dealing with the point sources B_1 to B_4 an obvious choice for the origin O is the midpoint of the set, then the vector



Polar Diagram in Cartesian Form
(obtained by multiplying together the two dotted curves in Fig 6.13)



(b)
Complete Polar Diagram in Polar Form

FIG. 6.14. COMPLETE HORIZONTAL POLAR DIAGRAM OF FIG. 6.11

diagrams of the fields from these sources will take the form shown in Fig. 6.12. These diagrams show that the resultants of E_1 and E_4 and of E_2 and E_3 are always in phase or anti-phase. Hence the resultants of each of the two pairs may be added as shown in Fig. 6.13 (b).

The multiplication of the dotted curves in Figs. 6.13 (a) and (b) gives Fig. 6.14 (a), which is shown in polar form in Fig. 6.14 (b), where use has been made of the fact that the diagram is the same in each quadrant.

(c) *Effect of Spacing in Arrays*

A number of the fundamental properties of a cophasal linear array can be readily deduced from vector diagrams of the component fields. Fig. 6.15 shows a simple example of such an array—in this case we have five elements uniformly spaced at intervals of 0.5λ . In addition, a number of diagrams

are given showing the relative phases of the field components for various bearing angles.

When $\phi = 0^\circ$ all five field vectors are in phase, but as ϕ increases they begin to "unfold" until when $\phi = 23.6^\circ$ they are evenly spaced and hence their resultant is zero. A further zero resultant occurs when E_1 and E_5 have rotated through

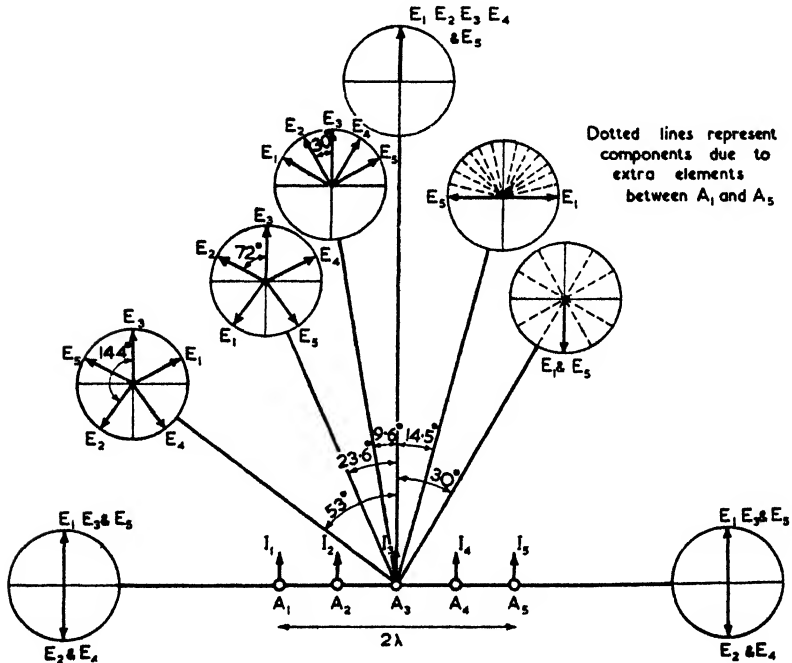


FIG. 6.15. DIAGRAM FOR ILLUSTRATING THE PROPERTIES OF COPHASAL LINEAR ARRAYS

288° and E_2 and E_4 through 144° . These pairs retain their 2 : 1 difference in rate of spinning all the time, since the relative rates of spin are determined entirely by the antenna spacing. Finally, when $\phi = 90^\circ$, the resultant is one-fifth of its value at $\phi = 0^\circ$.

If we were to insert a large number of elements between the existing ones the array would be equivalent to a uniform sheet of current. On the vector diagram the angle between vectors E_1 and E_5 would contain a correspondingly greater number of field components and likewise for the angular space between E_5 and E_3 . It is easy to realize that this will hardly affect the

main forward lobe of the polar diagram for values of ϕ which are less than $\pm 10^\circ$. Neither is the remainder of the main lobe affected to any great extent, for instead of the first zero occurring at $\phi = \pm 23.6^\circ$, it will be at $\phi = \pm 30^\circ$, i.e. when E_1 and E_5 have rotated through 180° . The "filling in" between the five original rotating vectors by further vectors corresponding to the extra antenna elements increases the uniformity of the vector distribution, with the result that for large values of ϕ the resultant can no longer be as great. This is demonstrated, for example, in the direction $\phi = 90^\circ$, for which the resultant is now zero instead of one-fifth of the maximum.

The diagrams in the negative quadrant have been chosen to illustrate the fact that if we have two antennae only then the main lobe is twice as sharp as that caused by a uniform current distribution. In this case A_1 and A_5 have been chosen as a pair and it is obvious that the forward lobe becomes zero when E_1 and E_5 have rotated through 90° (which for these spacings means $\phi = \pm 14.5^\circ$). But if the intervening angular space were to be filled in by a large number of further vectors, they would have to rotate through 180° for the resultant to be zero (this occurs for $\phi = \pm 30^\circ$). Hence the ratio of the beam widths in the two cases is very nearly 2 : 1. We have considered a pair of antennae separated by 2λ ; for wider spacings the approximation to this ratio would be even closer.

In the above examples considerable use was made of symmetry—a feature which should always be exploited as fully as possible. When dealing with unsymmetrical arrays the use of spinning-vector diagrams is almost essential. If, in addition, a calculating machine is available, the combination provides a very quick and flexible technique for the determination of polar diagrams or, what is normally much more difficult, for the determination of a practical array to produce a given diagram.

The "inverse" problem of determining the array to produce a given polar diagram has been considered in a number of articles among which that by Wolff⁽³⁶⁸⁾ is a good example. Assuming linear arrays he obtains the result in the form of a Fourier series which specifies pairs of antennae. From an engineering point of view it is nearly always simpler to make an approximate estimate of the required array and then to calculate a number of polar diagrams, based on practical configurations, after which the best compromise may be chosen.

6.2. GAIN OF DIRECTIVE SYSTEMS

(a) *A General Definition*

The gain of a directive antenna system may be defined on a power basis taking as our standard radiator a hypothetical omnidirectional antenna (sometimes referred to as an "isotropic" radiator). Then the directivity is given by the ratio of the power that must be supplied to the isotropic radiator to the power supplied to the directive antenna, when both antennae radiate the same power per unit solid angle in the direction of maximum radiation for the latter antenna, i.e. both antennae give the same field strength in this direction.

To compute this ratio it is convenient to surround the antenna by a sphere—a hemisphere when the ground is taken into account—and to calculate the power per unit area transmitted through this sphere over the different parts of its surface. This power is given by Poynting's vector \mathbf{S} which, in the M.K.S. system, is in watts per square metre. If the field strength E is in volts per metre, then

$$|\mathbf{S}| = E^2/z_{00} = 0.00265 E^2 \quad . \quad . \quad . \quad (6.4)$$

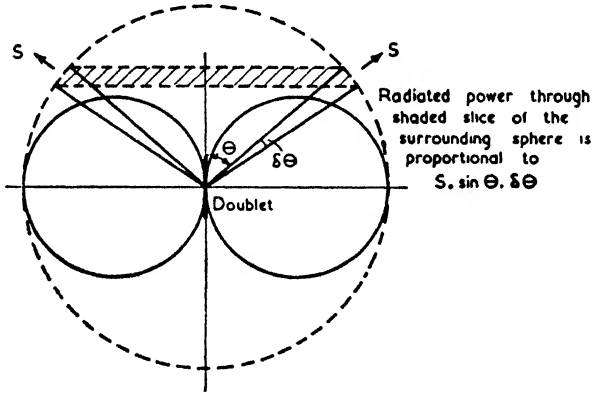
By integration the total power may be found, the expression being of the form $W = \int S da$. This value is compared with the value that would be obtained if the whole surface of the sphere were transmitting a uniform power density S_m , where S_m is the value of the Poynting vector at the point of maximum radiation and equals E_m^2/z_{00} . The power W_0 obtained in this way is that required for the isotropic radiator. Hence the power gain with respect to an omnidirectional antenna is given by

$$G_0 = \frac{W_0}{W} = \frac{\int S_m da}{\int S da} \quad . \quad . \quad . \quad (6.5)$$

There is obviously no need actually to calculate the powers involved; all that is required is that their ratios should be determined.

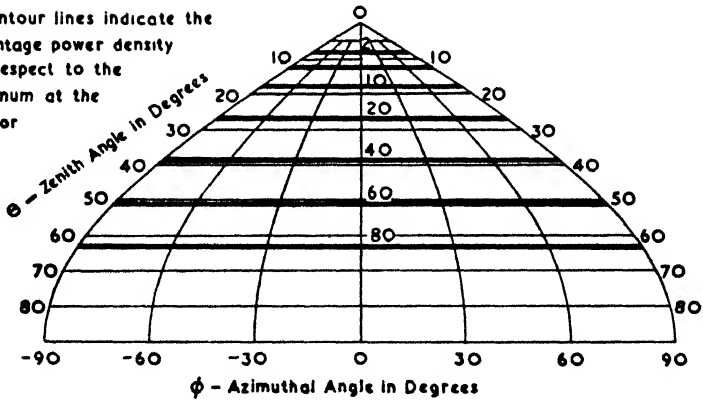
As an example we may take the simplest of all cases, that of a doublet in free space. Such an antenna has a polar diagram as shown in Fig. 6.16 (a) in the plane containing the dipole and a circular pattern in the equatorial plane. The power radiated is everywhere proportional to E^2 , but Fig. 6.16 (a) cannot be used directly since the surface area of the surrounding sphere decreases towards the poles for a given element of

angle $\delta\theta$. This decrease is proportional to $\sin \theta$. Hence by weighting the values of $S da$ by this amount we arrive at the correct total power radiated, but for making a calculation of



Polar diagram in a meridian plane

The contour lines indicate the percentage power density with respect to the maximum at the equator



(b) Power Distribution Diagram

FIG. 6.16. DIAGRAMS FOR THE INTEGRATION OF THE TOTAL POWER RADIATED FROM A DOUBLET

the gain we require only the total power *relative* to that in the maximum direction and this may be obtained by taking the square of the relative field strengths.

The proportioning by $\sin \theta$ can be done by drawing a power distribution diagram in which the lines of latitude are equally

spaced and the lines of longitude follow a sine law. A diagram of this nature is shown in Fig. 6.16 (b), and it embraces one-quarter of the whole sphere. In a complicated case, such as is shown in Fig. 6.58, the total power evaluation can be carried out by a planimeter to a degree of accuracy depending on the number of subdivisions, but in this simple example we have

$$\begin{aligned} W &= \frac{8}{z_{00}} \int_0^{\pi/2} E^2 \sin \theta \, d\theta \\ &= \frac{8E_m^2}{z_{00}} \int_0^{\pi/2} \sin^3 \theta \, d\theta \\ &= \frac{16}{3} E_m^2 / z_{00} \end{aligned}$$

The total power that would be radiated if the field strength were everywhere equal to E_m , the maximum field strength, is

$$\begin{aligned} W_0 &= \frac{8}{z_{00}} \int_0^{\pi/2} E_m^2 \sin \theta \, d\theta \\ &= \frac{8}{z_{00}} E_m^2 \end{aligned}$$

Hence the power gain of an elementary dipole is

$$G_0 = \frac{W_0}{W} = 1.5 \text{ (i.e. } 1.76 \text{ db)} \quad . \quad . \quad (6.6)$$

Similarly it may be shown that the power gain of a half-wave dipole is

$$G_0 = 1.64 \text{ (i.e. } 2.15 \text{ db)} \quad . \quad . \quad (6.7)$$

The latter figure is based on the assumption of a perfectly sinusoidal current distribution and corresponds to a figure for the loop radiation resistance of 73.13 ohms.

The power gain for various directive antennae is given in the following sections. For a large array of the type shown in Plate No. XI (facing page 302) the gain is 150, i.e. 21.76 db.

With a directive microwave antenna, the gain may be measured in a relatively simple manner by pointing the antenna towards a large reflecting sheet (which is a few wavelengths away) and then measuring the standing wave ratio along the feeder to the antenna. It is essential that in the absence of the reflecting sheet the antenna should be correctly matched to its feeder. The method appears to have been first

devised by E. M. Purcell, of the Massachusetts Institute of Technology, and is described in an article by Pippard, Burrell and Cromie,⁽⁷¹⁾ who also show that the results are liable to errors of up to 10 per cent unless the influence of re-radiation is allowed for by taking a series of measurements at varying distances.

The reflecting sheet should be far enough away for the wavefront striking it to be sensibly plane—i.e. the greatest departure from planarity should not exceed $\lambda/4$. If we take the gain of the antenna to be G_0 , then the gain of the image will also be G_0 , so that Poynting's vector at the image will be

$$S = \frac{G_0 W}{16\pi x^2}$$

where x = distance between antenna and reflecting sheet,

W = total power radiated.

This power density is, of course, that received at the antenna itself and hence the power reflected back into the antenna is given by

$$SA_e = \frac{G_0^2 \lambda^2 W}{64\pi^2 x^2}$$

where A_e = effective area of absorption as given by eqn. (5.4)

$$= \frac{G_0 \lambda^2}{4\pi}$$

The voltage reflection coefficient, $|B|/|A|$, is given by dividing the reflected power by the radiated power and taking the square root of the resultant. Hence

$$|B|/|A| = \frac{G_0 \lambda}{8\pi x}$$

The reflection coefficient is obtainable directly from a measurement of the standing-wave ratio along the feeder (*see* equation (10.43)) and application of the above equation will give the power gain of the antenna.

(b) *A Practical Definition*

In some cases it is more instructive to know the gain of a system as compared with the simplest practical form of antenna, i.e. a half-wave dipole. The latter is therefore often used as a standard for comparison using the field strength in

the equatorial plane of the dipole. This comparison is sometimes made in the form of a field strength ratio which may lead to confusion with power ratios; but if the result is expressed in decibels then no error can arise on that account. It will be noticed from (6.7) that if the gain is referred to a half-wave dipole (which we shall call G_H) then

$$G_H = G_0 - 2.15 \text{ db} \quad (6.8)$$

Unfortunately there are also other practical definitions which are sometimes used and for these a horizontal dipole is taken to be some specified height above a perfect earth. The height is either $\lambda/2$ or that of the centre of the antenna system. In the latter case no comparison can be made with the previous definitions, but for the half-wave dipole $\lambda/2$ above the earth we have $G_0 = 8.2 \text{ db}$. Obviously standards which include earth reflections—even if assumed to be from a perfectly conducting earth—can claim to be more “practical” than any free-space standard. Nevertheless it is less confusing to keep to free-space definitions and in this chapter we shall use G_H as our measure of gain.

Correlation between Mutual Impedance and Gain

If the real parts of the mutual impedance between the elements of an array are known, the gain may be determined without integration over a sphere. In such cases we simply compute the input power to each element knowing the currents in the system (these must be known in the first place to derive the polar diagram). The mutual impedance between the elements of an array may be determined by the induced e.m.f. method described in Vol. I, § 5.2, so that such a gain calculation is equivalent to integrating over the surface of the conductors in the system instead of over the surface of a surrounding sphere.

The correlation between mutual impedance and gain is illustrated by the following simple examples.

(a) *Two Parallel Dipoles Fed in Anti-phase*

In Fig. 6.17 we have the case of two parallel dipoles fed with equal currents in anti-phase which results in the familiar figure-of-eight polar pattern in the equatorial plane of the dipoles. When the spacing is small, say not greater than $\lambda/10$, the pattern follows a simple sine law whatever the spacing

may be. Looking at the vector diagram of Fig. 6.17 (b) we see that if the spacing is halved the resultant of E_1 and E_2 is also halved for all values of ϕ . Yet if there are no dissipative losses in the system *the total radiated energy must be the same* for cases (i) and (ii). It follows therefore that the magnitudes of E_1 and E_2 in case (ii) must be double their values in case (i), i.e. the currents in the two antennae are doubled for the same

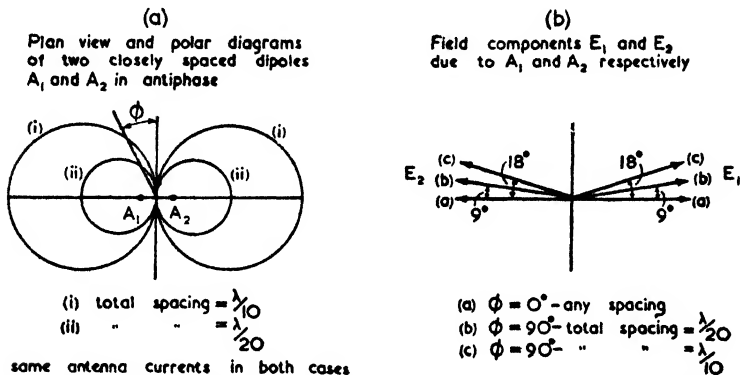


FIG. 6.17. DIAGRAM FOR ILLUSTRATING THE CORRELATION BETWEEN THE MUTUAL IMPEDANCE AND THE SCALE FACTOR OF A POLAR DIAGRAM

input power. Hence the radiation resistance of each antenna must be one-quarter of the value it has in case (i).

In general, the radiation resistance of each antenna decreases with the square of the distance of separation at close spacings. The case of a horizontal half-wave dipole above a perfect conductor is just like the above example except that energy is radiated over a hemisphere only, and from Fig. 3.14 we see that the radiation resistance varies in the expected manner for heights which are a small fraction of a wavelength.

If the half-wave dipole is situated at a height of $\lambda/2$ the radiation resistance is approximately the same as that in free space; in which case the maximum field is double that of a free-space dipole because of the image of the dipole in the ground, and since $G_0 = 2.15$ db for a half-wave dipole the total gain is 8.15 db. (Making an allowance for the slight difference in radiation resistance brings this figure up to the previously mentioned value of 8.2 db.)

(b) Two Parallel Dipoles Fed in Phase

For this simple case it is apparent that, as the dipoles are brought closer and closer together, the radiation pattern

becomes a circle in the equatorial plane, thus being identical with the single dipole pattern. Consequently the current in each of the two dipoles must be half that of a single dipole fed with the same total power; therefore the radiation resistance of each dipole is doubled as the antennae are brought together. This conclusion is substantiated by the curve of mutual impedance given in Fig. 3.15.

If the dipoles are separated by a *large number of wavelengths* the polar diagram has the form shown in Fig. 6.18 (b). When

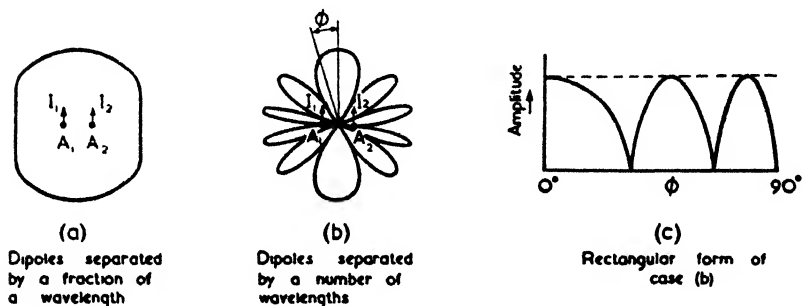


FIG. 6.18. DIAGRAMS FOR THE DISCUSSION OF THE MUTUAL IMPEDANCE BETWEEN TWO COPHASAL DIPOLES

the number of lobes is very high each one follows almost a perfect sine law on plotting field strength versus angle of exploration—this can be appreciated from a consideration of spinning field vectors, for in this case the number of complete revolutions is so high that *the rate of spin of the vectors is approximately uniform over any one complete revolution.*

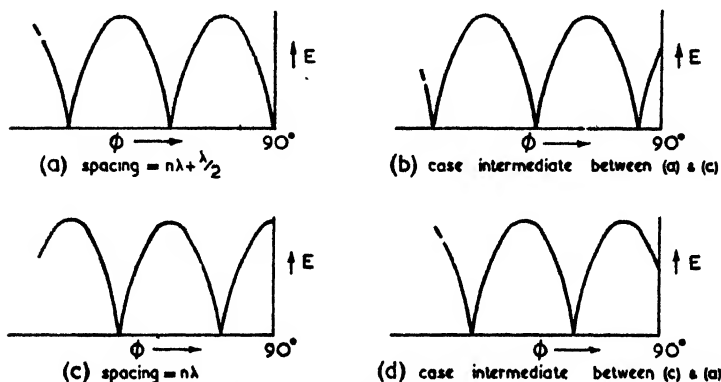
Thus the lobes have a pattern in rectangular co-ordinates as shown in Fig. 6.18 (c). In evaluating the total power according to the methods described on antenna gain, the increase in the relative widths of the lobes as $\phi \rightarrow 0^\circ$ and also the decrease in surface area of the surrounding sphere of integration can both be neglected (the number of lobes is supposed to be great enough for uniform conditions to prevail over any small sample of solid angle). Hence the total power radiated equals the power per unit solid angle along a direction of maximum radiation multiplied by the r.m.s. value of a sine wave. That is

$$G_0 = \sqrt{2} \text{ (i.e. 3 db)}$$

The lobe maxima represent directions for which E_1 and E_2 are in phase. Therefore $(I_1 + I_2) = I\sqrt{2}$ where I is the current in a single dipole fed by the same total power. We

can therefore deduce immediately that R_1 and R_2 , the radiation resistances of the two dipoles, must both equal R , the radiation resistance of a single dipole.

The above result was, of course, only to be expected, but the correlation with the polar diagram should be noted. We can now picture why the mutual impedance between two dipoles follows the curve shown in Fig. 3.15. The oscillations in this



The above diagrams are enlarged portions of Fig. 6.18 (c) when the spacing is several wavelengths

FIG. 6.19. DIAGRAMS FOR THE DISCUSSION OF THE CORRELATION BETWEEN THE MUTUAL IMPEDANCE AND POLAR DIAGRAMS

curve are directly related to the formation of further lobes which "come in" from the direction of $\phi = \pm 90^\circ$ as the separation is increased. This may be explained in the following manner.

Whenever there is an integral number of half lobes in the plot of E versus ϕ in the range of $\phi = 0^\circ$ to 90° , the radiation resistance of each dipole equals that of a single dipole (i.e. the mutual resistance is zero). At $\phi = 0^\circ$ there is always a lobe maximum; hence for zero mutual resistance there must be either zero radiation or a lobe maximum at the point $\phi = 90^\circ$. The first condition, namely of zero radiation, is shown in Fig. 6.19 (a); this occurs when the spacing is an odd number of half wavelengths. As the spacing is increased (Fig. 6.19 (b)) a new lobe commences—the others being squeezed up a little more—and the mean power is decreased for a given peak value of E ; thus R_1 and R_2 are decreased, i.e. the mutual resistance is negative. Increasing the spacing still further completes half a lobe so that the mutual resistance is

again zero; this occurs when the spacing is an integral number of wavelengths. Further spacing (Fig. 6.19 (d)) increases the mean power and the mutual impedance becomes positive.

Gain of Linear Arrays

Provided the elements of an array have negligible mutual coupling, the power gain in the direction of maximum radiation (assuming that all the field components are in phase in this direction) is simply equal to the number of elements. For instance, if the number of elements is n and each carries a current of strength I , then the power radiated is

$$W_n = nRI^2$$

where R is the radiation resistance of each element. To obtain the same total field strength from a single element the current would have to be equal to nI , and hence the power radiated would be

$$W_1 = R(nI)^2$$

Consequently the power gain of such an array is given by

$$W_1/W_n = n \quad . \quad . \quad . \quad (6.9)$$

In most practical arrays, however, there is appreciable mutual coupling between the individual elements, in which case the above formula will no longer be true—unless the algebraic sum of the mutual resistance components happens to be relatively small (a state of affairs which is true of a Kooman array, for example). When an “averaging out” of the mutual resistances does not occur, a correction factor must be applied to equation (6.9).

However, a knowledge of the mutual impedances is not essential since the gain may be determined from the polar diagram by using the method of integration of the polar diagrams. In this way Sterba⁽¹⁷⁷⁾ obtained valuable curves showing the gain of various linear arrays and combinations of such arrays. Fig. 6.20 (a) shows the gain of broadside arrays of varying lengths for different spacings between the elements, while Fig. 6.20 (b) shows similar curves for end-fire arrays—the division into “broadside” and “end-fire” arrays is obvious from Figs. 6.21 (a) and 6.21 (b), which show typical cases. The gain curves in both figures assume that the elements are doublets; therefore they are only approximately correct if half-wave dipoles are used.

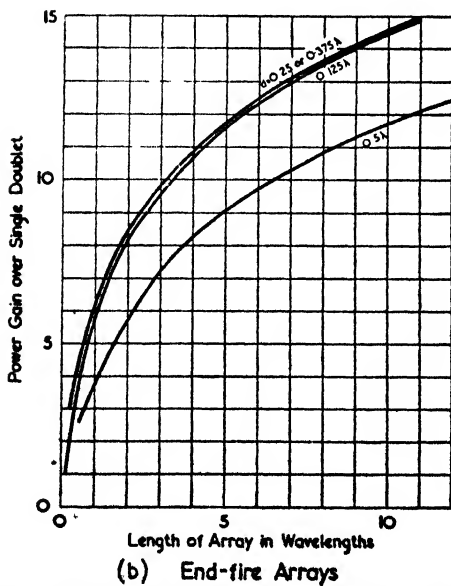
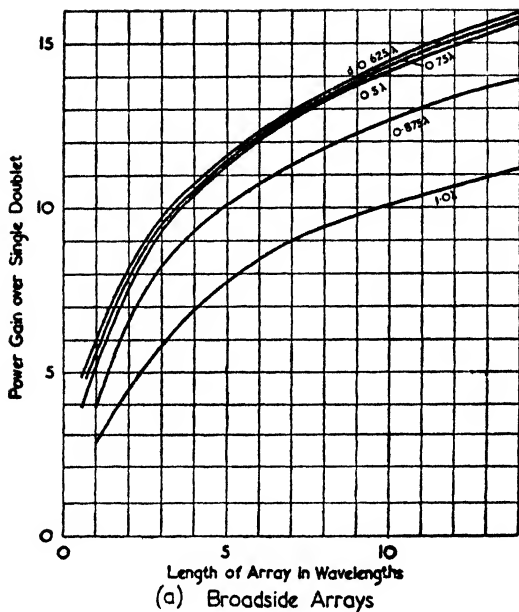


FIG. 6.20. POWER GAIN CURVES FOR ARRAYS OF DOUBLET

A notable feature of these curves is that the gains for broadside and end-fire arrays of equal length are very nearly the

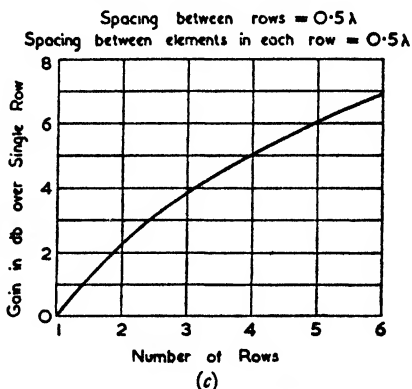


FIG. 6.20 (c). GAIN OBTAINED BY STACKING BROADSIDE ARRAYS OF DOUBLETS WHOSE SPACING IS 0.5λ
(A row must consist of at least three doublets)

same. There is an appreciable difference, however, in the widest spacings which may be employed whilst still obtaining the maximum gain for any given length of array. With end-fire

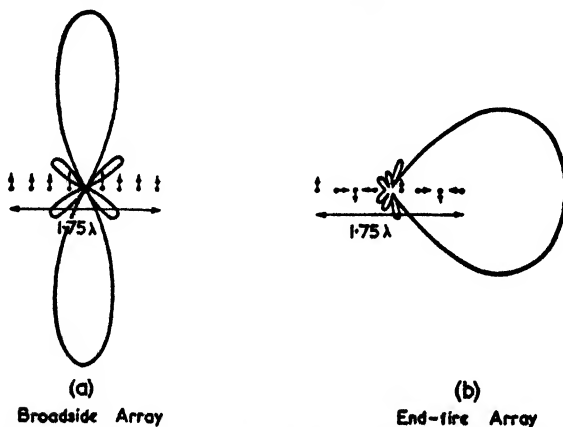


FIG. 6.21. EXAMPLES OF BROADSIDE AND END-FIRE ARRAYS

arrays a spacing of 0.375λ is needed, but for broadside arrays a spacing of 0.75λ will suffice. (In this connection it is interesting to recall some observations made in the previous section on the changes in the polar diagram caused by increasing the

number of elements per unit length in a cophasal array (i.e. a broadside array)—it appeared that the main lobe altered relatively little as the spacing between adjacent elements was decreased from the initial value of 0.5λ and this fact alone shows that the gain remains approximately constant for close spacings.)

For broadside arrays a spacing of 0.5λ is particularly convenient since the right phase relationship is easily obtained by the feeder lines; also the total impedance is easy to estimate since the elements are all in parallel. Fig. 6.20 (c) shows the approximate increase in gain for arrays of this spacing when several rows of elements are stacked one above the other. The increase actually depends on the number of elements in a row, but the gain curve is sufficiently accurate to make initial estimates.

At a distance of a wavelength or so from a rectangular array the field will be approximately that due to an infinite sheet of current. By making an exact calculation of the field it would be possible to monitor the whole array at short distances in front of it and at ground level. Calculations of this nature have been made by Moullin⁽¹⁷³⁾ who shows the departure from the infinite-sheet value for various arrays.

Maximum Gain of Linear Arrays

Theoretically the gain of an array of given dimensions can be increased without limit, but as the gain is increased so the radiation resistance of each element is decreased, so that in practice the dead-loss resistance becomes such a large proportion of the total resistance that the gain actually decreases. The principles involved are not without interest, however, and they can be demonstrated in the following simple way.

In Fig. 6.22 (a), a_1 and a_2 are the two end elements of an array, while close to them are the pair b_1 and b_2 which are fed with slightly weaker currents in antiphase. Fig. 6.22 (b) shows the two main lobes produced by each pair of elements and, since they are in phase opposition, it is obvious that the resultant forward lobe has a narrower beam width than either of the two component beams. The side lobes can be reduced by adding further pairs of elements in between the outer pairs, which means that for a given power input the gain of the forward lobe will be considerable. With this state of affairs the end elements carry considerable currents since even the difference current, δI , must be great. It should be noted that

the radiation resistance of each element will be very low, for here we have the case of closely spaced elements with almost equal currents in antiphase.

The corresponding continuous distribution of current is of the form shown in Fig. 6.22 (c). If one could only achieve such a distribution with a vertical radiator above the ground (the image in the ground forming half the array in this case) then the service area of a broadcast station could be considerably

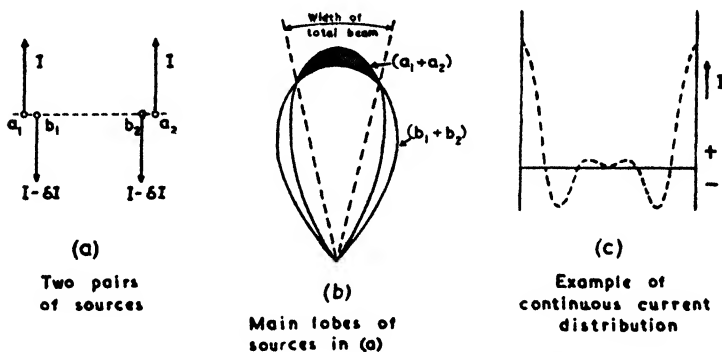


FIG. 6.22. DIAGRAMS FOR ILLUSTRATING THE MAXIMIZING OF THE GAIN FROM LINEAR ARRAYS

increased. A mathematical treatment of the problem has been given by Bouwkamp and de Bruign⁽³⁵⁾ and by Schelkunoff.⁽²⁰⁾

6.3. LONG-WIRE ANTENNAE

The radiation from a wire which is several half-wavelengths long is highly directional on account of the appreciable space phasing which exists between the extremities of the wire. The polar diagram obtained will be bidirectional if the wire carries a standing wave system (i.e. if the wire is open- or short-circuited) or unidirectional if the wire carries a travelling wave (i.e. if the wire is terminated by a resistance equal to its characteristic impedance). It is therefore convenient to consider long-wire antennae in two groups according to whether the radiator is resonant or non-resonant.

Resonant Long Wire

The radiation from resonant wires which are not an integral number of half-wavelengths long has been analysed by Alford.⁽²⁷⁾

We shall confine ourselves, however, to the simpler case in which the wire is m half-wavelengths long, i.e. it is being excited in its m th mode.

With this proviso we find that the polar coefficient can readily be obtained in the same manner as was described in Vol. I, § 4.4, for the single half-wave case—all that needs to be done is to change the limits of integration. The integration leads to the following formulae—

$$P(\theta) = \frac{\cos\left(\frac{m\pi}{2} \cos \theta\right)}{\sin \theta} \quad (\text{when } m \text{ is odd}) \quad (6.10a)$$

$$P(\theta) = \frac{\sin\left(\frac{m\pi}{2} \cos \theta\right)}{\sin \theta} \quad (\text{when } m \text{ is even}) \quad (6.10b)$$

In either case the electric intensity is given by equation (4.49), Vol. I, so that

$$E_{\theta} = \frac{60}{r} I_l P(\theta) \quad . \quad . \quad . \quad (6.11)$$

where E_{θ} = field strength in volts/metre,
 r = distance in metres,
 I_l = loop current in amperes.

It will be noticed that the numerators of the equations for $P(\theta)$ resemble the height factors $F(H, \theta)$ as given by equations (6.2) and (6.3). The only difference is that in the case of long wires we are mainly interested in values of θ ranging from 0° to 30° whereas for height factors the interesting range for θ is from 60° to 90° . Equations (6.10a) and (6.10b) may therefore be obtained from the height factor curves on dividing by $\sin \theta$. The latter step may be performed by using logarithmic graph paper in the manner described in § 3.1.

Fig. 6.23 shows the polar diagrams for $m = 1, 2, 3$ and 4 , together with the corresponding current distribution. Due to feeding the antenna at one point only, the current distribution is not quite uniform in practice. This results in a certain amount of asymmetry in the polar diagram—an effect which was examined experimentally by Bergmann,⁽³⁴⁾ but the more recent experiments of McPetrie and Saxton⁽¹¹⁹⁾ show very little asymmetry on this account.

As the length of the wire is increased so the main lobe comes nearer to the axis of the wire. The angle at which this lobe

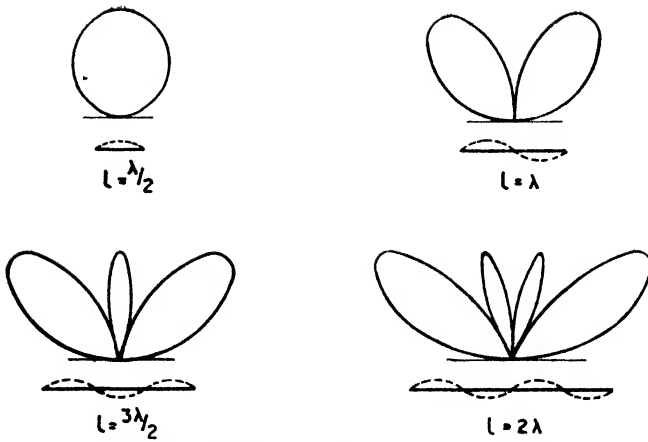


FIG. 6.23. POLAR DIAGRAMS OF RESONANT LONG-WIRE ANTENNAE

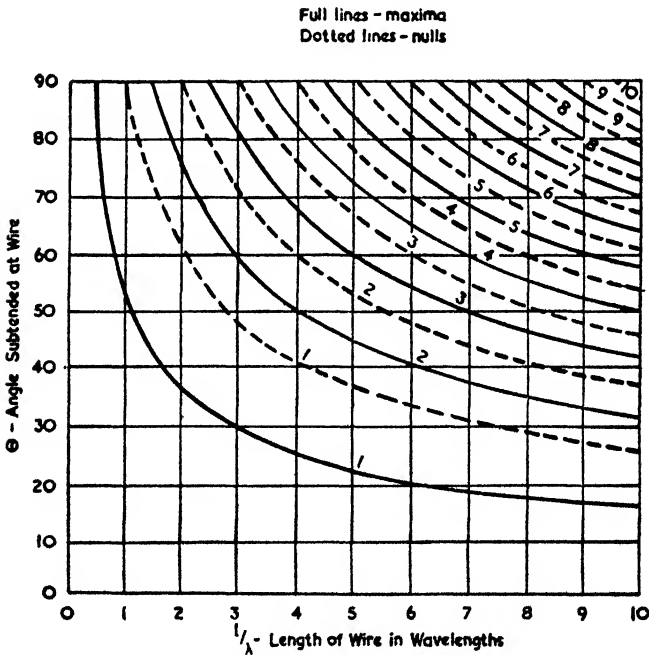


FIG. 6.24. ANGULAR POSITION OF LOBE MAXIMA AND NULLS FOR RESONANT WIRES

occurs and also the angular position of the other lobes may be found from the curves of Fig. 6.24.

The radiation resistance for a wire which is an integral number of half-wavelengths long may be obtained by the same methods as were used to derive equation (5.19), Vol. I. Proceeding on these lines we obtain

$$R_{lr} = 30C(2\beta l) \quad . \quad . \quad . \quad (6.12)$$

If $l > \lambda$, the cosine integral part of $C(2\beta l)$ may be neglected, so that the radiation resistance is given simply by

$$R_{lr} = 17.32 + 30 \log_e 2\beta l$$

or

$$72.45 + 30 \log_e m$$

where $m =$ mode of excitation, i.e. the number of half-wavelengths.

To determine the gain of the major lobe we evaluate equation (6.5) by substitution for S_m according to (6.11) and using the input power for the denominator of (6.5). If θ_m is the angular direction of the maximum radiation then

$$S_m = \frac{E_{\theta}^2}{z_{00}} = \frac{30}{\pi r^2} I_l^2 P^2(\theta_m)$$

Then the gain over an omnidirectional source is given by

$$\begin{aligned} G_0 &= 4\pi r^2 \frac{30}{\pi r^2} \frac{I_l^2 P^2(\theta_m)}{I_l^2 R_{lr}} \\ &= \frac{120}{R_{lr}} P^2(\theta_m) \quad . \quad . \quad . \quad (6.13) \end{aligned}$$

Fig. 6.25 shows both the radiation resistance and the value of G_H for values of m from 1 to 14. The power gain, G_H , is expressed with respect to a half-wave dipole (a more practical comparison than that given by an omnidirectional source) and is given by $G_H = 0.61G_0$.

For lengths of wire which are not an integral number of half-wavelengths, the radiation resistance varies according to the position of the input terminals. In practice the resonant lengths are slightly shorter than $m\lambda/2$. An approximate formula for the resonant length is

$$l = (m - 0.05)\lambda/2 \quad . \quad . \quad . \quad (6.14)$$

In spite of the fact that the resonant frequencies are therefore not exact multiples of each other, long-wire antennae make good radiators at harmonics of the lowest operating frequencies.

Thus a 40 m wire, which is a resonant half-wave radiator at 3.5 Mc/s, will operate as a long-wire radiator on the 7, 14 and 28 Mc/s bands. With such multi-band working, the feeder line cannot be matched at all the operating frequencies, so that the system requires a tunable transmission line.

All the formulae given above are for free-space conditions and in practice the effect of ground reflections must be taken

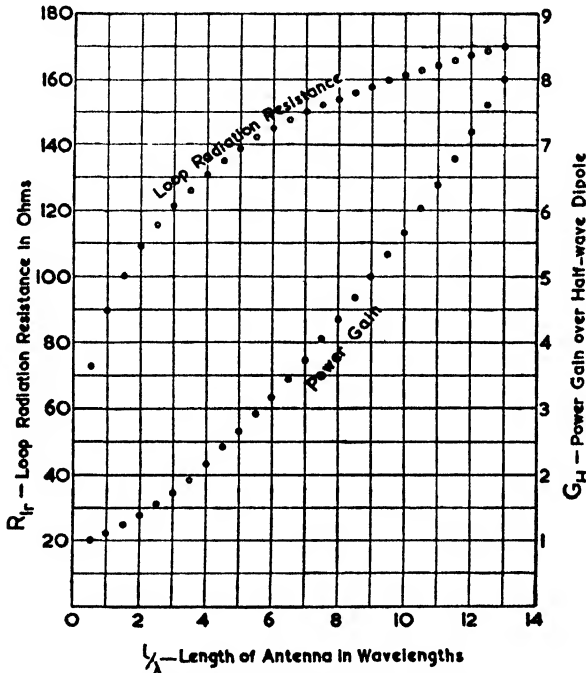


FIG. 6.25. LOOP RADIATION RESISTANCE OF A RESONANT WIRE ANTENNA AND POWER GAIN OF MAJOR LOBE

into consideration when calculating the overall polar diagram. This can be done by means of the height factor curves of Figs. 6.4 to 6.7. Although there is no radiation in a direction along the actual axis of the wire, for short-wave communication the wire is pointed towards the other station, since the required radiation is at an angle of, say, 20° to the horizontal.

The radiation resistance is also affected by the ground, but no appreciable change is caused if the height of the wire is greater than about 0.3λ . The variation of radiation resistance with height is shown in Fig. 6.26 for $l = 4\lambda$ and 8λ . These

curves were obtained with the aid of the mutual impedance curves given by Carter.⁽⁴³⁾

It should be remembered that the polar diagrams given

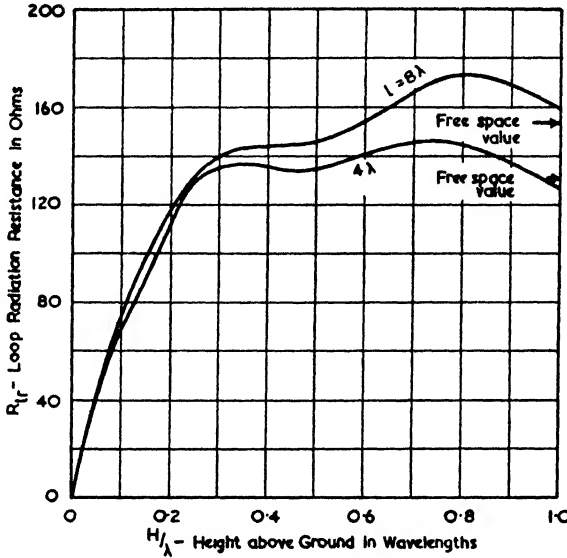


FIG. 6.26. VARIATION OF LOOP RADIATION RESISTANCE WITH HEIGHT ABOVE THE GROUND FOR RESONANT WIRES OF LENGTHS 4λ AND 8λ

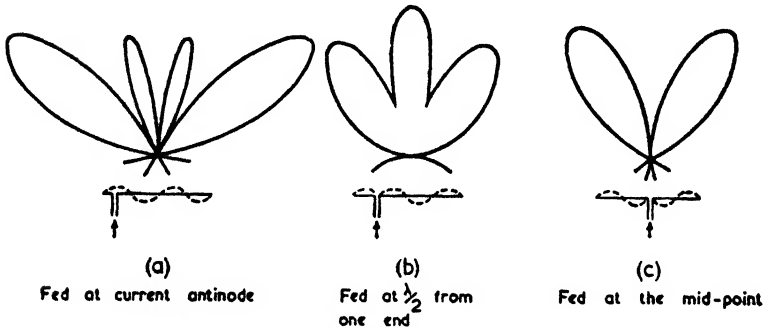


FIG. 6.27. VARIATION OF POLAR DIAGRAM OF A WIRE 2λ LONG WITH POSITION OF FEED POINT

by Figs. 6.23 and 6.24 apply only if the antenna is fed at a current antinode or at an extreme end. The latter form of feeding is popular with amateurs since it permits multi-band working. As an example of the variations in the polar diagram

caused by feeding at different points, we may take the case $m = 4$ which is illustrated in Fig. 6.27 for three different input terminals.

Resonant Wires with Alternate Phases Suppressed

The simple resonant wire tends to concentrate the radiation along the axis of the wire, but if the alternate phases are

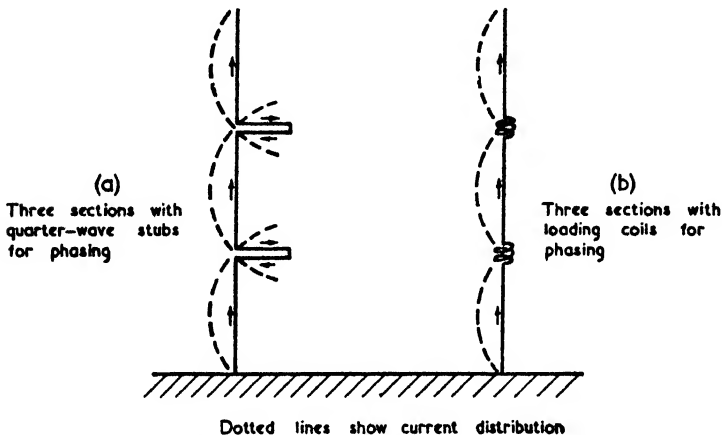


FIG. 6.28. EXAMPLES OF THREE-SECTION FRANKLIN ANTENNAE

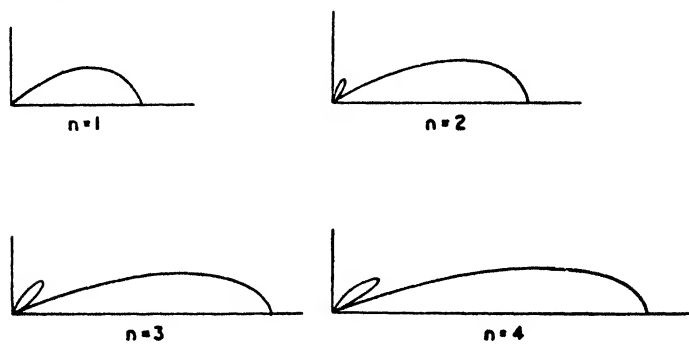
suppressed the opposite effect occurs, i.e. the radiation is concentrated in the equatorial plane. Fig. 6.28 shows two such cases, the suppression being obtained in case (a) by means of quarter-wave stubs and in (b) by loading coils. The concentration in the equatorial plane is illustrated by Fig. 6.29, which shows the polar coefficients for $n = 1, 2, 3$ and 4, where n is the number of half-wave elements.

This type of antenna is known as the Franklin antenna and has been employed frequently by the Marconi Company in the form of arrays of such antennae. The Franklin antenna would also form an ideal radiator for medium-wave broadcast purposes, were it not for the mechanical difficulties of erecting sufficiently high masts at these wavelengths.

Assuming the idealized case of equal current loops spaced exactly half a wavelength apart, it can be shown⁽²²⁾ that the loop radiation resistance is given by

$$R_{lr} = (-1)^{n-1} 30 [C(2\beta l) - 4C(2\beta l - \beta\lambda) + 8C(2\beta l - 2\beta\lambda) - \dots] \quad (6.15)$$

The values of R_{lr} for $n = 1$ to 10 are shown plotted in Fig. 6.30 together with the figure of merit of such a radiator when



$n =$ number of half-wave elements

FIG. 6.29. VERTICAL POLAR DIAGRAMS OF FRANKLIN ANTENNAE

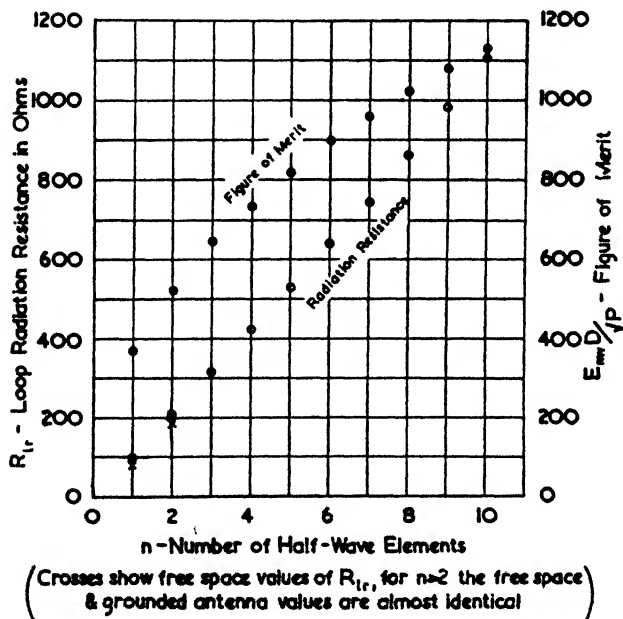


FIG. 6.30. LOOP RADIATION RESISTANCE AND FIGURE OF MERIT OF A FRANKLIN ANTENNA

placed vertically above the ground (the latter values are based on a curve given by Brown⁽³⁹⁾). When a Franklin antenna

consisting of one or two elements only is placed above the ground, the radiation resistance is somewhat modified. These modified values are shown by crosses in Fig. 6.30.

The polar diagram of a Franklin array in a vertical plane can be calculated by multiplying the dipole pattern by that produced by a line of cophasal sources whose separation is half a wavelength. This multiplication may be performed by using the appropriate height factor curves in the manner described in § 6.1. Alternatively the formula for a row of collinear cophasal sources may be used; if the number of

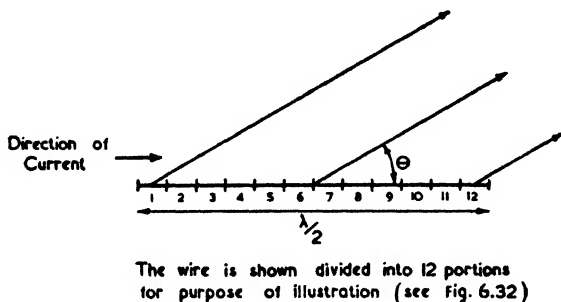


FIG. 6.31. DIAGRAM FOR THE ANALYSIS OF A TRAVELLING-WAVE RADIATOR

sources is n and the distance between adjacent sources is $\lambda/2$, the polar pattern is given by

$$F(\theta) = \frac{\sin(n\pi \cos \theta)}{\sin((\pi/2) \cos \theta)} \quad (6.16)$$

where n = number of half-wave elements (the effective number is $2n$ due to the images in the ground),
 θ = zenith angle.

Non-resonant Wires

The directive antennae described so far have all been excited by standing waves, but this is not an essential condition since travelling-wave systems also produce radiation. Their disadvantage lies in the fact that some form of terminating resistance is required, for without such a termination reflections would take place, thereby bringing us back to the case of a standing-wave antenna. Because of their termination, travelling-wave systems dissipate about half the total power in the form of heat. Nevertheless, they have a considerable number of uses, for they possess the virtue of exceptionally

wide bandwidths (frequency ranges of as much as 3 : 1 can be covered by one antenna) together with highly directive polar patterns.

Let us consider a conductor which is half a wavelength long (Fig. 6.31) and along which flows an unattenuated travelling

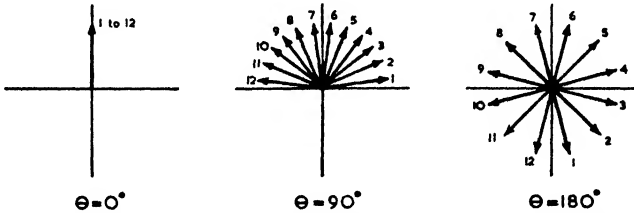


FIG. 6.32. DIAGRAMS OF THE FIELD COMPONENTS FOR THE RADIATOR SHOWN IN FIG. 6.31

wave. Then at each portion of the conductor the current will reach the same peak value but at a time dependent on the distance along the conductor. From the point of view of field strength at some distant point, we may take equal r.m.s. values for each portion and consider only the relative phases.

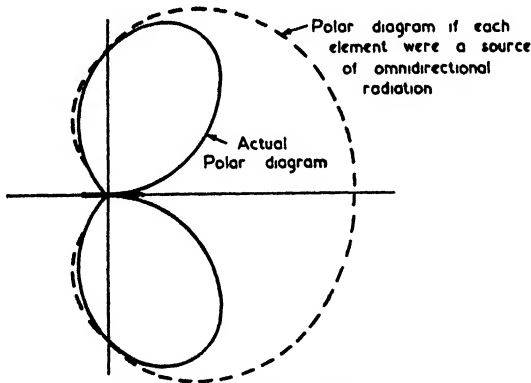


FIG. 6.33. POLAR DIAGRAM OF RADIATOR IN FIG. 6.31

The conductor is shown divided into twelve portions for convenience so that the vector diagrams for $\theta = 0^\circ$, 90° and 180° will be as shown in Fig. 6.32, provided that the radiation from each element is omnidirectional.

It is apparent from these diagrams that if each portion were to radiate uniformly in all directions the polar pattern would be of the form shown dotted in Fig. 6.33. Actually the radiation

from each element of length is proportional to $\sin \theta$ so that the polar diagram is the full curve in Fig. 6.33.

Were we to take any other length of conductor the radiation (neglecting the sine law for the moment) would always be a maximum in the direction in which the wave is travelling and zero, or very low, in the opposite direction. Fig. 6.34 shows the polar diagram for conductor lengths of 1λ and 4λ . The angle of the main lobe for wires of several wavelengths is much

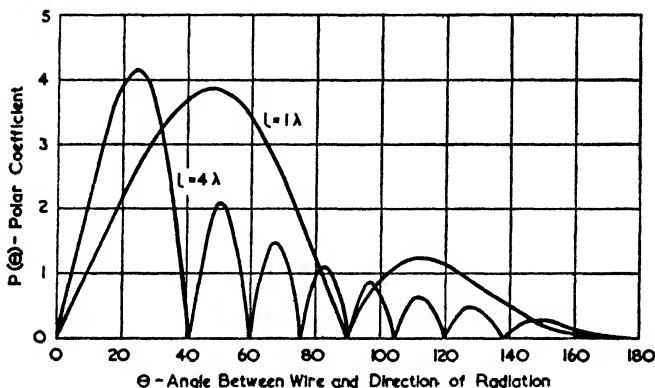


FIG. 6.34. POLAR DIAGRAMS OF WIRES OF LENGTHS 1λ AND 4λ CARRYING A TRAVELLING WAVE

the same as in the corresponding stationary wave case. Even for a 1λ line the difference is not great ($\theta = 45^\circ$ instead of 54° as in the stationary case).

In practice, the current is attenuated along the wire because of radiation losses, but this effect can be neglected without appreciable error. If the r.m.s. current at the input is I , then the field at a distance r due to a travelling wave along a wire of length l is given by equation (4.54), Vol. I, which is

$$E = \frac{60I}{r} \frac{\sin \theta}{(1 - \cos \theta)} \sin \left[\frac{\beta l}{2} (1 - \cos \theta) \right] \quad (6.17)$$

The polar coefficient is therefore

$$P(\theta) = \frac{\sin \theta}{(1 - \cos \theta)} \sin \left[\frac{\beta l}{2} (1 - \cos \theta) \right] \quad (6.18)$$

This expression may be compared with those given for stationary waves on wires of odd or even number of half-wavelengths (equations (6.10a) and (6.10b)). When θ is small

the polar coefficients of all three reduce to $\theta^{-1} \sin(m\pi\theta^2/4)$, which demonstrates the statement that the major lobe occurs at the same angle for both cases if the wire is several wavelengths long. The angle at which the major lobe occurs is given in Fig. 6.35, together with the radiation resistance.

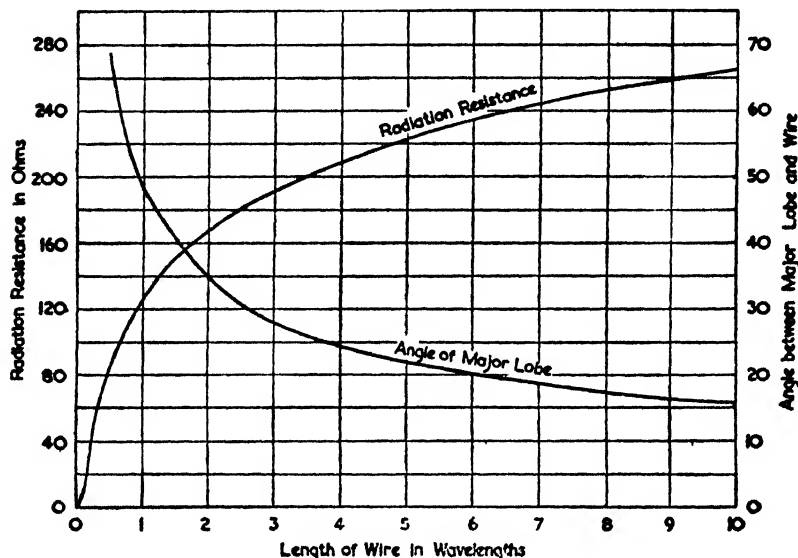


FIG. 6.35. ANGLE OF MAJOR LOBE AND RADIATION RESISTANCE OF A WIRE CARRYING A TRAVELLING WAVE

The radiation resistance is given by (see, for instance, refs. (20) and (27))

$$R_r = 60 \left[C(\beta l) - 1 + \frac{\sin 2\beta l}{2\beta l} \right]. \quad (6.19)$$

Since the wire carries a travelling wave, the radiation resistance is the same at all points along the wire (the attenuation of the current due to radiation being neglected). When $l > \lambda$, the above formula simplifies to

$$R_r = 60[\log_e 2\beta l - 0.423] \quad (6.19a)$$

It should be noted that for a practical application of the non-resonant wire, arrangements must be made to permit a return current, the radiation from which must not cancel that from the outgoing current along the wire. One way of doing this is to pull the two sides of a terminated transmission line apart until the line has a diamond shape (thus producing a

rhombic antenna); another way is to lift up the middle of a line using the ground for the return circuit (this leads to the inverted-V type of antenna).

6.4. LONG-WIRE ARRAYS

Under this heading we shall discuss various combinations of long-wire radiators (whether resonant or non-resonant) except for the rhombic antenna which, owing to its wide application, is considered in more detail in the next section.

The Echelon Antenna

If a number of long wires are arranged in echelon formation (Fig. 6.36) the combined radiation can be made to be substantially unidirectional.

To analyse such an array it is simplest to consider first of all the case of only two parallel wires of equal length as shown in Fig. 6.36 (a). The wires carry standing currents and are fed 180° out of phase; also the degree of stagger between them is such that the line joining their ends makes an angle of $(90^\circ - \theta_m)$ with the central axis where $\theta_m =$ angle of major lobe for a single wire. There would therefore be strong radiation in the direction marked B were it not for the fact that the currents at corresponding points on the wire are out of phase. Consequently the radiation towards B is sensibly zero and the same holds true for the reverse direction B' .

On the other hand we wish the radiation towards A and A' to be additive and this can be done by so spacing the wires that the distance b equals half a wavelength. Thus the required characteristics are given by making

$$\begin{aligned} s &= (\lambda/4) \sec \theta_m \quad . \quad . \quad . \quad (6.20) \\ d &= (\lambda/4) \operatorname{cosec} \theta_m \end{aligned}$$

If we take the particular case $l = 8\lambda$, then $\theta_m = 17.5^\circ$ so that the values of s and d are 0.26λ and 0.82λ respectively. A more practical size for small installations is $l = 3\lambda$, which gives $\theta_m = 30^\circ$, $s = 0.29\lambda$ and $d = 0.5\lambda$.

In major installations it is desirable to remove one of the main lobes so that the system becomes unidirectional instead of bidirectional. This can be done by adding a second pair of wires in the manner shown in Fig. 6.36 (b) where L_1 and L_2 denote one pair and L_3 and L_4 the other pair. The second pair

of wires are fed with 90° phase difference with respect to the first and since the spacing along the direction θ_m is equal to $\lambda/4$ (i.e. half that between the two wires of a pair) the phases of corresponding current elements will add in the direction A and cancel in the direction A' . In fact we obtain a system in which corresponding current elements are 90° behind that

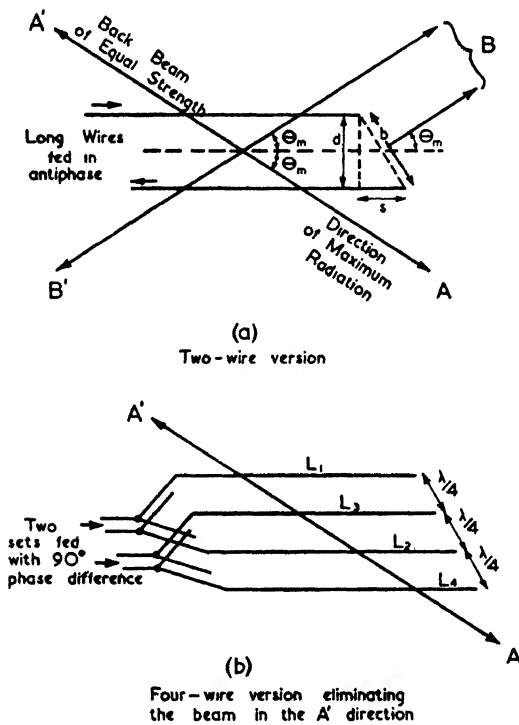


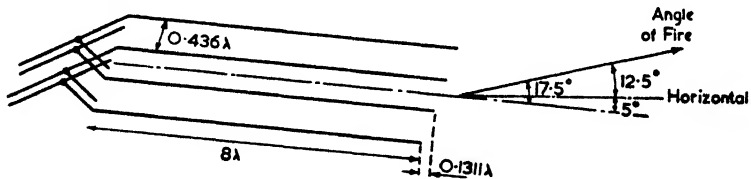
FIG. 6.36. THE ECHELON ANTENNA

in the previous wire when considered in direction A , this phase difference being neutralized by the space phasing of 90° .

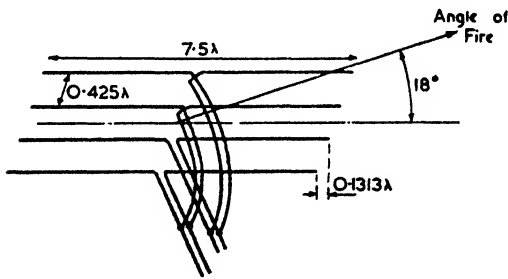
A further refinement is to neutralize the radiation from the feeders to the wires (on account of the appreciable spacing between pairs of long wires this radiation is not negligible). This can be done by the addition of extra branches to the feeder system as shown.

Fig. 6.37 (a) shows an application of the above principles to an array set up in a vertical plane and therefore giving a vertically polarized wave at a distance. In order to lower the

beam produced, the wires themselves are not horizontal but are inclined at an angle of 5° . This type of antenna is a development by the Radio Corporation of America and is described in detail together with other long-wire antennae in a comprehensive article by Carter, Hansell and Lindenblad.⁽¹⁶⁴⁾ They designated this particular form by the title "Model B."



(a)
R.C.A. Type B Array
(the wires lie in a vertical plane)



(b)
R.C.A. Type C Array
(the wires lie in a vertical plane)

FIG. 6.37. TWO FORMS OF ECHELON ANTENNA
(Carter, Hansell and Lindenblad, *Proc. I.R.E.*, Oct., 1931)

The R.C.A. Model C is shown in Fig. 6.37 (b) and is the horizontal variation of Model B. Model C is an odd number of half-wavelengths long, so that it may be fed at the centre as shown. Receiving tests conducted with Model C showed that it should be at a height of at least one wavelength above the ground in order to obtain full gain from the array.

The polar diagrams and the gains of these echelon antennae may be deduced from the corresponding values for each single wire. To make the calculation more exact, the mutual impedances should be allowed for. A discussion of this type of calculation is given by Carter,⁽⁴⁸⁾ who deduces that for a

four-element array with $l = 8\lambda$ the power gain $G_H = 16.4$ (the gain of a single wire of the same length is 4.42).

Experimental values obtained by Carter, Hansell and Lindenblad⁽¹⁸⁴⁾ on the antennae of Fig. 6.37 are as follows—

Model B $G_H = 16$ (i.e. 12 db)

Model C $G_H = 17.5$ (i.e. 12.4 db)

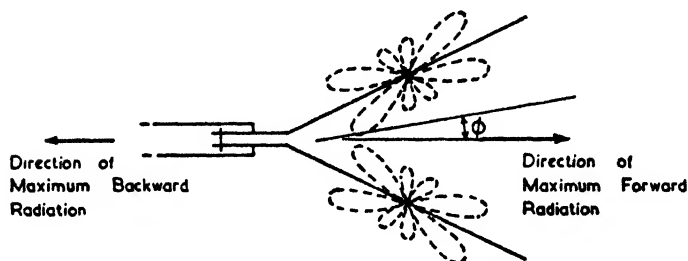


FIG. 6.38. A RESONANT-V ANTENNA

With an array of such units the power gain is approximately proportional to the number of units.

Resonant-V Antennae

If two long-wire antennae are arranged in a horizontal V shape as shown in Fig. 6.38 and fed in anti-phase at the apex, the resultant polar diagram is horizontally polarized in the plane of the V and also in the plane of symmetry through the bisector of the V. At all points outside these planes the polarization is elliptical. The geometry of the field from such an arrangement of wires is considered in detail in the next section in regard to radiation from rhombic antennae which are essentially two V's joined end to end. (The fact that rhombics carry a travelling wave instead of a standing wave does not affect the polarization.)

It is obvious that in order to secure the greatest possible forward radiation the semi-angle between the wires should equal the angle of the major lobe from each wire. The latter may be obtained from Fig. 6.24 for any specific length of wire.

The main difference in the two cases is that whereas the rhombic radiates a strong signal in one direction only, the resonant-V antenna is bidirectional. The bidirectional characteristic of the V antenna follows from the fact that a distant point whether directly in front or directly behind the V has a

field which is derived from the same effective configuration of radiating elements. This can be appreciated by moving one wire parallel to itself until a new apex is formed by the meeting of the ends which were formerly at the extremities of the V.

A bidirectional characteristic is seldom required; for a single point-to-point service it is both wasteful and liable to cause echoes at the receiving station due to signals which travelled via the longer great circle path. To make the beam unidirectional a second V may be mounted at an odd number

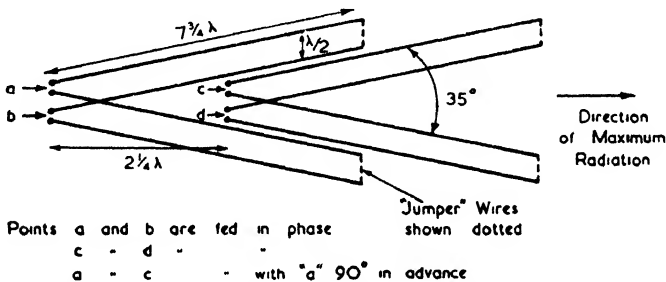


FIG. 6 39 AN OMNIDIRECTIONAL ARRAY OF FOUR V ANTENNAE

of quarter-wavelengths behind the first. This second V is fed with a current whose phase is at 90° with respect to that at the terminals of the first V. If the spacing were equal to $(\lambda/4 + n\lambda)$, where n is any integer, then a phase lead of 90° in the second antenna would give forward directivity and negligible backward radiation; if the spacing were $(3\lambda/4 + n\lambda)$ the same phasing would reverse the directivity.

A complete unit of V antennae as used by the R.C.A. consists of four V's arranged as shown in Fig. 6.39. In each case the lower antenna is about half a wavelength below the upper one and is fed in the same phase. This layout can be readily adapted for de-icing by adding "jumper" wires (shown by the dotted lines in Fig. 6.39) which give a d.c. path through the system and thereby permit a heating current of frequency 50 or 60 c/s to be passed through the antenna wires. The radiation from a jumper wire is negligible since the high-frequency currents flow in opposite directions toward the centre of the wire.

The power gain of the unit shown in Fig. 6.39 over a half-wave dipole is about 40, i.e. $G_H = 16$ db. For a number of units arranged side by side the power gain is proportional to the number of units.

The polar diagrams of two V antennae of lengths λ and 8λ are shown in Fig. 6.40 for both the vertical and the horizontal planes. In the case of the pattern in the horizontal plane, the field strength is best expressed in terms of the field due to each individual leg as given by equation (6.11); this leads to—(see Carter, Hansell and Lindenblad⁽¹⁶⁴⁾)—

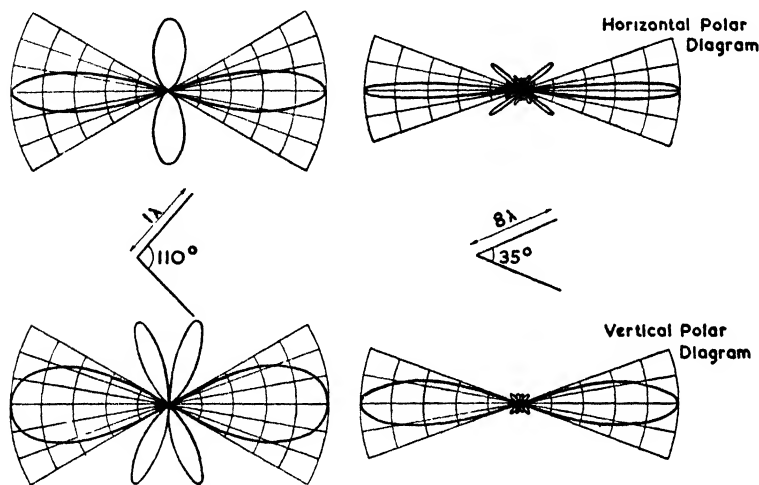


FIG. 6.40. POLAR DIAGRAMS OF RESONANT V ANTENNAE OF LENGTHS $l\lambda$ AND 8λ

$$E = \sqrt{[E_a^2 + E_b^2 - 2E_aE_b \cos(\beta l \sin \psi \sin \phi)]} \quad (6.21)$$

where E_a , E_b = field strength due to wires a and b respectively,
 ψ = semi-angle between wires,
 ϕ = azimuthal angle (Fig. 6.38).

The field strength in a vertical plane through $\phi = 0^\circ$ is given by

$$E = \frac{120I_l}{r} \left[\frac{\sin\left(\frac{\beta l}{2} \cos \psi \sin \Delta\right) \sin \psi}{1 - \sin^2 \Delta \cos^2 \psi} \right] \quad (6.22)$$

where I_l = loop current in amperes,
 r = distance in metres,
 Δ = angle of elevation.

Non-resonant Inverted-V

If a long wire carrying a travelling wave were inclined to the ground it would give maximum radiation along the ground if

the angle the wire made with the ground were equal to the angle of the major lobe as given by Fig. 6.35. By combining two such wires as shown in Fig. 6.41 we obtain accessible terminals for both the generator and the load. Inverted-V antennae of this type were described by Bruce⁽¹⁶¹⁾ and are sometimes known as Bruce antennae. Unfortunately confusion can arise out of the fact that rhombic antennae are also sometimes named after him (rhombic antennae are closely related to inverted-V's and are also described in the aforementioned reference).

A simple rule to remember with inverted-V antennae is that the length of each wire should exceed its projection on the

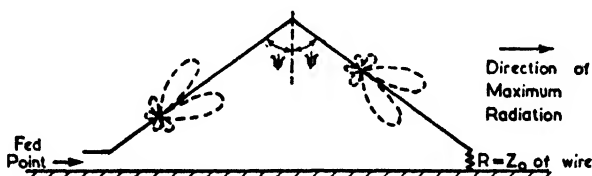


FIG. 6.41. A NON-RESONANT INVERTED-V ANTENNA

ground by half a wavelength. The basis for this rule may be reasoned out from a consideration of induced voltages in the receiving case. The very wide bandwidths obtainable with a long V antenna are obvious from a study of Fig. 6.35, which shows that the direction of maximum radiation varies very little with moderate changes in frequency if l is greater than, say, six wavelengths.

The inverted-V antenna may be thought of as a rhombic of which one-half is provided by the image in the ground. All the formulae applicable to rhombic antennae could therefore be used for the inverted-V, were it not for the finite ground conductivity which modifies the polar pattern in a vertical plane. This modification is very dependent on the ground conductivity since the radiation in the main direction of the inverted-V is vertically polarized.

One of the uses of an inverted-V antenna occurs when rhombic antennae are being used on the same site and it is desired to keep the interaction as small as possible. Plate X shows one end of the Belfast-Stranraer radio-telephone link, which uses arrays of rhombics and also arrays of inverted-V antennae at each terminus.

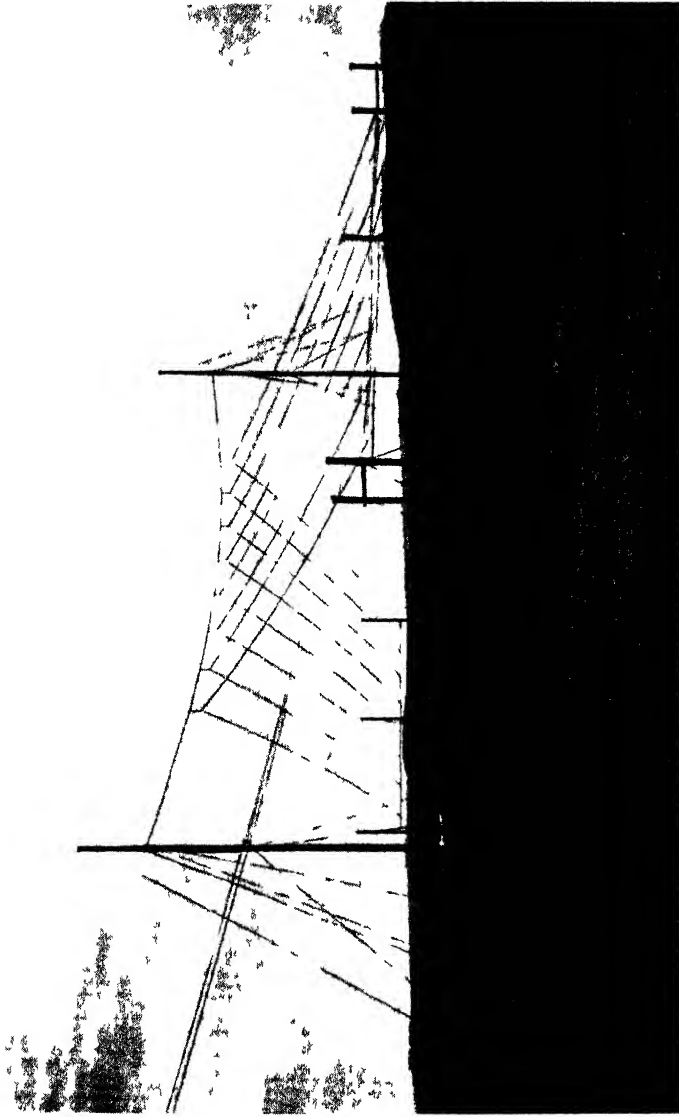


PLATE X AN ARRAY OF INVERTED-V ANTENNAE AT BALLYCOMRIN FOR RADIO TELEPHONE
COMMUNICATION ON THE BEIFAST STRANRAER LINK
(Courtesy of Standard Telephones & Cables Ltd)

6.5. RHOMBIC ANTENNAE

Free-space Conditions

Four wires arranged in a diamond shape, as shown in Vol. I, Fig. 4.10, form a rhombic antenna and are the free-space equivalent of an inverted-V antenna with its image in a perfectly conducting ground. The radiation pattern of each side is shown by the small polar diagrams in the figure and with correct phasing four of the main lobes would augment each other in the direction shown. This phasing is automatically secured when the wires are fed with a go-and-return

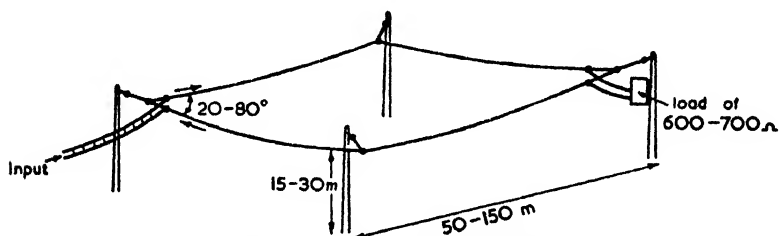


FIG. 6.42. A PERSPECTIVE SKETCH OF A RHOMBIC ANTENNA

current in the manner shown. The directing of the main lobes along the central axis is a separate problem and is considered later under the heading of "optimum dimensions."

In practice a rhombic antenna is mounted above the ground as shown in Fig. 6.42 at heights varying between one-third of a wavelength and one wavelength or more. With this type of antenna, gains of the order of 20 db over a half-wave dipole in free space may be obtained, the corresponding beam angle being about 10° to 15° above the horizontal. Rhombics also have the advantage that as the frequency is decreased so the angle of fire is automatically increased, and this happens to be just what is required for long-distance short-wave communication.

The equations for the radiation pattern and gain of rhombic antennae are developed in § 4.5, Vol. I, for the free-space case. When a rhombic is mounted horizontally above the ground it may be considered to have a negative image below the ground and the combined field strength is double that of the free-space case multiplied by the height factor for negative images as given by equation (6.3). Hence the total field strength is given by the following formulae which use the symbols shown in Fig. 6.43.

(a) *Field Strength and Polar Diagram in a Vertical Plane through $\phi = 0^\circ$* (Δ , the angle of elevation, is the independent variable)

$$E = \frac{480I}{r} F_1 F_2 F_3 \quad . \quad . \quad . \quad (6.23)$$

If the characteristic impedance of the rhombic is 600 ohms

$$E_{mV} = \frac{620\sqrt{P}}{D} F_1 F_2 F_3 \quad . \quad . \quad . \quad (6.24)$$

also the power gain is then

$$G_H = [2.8 F_1 F_2 F_3]^2 \quad . \quad . \quad (6.25)$$

In the above formulae

E = field strength in volts/metre,

E_{mV} = field strength in millivolts/metre,

I = current in amperes,

P = input power in kilowatts,

r = distance in metres,

D = distance in kilometres,

F_1 = height factor (equation (6.3)),

F_2 = asymmetry factor (equation (4.59), Vol. I),

F_3 = length factor (equation (4.59), Vol. I),

G_H = power gain over half-wave dipole in free space.

The three functions F_1 , F_2 and F_3 are given in Figs. 3.8 (or 6.6), 6.44 and 6.45 respectively—in each case the ordinates are plotted on a logarithmic scale and furthermore these scales are equal. Consequently the three factors may be multiplied together by simple addition on tracing paper (the method is described in § 3.2).

(b) *Field Strength and Polar Diagram in a Plane through $\Delta = \text{constant}$* (ϕ , the azimuthal angle, is the independent variable)

$$E = \frac{480I}{r} F_1 F_4 F_5 \quad . \quad . \quad . \quad (6.26)$$

If the characteristic impedance of the rhombic is 600 ohms

$$E_m = \frac{620\sqrt{P}}{D} F_1 F_4 F_5 \quad . \quad . \quad . \quad (6.27)$$

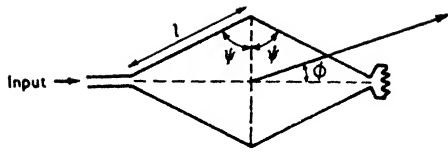
also the power gain is then

$$G_H = [2.8 F_1 F_4 F_5]^2 \quad . \quad . \quad (6.28)$$

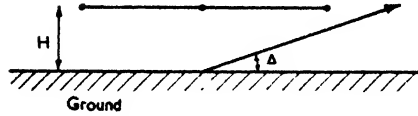
In the above formulae,

F_4 = asymmetry factor (equation (4.61), Vol. I),

F_5 = length factor (equation (4.61), Vol. I).



(a) Plan View



(b) Elevation

FIG. 6.43. DIAGRAMS SHOWING CO-ORDINATES AND DIMENSIONS FOR A RHOMBIC ANTENNA

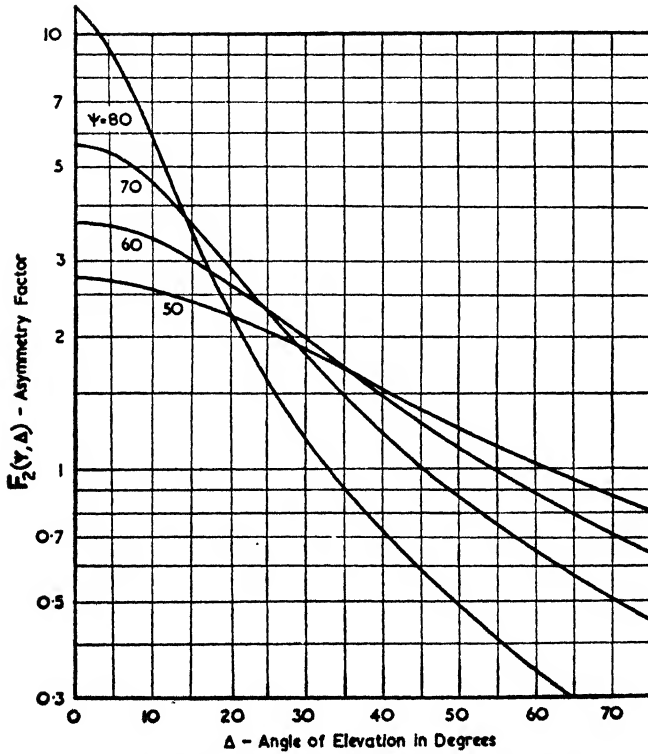


FIG. 6.44. ASYMMETRY FACTOR $F_2(\psi, \Delta)$ FOR DETERMINING THE VERTICAL POLAR DIAGRAM OF A RHOMBIC ANTENNA

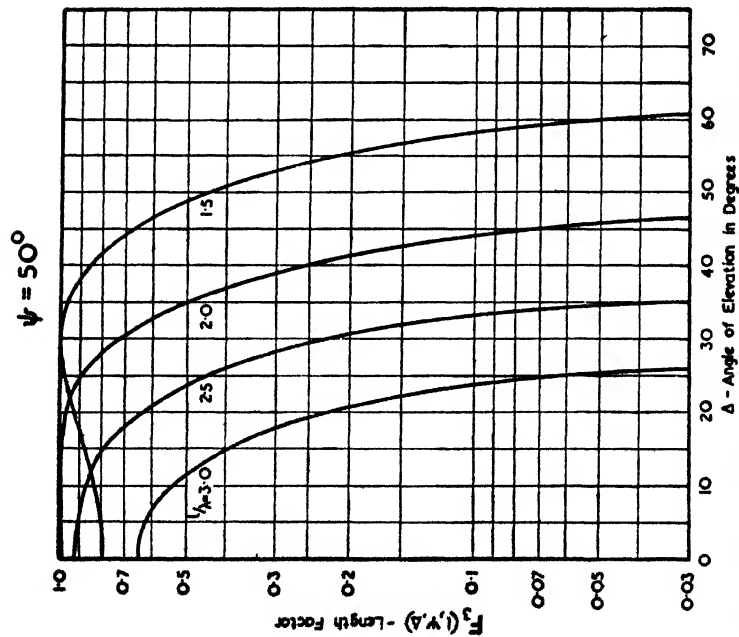


FIG. 6.45 (a). LENGTH FACTOR $F_3(l, \psi, \Delta)$ FOR DETERMINING THE VERTICAL POLAR DIAGRAM OF A RHOMBIC ANTENNA, $\psi = 50^\circ$

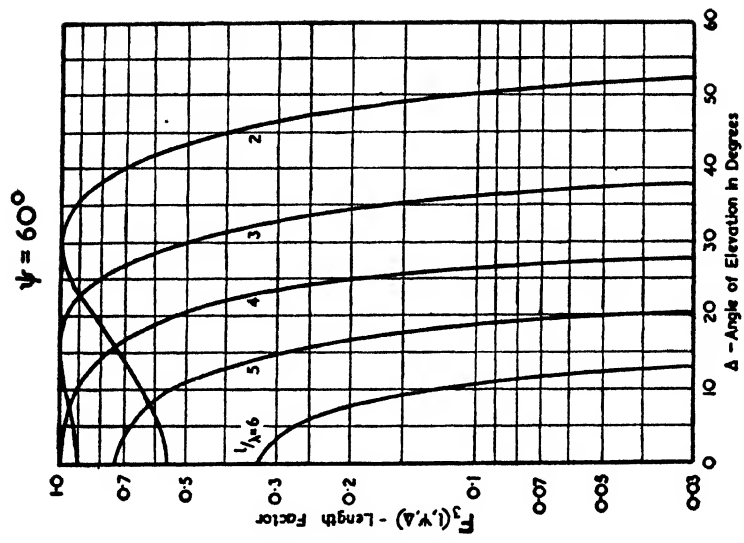


FIG. 6.45 (b). LENGTH FACTOR $F_3(l, \psi, \Delta)$ FOR DETERMINING THE VERTICAL POLAR DIAGRAM OF A RHOMBIC ANTENNA, $\psi = 60^\circ$

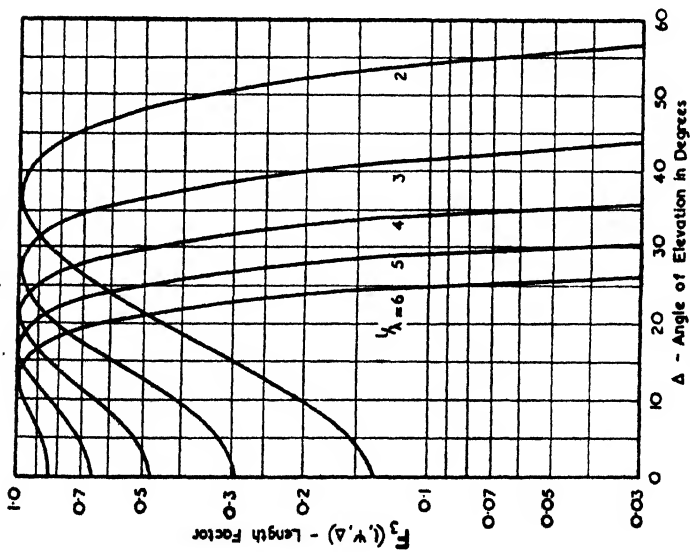
$\psi = 70^\circ$ 

FIG. 6.45 (c). LENGTH FACTOR F_3 (l, ψ, Δ) FOR DETERMINING THE VERTICAL POLAR DIAGRAM OF A RHOMBIC ANTENNA, $\psi = 70^\circ$

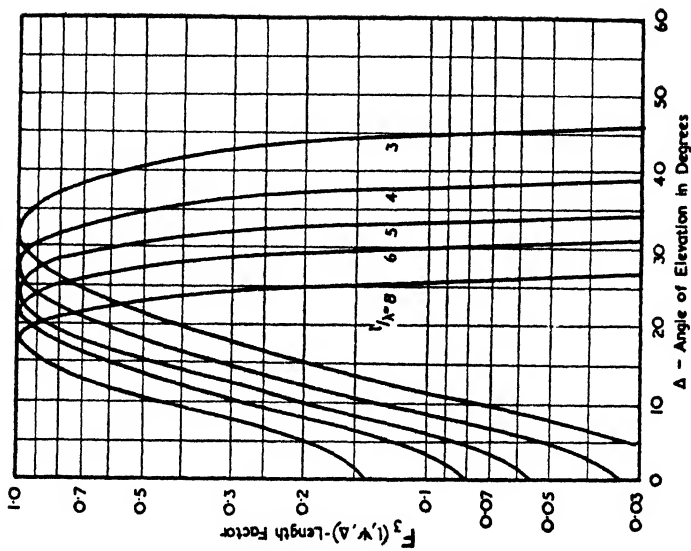
 $\psi = 80^\circ$ 

FIG. 6.45 (d). LENGTH FACTOR F_3 (l, ψ, Δ) FOR DETERMINING THE VERTICAL POLAR DIAGRAM OF A RHOMBIC ANTENNA, $\psi = 80^\circ$

Again the product of the factors may be determined graphically. We use Fig. 6.46 for F_4 and Fig. 6.47 for F_5 —the height factor F_1 is obtained from either Fig. 3.8 or 6.6 as before.

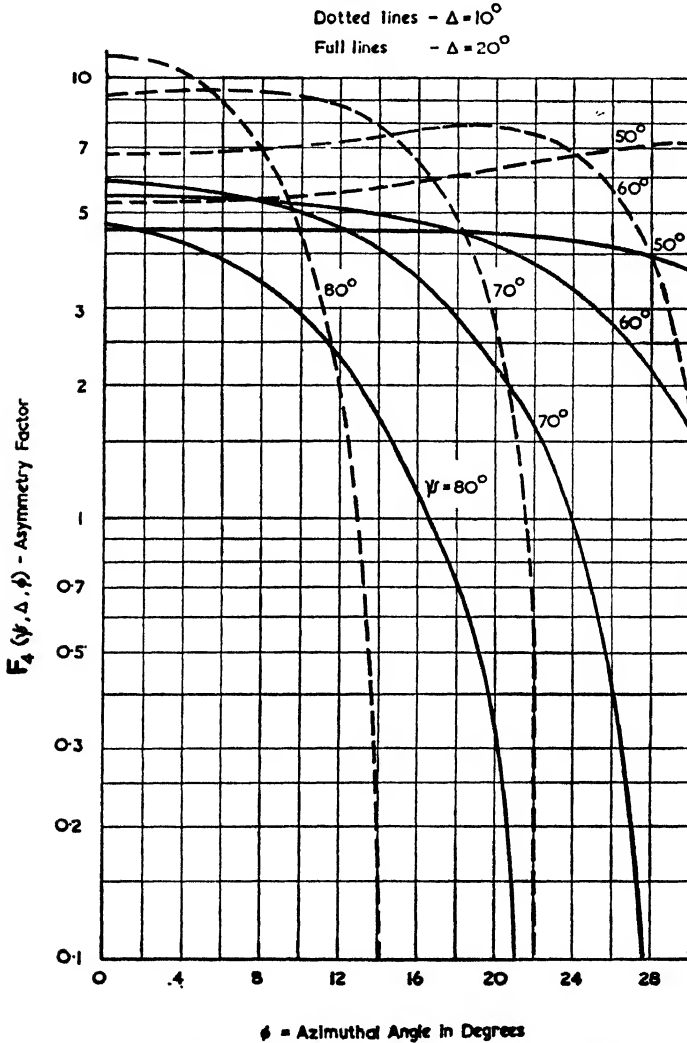


FIG. 6.46. ASYMMETRY FACTOR $F_4(\psi, \Delta, \phi)$ FOR DETERMINING THE HORIZONTAL POLAR DIAGRAM OF A RHOMBIC ANTENNA

The graphs for F_4 and F_5 are plotted for two typical values of Δ , namely 10° and 20° . The appropriate value in any

particular case can be determined by inspection of the vertical polar diagram. Actually the "horizontal" polar diagram varies relatively slowly with varying values of Δ , so that it is

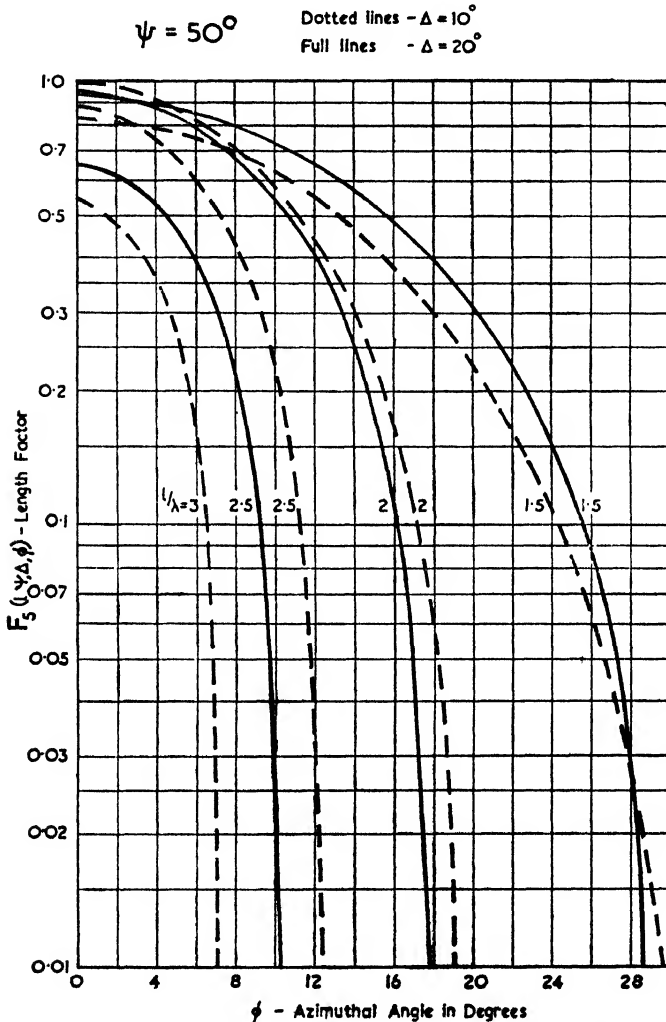


FIG. 6.47 (a). LENGTH FACTOR $F_s(l, \psi, \Delta, \phi)$ FOR DETERMINING THE HORIZONTAL POLAR DIAGRAM OF A RHOMBIC ANTENNA, $\psi = 50^\circ$

sufficiently accurate to take either 10° or 20° for Δ according to which is the nearer to the angle of fire.

It will be noticed that if we put $\Delta = 0^\circ$ the height factor F_1 becomes zero. By selecting some value of Δ which corresponds roughly to the angle of fire we obtain a more accurate

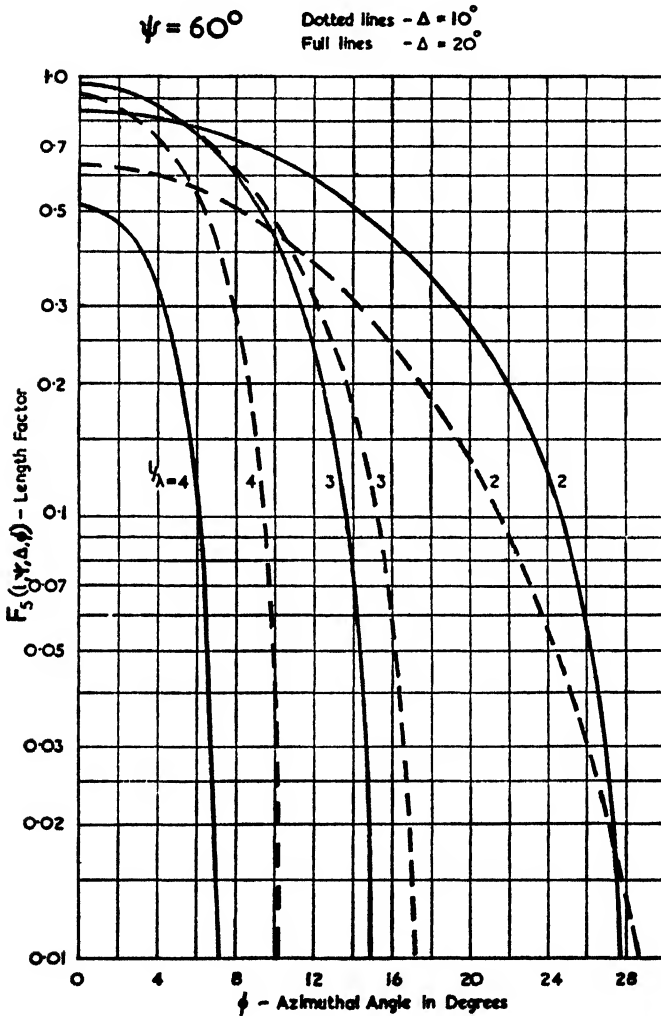


FIG. 6.47 (b). LENGTH FACTOR $F_s(l, \psi, \Delta, \phi)$ FOR DETERMINING THE HORIZONTAL POLAR DIAGRAM OF A RHOMBIC ANTENNA, $\psi = 60^\circ$

“horizontal” polar diagram as well as avoiding the $F_1 = 0$ difficulty. The increase in accuracy is not great since the

polarization is only truly horizontal in the planes for which $\Delta = 0^\circ$ and $\phi = 0^\circ$.

Experimental verifications of the rhombic equations were

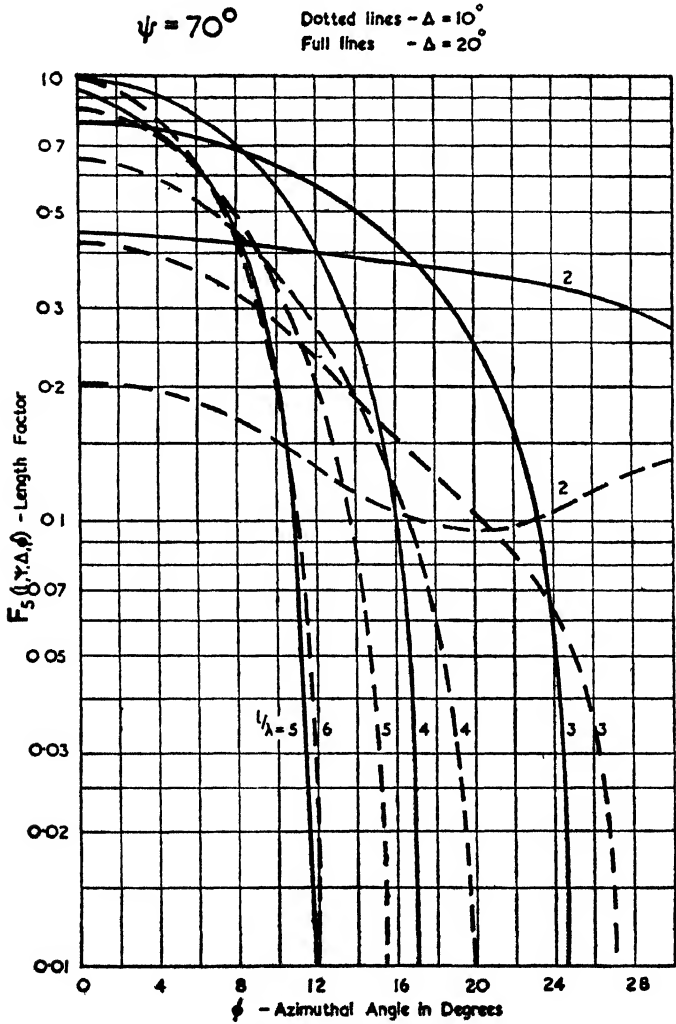


FIG. 6.47 (c). LENGTH FACTOR $F_5(l, \psi, \Delta, \phi)$ FOR DETERMINING THE HORIZONTAL POLAR DIAGRAM OF A RHOMBIC ANTENNA, $\psi = 70^\circ$

obtained in an important paper by Bruce, Beck and Lowry.⁽¹⁸²⁾ Fig. 6.48 shows some of their results.

Design of Rhombic Antennae

If the height, H , above the ground, the length, l , of each side and the semi-included angle, ψ , are all known, then equations

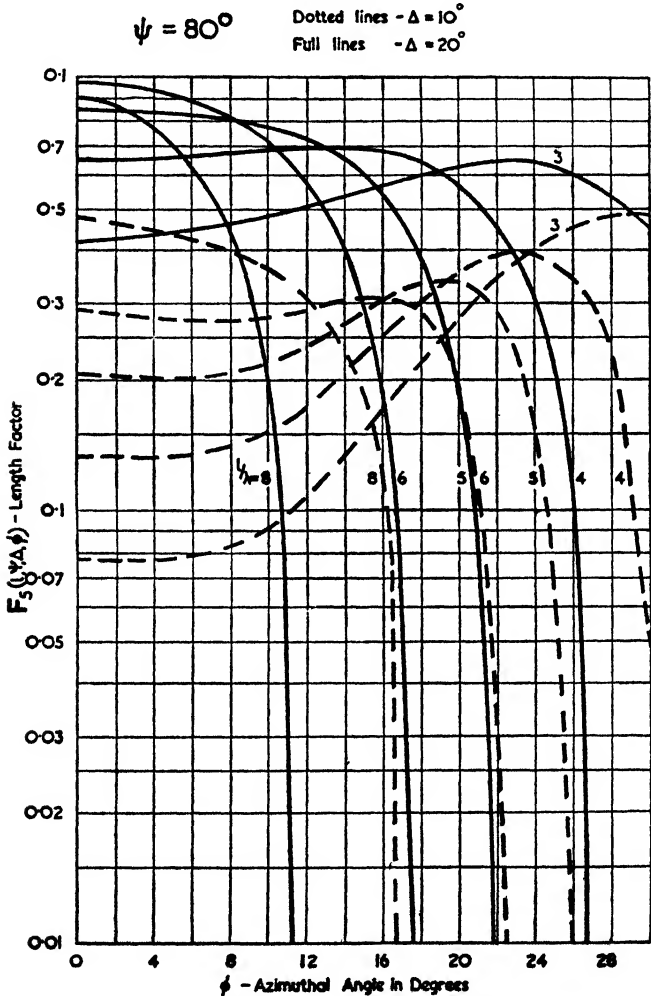


FIG. 6.47 (d). LENGTH FACTOR $F_5(l, \psi, \Delta, \phi)$ FOR DETERMINING THE HORIZONTAL POLAR DIAGRAM OF A RHOMBIC ANTENNA, $\psi = 80^\circ$

(6.25) and (6.28) give both the polar diagrams in the two important planes and the gain over a half-wave dipole in free

space. The power gain obtained in this way is based on a nominal value of 600 ohms for the characteristic impedance of the wires composing the rhombic. With most designs the characteristic impedance has a value somewhere between 600 and 800 ohms, the power gain being inversely proportional to the value of this impedance.

When the actual field strength in a given direction is required we use equations (6.23) and (6.26) or equations (6.24) and

$$\begin{aligned} \text{Dimensions of rhombic} \quad l &= 3.25 \lambda \\ \psi &= 58^\circ \\ H &= 0.5\lambda \text{ (curve a)} \\ &= 1.0 \lambda \text{ (curve b)} \end{aligned}$$

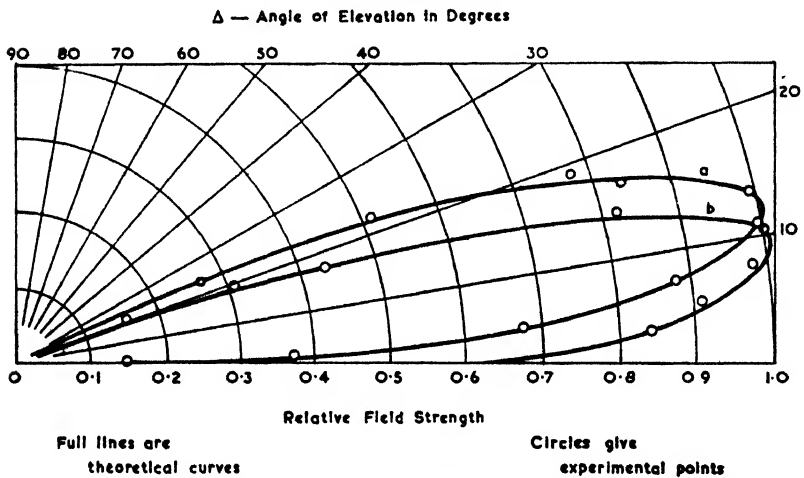


FIG. 6.48. VERTICAL POLAR DIAGRAMS OF A RHOMBIC ANTENNA
(Bruce, Beck and Lowry, *Proc. I.R.E.*, Jan., 1935)

(6.27), according to whether the input current or input power is known. In the latter case a correction for the characteristic impedance may be needed if this differs appreciably from the assumed value of 600 ohms.

With a little experience, one can soon select appropriate values for H , ψ and l from the curves provided. In most problems the angle of fire is known and also the horizontal beam width. The problem may then be approached by taking the optimum value for H (as determined by Figs. 3.8 or 6.6) and then selecting ψ and l so that not only is the correct angle of fire given, but also the beam width obtained from equation (6.26) is adequate.

The above procedure may appear to be too much on a "cut and try" basis, but the fact remains that in practice one

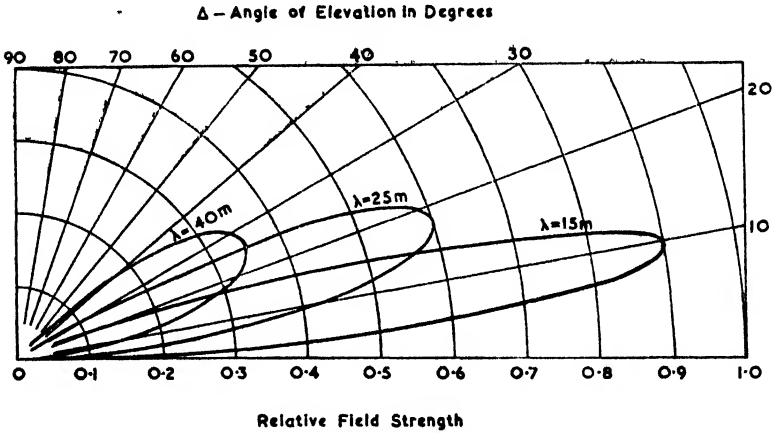


FIG. 6.49 (a). THEORETICAL VERTICAL POLAR DIAGRAMS OF A RHOMBIC ANTENNA FOR THREE DIFFERENT WAVELENGTHS

is often restricted in one dimension or another. In many cases rhombics are usually required to work over a range of frequencies so that optimum dimensions are only possible over

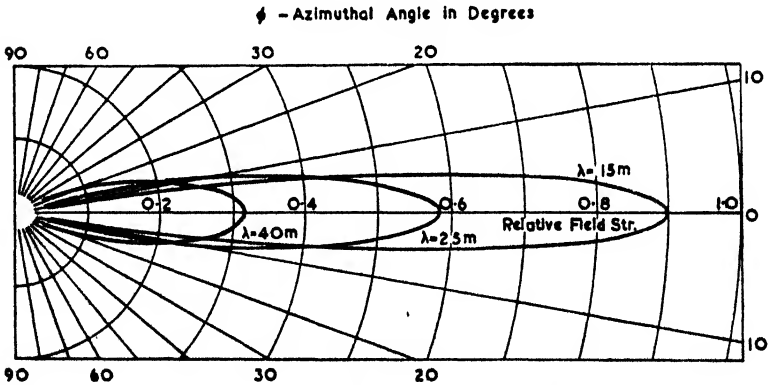


FIG. 6.49 (b). THEORETICAL HORIZONTAL POLAR DIAGRAMS OF A RHOMBIC ANTENNA FOR THREE DIFFERENT WAVELENGTHS

part of the working range. When operation over a band is required, a good rule is to design the rhombic for the geometric mean of the extreme frequencies. The frequency range which may be covered varies with the size of the antenna—if the

sides are one or two wavelengths long a range of 2 : 1 is the limit, but if the sides are several wavelengths long a range of 3 : 1 becomes practicable. Fig. 6.49 gives the performance of a typical rhombic antenna over a range of frequencies.

Optimum Dimensions

To obtain the maximum gain at a given angle of elevation the functions F_1 , F_2 and F_3 in equation (6.25) are differentiated with respect to Δ . This leads to the following formulae—

$$H = \frac{\lambda}{4 \sin \Delta} \quad . \quad . \quad . \quad . \quad (6.29)$$

$$\psi = \sin^{-1} (\cos \Delta) \quad . \quad . \quad . \quad (6.30)$$

$$l = \frac{\lambda}{2(1 - \cos \Delta \sin \psi)} \quad . \quad . \quad (6.31)$$

The value for H is the lowest optimum height (it is only on ultra-short waves that one of the higher order optima might be used), and l is maximized for the major lobe of the polar pattern. From the second equation we see that the optimum angle of inclination, ψ , is the complement of the angle of fire, a feature which is quite independent of H but not of l , since equation (6.31) was used in the derivation of this relation.

Substituting (6.30) in (6.31) gives

$$l = \frac{\lambda}{2 \sin^2 \Delta} \quad . \quad . \quad . \quad (6.32)$$

For any given angle of fire we can therefore maximize H , ψ and l by the equations given above. On doing this and taking the complete vertical pattern we find that the lobe maximum is actually below the chosen angle (see Fig. 6.50). In order to obtain the lobe maximum at the angle of fire, the differential coefficient of E (equation (6.23)) with respect to Δ must be zero. This occurs when

$$l = \frac{0.371 \lambda}{1 - \cos \Delta \sin \psi}$$

Substituting this value in the equation for E and maximizing with respect to ψ gives

$$\sin \psi = \cos \Delta$$

Consequently the desired result can be obtained merely

by decreasing l to 74 per cent of its previous value, the "alignment" value for l being

$$l = \frac{0.371\lambda}{\sin^2 \Delta} \quad (6.33)$$

Strangely enough the alignment design results in a decrease in field strength at the angle Δ , the decrease being of the order of 15 per cent. The origin of this anomaly lies in the

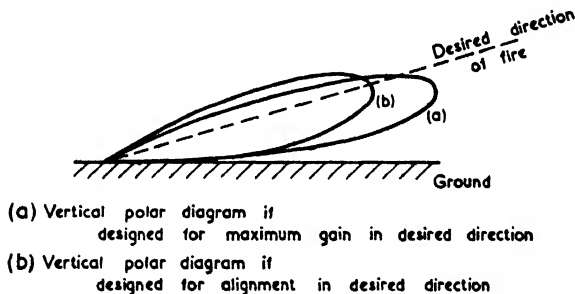


FIG. 6.50. COMPARISON OF ALIGNMENT DESIGN AND MAXIMIZED DESIGN FOR A RHOMBIC ANTENNA

cupped shape in the region of small Δ values of the length factor curves in Fig. 6.45. The alignment design is therefore of more use for receiving than for transmitting rhombics.

The optimum dimensions as given by equations (6.29) to (6.33) are shown plotted in Fig. 6.51 for angles of elevation between 0° and 45° . From these curves it is obvious that when the angle of fire is small, say 10° to 15° , the optimum side length will be too great for practical erection. (The practical limit for sides suspended between two poles is about 150 m.)

Some General Features of Rhombic Antenna Design

The following paragraphs outline a few of the more secondary considerations in rhombic antenna design. For a full account of rhombics, including mechanical design features, the reader may refer to *Rhombic Antenna Design*, by A. E. Harper.⁽⁸⁾

(a) Use of Multiple Wires

In the analysis given above it has been assumed that the characteristic impedance of a rhombic antenna is uniform. Obviously this cannot be true, since the spacing between the wires is far greater in the middle (on account of the logarithmic

form of the formula for the characteristic impedance, the error is not so great as might be supposed). A more uniform characteristic impedance may be obtained by making the sides of

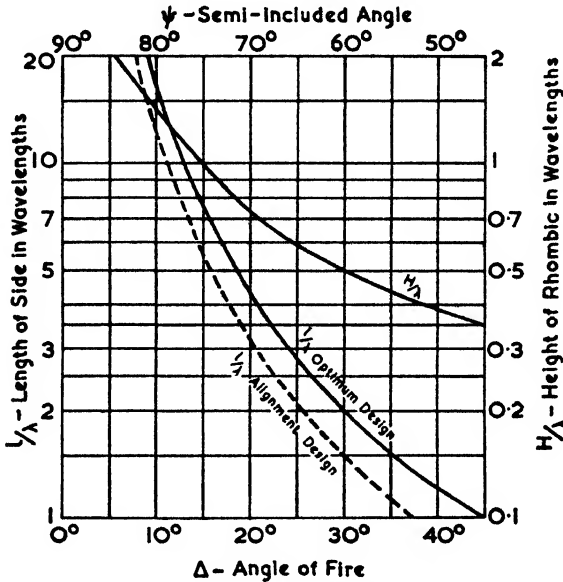


FIG. 6.51. DIMENSIONS FOR OPTIMUM DESIGN OF A RHOMBIC ANTENNA FOR A GIVEN ANGLE OF FIRE

two or more wires which are together at the input and output ends but which diverge towards the middle, as shown in Fig. 6.52. A suitable spacing between the outermost wires at

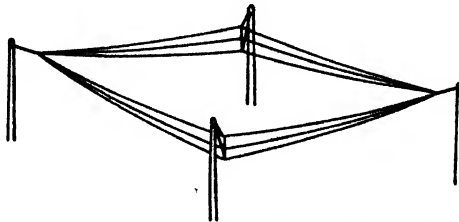


FIG. 6.52. RHOMBIC WITH TREBLE-WIRE SIDES FOR IMPROVING THE UNIFORMITY OF INPUT IMPEDANCE OVER THE WORKING RANGE OF FREQUENCIES

the middle is about 20 per cent of their mean height above the ground.

By using multiple wires the input impedance can be kept constant to, say, 600 ± 50 ohms over a 3 : 1 range in frequency,

whereas the same antenna with single wires would show an impedance range of about 700 ± 100 ohms over the same range (the higher impedance values occur at the low-frequency end of the working range).

(b) *Terminating Resistance*

The best value for the terminating resistance must be found experimentally if a particularly even input impedance characteristic is desired. In general the value required will be some 100 to 300 ohms greater than the input resistance—the smaller increase occurs with the bigger rhombics. Thus to achieve a mean input resistance of 600 ohms a terminating resistance of about 700 ohms would be required for a single-wire rhombic for which $l = 150$ m, $\psi = 75^\circ$, whereas a value of about 900 ohms would be needed if $l = 50$ m, $\psi = 50^\circ$.

For receiving antennae a simple resistor will suffice, but for transmitting antennae it is impracticable to use resistors if more than about 2 kW are to be dissipated in the termination. Hence for greater powers open dissipative transmission lines must be used; these may consist either of iron wire or, what is preferable from a weathering point of view, of stainless steel wire. The necessary data for calculating the performance of such dissipative lines will be found in §§ 10.4 and 10.6.

(c) *Supporting Masts*

It is immaterial whether wood or steel masts are used. Furthermore the supporting guys need not be insulated, but in this case care should be taken to ground the wires efficiently or else a noticeable change in the polar pattern will occur. If wooden posts are used these are normally thick enough not to need guys except for a back-stay.

6.6. ARRAYS OF HORIZONTAL ELEMENTS

Over a perfectly conducting earth vertical radiators would be preferred for long-distance transmission, whether it be for direct transmission or for propagation via the ionosphere. In actual fact the finite conductivity of the ground greatly reduces the radiation at grazing angles as shown, for example, by the curves in Fig. 3.13. Even at angles of elevation of the order of 10° to 30° (as used for long-distance sky-wave transmission), the radiation with vertical polarization is more likely to be *less* than that obtained with horizontal polarization.

Experiments carried out by the B.B.C.⁽¹⁷⁰⁾ on long-distance sky-wave transmission lead to the conclusions that horizontal radiators give both better field strength and less fading. (There appears to be no theoretical justification for the improvement in fading.) Nevertheless vertical radiators have been used with success in many installations and such arrays will be considered in the next section.

Kooman Arrays

The above name is often given to arrays of horizontal half-wave dipoles, on account of their being patented by Kooman in 1927. They were originally used by the Netherlands P.T.T. and also by the Telefunken Company, who called them "tannenbaum" (pine-tree) arrays.

The dipoles are normally end-fed; hence they might also be considered to be arrays of centre-fed full-wave dipoles. For the sake of economy two or three complete arrays are usually suspended together between two masts. The combined system may then be referred to as a "curtain" of antennae. Some engineers reverse this terminology and call the whole system between two masts an "array" and the individual sets of antennae a "curtain"—we shall keep to the former definitions. A typical curtain of Kooman arrays is shown in Plate XI, in which a curtain of reflectors carries a parasitically excited dipole one-quarter of a wavelength behind each driven dipole; the arrangements are such that the roles of reflector and driven antenna may be reversed.

A convenient classification of these arrays has been devised. The first letter of the code is an *H*, indicating horizontal elements; the second is *R* to indicate a reflecting curtain; the third letter is another *R* if the reflector can be reversed, and the fourth (or third) letter an *S* to indicate that the beam is slewable electrically. The figures which follow indicate firstly, the number of half-wave dipoles in a horizontal plane, secondly, the number in a vertical plane, and thirdly, the height in wavelengths of the lowest dipoles above the ground. Thus assuming the antennae in Plate XI are reversible and slewable both arrays would be coded $HRRS_{4/4/1}$.

Fig. 6.53 (*a*) shows an $H_{2/4/1}$ array. This configuration is particularly useful since the impedance of a thin full-wave dipole fed at the centre is about 4 000 ohms; hence four full-wave dipoles in parallel give an impedance of about

500 ohms, which is a suitable value for feeding by two-wire lines. It should be noted that the antennae may be considered in parallel, since they are spaced at intervals of $\lambda/2$ along the feeder; also the feeder is twisted round between each full-wave dipole so as to obtain the correct phase relationship for broad-side radiation.

Two such arrays side by side form an $H_{4/4/1}$ array as shown in Fig. 6.53 (b), whereupon a transmission line feeding them

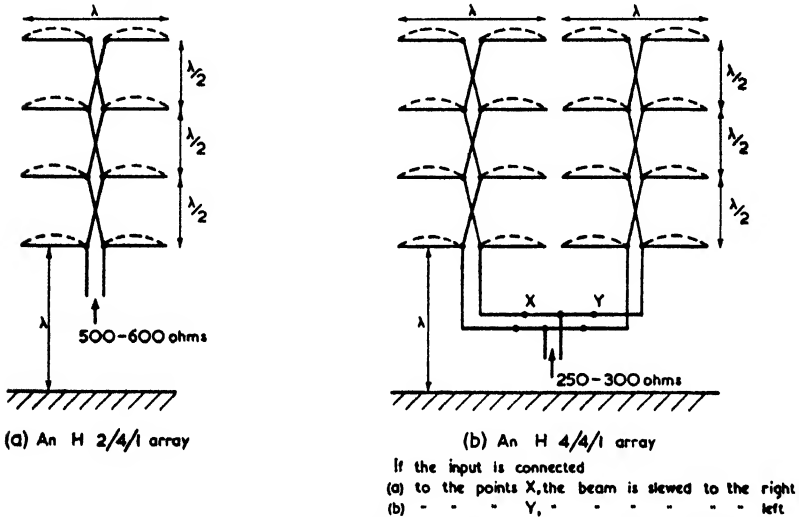


FIG. 6.53. ARRAYS OF HORIZONTAL DIPOLES (OR "KOOMAN ARRAYS")

both should have a characteristic impedance of the order of 250 ohms, i.e. a four-wire line would be more suitable. The beam produced by a $4/4/1$ array may be slewed horizontally to either side by altering the phase relationship between the two halves. Consideration of the component vectors shows that such slewing will cause a large secondary lobe to appear on the opposite side to which we are slewing the beam. In fact, if the relative phases of the two halves are altered by $\pm 90^\circ$ from the equiphase position, two lobes of equal magnitude will appear on either side of the main direction.

(a) Horizontal Polar Diagram

The polar pattern in a horizontal plane is given by the curves of Fig. 6.54 which are for n dipoles spaced $\lambda/2$ between centres (for other spacings similar curves may be constructed



PLATE XI CURTAIN OF TWO TYPE HR4 1 KOOMAN ARRAYS AT DAVENTRY
(courtesy of the B.B.C.)

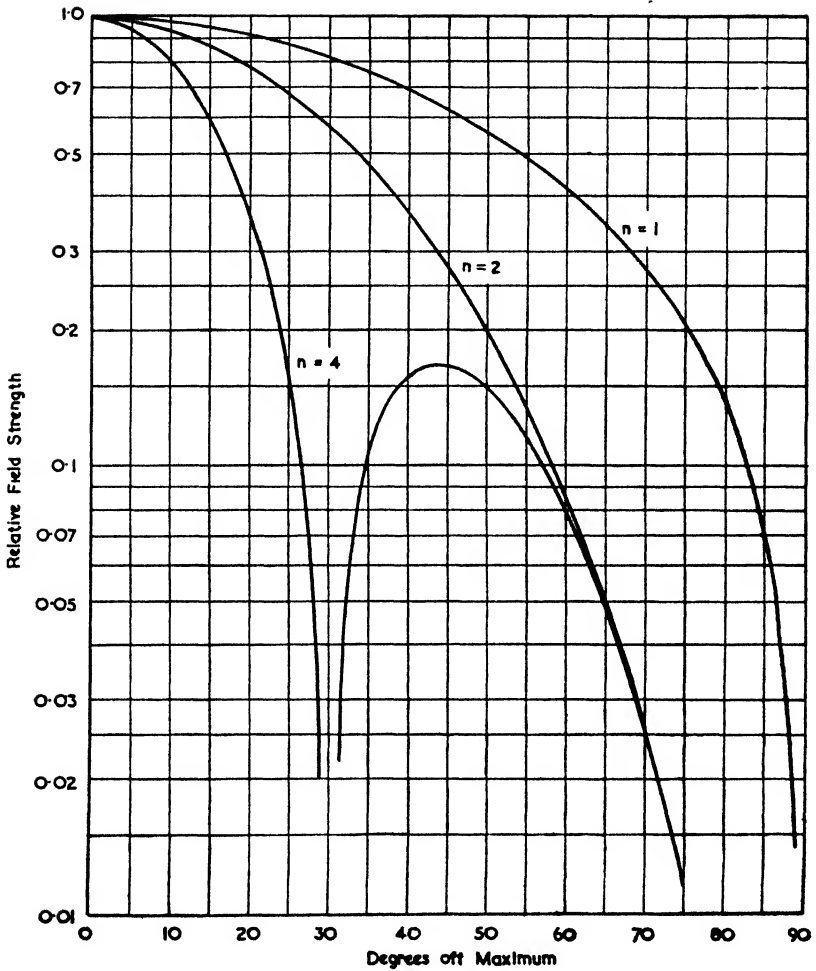


FIG. 6.54. HORIZONTAL POLAR DIAGRAMS OF KOOMAN ARRAYS

by the method described in the previous section). The corresponding formulae for $\lambda/2$ spacing are as follows—

$$\begin{aligned}
 n = 1 \quad F(\phi) &= \frac{\cos((\pi/2) \sin \phi)}{\cos \phi} \\
 n = 2 \quad F(\phi) &= \frac{\cos^2((\pi/2) \sin \phi)}{\cos \phi} \\
 n = 3 \quad F(\phi) &= \frac{\cos((\pi/2) \sin \phi)}{\cos \phi} \left[\frac{1}{3} + \frac{2}{3} \cos(\pi \sin \phi) \right] \\
 n = 4 \quad F(\phi) &= \frac{1}{2} \left[\frac{\cos^2((\pi/2) \sin \phi)}{\cos \phi} \right. \\
 &\quad \left. + \frac{\cos((\pi/2) \sin \phi)}{\cos \phi} \cos\left(\frac{3}{2} \pi \sin \phi\right) \right]
 \end{aligned}$$

To find the degree of slewing obtained by varying the phasing we find the polar diagram of two point sources situated at the centres of the two halves and phased according to the new phase relationship; then this diagram is multiplied by the diagram of half the total array. The maximum possible slew is not great, in fact, with a phasing of $\pm 90^\circ$ the slew of two sources separated by 1λ is only 30° and this is reduced to $21\frac{1}{2}^\circ$ after multiplication by the $n = 2$ curve. Fig. 6.55 gives two examples of a slewed polar pattern and Fig. 6.56 shows an experimental curve obtained by Page.⁽¹⁷⁴⁾

(b) *Vertical Polar Diagram*

The vertical polar diagram of the array in free space may be readily determined by the methods given in the beginning of this chapter. The complete diagram is then obtained by multiplying the free-space curve (which is sometimes referred to as the "frame factor") by the appropriate height factor curve of Figs. 6.6 and 6.7, where the height in question is that of the centre of the array.

Thus for an $H_{4/4/1}$ array the height would be 1.75λ and the vertical polar diagram as shown in Fig. 6.57.

This simple multiplication of the frame factor by the height factor is only possible because polarization is horizontal. Consequently the errors made by assuming perfect reflection are quite small—particularly at low angles of elevation where the major lobe is formed.

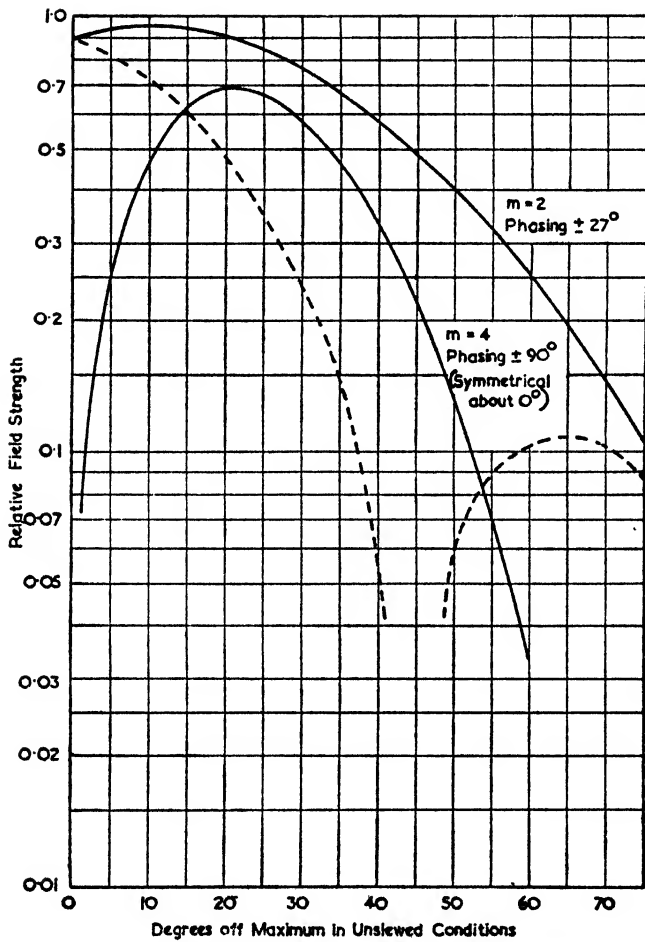


FIG. 6.55. HORIZONTAL POLAR DIAGRAMS OF SLEWED KOOMAN ARRAYS

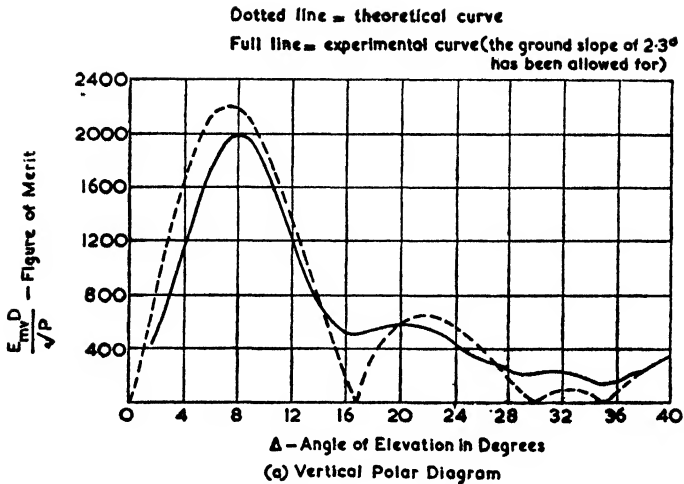


FIG. 6.56 (a). THEORETICAL AND EXPERIMENTAL VERTICAL POLAR DIAGRAMS OF AN HRRS/4/4/1 TYPE ARRAY
(Page, *Jour. I.E.E.*, June, 1945)

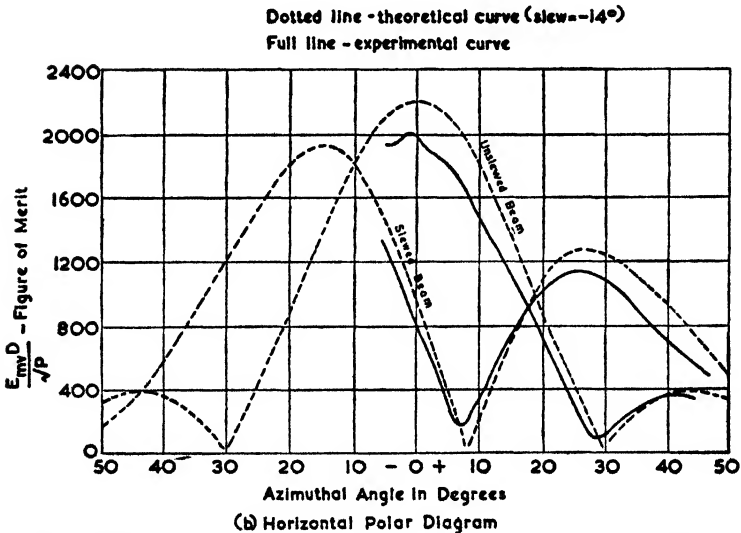


FIG. 6.56 (b). THEORETICAL AND EXPERIMENTAL HORIZONTAL POLAR DIAGRAMS OF AN HRRS/4/4/1 TYPE ARRAY
(Page, *Jour. I.E.E.*, June, 1945)

(c) Gain of Array

The gain of a Kooman array may be obtained by preparing a power distribution diagram as described in the previous

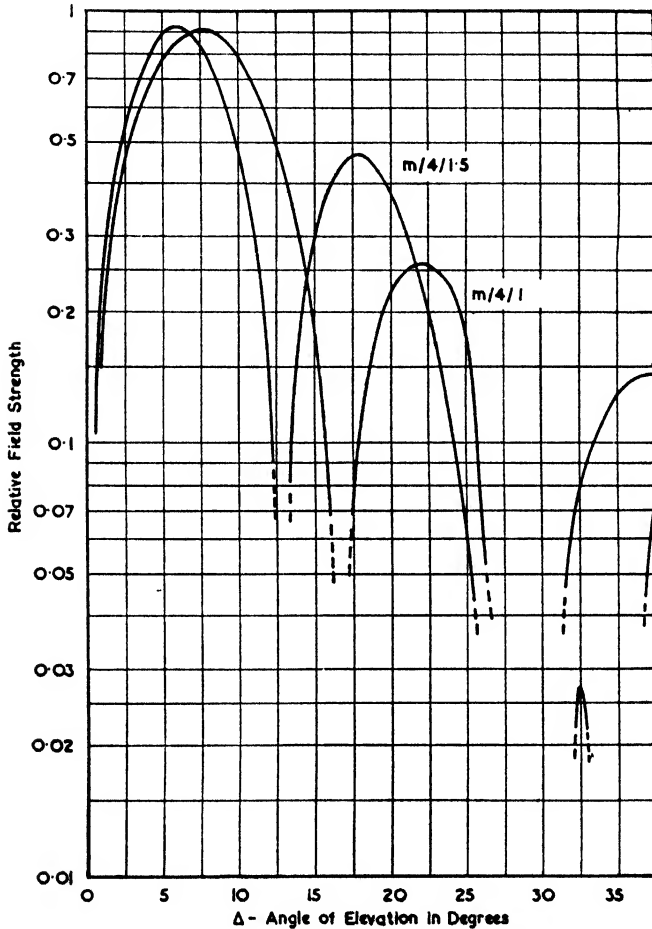


FIG. 6.57. VERTICAL POLAR DIAGRAMS OF $H_{m/4/1}$ AND $H_{m/4/1.5}$ ARRAYS

section and illustrated in Fig. 6.16 for an elementary dipole. The corresponding diagram for an $H_{4/4/1}$ array is shown in Fig. 6.58. This is based on a diagram given by Hayes and MacLarty⁽¹⁷⁰⁾ who obtain a gain of $G_0 = 19$ db by integration on this diagram.

Alternatively the gain calculation may be based on the

determination of the radiation resistance of each dipole using the table of mutual resistances given on p. 105.

If this is done for an $H_4/4/1$ array the total radiation resistance of the whole array proves to be 34.2 ohms in excess of that for sixteen half-wave dipoles widely separated in space. Thus the values of all the antenna currents are reduced by a factor of 0.986 on account of the mutual resistances. This means a power loss of only 0.012 db, so that the mutual terms obviously tend to balance out and can be neglected. This feature applies only in certain cases and is due in the present

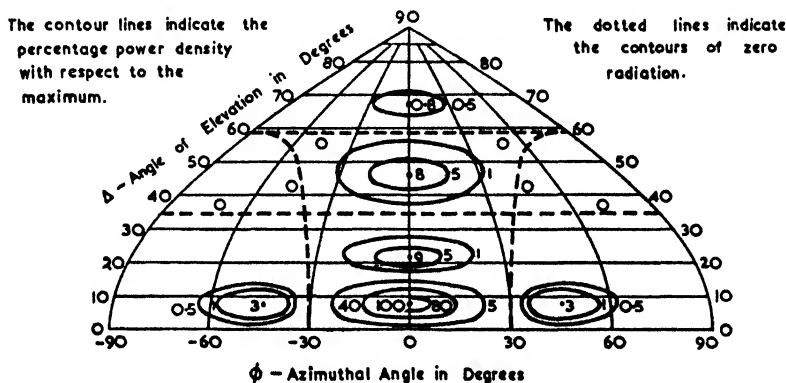


FIG. 6.58. POWER DISTRIBUTION DIAGRAM OF AN $H_4/4/1$ ARRAY
(Hayes and MacLarty, *Jour. I.E.E.*, Sept., 1939)

instance to the fact that the mutual resistance of adjacent collinear dipoles is positive while that of broadside or diagonally placed dipoles is negative by roughly the right amount to give cancellation. The mutual impedances may therefore be neglected for arrays in which the spacing is 0.5λ if the array has both rows and columns and if the total number of dipoles is at least 4.

The above rule makes the gain computation quite simple. In terms of power, G_H is equal to the total number of half-wave dipoles multiplied by 4 (the factor 4 allows for ground reflections). The value thus obtained is reduced by some quite small factor which is given by the vertical polar diagram. The reduction factor is simply due to the fact that, for the angle of elevation at which the frame and its image are in phase, the frame polar diagram is no longer quite at its maximum—the reduction is given directly on obtaining the vertical polar diagram by the graphical means previously described.

For example an $H_4/4/1$ array has a power gain of $4 \times 4 \times 4$ which is reduced by the factor $(0.91)^2$ as obtained from the vertical polar diagram of Fig. 6.57. Hence

$$\begin{aligned} G_H &= 64 \times 0.828 \\ &= 52.9 \text{ (i.e. } 17.2 \text{ db)} \end{aligned}$$

Using equation (6.6) gives the gain over an omnidirectional antenna as

$$G_o = 19.35 \text{ db}$$

which is in good agreement with the value given by Hayes and MacLarty.

The above method therefore provides an extremely simple way of determining the gain of an array. Indeed to a first

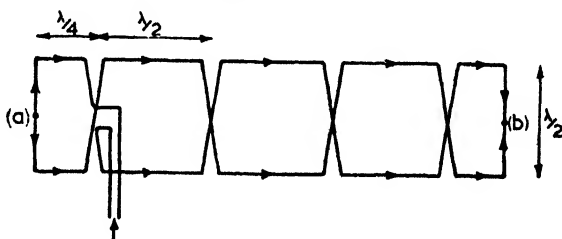


FIG. 6.59. A HORIZONTAL STERBA ARRAY

approximation the power gain is simply $4n$, where n is the total number of elements.

The increase in gain obtained by adding an array of reflectors behind the driven array may be taken to be 3 db, i.e. the forward field strength is increased by $\sqrt{2} : 1$. This figure represents the theoretically ideal case but it is also closely approximated to in practice with a large array.⁽¹⁷⁰⁾

On slewing the beam the gain is reduced by a factor which can readily be deduced from the horizontal polar diagram. Thus slewing an $H_4/4/1$ array by 11° (corresponding to a phasing of $\pm 30^\circ$) will reduce the gain by 0.35 db.

Horizontal Sterba Arrays

The horizontal Sterba array is closely allied to horizontal dipole arrays since it is virtually a set of such dipoles connected in the form of a continuous loop (Fig. 6.59). To obtain correct phasing at the ends quarter-wave sections must be used—thus points (a) and (b) in Fig. 6.59 are current nodes. The complete loop is fed at a current antinode.

In view of the continuous d.c. path provided by such an arrangement the whole set of elements can have a d.c. or low-frequency current passed through it for de-icing purposes. A complete array might consist of two complete loops separated by a vertical distance of $\lambda/2$.

The polar diagram of such an array is obviously very nearly the same as that of a Kooman array of the same overall dimensions, the only differences being due to the existence of

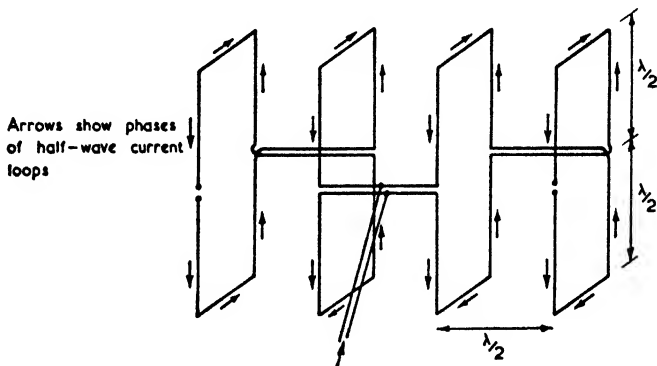


FIG. 6.60. A WALMSLEY ARRAY

the quarter-wave elements at the ends which would tend to make the horizontal polar diagram just a little more directive.

A reflector curtain consisting of an identical set of elements and spaced a quarter of a wavelength behind the driven elements is normally used. The resultant gain is of the order of 3 db.

The Walmsley Array

This type of array is used by the British General Post Office and takes the form shown in Fig. 6.60 for a four-unit array. A single unit by itself has an appreciable radiation from the half-wavelength sides—about 16 per cent of the total power is lost in this way. If a row of such units were arranged horizontally the radiation from the sides would tend to be neutralized (apart from the end elements). With a set of vertical units as shown in Fig. 6.60 this is not so, and steps have to be taken to reduce this undesired radiation.

Walmsley⁽¹⁷⁹⁾ describes how this was done by placing parasitic elements alongside the offending elements so that the power radiated in this way was reduced to 17 per cent of its

former value. To achieve this the parasitic wires were placed $\lambda/16$ away from the side elements and had a length of approximately $\lambda/2$.

When this radiation from the shorter sides has been made small each unit may be seen to consist of two full-wave dipoles spaced half a wavelength apart. The impedance at the feed-points is therefore of the order of a few thousand ohms—hence the need for feeding four units in parallel from one transmission line. A large array may consist of as many as forty-eight pairs of full-wave dipoles.

These arrays are best suited to operate as a bidirectional beam, for the spacial distribution of the radiating elements is such as to make any reflector curtain relatively inefficient.

6.7. ARRAYS OF VERTICAL ELEMENTS

Any of the previously mentioned arrays can be arranged so that their radiating elements are vertical. Such an arrangement is uncommon for a Kooman array but Sterba arrays are quite often used in the vertical form.

The best known of all vertical arrays is the Franklin array, of which a photograph is shown in Plate XII.

The Franklin Array

The principle of the Franklin antenna (also known as the Marconi-Franklin antenna) was discussed in § 6.4 and illustrated in Fig. 6.28, which shows a set of vertical half-wave dipoles whose currents are all in phase. To obtain this phase relationship by feeding each column of antennae at the base only, the collinear elements must be joined by a phasing device which is equivalent to half a wavelength of conductor and this may be either a phasing coil or a quarter-wave line. There is a third type of connection which leads to what is known as a folded Franklin antenna and this has the advantage of being easier to erect as well as having greater radiation efficiency. A sketch showing typical dimensions of the folded type is given in Fig. 6.61, from which it can be seen that it consists effectively of a column of overlapping half-wave dipoles whose centres are 0.35 to 0.4λ above each other and whose ends are connected by a folded wire $\lambda/2$ long.

A large array may consist of six dipoles to each column and six columns spaced $\lambda/2$ apart, when quite a good approximation

to a uniform sheet of current is obtained. To improve the forward directivity a curtain of reflectors may be added one-quarter of a wavelength behind. Such reflectors are spaced at intervals of only $\lambda/4$ and help to broaden the tuning of the array (see Ladner and Stoner⁽¹⁸⁾).

For a small array of, say, four columns each 30 m high, the

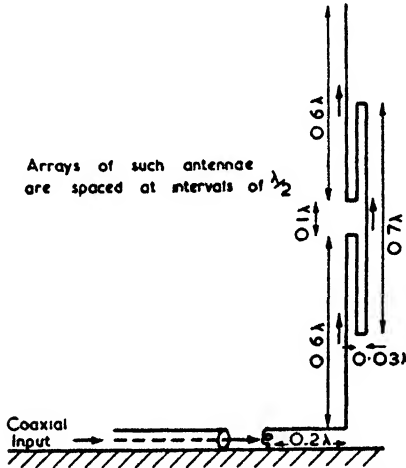


FIG. 6.61. A FOLDED FRANKLIN ANTENNA

spacing between the energized columns may also be reduced to $\lambda/4$.

Franklin arrays are easily fed by coaxial lines for which purpose coupling units of the type indicated in Fig. 6.61 can be used.

The Series Phase Array

A series phase array is one which carries a travelling wave and is folded at intervals to produce radiating elements as shown in Fig. 6.62. These elements radiate with the same polar diagram as a standing-wave antenna of the same height. Arrays formed in this way are very flexible since, by a suitable choice of phasing between adjacent elements, the polar diagram of the system as a whole can be made to give a variety of both broadside and end-fire patterns. In their usual form they function as end-fire arrays of vertical elements, in which case the radiation from the wires joining the elements is small due to their proximity to the ground.

The radiation from a folded wire carrying a travelling wave

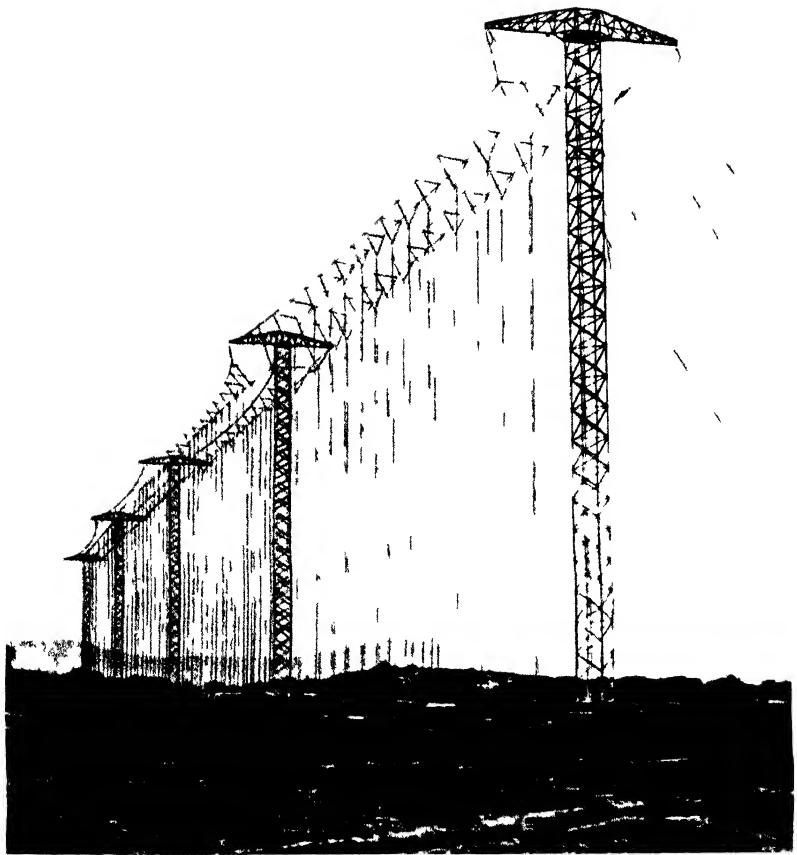
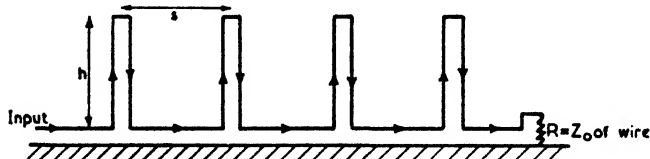


PLATE XII ARRAY OF FRANKLIN ANTENNAE AT BODMIN CORNWALL
(Courtesy of Marconi Wireless Telegraph Co Ltd)

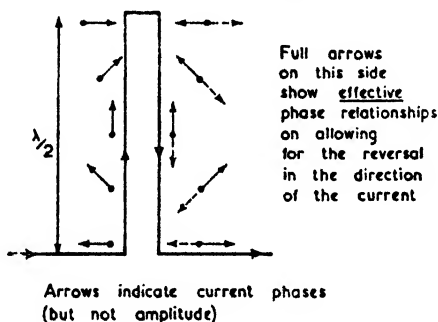
may be studied by means of Fig. 6.63, which has vector diagrams giving the phase relationships of the currents along the wire. The dotted vectors on the right-hand side show the phase relationship as it would be *were it not for the reversal due*



The arrows only indicate the direction in which the current is travelling. The actual relative phases at any one moment depend on the dimensions of h and s

FIG. 6.62. A SERIES PHASE ARRAY

to the current travelling in the opposite direction. The effective phases from the point of view of radiation are shown by the full vectors. These indicate that the net effect is just as if there were a standing wave on the wire with a current antinode at the top. This is true whatever the length of folded wire may be.



Arrows indicate current phases (but not amplitude)

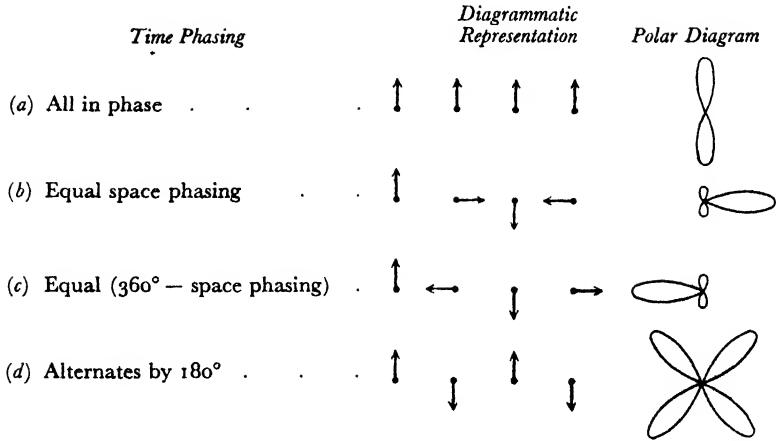
FIG. 6.63. DIAGRAM ILLUSTRATING THE CURRENT PHASES ALONG A FOLDED ELEMENT OF LENGTH $\lambda/2$

The phase relationship between adjacent wires is obviously dependent on the length $2h$ as well as on the spacing d .

Since it is also possible to make the electrical length of the feed between each radiating element differ from the free-space distance, a great variety of arrangements is possible. Examples of some of these arrangements are tabulated on page 314 for the case of four elements spaced at intervals of $\lambda/4$.

A comparison of cases (b) and (c) shows how an end-fire beam may be reversed.

The case in which the time phasing equals the space phasing



is met in practice by any array of folded elements whose heights are $\lambda/2$ and whose feed wires run straight from one element to the next. Such elements therefore provide a convenient basis for end-fire arrays.

As is usual in the case of linear arrays the spacing between the elements is not at all critical—suitable values are $d = \lambda/4$ or $\lambda/6$.

Fig. 6.21 (b) shows the horizontal polar diagram for an eight-element array for which $d = \lambda/4$, i.e. the overall length is 1.75λ . In practice the attenuation of the travelling wave due to radiation alters the theoretical polar diagram a little. The changes to the major lobe are small—only the minor lobes are appreciably altered, the effect on them being an “averaging out” process, i.e. the nulls disappear and the maxima are reduced. Fig. 6.21 (b) is valid for any height of antenna, but the vertical polar diagram depends not only on the height but also on the ground conductivity and the wavelength.

Assuming a perfectly conducting ground, the vertical polar diagram may be obtained by multiplying Fig. 6.21 (b) by the vertical polar characteristic of each element. An indication of the modifications introduced by the finite conductivity of the ground can be obtained from Fig. 3.13.

The following typical gain figures obtained in practice with the end-fire system are given by Ladner⁽¹⁷¹⁾—

$$\begin{array}{l}
 \text{Length of Array} = 4\lambda \\
 \text{Single array} \quad G_H = 10 \text{ db} \\
 \text{Two parallel arrays} \quad G_H = 14 \text{ db} \\
 \text{Four parallel arrays} \quad G_H = 18 \text{ db}
 \end{array}$$

CHAPTER VII

D.F. Antennae

THE art of position and direction finding by means of radio waves has been developed so much in recent years that we now have a great variety of different systems for this purpose. It is possible to classify all these systems in four distinct categories. These are as follows—

- (a) reception of minimum signal (“null” methods),
- (b) reception of maximum signal,
- (c) reception of equal signals from two different polar patterns,
- (d) time or phase measuring systems.

As far as the antenna design of these systems is concerned, the problem is mainly one of obtaining suitable polar patterns. For null systems the most common polar pattern is a figure-of-eight and this is readily obtainable by means of a loop antenna or two spaced vertical antennae. The present chapter is limited entirely to antennae of this type for even a brief discussion of direction-finding systems in general would be unduly long.

Since a full account of the principles underlying the derivation of polar patterns has been given in § 6.1, no further discussion of the principles as such will be included in the following sections.

7.1. THE LOOP ANTENNA

Characteristics of a Small Loop

A single loop antenna whose diameter is but a small fraction of a wavelength has a polar diagram as shown in Fig. 7.1 (c). The reason for this pattern is easily appreciated if we consider the case of a square loop as shown in Fig. 7.1 (a) along the vertical sides of which flow currents i_a and i_b (the currents are

equal because the sides of the loop are only a small fraction of a wavelength long). Hence the field at a point in the horizontal plane is given by the vector sum of E_a and E_b which represent the electric field intensities due to i_a and i_b respectively. Along the axis of the loop ($\phi = 0^\circ$ or 180° in Fig. 7.1 (c)) the two field components will be in antiphase since the currents flow in opposite directions—therefore the resultant field is zero. In other directions the resultant E has a value which is given by $2E_a \sin [(\beta d/2) \sin \phi]$ and when $\phi = 90^\circ$ or 270° this has a

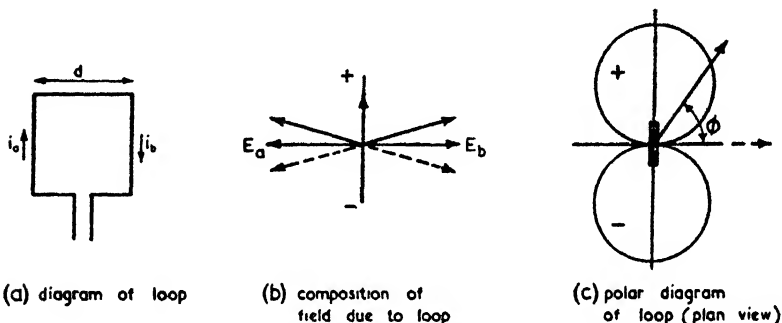


FIG. 7.1. CHARACTERISTICS OF LOOP TRANSMITTING ANTENNA

maximum value of $E_a \beta d$, where βd is the distance between the sides in radians.

The field strength in a horizontal plane due to a given current flowing round the loop may be found quite readily by means of equation (4.41), Vol. I. From this equation we see that the field in the equatorial plane due to a short filament of current of moment Id is given by

$$E_a = j \frac{60\pi}{\lambda r} e^{-j\beta r} Id$$

where r = distance to the field point in metres,
 I = r.m.s. current in amperes.

The total field E due to both sides of the loop is $E_a \beta d$ at the maximum points and is proportional to $\sin \phi$, hence

$$E = \frac{120\pi^2}{\lambda^2} \frac{I}{r} A \sin \phi. \quad (7.1)$$

In the above equation all the units conform to the M.K.S. system and A is the area in square metres. If the loop consists of n turns, all carrying equal currents, then the value of E is multiplied by n . The formula is also true for any shape of

loop, provided the dimensions are small in comparison with a wavelength.

When the loop is acting as a receiver of energy, the phases of the induced currents in the sides are best considered with reference to the phase that a current induced in a vertical antenna would have if placed at the centre of the loop. Thus the current phases in the presence of an incident wave are as shown in Fig. 7.2 (b).

Since i_a and i_b act in opposition around the loop the phase

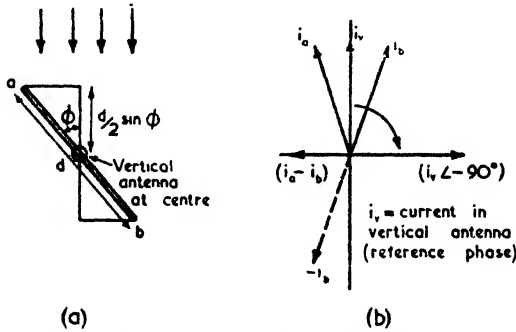


FIG. 7.2. RECEPTION DIAGRAMS FOR LOOP ANTENNA

of one of them must be reversed in the vector diagram in order to obtain the correct resultant.

It will be observed that the resultant loop current is in phase quadrature with the current in the reference antenna. This property may be used if i_a and i_b are slightly unequal (in which case the resultant has a small component in phase with i_v) by injecting just sufficient current in antiphase from a vertical antenna to balance out the component along i_v —this results in a second order inaccuracy in the direction of zero loop signal, an effect which is, however, preferable to a broad minimum.

The induced e.m.f.'s in the sides are both equal to Ed where E is the field strength of the incident wave, and since $\beta d \ll 2\pi$ their resultant is given by

$$\begin{aligned}
 e &= 2 Ed \sin \left(\frac{\beta d}{2} \sin \phi \right) \\
 &= \frac{2\pi}{\lambda} AE \sin \phi \quad . \quad . \quad . \quad (7.2)
 \end{aligned}$$

The loop e.m.f. is therefore proportional to A , the area of the loop, and to $\sin \phi$. This is true for all small loops whatever

their shape may be, since their cross-section may be subdivided into small squares. If the loop has n turns, then the right-hand side of (7.2) is multiplied by n . Consequently the effective height of such a loop when in the position of maximum reception is given by

$$h_e = \frac{2\pi}{\lambda} nA \quad . \quad . \quad . \quad . \quad (7.3)$$

A further useful loop parameter is the "pick-up" factor; it is the ratio of the voltage, V (produced at some specified terminals) to the field strength, E . The terminals chosen are those across the first tuned circuit; they are therefore likely to be the input terminals to the amplifier. In the case of a tuned loop, the pick-up is simply given by the product of the effective height and the magnification of the frame inductance, that is

$$\begin{aligned} \left| \frac{V}{E} \right| &= h_e Q \\ &= \frac{2\pi}{\lambda} nA Q \quad . \quad . \quad . \quad . \quad (7.4) \end{aligned}$$

The pick-up factor may be increased by an iron-cored loop. This type of loop has been discussed by Burgess,⁽³⁷⁵⁾ who arrives at the following conclusions—

(a) the permeability of the iron dust should be as high as possible;

(b) the core should be elongated in the direction of the axis of the loop;

(c) the core may be hollowed to an appreciable extent without a significant reduction in the performance;

(d) the loop should be slightly spaced from the core to prevent excessive dielectric losses;

(e) stranded wire helps to reduce the copper losses with the core inserted.

As an example he quotes the D.F. loop used on German aircraft. This had a hollow spheroidal core (the ratio of the two axes being 4 : 1) whose permeability was 50. With a hole occupying 40 per cent of the central cross-sectional area the pick-up factor was increased by ten, due to the core. Had the core been solid the increase in the pick-up would have been 10.6 instead of 10; thus the loss in pick-up due to hollowing the core is quite small.

Direction Finding Properties of a Loop

The polar diagram of a loop shows the greatest rate of change of signal with angle of rotation in the regions $\phi = 0^\circ$ or 180° (Fig. 7.1) so that if the loop is used to obtain the bearing of some transmitter the greatest accuracy is obtained by turning the loop until the received signal is a minimum.

On performing this operation there remains an ambiguity of 180° in the direction, but this may be resolved by adding

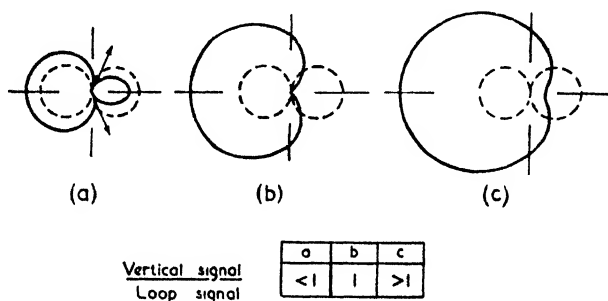


FIG. 7.3. MODIFICATION TO THE POLAR DIAGRAM OF A LOOP ANTENNA DUE TO THE PRESENCE OF AN IN-PHASE "VERTICAL" SIGNAL

a signal which is received on a simple vertical antenna. When this "vertical" signal has the appropriate strength and has its phase changed by 90° , the polar diagram is transformed from a figure-of-eight to a cardioid as shown in Fig. 7.3 (b). The null point of this cardioid is at right angles to the two nulls given by the loop itself. The direction of the right angle with respect to the actual bearing depends on whether the phase of the vertical signal has been advanced or retarded by 90° . The phase relationships are shown in Fig. 7.2 (b).

The desired 90° phase change to the signal from the vertical antenna can be obtained in a number of ways in the circuits coupling the loop and the vertical antenna to the grid of the first valve. For details of such circuits the reader may refer to the two books mentioned in the introduction.

"Antenna Effect" or "Vertical"

In addition to the signal caused by the phase difference between the two sides of the loop, there will also be a signal whose phase is the same as that obtained in a vertical antenna

situated at the centre of the loop, i.e. the loop as a whole acts as a vertical receiving antenna. The signal obtained in this manner is obviously independent of the orientation of the loop so that the directional properties of the loop are impaired. This phenomenon is known as "antenna effect" or "vertical."

The effect on the polar diagram of the loop depends on whether the "vertical" component is in phase or in phase quadrature with the loop signal. In the former case the resultant pattern is as shown in Fig. 7.4, in which the zeros are replaced by broad minima; in the latter case the pattern is given by Fig. 7.3 (a) which shows that the two minima have been displaced in opposite directions.

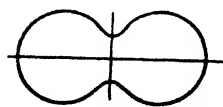


FIG. 7.4. BROADENING OF MINIMA DUE TO VERTICAL SIGNAL IN PHASE-QUADRATURE

In practice the undesired vertical signal will have some intermediate phasing so that the bearings become both inaccurate and less distinct. The reduction of the antenna effect in a loop is therefore of prime importance, especially for small loops—since the vertical signal is proportional to the height of the loop, whereas the loop signal is proportional to the area of the loop.

To reduce the vertical component, the loop should be

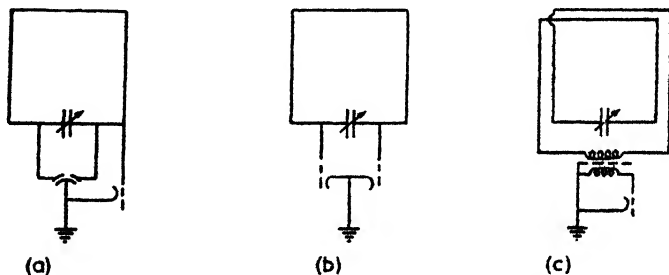


FIG. 7.5. THREE CIRCUITS FOR REDUCING "VERTICAL"

balanced with respect to earth and this can be done in a number of ways of which three are illustrated in Fig. 7.5.

Another method of reducing vertical is to enclose the loop in a shield which completely surrounds it except for a small gap (Fig. 7.6); in this way the loop itself is enclosed in an electrostatic shield. A screen of this nature prevents the pick-up of vertical signal in the loop but makes no difference to the loop signal.

To understand the effect of the screen it is probably easiest

to consider the loop from a transmitting point of view. Thus in Fig. 7.6 (b) we have a loop current in the centre conductor of i_a' or i_b' according to which side of the gap we are considering. Since the centre conductor is continuous $i_a' = i_b'$.

Boundary conditions inside the shield (which, with the loop, forms a coaxial line) demand that the currents on the inside of the screen must equal those in the corresponding portions of the inner conductor, hence $i_a'' = i_a'$ and $i_b'' = i_b'$, so that we have $i_a'' = i_b''$. The currents on the outside of the shield

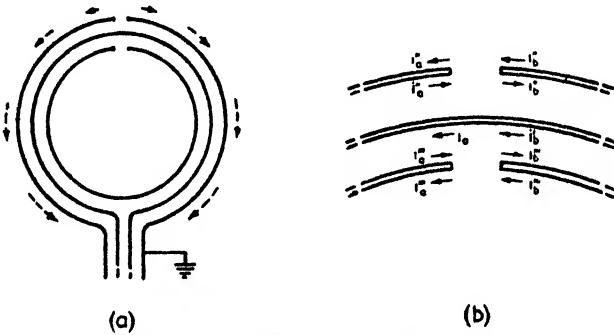


FIG. 7.6. SHIELDED LOOP ANTENNA

must equal those on the inside, for the currents round the edges must be continuous, i.e. $i_a''' = i_a''$ and $i_b''' = i_b''$. Consequently $i_a''' = i_b'''$ and therefore the current is continuous around the outer surface of the screen just as if the gap were non-existent. We have, in fact, got unity coupling between the inner loop and the outside of the shield.

For the loop to be acting as a vertical antenna there should be lines of electric force from the loop to the surrounding earth, i.e. the inner conductor should play the same role as the vertical conductor shown in Fig. 1.5. This is clearly impossible because of the surrounding electrostatic shield. In fact, if we were to excite the loop with respect to earth (and therefore with respect to the earthed shield), the lines of electric force would be confined entirely to the space between the two conductors. The two modes of operation correspond to placing

- (a) a generator in series with the loop, or
- (b) a generator between the loop and the shield.

Of these only the first mode is capable of external radiation for the reasons given above. Hence, in view of the reciprocity between transmission and reception, a screened loop will be

responsive to the circulating current due to the vector difference between the induced e.m.f.'s in each side of the screen, but it will not have any pick-up due to the vector sum of such e.m.f.'s. It will be noticed that, although Fig. 7.6 shows the gap in the screen as being at the top of the loop system, the above arguments hold for any other position of the gap.

Crossed-loop Antenna

In order to obtain a high sensitivity on a loop direction finder the area of the loop should be as great as possible, but this

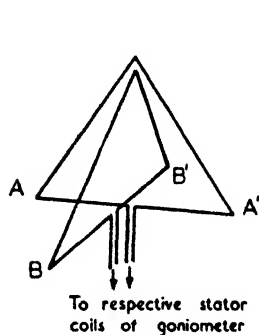


FIG. 7.7. BELLINI-TOSI
CROSSED LOOPS

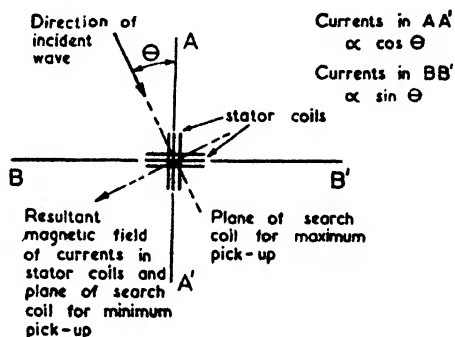


FIG. 7.8. ANGULAR POSITION OF GONIOMETER
COIL WITH RESPECT TO THE DIRECTION OF
THE RECEIVED SIGNAL

leads to loop sizes which cannot be designed for rotation. This difficulty is avoided by the Bellini-Tosi system which employs two fixed crossed loops at right angles as shown in Fig. 7.7. Each loop is in series with a coil and these two coils are at right angles to each other while between them is a rotatable search coil. Bearings are taken by rotating the search coil as if it were a rotating-loop antenna. The coil assembly as a whole is known as a "radiogoniometer" or simply a "goniometer." The currents flowing in the two fixed coils of the goniometer are equal to the loop currents and these are proportional to the sine and the cosine of the angle the incident wave makes with one of the loops (Fig. 7.8 (a)). If I_m is the current in a single loop when the loop is in the plane of the incident wave, then the loop currents are $I_m \sin \phi$ and $I_m \cos \phi$. The search coil is therefore in a magnetic field which has two components at right angles proportional to $I_m \sin \phi$ and $I_m \cos \phi$. In the position of maximum flux linkage the

total flux through the search coil is proportional to $(I_m^2 \sin^2 \phi + I_m^2 \cos^2 \phi)^{\frac{1}{2}}$ and this expression equals I_m . Hence the maximum pick-up of the search coil is independent of ϕ and depends only on the strength of the incident field. The minimum pick-up is at right angles to this position and should theoretically be equal to zero.

As a result of the extra coils and the imperfect coupling between them and the search coil, the pick-up of a Bellini-Tosi system is such that each of the crossed loops must have an area of more than twice that of a single loop antenna in order to have an equal sensitivity. The two loops may be tuned

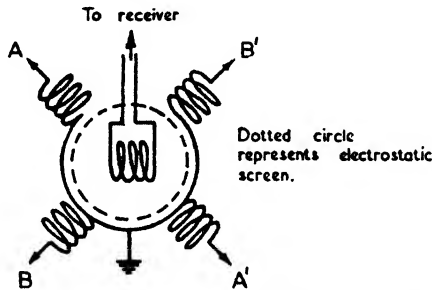


FIG. 7.9. APERIODIC GONIOMETER SYSTEM

separately, but this necessitates careful balancing of the two tuned systems to avoid amplitude and phasing errors which would give blurred minima or false bearings or both. An aperiodic system in which only the search coil is tuned is therefore to be preferred.

Fig. 7.9 shows the goniometer circuit for an aperiodic system. The two mid-points of the fixed coils are joined together and earthed, while the search coil is surrounded by an electrostatic shield (which must not form a complete loop). These two measures considerably reduce the antenna effect in the system.

To obtain a good signal-to-noise ratio, tight coupling must be employed between the search and field coils and this in turn introduces errors due to the non-uniformity of the field in which the search coil is immersed. The error will obviously be zero when the search coil is in the plane of either field coil or at 45° to the field coils. It is therefore zero in eight positions and attains maximum values between these positions; hence this form of coupling error is known as "octantal error." The errors may be reduced to less than $\frac{1}{3}^\circ$ by winding the field coils in a special non-uniform manner; at the same time

the coefficient of coupling can be maintained to a value as high as 75 per cent.

Errors Due to Polarization

When dealing with a wave travelling horizontally (E_1 in Fig. 7.10) a receiving loop rotated about a vertical axis gives the correct bearing even if there be some horizontal polarization present; but should the wave be incident at some angle other than 90° from the vertical, then the presence of a horizontal component will cause false readings. Thus E_2 and E_3 in Fig. 7.10 make no difference to the reading but E_4 does produce a resultant e.m.f. round the loop. These facts can be appreciated either by considering the sum of the induced e.m.f.'s round the sides, or by considering the magnetic flux threading the loop. It is apparent that in the extreme case of E_4 greatly exceeding all the other fields, the plane of the loop would have to be at right angles to E_4 for minimum pick-up, i.e. the bearing obtained on E_1 would be 90° in error.

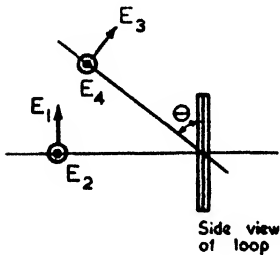


FIG. 7.10. DIAGRAM FOR POLARIZATION ERRORS

In practice, a field such as E_4 can arise from the horizontal component of a sky wave which has suffered reflection and changes in polarization from the ionosphere. This particular form of error was first observed on medium and long waves for which ionospheric reflections are only appreciable at night and hence the phenomenon came to be known as "night effect."

Undesired horizontal polarization of the above nature can also occur when taking bearings of an aeroplane which is using a trailing wire antenna. In this case the abnormality is called "aeroplane effect."

If bearings are taken on an aeroplane, polarization errors due to night effect are less than on the ground, provided the transmission is over a fairly long distance. This is due to the improved signal strength of the ground wave at greater heights.

Standard Wave Error

In order to provide a simple basis for comparing the relative freedom of different D.F. antennae from polarization errors, a standard form of incident wave of mixed polarization has been adopted (it was originally used in a paper by Barfield⁽¹⁸¹¹⁾).

This standard wave has an angle of incidence of 45° while the horizontal and vertical components are of equal intensity, for example in Fig. 7.10 the angle θ would be 45° , E_3 and E_4 would be equal. The relative phases of the two components are such that the *e.m.f.'s induced by them are in phase*. This definition has been chosen simply for convenience. It means that the incident wave must, in general, be elliptically polarized—for the horizontal and vertical components undergo different phase changes on reflection from the surface of the earth. The error resulting from such a standard wave is known as the “standard wave error” and for the case of a simple loop is equal to 35.3° .

The standard wave error is a function of the wavelength and the ground constants, though it so happens that in the case of a simple loop the departure from the value of 35° is relatively small under different conditions—provided the diameter of the loop and its height above the ground are both small in comparison with a wavelength.

7.2. PERFORMANCE OF D.F. LOOPS

The performance of all receiving systems is limited by signal-to-noise considerations. This is particularly true of D.F. loops since they are operated in the region of minimum received signal. A convenient criterion to adopt is to specify the field strength required to equal the noise level when the loop is rotated to $\pm 1^\circ$ from the zero signal angle. Assuming that a signal is just audible when it equals the noise level (or rather that the L.F. modulation of this signal is audible), then this field strength will result in a silence zone of $\pm 1^\circ$. We shall call this figure the “sensitivity” of the system and denote it by the symbol E_s .

If the received wavelengths exceed 10 m the noise due to the first valve may be neglected; in this case the value of E_s depends entirely on the antenna and input circuits (for a given overall bandwidth). Furthermore the thermal noise is due solely to the ohmic resistance of the loop for the radiation resistance is negligible in comparison.

The radiation resistance of a loop whose diameter is small compared with a wavelength is given by

$$R_r = 790 \left(\frac{h_e}{\lambda} \right)^2 \quad (7.5)$$

where h_e = effective height of loop as given by (7.3).

This value is obtained from equation (4.44), Vol. I, on substituting the effective height for the length of the linear radiator carrying a uniform current, since the radiation patterns of the loop and the short linear radiator are identical in shape. With typical loops for long and medium wavelengths the value for R_r is well below one thousandth of an ohm.

Calculation of Signal-to-noise Ratio

The thermal noise voltage in the loop is given by equation (5.6), which shows that the series noise e.m.f. is given by

$$e_n = \sqrt{4kTRB} \text{ volts} \quad . \quad . \quad (7.6)$$

At normal temperatures the value of this thermal e.m.f. becomes

$$e_n = 0.004 \sqrt{BR} \mu\text{V} \quad . \quad . \quad (7.7)$$

This value has to be compared with the induced signal e.m.f. in the loop which can be expressed (by means of equations (7.2) and (7.3)) as

$$e_s = h_e E \sin \phi \text{ volts} \quad . \quad . \quad (7.8)$$

where h_e = effective height of loop

$$= \frac{2\pi}{\lambda} nA$$

In the position of maximum pick-up $\phi = 90^\circ$, so that the signal-to-noise ratio becomes

$$\frac{e_s}{e_n} = \frac{2\pi nA}{\lambda} \sqrt{\frac{Q}{\omega L}} \frac{E}{\sqrt{4kTB}} \quad . \quad . \quad (7.9)$$

It is apparent from the above formula that, for a good signal-to-noise ratio, both Q and nA/\sqrt{L} should be as large as possible. The latter quantity has been discussed by Burgess,⁽³⁷⁵⁾ who introduces the idea of an "electrical volume" which is given by $4\pi n^2 A^2/L$. From such considerations he deduces that the optimum solenoid is one whose ratio of length to diameter is 0.45, and also that two windings connected in parallel can give an improvement (due to the increased number of turns for a given inductance).

It was pointed out in § 5.3 that atmospheric noise predominates over the thermal noise in the antenna circuit on long and medium waves, and this is more or less true even for loops if they are used in the position of maximum pick-up.

But for D.F. purposes we use loops in the region of *minimum* pick-up and under these circumstances the thermal noise in the loop and the coupling circuits is mostly the more important factor. With this in mind we may base our calculations on equation (7.9) after due allowance has been made for the pick-up position of the loop.

What is of particular significance is the sensitivity, E_s , of the system as defined in the beginning of this section. To illustrate the calculation we will take the case of a typical loop.

Example

A loop consists of twelve turns of 60 cm diameter and has a Q of 100. The loop is tuned by a capacitor (whose losses we may neglect) and together they form the input circuit to the first valve. We wish to find the field strength E_s at which the S/N ratio is unity when the loop is 1° off the true bearing. The carrier frequency is 300 kc/s and the receiver bandwidth is ± 2 kc/s.

The effective height of the loop at 300 kc/s is given by

$$h_e = \frac{2\pi \times 12 \times 0.263}{1\ 000} \text{ m} = 2.0 \text{ cm}$$

The noise e.m.f. is given by (7.7) on inserting 4 kc/s for B and 4.24 ohms (equals $\omega L/Q$) for R . Hence

$$\begin{aligned} e_n &= 0.004 \sqrt{4 \times 4.24} \\ &= 0.0165 \mu\text{V} \end{aligned}$$

This must equal the induced signal e.m.f. as given by equation (7.8), therefore

$$h_e E \sin \phi = 0.0165$$

Putting $\phi = 1^\circ$ and writing E_s for E , we have

$$\begin{aligned} E_s &= 0.0165 \times 57 \times 50 \\ &= \underline{\underline{47 \mu\text{V/m}}} \quad (f = 300 \text{ kc/s}) \end{aligned}$$

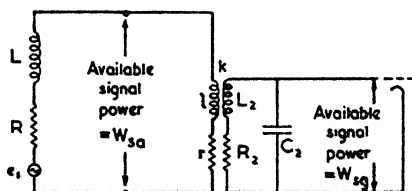
In general, any value below $50 \mu\text{V/m}$ is satisfactory. At higher carrier frequencies the value of E_s will decrease since $e_n \propto \sqrt{f}$ and $e_s \propto f$ while the Q of the frame is roughly constant. If Q is constant then $E_s \propto 1/\sqrt{f}$, e.g. at twice the frequency we have

$$E_s = \underline{\underline{33.1 \mu\text{V/m}}} \quad (f = 600 \text{ kc/s})$$

It should be noticed that for the above simple case the S/N ratio is determined directly by the series e.m.f.'s since both e_s and e_n are multiplied by Q . The value of Q only enters into the calculation of the series resistance R .

Effect of Goniometer on Signal-to-noise Ratio

When a goniometer is introduced between the pick-up loops and the grid of the first valve the signal-to-noise ratio is bound



$$\begin{aligned} Z_1 &= \text{total primary impedance} \\ &= R_1 + j\omega L_1 \\ &= (R+r) + j\omega(L+l) \end{aligned}$$

$$q = \frac{\omega l}{r}$$

$$Q_2 = \frac{\omega L_2}{R_2}$$

FIG. 7.11. EQUIVALENT CIRCUIT OF CROSSED LOOPS AND GONIOMETER FOR SIGNAL-TO-NOISE CALCULATIONS

to deteriorate. This deterioration may be measured in terms of "noise figures" as defined on p. 210. If the available signal power at the antenna terminals is W_{sa} and that at the grid terminals is W_{sg} , then the noise figure of the coupling network is given by

$$N = W_{sa}/W_{sg} \quad (7.10)$$

The available noise power is unchanged by the addition of the network. This follows from equation (5.7) when taken in conjunction with Thevenin's theorem. Indeed for all passive networks whose resistive elements are at the same ambient temperature, the above simplified form of equation (5.11) applies.

In dealing with a goniometer we have *two* crossed loops as the source of signal, but since both the induced e.m.f.'s in the loops and the induced e.m.f.'s in the field-coils of the goniometer follow a sine law for one loop (or field-coil) and a cosine law for the other loop (or field-coil), the equivalent circuit may be greatly simplified. This simplification is effected by considering the crossed loops as a single loop and the

field-coils as a single coil whose coupling with the search coil is constant. The equivalent circuit therefore becomes as shown in Fig. 7.11.

Referring to this figure we have

$$N = \frac{W_{sa}}{W_{sp}} = \frac{R_1 + \left| \frac{Z_1}{\omega M} \right|^2 R_2}{e_s^2} \cdot \frac{e_s^2}{R}$$

$$= 1 + r/R + \left| \frac{Z_1}{\omega M} \right|^2 R_2/R$$

On making the following substitutions

$$k = \frac{M}{\sqrt{(L_2 l)}}, \quad q = \frac{\omega l}{r}, \quad Q_2 = \frac{\omega L_2}{R_2}$$

we obtain

$$N = 1 + \frac{|\mathcal{Z}|^2}{k^2 \omega l Q_2 R} + \frac{\omega l}{R} \left(\frac{1}{q} + \frac{1}{k^2 Q_2} + \frac{1}{k^2 Q_2 q^2} \right)$$

$$+ \frac{2}{k^2 Q_2} \left(\frac{X}{R} + \frac{l}{q} \right) \quad \dots \quad (7.11)$$

Examination of the above expression shows that k , q and Q_2 should all be as large as possible for the best results. These conclusions are quite consistent with simple physical arguments, as is also the fact that N is independent of C_2 .

An interesting deduction from (7.11) is that for given values of k , q and Q_2 there exists an optimum value of ωl which is given by

$$\omega l_{\text{opt}} = |\mathcal{Z}| \left[1 + \frac{1}{q^2} + \frac{k^2 Q_2}{q} \right]^{-1} \quad \dots \quad (7.12)$$

The term $1/q^2$ may be neglected in the above expression, and since $\omega l \gg R$ we have

$$l_{\text{opt}} = \frac{L}{\sqrt{(1 + k^2 Q_2/q)}} \quad \dots \quad (7.13)$$

The expression for l_{opt} is therefore independent of frequency.

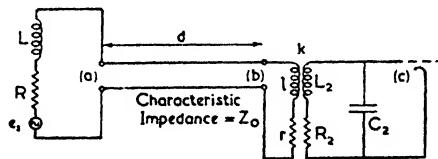
In practice Q_2 is likely to be about four times greater than q (due to the shape of a goniometer the magnification values of the coils are essentially low). As for k^2 , a likely value is 0.7. Hence the value of l_{opt} will generally prove to be equal to about $L/2$.

The direct application of the above results is limited to cases in which there are no transmission lines between the loops

and the goniometer. In the majority of cases, however, transmission lines are used so that the problem is more complicated. We will consider first of all the insertion of a line whose attenuation constant is zero.

Insertion of Lossless Line

If a transmission line is added as shown in Fig. 7.12 the impedance of the loop will be transformed from Z to Z' . The transformation is given by equation (7.15), or, alternatively,



N' = noise figure between terminals (a) and (b)
 N'' = " " " " (b) and (c)

FIG. 7.12. EQUIVALENT CIRCUIT OF CROSSED LOOPS AND GONIOMETER WITH TRANSMISSION LINE INSERTED

a circle diagram of impedance as described on p. 457 may be used.

As a result of this transformation the loop may be found to resonate within the band of operation. For instance, if 30 m of line were used, the loop specified in the previous example (p. 327) would have to be reduced from twelve turns to six turns to keep the resonant frequency above 600 kc/s. On the other hand, too few turns would result in a serious decrease in the overall signal-to-noise ratio.

It will be found that with some combinations of loop and line the presence of the line actually improves the signal-to-noise ratio at the grid. This is due to the transformer action of the transmission line which, in the present instance, has been assumed to be lossless.

Insertion of Line with Losses

The general observations made in the previous paragraphs with respect to a perfect line still apply when the line losses are taken into account. The impedance transformation will differ only slightly, but the line losses will result in a noise figure which may be calculated according to equation (7.10).

Using the same notation for the line constants as employed in Chapter X, we have the following relationships (Fig. 7.12)—

$$\frac{e}{e'} = \cosh Pd + \frac{Z}{Z_0} \sinh Pd \quad (7.14)$$

where e' = voltage at goniometer end of line,

$$Z' = R' + jX' = Z_0 \frac{Z \cosh Pd + Z_0 \sinh Pd}{Z_0 \cosh Pd + Z \sinh Pd} \quad (7.15)$$

where Z' = impedance looking left from goniometer.

It is only the resistive component of Z' which determines the available signal power, and if the imaginary part of Z_0 does not exceed ± 2 per cent of the real part the value of this component is given by

$$R' = R \left| \frac{e'}{e} \right|^2 \left[\cosh 2\alpha d + \frac{\sinh 2\alpha d}{2R} \left(Z_0 + \frac{|Z|^2}{Z_0} \right) \right]$$

The noise figure of the transmission line is therefore given by

$$N' = \left(\frac{e}{e'} \right)^2 \left(\frac{R'}{R} \right) = \cosh 2\alpha d + \frac{|Z| \sinh 2\alpha d}{2R} \left(\frac{Z_0}{|Z|} + \frac{|Z|}{Z_0} \right) \quad (7.16)$$

If $\alpha = 0$ then the above equation gives $N = 1$ which is, of course, correct on physical grounds. When αd is small, i.e. less great than 0.1, there is no need to use hyperbolic tables since we then have

$$\begin{aligned} \cosh 2\alpha d &\doteq 1 \\ \sinh 2\alpha d &\doteq 2\alpha d \end{aligned}$$

However, in calculating Z' which replaces Z in equations (7.11) and (7.12), the exact transmission-line formula as given in equation (7.15) must be used.

If $|Z| \doteq Z_0$, in addition to αd being less great than 0.1, equation (7.16) reduces to

$$N' = (1 + \alpha d Q) \quad (7.17)$$

The interpretation of the above expression is interesting, for it shows that a large Q -value is detrimental to a low N -value. On the other hand a low Q -value is detrimental to a good signal-to-noise ratio at the antenna terminals! There is no way out of the impasse—the only compensation is that the signal-to-noise ratio at the goniometer end of the line is very insensitive to variations in the Q -values of the loop.

In the following example the above approximate formula has not been used, though it could have been employed without introducing appreciable error.

Example

Each of the crossed loops has the following characteristics (they will be considered as if they were one loop for the reasons given on p. 328—hence Fig. 7.12 applies for this example).

Radius	$a = 30 \text{ cm}$
Number of turns	$n = 6$
Inductance	$L = 56.2 \mu\text{H}$
Magnification	$Q = 100$

The loop is followed by 30 m of twin coaxial line whose characteristics are—

Characteristic impedance	$Z_0 = 140 \text{ ohms}$
Attenuation constant	$\alpha = 0.012 \text{ db/m at } 1 \text{ Mc/s}$ (over moderate ranges of frequency α varies as \sqrt{f})

The characteristics of the goniometer are as follows—

Stator coils	$q = 30$
Rotor coil	$Q_2 = 30$
Stator inductance	$l = 70 \mu\text{H}$

From the value of α given above we can deduce that $\alpha = 0.00107$ nepers per metre at 600 kc/s. Therefore at a frequency of 600 kc/s, equation (7.16) gives

$$N' = \cosh 0.0644 + 50 \sinh 0.0644 \left(\frac{140}{112} + \frac{112}{140} \right) = 8.0$$

From equation (7.15) we have

$$Z' = 108.5 + j658 \text{ ohms}$$

(the corresponding lossless line formula would have given a value of R' which was 7 times too small)

On substituting Z' for Z in equation (7.11) we find that the noise figure for the second stage is

$$N'' = 2.5$$

The overall noise figure is given by equation (5.15) which in this case reduces to $N = N'N''$ since $N_1 = 1/G_1 = N'$. We therefore have

$$N = 20$$

The value of the initial signal-to-noise ratio is the same as that obtained in the previous example on p. 327, in spite of a change in the number of turns. This is because we have assumed the same Q and area of cross-section whereupon h_s and \sqrt{R} both vary directly with n . Therefore

$$\begin{aligned} E_s &= 33.1 \times \sqrt{20} \\ &= \underline{\underline{148 \mu\text{V/m}}} \quad (f = 600 \text{ kc/s}) \end{aligned}$$

The table below affords a direct comparison of the sensitivity figure E_s for different circuits (all refer to the loop, line and goniometer stipulated in the above example unless otherwise stated).

Type of Circuit	Sensitivity E_s in $\mu\text{V/m}$	
	300 kc/s	600 kc/s
(a) Loop directly on grid of first valve	47	33
(b) With goniometer and 30 m of <i>lossless</i> line	249	114
(c) As for (b) but allowing for line losses	274	148
(d) With goniometer but no line	268	160
(e) As for (b) but q and Q_s doubled	179	84
(f) As for (e) but Q also doubled	176	82

The conclusions to be drawn from the above figures are—

1. The introduction of a goniometer of typical Q -values increases the value of E_s appreciably—in the above case by as much as five times. Even if the goniometer has exceptionally high Q -values, E_s is increased by a factor of about 3. (The relatively poor magnification factors of goniometer coils are partly due to the need of spacing the windings to compensate for octantal error.)

2. The insertion of a transmission line makes relatively little difference to the sensitivity figure even when the attenuation of the line is taken into account. Indeed the transforming action of the line may cause some lowering of the value of E_s .

3. Once a goniometer has been introduced there is little to be gained by striving for higher magnification factors in the loop coils themselves.

4. If a goniometer is added, the only way of restoring the original signal-to-noise performance of the receiver is to increase the diameter of the loop. If we assume a loop whose radius

is large compared with the width across the windings, then for a given value of inductance an^2 is constant. By further assuming that Q is constant, we find the signal-to-noise voltage ratio at the antenna terminals varies as $(a)^{3/2}$. This indicates that the signal-to-noise ratio varies at least in proportion to the diameter of the loop but not by as much as the area of the loop.

7.3. ADCOCK ANTENNAE

General Principles

Polarization errors could be avoided if we omitted the horizontal members of the loop and used only two spaced vertical

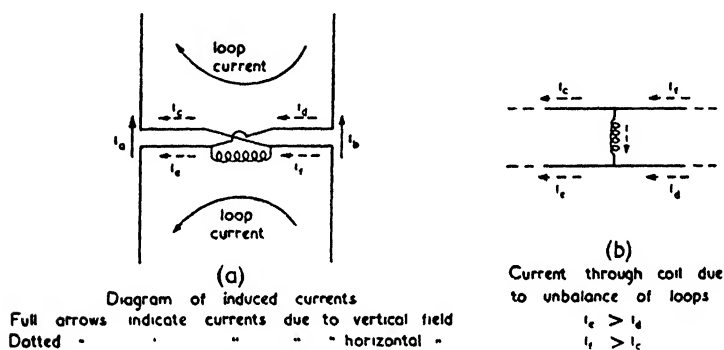


FIG. 7.13. THE PRINCIPLE OF THE ADCOCK ANTENNA

antennae. Systems based on this principle are known as Adcock antennae, after the name of their inventor.

The signals in the two vertical members must be brought together in some way without introducing pick-up from horizontal electric fields; this requirement may be fulfilled to a large extent by using parallel or coaxial transmission lines. A basic form of Adcock antenna system is shown in Fig. 7.13 (a), together with arrows indicating its response to vertical and horizontal fields.

In the case of the vertically polarized field the currents i_a and i_b obviously flow in opposition through the coil so that the output is a measure of the difference signal and thereby resembles the case of a loop antenna. With a horizontal electric field the currents are such that

$$i_c + i_e = i_f + i_d$$

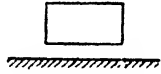
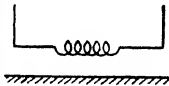
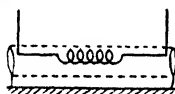
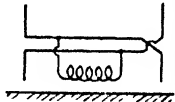
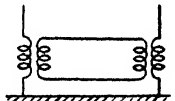
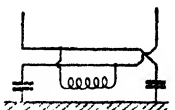
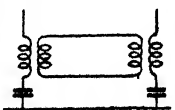
provided the spacing between the two conductors of the transmission line is small enough in comparison with a wavelength for the phase differences in the induced currents in the two sides to be negligible. If the system is completely balanced (as would be the case if it were far removed from neighbouring objects or the ground), then $i_c = i_e$, and there can be no output due to the horizontal pick-up. If, however, the system is unbalanced so that $i_e > i_a$, then $i_f > i_c$ and we have a resultant current through the transformer as shown by the dotted arrow in Fig. 7.13 (b). This is equivalent to saying that the "loop" current in the lower half of the system is greater than that in the upper half. Such a situation arises in the presence of the ground when the capacitance to ground of the lower elements permits an increase in the circulating current in that portion of the system.

From the above considerations it is apparent that an "H" type of Adcock system should be balanced as far as possible, and that loop currents should be kept as low as possible. For ultra-short-wave reception elevated half-wave dipoles are quite easily erected, but for medium- and long-wave reception it is more convenient to use the upper half of the configuration shown in Fig. 7.13 (a) and to mount this just above the ground as shown in the table on p. 336—the antenna is then referred to as a "U"-type Adcock antenna.

If the earth were a perfect conductor the "U"-type would have no polarization error at all apart from a very small amount due to the finite height of the horizontal link above the ground. In practice the finite ground conductivity causes this type to have standard wave errors ranging from 10° to 30° over soil and from 1° to 7° over sea water (for wavelengths between 10 and 10 000 m). The smallest errors occur for wavelengths of the order of 100 m and the greatest at the extremes of the aforementioned range.

Comparison of Different Types

Various modifications of the simple "U"-type Adcock antenna have been devised with the object of reducing the standard wave error still further. These are shown diagrammatically in the second column of the table on p. 336. The experimental results given in this table were obtained by Barfield⁽¹⁸¹⁾, who carried out an extensive investigation into the relative merits of the different systems.

Type	Diagram	Height of Horizontal Members in Metres	Standard Wave Error in Degrees	Pick-up Factor in Metres
Loop		$\ll \lambda$	35	10 to 20
"U"		0.5	12	100 to 200
Screened "U"		0.5	6	100 to 200
Elevated or "H" type		15	2	100 to 200
Coupled		0.5	1	50 to 100
Balanced		2.0	6	100 to 200
Balanced Coupled		2.0	< 1	50 to 100

(Experimental comparison of loop and Adcock systems for $\lambda = 300$ m, $g = 0.017$ (after Barfield, ref. (181)). The loop is 1 metre square and all the other systems are 24 m high. For further information see text.)

Neither the loop antenna nor the elevated-type Adcock show appreciable changes in the standard wave error for different soil conductivities. The screened U-type must have the screen earthed at both ends—if the screen is left unearthed no improvement at all is obtained.

The pick-up factors quoted are defined on p. 318, and for a simple loop the factor is given by equation (7.4). For a given frame area this factor will not vary much when designed for different wavelengths, since the Q of the frame will be roughly the same at different wavelengths while the number of turns tends to be proportional to λ .

The pick-up factors for the Adcock antennae represent favourable cases, particularly since the factor is a maximum in the region of 300 m with normal practical heights and spacings. The antennae themselves are untuned and the voltage is measured across a tuned secondary. For a given antenna the pick-up factor will vary as the cube of the frequency (or the fourth power in the case of a coupled system) whereas with a loop antenna the variation is only with the first power. To counteract these variations with frequency in an Adcock system, coil changes should be made at fairly frequent intervals.

A variation of the screened U-type is the buried U-type Adcock antenna in which the horizontal members are buried a metre or so below the ground. Such a system can give a better performance than the screened type, but owing to the penetration of radio waves into the earth the shielding is by no means perfect (a wire screen on the surface of the ground may be used to improve the shielding).

The coupled type owes its good performance to the fact that the impedance presented to loop currents is high. To keep this as high as possible the capacitance between the windings of the transformer is made small or else an electrostatic shield may be used. Still further improvement may be obtained by also balancing the system with capacitors as shown in the last diagram of the table on p. 336. A balanced circuit of this nature is only strictly correct for one frequency, but satisfactory balancing is obtained over a frequency range of 4 : 1.

Spaced-loop Antennae

A spaced-loop antenna system as shown in Fig. 7.14 will have the same virtues as an Adcock system when taking bearings

along a line AA' or vice versa. In these directions the phase-opposite connection of the two loops will cause a zero in the

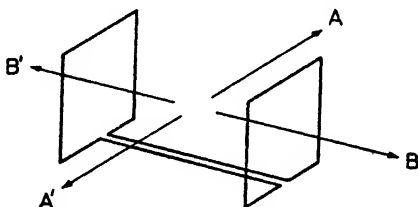


FIG. 7.14. THE SPACED-LOOP ANTENNA

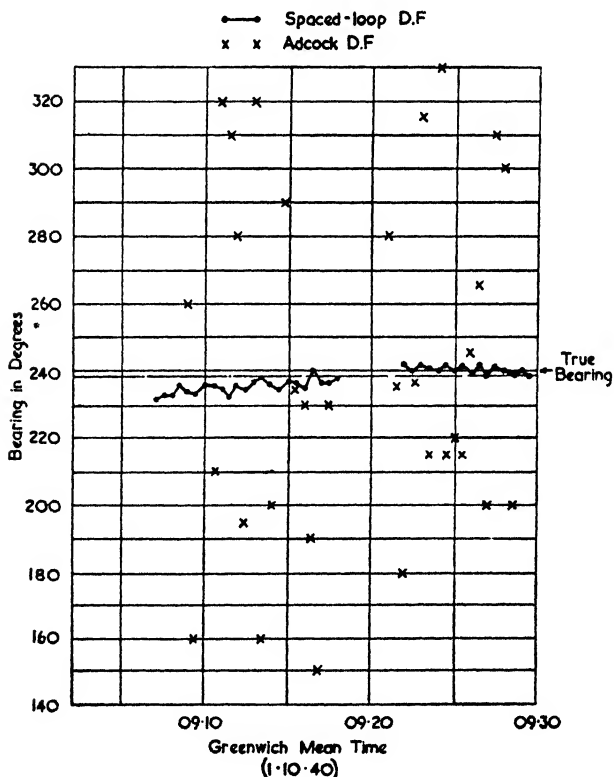


FIG. 7.15. SIMULTANEOUS BEARING OBSERVATIONS ON A SPACED-LOOP AND AN ADCOCK DIRECTION-FINDER
(Ross, *Jour. I.E.E.*, Mar., 1947)

polar pattern despite the fact that each loop in itself has a maximum pick-up. At the same time the loops are obviously

insensitive to horizontal polarization. The polar diagram also has two zeros in the directions BB' and $B'B$, but for both these cases there is no protection against horizontal polarization.

This system has the advantage that—unlike simple vertical antennae—the spaced elements have a pick-up which does not vary with the angle of incidence of the oncoming waves.

As a result the polarization error does not increase rapidly with decreasing angles of incidence as is the case with an Adcock antenna. The spaced-loop system is therefore particularly useful when bearings are being taken of sky waves which have originated from transmitters less than 500 km away.

This type of direction-finder has been discussed recently by Ross,⁽¹⁹⁶⁾ who gives the results shown in Fig. 7.15.

Antennae for Ships, Aircraft and Automobiles

ALTHOUGH the principles of design remain fundamentally the same, various special considerations come into play when an antenna is mounted on a moving structure such as a ship, an aircraft or an automobile. The problems involved are often made more difficult by the fact that very little concession can be made to the requirements of the radio engineer. In this chapter we shall therefore consider some of the particular problems which arise when antennae are used under the above conditions.

8.1. D.F. LOOPS FOR SHIPS

Influence of Ship's Structure on D.F. Bearings

Even in the most favourable positions aboard a ship, the D.F. antenna will be affected by the presence of induced currents in the rigging, masts, hand-rails and other metallic parts of the ship's structure. These currents cause secondary fields whose effect on the D.F. antenna varies with the heading of the ship. As a result the D.F. bearings obtained are inaccurate unless steps are taken to mitigate the effect of these secondary fields.

The measures that may be taken to reduce the errors consist in breaking up the offending wires by means of insulators, bonding the structure to the hull of the ship, or the erection of some compensating loop. Even when such measures have been taken, there often remains a residual error and this may be further decreased by the provision of a cam to the indicator mechanism or by the use of calibration charts. Whatever measures may be adopted they should be tried under conditions which represent as far as possible the normal sea-going state of the ship, i.e. rigging, cranes and other movable structures should be in their sea-going positions.

The interfering secondary fields may be divided into two groups according to whether they are mainly in phase quadrature or mainly in phase with the primary field. When the structure responsible for the secondary field is distinctly off tune, it will give a phase quadrature field if it is a vertical radiator but an in-phase field if it is some form of loop. The

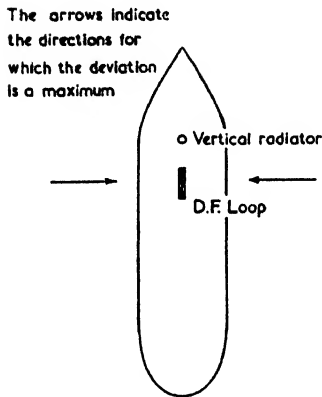


FIG. 8.1. SEMICIRCULAR ERROR DUE TO RERADIATION FROM A VERTICAL WIRE OR MAST

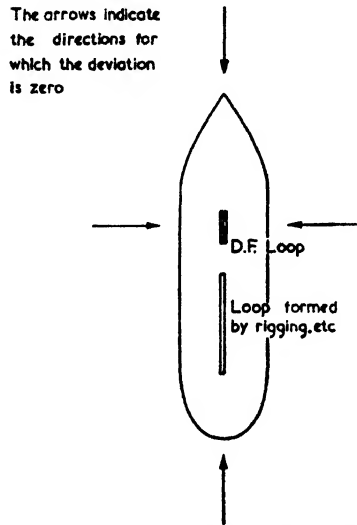


FIG. 8.2. QUADRANTAL ERROR DUE TO RERADIATION FROM A LOOP STRUCTURE

former type of field leads to broad minima which can be compensated for by the balancing control (the setting of the control will, however, vary with the bearing) whereas an in-phase field causes deviation errors. The situation may be summarized by the table shown on the next page and by Figs. 8.1 and 8.2.

Since the errors due to a loop repeat every quadrant the loop gives rise to what is known as "quadrantal error." An important point with regard to quadrantal error is that the signs of the errors in each quadrant are reversed if the tuning of the loop is made to fall on the opposite side of f . Thus the errors due to an open loop tuned to a frequency above f (the mast-hull structure forms a notable example of such a loop) may be compensated for by the deliberate provision of a closed loop tuned below f . (In the foregoing remarks it is assumed

that the loops in question are in the same plane, since turning a loop at right angles will, in itself, alter the signs of the errors.) Fig. 8.3 shows a compensating loop circuit.

The provision of compensating loops is discussed by Solt⁽²¹⁹⁾ who, among his examples, gives the curves shown in Fig. 8.4, which indicate the very useful degree of compensation obtained in this way. In practice the addition of a compensating loop

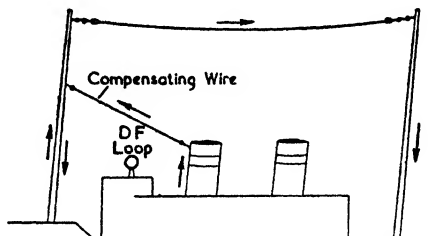


FIG. 8.3. COMPENSATING LOOP TO COUNTERACT MAST-HULL CIRCULATING CURRENTS

must be made with some care, since any resonance within the band of operating frequencies would completely spoil the compensation.

Secondary Field	Source of Secondary Radiation	Natural Frequency of Secondary Radiator	Errors Repeat every	Type of Error
In phase quadrature	Vertical conductor Open loop	Above f Below f At f	Semicircle Quadrant	Indistinct minima (correct by balancer control)
In phase	Vertical conductor Open loop Closed loop	At f Above f Below f Below f	Semicircle Quadrant	Bearings deviated from true position

(Frequency of incident wave = $f c/s$)

The effects of vertical conductors and loops are not quite so simple as the above table might lead one to believe. For one thing, the phasing will be modified by the distance between the secondary source and the D.F. loop; also the effect of such phasing will vary with frequency. Another point is that the loop circuits will also exhibit some antenna effect.

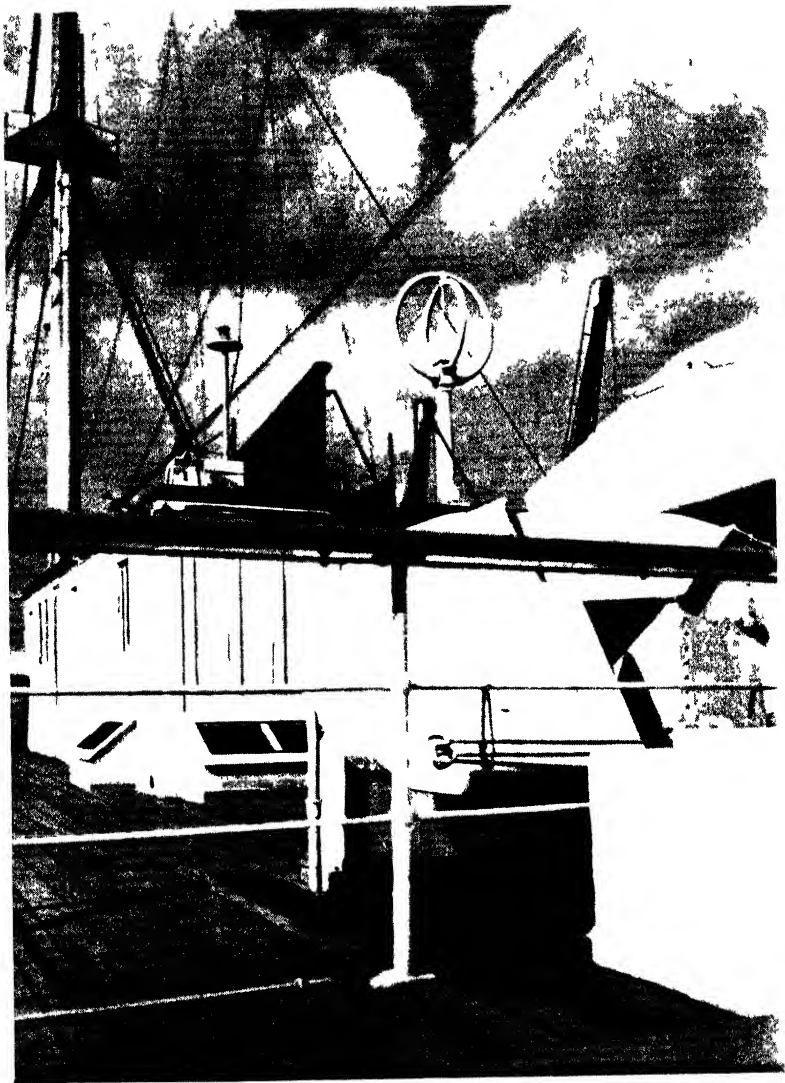


PLATE XIII. THE CROSSED-LOOP D F. ANTENNA ON S S. "ORION"
(*Courtesy of Marconi International Marine Comm Co, Ltd*)

Indeed, in the directions of the greatest quadrantal error the minima may suffer appreciably owing to an in-phase field component. This obscuring of the minima in the regions of maximum deviation is also cured to a large extent by the provision of a suitably designed compensating loop.

Whenever the D.F. loops are small enough to be screened this should be done, since screening has the advantage of

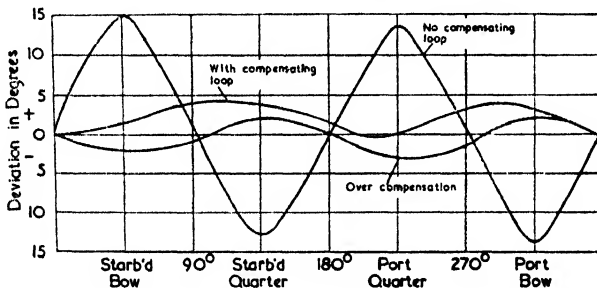


FIG. 8.4. REDUCTION OF QUADRANTAL ERROR BY MEANS OF A COMPENSATING LOOP
(Solt, *Proc. I.R.E.*, Feb., 1932)

reducing antenna effect and precipitation static as well as of providing a weatherproof housing. An example of a pair of screened crossed loops is shown in Plate XIII; they are essentially a small form of Bellini-Tosi loops, though one usually associates the name with large unscreened loops.

Bellini-Tosi Loops

All the early direction finding on ships was done by crossed loops of considerable size (on large ships each loop might have an area of some 50 m²). Such loops are known as Bellini-Tosi loops and have the advantages of a better pick-up factor and greater freedom from quadrature effect.

The essential features of such loops are that they should have equal areas, be at right angles to each other, and that each loop should be symmetrical about a vertical axis. The loops need not have similar shapes, neither do they need to have the same central vertical axis. It is obvious therefore that a great variety of loop arrangements could be devised—for a selection of such arrangements the reader may refer to the book by Keen⁽¹¹⁾ who deals at some length with Bellini-Tosi loops.

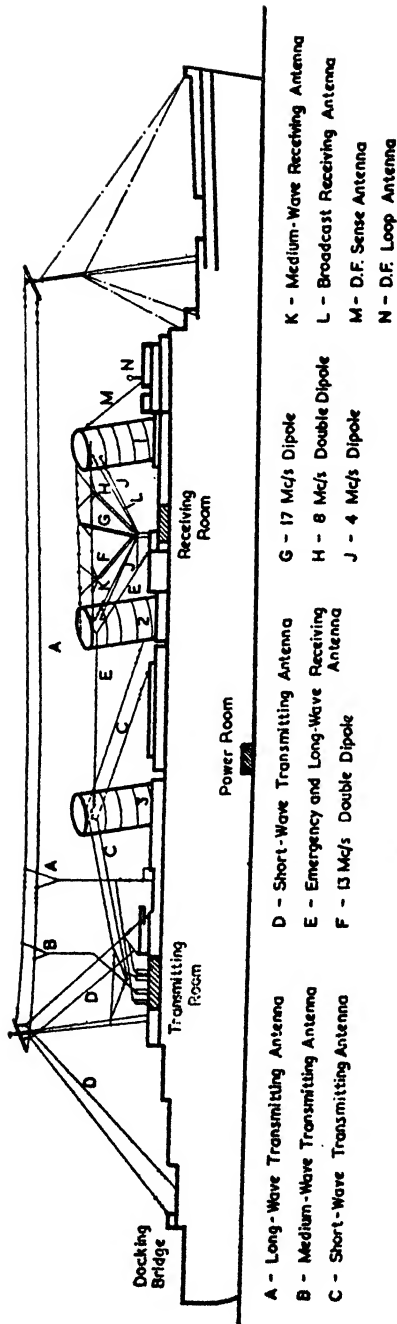


FIG. 8.5. LAYOUT OF ANTENNAE ON R.M.S. "QUEEN MARY"
 (Loring, McPherson and McAllister, *Jour. I.E.E.*, Sept., 1937)

- | | | |
|--------------------------------------|---|-----------------------------------|
| A - Long-Wave Transmitting Antenna | D - Short-Wave Transmitting Antenna | K - Medium-Wave Receiving Antenna |
| B - Medium-Wave Transmitting Antenna | E - Emergency and Long-Wave Receiving Antenna | L - Broadcast Receiving Antenna |
| C - Short-Wave Transmitting Antenna | F - 13 Mc/s Double Dipole | M - D.F. Sense Antenna |
| | G - 17 Mc/s Dipole | N - D.F. Loop Antenna |
| | H - 8 Mc/s Double Dipole | |
| | J - 4 Mc/s Dipole | |

Whatever site is selected on the ship, the stray capacitances should be both as small and as symmetrical as possible; also it should not be necessary to move the loops when taking on cargo. A rotating loop (or a pair of small crossed loops as shown in Plate XIII) is therefore an obviously much more convenient structure, particularly on board relatively small ships. Provided the quadrantal error of a small loop can be compensated for and the signal-to-noise ratio be kept low enough, there is nothing to be gained by the use of large unscreened loops. Consequently large loops are rarely used nowadays.

8.2. COMMUNICATION ANTENNAE ON SHIPS

The provision of suitable antennae for communication purposes on board a ship raises more difficulties than on a land station. On the whole it is the receiving antennae which are the most difficult to design and locate; this is because they will have currents induced in them both by the transmitting antennae and by the electrical machinery on board. In particular, when sailing in tropical regions the large number of fans operating can raise the noise level to a serious extent.

On large ships the problem of separating the transmitting and receiving antennae is fairly simple. Fig. 8.5 shows the layout of the antennae on the *Queen Mary*. As usual, the long- and medium-wave transmitting antennae are of the T or inverted-L types and their top portions are suspended between the two masts. For short-wave transmission inverted-V antennae are mainly used, the top of the aft funnel forming one point of support. The short-wave receiving antennae are horizontal dipoles suspended between the first two funnels, while those for long and medium waves are sloping wires between the same two funnels.

In spite of the advantages of inverted-V transmitting antennae—they are so obviously suited to mounting on a ship—they have since been superseded on the *Queen Mary* by horizontal dipoles. The reason for this is that the inverted V's were found to be too directional. In addition it has been found that horizontal antennae are less subject to losses and distortions to the polar diagram, since the induced currents in the neighbouring metallic structures are not so great. On a small ship it is often necessary to use the same antenna for both transmission and reception. A further simplification

consists of making the antenna in the form of an all-wave antenna, the top portion acting as a top capacitor on long and medium waves but as a double-wire dipole feeding to a transmission line on short waves.

8.3. AIRCRAFT ANTENNAE FOR D.F. AND LANDING SYSTEMS

The design of D.F. loops for aircraft has followed the same course as in the case of ships, i.e. the use of large loops has been superseded by small screened loops. With aircraft, however, the trend has been even more definite since the modern all-metal plane precludes the use of large loop structures.

In the days of wood and fabric biplanes, the wires for a loop antenna could be run along the top wing, down an end strut and back again via the lower wing and a strut at the farther end. If the aircraft were heading towards the transmitter, the loop would be in a position of minimum pick-up; thus it was necessary to slew the plane from side to side occasionally to verify that the heading was correct. The method was improved upon by providing a small auxiliary coil whose plane was in the line of flight; hence when heading towards the transmitter this coil was at maximum pick-up. On adding the signals from the larger main loops, first in one sense and then in the opposite sense, an overlapping pattern of reception was produced which made it unnecessary to slew the plane. The smaller loop acted virtually as a sense-determining loop and was usually termed the "main" loop, i.e. the normal terminology with regard to "main" and "auxiliary" was the reverse of that given above.

The slow speed of early aircraft also made it possible to mount Bellini-Tosi loops on top of them. On biplanes the crossed loops were mounted between the wings, while on monoplanes one loop was fixed in the plane of the fuselage and the other along the wing—the central support for both loops being a short mast.

Present-day practice is to mount a screened rotatable loop either above or below the fuselage. The former position is convenient for small aircraft of the private type, while the latter is more suitable for commercial airliners. Plate XIV shows a typical D.F. loop mounted below the fuselage. An extra advantage of the rotatable screened loop is that it may be used for ordinary reception purposes when precipitation

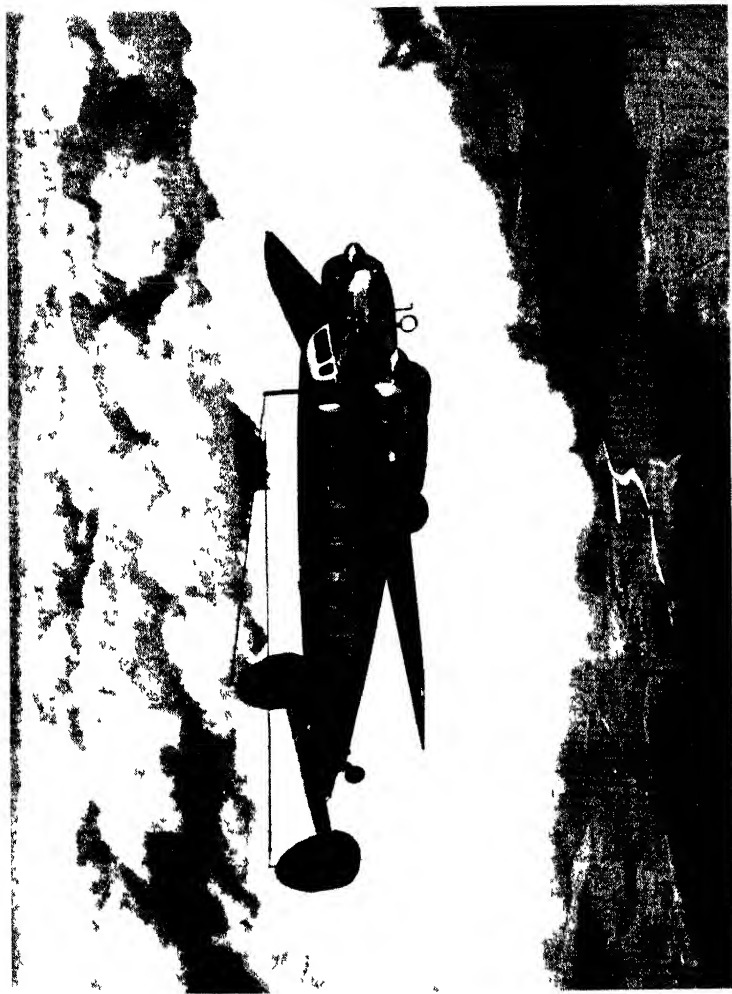


PLATE XIV A LOCKHEED "ELECTRA" SHOWING THE MOUNTING OF THE
D.F. LOOP AND THE V-TYPE COMMUNICATION ANTENNA

Courtesy of British Airways, Ltd.

static is marring the reception on other antennae. Indeed this ability to be able to use the loop for normal reception is a regulation requirement in some countries.

One trouble that may beset a rotating loop is that heavy ice formation can freeze it to the fuselage. For this reason loops have been mounted in the nose of some commercial aircraft (the nose being non-metallic), in which position all aerodynamical drag is also eliminated. Unfortunately such nose installations are subject to large deviation errors. Another method that has been used to combat ice formation and drag is to make the whole loop retractable. An example of a retractable loop is given in the book by Keen⁽¹¹⁾ in which is shown a picture of such a loop of 13 in. diameter as fitted to an Imperial Airways flying-boat. Yet a further method is to fit the loop in a bulge in the perspex dome over the cockpit. This arrangement is employed in the De Havilland "Dove," of which a sketch is shown later, in Fig. 8.10.

As in the case of ship installations, the D.F. loops on aircraft are subject to deviation errors. If the loop is mounted below the fuselage a calibration on the ground is useless, but if it is mounted on top of the fuselage a ground calibration will give useful—though not necessarily quite accurate—indication of the deviation errors.

Homing Systems and Automatic Direction Finders

The method described in the previous paragraphs of obtaining a right-left indication from a transmitter received a number of extensions which resulted in "homing devices" in which the indication was given in the form of a pointer (such a system has also been called a "radio compass"). In order to take bearings of transmitters at *any* angle with respect to the aircraft it becomes necessary to rotate the loop in some manner; the system is then known as an "automatic direction finder."

The required polar patterns for a homing device are obtained by forming two cardioid polar diagrams as shown in Fig. 8.6. Each of these is obtained by the usual device of adding an in-phase signal from a vertical antenna to the loop signal. By either mechanical or electrical commutation the phase of one of the component signals is changed by 180° at regular intervals, thereby producing the complementary pattern. Such a homing device is particularly suited to small aircraft, in which case the loop projects above the pilot's cabin. When

used for homing, the loop is fixed with its plane at right angles to the direction of flight.

The disadvantage of a homing device is that, in the presence

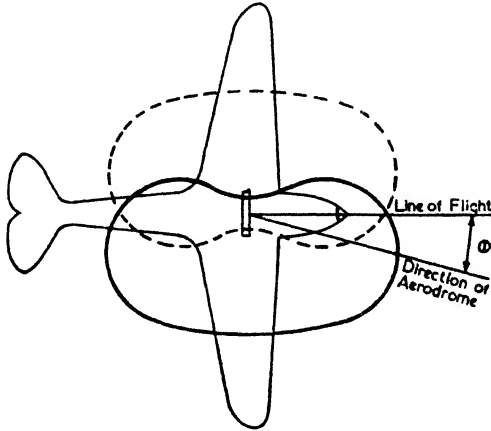


FIG. 8.6. PRINCIPLE OF KEYED PATTERN HOMING

of a cross wind, the aircraft will follow a curved course over the ground as shown in Fig. 8.7. With care the additional use of a magnetic compass can minimize this drifting off the

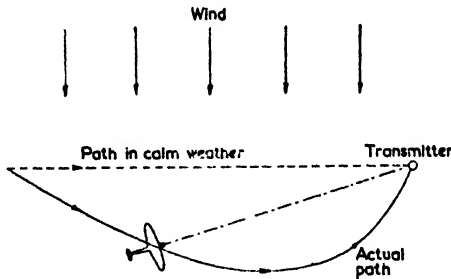


FIG. 8.7. PATH FOLLOWED BY HOMING AIRCRAFT IN PRESENCE OF A SIDE WIND

straightest course, but this detracts from the simplicity of the original idea.

The functions of the radio compass have been extended in an interesting manner by Busignies to provide an automatic direction finder. The system works on the principle of rotating the loop at, say, 300 r.p.m. This causes the signal strength of the station to which the receiver is tuned to vary cyclically

with the loop rotations—the maximum pick-up occurring when the loop is in line with the station and the minimum when it is at right angles. The rectified output therefore varies cyclically, so that by comparing the phase of the output with the phase of the a.c. generator used for rotating the loop we obtain a direct measure of the bearing with respect to the aircraft. A discussion of the phase comparison and of the method of resolving the 180° ambiguity is beyond the scope of this book—the reader will find them described in an article by Busignies⁽²⁰⁸⁾.

An automatic direction finder used extensively in America is one in which the loop is driven by a motor which causes the loop (and therefore the keyed cardioid patterns) to rotate until the equi-signal direction is found. This position is registered by a pointer geared to the motor.

Radio Altimeter Antennae

The principles of the radio altimeter have been discussed in a number of articles in recent literature, in particular a description will be found in the book by Sandretto.⁽¹⁹⁾ From the antenna point of view, the main requirement is a wide bandwidth—a typical frequency excursion for the transmitter is ± 25 Mc/s with a mean of 500 Mc/s. Thus the required bandwidth exceeds that obtainable by ordinary thick antennae.

In order to meet the requirements a tuning stub must be used and this may be calculated in the manner described in § 10.7. The tuning stub was incorporated in the antenna in a very neat manner by the Western Electric Co., who used the circuit shown in Fig. 8.8. To reduce the effect of icing, a perspex casing was fitted over the radiating portion. An alternative form can be made by filling a tuning stub of appropriate length with polythene and surrounding the feed point with the same material; this gives a weatherproof construction of small dimensions.

The polar diagram of an altimeter antenna of the type shown in Fig. 8.8 is almost ideal since all the energy is directed downwards, yet the beam it produces is not too narrow (a narrow beam would cause the signal to be lost if the plane banked sharply). The transmitting and receiving antennae are usually identical; they are either mounted one on each wing, or separated by about 2 m under the belly of the aircraft. The exact spacing depends on the degree of coupling required

between them. In cases where direct injection is employed, this coupling is made as weak as possible.

An obvious improvement on the above type of antenna would be obtained by the use of two slot antennae. Actually

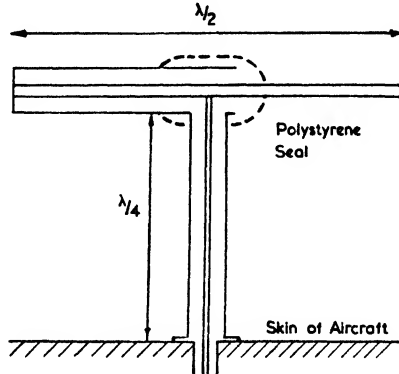


FIG. 8.8. ALTIMETER ANTENNA WITH QUARTER-WAVE STUB INCORPORATED IN ONE HALF OF THE DIPOLE

this is not quite so simple as it sounds, for the box behind the slot must take up an appreciable space; moreover, the slot may weaken the skin stressing. Consequently the provision

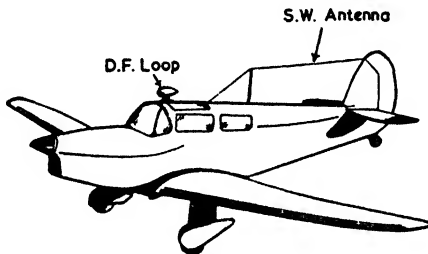


FIG. 8.9. TYPICAL ANTENNA LAYOUT ON A SMALL AIRCRAFT

of slot antennae cannot be introduced as an afterthought—they must be fitted in with the general design of the aircraft.

Marker Beacon Antenna

Marker beacons operate on wavelengths between 2 m and 8 m, and their transmitting antenna is a horizontal dipole (or an array of dipoles) lying in the direction of approach for the

aircraft. Reception is obtained conveniently therefore on a half-wave dipole consisting of two lengths of wire which are suspended below the fuselage on short masts some 30 cm long. The dipole is therefore quite near the body of the plane; hence its input impedance is low, but this is unimportant compared with the aerodynamical advantages gained.

Antennae for Approach Systems

A simple vertical rod 1 m high forms an effective antenna for approach systems using vertical polarization and working on wavelengths of about 8 m. Beam approach systems on about 3 m wavelengths are often horizontally polarized, in which case one of the simpler forms of loop antennae (*see* Fig. 3.28) may be used, the mounting position being somewhere above the control cabin, as in the case of the vertical rod.

For the B.A.B.S. (beam approach beacon system) method of landing a ground beacon is interrogated from the plane and the return signal is received on two keyed antennae whose polar patterns overlap in the forward direction. To achieve the correct pattern the two receiving antennae are mounted on either side of the nose of the plane together with director elements. Plate No. XV shows the port-side receiving system and also the quarter-wave transmitting antennae under the nose of a B.O.A.C. "York" aircraft.

8.4. AIRCRAFT ANTENNAE FOR COMMUNICATION CHANNELS

The antennae used for communication purposes fall into four main groups: (1) trailing wires for long, medium and short waves, (2) a wire from a short mast near the nose to the tail fin for short waves, (3) whip antennae for ultra-short waves and (4) antennae formed by exciting some portion of the metal skin of the aircraft. The various forms are illustrated in Figs. 8.9 and 8.10, together with the other types of antennae normally found on such aircraft.

Trailing-wire Antennae

The trailing-wire antenna formed the earliest solution to a transmitting antenna for long and medium wavelengths. A typical installation is shown in Fig. 8.11, from which it can

be seen that for a speed of 250 km per hour (about 150 m.p.h.) the distance of the weighted end below the aircraft will be roughly one-third of the length of the wire.

It will be noticed that the farther away from the aircraft one goes, the more vertical the wire becomes—at the same

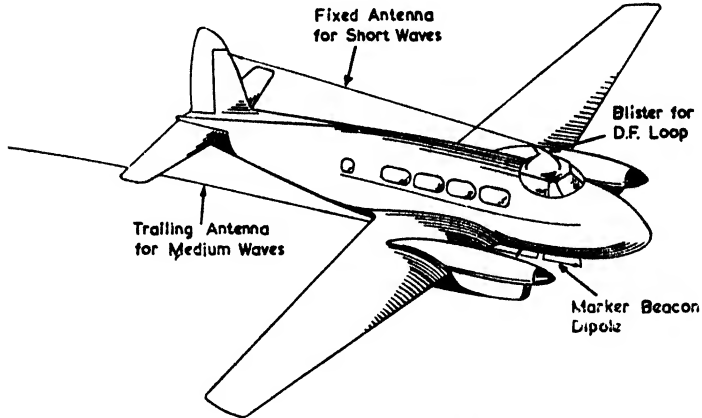


FIG. 8.10. EXAMPLE OF ANTENNA LAYOUT ON A COMMERCIAL AIRCRAFT

time the current in the wire diminishes. Consequently the effective height of the antenna is only about one-quarter of the actual height, i.e. in Fig. 8.11 the effective height will be about 4 m.

The wire itself is made of stranded steel about 1.25 mm

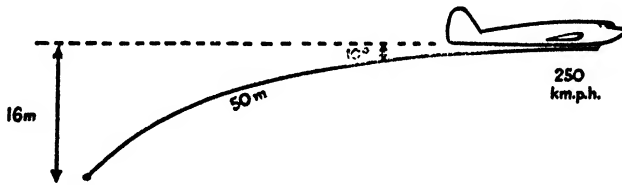


FIG. 8.11. DIAGRAM OF A TRAILING-WIRE ANTENNA

(50 thou.) diameter and is wound out through a "fairlead" which is an insulated tube projecting some 0.5 m below the fuselage. An obvious position for the fairlead is at the front of the aircraft below the radio gear. Unfortunately this position causes the antenna to run roughly parallel to the fuselage for some distance (particularly at high speeds) with the undesirable results of increasing the capacitance at the base of the antenna

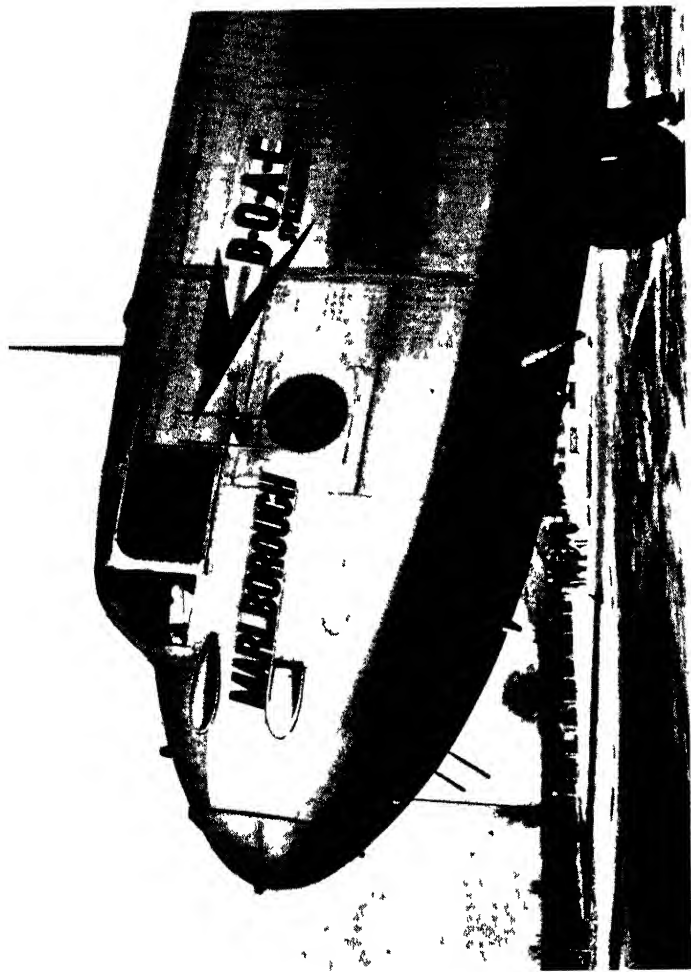


PLATE XV A B O A C SPEEDBIRD YORK AIRCRAFT SHOWING COMMUNICATION AND
NAVIGATIONAL ANTENNAE

The B A B S transmitting antenna may be seen and also the 1111 single receiving antenna
which have directors in front

(Courtesy of B O A C)

and increasing the losses due to induced currents in the aircraft. There is therefore some advantage to be gained by placing the fairlead about midway down the fuselage if such an arrangement is not mechanically too inconvenient. In Plate No. XV the fairlead can be seen under the nose of the aircraft on the port side.

Experiments by Bovill⁽²⁰⁵⁾ indicated that at a wavelength of 900 m the capacitance of a trailing antenna of 60 m (200 ft) varied between 350 and 450 $\mu\mu\text{F}$ according to the type of aircraft. At the wavelength in question the capacitance would differ very little from the static capacitance since the total length of the antenna would be about $\lambda/15$. The static capacitance of the wire in free space may be found directly from Fig. 2.6; in this case $l/a = 96\ 000$, so that $C = 305\ \mu\mu\text{F}$. The measured values exceed this owing to the proximity of some of the wire to the body of the aircraft.

The radiation resistance at a wavelength of 900 m is but a small fraction of an ohm, but measurements show that the total resistance lies somewhere between 5 and 20 ohms. Hence the antenna is inherently very inefficient. These high losses cannot be attributed to the use of steel wire but appear to be due to losses in the fairlead and the body of the aircraft.

At a wavelength of 600 m (which is used for distress signals over the sea) the antenna capacitance will be slightly greater, while the total resistance tends to decrease in spite of the radiation resistance being doubled. This decrease in the total resistance continues with decreasing wavelengths until, in the case of a 50 m wire, a minimum is reached at about 700 kc/s (430 m). For still shorter wavelengths the total resistance increases again owing to the fact that the radiation resistance now becomes appreciable. A typical curve is shown in Fig. 8.12; this was obtained by interpolation from the experimental results of Hyland.⁽²¹³⁾ At the quarter-wave resonance condition the resistance is between 10 and 20 ohms, the value being such that it lies between that obtained with a resonant fixed aircraft antenna and that obtained with a vertical quarter-wave antenna above the ground. The net result is to give a total resistance which does not vary very widely over the whole wavelength range of 200 to 900 m.

If the wire can be let out to various lengths the matching problem over a wide range of frequencies is simplified, so that the trailing antenna can then also be used for short-wave transmission. An ideal arrangement is to provide an automatic

motor mechanism which lets out just the right length of wire to suit the selected wavelength. However, such a refinement is only economical on a commercial airliner but these are tending to give up trailing wires for the reasons mentioned below.

The trailing-wire antenna has a number of disadvantages which are tending to make it obsolete except for emergency use or for communication with ships. It causes considerable dynamical drag (a feature which cannot be overlooked in

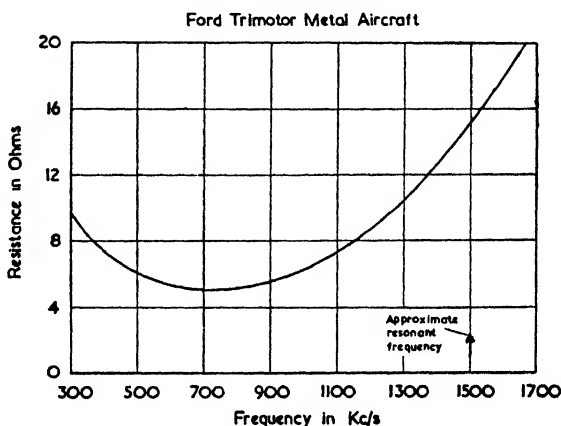


FIG. 8.12. RESISTANCE OF A 50 METRE TRAILING-WIRE ANTENNA
(Hyland, *Proc. I.R.E.*, Dec., 1929)

high-speed aircraft); the strains on the wire are such that renewals are frequent; it has sufficient horizontal polarization to cause bad D.F. errors (this type of error is known as "aeroplane effect"); in concentrating on landing, a single pilot can easily forget to wind the antenna in; the tail end of the wire is very susceptible to icing.

Since the introduction of short and ultra-short waves for communication purposes the main advantage of the trailing wire—namely that of a better effective height for medium waves—is no longer so important. Also the increased size of commercial aircraft has made the provision of reasonably efficient fixed antennae easier, so that even on medium waves a serviceable result can be obtained with a fixed wire. Of course, for reception purposes the difference between trailing- and fixed-wire antennae may be negligible, since the signal-to-noise ratio then becomes the important consideration and

this seldom depends on antenna efficiency when medium waves are concerned.

Fixed-wire Antennae

Because of the disadvantages of trailing-wire antennae mentioned above, fixed antennae stretched along the length of the fuselage at a height of about 1 m have been tried instead. With such a fixed antenna the range of communication with 100 W into the antenna is reduced to perhaps only 100 km, which is half the range possible with a trailing antenna; nevertheless the convenience of the fixed wire makes it an attractive proposition.

The effective height of the fixed wire is roughly equal to its height above the fuselage, and since this is limited to 1 m or so for aerodynamical considerations, the effective height is only one-third or one-fourth that of a trailing-wire antenna. Also the capacitance of the wire is reduced by about the same amount as compared with the trailing type. As a result of the low capacitance values, the peak voltage at the antenna input may have values as high as 20 000 V. The fixed-wire antenna is therefore a highly inefficient form of radiator for medium and long wavelengths.

At short wavelengths, however, the fixed-wire antenna is not nearly so inefficient and it is at such wavelengths that the fixed-wire type finds its main use. Two typical installations are shown in Fig. 8.13, together with the corresponding typical impedance curves.

Case A is that of a small and relatively slow aircraft in which a tall mast of 1 m to 2 m is used, the total length of wire being about 6 m. This results in an inverted-L antenna for which the quarter-wave resonance occurs at wavelengths of about 4.2 times the length of wire, i.e. the resonant frequency f_0 is in the neighbourhood of 12 Mc/s.

The radiation resistance of such an antenna could be calculated to a useful degree of approximation by treating it as an inverted-L antenna whose "ground" is the metal fuselage of the aircraft. The appropriate curves for this calculation are given in Fig. 2.5. With a metal fuselage the ground is so highly conducting that the base resistance, R_b , is hardly any greater than the radiation resistance (at least for frequencies above $0.4 f_0$).

To estimate the base reactance X_b , one can assume tentatively a characteristic impedance of 500 ohms and then apply

equation (2.1). Such a value for the characteristic impedance will lie between the free-space value and that which would be obtained if the top of the fuselage were an infinite conducting sheet.

Case B of Fig. 8.13 represents the long sloping wire as used in many commercial aircraft to-day. The length of wire would be about 15 m, so that the resonant frequency is of the order of 5 Mc/s. Owing to the close proximity of much of the wire

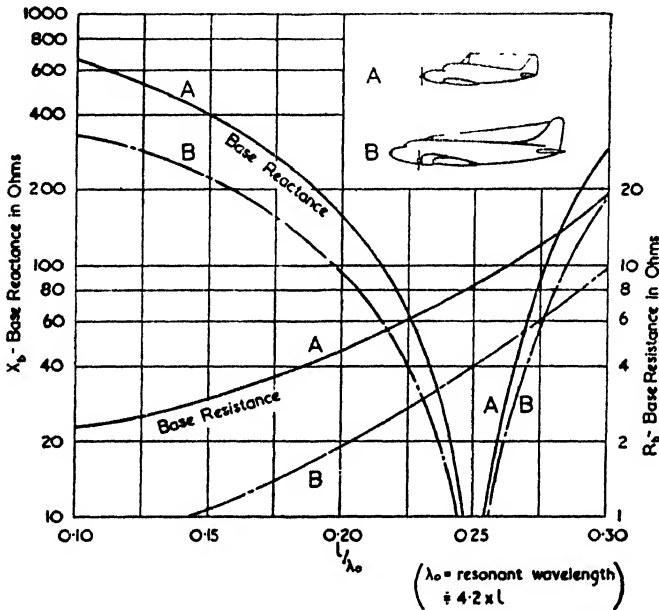


FIG. 8.13. AVERAGE CHARACTERISTICS OF FIXED AIRCRAFT ANTENNAE

to the fuselage, the characteristic impedance of the wire is lower and hence the reactive impedance is also lowered. The absence of a mast at the front end decreases the radiation resistance in comparison with case A for corresponding fractions of f_0 .

With a sloping antenna the radiation resistance may be estimated by considering an equivalent antenna whose vertical and horizontal portions are about 0.8 times the vertical and horizontal projections of the actual antenna. A more refined approximation on these lines may be found in the book by Sandretto.⁽¹⁹⁾ For estimating the reactance, a characteristic

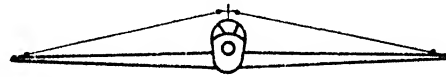
impedance whose value lies between 300 and 350 ohms may be assumed.

In view of the different shapes of aircraft it is impossible to give fairly exact figures on the antenna characteristics. When the aircraft has a double tail the antenna may be constructed with a V top, thereby increasing the antenna capacitance and broadening the bandwidth. An antenna of this type is shown in Plate No. XIV.

Another form of fixed-wire antenna is one which runs along the length of the wing in the manner shown in Fig 8.14 (a). The general form is that of a low T-antenna and the impedance characteristic is roughly the same as that of a sloping-wire antenna (type B, Fig. 8.13) whose length is some 30 to 50 per cent longer than half the top of the T.

There is some difficulty in measuring the polar diagram of an aircraft antenna; measurements on the ground cannot be relied upon, while flight tests are costly and their results require careful interpretation. For this reason Haller⁽²¹⁰⁾ constructed a high platform

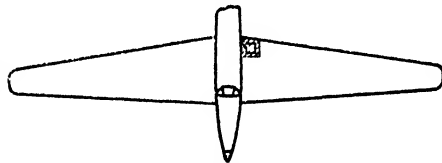
on which one-tenth scale models could be placed (the wavelength used for the tests was also one-tenth of the working wavelength). When performed with a fixed antenna along the length of the fuselage, these tests showed that at frequencies up to about the quarter-wave resonant frequency the horizontal polar diagram was substantially a circle and the polarization predominantly vertical. At higher frequencies the increased radiation from the horizontal portion introduces an appreciable proportion of horizontal polarization in certain directions, but for communication purposes the antenna may still be considered as an omnidirectional radiator of vertically polarized waves.



(a)
Sloping T-type Antenna



(b)
Shunt-Excited Metal Wing



(c)
Metal Wing Excited by Coil in Cut-away
Portion Covered with Dielectric

8.14. THREE TYPES OF WING ANTENNAE

Finally a few mechanical points might be mentioned. With fixed-wire antennae, the diameter of the wire is about 1 to 1.25 mm (40 to 50 thou.) and the material is stranded steel. It is advantageous to use copper-clad steel since the resistance reaches quite low values on some parts of the short-wave range. Special streamlined insulators are available for aircraft use; these both decrease the wind resistance and reduce the possibility of icing.

Shunt-excited Wing

An obviously attractive idea is to use the actual wing of an aircraft as the antenna. Since it is impracticable to insulate the wings from the fuselage, the wing antenna may be shunt fed in the manner shown in Fig. 8.14 (*b*).

The impedance curve of such an antenna has a resistance component which is rather similar to curve *A* in Fig. 8.13 (the corresponding fixed antenna has a length equal to one-half of the wing span). The reactive component, however, is quite different and is inductive for all frequencies below the full-wave resonant frequency. For example, the curves given by Haller⁽²¹¹⁾ showed an inductive impedance of 600 ohms when the whole wing was at half-wave resonance. An inductive input impedance at the first resonant point is quite normal for all shunt-fed antennae—whether grounded or not—and calls for a series tuning capacitor.

Nowadays commercial aircraft are often designed for flying speeds in the region of 500 km/hr and at such speeds even the wire feed shown in Fig. 8.14 (*b*) is objectionable. In such cases the feeder system may be completely suppressed by using a loop for excitation where this loop is inside either the leading or trailing edge of the wing. For this purpose the portion of the wing which encloses the loop must be non-metallic (*see* Fig. 8.14 (*c*)). The area of the loop would be about 0.2 m² for an aircraft of the size shown in Fig. 8.10 and might consist of, say, three turns of copper tubing in which case the input impedance would be of the order of $5 + j100$ ohms.

It is interesting to note that with the above form of excitation the fuselage must also be excited to some extent; in fact we have virtually made a horizontal turnstile antenna out of the surface of the aircraft. Nevertheless practical tests indicate that there is also an appreciable vertically polarized field from such antennae. For further information the reader may consult a paper by Johnson.⁽³⁸⁷⁾

Whip Antennae

The use of ultra-short waves for communication has made it possible to use a very simple form of omnidirectional radiator which consists of a non-rigid vertical rod projecting above the fuselage. At a frequency of 125 Mc/s the length of such a rod will only be about 60 cm.

A typical requirement for such an antenna is that it should cover a range of ± 10 Mc/s without being re-tuned. This may be achieved by means of a tuning stub in the manner described in § 10.7. In this way the input impedance about the quarter-wave resonance point may be kept reasonably constant.

If the whip is mounted too near the tail fin, a serious decrease in the backward radiation may occur, but this is not a favourable position unless the transmitter is mounted in the tail of the aircraft and remotely controlled. A very convenient position in practice is just at the back of the cockpit, in which case an appreciable portion of the "ground" below the whip may consist of the cockpit. If this is so, all calculations based on the assumption of a quarter-wave rod above a large conducting sheet are invalidated and the impedance characteristics must be determined experimentally.

It is to be expected that, for certain positions in flight, the structure of the aircraft would screen off some of the radiation from the plane. Although this effect has been observed, it does not appear to be an important limitation. For a recorded case of such screening, together with some curves showing relative field strength versus distance, the reader may consult the book by Sandretto.⁽¹⁸⁾

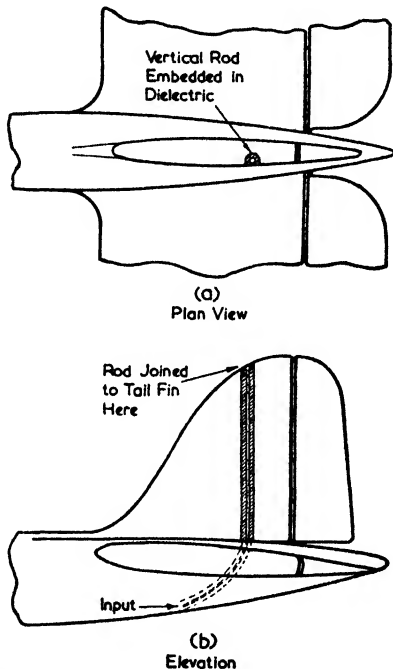


FIG. 8.15. FOLDED UNIPOLE METHOD OF EXCITING A TAIL FIN

A suppressed form of ultra-short-wave antenna may be formed by exciting the tail fin or some portion of it. For example, if the tail is of plastic material the leading edge may be covered with copper foil. By making a vertical recess in a metallic fin as shown in Fig. 8.15 the whole fin can be excited as if it were half a folded dipole (the other half being supplied

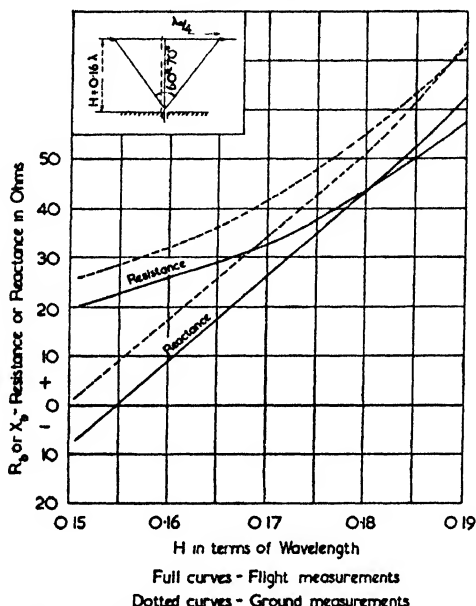


FIG. 8.16. EXPERIMENTAL IMPEDANCE CURVES OF A THREE-WIRE FAN ANTENNA

(Bennett, Coleman and Meier, *Proc. I.R.E.*, Oct., 1946)

by an internal quarter-wave stub in series with the vertical feeder). The vertical feeder should be enclosed in polythene to aid the streamlining and to reduce precipitation static.

At distances of over 20 km from the ground station the field strength may be calculated by means of the ordinary ray theory as outlined in § 9.5, but, nearer in, the field strength is less predictable due to the structure of the aircraft modifying the radiation pattern. Fortunately at short range the field strength is high enough for the fluctuations in signal strength to be unimportant.

Fan Antennae

In order to obtain even wider bandwidths than is possible with a whip antenna and tuning stub, a set of wires spread out

fanwise may be used. Such an arrangement is the practical equivalent to a "thick" antenna which, as is well known, results in a wider bandwidth.

Fan antennae are described (among others) in a detailed article by Bennett, Coleman and Meier.⁽²⁰⁴⁾ Their prototype fan antenna is shown in Fig. 8.16, together with impedance curves for both ground and flight measurements. Fig. 8.17 shows a three-wire fan antenna as installed on the tail of a

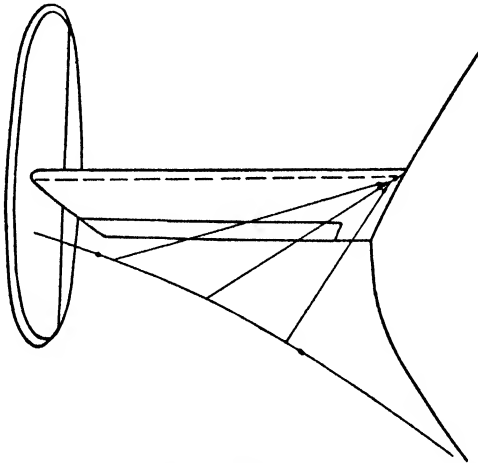


FIG. 8.17. FAN-TYPE ANTENNA MOUNTED ON TAIL OF AIRCRAFT

large aircraft. With this type of antenna, bandwidths of ± 15 per cent are realizable for a limiting standing wave ratio of 1.5 to 1 (the authors take 2 : 1 as their criterion, for which value bandwidths of over ± 20 per cent are feasible).

8.5. AUTOMOBILE ANTENNAE

On long and medium waves the effect of the metal body of a car on the field distribution is not very great. This is to be expected, for the dimensions of the car are small in comparison with a wavelength so that no resonances can be set up. The maximum differences due to the body are about ± 50 per cent on the original field strength; this is of no importance for communication purposes but needs consideration if accurate field strength measurements are required.

Figs. 8.18 and 8.19 show some of the results of tests conducted

by DeWitt and Omberg⁽²⁰⁷⁾ on the influence of a car body on the field strength. It will be seen that above the roof the field is actually some 10 to 30 per cent greater, depending on the orientation of the car, while at the sides there is a diminution of some 40 per cent along those sides which are at right angles to the plane of the wavefront. These changes to the field were

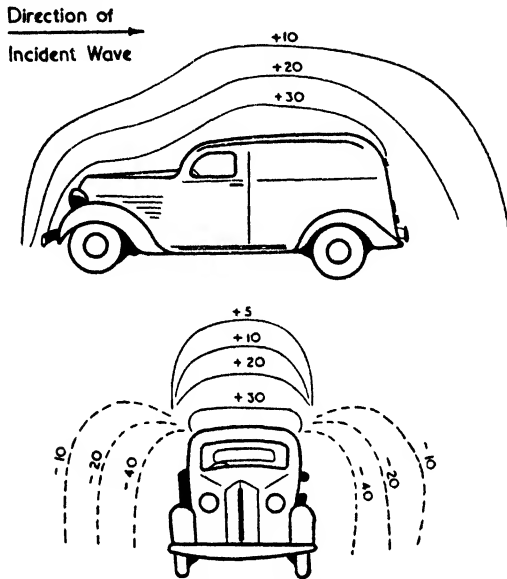


FIG. 8.18. PERCENTAGE CHANGE IN FIELD STRENGTH ON MEDIUM WAVES DUE TO PRESENCE OF AN ALL-METAL TRUCK
(DeWitt and Omberg, *Proc. I.R.E.*, Jan., 1939)

found to be independent of frequency within the broadcast band; they can be attributed to induced currents in the metallic surfaces (or continuous loops of metal). The strength and direction of these induced currents follow the same general laws as those applicable to a D.F. loop, i.e. an isolated surface which was parallel to the ground or to the plane of the wavefront would not have any induced currents.

The four main positions for car antennae are shown in Fig. 8.20. Of these only the under-car type has the advantage of being concealed but in other respects it is the worst form of antenna. That such a form of antenna is at all practicable is due largely to the fact that medium waves penetrate for a distance of some metres into the ground, so that from a

pick-up point of view it is almost immaterial—if the antenna is above or below the car. (This statement is not true for very wet or reinforced concrete roads for which the pick-up is sometimes reduced to about one-third of its normal value.)

An under-car type of antenna is very liable to damage unless it is strongly made and suspended by means of flexible rubber straps, but its greatest disadvantage is that it is situated in a region of high noise fields. The noise fields are partly

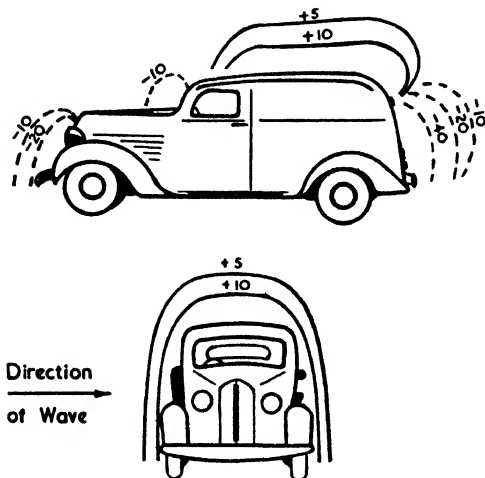


FIG. 8.19. PERCENTAGE CHANGE IN FIELD STRENGTH ON MEDIUM WAVES DUE TO PRESENCE OF AN ALL-METAL TRUCK
(DeWitt and Omberg, *Proc. I.R.E.*, Jan., 1939)

due to the ignition system and partly to the discharges of static fields set up by the action of the rotating wheels. The mechanism of this "tyre static" is that the tyres become charged by the rubbing action on the road, whereupon these charges leak on to portions of the wheel which are insulated from the main body of the chassis by virtue of oil films. The noise field is generated when such capacitors are discharged either by the potential being great enough to puncture the oil film, or through causes such as sparking across to the brake drums.

A further type of noise to which the under-car antenna is especially prone is intermittent contact noise caused by poor bonding of the metal portions of the car. Intermittent contacts are liable to result in changes in the effective height and therefore in the pick-up of the antenna.

Both the scuttle and bumper types of aerial are unfavourably

situated with regard to local noise fields. They both have a greater effective height than the normal type of over-car antenna, but this is counteracted to some extent by the capacitance of the lower portion to the body in the case of the scuttle type, and by the capacitance of the input lead in the case of the rear bumper version. The performance of the bumper antenna can be improved by fitting the radio in the rear of the car but this leads to complications in the design of the controls for the radio equipment.

The over-car antenna has everything to recommend it from an electrical point of view, furthermore the characteristics of

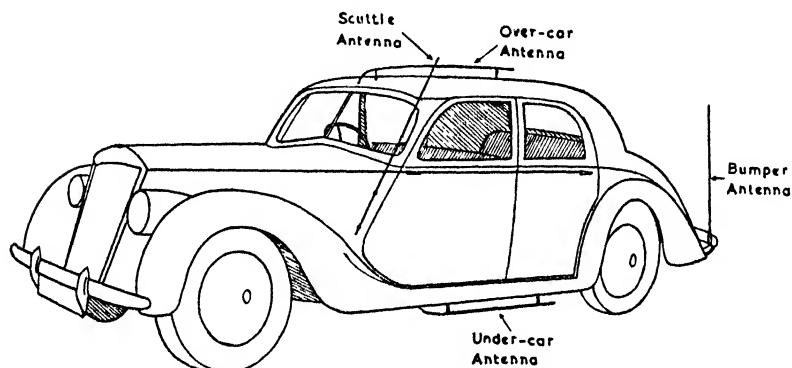


FIG. 8.20. FOUR TYPES OF AUTOMOBILE ANTENNAE

such antennae may be predicted to a satisfactory degree by standard theoretical methods. For instance, the capacitance of the horizontal portion may be calculated by taking double the capacitance of a parallel-wire line of equal length and of spacing equal to that between the horizontal portion and its image in the metal roof. Also the effective height is approximately equal to the actual height as is the case with a normal inverted-L antenna whose top is long relative to the vertical portion. (Thus a typical over-car antenna will have a capacitance of about $50 \mu\mu\text{F}$ and an effective height of 10 cm.)

Sometimes an over-car antenna takes the form of a short vertical rod some 30 to 40 cm high without any horizontal portion. In such cases the antenna will have a capacitance of about $5 \mu\mu\text{F}$ and an effective height of half the actual height.

The reduction of the local noise field surrounding a car is a complex problem and involves some trial and error with regard to the running of leads, bonding, etc.; but the most

effective single measure that can be taken is to fit non-inductive resistors of about 10 000 ohms resistance in series with each sparking-plug lead. In this way the sparking current is made to take the form of a highly-damped pulse instead of having the usual oscillatory waveform.

Propagation of Radio Waves

BROADLY speaking, we may divide the propagation characteristics of radio waves into three groups—those for which the ground is a good conductor (long and, to a lesser degree, medium waves), those which are reflected efficiently by the ionosphere (short waves), and those for which the ground is a dielectric (ultra-short waves and, to a greater degree, microwaves). These characteristics are used to obtain good radiation along the surface of the earth in the case of long and medium waves, long-distance transmission via the ionosphere on short waves and quasi-optical transmission on the still shorter wavelengths.

General solutions of the propagation of radio waves (excluding the effect of the ionosphere) have been given by Norton⁽²⁷¹⁾ and Burrows and Gray.⁽²³⁴⁾ These solutions deal with antennae of either form of polarization and of any height, wavelength, or ground constants. The calculations are necessarily involved, but fortunately in the large majority of practical cases a much simpler analysis will suffice. This is due to the following facts—

(a) on long and medium waves the antenna is normally a vertical radiator on the ground,

(b) on short waves ionospheric propagation is usually required so that the surface wave at the point of reception is negligible,

(c) on ultra-short and microwaves the surface wave is negligible at even short distances.

The five sections which deal with propagation at specific wavelengths are preceded by one outlining the analysis of the wave into surface, space and sky waves. An appreciation of the general principles of this resolution is essential for an understanding of field strength formulae.

9.1. SURFACE, SPACE AND SKY WAVES

In general, the field strength at any point may be resolved into three distinct components—these are (a) a surface wave, (b) a space wave, and (c) a sky wave. The second of these components can be further resolved into a direct ray and a ray

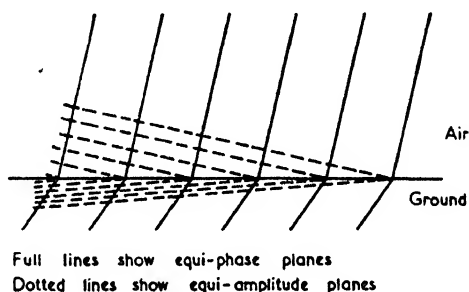
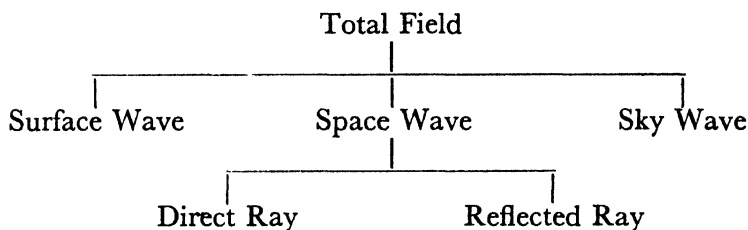


FIG. 9.1. THE STRUCTURE OF A SURFACE WAVE

reflected off the ground. To make this classification clearer it can be put in the form of a family tree—



In the great majority of practical cases at least one of these components is either negligible or non-existent; this simplifies considerably the field strength calculations. The properties of these components may be summarized as follows—

(a) *The Surface Wave*

This component consists of a wave which travels along the ground in a tilted manner as shown in Fig. 9.1.

It might appear from this figure that there ought to be a reflected ray off the ground. Actually there is not, for the surface wave is a non-homogeneous wave, i.e. the equiphase planes do not coincide with the equi-amplitude planes. As a result the wave is capable of travelling along the ground

without reflection, but a certain proportion of the total energy is continually propagated into the ground. This proportion depends on the horizontal component of the electric vector which is elliptically polarized. The polarization of this vector for different wavelengths is shown in Fig. 9.2, while Fig. 2.25

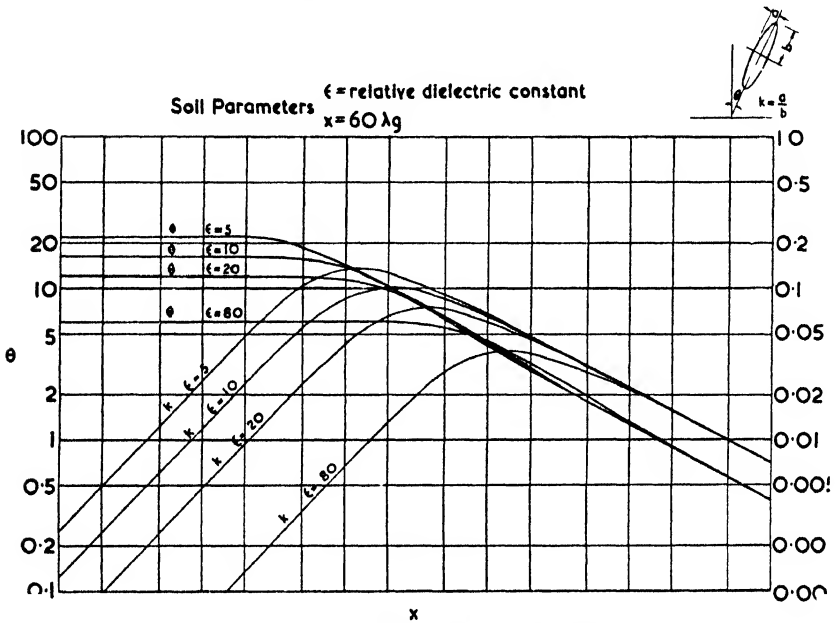


FIG. 9.2. THE TILT AND POLARIZATION OF THE SURFACE WAVE FOR VARIOUS GROUND CONSTANTS
(Norton, *Proc. I.R.E.*, Sept., 1937)

gives the depth of penetration of the wave into the ground for various conductivities.

The field strength decreases exponentially both above and below the surface of the earth. Below the ground the reduction in field strength becomes appreciable in a fraction of a wavelength, while above the ground a similar reduction takes place in a few wavelengths. These variations in field strength are, of course, superimposed on a general reduction in field strength as we move farther away from the source.

The surface wave from a vertical antenna is far stronger than that from a horizontal antenna at the same height, and in both cases it decreases with the height of the antenna above the ground. Thus with a half-wave dipole the surface wave

may be neglected at a distant point if the dipole is vertical and at least one wavelength above the ground; but if it is horizontal, the dipole need only be about one-eighth of this height above the ground.

In practice the surface wave is the only component in which we are interested when dealing with the reception of local broadcasting on medium waves. At greater distances the sky waves must also be taken into consideration, until at distances above, say, 300 km, it is only the sky wave that counts.

As the wavelength becomes shorter, so the surface wave becomes weaker. For example, even with a vertical antenna a range of only 30 km is obtained on a wavelength of 60 m, whereas if the wavelength were 550 m the range would be ten times as great (these remarks assume a received field strength of $100 \mu\text{V/m}$). The surface wave is therefore rarely relied upon when using short wavelengths and not at all in the case of all ultra-short or microwaves.

(b) *The Space Wave*

The space-wave component consists of the sum of the direct ray and the ray reflected from the ground. These rays are shown in Fig. 1.9, which gives the geometry of the space wave at a point P when the radiation is due to an element of current ds . For a perfectly conducting ground the image of ds is in phase for vertical elements and out of phase for horizontal elements, but in the general case of finite conductivity the complete reflection coefficients as given by Fresnel's formulae must be used.

To find the field due to a complete antenna, we have to calculate the sum of the field strengths due to all such elements and, in general, this would involve different reflection coefficients according to the angle of incidence of the reflected ray. Fortunately in most practical problems the antenna can be assumed to be a point source (whose polar diagram is that of the actual antenna) so that the reflection coefficient varies only with the angular position of the field point and not also for each element of current.

Space-wave calculations find their main use in ultra-short wave and microwave propagation. At such wavelengths the sky wave is normally non-existent, and in addition the surface wave is negligible except in the immediate neighbourhood of the antenna.

At medium wavelengths the space wave must be taken into account for all angles greater than a degree or so above the ground. A typical polar pattern of a grounded vertical radiator is shown in Fig. 1.10 in which the dotted line indicates the *total* field obtained on including the surface wave. Near grazing incidence the space wave is proportional to $(1 + R_v)$, where R_v is the reflection coefficient for vertically polarized waves and equals -1 when θ , the angle of incidence, is 90° . If,

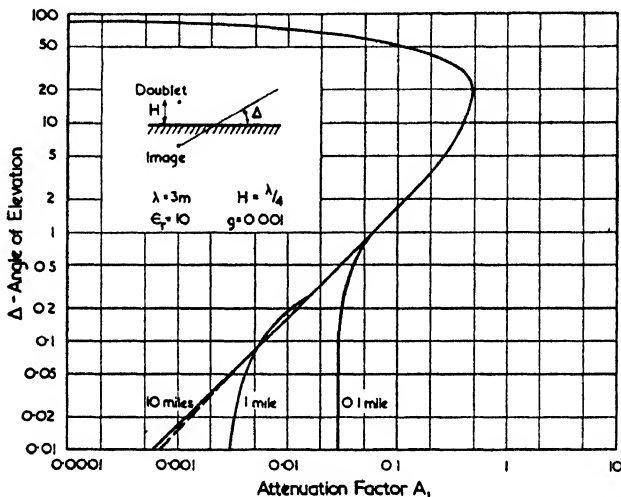


FIG. 9.3 (a). THE FIELD DUE TO AN ELEVATED VERTICAL DOUBLET ABOVE A GROUND OF FINITE CONDUCTIVITY
(Norton, *Proc. I.R.E.*, Sept., 1937)

however, the conductivity were infinite, then R_v would equal $+1$ when $\theta = 90^\circ$ so that the space wave would be a maximum along the surface.

The surface wave, on the other hand, is proportional to $(1 - R_v)$. Consequently it has a large value for finite conductivity, but is zero for infinite conductivity; hence for the latter case the space wave gives the whole of the radiation pattern.

The relative values of space- and surface-wave components for an elevated doublet are shown in Fig. 9.3 for various wavelengths. It will be noticed that in some cases the combined field is actually *less* than that due to the space wave alone—this effect was also found by Wwendensky.⁽²⁹²⁾

On account of the water vapour content in the earth's

atmosphere, a horizontally-propagated radio wave follows a curved path which partially compensates for the earth's curvature. To allow for this in space-wave calculations it is usual to assume that the paths of the rays are straight but that the radius of the earth is 33 per cent greater than the true radius.

The use of this "apparent radius" of the earth gives correct results for average conditions when atmospheric refraction is

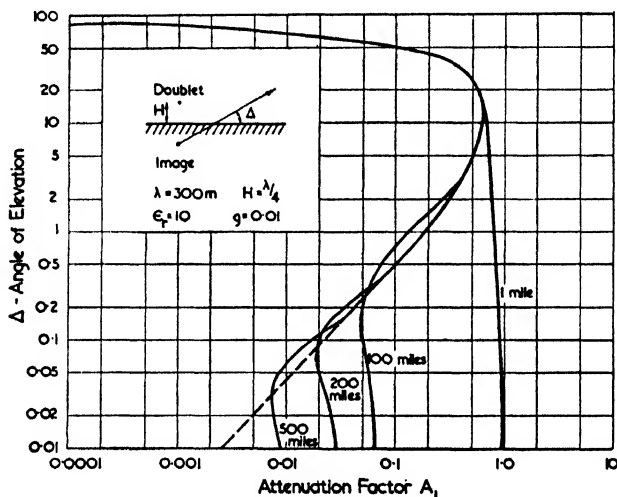


FIG. 9.3 (b). THE FIELD DUE TO AN ELEVATED VERTICAL DOUBLET ABOVE A GROUND OF FINITE CONDUCTIVITY (Norton, *Proc. I.R.E.*, Sept., 1937)

“normal.” Under certain atmospheric conditions, however, considerably more bending of the rays may take place and it is even possible for the rays to follow the curvature of the earth. The nature of this phenomenon (which is discussed on p. 428) is such that only microwaves and ultra-short waves can be affected in this manner.

(c) *The Sky Wave*

It is well known that the upper atmosphere contains two main ionized regions which are capable of reflecting radio waves. The lower one is the E layer (at a height of about 100 km) and is normally capable of reflecting waves at vertical incidence up to frequencies of the order of 2 to 5 Mc/s. The upper region is known as the F layer—or more precisely as

the F_2 layer—and is situated at heights which vary between 250 and 400 km. The F_2 region is capable of reflecting waves whose frequencies are as high as 3 to 12 Mc/s. In both cases the reflecting powers of the layers show marked diurnal, seasonal and yearly variations. These variations can be correlated with solar radiation and sunspot activity.

When the radio wave is incident at some oblique angle to the reflecting layers, the maximum frequency which can be reflected is increased by a factor of as much as 5 for the E layer and 3.5 for the F_2 layer, the corresponding skip distances being about 2 000 km and 3 500 km respectively.

The sky wave is a disadvantage on medium-wave broadcasting systems for it interferes with the surface wave, thereby causing fading at distances between 100 and 200 km. This interference is not apparent in the daytime owing to strong absorption of the sky wave in the lowest regions of the ionosphere. At night time, however, the sky wave is appreciable at broadcast frequencies so that, in addition to the region of fading referred to above, there is a secondary service area of relatively inferior reception which lies between radii of roughly 250 km and 750 km from the transmitter.

For wavelengths from 10 to 100 m the sky wave is of major importance since it provides the mechanism by which long-distance short-wave propagation takes place. An important feature of such propagation is that the attenuation may be hardly any greater than that for free space (i.e. the attenuation of the field strength is of the same order as the inverse distance law); consequently a reasonable field strength may be obtained with moderate powers over very great distances.

Reflections sometimes take place at frequencies in excess of 30 Mc/s; in fact the reception of television signals from Alexandra Palace (whose frequency is 47 Mc/s) has often been reported in the United States of America, but such propagation conditions are unreliable. It is therefore convenient to regard a wavelength of 10 m as forming the lower limit in wavelength for sky-wave propagation.

Finally it might be added that an entirely different form of reflection has been observed at wavelengths of the order of a few metres. The reflection in this case has taken place in the troposphere and is believed to be due to reflections from thin "clouds" of water vapour whose boundary forms a sufficiently sharp discontinuity of dielectric constant to give a weak but distinct reflection.

9.2. LONG WAVES

For long waves, in particular for wavelengths exceeding 5 000 m, the ground attenuation is very small, so that excellent long-distance propagation is possible. In addition, such waves suffer reflection at the lowest levels of the ionosphere (about 70 km) which, together with the ground, forms a sort of waveguide for the low-frequency radio energy. Inside this waveguide of two concentric spherical shells the waves propagate fairly efficiently, the only losses being those due to the spreading of the energy and to the attenuation at the two boundaries.

The theoretical treatment of such a case is exceedingly complicated for even the simpler case of diffraction round a spherical earth is quite difficult. The latter problem was examined in a number of investigations at the beginning of the century, of which that due to Watson⁽²⁸⁸⁾ is particularly important. Such investigations showed that the attenuation would take the form—

$$E \propto \sqrt{\left(\frac{\theta}{\sin \theta}\right)} e^{-\alpha D/\lambda^n}$$

where θ = angle subtended at the centre of the earth,
 α = an attenuation constant of the order of 0.003,
 D = distance in kilometres,
 n = a fractional index of the order of $\frac{1}{2}$.

A considerable amount of experimental work was done by Austin⁽²²⁴⁾ and others which resulted in an empirical formula of the same type as given above. This formula is known as the Austin-Cohen formula and, for day-time propagation over sea-water, is given by

$$E = 377 \frac{I h_e}{D} \sqrt{\left(\frac{\theta}{\sin \theta}\right)} e^{-0.0014 D/\lambda^{0.5}} \quad (9.1)$$

where E = field strength in millivolts/metre,
 h_e = effective height of antenna in kilometres,
 λ = wavelength in kilometres,
 D = distance in kilometres,
 θ = angle subtended at centre of earth in radians,
 I = antenna current at the base in amperes.

The relative attenuation for different wavelengths as given by the Austin-Cohen formula is shown in Fig. 9.4. In practice

the field strength is liable to vary within limits of one-half to twice that given by (9.1) particularly when there is an appreciable amount of land in the transmission path. Over land α is believed to have a value about double the sea-water value.

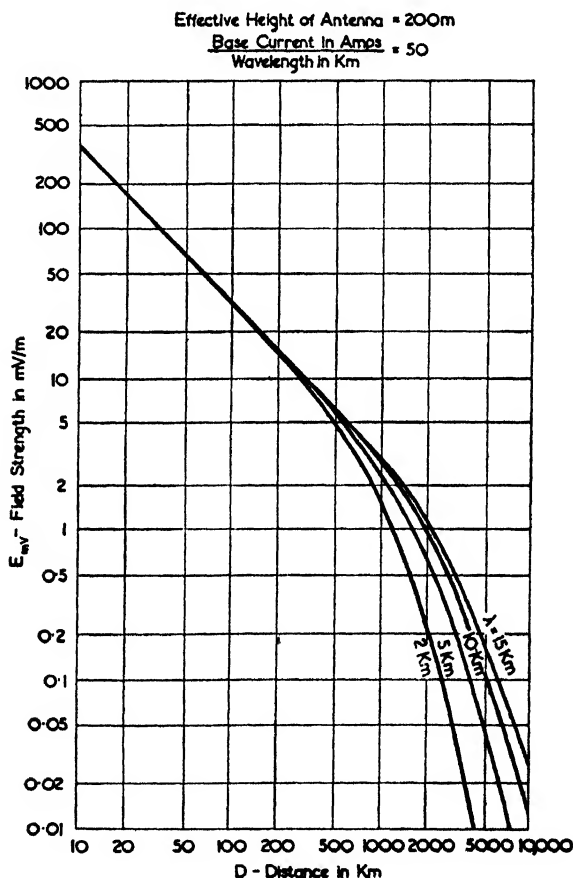
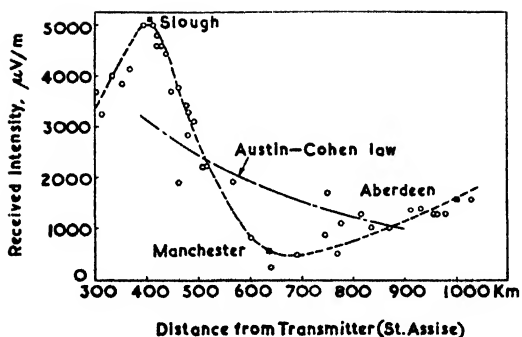


FIG. 9.4. FIELD STRENGTHS OVER SEA-WATER OF HIGH-POWER LONG-WAVE TRANSMISSIONS AS GIVEN BY THE AUSTIN-COHEN FORMULA

At distances less great than 1 000 km the field strength will oscillate about the calculated values, for then the surface and sky waves will interfere in a manner indicative of ordinary ray theory rather than following a waveguide mode of propagation. This effect was demonstrated by Hollingworth,⁽²⁸⁸⁾ one of whose curves is reproduced in Fig. 9.5.



$\lambda = 14.35 \text{ Km}$ $H = 75 \text{ Km}$

FIG. 9.5. OSCILLATIONS IN THE FIELD STRENGTH CURVE OF A LONG-WAVE TRANSMISSION AT MEDIUM DISTANCES FROM THE TRANSMITTER (Hollingworth, *Jour. I.E.E.*, May, 1926)

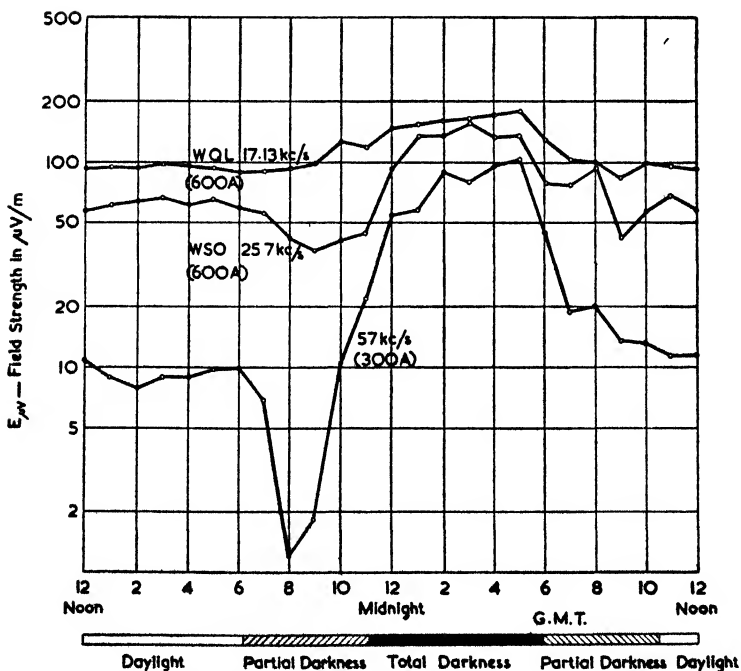


FIG. 9.6. FIELD STRENGTHS OF TRANSATLANTIC LONG-WAVE TRANSMISSIONS (Espenschied, Anderson and Bailey, *Proc. I.R.E.*, Feb., 1926)

One would also expect the field strength to vary with the ionospheric conditions and to show greater variations at the higher frequencies. Both these effects have been observed and are shown in Fig. 9.6, which is based on the experimental results of Espenschied, Anderson and Bailey⁽⁹⁷⁾ (their curve for 57 kc/s has been doubled in height to give the field strength that would be obtained with twice the current, thereby bringing this curve in line with the other two cases; it is not clear, however, whether the same effective antenna height was used in all three cases). The highest frequency shows a distinct diminution of field strength during the daylight hours; this is, no doubt, due to the increased absorption experienced in the lower regions of the ionosphere.

The relationship between the Austin-Cohen formula and that for propagation over a perfectly conducting flat earth is worthy of note. To start with we may obtain the free-space field strength of an element of current from equation (4.41), Vol. I, which (omitting the phasing term and putting $\theta = 90^\circ$) gives

$$E = \frac{\beta^2}{4\pi\epsilon r} M$$

M is the dipole moment and equals $il/j\omega$, where i is the instantaneous current in amperes and l the length of the current element. Therefore the magnitude of the field strength is given by

$$E = z_{00} \frac{il}{2\lambda r}$$

where $z_{00} =$ intrinsic impedance of free space,
 $= 120\pi$ or 377 ohms.

In the above formula all the units are in the M.K.S. system (z_{00} has been substituted for $\beta/\epsilon\omega$). The same element of current above a perfectly conducting earth would give twice the field strength—not $\sqrt{2}$ times as for the constant power case, since keeping the current constant has doubled the radiation resistance and the power. For the general case of a vertical antenna carrying an r.m.s. current of I amps at the base and of effective height h_e , we substitute Ih_e for il , whereupon E is in r.m.s. volts and is given by

$$E = 377 \frac{Ih_e}{r} \text{ volts/metre} \quad . \quad . \quad (9.2)$$

On making due allowance for the use of metres in the above equation instead of kilometres, it is apparent that the Austin-Cohen formula is identical with (9.1) for short distances. It should be noted, however, that the Austin-Cohen formula is not accurate for short distances because of the oscillations in the field strength versus distance curves due to the sky wave.

9.3. MEDIUM WAVES

There are two important requirements for the propagation characteristics of long- and medium-wave transmitters—

(a) that the field strength from the surface wave should be as great as possible, i.e. the highest possible horizontal figure of merit is desired,

(b) that the ratio of the field strength of the surface wave to that of the sky wave should be as great as possible.

The first of these requirements obviously indicates the need for a high antenna efficiency and as much input power as the economics of the situation will permit. It is important that the available radiated energy should be directed along the surface of the earth as far as possible and this may be achieved by using a vertical radiator whose height is 0.64λ (see Fig. 2.28).

The second requirement is usually more important than the first for, with radiated powers in excess of, say, 1 kW, the service area is limited by fading due to interaction between the surface and sky waves rather than by lack of adequate field strength. In order to obtain the greatest ratio of surface wave to sky wave, the polar characteristics of the antenna should be such that the radiation at angles of about 30° from the vertical should be as low as possible. This condition is fulfilled by vertical radiators whose heights lie between 0.52λ and 0.57λ (Fig. 2.29). The actual height employed depends on the ground characteristics and the wavelength.

It will be noticed that the optimum anti-fading height is not very different from the optimum height for horizontal radiation. The two requirements must obviously lead to much the same answer.

Field Strength along the Ground

The field strength along the ground is entirely due to the surface wave which, for a large number of practical cases, is given simply by equations (1.5) and (1.6).

Combining these two equations, we find that the field strength due to a *short vertical radiator* is

$$E_{mV} = \frac{300\sqrt{P_r}}{D} A_1 \quad (9.3)$$

where E_{mV} = field strength in millivolts/metre,
 P_r = radiated power in kilowatts,
 D = distance from radiator in kilometres,
 A_1 = Sommerfeld's attenuation constant

$$\dot{\div} \frac{2 + 0.3\rho}{2 + \rho + 0.6\rho^2}$$

ρ = numerical distance

$$\dot{\div} \frac{\beta r}{120\lambda g}$$

The attenuation constant, A_1 , is given by the full curve of Fig. 9.7, while the dotted curve in the same figure shows the approximation to it as given by Van der Pol's formula. These curves are valid only when $60\lambda g$ is at least twelve times $(\epsilon_r + 1)$, but this is true for virtually all cases in which the wavelength exceeds 200 m (abnormally rocky districts provide the sole exception). The more general case may be treated according to the methods of Norton⁽²⁷¹⁾ and Burrows and Gray,⁽²³⁴⁾ who use a modification of Sommerfeld's numerical distance.

If the radiator is not short, the factor of proportionality given by Fig. 2.28 must be used. This factor shows an increase of 4.3 per cent for a $\lambda/4$ antenna (*N.B.* equal *radiated* powers are assumed; in practice the efficiency of a short antenna will be low). Short antennae give a simple cosine law for the vertical radiation pattern and form a convenient standard for field strength curves.

Taking the general case of a simple vertical antenna whose efficiency is η leads to the following modification of equation (9.3)—

$$E_{mV} = \frac{300\sqrt{(\eta P)}}{D}, F(h)A_1 \quad (9.4)$$

where P = input power in kilowatts,

η = antenna efficiency

$$= \frac{R_r}{R_r + R_d}$$

R_r and R_d = radiation and dead-loss resistance respectively measured at the same point (e.g. at the base or at a current antinode),

$F(h)$ = relative horizontal field strength for antenna of height "h" when $\eta = 100\%$ (Fig. 2.28).

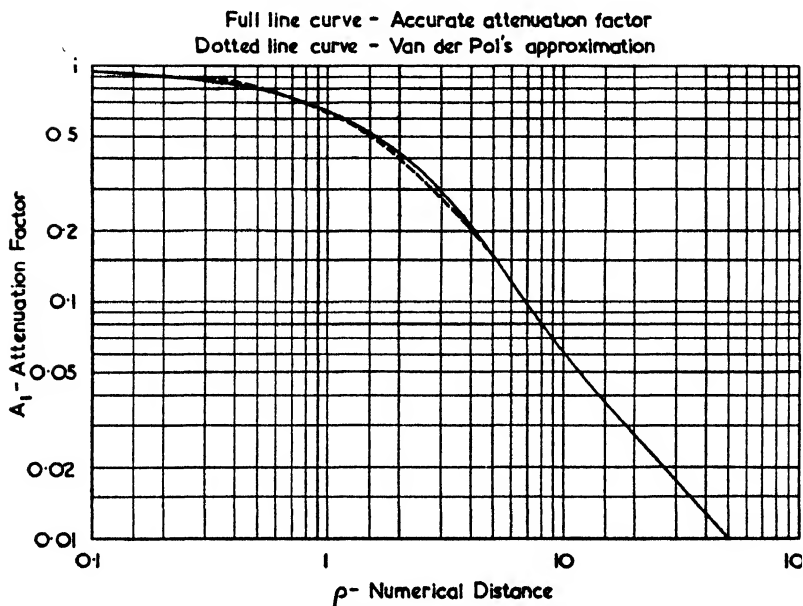


FIG. 9.7. THE SOMMERFELD ATTENUATION CONSTANT A_1 AS A FUNCTION OF THE NUMERICAL DISTANCE

An example which illustrates the application of the above formula is given on p. 381.

For both equations (9.3) and (9.4) the earth has been assumed to be flat. The validity of this assumption depends on the wavelength, for longer waves will be diffracted more easily round the earth. The maximum distance for plane earth conditions to hold may be taken to be equal to $12(\lambda)^{\frac{1}{2}}$ km. This function is shown plotted in Fig. 9.8.

It happens that the radius at which fading commences at night time is roughly the same distance as the maximum distance for the plane earth assumption. Equation (9.4) may therefore be used with reasonable accuracy for all places within the normal service area of a medium-wave broadcast station.

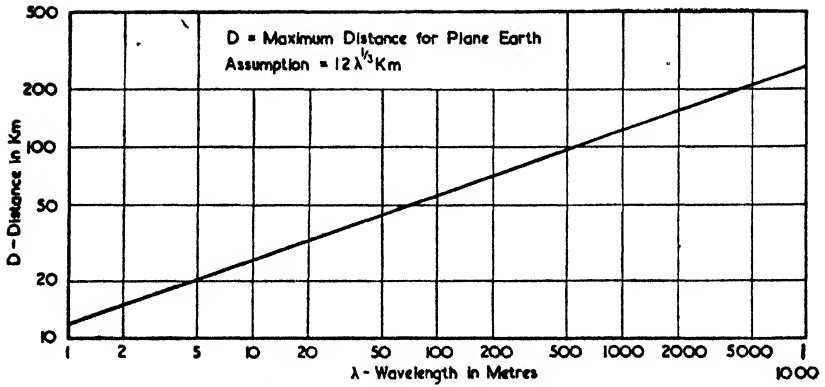


FIG. 9.8. MAXIMUM DISTANCE FOR THE VALIDITY OF THE ASSUMPTION OF A PLANE EARTH

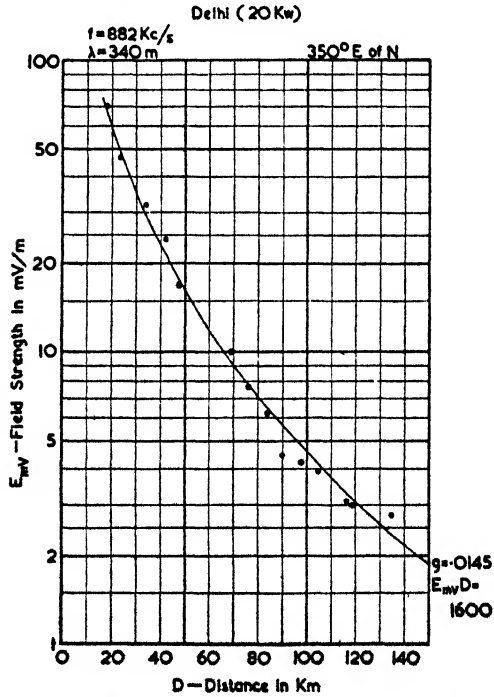


FIG. 9.9. EXPERIMENTAL FIELD STRENGTH VALUES OF A MEDIUM-WAVE TRANSMITTER
(All India Radio Report, 1940)

The example given in Fig. 9.9 shows experimental points obtained from the Delhi transmitter (*Report on the Progress of Broadcasting in India, Delhi, 1940*), together with a calculated curve assuming a figure of merit of 1 600 mV/m at 1 km and a ground conductivity of 0.0145 mhos/m. The figure of merit was obtained from the reference cited and the conductivity figure was selected to give the best fit.

Spherical Earth and Refraction Effects

On long wavelengths we are often interested in the field strength at considerable distances from the transmitter, whereupon it becomes necessary to allow for the curvature of the earth. This may be done by multiplying (9.4) by a "shadow factor," A_2 , which is a function of the wavelength, the distance and the radius of the earth. In particular A_2 is a function of the spherical earth distance parameter, ζ , which is given by

$$\zeta = \frac{\beta r}{(\beta k a)^{\frac{1}{2}}} = 4.43 \times 10^{-5} \lambda^{-\frac{1}{2}} r \quad . \quad . \quad (9.5)$$

or

$$4.43 \times 10^{-2} \lambda^{-\frac{1}{2}} D$$

where a is the radius of the earth and k is a factor of $4/3$ to allow for refraction as mentioned on p. 416. All lengths are in metres except D which is in kilometres.

Introducing the shadow factor modifies equation (9.4) to

$$E_{mV} = \frac{300 \sqrt{(\eta P)}}{D} F(h) A_1 A_2 \quad . \quad . \quad (9.6)$$

The curves of Fig. 9.10 show the shadow factor A_2 for two extreme cases. Curve (1) is for a perfectly conducting earth and curve (2) for a perfect dielectric earth (curve (2) also holds for *horizontal* polarization with *all* types of earth). Intermediate cases are difficult to derive though a set of graphs from which the shadow curves of such cases may be deduced have been published by Burrows and Gray.⁽²³⁴⁾ The situation may be summarized as follows (vertical polarization is assumed in all cases)—

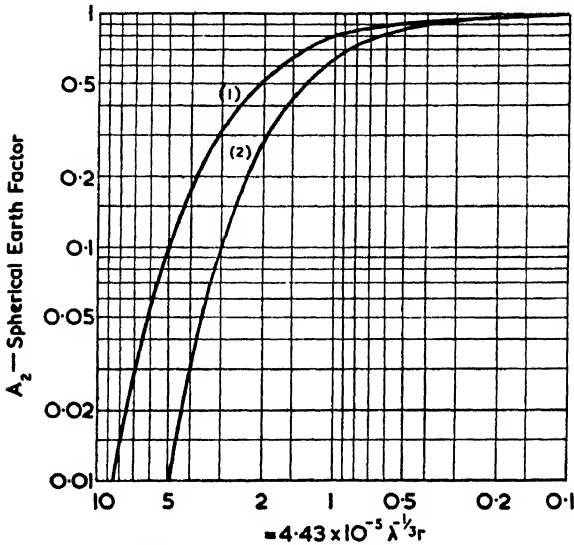
- (i) Curve (1) is accurate for long waves over sea-water.
- (ii) Curve (1) is fairly accurate for long waves over good conducting ground or for medium waves over sea-water.
- (iii) Curve (1) is a *rough* approximation for long waves over badly conducting ground, or for medium waves over

good conducting ground. (In such cases the exact curve does not necessarily lie between curves (1) and (2), but may lie outside the (1) curve in some regions.)

(iv) For medium waves and poor ground conductivity the exact curve lies between (1) and (2).

(v) For short waves curve (2) is a fair approximation.

(vi) For ultra-short waves curve (2) is almost exact.



- (1) Vertical Polarization if earth is perfect conductor
 (2) Vertical Polarization if earth is perfect dielectric
 or Horizontal Polarization for any ground constant

FIG. 9.10. SHADOW FACTOR CURVES FOR IDEALIZED EARTH CONSTANTS
 (Burrows and Gray, *Proc. I.R.E.*, Jan., 1941)

Fortunately the shadow factor is mainly required for medium- and long-wave propagation over sea water, in which case curve (1) applies with good accuracy.

Field strength curves allowing for the curvature of the earth were published by Norton⁽²⁶⁹⁾ and are reproduced here in Figs. 9.11, 9.12 and 9.13. In every case the antenna is assumed to have a horizontal figure of merit of 300 mV/m at 1 km—this corresponds to the case of a short vertical radiator ($h < \lambda/10$) whose dead-loss resistance is negligible in comparison with the radiation resistance. The ground conductivity may be estimated from the table given in Appendix I, p. 475.

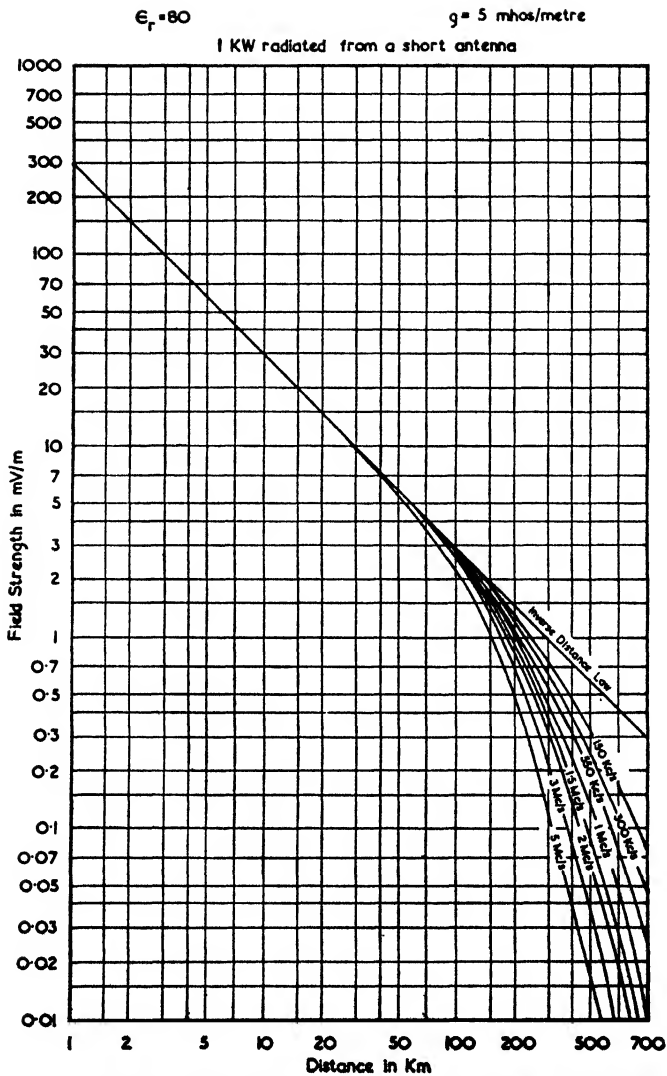


FIG. 9.11. FIELD STRENGTHS OF A VERTICAL RADIATOR—TRANSMISSION OVER SEA-WATER
(Norton, *Proc. I.R.E.*, Oct., 1936)

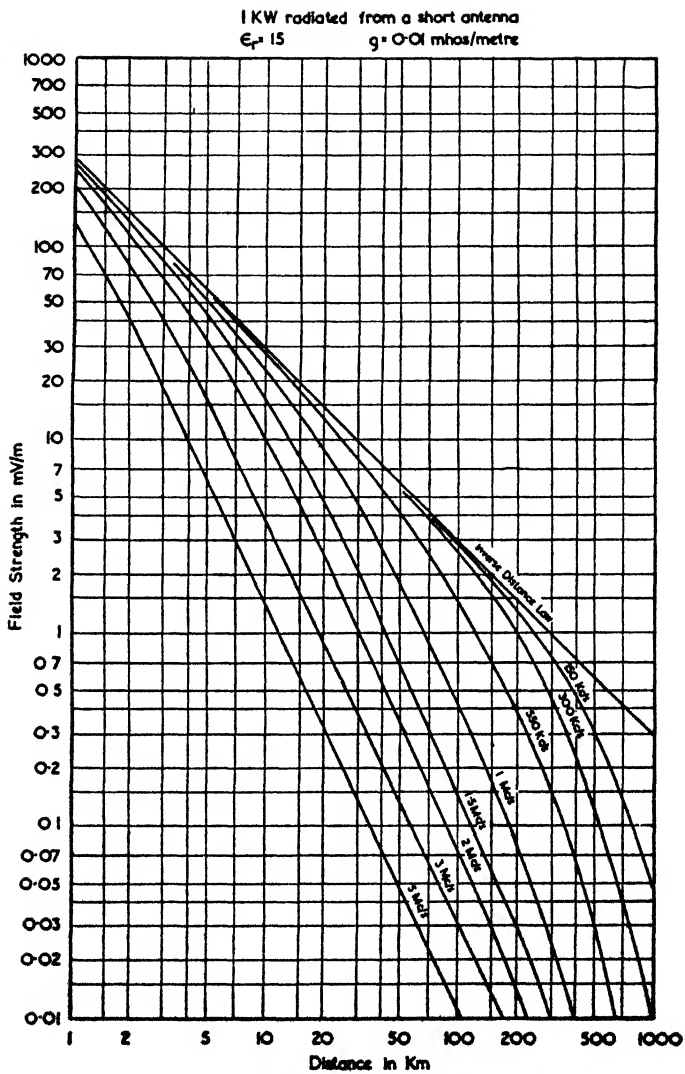


FIG. 9.12. FIELD STRENGTHS OF A VERTICAL RADIATOR—TRANSMISSION OVER SOIL OF GOOD CONDUCTIVITY
 (Norton, *Proc. I.R.E.*, Oct., 1936)

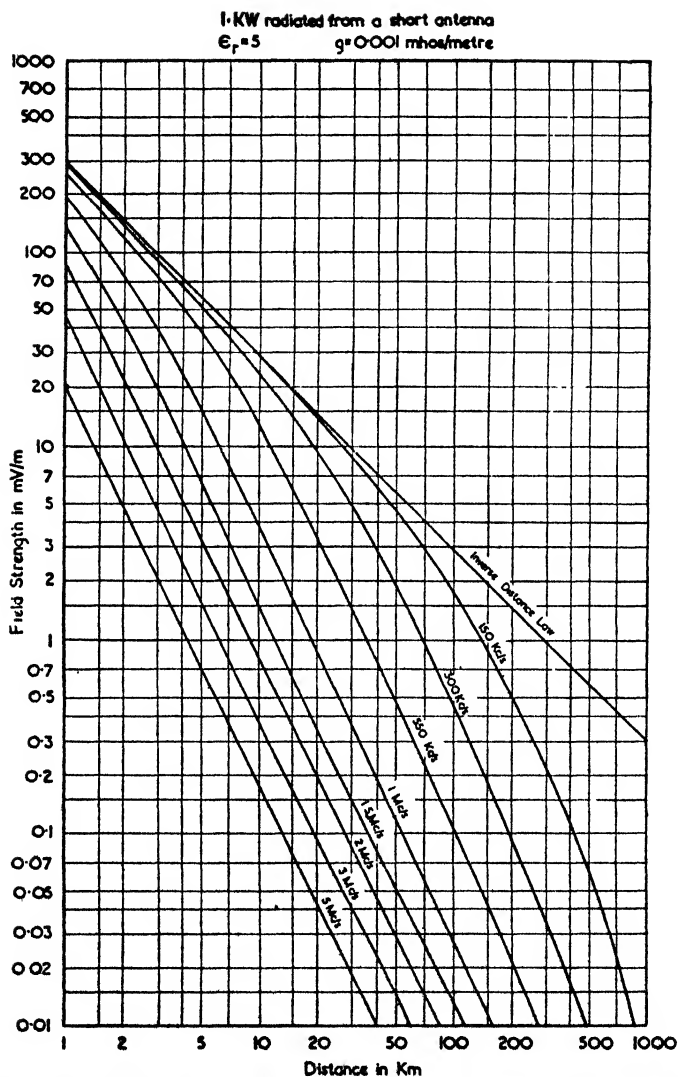


FIG. 9.13. FIELD STRENGTHS OF A VERTICAL RADIATOR—TRANSMISSION OVER SOIL OF BAD CONDUCTIVITY
 (Norton, *Proc. I.R.E.*, Oct., 1936)

Calculation of Fade-free Radius

In order to make an estimate of the probable fade-free radius of a broadcasting station, some assumption must be made as to the minimum permissible ratio of direct to indirect radiation. The highly arbitrary nature of such an assumption will be realized when one considers that the true criterion is whether or not the average listener would notice the fading—a feature which depends on the receiver, the receiving antenna, the ground constants and a number of other factors—quite apart from the psychological aspects of the problem.

It is therefore customary to take some arbitrary ratio such as 2 : 1 or 3 : 1 for the minimum direct to indirect field

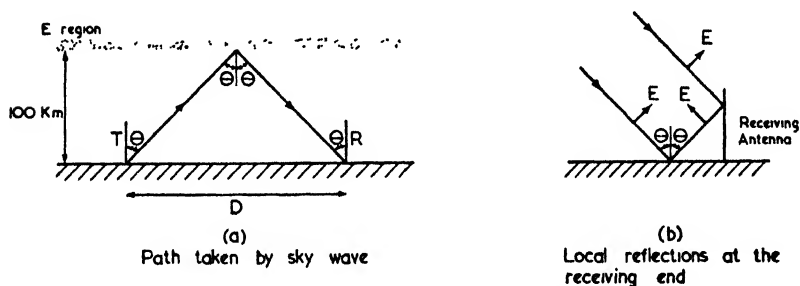


FIG. 9.14. GEOMETRY OF SKY WAVE FOR FADE-FREE RADIUS CALCULATIONS

strengths. It will be found that the calculated fade-free radius does not vary much with the assumed ratio, for the field strength along the ground falls off fairly rapidly at such distances whereas the sky-wave signal increases rapidly in the same region.

A more precise criterion is obtained by considering the induced e.m.f.'s in the antenna, in which case the effective field strength of the sky wave is doubled and multiplied by $\sin \theta$ (when $D = 100$ km, $\theta = 30^\circ$, and the two criteria coincide). This process allows for the ground reflections from the sky wave (such reflection is absent in the case of the surface wave). The geometry of the problem is shown in Fig. 9.14 (a) and (b). If the receiving antenna is short in comparison with a wavelength, the direct and reflected components of a vertically polarized sky wave augment each other in a vertical direction but cancel in a horizontal direction. The correctness of assuming that the reflected ray is due to a "positive image" can be judged by an examination of the curves in Figs. 9.34

and 9.35. From these curves we see that this is a reasonable approximation for wavelengths above 200 m and values of θ below 75° —provided the ground conductivity is not very low.

The case of a vertically polarized sky wave gives the greatest possible interference, and in these circumstances the induced e.m.f. due to the sky wave is given by

$$e_2 = 2E_2h_e \sin \theta$$

where E_2 = field strength of sky wave,
 h_e = effective height of receiving antenna.

The corresponding surface wave e.m.f. is

$$e_1 = E_1h_e$$

where E_1 = field strength of surface wave.

Hence
$$\frac{e_1}{e_2} = \frac{E_1}{2E_2 \sin \theta} \quad (9.7)$$

If we take our definition of fade-free radius to be such that $e_1/e_2 = 2$, then the worst possible fluctuations in the total signal strength will be 3 : 1.

The relative strength of the sky wave is determined from the vertical polar pattern of the transmitting antenna, and a reflection coefficient of unity may be assumed for the E layer in order to take the most unfavourable case.

The polar pattern of the transmitting antenna is given by the curves of Fig. 2.29 so that the induced e.m.f. due to the sky wave is

$$e_2 = \frac{600\sqrt{(\eta P)}}{D} F(h)F(\theta) \sin^2 \theta h_e \text{ millivolts} \quad (9.8)$$

where $F(h)$ = relative horizontal field strength (Fig. 2.28),
 $F(\theta)$ = standardized polar coefficient (Fig. 2.29),
 θ = angle of incidence (Fig. 9.14).

Of the two “ $\sin \theta$ ” factors in the above equation one is due to the resolution in a vertical direction, the other is due to the total path length being equal to $D \operatorname{cosec} \theta$. Taking the E layer to be 100 km high and assuming a negligible path length in the layer itself, we have the simple relationship

$$\theta = \tan^{-1} \frac{D}{200} \quad (9.9)$$

This is shown plotted in Fig. 9.15 over the range which is of interest in practical computations.

The surface-wave induced e.m.f. corresponding to (9.8) is

$$e_1 = \frac{300\sqrt{(\eta P)}}{D} F(h) A_1 A_2 h_e \text{ millivolts} \quad (9.10)$$

Since the determination of the fade-free radius depends on the ratio of (9.8) to (9.10), it would be possible to eliminate the common factors in these two expressions, but we are also interested in the absolute field strengths so that in practice it

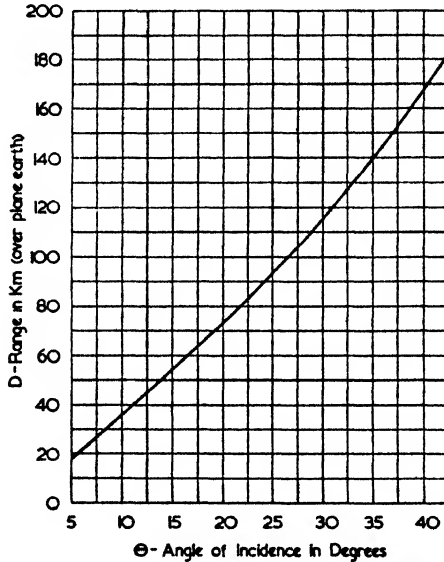


FIG. 9.15. ANGLE OF INCIDENCE OF SKY WAVES REFLECTED FROM THE E LAYER

is preferable to work out both equations expressing the results in effective field strengths, i.e. we put $h_e = 1$ m. A useful short cut, however, may be taken when comparing different anti-fade antennae by keeping $F(h)$ constant. This does not cause much error in the field strength curves and has the advantage that the ground-wave curves need not be redrawn for every small change in antenna height.

The curves of Fig. 9.16 give the ground- and sky-wave fields for determining the fade-free radius of a transmitter working on a wavelength of 550 m and a radiated power of 1 kW. All the curves are based on a value of $F(h)$ of 1.33, i.e. $E_{m\gamma} D / \sqrt{P} = 400$, so that the absolute scale is 25 per cent too high for a short antenna and a few per cent too low for a

0.57λ antenna. In order to determine when the ratio of ground to sky wave is 3 : 1, the effective value of the sky wave should be multiplied by 3, then the fade-free radius for the given conditions is determined simply by the intersection of

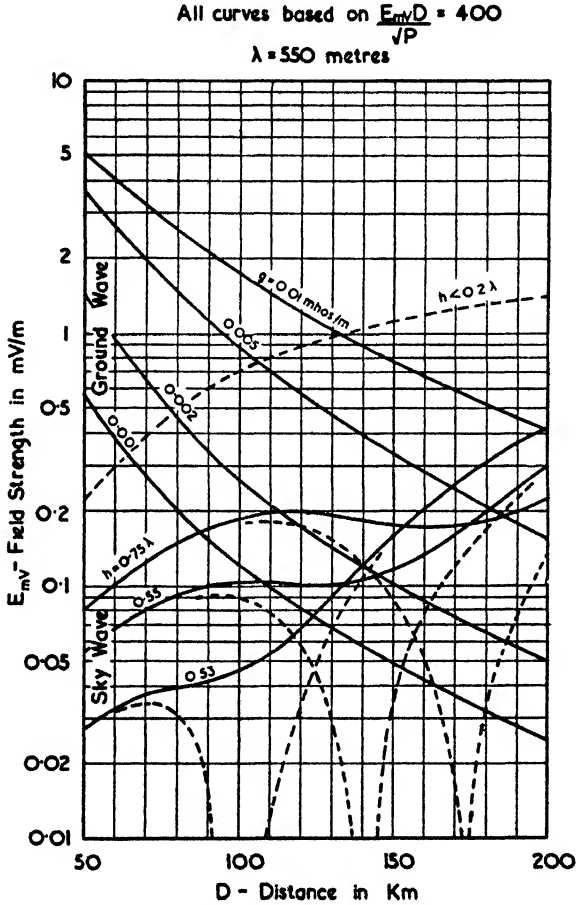


FIG. 9.16. PROPAGATION CURVES SHOWING THE VARIATION OF FADE-FREE RADIUS WITH GROUND CONDUCTIVITY, $\lambda = 550$ M

the ground- and sky-wave curves. It should be noted that these curves assume 100 per cent reflection in the ionosphere—in some publications 33.3 per cent or 50 per cent reflection is assumed, in which case the stipulated ratio is made correspondingly higher.

The great increase in fade-free radius resulting from the use

of antennae of heights of the order of 0.55λ is at once apparent from these curves. Also it will be noticed that when the ground conductivity is high, the best anti-fade antenna has a height of 0.57λ , but for poorer ground conductivity such a height

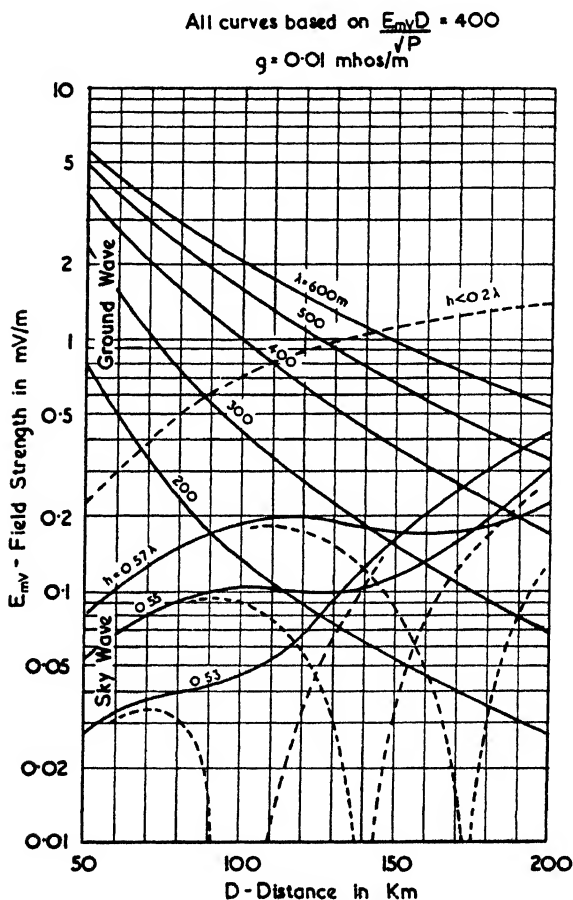


FIG. 9.17. PROPAGATION CURVES SHOWING THE VARIATION OF FADE-FREE RADIUS WITH WAVELENGTH, $g = 0.01$ MHOS/M

actually results in a decrease of the fade-free radius in comparison with a 0.53λ antenna. The optimum height therefore depends on the ground conductivity.

At the other extreme of the medium-wave broadcasting band the fade-free radius is much decreased due to the increased ground attenuation, and the optimum antenna heights

are lower for a given ground conductivity. Both these characteristics are illustrated by the curves of Fig. 9.17, which are for various wavelengths between 200 and 600 m.

The sky-wave curves in Figs. 9.16 and 9.17 assume a uniform mast radiator whose length is at least 50 times its breadth. With an idealized sinusoidal current distribution a typical sky-wave curve would resemble the dotted line in Fig. 9.18,

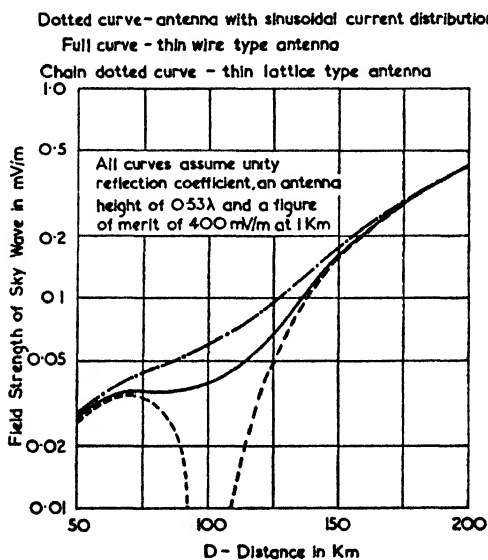


FIG. 9.18. COMPARISON OF SKY-WAVE CURVES FOR SINUSOIDAL AND PRACTICAL ANTENNA CURRENT DISTRIBUTIONS

but with a practical current distribution the curve will be modified as shown in curves (b) and (c). These show that the zero in the dotted curve is filled in to an extent depending on the type of mast.

Sky-wave Propagation

Beyond the region of fading due to interference between the surface and sky waves there is a region served by sky waves only. This may be termed the far-zone (the near-zone being the region of good surface-wave field strength). In this zone the broadcast service is only of second-rate quality though even this can be of distinct value in large sparsely populated countries. The various zones are illustrated in Fig. 9.19.

The far-zone comes into operation only during the night time for during the day the medium waves are strongly

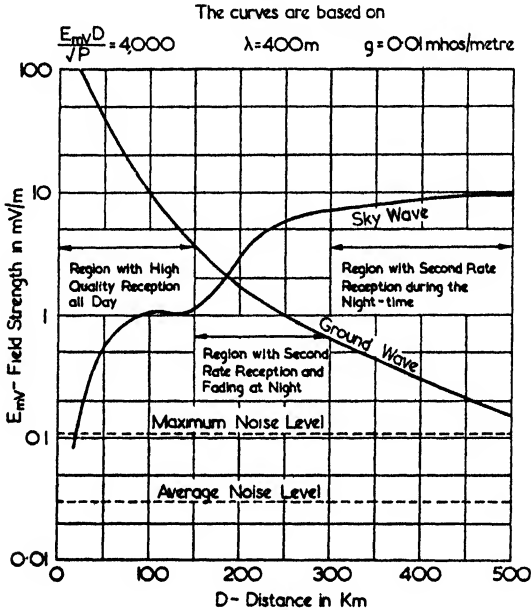


FIG. 9.19. THE SERVICE ZONES OF A TYPICAL BROADCAST STATION

absorbed in the lower regions of the ionosphere. A scale drawing of E layer reflections is given in Fig. 9.20, in which an allowance has been made for the fact that the waves

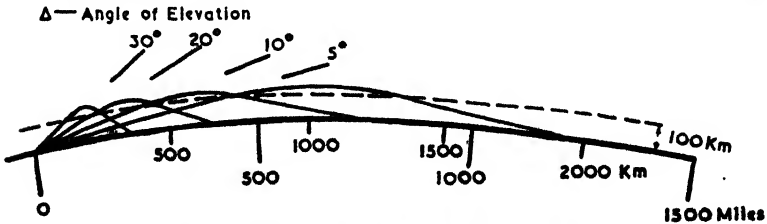


FIG. 9.20. PATHS TAKEN BY RAYS REFLECTED FROM THE E LAYER

penetrate into the ionosphere to varying degrees, depending on the angle of incidence.

A good deal of experimental data has been collected on the field strengths of the sky wave and this has been summarized

by the C.C.I.R. (International Radio Consultative Committee). The summary is shown in Fig. 9.21, together with two ground-wave propagation curves based on an earth conductivity of $g = 0.01$ mhos/m.

The sky-wave curves are for "quasi-maximum" values, that is to say, they give the value which is exceeded instan-

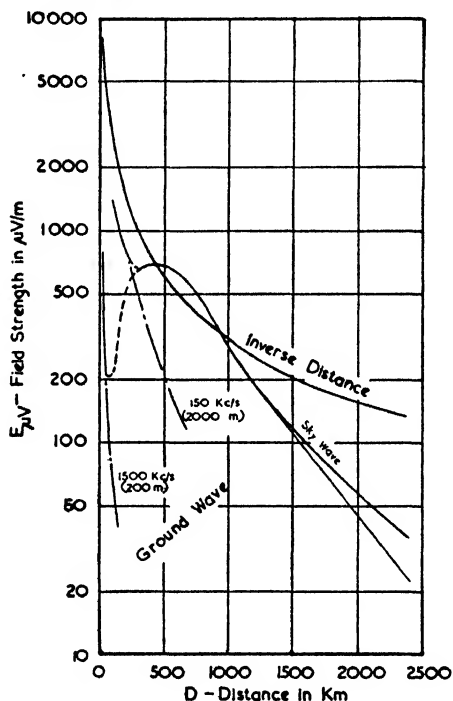


FIG. 9.21. NIGHT-TIME FIELD STRENGTHS IN THE FAR ZONE OF A MEDIUM-WAVE TRANSMITTER
(C.C.I.R. Report, Proc. I.R.E., Oct., 1938)

taneously about 5 per cent of the time. The "medium values," which are defined as the field strengths exceeded instantaneously 50 per cent of the time, are about 0.35 of the quasi-maximum values.

There are two sky-wave curves, one for propagation not close to the magnetic poles (mostly north-to-south transmissions), the other for propagation near the magnetic poles (mostly east-to-west transmissions).

It will be noticed that between 500 and 1 000 km the sky wave actually exceeds the values given by the inverse distance

law. This apparent violation of the fundamental laws of propagation is due to the trapping of the waves between the ionosphere and the ground which prevents the wavefront from expanding in the normal manner. Another way of looking at the phenomenon is to consider the increase in the effective field due to ground reflections (as was done in deriving equation (9.7)). This point of view also indicates in a crude way the range over which the inverse square law is likely to be exceeded since—

(a) at distances of less than 500 km the vertical resultant is smaller and also the radiation from the antenna is somewhat less;

(b) at distances in excess of 1 000 km the angle of incidence is as great as the Brewster angle or even greater, so that the ground reflections no longer augment the downcoming rays.

9.4. SHORT WAVES

With but few exceptions, radio waves whose wavelengths lie between 10 and 100 m are used for propagation via the ionosphere. This is because at these wavelengths the surface wave is weak (even with vertical radiators) while, on the other hand, it is not feasible to erect antennae which are several wavelengths above the ground—as is done at still shorter wavelengths. In short-wave propagation the earth is therefore used merely as a reflector to aid in projecting the radio beam upwards at some suitable angle. Also, in the case of multiple hops, the earth acts as the lower reflecting surface between the points of transmission and reception.

For the few cases in which short-wave transmissions are used with vertical radiators to obtain as good a surface wave as possible, the range may be determined in the manner outlined in the previous section for medium- and long-wave transmissions.

The design of a long-distance short-wave system requires a knowledge of the following—

1. The great-circle distance between the points of transmission and reception.
2. The bearing of the point of reception.
3. An estimate of the angle of fire in the vertical plane to give a downcoming ray directed at the point of reception.
4. The horizontal beam width needed to give adequate coverage of the district over which reception is required (or,

in the case of point-to-point communication systems, to give sufficient margin to allow for deviations from the great-circle route).

5. The critical frequency of the ionosphere or, what is the practical equivalent, the maximum usable frequency for the range in question. In either case the values are those at the point of reflection. For multihop transmission the *lowest* critical frequency at any of the points of reflection is the required value.

Great-circle Distances and Bearings

It is not possible to develop the surface of a sphere on a flat sheet of paper—that is to say, if the surface of a globe could be cut and detached it would not be possible to lay any finite portion of it on a flat surface. Therefore the basis of all map construction is the projection of the sphere on a surface which is capable of development. A suitable surface is a conical one and this is usually used in a modified form called *Lambert's Projection* in which the cone passes through two lines of latitude (known as the “standard parallels”). The standard parallels are naturally chosen to lie towards the top and bottom of the area which is to be charted. The compromise thus effected is very satisfactory for areas even as large as the United States, for which the maximum scale error is less than 3 per cent, and generally less than $\frac{1}{2}$ per cent. Moreover, a straight line on this projection may be taken as a great circle for maps up to the size mentioned above.

If the distances involved are too great for a map to be used, both great-circle distances and bearings may be found from a gazetteer by the use of spherical trigonometry. The appropriate formulae are as follows—

$$\cos D_{AB} = \sin L_A \sin L_B + \cos L_A \cos L_B \cos LO_{AB} \quad (9.11)$$

$$\sin B_{AB} = \cos L_B \operatorname{cosec} D_{AB} \sin LO_{AB} \quad (9.12)$$

$$\sin B_{BA} = \cos L_A \operatorname{cosec} D_{AB} \sin LO_{AB} \quad (9.13)$$

where D_{AB} = great-circle distance in degrees and minutes
(1 minute = 1 nautical mile = 1.853 km),

$L_{A, B}$ = latitude of station *A* or *B* (positive for N and negative for S latitudes respectively),

LO_{AB} = difference in longitude between *A* and *B*
(positive for bearings E of N),

$B_{AB, BA}$ = bearing of *B* from *A* or of *A* from *B* (positive direction being clockwise).

Taking, for example, London ($51^{\circ} 31' N$, $0^{\circ} 6' W$) and New York ($40^{\circ} 43' N$, $74^{\circ} 1' W$), we have

London to New York = $50^{\circ} 7' = 5\,570$ km

Bearing of New York from London = $288^{\circ} 24'$

Bearing of London from New York = $51^{\circ} 11'$

For many purposes it is convenient to use a globe and paste a transparent piece of material marked out in degrees over the point of transmission, then both great-circle distances and bearings may be found roughly, but very quickly, with the aid of a piece of string. By such means it is easy to observe

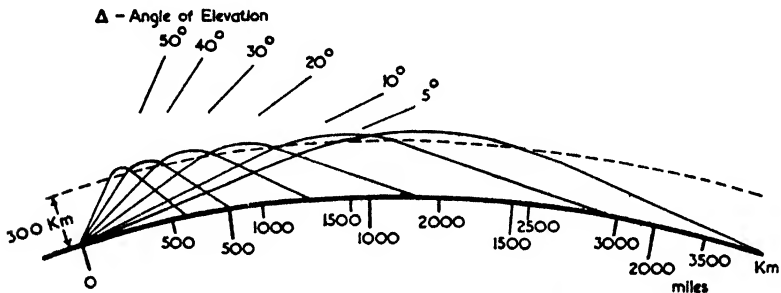


FIG. 9.22. PATHS TAKEN BY RAYS REFLECTED FROM THE F LAYER

the coverage obtained for broadcast services with different degrees of horizontal beam width.

A globe also has the advantage that the local time at the point, or points, of reflection can readily be noted—for they are usually marked with meridian lines every 15° , i.e. at intervals which are equivalent to one-hour intervals in time.

The range of the ionosphere wave can be noted directly on the globe by means of a piece of cardboard cut out and marked as shown in Fig. 9.22.

Angle of Fire in the Vertical Plane

The angle of fire in the vertical plane is given by Fig. 9.22, which also has a curvature suitable for a 19 in. diameter globe. These ranges are based on the assumption of a reflecting layer at a height of 300 km, and an allowance based on the work of Appleton and Beynon⁽²²³⁾ has been made for the distance travelled in the ionosphere itself. For short distances no great

error is made by assuming immediate reflection at the ionized layers.

On long-distance transmissions the strongest signal may actually be due to a ray which has made several hops. This would be noticed by a high angle of arrival for the maximum signal. Studies of the angle of arrival have been made and

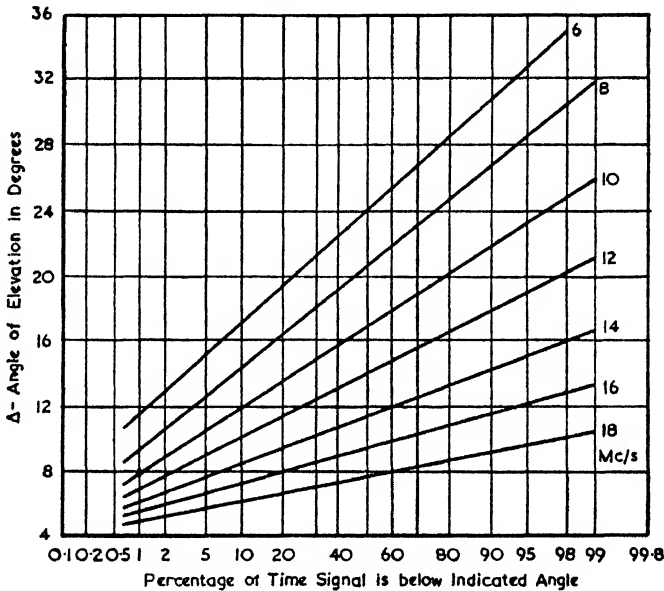


FIG. 9.23. ANGLE OF ARRIVAL OF TRANSATLANTIC SHORT-WAVE SIGNALS (Friis, Feldman and Sharpless, *Proc. I.R.E.*, Jan., 1934)

graphed on a statistical basis of which Fig. 9.23 is an example. In the latter figure it is apparent that the lower frequencies tend to arrive at higher angles—a feature which happens to be allowed for automatically in the polar characteristics of a rhombic receiving or transmitting antenna.

In view of the uncertainty of the optimum angle of fire and the variations which take place in the ionosphere, the beam width in a vertical plane of the polar diagram of transmission should not be too narrow. The beam produced by a typical rhombic antenna with sides a few wavelengths long is quite sharp enough for practical purposes.

For reflections from the E layer (at a height of 100 km) the corresponding curves to those of Fig. 9.22 are given in Fig. 9.20. In long-distance transmissions E-layer reflections come into

play only over a period of a few hours on either side of a summer noon, when the effect is to increase the maximum usable frequency by 10 to 30 per cent for distances between 500 and 1 500 km. Use of the E layer demands a shallower angle of fire for the best results, but this angle is usually fixed for a given antenna system at a given frequency, so in practice nothing can be done about it since the overall design will be based on F_2 layer reflections.

Horizontal Beam Width

Even when point-to-point communication is desired, the horizontal beam width of the transmitted radiation must not be too narrow. It has been found in practice that the horizontal angle of arrival of long-distance signals can show appreciable departures from the great-circle path. Observations made by Feldman⁽²⁴⁷⁾ showed that during periods of severe magnetic storms (which, almost invariably, have their counterpart in the ionosphere) the best signals from England arriving at New York were received from a south-easterly direction. The explanation lies in the fact that scattering of signals can take place from the ionosphere at such angles that the transmission "turns corners" and so arrives at the receiving end from an entirely unexpected angle. Such scattering is normally far too weak to rival the main signal, but during periods of great absorption on the great-circle path the scattered signal may actually be stronger. In the case quoted the great-circle path was nearer the polar regions where magnetic storms are more intense and frequent than elsewhere.

When a broadcast service over a whole country is required, the horizontal beam width is made wide enough to cover the whole area with only a few decibels of attenuation in that part of the polar pattern which is directed at the angular extremities of the country. The final choice of polar pattern depends on the distribution of the population in the country to be served and a number of other factors of an economic nature.

Maximum Usable Frequency

The term *maximum usable frequency* was explained in § 1.4, where it was defined as the highest frequency for which a single-hop transmission could be secured between two stations. This frequency, f_m , is related to the critical frequency, f_c , for vertical

incidence at the mid-point of the transmission path by the secant law, that is

$$f_m = f_c \sec \theta \quad (9.14)$$

where θ = angle of incidence at the ionized layer.

The relationship between θ and Δ , the angle of elevation of the transmitted ray, is given by

$$\cos \Delta = \left(1 + \frac{h}{a} \right) \sin \theta \quad (9.15)$$

where h = height of reflecting layer,
 a = radius of earth in same units as h .

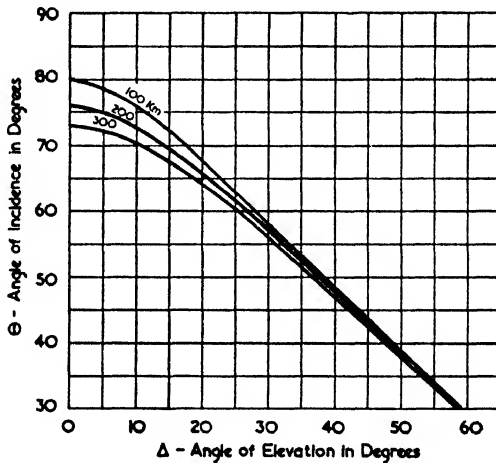


FIG. 9.24. ANGLE OF INCIDENCE AT A REFLECTING LAYER IN THE IONOSPHERE FOR A RAY HAVING A GIVEN ANGLE OF ELEVATION FROM THE GROUND

Fig. 9.24 shows the relationship for different values of h , from which we see that even if a radio beam is transmitted tangentially to the earth the maximum angles of incidence for the E and F_2 layers are 80° and 73° respectively.

The range of transmission, D , is related to h and θ as follows (see Fig. 9.25) —

$$\cos^2 \theta = \frac{(h + D^2/8a)^2}{(h + D^2/8a)^2 + D^2/4} \quad (9.16)$$

In evaluating the above expression, use has been made of the fact that for all practical values of D we can put $\sin D/2a = D/2a$. Together with (9.14) we have all the relevant data for obtaining f_m in terms of f_c , D and h . The relationship in terms of D is shown by the dotted lines of Fig. 9.26 for $h = 100$ and 300 km.

The above theory would be complete were it not for the fact that in practice—except for the case of sporadic E reflections—the reflecting boundary is never sharp. Therefore the

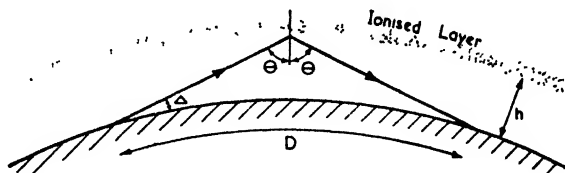


FIG. 9.25. DIAGRAM FOR EQUATIONS (9.15) AND (9.16)

rays actually travel for some distance into the ionized layer. In order to take account of this fact it is necessary to postulate some law for the vertical distribution of ionization—a suitable choice is a parabolic distribution. With this assumption

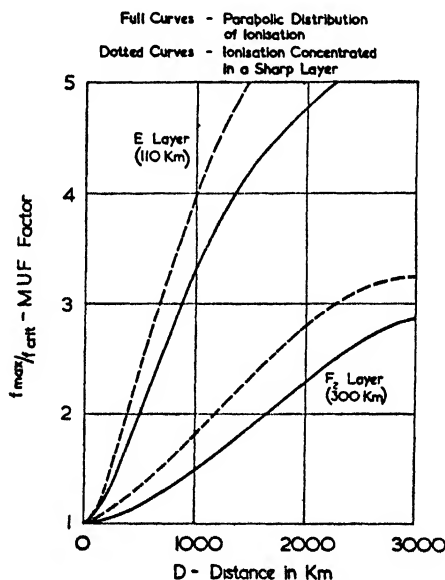


FIG. 9.26. VARIATION OF M.U.F. FACTOR WITH DISTANCE
(Appleton and Beynon, *Proc. Phys. Soc.*, July, 1940)

Appleton and Beynon⁽²²³⁾ have obtained sets of curves showing the M.U.F. factor (i.e. f_m/f_o) for different distances. Two typical curves of theirs are given by the solid lines in Fig. 9.26.

Multiplying the M.U.F. factor by the measured or predicted critical frequencies gives the final practical form of such curves

as shown in Figs. 9.27 to 9.31. The critical frequency varies not only with time but also with latitude and even with longitude. Only recently has sufficient data been acquired to give a fair indication of these variations with location. In Fig. 9.31 the curves are based on a study of available data showing the relative values of the critical frequencies (and therefore of the M.U.F.) at different latitudes. These curves are only a rough guide and as such will serve for all periods of the sunspot cycle. The variations with longitude are apparently due to the axis of the earth's magnetic field not coinciding with the axis of rotation, and at present the available data is too slight to permit generalizations.

The scale of relative critical frequencies in Fig. 9.31 has been chosen so that all curves pass through unity at latitude 40° . This is because for the majority of long-distance transmissions the latitude of Washington ($39^\circ 02' N$) is a better approximation than that of London. The Washington figures as given by the National Bureau of Standards have therefore been quoted in Figs. 9.27 to 9.30. They are reproduced here on a logarithmic scale, since it is very easy with such a scale to take any percentage of the M.U.F. Whenever the latitude at the point of reflection is appreciably different from 40° , a corrected curve should be prepared using Fig. 9.31 (for places in the Southern Hemisphere the reversal in the seasons must naturally be taken into account).

To use the M.U.F. curves we determine the difference between the local time and the time at the mid-point of the transmission path, then trace out the appropriate distance curve, having moved the top sheet bodily sideways by an amount equal to this time difference and upwards according to the percentage of the M.U.F. we wish to take.

Operating at the maximum usable frequency itself will cause the signal to be lost on some occasions. By taking 85 per cent of the M.U.F. greater certainty of communication is achieved, and by taking 50 per cent complete certainty could be obtained *were it not for absorption limitation setting in*. We therefore have to choose some percentage between the two limits mentioned and bias the choice according to the individual circumstances of the case. In order to show both 85 per cent and 50 per cent limits we draw in two sets of curves appropriate to these limits. When more than one hop is concerned we do the same thing for each point of reflection and finally take the lowest frequencies of the combined curve (i.e. where more than one

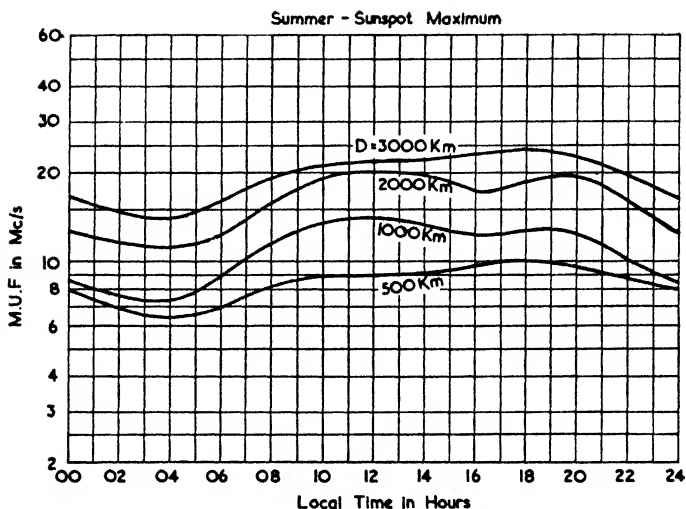


FIG. 9.27. THE DIURNAL VARIATION OF THE MAXIMUM USABLE FREQUENCY FOR LATITUDE 40° N, SUMMER, SUNSPOT MAXIMUM (National Bureau of Standards, 1940)

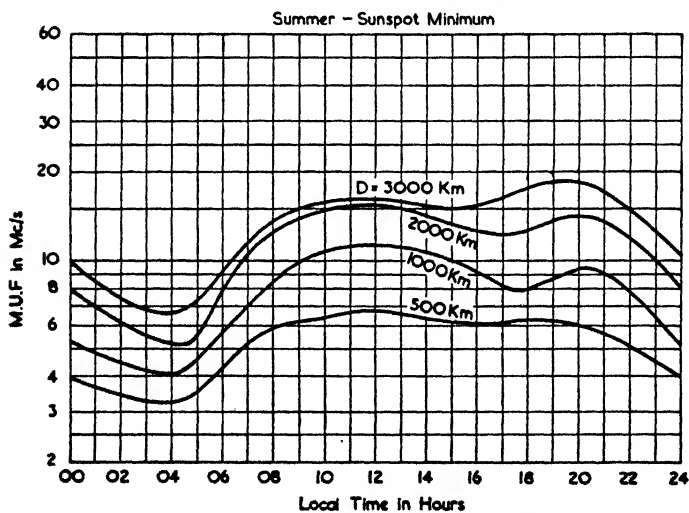


FIG. 9.28. THE DIURNAL VARIATION OF THE MAXIMUM USABLE FREQUENCY FOR LATITUDE 40° N, SUMMER, SUNSPOT MINIMUM (National Bureau of Standards, 1940)

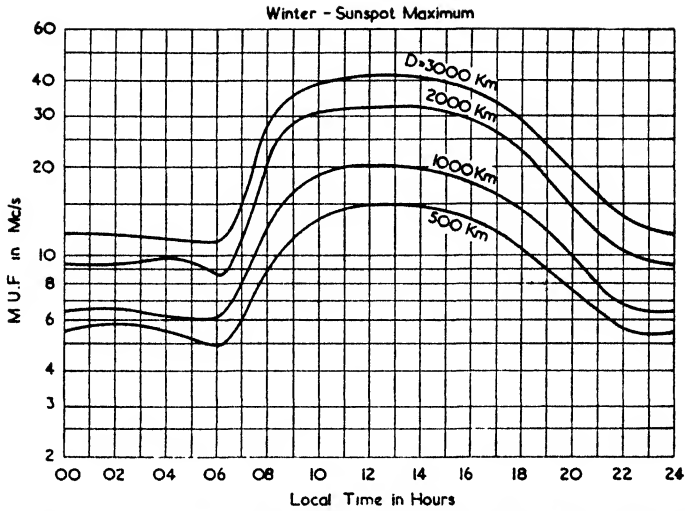


FIG. 9.29. THE DIURNAL VARIATION OF THE MAXIMUM USABLE FREQUENCY FOR LATITUDE 40° N, WINTER, SUNSPOT MAXIMUM (National Bureau of Standards, 1940)

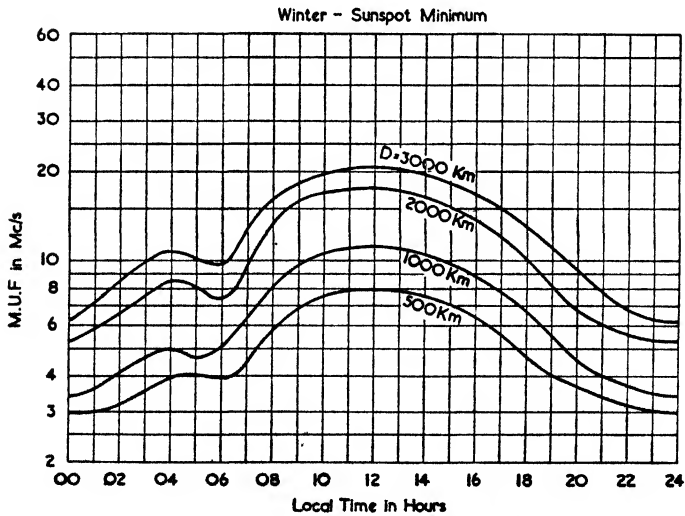


FIG. 9.30. THE DIURNAL VARIATION OF THE MAXIMUM USABLE FREQUENCY FOR LATITUDE 40° N, WINTER, SUNSPOT MINIMUM (National Bureau of Standards, 1940)

frequency is indicated the lowest is chosen). Whenever the combined curves show an appreciable range in frequency for some time of the day it is obvious that the transmission will be inferior—for when the selected frequency is reflected from the point which has the highest M.U.F. there will be appreciable absorption.

The published M.U.F. curves always refer to the *ordinary* ray. Thus a margin of safety is provided in the case of F_2 layer

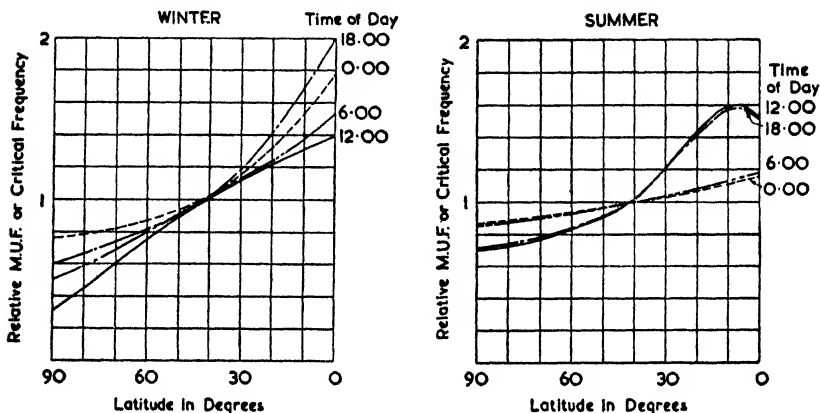


FIG. 9.31. LATITUDE CORRECTION FACTORS FOR CRITICAL AND MAXIMUM USABLE FREQUENCIES

reflections, since the critical frequency of the extraordinary ray in the F_2 layer is about 0.7 Mc/s higher than that of the ordinary ray. The exact relation between the critical frequencies is given by the following equation—

$$f_{ord}^2 = f_{ext}^2 - f_{ext}f_H$$

where f_H = gyro-frequency (1.3 Mc/s over England).

The extraordinary ray is much weaker with E-layer reflections because of the relatively high absorption due to the critical frequencies being nearer the gyro-frequency.

9.5. ULTRA-SHORT WAVES

General Features

At wavelengths below 10 m the propagation under normal circumstances is due entirely to the space wave, for the surface and the sky waves are either negligible or non-existent.

The criterion as to whether or not the surface wave may be neglected depends on the heights of the transmitting and receiving antennae. The surface wave may be neglected if both the heights exceed the following values—

$$\text{Vertical Polarization } h_T, h_R > \frac{\lambda}{4} |\epsilon'|^{\frac{1}{2}} \quad (9.17)$$

$$\text{Horizontal Polarization } h_T, h_R > \frac{\lambda}{4} |\epsilon'|^{-\frac{1}{2}} \quad (9.18)$$

where h_T and h_R = height of transmitting and receiving antenna respectively,

ϵ' = complex dielectric constant of the ground.

The above expressions are based on the work of Norton⁽²⁷¹⁾ and are sufficiently accurate for practical work. They may be further summarized into the following rules of thumb—

1. For vertical polarization the surface wave may be neglected over *all types of soil* if both the transmitting and receiving antennae are at least one wavelength above the ground. The surface wave may also be neglected over *sea-water* if both antennae are at least x wavelengths above the water, where x is the wavelength in metres (the minimum height for any frequency is 2 wavelengths).

2. For horizontal polarization the surface wave may be neglected over *all types of ground* (including sea-water) if both transmitting and receiving antennae are at least one-eighth of a wavelength above the ground.

In all cases where the above conditions are fulfilled and there are no sky waves present, only the evaluation of the space wave need be considered in order to determine the field strength. This evaluation may be based on the methods of geometrical optics in many practical cases, and this involves finding the vector sum of the direct ray and the indirect ray which has been reflected off the ground. When such methods fail (i.e. for line-of-sight and below line-of-sight propagation) the calculation must take into account the diffraction round the earth's curved surface. A discussion of the field strength under these conditions is given in the next section.

The simple ray method becomes inaccurate if the angle the reflected ray makes with the ground is less than $(\lambda/2\pi ka)^{\frac{1}{2}}$ radians, where ka is the apparent radius of the earth on allowing for refraction and equals 8.5×10^6 m. This function is plotted in Fig. 9.32. The ray calculation will not be seriously in error for

angles which are only 60 per cent of those given by the above curve, but for still smaller angles the error becomes appreciable.

By way of example, it might be mentioned that in the case of the television service from Alexandra Palace ($\lambda = 7.2$ m, height of transmitting antenna = 100 m) the ray theory is accurate for all heights of receiving antennae up to a radius of 20 km. At a radius of 30 km, which represents roughly the

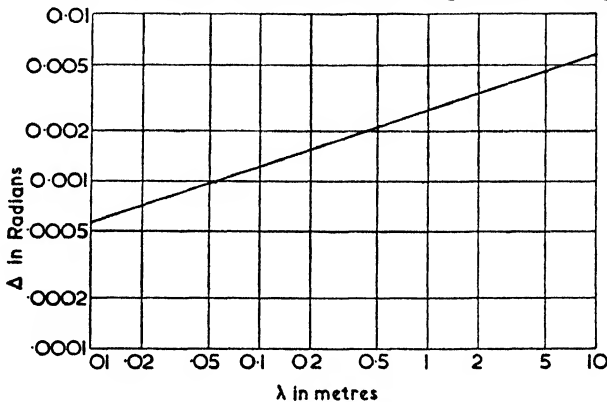


FIG. 9.32. GRAPH SHOWING THE SMALLEST ANGLE OF ELEVATION FOR WHICH RAY THEORY MAY BE ASSUMED

boundary for first-class reception, the ray theory still gives useful results.

Calculation of the Space Wave by Ray Theory

If ids is one of the current elements of an antenna (Fig. 1.9), then the field strength at P due to this element is given by the vector sum of the direct and indirect rays. In most practical cases, the difference in attenuation between the two rays due to their different path lengths is quite negligible; furthermore, the slight difference in their direction of polarization at the receiving end may also be overlooked. Consequently the field strength at P is given by

$$E = E_0(1 + R_{v,h} e^{-j\psi}) \quad (9.19)$$

where E_0 = field strength due to direct ray,

$R_{v,h}$ = reflection coefficient for vertical or horizontal polarization respectively,

ψ = numerical value of phase difference (in radians) between direct and reflected rays due to difference in path lengths.

The integration of the component field strengths due to each of the current elements may be simplified by assuming that the reflection coefficient does not vary with each element, i.e. by assuming that the source of radiation is concentrated at the centre of the transmitting antenna. With this assumption, equation (9.19) applies equally to the field due to the antenna as a whole if E_0 is the direct field due to the whole antenna. The polar pattern of the antenna must, however, be taken into account in cases where the directivity of the antenna system is great. Whether or not this latter refinement is necessary can easily be judged by computing the angular directions of the direct and reflected rays and noting the corresponding relative intensities of the vertical polar diagram of the antenna.

The value of $R_{v,h}$ is given in Vol. I by equations (3.52) and (3.53) for vertically and horizontally polarized waves respectively. Curves based on these formulae are shown in Figs. 9.33, 9.34 and 9.35 for ground conductivities similar to those used in Figs. 9.11 to 9.13.

In every case the value of R_v or R_h has phase as well as magnitude and may be expressed in the form $R_v = a_v e^{j\beta_v}$ or $R_h = a_h e^{j\beta_h}$. The phase angles are shown to a scale which represents the *phase advance* of the tangential component of the reflected electric field—the advantage of this convention is that it causes less confusion when dealing with field strength formulae. Another way of expressing the phase is to represent it as a *phase lag* on the perfect earth case (for which the horizontal electric components of incident and reflected rays are always 180° out of phase). The latter convention has the merit of being easier to remember since on purely physical grounds we should expect the phase to lag with imperfect conductivity, i.e. the charge movements on the surface lag with respect to the incident field when the conductivity is finite with the result that the re-radiation from them also lags. Diagrams illustrating the time phases of the electric vectors are given in Vol. I in Figs. 3.4, 3.5 and 3.6.

Although in Figs. 9.33 to 9.35 the phase angle of R_v is shown as approximating to 0° as $\theta \rightarrow 90^\circ$, the geometry of the case is such that the direct and reflected waves are actually tending to cancel each other (see, for example, Vol. I, Fig. 3.5 (b)). Thus for both vertically and horizontally polarized waves the reflection coefficients approximate, *in effect*, to -1 at angles near grazing incidence. This fact permits a useful

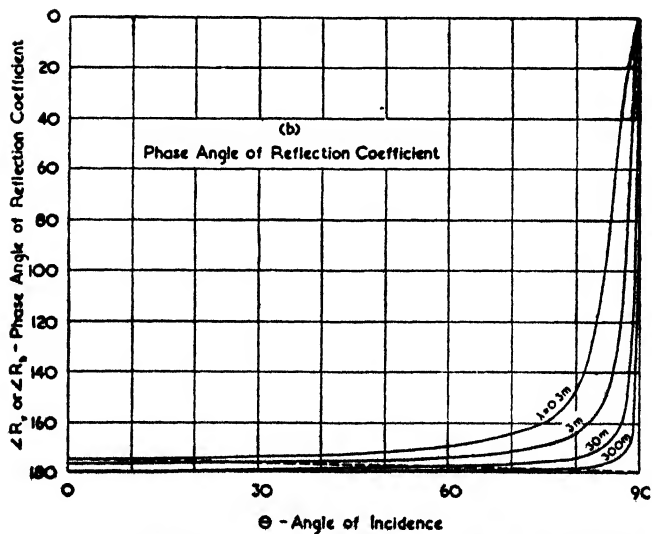
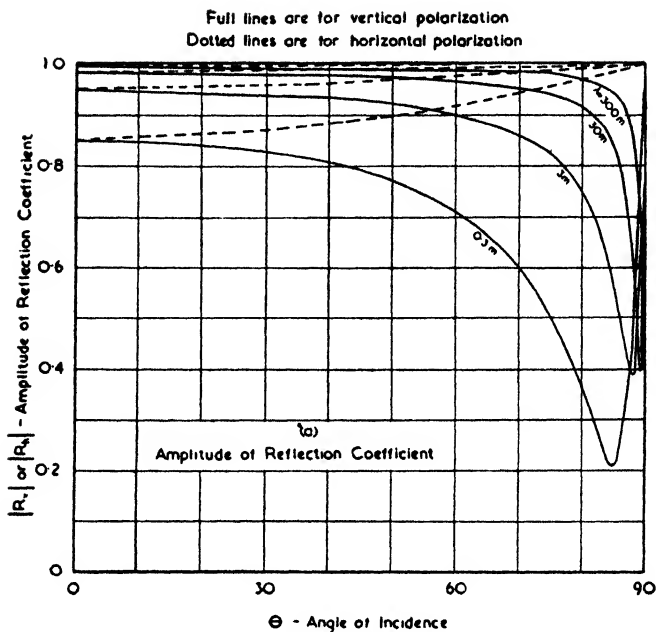


FIG. 9.33. VARIATION OF REFLECTION COEFFICIENTS WITH ANGLE OF INCIDENCE—SEA-WATER
 $\epsilon_r = 80, g = 5$ mhos/m.

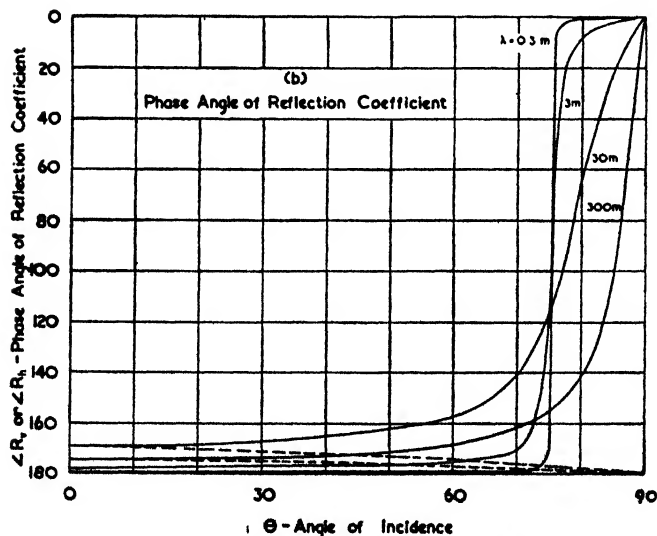
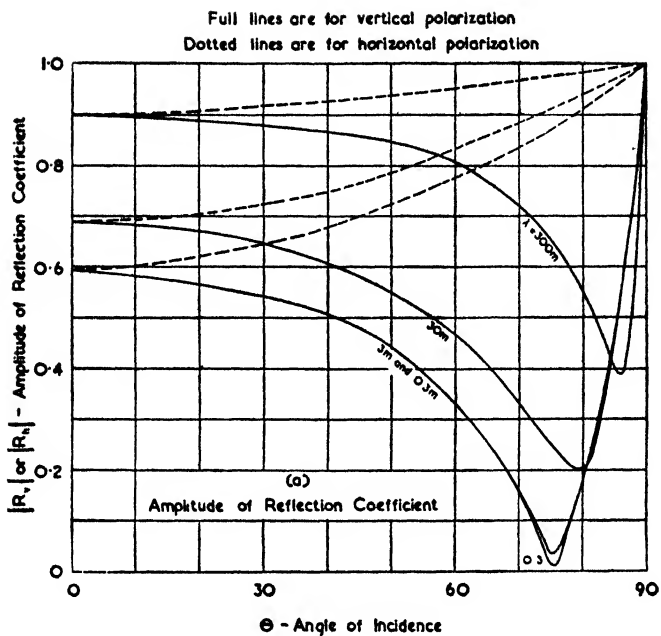


FIG. 9.34. VARIATION OF REFLECTION COEFFICIENTS WITH ANGLE OF INCIDENCE—SOIL OF GOOD CONDUCTIVITY

$$\epsilon_r = 15, \quad g = 0.01 \text{ mhos/m}$$

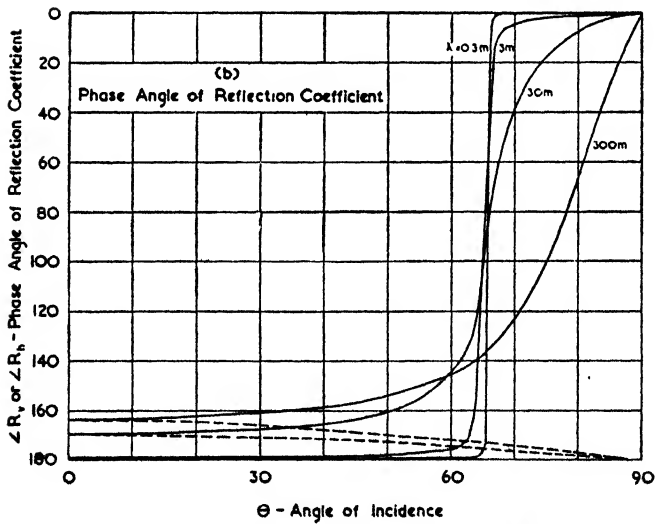
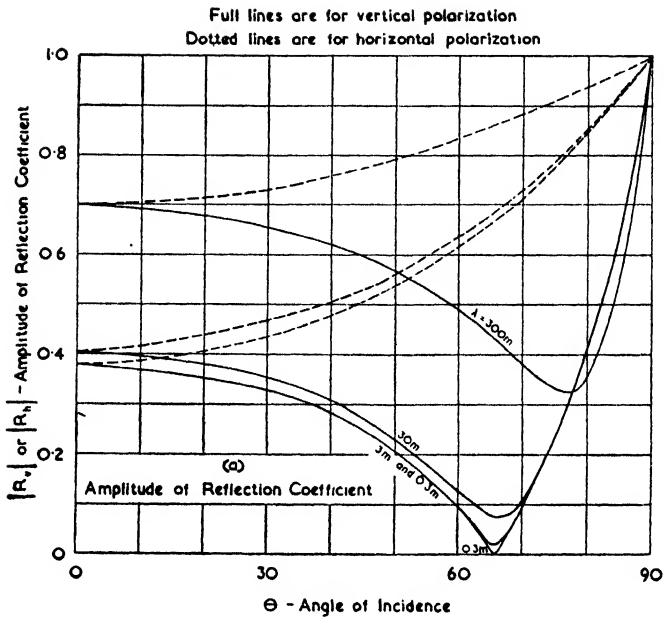


FIG. 9-35. VARIATION OF REFLECTION COEFFICIENTS WITH ANGLE OF INCIDENCE—SOIL OF POOR CONDUCTIVITY
 $\epsilon_r = 5, g = 0.001$ mhos/m

approximation to be made and leads to the simple field strength formula of equation (9.25) which is valid for a great many practical cases.

The geometry of the problem is shown in Fig. 9.36, from which we see that

$$r_1^2 = r^2 + (h_T - h_R)^2$$

$$r_2^2 = r^2 + (h_T + h_R)^2$$

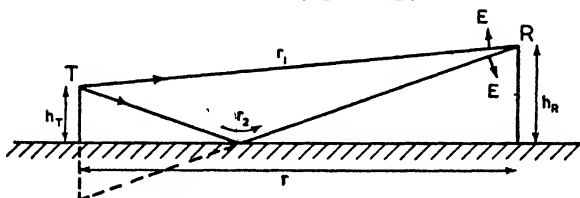


FIG. 9.36. DIAGRAM FOR SPACE-WAVE CALCULATIONS OVER A PLANE SURFACE

If $r \gg h_T + h_R$, which is true for most cases of practical interest, we have

$$r_1 = r + \frac{1}{2} \frac{(h_T - h_R)^2}{r}$$

$$r_2 = r + \frac{1}{2} \frac{(h_T + h_R)^2}{r}$$

Hence

$$\psi = \beta(r_2 - r_1) = \beta \frac{2h_T h_R}{r} \text{ OR } \frac{4\pi h_T h_R}{\lambda r} \quad (9.20)$$

Also, because $r \gg h_T + h_R$, we may write

$$\cos \theta = \frac{h_T + h_R}{r} \quad (9.21)$$

Example

The following example has been chosen to illustrate the application of the above formulae—

Let us suppose that in Fig. 9.36 T and R are vertical dipoles and that $h_T = 10$ m, $h_R = 5$ m, $r = 500$ m, $\lambda = 3$ m, power radiated, $W = 2$ watts.

Ground constants (sea-water) $\epsilon_r = 80$, $g = 5$ mhos/m.

Then equation (9.20) gives

$$\psi = 1.26 \text{ radians, or } 72^\circ$$

From (9.21) we find that

$$\theta = \frac{\pi}{2} - 0.033 \text{ radians}$$

$$= 88.1^\circ$$

The complex dielectric constant, as required for equation (3.52) of Vol. I, is $(\epsilon_r - j60\lambda g)$ which in this case equals $(80 - j900)$. Evaluating this equation or alternatively using the curves of Fig. 9.33 shows that $|R_v| = 0.39$ and $\angle R_v = 80^\circ$. The phase angle should be interpreted with care, for the geometry of the problem has to be taken into account. If the phase angle were in the region of zero, then Fig. 3.5 (b),

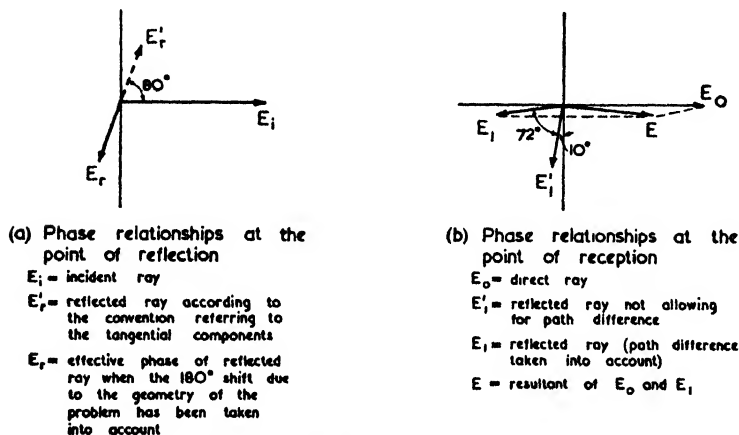


FIG. 9.37. PHASE DIAGRAMS OF FIELD INTENSITIES IN EXAMPLE

Vol. I, would represent the conditions, i.e. the effect would actually be that the reflected ray was in anti-phase (it is pointed out on p. 407 that a difficulty arises whatever convention one adopts). With the convention adopted here the 80° is taken positively with respect to the phase of the incident ray, and then the vector is reversed to allow for the geometry of the problem. The phases are shown in Fig. 9.37 (a).

In conjunction with the fact that $\psi = 72^\circ$ is the phase lag due to the path difference, we obtain the phase diagram shown in Fig. 9.37 (b) in which the magnitude of the resultant, E , is $0.62E_0$. The direct field E_0 is given by equation (1.2) and is

$$\begin{aligned} E_0 &= \frac{7\sqrt{W}}{r} \\ &= 19.8 \text{ mV/m} \end{aligned}$$

Therefore

$$E = 12.3 \text{ mV/m}$$

Field Strength Formulae

The example given above was purposely chosen to be as general as possible, since the application of the simplified formulae based on equation (9.19) which are given below will lead to incorrect results if the qualifying conditions are not satisfied.

In a great many cases ψ is small enough to write $e^{-j\psi} = (1 - j\psi)$. This condition is equivalent to stipulating $\sin \psi \doteq \psi$ and modifies (9.19) to

$$E = E_0(1 + R_{v,h} - R_{v,h}j\psi)$$

Provided $|R_{v,h}|$ is approximately equal to unity and $\angle R_{v,h}$ approximately equal to 180° (this takes into account the geometrical reversal in phase for vertical polarization) we can put the phase quadrature term equal to $j\psi$ so that

$$E = E_0(1 + R_{v,h} + j\psi) \quad . \quad . \quad (9.22)$$

On account of the approximations $\cos \theta = (h_T + h_R)/r$ and $\sin \theta = 1$, we may neglect $\epsilon' \cos \theta$ in comparison with $\sqrt{(\epsilon' - 1)}$ in the denominators of equations (3.52) and (3.53), Vol. I, for R_v and R_h , and write

$$R_v = \frac{\epsilon' \cos \theta - \sqrt{(\epsilon' - 1)}}{\sqrt{(\epsilon' - 1)}}$$

$$R_h = \frac{\cos \theta - \sqrt{(\epsilon' - 1)}}{\sqrt{(\epsilon' - 1)}}$$

where the negative sign in front of R_v has been dropped to allow for the geometrical reversal in phase. Inserting these values into equation (9.22) and using the values for ψ and E_0 as given by (9.20) and (1.2) respectively, we have

$$E_v = \frac{7\sqrt{W}}{r^2} \left[\frac{2\epsilon'(h_T + h_R)}{\sqrt{(\epsilon' - 1)}} + j \frac{4\pi h_T h_R}{\lambda} \right] \quad . \quad (9.23)$$

$$E_h = \frac{7\sqrt{W}}{r^2} \left[\frac{2(h_T + h_R)}{(\sqrt{(\epsilon' - 1)})} + j \frac{4\pi h_T h_R}{\lambda} \right] \quad . \quad (9.24)$$

For many cases which arise in practice, only the second term in the bracket is of importance; then $E_v = E_h$ (for horizontal polarization it is assumed that the transmitting and receiving antennae are broadside on), so that we are left with the simple expression

$$E_{v,h} = 88\sqrt{W} \frac{h_T h_R}{\lambda r^2} \quad . \quad . \quad (9.25)$$

In all three previous formulae the units are those of the M.K.S. system, i.e.

E = field strength in volts/metre,

W = power radiated in watts,

r = distance in metres,

$h_{T,R}$ = height of transmitter or receiver in metres,

λ = wavelength in metres.

Equation (9.25) is particularly simple and is much used in practice. It is therefore worth enumerating the conditions under which it may be used; they are as follows—

- (a) $h_T, h_R > \frac{\lambda}{8}$ (for horizontal polarization)
- $h_T, h_R > \lambda$ (for vertical polarization over land)
- $h_T, h_R > 2\lambda$ or λ^2 (for vertical polarization over sea water)
- whichever is the greater
(λ in metres)
- (b) $r > 10 (h_T + h_R)$ (for horizontal polarization)
- $r > 100 (h_T + h_R)$ (for vertical polarization)
- (c) $\frac{2\pi h_T h_R}{\lambda r} < \frac{1}{4}$
- (d) $r < 12\,000 \lambda^{\frac{1}{2}}$
- (e) $\frac{h_T + h_R}{r} > \left[\frac{\lambda}{2\pi r} \right]^{\frac{1}{2}}$

Condition (a) is discussed at the beginning of this section and is the requirement for neglecting the surface wave. Condition (b) ensures that the reflection coefficient approximates to -1 , (c) that $\psi = \sin \psi$, and (d) that plane earth conditions may be assumed. Finally, (e) stipulates the necessary condition for the use of ray theory—for, if the angle made with the reflecting surface is too small, the effect of diffraction cannot be neglected and ordinary ray theory becomes incorrect. Condition (e) is shown plotted in Fig. 9.32.

Of course in each of the above limitations the border line does not occur suddenly. As a rough guide one can say that any one of the above limits can be overstepped by 50 per cent or so without appreciable error, but if several of the limits are

exceeded simultaneously it is wise to consider the problem from first principles.

The use of equations (9.23) and (9.24) relaxes the second of the above limitations to $r > 3 (h_T + h_R)$ for horizontal polarization, and $r > 10 (h_T + h_R)$ for vertical polarization.

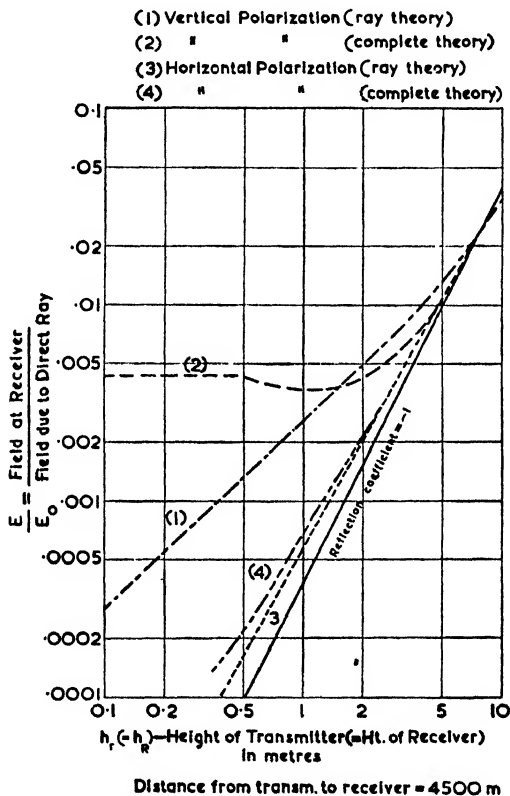


FIG. 9.38. THEORETICAL FIELD STRENGTH CURVES FOR TRANSMISSION ON A WAVELENGTH OF 7.5 M USING AN ELEVATED DIPOLE (McPetrie and Stickland, *Jour. I.E.E.*, Aug., 1940)

Furthermore, for vertical polarization the neglect of the surface wave will not prove important even if $h_R < \lambda$, provided $h_R > \frac{\lambda}{4}$ and $h_T > 3\lambda$ (h_T and h_R are interchangeable in these remarks).

An indication of the degree of error made by the use of these three formulae is given by Fig. 9.38, which is reproduced

from some curves by McPetrie and Stickland.⁽²⁵⁹⁾ The increased field strength near the ground with vertical polarization is a notable feature of these curves. Fig. 9.39 shows some of the experimental field strengths obtained by McPetrie and Saxton,⁽²⁵⁸⁾ together with a curve based on equation (9.25).

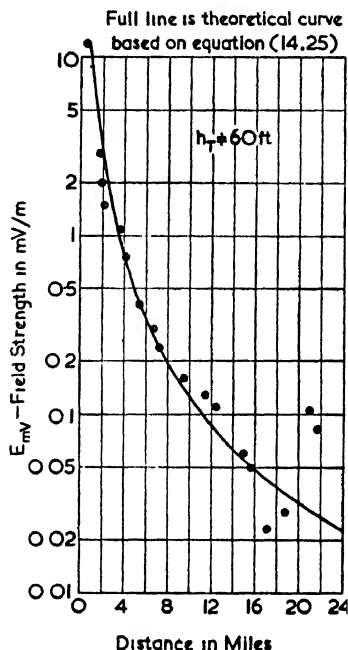


FIG. 9.39. EXPERIMENTAL FIELD STRENGTH VALUES OF A TRANSMISSION ON A WAVELENGTH OF 3 M

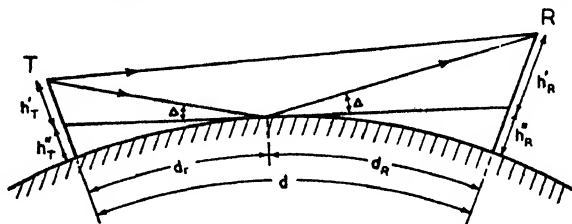
(McPetrie and Saxton, *Jour. I.E.E.*, Aug., 1940)

Effect of Spherical Earth

When taking into account the effect of earth curvature, we can also allow for the effect of refraction in a very simple manner. It was shown by Schelleng, Burrows and Ferrell⁽²⁸⁹⁾ that the degree of refraction associated with the average atmospheric conditions was such that a horizontal ray followed a curved path whose radius was four times that of the earth. They also showed that this could be allowed for by assuming the ray to be straight and increasing the radius of the earth by a factor of $4/3$, i.e. the earth is assumed to have an effective radius of 8 500 km.

The diagram for spherical earth transmission of the space

wave is as shown in Fig. 9.40. By finding the position of the tangent plane and using this as the new "earth," the method of calculation is reduced to that used for a plane earth. The only difference is that the reflected ray is decreased in magnitude by a divergence factor which allows for the fact that



When atmospheric refraction is taken into account, effective radius of earth = $\frac{4}{3} \times$ (actual value) = 8,500 Km

FIG. 9.40. DIAGRAMS FOR SPACE-WAVE CALCULATIONS OVER A SPHERICAL SURFACE

reflection is taking place from a curved surface. Thus the fundamental equation for the space wave (p. 406) is modified to

$$E = E_0(1 + SR_{v, h} e^{-j\psi}) \quad (9.26)$$

where S = spherical surface divergence factor.

$$\begin{aligned} 1/S^2 &= 1 + \frac{4h_T''r_R}{h_T'r} \\ &= 1 + \frac{2r_T r_R}{kar \tan \Delta} \end{aligned} \quad (9.27)$$

The first mentioned formula for S is usually more convenient for computation; the second indicates more clearly the degree of the dependence of S on the effective radius of the earth and on the distances involved.

In general, (9.26) must be solved according to the method outlined in the example at the beginning of this section, but where the appropriate simplifying conditions apply, the field strength can be obtained directly from equations (9.23), (9.24) or (9.25).

For all cases which arise in practice, the height of the tangent plane (Fig. 9.41) above the earth is given by

$$h = \frac{r^2}{2a} \quad (\text{without refraction})$$

or
$$\frac{r^2}{2ka} \quad (\text{allowing for atmospheric refraction})$$

Taking the form which allows for atmospheric refraction, and putting the distance in kilometres, we obtain the following simple formula—

$$h_{\text{metres}} = \frac{D^2}{17} \text{ km} \quad . \quad . \quad . \quad (9.28)$$

The values of h_T'' and h_R'' are given by the above equation for h on inserting r_T and r_R respectively for the distance D .

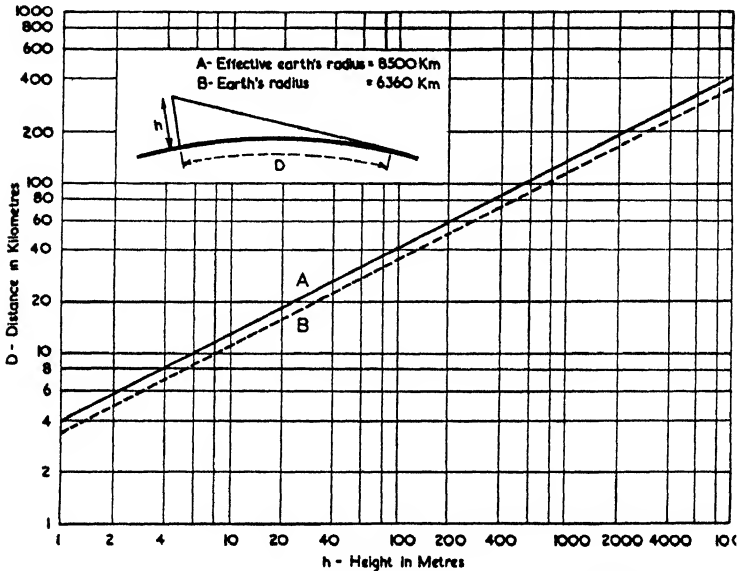


FIG. 9.41. RELATION BETWEEN HEIGHT ABOVE THE GROUND AND DISTANCE TO THE HORIZON

In a practical case r_T and r_R are at first unknown, though h_T , h_R and r will be given. The simplest way out of this difficulty is to use the curves of Fig. 9.42, which show the values of $\tan \Delta$ and the distance to the horizon for various values of height. For any two given height values we add the corresponding distances for equal values of $\tan \Delta$, thereby producing a combined curve from which we can read off the appropriate distance values. In Fig. 9.42 the limiting angles for which the simple ray theory holds are also indicated. This limitation corresponds to condition (e) on p. 414, and is shown as a complete curve in Fig. 9.32.

The above method of procedure is suitable for calculations concerning the received field strength in aeroplanes and also for

the transmission from one hill-top to another. In the latter case any local reflections on the hills have been allowed for in the effective polar diagram of the antenna system although in microwave work the directivity of the antenna system may be so high that the local hill reflections are negligible. In the following example the effect of local reflections has been

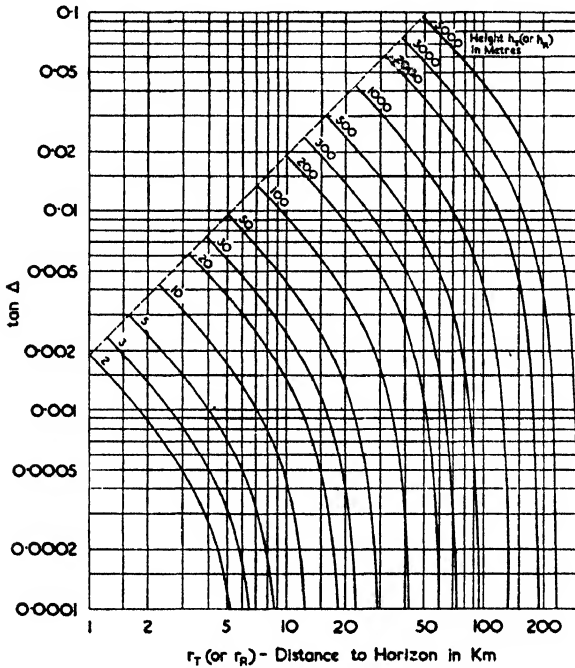


FIG. 9.42. RELATIONSHIP BETWEEN r_T (OR r_R) AND Δ IN FIG. 9.40

included; whether or not such reflections are present must be decided in any individual case by considering the polar pattern of each antenna in relation to the elevations along the transmission path.

Example

In Fig. 9.43 is shown an example of hillside-to-hillside transmission using horizontal polarization. From the curves of Fig. 9.42 we find that $r_T = 40$ km, $r_R = 30$ km, also $\tan \Delta = 0.005$. These values enable us to construct Fig. 9.44. (It should be noticed that exaggeration of the vertical scale has made the heights appear to be taken obliquely to the

occurring when transmissions to or from aeroplanes are concerned. For reception conditions the same considerations again apply, so that here also the polar diagram of the antenna should exhibit a maximum along the horizontal.

In our example, the polar patterns of the transmitting and receiving antennae would show a maximum along the horizontal if $h_T = 3.7$ m and $h_R = 2.8$ m. The antennae have therefore been placed at these heights and, since the polarization is horizontal, the full gain of 6 db along the lobe maximum may be assumed (neglecting any change in antenna impedance due to the presence of the ground). The field strength due to the direct ray is therefore given by twice the value in equation (1.2), i.e.

$$\begin{aligned} E_0 &= 2 \times \frac{7\sqrt{10}}{70\,000} \text{ V/m} \\ &= \underline{\underline{0.663 \text{ mV/m}}} \end{aligned}$$

At both the transmitting and receiving ends the angle between the direct and reflected rays is so small in comparison with the beam width of the polar diagram that it may be neglected. Also for horizontal polarization at such grazing angles we may safely assume $R_h = -1$. Hence the reflected ray produces a field intensity given by

$$E_1 = -SE_0e^{-j\psi}$$

$$\text{Here } \psi = \frac{4\pi \times 200 \times 150}{5 \times 70\,000} = 1.08 = 62^\circ$$

$$1/S^2 = 1 + \frac{4 \times 100 \times 30\,000}{200 \times 70\,000} = 2.17$$

$$\text{Hence } E_1 = -0.68 \angle -62^\circ E_0$$

The vector sum of E_0 and E_1 is such that

$$E = 0.60 \text{ mV/m}$$

Allowing for the directivity of the receiving system and for the effective "height" of the receiving dipole gives the induced series e.m.f. as

$$\begin{aligned} \epsilon &= 2 \times 0.60 \times \frac{2}{\pi} \times 5 \\ &= 3.8 \text{ mV} \end{aligned}$$

The above example shows the new features introduced by allowing for the earth's curvature, but it is simple in other

respects for, in general, it will be necessary to find the exact values for R_h (or R_v) for the local earth reflections as well as for the main reflection. In practice the effect of normal ground irregularities is often small; for instance, tests made with radio altimeters over reservoirs and over ordinary country show

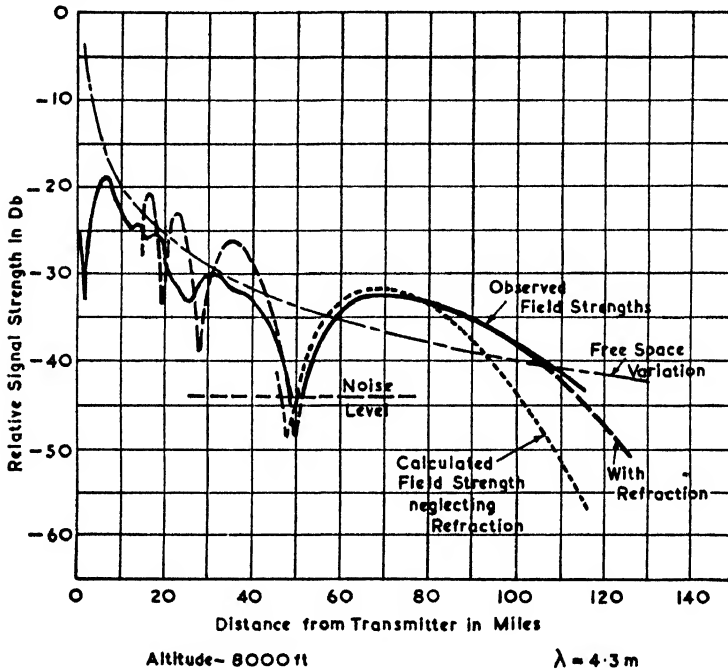


FIG. 9.45. RELATIVE FIELD STRENGTHS ON AN AEROPLANE FLIGHT
(Englund, Crawford and Mumford, *Proc. I.R.E.*, Mar., 1933)

differences which are usually within 6 db after allowing for the differences in the dielectric constants. The experiences of Selvidge⁽²⁸⁸⁾ may also be mentioned in this connexion; whilst carrying out diffraction experiments on ultra-short waves over sea water he found very little difference between calm conditions and those for which the waves were comparable with a wavelength.

Fig. 9.45 shows an experimental curve obtained by Englund, Crawford and Mumford⁽²⁴⁸⁾ for an aeroplane flight at an altitude of 8 000 ft. The agreement with the calculated values is particularly good when atmospheric refraction is taken into account. At distances of less than 40 miles the correspondence is not so good and the oscillations of field strength about the

free-space value are ill-defined. These oscillations are, of course, due to the aeroplane flying through the maxima and minima of the lobes produced by the direct and indirect rays; where these rays reinforce each other the increase above the free-space value is 6 db if the reflection coefficient is unity.

9.6. MICROWAVES

For many of the cases which arise in practice, the propagation of microwaves may be calculated on the basis of ray theory in precisely the same manner as was described in the previous section for ultra-short waves. Indeed, the range over which the simple ray treatment can be applied is increased, for the method applies to reflections whose angle with the ground is even smaller than for ultra-short waves (*see* Fig. 9.32).

The only difference that is likely to occur in the calculations is due to the fact that with microwaves the antenna system may be directive enough to make it necessary to allow for the polar diagram of the antenna when comparing the field strengths of the direct and reflected rays.

Field Strength Beyond the Optical Horizon

It is a well-known fact that the amount of diffraction round an obstacle of a fixed size is a function of the wavelength and that the diffraction decreases with decreasing wavelengths. Hence we should expect less diffraction on microwaves—a statement which is, of course, equivalent to the previously mentioned fact that the ray theory can be applied over a greater range of angles. The problem of diffraction has been studied by Eckersley⁽²³⁸⁾ and also by Van der Pol and Bremmer.^{(274) (275) (277)} The latter authors have made a comprehensive study of the propagation of radio waves from a vertical doublet round a spherical earth of finite conductivity. (A summary of their work is contained in the book by Bergmann and Lassen⁽⁶⁾.)

Van der Pol and Bremmer express their results in the form of the ratio of the Hertzian vector potential to that obtained under free-space conditions. For all practical cases this is equivalent to the ratio of the electric field strength, E , to the field strength, E_0 , which would be obtained under free-space conditions. Two of their sets of propagation curves are shown in Figs. 9.46 and 9.47—in each case the ordinates are in terms

of E/E_0 . These curves show that if both transmitting and receiving antennae are raised well above the ground then the shorter wavelengths give the greater values of E/E_0 at the optical horizon; on the other hand, if one antenna is on the

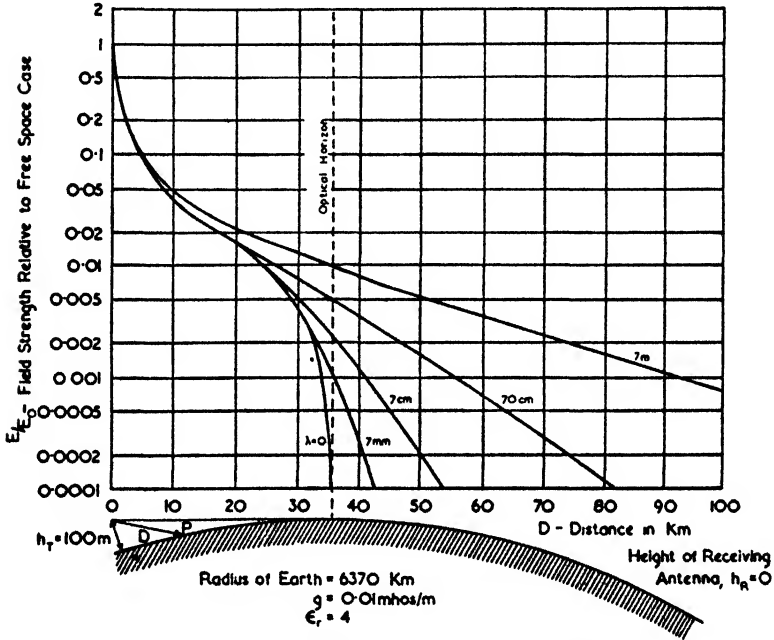


FIG. 9.46. FIELD STRENGTHS OF VERTICALLY POLARIZED RADIATION OVER A SPHERICAL CONDUCTING EARTH, CASE $h_T = 100$ M, $h_R = 0$ (Van der Pol and Bremmer, *Phil. Mag.*, Mar., 1939)

ground the converse is true. In either case the slope of E/E_0 in the diffraction zone increases as the wavelength is decreased.

The work of Domb and Pryce⁽²³⁶⁾ has considerably simplified the majority of field-strength calculations over a spherical earth. Their methods apply to all horizontally polarized waves and to vertically polarized waves over land if the wavelength is less than 50 m and over sea-water if the wavelength is less than 1 m.

For the antenna heights which occur in practice a good approximation to the attenuation of the field in the diffraction zone is given by

$$\text{Attenuation of } E/E_0 = \frac{26\,000}{\lambda^2 a^{\frac{1}{2}}} \text{ db/km} \quad (9.29)$$

where a = radius of curvature in metres.

This formula was confirmed experimentally by McPetrie and Ford⁽²⁸⁰⁾ for wavelengths between 9 cm and 12 m using hills whose curvatures ranged from 400 to 4 000 m. A comparison of this formula with the curves shown in Figs. 9.46

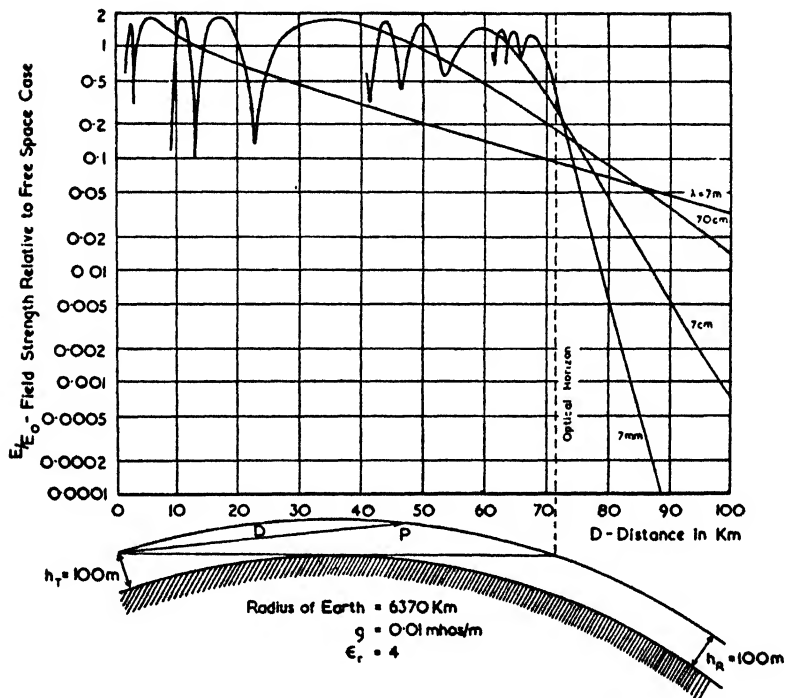


FIG. 9.47. FIELD STRENGTHS OF VERTICALLY POLARIZED RADIATION OVER A SPHERICAL CONDUCTING EARTH, CASE $h_T = 100$ M, $h_R = 100$ M (Van der Pol and Bremmer, *Phil. Mag.*, Mar., 1939)

and 9.47 (in which $a = 6.37 \times 10^6$ m) shows very satisfactory agreement at all wavelengths.

If “ a ” is put equal to the average effective radius of the earth, namely 8.5×10^6 m, we obtain the following useful formula—

$$\text{Attenuation of } E/E_0 = \frac{0.62}{\lambda^{\frac{1}{2}}} \text{ db/km} \quad (9.30)$$

Equation (9.30) makes it possible to construct a reasonably accurate “ E/E_0 versus distance” curve for various antenna heights by quite simple methods. We first calculate the curve

in the region over which ray theory holds (such calculations are discussed in detail in the previous section), and then add the curve given by equation (9.30) to give the best join with the ray theory curve. This process is greatly simplified if the E/E_0 scale is logarithmic—as shown in Figs. 9.46 and 9.47—for then the diffraction field curve is a straight line. To set the diffraction zone line at the right height we make it pass through the point representing the value of E/E_0 at the optical

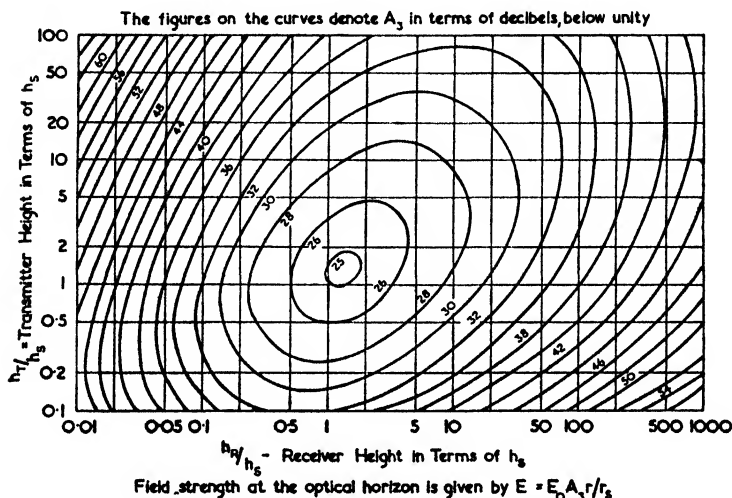


FIG. 9.48. CHART FOR COMPUTING THE FIELD STRENGTH AT THE OPTICAL HORIZON

(Domb and Pryce, *Jour. I.E.E.*, Sept., 1947)

horizon. Domb and Pryce⁽²³⁶⁾ have given a chart which greatly simplifies the calculation of this point. This chart is reproduced in Fig. 9.48 and is expressed in terms of a standard height, h_s , and a standard distance, r_s ; these are given by

$$h_s = \frac{1}{2}(a\lambda^2/\pi^2)^{\frac{1}{2}} \quad . \quad . \quad . \quad (9.31)$$

$$r_s = (a^2\lambda/\pi)^{\frac{1}{2}} \quad . \quad . \quad . \quad (9.32)$$

The chart gives the value of an attenuation factor which we shall call A_3 in terms of which the field strength relative to that in free space is given by

$$E/E_0 = r/r_s A_3 \quad . \quad . \quad . \quad (9.33)$$

where $E_0 = 7\sqrt{(WG_H)/r}$.

It will be noticed that A_3 varies very little with change in height in the region $h_T = h_R = h_s$. Taken in conjunction with the fact that $E_0 \propto r$ this means that, for a given antenna system and radiated power, the field strength at the optical horizon is roughly constant for different combinations of distance and antenna heights. This feature can be observed in

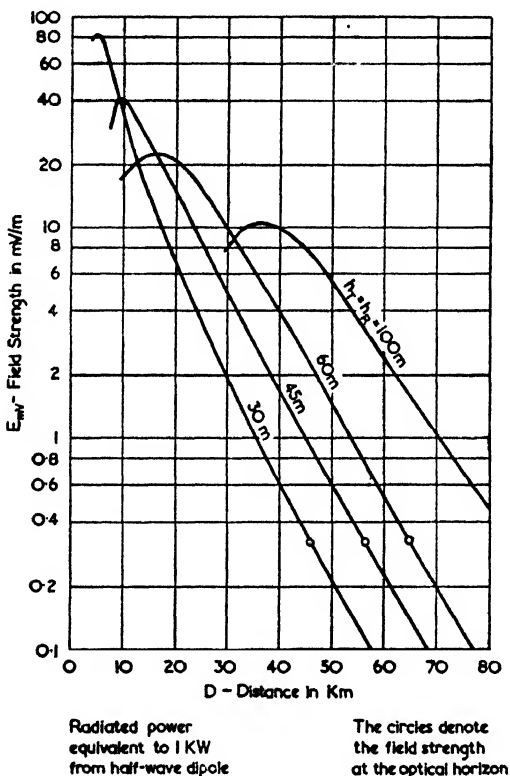


FIG. 9.49. THEORETICAL FIELD STRENGTHS FOR DIFFERENT HEIGHTS OF TRANSMITTING AND RECEIVING ANTENNAE USING A WAVELENGTH OF 60 CM

the curves of Fig. 9.49, which have been calculated by the method described above.

Although the propagation of microwaves is less favoured by diffraction phenomena, waves below 1 m wavelength are more favoured by the effects of refraction. Under special circumstances microwaves may be propagated over quite long distances. These circumstances are considered in the following paragraphs.

Super-refraction

In the course of propagation experiments with radar systems, it was found that centimetre waves occasionally gave ranges well beyond the optical horizon (for example a 50 cm radar on Malta has been known to give echoes from the coastline

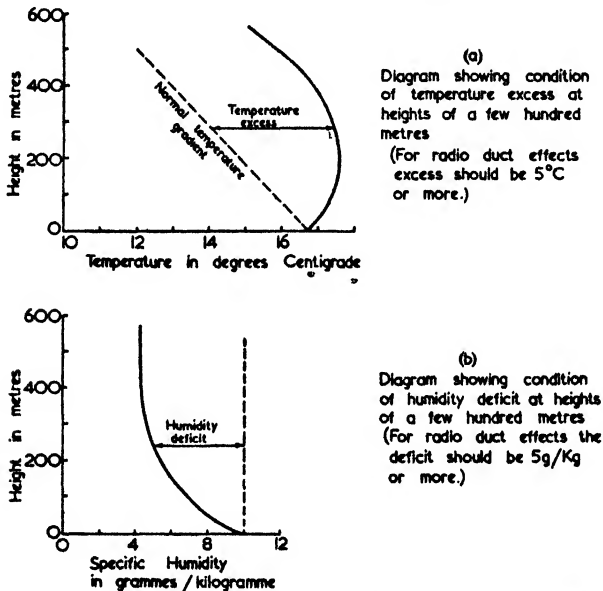


FIG. 9.50. ATMOSPHERIC CONDITIONS FOR PRODUCING SUPER-REFRACTION
(Booker, *Jour. I.E.E.*, Pt. III, No. 1, Mar.-May, 1946)

of Greece). The same effect was also observed on metre wavelengths but less frequently.

This phenomenon, which is called super-refraction, has been explained in terms of waveguide theory since the propagation is along a "radio duct" formed by the varying refractive index of the air next to the surface. A dielectric waveguide of this nature must have a depth of some 100 wavelengths or more and therefore differs in this respect from waveguides formed by metallic boundary surfaces (in which case the necessary depth is of the order of 1 wavelength). Since radio ducts are usually confined to heights between 20 and 200 m, this means that radio duct propagation is far more probable on micro-waves than on metre waves.

The necessary atmospheric conditions for the formation of these ducts are shown in Fig. 9.50 (a) and (b), which are based on data given in an article by Booker.⁽²²⁷⁾ Under normal circumstances the temperature of the atmosphere decreases by 9°C per kilometre of height, while the specific humidity (which is the ratio of the mass of water vapour to the mass of the volume of air containing it) is independent of height. It is the *degree of the departure from the normal conditions* which is important in this anomalous propagation; that is to say, it is the tem-

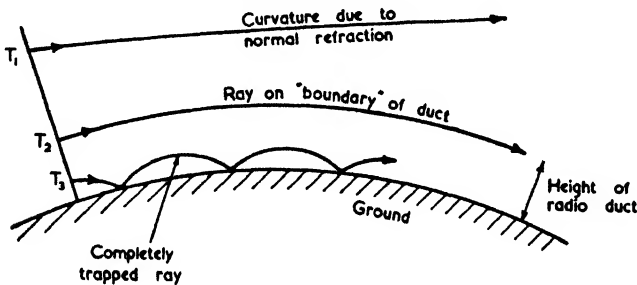


FIG. 9.51. EXAMPLES OF TRANSMISSION INSIDE, ALONG THE BOUNDARY OF, AND OUTSIDE A RADIO DUCT

perature excess and the humidity deficit shown in the above figures which are the determining features.

The top surface of a duct may be defined as the height at which a radio wave of given frequency just follows the curvature of the earth. This is illustrated by a ray propagated from T_2 in Fig. 9.51. Above this height the curvature decreases until it is simply that due to normal refraction, while below this height the ray is trapped entirely within the duct (these cases are shown by T_1 and T_3 respectively in Fig. 9.51).

According to Booker,⁽²²⁷⁾ the radius of curvature with normal refraction should be five times and not four times the radius of the earth. The figure of four times (which leads to the well-known value of 8 500 km for the apparent radius of the earth) indicates too great a bending of the waves for perfectly normal conditions and is really a compromise figure which makes some allowance for the abnormal conditions which often arise.

It should be noted that the effects of super-refraction are observed more readily with one-way communication systems than with radar systems. The latter are essentially two-way devices and therefore require a much greater increase in field

strength below the geometrical horizon to make the effects of super-refraction apparent.

The conditions leading to super-refraction and radio ducts are obviously determined by the prevailing weather conditions. If the lower atmosphere is well stirred up by wind then super-refraction is impossible. Warm, dry weather is the most favourable on the whole. In particular, super-refraction occurs readily over sea regions which are to the leeward of land masses. Under these circumstances the atmosphere over the sea can acquire an upper layer of warm, dry air which has drifted over from the land mass and is therefore most effective in the early evening.

The Radar Equation

The advent of radar, or radiolocation, as it was previously known, has greatly increased the interest in microwave propagation. In particular, it has created the problem of determining the range which can be obtained with a two-way transmission when the return signal is merely the reflected energy from some object. The equation expressing this range is commonly known as the radar equation and the first information to be released on this subject appears to have been an article by Fink.⁽²⁴⁸⁾

If the transmitted energy is W_t watts and the antenna power gain over an omnidirectional radiator is G_0 , then the magnitude of Poynting's vector at a distance r from the transmitter is given by

$$S_t = \frac{G_0 W_t}{4\pi r^2} \text{ watts/square metre}$$

The target will reradiate some of the incident energy back towards the transmitter and thus acts as a secondary source whose radiated power is σS_t , where σ is the effective cross-sectional area of the target for that particular direction. This effective area will be independent of the wavelength if the target size is large relative to one wavelength. The value of Poynting's vector at the radar station due to the reflected signal is therefore

$$S_r = \frac{\sigma S_t}{4\pi r^2} \text{ watts/square metre}$$

If the radar equipment has a receiving antenna whose effective area of absorption is A_r square metres, then the

received power will be $W_r = A_e S_r$, watts. On substituting for S_r and S_t and rearranging we obtain

$$r = \sqrt[4]{\left[\frac{\sigma A_e G_o W_t}{(4\pi)^2 W_r} \right]} \text{ metres} \quad . \quad . \quad (9.34)$$

When one antenna serves for both transmission and reception, as is often the case, then by equation (5.4) we have

$$G_o = \frac{4\pi A_e}{\lambda^2}$$

Under these circumstances equation (9.34) becomes

$$r = \sqrt[4]{\left[\frac{\sigma A_e^2 W_t}{4\pi \lambda^2 W_r} \right]} \quad . \quad . \quad (9.35)$$

In a radar system W_t will represent the peak power; hence it would appear that if the same total power were concentrated in a narrower pulse the range could be increased. This is not so, however, for with narrower pulses a greater receiver bandwidth is required and this results in an increase in the noise level. To overcome this increase in noise it is necessary to obtain a greater signal input power.

The optimum bandwidth for a pulse whose duration is equal to d microseconds is $1.2/d$ megacycles. Equation (5.7) shows that the available noise input is 4×10^{-15} watts per megacycle bandwidth and this becomes $N \times 4 \times 10^{-15}$ on allowing for the noise figure of the receiver (specimen noise figures are given in Fig. 5.5). Thus the total available noise input for a pulse duration of d microseconds is

$$W_n = \frac{4 \cdot 8N}{d} \times 10^{-15}$$

If we denote the minimum detectable received signal power by W_{min} then W_{min} will be some multiple of W_n , depending on whether the beam is scanning the target, and on losses between the antenna and first valve. With P.P.I. presentation W_{min} may be about 10 times W_n , but when the target is not being scanned we may put $W_{min} = W_n$ as representing the best possible case. Making the latter assumption we find that the maximum range under free-space conditions is

$$\begin{aligned} r_{max} &= \sqrt[4]{\left[\frac{\sigma A_e^2 W_t d}{4\pi \lambda^2 4 \cdot 8N} \times 10^{-15} \right]} \\ &\doteq \sqrt[4]{\left[\frac{\sigma A_e^2 W_t d}{2\pi \lambda^2 N} \right]} \times 10^{-4} \quad . \quad . \quad (9.36) \end{aligned}$$

A notable feature of the above equation is that r_{max} varies as $\sqrt[4]{W_t d}$, i.e. as the fourth root of the product of the peak power and the pulse duration. Thus the range is determined by the fourth root of the total energy content of the pulse.

The repetition frequency of the pulses will also affect the range to some extent, since a higher rate of repetition on the oscilloscope tends to improve the discrimination against noise.

As a guide to the order of the values of σ to be expected, one may take the following figures (those for shipping were obtained from an article by Byrnes⁽³⁵¹⁾)—

	<i>σ in square metres</i>
Buoy	1
Motor-boat	7
Twin-engined aircraft	30
Four-engined aircraft	80
Small two-masted vessel	150
Freighter or tanker	2 500

The value of σ may vary considerably with the aspect of the target, so that the above figures must be taken to represent quasi-maximum values.

Transmission Lines

EXCEPT in the case of microwave transmission, when waveguides are often used, antennae are almost invariably coupled to transmitters by means of transmission lines. Such lines form, therefore, an almost integral part of the antenna system.

When the line is used as a feeder, the normal aim is to "match" it so that there are no standing waves, or rather so that the standing wave ratio is below some stipulated value. The process of matching consists in supplying a load which is equal to the characteristic impedance of the line. Failure to do so will make the input end of the line appear reactive as well as resistive, but this may not matter (or can be compensated for); moreover, an appreciable mismatch can be tolerated before the increase in the line losses becomes excessive. All the same, an unmatched feeder is never to be preferred, since the input impedance will then vary with the length of line and the frequency; also the voltage antinodes may cause flash-over, and finally the heat generated at the current antinodes may exceed the safe rating.

Apart from their use as feeders, transmission lines may be employed as matching devices in the form of stubs or quarter-wave transformers; they may be used as filters or phasing sections, or they may be designed to provide an artificial load. The parallel line is simpler to construct and easier to test in the field but has the disadvantage of having a slight radiation field and somewhat greater attenuation. The coaxial line is particularly suitable for microwaves when the outer conductor may be a part of the supporting system.

10.1. BASIC TRANSMISSION-LINE EQUATIONS

An electromagnetic wave may be guided along two conductors in such a way as to cause but little attenuation with distance and to confine the transmitted energy to the immediate

neighbourhood of the conductors. When the separation between the conductors is a small fraction of a wavelength only one mode of propagation is possible—one in which all the lines of

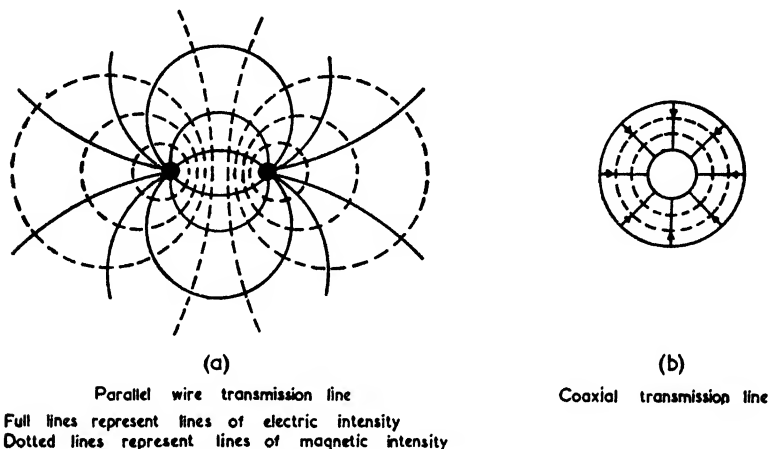


FIG. 10.1. FIELD DISTRIBUTIONS FOR PARALLEL-WIRE AND COAXIAL TRANSMISSION LINES OPERATING IN THEIR PRINCIPAL MODES

electric intensity start on one conductor and finish on the other. Field patterns of this nature are illustrated in Fig. 10.1, which shows the field distribution for the two most common

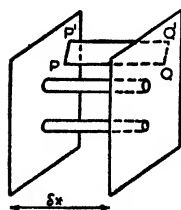


FIG. 10.2. DIAGRAM FOR DERIVATION OF TRANSMISSION-LINE EQUATIONS

forms of transmission. This mode of transmission is known as the "principal" or "dominant" mode and is uncritical as to the frequency transmitted. On the other hand a higher mode of transmission such as is shown in Fig. 5.11 (b), Vol. I, cannot be propagated unless the dimensions of the line exceed a certain minimum value which is a function of the frequency.

Fig. 10.2 illustrates a portion of a parallel-wire line which is supposed to consist of perfect conductors. In determining the equations for a transmission line excited in its principal mode we use the fact that the configuration of the lines of electric and magnetic force will be identical in magnitude and shape for both the sections shown. Consequently in evaluating the line integral of either E or H round a minute rectangle as shown in the figure (P and Q are corresponding points on the

two surfaces) the only components will be $(\partial E/\partial x)\delta x$ or $(\partial H/\partial x)\delta x$ respectively.

In both cases the curl of \mathbf{E} or \mathbf{H} is found by taking the limit of the line integral divided by the area. To obtain the value of curl \mathbf{E} the rectangle must be rotated to thread the maximum number of flux lines, i.e. PP' and QQ' are along lines of electric force, whereas to evaluate curl \mathbf{H} the sides PP' and QQ' are along lines of magnetic force. Maxwell's equations curl $\mathbf{E} = -\dot{\mathbf{B}}$ and curl $\mathbf{H} = \mathbf{J} + \dot{\mathbf{D}}$ therefore reduce to

$$\begin{aligned}\frac{\partial \mathbf{E}}{\partial x} &= -\dot{\mathbf{B}} \\ &= -\mu \dot{\mathbf{H}} \quad . \quad . \quad . \quad (10.1)\end{aligned}$$

and

$$\begin{aligned}-\frac{\partial \mathbf{H}}{\partial x} &= \mathbf{J} + \dot{\mathbf{D}} \\ &= g\mathbf{E} + \varepsilon \dot{\mathbf{E}} \quad . \quad . \quad . \quad (10.2)\end{aligned}$$

From a practical point of view it is easier to determine the voltage or the current than it is to find \mathbf{E} or \mathbf{H} . Now the instantaneous voltage, v , between the conductors is given by the line integral of \mathbf{E} taken from one conductor to the other, in which case \mathbf{B} refers to the total flux between the conductors and this total flux is, by definition, equal to the inductance between the lines multiplied by the instantaneous current i . If L is the inductance per unit length then this product equals $L\delta xi$, whereupon, on taking limits, we arrive at the line integral version of (10.1) which is

$$\frac{\partial v}{\partial x} = -L \frac{\partial i}{\partial t} \quad . \quad . \quad . \quad (10.3)$$

Equation (10.2) can be transformed by taking the line integral of \mathbf{H} round the wire which gives the total current i . On the right-hand side we transform the current density term to the total transverse conduction current which equals the transverse conductance, G , times the voltage, v ; also the total displacement current is given by $C\dot{v}$, where C is the capacitance per unit length. With these substitutions the equation becomes

$$\frac{\partial i}{\partial x} = -\left(Gv + C \frac{\partial v}{\partial t}\right) \quad . \quad . \quad (10.4)$$

The development of (10.3) and (10.4) has allowed for a leakage between the lines but not for resistance in the conductors. To allow for this resistance we may say that the

effect on the transverse field pattern is negligibly small but that there is a small tangential e.m.f. along the surface of the conductor. These assumptions leave equation (10.4) unchanged but add an e.m.f. to the right-hand side of (10.3) which may be expressed as the product of the conductor resistance per unit length and the current. We therefore obtain

$$\frac{\partial v}{\partial x} = - \left(Ri + L \frac{\partial i}{\partial t} \right) \quad . \quad . \quad (10.5)$$

where R is the *combined* resistance per unit length of the two conductors.

On making the usual assumption that the voltage and the current vary harmonically with time, i.e. that $v = Ve^{j\omega t}$ and $i = Ie^{j\omega t}$, we find that equations (10.4) and (10.5) become

$$\frac{dI}{dx} = - (G + j\omega C)V \quad . \quad . \quad (10.6)$$

$$\frac{dv}{dx} = - (R + j\omega L)I \quad . \quad . \quad (10.7)$$

These two equations were solved in Vol. I, § 3.3, where it was pointed out that their solution was analogous to that of the wave equation. The solutions are

$$V = V_0 e^{-Px} \quad . \quad . \quad (10.8)$$

$$I = I_0 e^{-Px} \quad . \quad . \quad (10.9)$$

where $P = \sqrt{[(R + j\omega L)(G + j\omega C)]} \quad . \quad . \quad (10.10)$

$$= \alpha + j\beta \quad . \quad . \quad . \quad (10.11)$$

P is known as the *propagation constant*, its real part, α , as the *attenuation constant*, and its imaginary part, β , as the *phase constant*.

The attenuation constant is a measure of the attenuation of the voltage or the current along the line and has the dimensions of nepers per unit length (to convert nepers to decibels, multiply by 8.686). The unit of length is the same as that used for R , L , G and C and would normally be the metre, but for lines of low attenuation the kilometre results in a more convenient value for α .

Points at which the voltage or the current has equal phases occur at intervals for which $\beta x = 2\pi$, and the distance between such points is equal to λ , the wavelength of the electromagnetic wave in the medium between the wires. The phase constant is therefore equal to $2\pi/\lambda$.

The most general solution to the transmission-line equations involves *two* arbitrary constants, so that instead of (10.8) we have

$$V = Ae^{-Px} + Be^{Px} \quad . \quad . \quad . \quad (10.12)$$

To obtain the corresponding current equation we may use (10.7) which gives

$$\begin{aligned} I &= \frac{P}{(R + j\omega L)} (Ae^{-Px} - Be^{Px}) \\ &= \frac{I}{Z_0} (Ae^{-Px} - Be^{Px}) \quad . \quad . \quad . \quad (10.13) \end{aligned}$$

where

$$Z_0 = \sqrt{\left(\frac{R + j\omega L}{G + j\omega C}\right)} \quad . \quad . \quad (10.14)$$

Z_0 is known as the *characteristic impedance* of the line and is, in general, a complex quantity, but for most practical cases $R \ll j\omega L$ and $G \ll j\omega C$ whereupon Z_0 is virtually a real quantity. In this book the designation R_0 is used for the real part of Z_0 whenever Z_0 is definitely complex and we wish to refer specifically to the real part of the characteristic impedance.

Comparing (10.12) and (10.13) shows that if $B = 0$, then $\frac{V}{I} = Z_0$, but if $A = 0$ then $\frac{V}{I} = -Z_0$. The former case represents conditions for which there is only a forward-travelling wave, whereas in the latter case there is only a backward-travelling wave. The difference in the sign of Z_0 for the two cases is due to the fact that with the forward-travelling wave we are looking into a load, but with the backward-travelling wave we are looking into a generator (in practice the "generator" will be due to the reflection from an unmatched load).

10.2. TRANSMISSION-LINE CONSTANTS

(a) Capacitance per Unit Length

The simplest case to calculate is that of a coaxial line as shown in Fig. 10.1 (b) because the symmetry of the field permits direct application of the divergence law.

We may imagine the inner conductor to be surrounded by a concentric cylinder of radius r such that $a < r < b$ (see Fig. 10.3); then the lines of electric force are everywhere normal to the surface of this cylinder. Hence if the charge per

unit length is q , the electric intensity E at the surface of the cylinder is given by (see Vol. I, § 2.1)

$$2\pi rE = q/\epsilon$$

The potential difference between the outer and inner conductors is therefore given by

$$V = \int_a^b E dr = \frac{q}{2\pi\epsilon} \log_e \frac{b}{a}$$

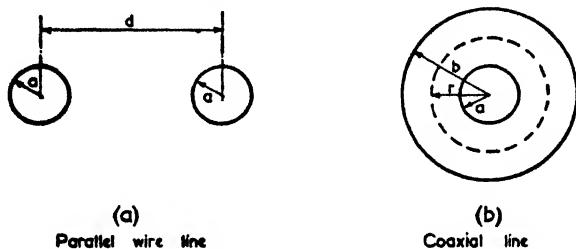


FIG. 10.3. DIAGRAM SHOWING DIMENSIONS USED IN TRANSMISSION-LINE FORMULAE

Hence the capacitance per unit length of a coaxial line is

$$C = \frac{2\pi\epsilon}{\log_e b/a} \text{ farads/metre} \quad . \quad . \quad (10.15)$$

The corresponding formula for the two-wire case of Fig. 10.1 (a) cannot be derived quite so simply. The result,⁽²⁰⁾ which is a two-dimensional solution of Laplace's equation, is as follows—

$$C = \frac{\pi\epsilon}{\cosh^{-1}(d/2a)} \quad . \quad . \quad (10.16)$$

If $d > a$, which is often the case in practice, this becomes

$$C = \frac{\pi\epsilon}{\log_e (d/a)} \text{ farads/metre} \quad . \quad . \quad (10.17)$$

In the case of a parallel-wire line the presence of the ground will modify both the capacitance and the inductance per unit length. According to Terman,⁽²³⁾ the capacitance of a parallel-wire line whose height above the ground is h , is increased by an amount which is the same as would result if the spacing, d , were decreased to $d/\sqrt{[1 + (d/2h)^2]}$.

(b) *Inductance per Unit Length*

It can be shown (*see ref. 1*) that the capacitance and inductance per unit length of a transmission line are related in a simple manner to the velocity of propagation in the dielectric surrounding the conductors. If the aforementioned quantities are denoted respectively by C , L and v , the relation is

$$v = \frac{1}{\sqrt{LC}}$$

In the above equation L is the *external inductance*, the internal inductance of the conductors not being included. This makes no difference in the case of conductors of low permeability, but with a line consisting of, say, a pair of iron wires the internal inductance would make a small but distinct contribution to the total inductance.

The velocity of propagation is also given in Vol. I by equation (3.38) as

$$v = \frac{1}{\sqrt{(\mu\epsilon)}}$$

The inductance per unit length is therefore given in terms of the capacitance per unit length by the following equation

$$L = \frac{\mu\epsilon}{C} \quad . \quad . \quad . \quad (10.18)$$

It should be remembered that μ and ϵ are in M.K.S. units. For air dielectric, we have $\mu = \mu_0 = 4\pi \times 10^{-7}$ H/m, and $\epsilon = \epsilon_0 = (1/36\pi) \times 10^{-9}$ F/m.

Using equations (10.15), (10.17) and (10.18) we obtain the following values for inductance per unit length—

Coaxial line

$$L = \frac{\mu}{2\pi} \log_e \left(\frac{b}{a} \right) \text{ henrys/metre} \quad . \quad . \quad (10.19)$$

Parallel-wire line

$$L = \frac{\mu}{\pi} \log_e \left(\frac{d}{a} \right) \text{ henrys/metre} \quad . \quad . \quad (10.20)$$

The inductance of a set of parallel wires may be found directly by means of a "Stream function" which is a vector potential taken in one direction only. For examples of such calculations the reader may refer to Schelkunoff's *Electromagnetic Waves*.⁽²⁰⁾

(c) *Resistance per Unit Length*

At high frequencies the depth of penetration of the current into the conductor is small in comparison with the radius of the conductor. It is then justifiable to make the assumption that the effective resistance is equal to the d.c. resistance of a cylinder whose outer radius equals that of the conductor and whose thickness is equal to the "skin depth." Using the results of Vol. I, § 3.4 (c), we find that R , the resistance per unit length of a single wire whose circumference is $2\pi a$, is given by

$$R = R_m / 2\pi a \\ = \frac{1}{2\pi a} \sqrt{\frac{\pi \mu f}{g}} \text{ ohms/metre} \quad . \quad . \quad (10.21)$$

In the case of concentric lines, the current distribution is unaffected by the presence of the symmetrically disposed outer conductor, so that the total resistance per unit length is given by

$$R = \frac{R_m}{2\pi} \left[\frac{1}{a} + \frac{1}{b} \right] \text{ ohms/metre} \quad . \quad . \quad (10.22)$$

where a = radius of inner conductor in metres,

b = inner radius of outer conductor in metres.

With parallel transmission lines the current distribution is slightly modified (a phenomenon which is known as "proximity effect"), but for all practical purposes it is legitimate to neglect this, so that the total resistance per unit length is

$$R = \frac{R_m}{\pi a} \text{ ohms/metre} \quad . \quad . \quad (10.23)$$

(d) *Conductance per Unit Length*

Parallel transmission lines usually have air as the dielectric and have as few insulators as possible. In these circumstances the conductance losses are not a major factor. With concentric lines, however, solid dielectrics are often used where the power to be transmitted does not exceed a kilowatt or so.

If the conductivity of the dielectric is g we find, for the concentric line case, that the conductance is

$$G = 2\pi \frac{g}{\log_e \frac{b}{a}} \text{ mhos/metre}$$

In practice the characteristics of a dielectric are usually expressed in terms of a "power factor" which equals $G/\omega C$ when $G \ll \omega C$, and is therefore the inverse of the Q of the medium. On inserting the value for C according to equation (10.15) we then have

$$\begin{aligned} G &= \frac{\omega C}{Q} \\ &= \frac{2\pi\omega\epsilon}{Q \log_e \frac{b}{a}} \end{aligned} \quad (10.24)$$

where $\epsilon =$ dielectric constant of medium in M.K.S. units
 $= \epsilon_r \epsilon_0$

(e) Attenuation Constant

It is apparent from equations (10.8) to (10.11) that the voltage and current along a transmission line are attenuated by a factor $e^{-\alpha x}$ where α is the attenuation constant and x the distance along the line. When αx is equal to unity the attenuation factor is $1/2.7$, i.e. 1 neper or 8.686 decibels, hence α is the attenuation in nepers per unit length. At radio frequencies the primary constants are such that $\omega L \gg R$ and $\omega C \gg G$; consequently the evaluation for α from equation (10.10) gives

$$\begin{aligned} \alpha &= \frac{R}{2\sqrt{L}} + \frac{G}{2\sqrt{C}} \\ &= \frac{R}{2Z_0} + \frac{G}{2} Z_0 \end{aligned} \quad (10.25)$$

In the latter expression we have used the fact that Z_0 is real and equal to $\sqrt{L/C}$ under the conditions stipulated above. The equation shows that the relative contribution of the conductance to the total attenuation increases with the characteristic impedance. To quote a practical case⁽³²⁸⁾ involving 4-wire lines, the leakage losses at 20 Mc/s were 67 per cent of the copper losses for $Z_0 = 550$ ohms, and 39 per cent for $Z_0 = 320$ ohms. It should be noted that these increases above

the copper loss figures included the *whole* of the extra losses and that with perfectly clean, dry insulators the losses would be smaller. In general an assessment of the copper losses will

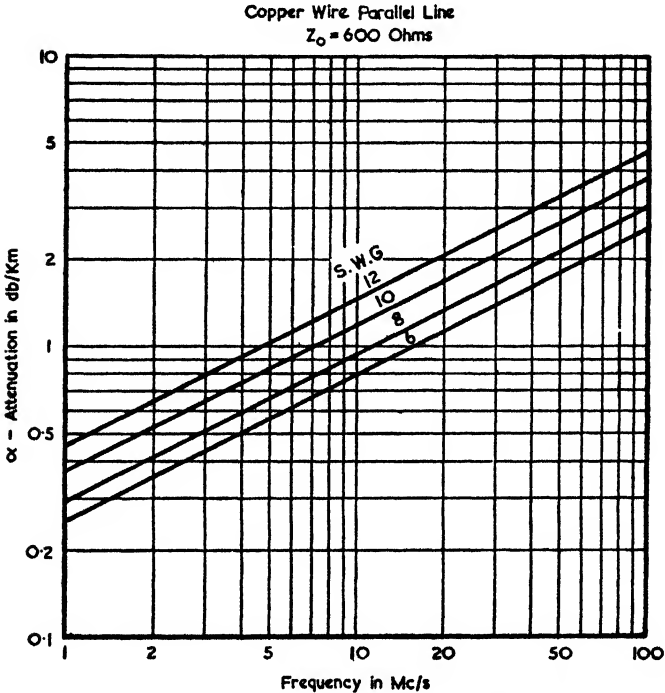


FIG. 10.4. ATTENUATION CONSTANT OF PARALLEL-WIRE COPPER LINES

either suffice or give a first approximation to the total losses; the attenuation constant is then given by

$$\begin{aligned} \alpha &= \frac{R}{2Z_0} \text{ nepers/metre} \quad . \quad . \quad . \quad (10.26) \\ &= \frac{R_m}{2\pi a Z_0} \text{ (parallel lines)} \\ &\text{or } \frac{R_m}{4\pi Z_0} \left[\frac{1}{a} + \frac{1}{b} \right] \text{ (concentric lines)} \end{aligned}$$

The value of α given above is the attenuation constant for *some particular transmission-line configuration*; it should not be confused with the attenuation constant of the *medium* which is the real part of the "intrinsic propagation constant" discussed

in Vol. I, §§ 3.3 and 3.4. The equation for R_m given in Vol. I, equation (3.42) and again in (10.21) shows that R_m varies as the square root of the permeability of the metal.

Consequently iron and steel wires have appreciable attenuation and are therefore suitable for dissipative lines such as terminating networks for rhombic antennae. Typical values are as follows—

Copper wire

$$R_m = 2.61 \times 10^{-7} \sqrt{f} \text{ ohms}$$

Iron wire

$$R_m = 8.89 \times 10^{-6} \sqrt{f} \text{ ohms}$$

Stainless steel wire (USS12)

$$R_m = 1.16 \times 10^{-5} \sqrt{f} \text{ ohms}$$

where f = frequency in cycles/second.

Inserting these values in equation (10.26) gives the curves shown in Figs. 10.4 and 10.5, in which the attenuation is given in db per kilometre.

The presence of standing waves (which are discussed in the next section) increases the total losses. If the line has a standing wave whose ratio is ρ , then the current at a distance x from a current minimum is given by

$$I^2 = I_{min}^2 \frac{\rho^2 \tan^2 \beta x + 1}{\tan^2 \beta x + \rho}$$

By finding the losses for a small element dx , and by integrating between $x = 0$ and $\lambda/4$ (thereby obtaining a complete sample of the r.m.s. current variations) we obtain the following ratio—

$$\frac{\text{Attenuation for standing wave}}{\text{Attenuation for travelling wave}} = \frac{1}{2} \left(\rho + \frac{1}{\rho} \right) \quad (10.27)$$

For example, with standing wave ratios of 1.1 and 1.5 the percentage increases in losses are 0.45 per cent and 8.3 per cent respectively.

It should be noted that equation (10.27) applies to a line which is not in itself highly dissipative, i.e. the value of ρ is fairly uniform along the line; a practical case of this nature is that for a transmission line feeding an antenna array. If a highly dissipative line were used (e.g. the terminating load of

a rhombic) the value of ρ would vary greatly along the line. Equation (10.27) also assumes that the line is an appreciable number of quarter-wavelengths long.

For a given conductor material there exists an optimum characteristic impedance for which the attenuation constant

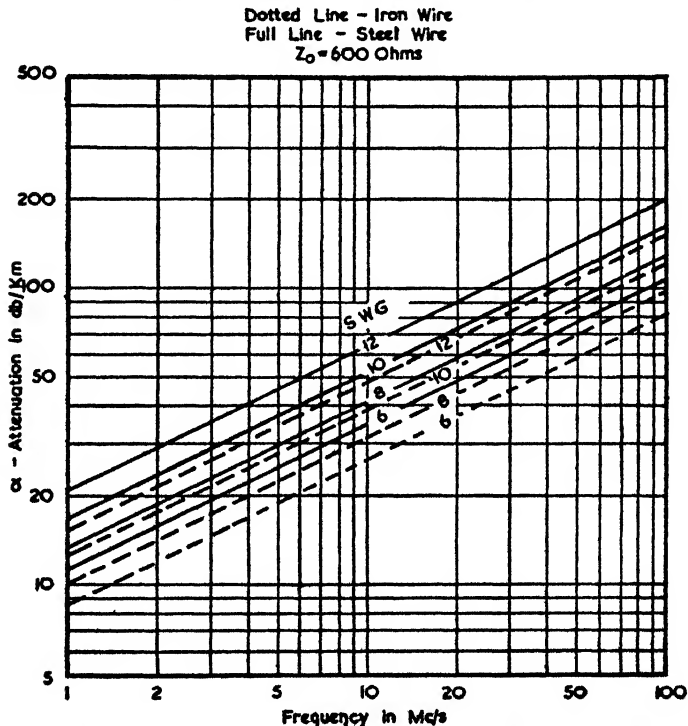


FIG. 10.5. ATTENUATION CONSTANT OF PARALLEL-WIRE IRON AND STEEL LINES

is a minimum. In the case of copper and concentric lines this value of Z_0 is 77 ohms (corresponding to a ratio of 3.6 for b/a); however, the attenuation is within 5 per cent of the minimum value throughout the range $Z_0 = 57$ to 100 ohms, i.e. the optimum design is quite uncritical. With air-spaced parallel lines minimum attenuation occurs when $Z_0 = 175$ ohms (see ref. 9), but again the values are uncritical. In practical cases, where the feeding of energy to antennae is involved, the conditions for minimum attenuation with cross-section do not even come into consideration since good matching, short

lengths and adequate power-handling capacity are more important features.

(f) *Phase Constant*

The expansion of the right-hand side of (10.10) in terms of $R/\omega L$ and $G/\omega C$ gives high powers of these ratios for the imaginary component. Therefore the value of the phase constant, β , is given to a high degree of approximation by $\beta = \omega\sqrt{LC}$ when $R \ll \omega L$ and $G \ll \omega C$. The value of \sqrt{LC} is equal to the velocity of the waves in the dielectric surrounding the wires; hence $\beta = 2\pi/\lambda$, where λ is the wavelength in the dielectric.

Reference to equations (10.8) and (10.9) shows that if the attenuation were zero the voltage and current values would repeat themselves in phase and magnitude at intervals for which $e^{-\gamma(x_1 - x_2)}$ equals 2π , i.e. at intervals for which $(x_1 - x_2) = \lambda$. At intervals of $\lambda/2$ the magnitudes are equal but the voltage (or current) is in antiphase.

(g) *Propagation Constant*

The propagation constant is defined by equation (10.10) as the square root of the product of the series impedance and the shunt admittance per unit length. In general \tilde{P} is complex, the real part being the attenuation constant and the imaginary part the phase constant, as shown by equation (10.11).

(h) *Characteristic Impedance*

Equation (10.14) shows that the characteristic impedance is given by the square root of the ratio of the series impedance to the shunt admittance. At high frequencies Z_0 is substantially a real number whose value is given by $\sqrt{L/C}$. We obtain therefore the following values for the characteristic impedance of a transmission line (the dimensions are shown in Fig. 10.1)

Coaxial line

$$\begin{aligned} Z_0 &= \frac{1}{2\pi} \sqrt{\left(\frac{\mu}{\epsilon}\right)} \log_e \frac{b}{a} \text{ ohms} \quad . \quad . \quad (10.28) \\ &= 60 \log_e \frac{b}{a} \text{ (air dielectric)} \end{aligned}$$

or

$$138 \log_{10} \frac{b}{a}$$

Parallel-wire line

$$Z_0 = \frac{1}{\pi} \sqrt{\left(\frac{\mu}{\epsilon}\right)} \log_e \frac{d}{a} \text{ ohms.} \quad (10.29)$$

$$= 120 \log_e \frac{d}{a} \text{ (air dielectric)}$$

or $276 \log_{10} \frac{d}{a}$

In the above expressions we could have substituted z_0 , the intrinsic impedance of the medium, for $\sqrt{(\mu/\epsilon)}$, but the form

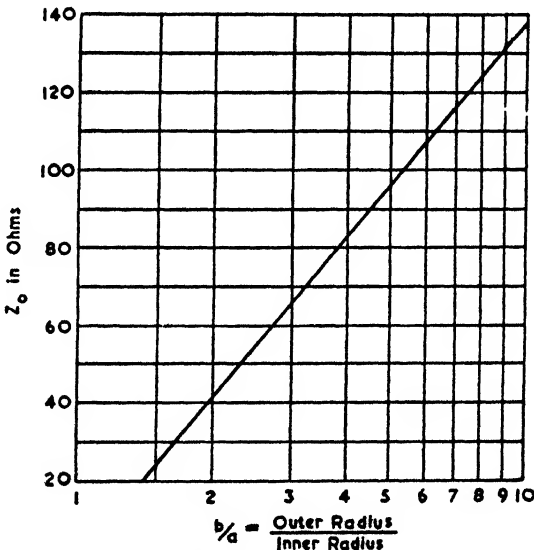


FIG. 10.6. CHARACTERISTIC IMPEDANCE OF COAXIAL LINES

given above shows the dependence of Z_0 on μ and ϵ more clearly. Graphs of Z_0 are given in Figs. 10.6 to 10.9 for concentric lines, two-wire parallel lines and two forms of four-wire lines.

When dealing with transmission lines of unusual cross-section the characteristic impedance may be determined graphically by plotting the electric and magnetic lines of force. This field plotting technique is described in a paper by R. W. D. Oughby⁽³⁴⁷⁾ who gives the examples shown later in Figs. 10.10 and 10.12.

Essential feature of such plotting is that we fill the area

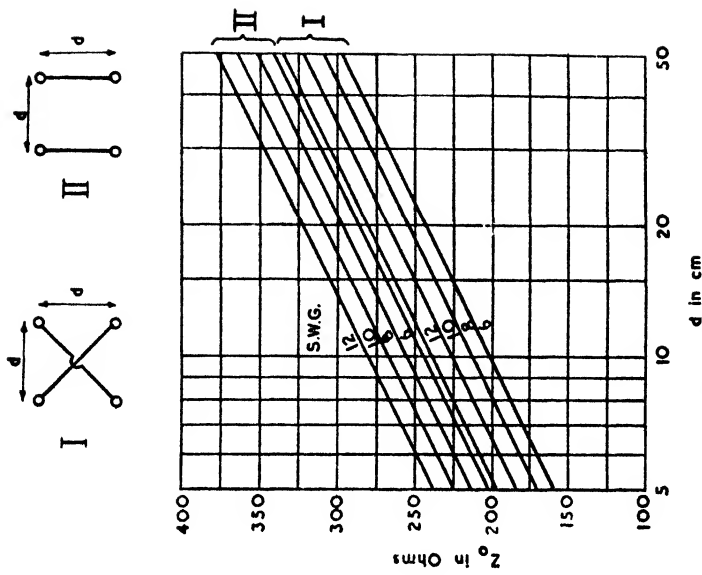


FIG. 10.8. CHARACTERISTIC IMPEDANCE OF FOUR-WIRE LINES

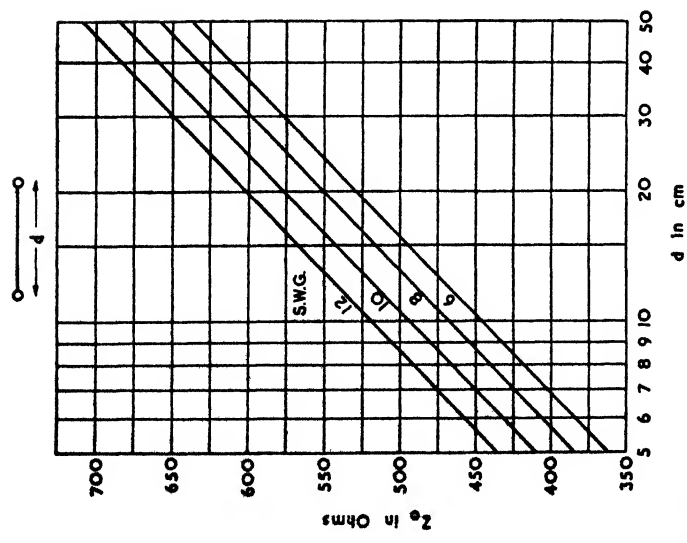


FIG. 10.7. CHARACTERISTIC IMPEDANCE OF PARALLEL-WIRE LINES

of cross-section occupied by the dielectric with "curvilinear squares," that is, with curvilinear cells which on further subdivision tend to become perfect squares. To illustrate what is meant by a curvilinear square, consider a cell (which must be a portion of an *orthogonal* system) as shown in Fig. 10.10 (a).

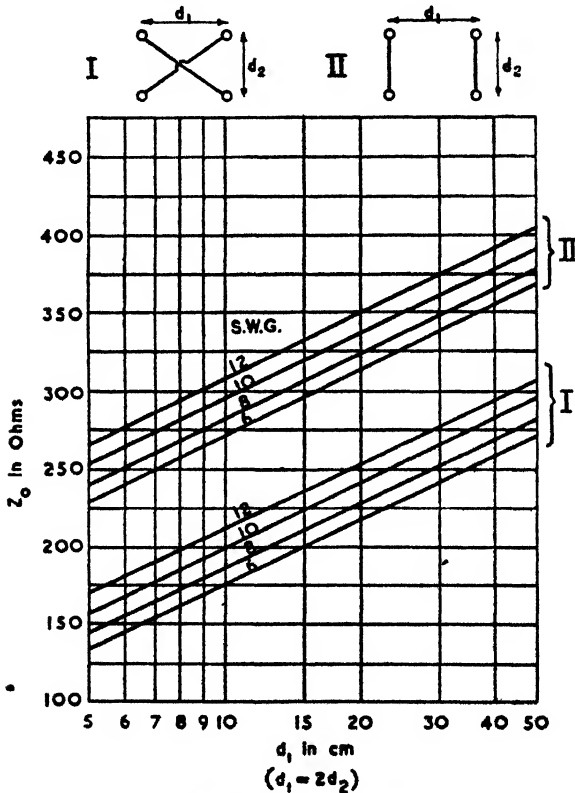


FIG. 10.9. CHARACTERISTIC IMPEDANCE OF FOUR-WIRE LINES

On sub-dividing such a cell into equal portions, we see that the ultimate figure is a rectangle. If, however, this is done with the cell shown in Fig. 10.10 (b) the ultimate shape is a square, hence the cell is a curvilinear square.

When the dielectric is air, each curvilinear square represents an impedance of 377 ohms. If two such cells are in series, i.e. if the common boundary line is a line of magnetic force, then their combined impedance is twice 377 ohms. For two cells in parallel, i.e. where the common boundary line is a

line of electric force, the combined impedance is half of 377 ohms. So for any configuration of cells we determine the

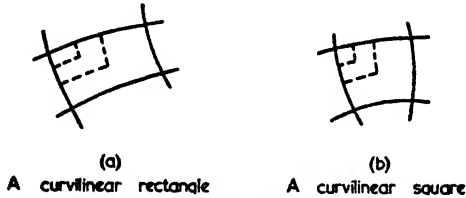


FIG. 10.10. ILLUSTRATIONS OF CURVILINEAR RECTANGLE AND SQUARE

impedance simply by multiplying 377 by the number of series elements and dividing by the number of parallel elements.

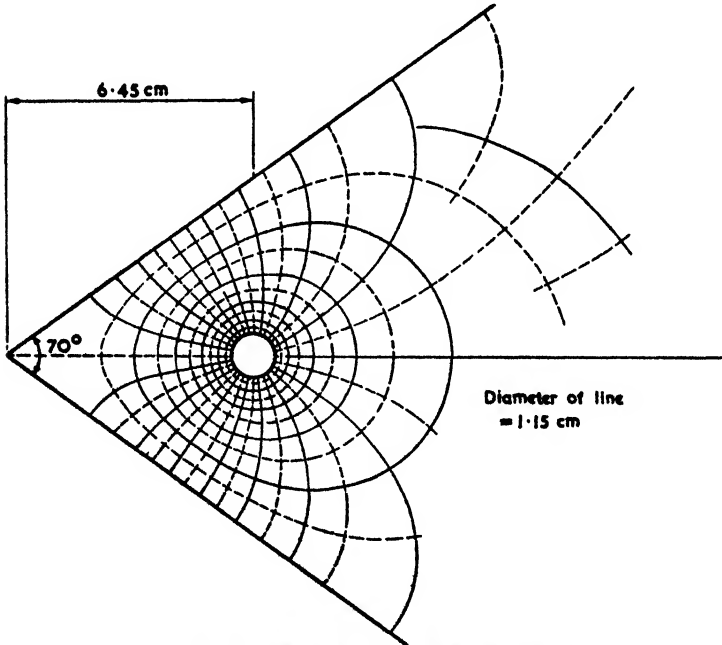
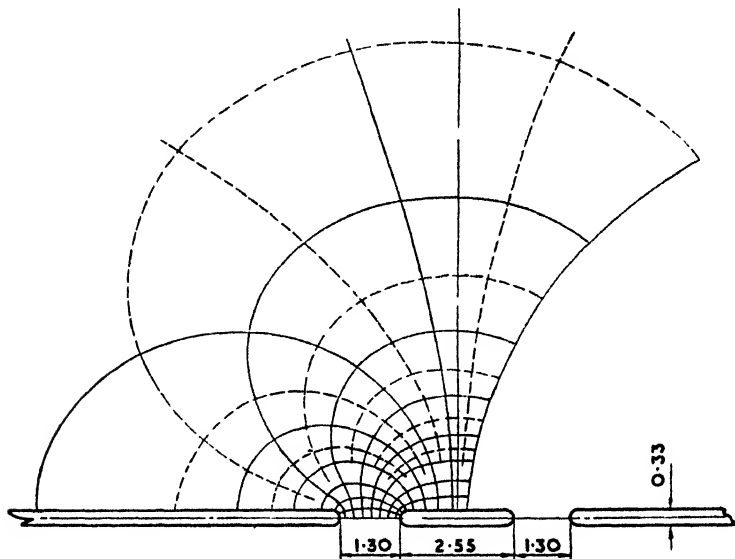


FIG. 10.11. FIELD DISTRIBUTION IN THE CROSS-SECTION OF A TRANSMISSION LINE CONSISTING OF A CYLINDRICAL CONDUCTOR AND TRIANGULAR TROUGH

Having sketched the principles of the method, let us take a specific example. In Fig. 10.11 will be seen the cross-section of a transmission line consisting of an angle piece and a circular rod.

We know that the lines of \mathbf{E} and \mathbf{H} must satisfy the boundary conditions as discussed in Vol. I, § 3.2. Since inside the metal conductors the electric intensity is exceedingly small and furthermore the *tangential* electric intensity is continuous across the boundary, it follows that the tangential components of \mathbf{E} are negligible. Consequently, the lines of electric intensity



All dimensions are
in centimetres

Strip Transmission Line

$$N = 4 \times 7.25$$

$$V = 8$$

$$Z = 377 \times 8 / 29 \approx 108 \text{ ohms}$$

FIG. 10.12. FIELD DISTRIBUTION IN THE CROSS-SECTION OF A STRIP TRANSMISSION LINE

align normally on the conductors. As for the lines of magnetic force, they must form an orthogonal system with the electric lines.

The procedure is therefore to sketch in tentatively some lines of \mathbf{E} and then an orthogonal system of \mathbf{H} lines. The cells formed in this way should be curvilinear squares. If they are not, we must re-proportion our distribution of lines. There is no objection to being left with some *fractional* value of a curvilinear square, for such fractions are simply included in the final ratio. Carrying out this process produced the family of curves shown in Fig. 10.11, in which the full lines show 15 sets of cells in

parallel and 5 sets in series. Thus we find that the characteristic impedance is

$$\begin{aligned}\zeta_0 &= 377 \times \frac{1}{1\frac{1}{2}} \\ &= 126 \text{ ohms}\end{aligned}$$

To achieve greater accuracy a finer sub-division is needed, but eventually the necessary drawing accuracy becomes too difficult to attain.

It is actually quite easy to obtain a result accurate to 5 per cent by this apparently crude trial-and-error method, while with care an accuracy of 2 per cent may be obtained. Field plotting therefore provides a convenient method for calculating the characteristic impedance of a line of uniform cross-section. A further example of field plotting is shown in Fig. 10.12.

10.3. REFLECTION, VOLTAGE AND CURRENT EQUATIONS

Reflection Coefficients

In equations (10.12) and (10.13) the constants A and B are proportional to the amplitudes of the forward- and backward-travelling waves respectively; consequently the reflection coefficient of a line terminated by some arbitrary impedance, ζ_R , is given by the ratio B/A . The impedance in the general case is obtained by dividing (10.12) by (10.13) which gives

$$\zeta_x = \frac{V_x}{I_x} = \zeta_0 \frac{Ae^{-Px} + Be^{Px}}{Ae^{-Px} - Be^{Px}} \quad (10.30)$$

If the line is cut at a point $x = l$ and a terminating impedance, ζ_R , is inserted then

$$\zeta_R = \zeta_0 \frac{Ae^{-Pl} + Be^{Pl}}{Ae^{-Pl} - Be^{Pl}}$$

On rearranging this expression we obtain

$$\frac{Be^{Pl}}{Ae^{-Pl}} = \frac{\zeta_R - \zeta_0}{\zeta_R + \zeta_0} \quad (10.31)$$

By putting $l = 0$ we find that the voltage reflection coefficient is given by

$$\frac{B}{A} = \frac{\zeta_R - \zeta_0}{\zeta_R + \zeta_0} \quad (10.32)$$

The corresponding current reflection coefficient is given by $-B/A$ and is therefore the negative of the above expression. It is apparent that in general $\frac{B}{A}$ is a complex number.

Impedance of Terminated Line

If a line is terminated as shown in Fig. 10.3 (c) the input impedance is given by putting x equal to zero in equation (10.30) thereby giving

$$Z(l) = Z_0 \frac{A + B}{A - B}$$

On using equation (10.31) we have

$$Z(l) = Z_0 \frac{1 + \frac{Z_R - Z_0}{Z_R + Z_0} e^{-2Pl}}{1 - \frac{Z_R - Z_0}{Z_R + Z_0} e^{-2Pl}}$$

This expression may be put into a more convenient form by using hyperbolic functions, when the following well-known formula is obtained—

$$Z(l) = Z_0 \frac{Z_R \cosh Pl + Z_0 \sinh Pl}{Z_R \sinh Pl + Z_0 \cosh Pl} \quad (10.33)$$

Two useful derivations from the above formula are obtained for the cases $Z_R = 0$ (short-circuited line) and $Z_R = \infty$ (open-circuited line). They are as follows—

$$(a) \quad Z_R = 0 \quad Z(l) = Z_0 \tanh Pl \quad (10.34)$$

$$(b) \quad Z_R = \infty \quad Z(l) = Z_0 \coth Pl \quad (10.35)$$

If the transmission line has no dissipation, $\alpha = 0$, so that $P = j\beta$ and the above formulae reduce to trigonometrical functions as follows—

$$(a) \quad Z_R = 0 \quad Z(l) = jZ_0 \tan \beta l \quad (10.36)$$

$$(b) \quad Z_R = \infty \quad Z(l) = -jZ_0 \cot \beta l \quad (10.37)$$

For a non-dissipative line Z_0 is necessarily real, and therefore the above two formulae result in pure reactances. A plot of the reactive impedances is shown in Fig. 10.13 for $l = 0$ to $l = \lambda$. It will be noticed that a line which is one-quarter of a wavelength long is a short circuit at its input end if the termination is an open circuit and vice versa. This property of a $\lambda/4$ line is often used for keying arrangements in which the termination is keyed from the open- to the short-circuited

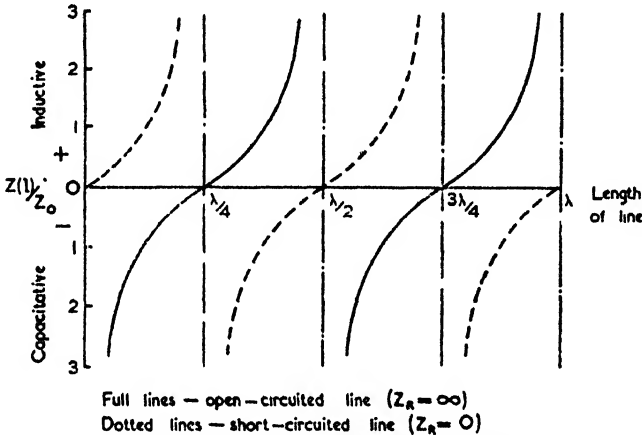


FIG. 10.13. REACTANCE CURVES FOR A NON-DISSIPATIVE LINE

conditions by means of a relay or a spark gap. In radar circuits, for instance, a spark-gap method may be used to switch the antenna system either on to the transmitter or on to the receiver in extremely short intervals of time.

Whether there is dissipation present in the line or not, we have the following simple relationship between the short-circuited input impedance ($Z_{s/c}$) and the open-circuited input impedance ($Z_{o/c}$)

$$Z_{s/c} Z_{o/c} = Z_0^2 \quad . \quad . \quad . \quad (10.38)$$

This relationship provides a method of measuring the characteristic impedance of a line experimentally.

Voltage and Current Equations

The voltage and current at any point along a transmission line (see Fig. 10.3 (c)) may be expressed in terms of V_S , the voltage at the sending end. They may be deduced from

equations (10.12), (10.13) and (10.32), which give the following formulæ—

$$V_x = V_S \frac{Z_R \cosh P(l-x) + Z_0 \sinh P(l-x)}{Z_R \cosh Pl + Z_0 \sinh Pl} \quad (10.39)$$

$$I_x = \frac{V_S}{Z_0} \frac{Z_R \sinh P(l-x) + Z_0 \cosh P(l-x)}{Z_R \cosh Pl + Z_0 \sinh Pl} \quad (10.40)$$

When standing waves are present the voltage and current values go through maxima and minima (a voltage maximum corresponding to a current minimum and vice versa). For a non-dissipative line these are related as follows—

$$\frac{V_{max}}{I_{max}} = \frac{V_{min}}{I_{min}} = Z_0$$

Since Z_0 is real, the impedance at the points of maxima and minima will also be real and given by

$$\frac{V_{max}}{I_{min}} = \rho Z_0 \quad \text{and} \quad \frac{V_{min}}{I_{max}} = \frac{Z_0}{\rho} \quad (10.41)$$

where ρ = standing wave ratio

$$= \frac{V_{max}}{V_{min}} \quad \text{or} \quad \frac{I_{max}}{I_{min}} \quad (10.42)$$

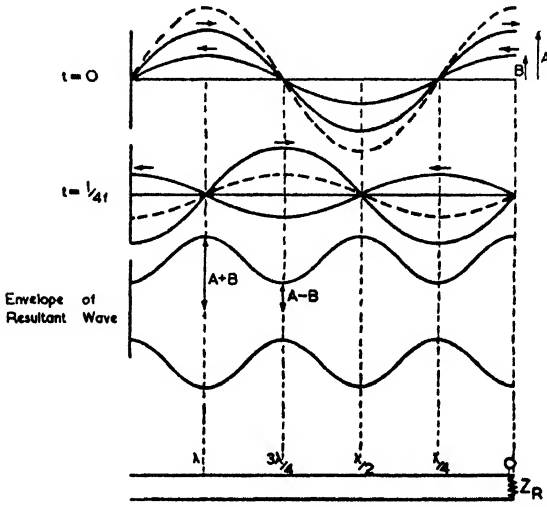
Standing Wave Ratio

Equation (10.12) showed that the voltage V_x across any part of the line was due to the sum of a forward wave Ae^{-Px} and a backward wave Be^{Px} . If the line is non-dissipative these components become $Ae^{-j\beta x}$ and $Be^{j\beta x}$, showing that the moduli of the two components are unaffected by the value of x which is a measure of the distance along the line. V_x also has a time variation of the form $e^{j\omega t}$ for the instantaneous voltage is $v_x = V_x e^{j\omega t}$, of which we take either the real or the imaginary part to give a harmonic variation in time. Somewhere along a sufficiently long line, therefore, the sum of the forward and backward waves must give voltage maxima and minima spaced at intervals of $\lambda/4$. A diagram illustrating this for two chosen intervals of time is given in Fig. 10.14.

It is apparent from such a diagram that the standing wave set up has a peak amplitude of $|A| + |B|$ at the voltage maxima and $|A| - |B|$ at the voltage minima. Hence the standing wave ratio is

$$\rho = \frac{V_{max}}{V_{min}} = \frac{|A| + |B|}{|A| - |B|} \quad (10.43)$$

The ratio $\frac{|B|}{|A|}$ is given by equation (10.32) if Z_R and Z_0 are both real. If Z_R is the impedance at a voltage maximum then



The dotted lines indicate the sum of the two waves
 A = amplitude of incident wave
 B = amplitude of reflected wave
 A = 2B

FIG. 10.14. DIAGRAMS SHOWING FORMATION OF A STANDING WAVE FROM TWO TRAVELLING WAVES

Z_R is real and may be written R_R . We therefore obtain (on putting $Z_0 = R_0$ to show that Z_0 is real)

$$\rho = \frac{R_R}{R_0} \quad (10.44)$$

Hence the standing wave ratio is equal to the ratio of the impedance at a voltage maximum to the characteristic impedance. If the impedance at a voltage minimum is considered instead, then the inverse relationship holds.

10.4. IMPEDANCE DIAGRAMS

Rectangular Form of Impedance Chart

In most practical cases sufficient accuracy can be obtained by the use of a transmission-line impedance chart as shown

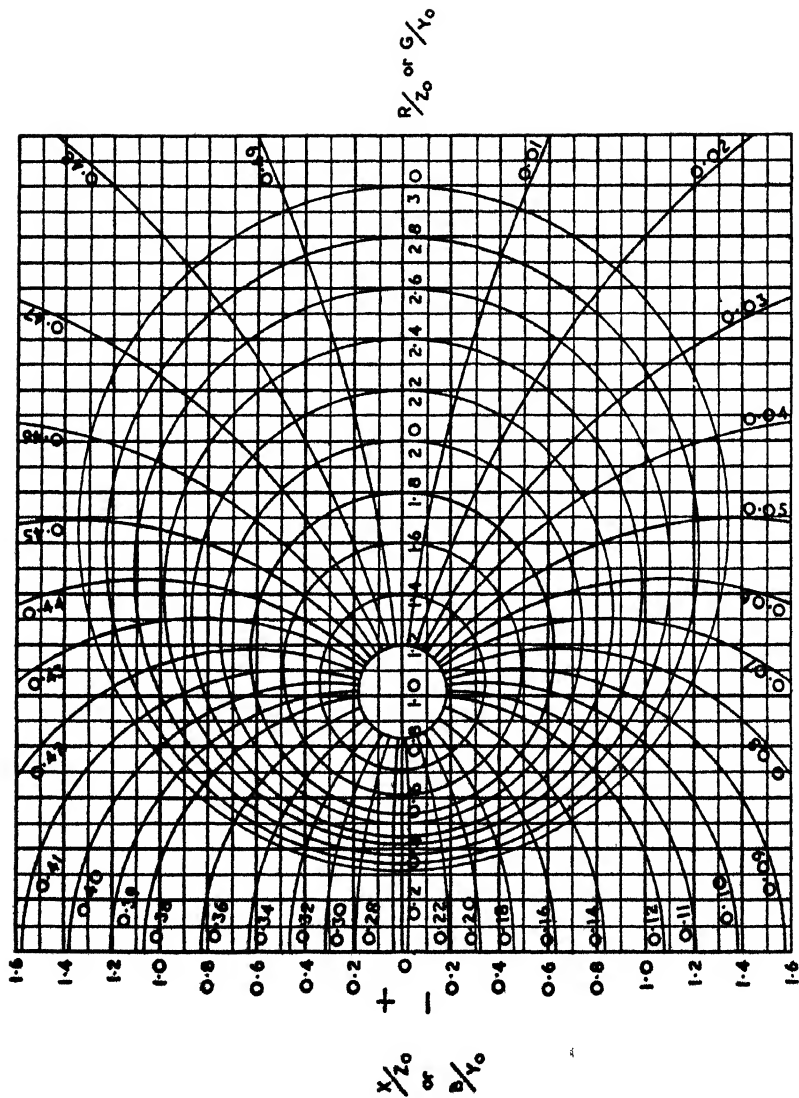


FIG. 10.15. CARTESIAN FORM OF CIRCLE DIAGRAM OF IMPEDANCE

in Fig. 10.15, which is known as the circle diagram of impedance. This particular form uses rectangular co-ordinates for the real and imaginary parts of the series impedance, but the polar version as shown in Fig. 10.16 (it is described by Smith⁽³⁸⁹⁾ and also by Willis Jackson and Huxley⁽³⁹¹⁾) is even more convenient if a separate rotating arm is available. In addition, the polar version has the merit of catering for *all* values of impedance.

The circle diagram is standardized in terms of Z_0 , so that an impedance of, say, $900 - j480$ would be read as $1.5 - j0.8$ if Z_0 were 600 ohms.

It can be shown⁽⁹⁾ ⁽²¹⁾ that the circles which have the real axis as a diameter are circles of constant αl (where αl is the total one-way attenuation along a line of length l , while those which pass through the point $1 + j0$ and have the imaginary axis as a diameter are circles of constant βl (where βl is the distance along the line in radians—it should be noted that the value of βl changes by $\pi/2$ on passing through $l + j0$). It is therefore convenient to refer to them as the “ αl ” and “ βl ” circles respectively.

If a line has no attenuation, the input impedance is found by travelling along one of the αl circles for a distance equal to the length of line, the said distance being given by the difference in the βl values. The process may be appreciated by the following example—

Example

In Fig. 10.17 we have a line of characteristic impedance 600 ohms, whose length at 30 Mc/s is 0.34 of a wavelength. It is terminated by a resistance of 1 430 ohms in series with a capacitance of $13.6 \mu\mu\text{F}$.

The impedance of C at 30 Mc/s is 390 ohms. Hence the terminating impedance is given by

$$\begin{aligned} Z_R &= 1\,430 - j390 \text{ ohms} \\ &= 2.38 - j0.65 \text{ in terms of } Z_0 \end{aligned}$$

Reading on the diagram of Fig. 10.15 shows that this represents a point which is given by the intersection of the βl curve of 0.02 λ with the αl circle which passes through

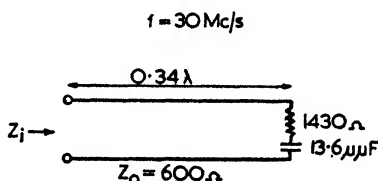


FIG. 10.17. FIGURE FOR EXAMPLE—
TRANSMISSION-LINE CALCULATION

$R/Z_0 = 2.6$ on the real axis. We follow this αl circle in a clockwise direction until it is intersected by the βl curve whose value is $(0.02\lambda + 0.34\lambda)$. At this point we find that $R = 0.58Z_0$ and $X = 0.64Z_0$, i.e. $R = 346$ ohms and $X = 384$ ohms. Hence

$$\underline{\underline{Z_i = 346 + j384 \text{ ohms}}}$$

Had the length of line been 0.23λ or 0.48λ the impedance would have been purely resistive, the values being $R = 0.384Z_0$ and $R = 2.6Z_0$ respectively. It is apparent that whatever length we make the line the impedance will never be less than $0.384Z_0$ and never greater than $2.6Z_0$. Also at such points the input impedance is purely resistive and the r.m.s.

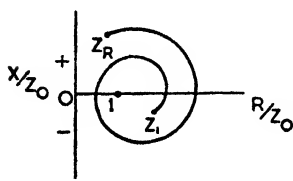


FIG. 10.18. IMPEDANCE DIAGRAM FOR A DISSIPATIVE TRANSMISSION LINE

voltages are a minimum and a maximum respectively, while the currents are a maximum and a minimum. Since the line itself dissipates no power, it follows that equal powers are dissipated in either case; hence the ratio of V_{max}/V_{min} or I_{max}/I_{min} is equal to 2.6. In the previous section these ratios were defined as the standing wave ratio; so we come to the conclusion that the standing wave ratio, ρ , is given by the intercepts of the αl circle with the real axis.

Hence the αl circles might also be termed circles of constant standing wave ratio, and this is perhaps the better definition, for the attenuation constant of the line itself is zero if we keep to a given circle—the value of αl has really been derived for some imaginary length of attenuating line whose input impedance equals that of the termination Z_R . If the transmission line under consideration were not non-dissipating then, instead of travelling on a constant αl circle, we should have to spiral inwards, cutting across circles whose values of αl became greater and greater as we came inwards. A spiral of this nature is shown in Fig. 10.18, while in Fig. 10.19 are shown the formulae for determining the αl and βl circles. For a fuller account (in which the derivation of these curves is also given) the reader may refer to the book by Slater⁽²¹⁾.

Exactly the same curves may be used for admittances of the form $G + jB$, where G is the conductance and B the susceptance. In this case the values will be standardized in terms of Y_0 , the characteristic admittance of the line, where

Exactly the same curves may be used for admittances of the form $G + jB$, where G is the conductance and B the susceptance. In this case the values will be standardized in terms of Y_0 , the characteristic admittance of the line, where

$Y_0 = 1/Z_0$. The advantage of the admittance form of the circle diagram is that the value of a stub which is in parallel across the line can then be readily calculated, for, as is well known, admittances which are in parallel may be added together.

Yet another virtue of the circle diagram is that it may be used for converting impedances into admittances. For this purpose we use the impedance inverting properties of a quarter-wave length of line. Thus the impedance $R/Z_0 + jX/Z_0$ is equal to the admittance $G/Y_0 + jB/Y_0$ where G/Y_0 and B/Y_0 are given by travelling round an al circle for a distance of $\beta l = 0.25\lambda$ and then reading the chart as an admittance

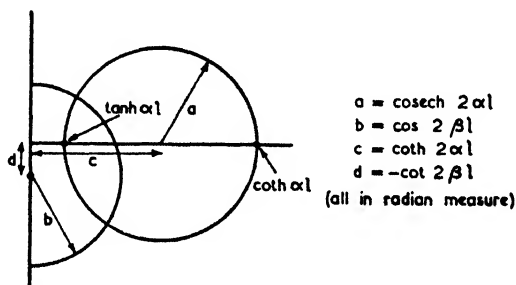


FIG. 10.19. CONSTRUCTION OF CARTESIAN FORM OF IMPEDANCE DIAGRAM

diagram. The method will be illustrated by the following example.

Example

Let us suppose that in the example of Fig. 10.17 we wish to find the length of line which will tune out the reactance of Z_i .

From the point $0.58 + j0.64$ which represents Z_i and is on $\beta l = 0.36\lambda$ we travel along the al circle (in this case the circle passing through $R = 2.6Z_0$) until $\beta l = 0.36\lambda + 0.25\lambda$, which equals 0.11λ on subtracting half a wavelength. (It should be noted that since the impedance conditions repeat themselves every half-wavelength, such a subtraction can always be performed.)

The new point is $0.77 - j0.85$ and this equals $G/Y_0 + jB/Y_0$, so that $G + jB = (1.28 - j1.42)10^{-3}$ mhos on putting $Y_0 = 1/Z_0$. To reduce the reactance to zero, we must therefore add an admittance equal to $+j1.42 \times 10^{-3}$ mhos, i.e. an impedance equal to $-j707$ ohms or $-j1.175Z_0$.

At a frequency of 30 Mc/s such an impedance would be given by a capacitance of $75 \mu\mu\text{F}$.

The required length of stub is given by equations (10.36) and (10.37) for short- and open-circuited stubs respectively, and if the characteristic impedance of the stub is the same as that of the line, we have for an open-circuited stub

$$\begin{aligned}\beta l &= \cot^{-1} (1.175) \\ &= 0.705 \text{ radians}\end{aligned}$$

i.e. $l = \underline{\underline{0.112\lambda}}$

The calculation can be carried through entirely by means of the circle diagram, by making use of the fact that the imaginary axis corresponds to a circle of infinite radius for which $\alpha l = 0$. This provides us with a method of inverting susceptances and of finding the line lengths of stubs (assuming, of course, that the diagram happens to cover the values in question). Thus in the present case we take $B/Y_0 = -j0.85$ and travel along the imaginary axis until the value of l is increased by 0.25λ , i.e. we go from $l = 0.138\lambda$ to $l = 0.388\lambda$. At the latter point we find X/Z_0 and this equals $+j1.175$. Hence the required stub has a reactance of $-j1.175Z_0$ as previously calculated.

The length of this stub is given by the value of l at the point $X/Z_0 = -j1.175$. This value is such that $l = \underline{\underline{0.112\lambda}}$, which agrees with the previous figure. The stub in question is obviously open-circuited since for smaller l -values the negative reactive impedance increases.

Matching Two Impedances

It is apparent from the impedance chart that any two real impedances R_1 and R_2 can be matched by means of a quarter-wave section of line whose characteristic impedance Z_0 is the geometric mean of the two resistances, i.e. $Z_0^2 = R_1 R_2$. Thus an antenna whose impedance is 72 ohms could be matched to a line of characteristic impedance 600 ohms by means of a $\lambda/4$ section of line for which $Z_0 = 208$ ohms (Fig. 10.20 (a)).

Such a matching section is, however, only accurate for one frequency, since at neighbouring frequencies the line is either shorter or longer than $\lambda/4$. By performing the matching in two steps a wider range of frequencies can be catered for. In the example given above we should use two $\lambda/4$ sections having $Z_0' = \sqrt{(72 \times 208)}$ and $Z_0'' = (\sqrt{208 \times 600})$.

That an improvement is obtained can be appreciated by considering Fig. 10.21. If the frequency is on the high side, the first section is longer than $\lambda/4$ so that we travel along the αl circle to a point p_1 . On considering the second section, the position of p_1 tends to compensate for the fact that the second

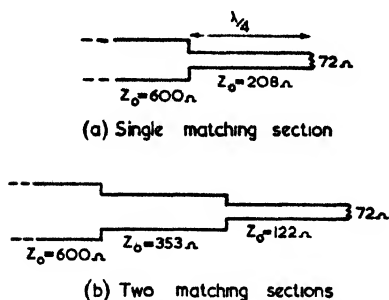


FIG. 10.20. EXAMPLES OF QUARTER-WAVE MATCHING SECTIONS

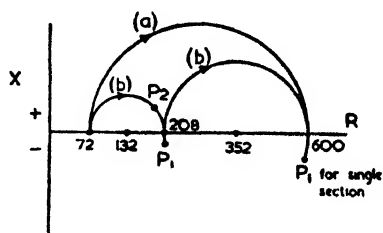


FIG. 10.21. IMPEDANCE DIAGRAMS FOR MATCHING SECTIONS SHOWN IN FIG. 10.20

section is also longer than $\lambda/4$. Consequently the final impedance is nearer 600 ohms than it would be with a single section only. For lower frequencies we come to some point such as p_2 , and here again a certain amount of compensation occurs between the two sections.

Considerations of this nature show that the best match over a band of frequencies is obtained by having a tapering transmission line of slowly varying characteristic impedance (for the best results the line must be long in comparison with a wavelength).

In the general case involving the matching of two complex impedances, we construct a circle whose centre lies on the real axis and whose circumference passes through the two points Z_R and Z_S (Fig. 10.22). Then Z_0 is given by the geometric mean of the two intersections with the real axis, and the length of line required is found either by geometrical constructions based on the curves and formulae of Fig. 10.19 or by scaling the original figure to fit a given impedance chart. Usually it is better practice to tune out the reactances of Z_R and Z_S before introducing a matching section.

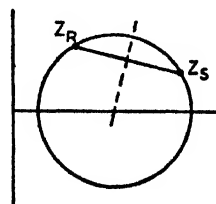


FIG. 10.22. IMPEDANCE DIAGRAM FOR MATCHING TWO IMPEDANCES

Tuning Out Reactances

For any position on the impedance charts of Figs. 10.15 or 10.16 it is possible to add a reactance whose value completely cancels that indicated by the point in question. If we use a line whose length is such that the real part of the impedance equals Z_0 , then on adding the cancelling reactance the final impedance is Z_0 . For example, in Fig. 10.23 we start with an impedance represented by the point P , add a length of line given by PP' ; then a reactance equal and opposite to that of P' brings us to Z_0 .

It must not be forgotten when dealing with the reactance and resistance values that *the elements are in series*. In practice

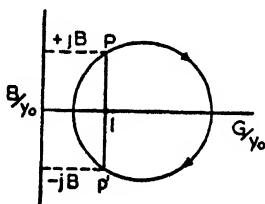


FIG. 10.23. TUNING OUT OF REACTANCE AS SHOWN BY THE IMPEDANCE DIAGRAM

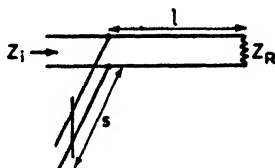


FIG. 10.24. DIAGRAM OF SINGLE-STUB TUNING CIRCUIT

it is often more convenient to introduce a shunt reactance and in this case the circle diagram should be used in terms of admittance. For example, if a line is shunted by a capacitance (due to a dielectric spacer, for instance) whose susceptance is $+jB$ (denoted by P in Fig. 10.23), then on transversing about a quarter of a wavelength of line we arrive at the point P' where the addition of a similar shunt capacitance would bring us back to $G/Y_0 = 1$. The correct spacing of line discontinuities can therefore result in compensating effects which leave the effective admittance of the line unchanged. In order to obtain better compensation over a range of frequencies either the capacitances of the spacers or their distance apart may be varied, or both factors can be varied. A number of such arrangements have been described in patent specifications.

The input impedance of a line can always be made equal to Z_0 if we have at our disposal an adjustable stub at an adjustable distance along the line. Referring to Fig. 10.24, we make " l " such that the conductance looking towards Z_R is equal to Y_0 and adjust " s " so as to tune out the susceptance.

In most practical cases, however, it is inconvenient to provide an adjustable length of line so that extra tuning stubs at fixed positions are to be preferred. To cover all possibilities it is necessary to employ *three* stubs, but two will cover the majority of requirements; the latter arrangement is sometimes called a double-shunt tuner.

The double-shunt tuner has been described by Slater,⁽²¹⁾ whose method we shall follow in the explanations given below.

In Fig. 10.25 (a) we have stubs at P' and P'' separated by a distance l . At P' the admittance Y_1 is $G_1 + jB_1$ where B_1 is

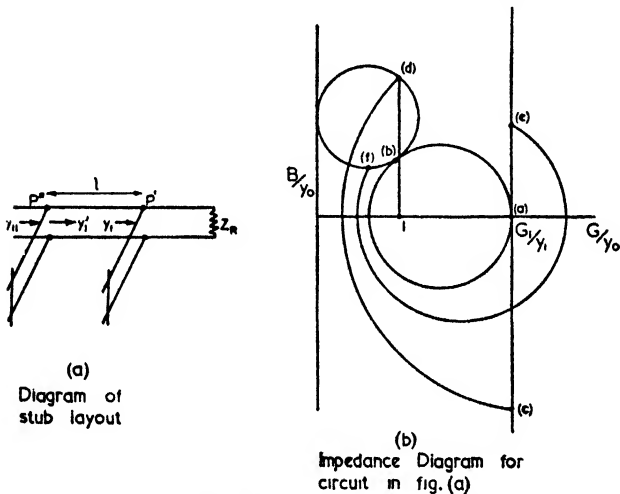


FIG. 10.25. DIAGRAM OF TWO-STUB TUNING CIRCUIT

adjustable by means of the first stub. Fig. 10.25 (b) shows the admittance diagram in which (a) is the point G_1/Y_0 and (c) is the point $G_1/Y_0 + jB_1/Y_0$. The admittance Y_{11} is given by the point (b), which is such that (a) (b) represents a line of length equal to l . We draw a circle touching the admittance circle at the point (b) and also the imaginary axis, then all admittance circles cutting the line (a) (c) and the second circle will represent a line of length l between the intercepts. For example, the portions (c) (d) and (e) (f) both represent line lengths equal to l .

In the diagram (d) is vertically above $G/Y_0 = 1$, so that the appropriate shunt admittance at this point will make Y_{11} equal to Y_0 . Therefore the first stub should have a length corresponding to (a) (c). It is apparent from this diagram that the

matching cannot be carried out at all if the circle touching the imaginary axis is not cut by the vertical line through the point $1 + j0$. A spacing between the stubs such that $l = \lambda/8$ will cover a wide range of values for impedance matching.

10.5. PRACTICAL CONSIDERATIONS

The following paragraphs deal with some of the more purely practical aspects of transmission-line design. For further details the reader may consult papers by Sterba and Feldman,⁽³⁴³⁾ Cork and Pawsey,⁽³²⁴⁾ and McLean and Bolt.⁽³³⁵⁾

The relative merits of coaxial and open-wire lines are such that both types are still in use and both types have their protagonists. Broadly speaking, the coaxial type is to be preferred for medium-wave broadcasting, while open-wire lines function adequately on short-wave transmitting systems ("open-wire" lines would include lines such as an unbalanced 6-wire line with a centre conductor—such lines form an alternative to a solid coaxial line). For reception purposes the coaxial line or the shielded pair are to be preferred on account of their freedom from pick-up of noise.

Power-handling Capacity

In order to reduce the likelihood of flashover or corona to a minimum, it is obviously an advantage to employ transmission lines whose proportions are such that the voltage gradient between the conductors is a minimum. With a given power input, this can be shown⁽⁹⁾ to call for a ratio of b/a of 1.65, i.e. $Z_0 = 30$ ohms (if a given *input voltage* is assumed $b/a = 2.72$ and $Z_0 = 60$ ohms). This ratio for the minimum voltage gradient is not critical. For a characteristic impedance of 50 ohms the voltage gradient is only about 10 per cent greater than the minimum. In any case it must be remembered that these ratios are for perfectly smooth conductors. In practice the voltage gradient may be more a function of the roughness of the surfaces rather than of the ratio of b/a , hence the above-mentioned proportions are mainly of academic interest.

From experiments at power frequencies it has been found that discharges occur from the centre conductor if the peak voltage gradient exceeds about 30 kV/cm. This is reason to believe that at radio frequencies the permissible electric stress is roughly the same. In practice the greatest stresses will occur

in the neighbourhood of the supporting insulators; for example, Sterba and Feldman⁽³⁴³⁾ found that a line of 6 cm outer diameter broke down near the insulators with 9 000 r.m.s. volts. This represents a peak voltage gradient of only 6 kV/cm if based on the conductor separation.

With parallel transmission lines it would appear from the results obtained by McLean and Bolt⁽³³⁵⁾ that the corona breakdown voltage varies but little with spacing (their minimum spacing was 9 cm). Using No. 6 S.W.G. they found that

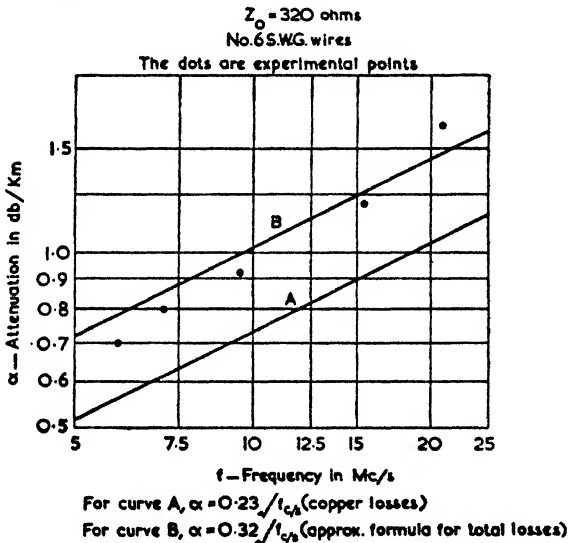


FIG. 10.26. ATTENUATION OF FOUR-WIRE TRANSMISSION LINE
(McLean and Bolt, *Jour. I.E.E.*, May, 1946)

the maximum working voltage was 30 kV peak between the two wires. Their results also showed that the same peak voltage is the approximate upper limit for 12 in. rod insulators (these were used to support the lines, there being no spacers between the lines themselves) while the fitting of these rods with corona rings more than doubled this permissible voltage.

With large transmission lines, therefore, the choice of line rests on the permissible attenuation rather than on limitations due to corona. Curves showing the attenuation for different lines over a wide range of frequencies are given in Figs. 10.4 and 10.5. Due to insulator and leakage losses the total losses will be some 20 to 60 per cent higher than those given in these figures. An example is shown in Fig. 10.26 which is taken

from the curves given by McLean and Bolt.⁽³³⁵⁾ In their article it is also stated that the average length of open-wire line at B.B.C. short-wave stations is 0.6 km, which results in a power loss of 18 kW per 100 kW at a frequency of 17.8 Mc/s. It is obviously advantageous to place the antennae that are working at the highest frequencies nearest to the transmitters; by doing this the B.B.C. keep the efficiency of all lines at approximately 82 per cent.

Radiation Losses

The radiation from coaxial lines (or twin screened lines) is negligible and would be zero if the walls were perfect conductors. It is only from open ends that any radiation into space takes place. The radiation from an open end has been calculated to be⁽⁷⁷⁾

$$R_{ir} = \frac{20\pi^2 A^2}{\lambda^4} \quad . \quad . \quad . \quad (10.45)$$

where A = area of opening.

In practice λ is usually many times the outer radius of the line, so that the radiation losses from an open end are quite small.

With open-wire transmission lines the radiated power is increased if standing waves are present, but to obtain any significant radiation losses the lines must be appreciably unbalanced. Sterba and Feldman⁽³⁴⁸⁾ give the power radiated from a balanced line carrying a travelling wave only as

$$W = 160 \left(\frac{\pi d}{\lambda} \right)^2 I^2 \quad . \quad . \quad . \quad (10.46)$$

Hence the radiation resistance of the line is given by

$$R_r = 1580 d^2 / \lambda^2 \quad . \quad . \quad . \quad (10.47)$$

Comparing this with equation (4.44), Vol. I, shows that R_r is equal to twice the radiation resistance of a uniform filament of current of length d . This statement immediately indicates the minute amount of radiation from a parallel wire for which $d < \lambda$. The above formulae apply to any length of line provided only that $d < 0.1\lambda$ and that the line length is greater than $20d/\lambda$. Fig. 10.27 shows the power radiated from lines for which $Z_0 = 600$ when the transmitted power is 1 kW.

If the line is balanced but carries a standing wave the radiation loss is increased to an extent depending on the amplitude of the standing wave and its position with respect to the ends

of the line. For a pure standing wave the radiation is a maximum when the current is zero at both ends. It is then given by

$$W = 120 \left(\frac{\pi d}{\lambda} \right)^2 I_p^2 \quad . \quad . \quad . \quad (10.48)$$

where $I_p = \text{peak current in amperes.}$

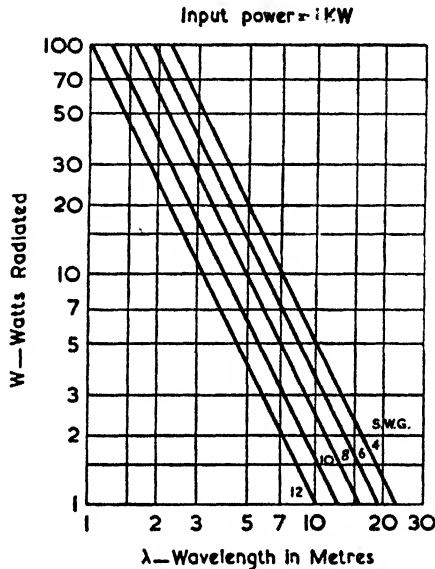


FIG. 10.27. RADIATION FROM A LONG PARALLEL-WIRE TRANSMISSION LINE WHOSE CHARACTERISTIC IMPEDANCE IS 600 OHMS (Sterba and Feldman, *Proc. I.R.E.*, July, 1932)

The radiation is a minimum when the current is a maximum at each end, and is then expressed by

$$W = 40 \left(\frac{\pi d}{\lambda} \right)^2 I_p^2 \quad . \quad . \quad . \quad (10.49)$$

If the line is *unbalanced*, the radiation may become appreciable. Sterba and Feldman⁽³⁴³⁾ have shown that for lines whose height above the ground is h , the power radiated by an unbalanced current of I amperes (r.m.s.) is given approximately by

$$W = 80I^2 \quad \text{if } h = \lambda/4 \quad . \quad . \quad (10.50)$$

$$W = 125I^2 \quad \text{if } h = \lambda/2 \quad . \quad . \quad (10.51)$$

The length of line should exceed four times the height in either case. In practice the losses have been found to exceed

these values and the extra losses are probably due to the imperfect conductivity of the ground.

As an example let us consider a parallel-wire line of No. 6 S.W.G. whose characteristic impedance is 600 ohms and which is transmitting 10 kW of power at a frequency of 20 Mc/s.

Reading from Fig. 10.27, we find that the radiated power is $1.6 \times 10 = 16$ watts.

If the line were unbalanced so that the currents were 5.0 amp and 3.2 amp, then the radiated power due to the balanced currents would be decreased by some 40 per cent but the unbalanced current of 1.8 amp would radiate about 260 watts—a far greater loss than that due to the balanced components.

Dissipative Transmission Lines

When open-wire transmission lines are used as loads the two main requirements are that the input impedance should be sensibly resistive and secondly that the wires are not heated unduly. Both these requirements can be met by the simple expedient of using very long lines, but this would often be very uneconomical. It is good practice, therefore, to grade the line so that the power loss per unit length is approximately constant. For convenience the end of the line is usually left open-circuited or short-circuited (the reflected wave travelling back to the generator will be attenuated by the same amount as the forward wave). The total length required can be reduced if one goes to the trouble of making an exponential line; such a line has been described by Burrows.⁽³²¹⁾

The input impedance of a dissipative line is given by equation (10.34) or (10.35), according to whether the end is short- or open-circuited, and the corresponding impedance diagram takes the form of a spiral as shown in Fig. 10.18. As this spiral comes towards the centre it crosses the family of constant αl circles whose intercepts with the real axis are shown in Fig. 10.19. When calculating the attenuation we are not interested in the actual input impedance, so αl can be calculated by its intercepts with the real axis and these are related directly with the standing wave ratio, ρ , as follows—

$$\rho = \coth \alpha l \quad . \quad . \quad . \quad (10.52)$$

If we stipulate a certain value of ρ , then the value of l can be obtained for a line whose attenuation coefficient is known. The resultant input impedance is not necessarily resistive but

this is immaterial as far as the standing wave ratio is concerned. It will be realized that this particular standing wave exists only in the immediate neighbourhood of the input end of the line, since farther down the line the standing wave ratio increases.

A point that must not be overlooked is that whereas ρ defines the input impedance (which lies on one of the αl circles) and therefore allows for the reflected wave as well as the forward wave, the value of αl refers to the attenuation for *one-way* propagation only.

Example

A line is required whose losses are such that the input impedance corresponds to a standing wave ratio of 2. (It does not matter whether the line is open- or short-circuited; in both cases perfect reflection occurs at the end.) From equation (10.43) we have

$$\rho = 2 = \frac{|A| + |B|}{|A| - |B|}$$

where $|A|$ = amplitude of forward-travelling wave,
 $|B|$ = amplitude of reflected wave.

Hence $\frac{|A|}{|B|} = 3$.

The *two-way* attenuation is therefore such that the voltage or current amplitudes are decreased by a factor of 3. This corresponds to an attenuation of 9.54 db.

From equation (10.52) we have

$$\coth \alpha l = 2$$

i.e.

$$\alpha l = \underline{4.77 \text{ db}}$$

This is the *one-way* attenuation value.

The following table presents some figures of practical value as given by equation (10.52). Appropriate values for α may be obtained from the curves of Fig. 10.5.

Standing Wave Ratio ρ at Input Terminals	One-way Attenuation αl , in nepers	One-way Attenuation αl , in db	Two-way Attenuation $2\alpha l$, in db
1.05	1.86	16.1	32.2
1.10	1.52	13.2	26.4
1.15	1.33	11.55	23.1
1.20	1.20	10.4	20.8

Heat Dissipation

When designing attenuating lines for loads (for example, the terminating load for a rhombic antenna) the temperature rise of the conductors must be taken into account in cases where the power dissipated is great.

Fig. 10.28 shows the temperature of the wire for a number of different power dissipations with varying conductor radius.

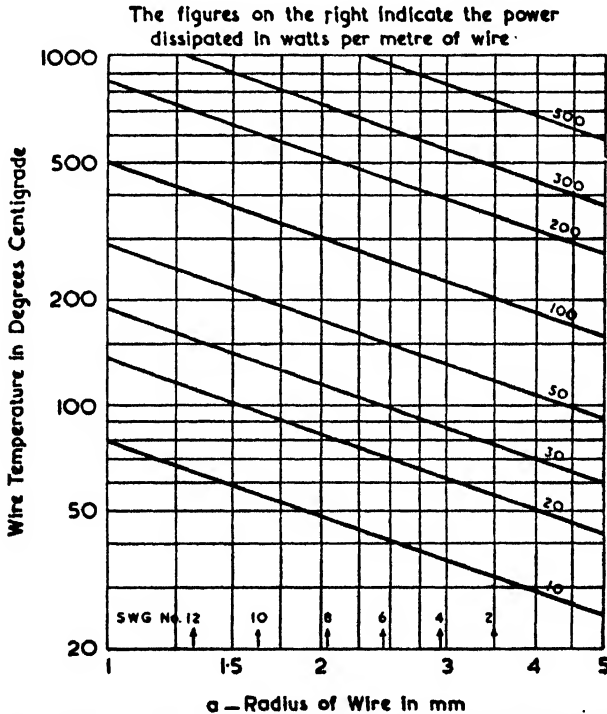


FIG. 10.28. TEMPERATURE OF A DISSIPATIVE WIRE SITUATED IN FREE AIR

These curves have been calculated from data given in an article by Barnes⁽⁸⁴⁹⁾ and apply to wire with a matt surface (it is immaterial whether the conductor is solid or hollow).

10.6. USE OF STUB TO INCREASE ANTENNA BANDWIDTH

One of the most useful applications of transmission lines to antenna design is in the use of a tuning stub at the input

terminals of an antenna to increase the bandwidth. Such a device is particularly suitable for ultra-short and microwave antennae; it should not be confused with a "detuning stub" (as shown in Fig. 3.42) whose purpose is merely to provide a high impedance to waves travelling along the outside of the coaxial feeder.

The action of a tuning stub is readily seen if we consider a half-wave antenna, such as the one shown in Fig. 10.29, and remember that the input impedance of the antenna is similar to that of an open-circuited but dissipative transmission line. A *short-circuited* transmission line of the same length will obviously tend to cancel the variations in reactance with frequency—it is simply a question of figuring out a suitable length and characteristic impedance for this stub. The manner in which this may be done is illustrated in the following example.

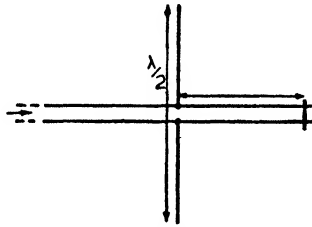


FIG. 10.29. USE OF STUB IN PARALLEL WITH INPUT TERMINALS TO INCREASE BANDWIDTH OF ANTENNA

Example

A whip antenna suitable for mounting on an aircraft to form a quarter-wave antenna (the fuselage being the "earth") is required to operate over a band of frequencies in the region of 125 Mc/s. The length of the whip divided by the mean radius is equal to 200. Assuming that a standing wave ratio of 1.5 can be tolerated, it is required to find the bandwidth obtainable by means of a tuning stub and also the characteristics of the stub.

By interpolation from the curves of Figs. 3.1 and 3.2 we can prepare an admittance diagram of the antenna as shown in Fig. 10.30 (the necessary inversions from impedance to admittance may be performed with the aid of a circle diagram as described on p. 457). With the same figures we also prepare the curves of conductance and susceptance plotted against fractions of a wavelength as shown in Fig. 10.31.

On the admittance diagram the value of Y_0 is 0.02 mhos, since the characteristic impedance of the transmission line is 50 ohms. The choice of 50 ohms lies in the fact that on resonance the antenna has an impedance of about 35 ohms, and this results in a standing wave ratio of 1.43, i.e. within the limit of 1.5. At frequencies on either side of the resonant

point the antenna impedance will be greater than the maximum tolerable impedance (assuming a purely resistive input), being 75 ohms for a standing wave ratio of 1.5.

The standing wave ratio circle, $\rho = 1.5$, has been marked in on the admittance chart. So long as the admittance falls within this circle ρ will not exceed 1.5. From a study of the

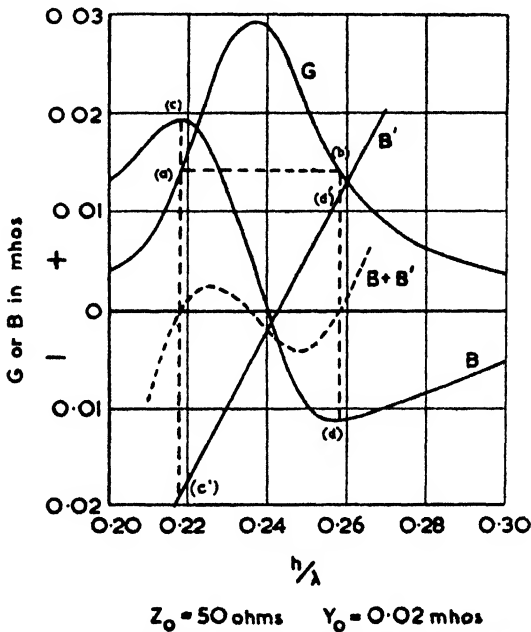


FIG. 10.30. ADMITTANCE DIAGRAM OF WHIP ANTENNA

full curve of Fig. 10.31, together with the corresponding curves of Fig. 10.30, it is apparent that the bandwidth is from 0.237λ to 0.247λ , i.e. about ± 2 per cent.

If the susceptance is made equal to zero at the ends of the band, then the corresponding conductance values must be such that $G/Y_0 = \frac{2}{3}$ in order that $\rho = 1.5$. A convenient value to take is $G = 0.014$ mhos, i.e. $G/Y_0 = 0.7$. We therefore draw a line at this value intersecting the conductance curve at the points (a) and (b). The corresponding susceptance values are (c) and (d) and these are tuned out by two equal and opposite susceptances (c') and (d') due to the tuning stub.

In drawing in the susceptance curve of the tuning stub, use can be made of the fact that $\cot \beta l = (\pi/2 - \beta l)$ in the region

of $\beta l = \pi/2$, hence a straight line may be drawn joining (c') and (d'). The susceptance of the stub is given by

$$\begin{aligned} B' &= Y_0' \cot \beta l \\ &= Y_0' \beta l \end{aligned}$$

The value of Y_0' is therefore given by the slope of (c') (d')

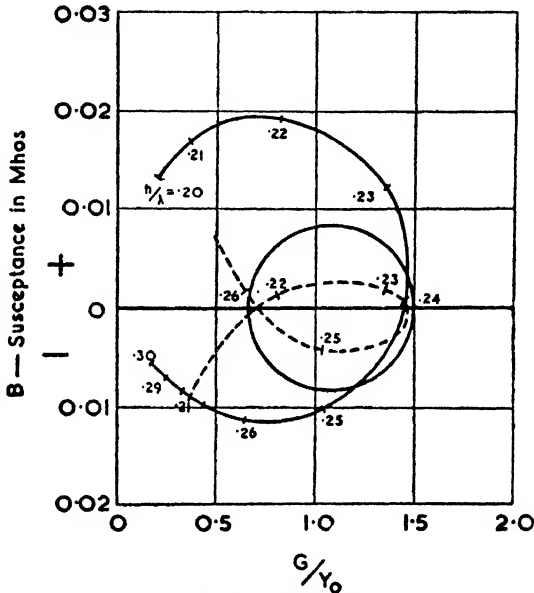


FIG. 10.31. CIRCLE DIAGRAM OF ADMITTANCE FOR WHIP ANTENNA

and that of l by the intercept with the real axis. From Fig. 10.16 we find that

$$Y_0' = 0.123 \text{ mhos}$$

i.e.

$$Z_0' = 8.1 \text{ ohms}$$

$$l = 0.243\lambda$$

The combined susceptance curve is shown dotted and is marked $B + B'$. With the aid of this curve and the conductance curve we can construct a new admittance curve as shown by the dotted curve of Fig. 10.31. It is obvious from this last curve that a far greater proportion of the admittance characteristic now lies within the $\rho = 1.5$ circle. From a study of this curve and the corresponding curves of Fig. 10.30 we find

that the limits are now 0.259 and 2.217λ , i.e. about ± 8 per cent.

The mid-point of this band is 0.238λ and this is to correspond to a frequency of 125 Mc/s. Hence the height, h , of the antenna is given by

$$\begin{aligned} h &= 0.238\lambda = 0.238 \times 2.4 \text{ m} \\ &= 0.572 \text{ m} \end{aligned}$$

$$\begin{aligned} \text{Also } l &= \lambda/4 \text{ at } 2.4 \times \frac{0.238}{0.243} \text{ m} \\ &= 0.587 \text{ m} \end{aligned}$$

A dielectric-filled line must be used for the stub in order to obtain the very low characteristic impedance. Consequently

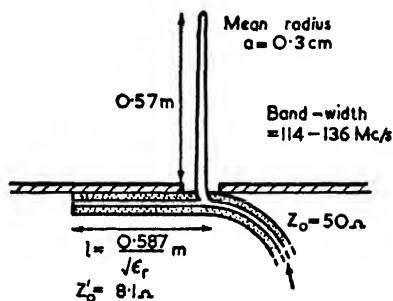


FIG. 10.32. DIAGRAM OF WHIP ANTENNA DESIGNED WITH STUB FOR WIDENING BANDWIDTH

the actual stub length will be shorter than the above calculated value by a factor of $\sqrt{\epsilon_r}$.

The results are summarized in Fig. 10.32.

APPENDIX I

DIELECTRIC CONSTANT AND CONDUCTIVITY TABLES

The figures in Table I are based on a survey of available data, together with some personal experience of the electrical characteristics of the ground. Ground constants have also been published in some of the books and articles quoted in the bibliography.^{(15) (23) (246)}

In calculating the complex dielectric constant ϵ' from the equation $\epsilon' = \epsilon_r - j60\lambda g$, λ is the wavelength in metres and g is the conductivity in mhos per metre, but for purposes of comparison the conductivity is also given in e.m.u.

TABLE I: TYPICAL GROUND CONSTANTS

Type of Ground	Relative Dielectric Constant ϵ_r	Conductivity g	
		Mhos/metre	E.M.U.
Exceptionally well-watered pastoral land with rich soil	20	0.03	3×10^{-13}
Pastoral land with good soil	15	0.01	1×10^{-13}
Pastoral land with low hills	10	0.005	5×10^{-14}
Hilly country with moderate vegetation	5	0.002	2×10^{-14}
Built-up urban districts	5	0.001	1×10^{-14}
Exceptionally hard, rocky country, sparsely vegetated	5	0.0002	2×10^{-16}
Sea water	80	4 to 5	$4 \text{ to } 5 \times 10^{-11}$
Fresh water	80	0.01 to 0.001	1×10^{-13} to 1×10^{-14}

TABLE II: METALS AND INSULATORS

Material	Relative Dielectric Constant ϵ_r	Conductivity g in mhos/metre
Copper		5.8×10^7
Silver		6.14×10^7
Iron.		1.0×10^7
Steel		0.5 to 1×10^7
Porcelain	5 to 6.5	3×10^{-12}
Glass	6 to 9	1×10^{-12}
Pyrex glass	2.6 (3 Mc/s) 4.5 (30 kc/s)	$< 1 \times 10^{-12}$

TABLE III: POWER FACTORS OF INSULATORS

Material	Relative Dielectric Constant, ϵ_r	Power Factor Multiplied by 10^4		
		50 c/s	1 Mc/s	50 Mc/s
Pyrex glass	3.0 (approx.)	—	35	—
Porcelain	5 to 6.5	170 to 250	70 to 120	—
Steatite	5.5 to 6.5	25 to 30	15 to 20	—
Frequenta, Calit or Calan	5.5 to 6.5	10 to 15	3 to 5	2 to 3
Quartz	4.7	1	1	1.1

(from Bruckmann⁽⁷⁾.)

APPENDIX II

THE M.K.S. SYSTEM

THE M.K.S. system of electrical units was proposed by Giorgi in 1901 and adopted by the I.E.C. in 1935 at a conference held at Scheveningen. The system uses the metre, the kilogram and the second as its fundamental units. It has the great advantage of replacing the three existing systems (the c.m.u., the e.s.u. and the practical system) by one system only which, moreover, is the same as the present practical system so far as the fundamental units are concerned. The sole exception is the unit of magnetic flux which in the M.K.S. system is the *weber* and equals 10^8 maxwells.

Secondary units involving the primary ones per unit of length or area are necessarily different (e.g. volts/centimetre becomes volts/metre).

There are no powers of 10 or of c to remember, but the permeability and the dielectric constant must be included in all formulae. In the case of air or free space they have the values

$$\mu_0 = 4\pi \times 10^{-7} \text{ henrys/metre}$$

$$\epsilon_0 = \frac{1}{36\pi} \times 10^{-9} \text{ farads/metre}$$

For a full description of the M.K.S. system and of the modifications it introduces in the older forms of the electromagnetic equations, the reader may refer to an article by Williams.⁽³⁸⁷⁾ The two tables below summarize the main features of the system.

TABLE I: THE M.K.S. SYSTEM OF UNITS

Quantity	Unit	Dimensional Equivalent
Length	Metre	
Mass	Kilogram	
Time	Second	
Energy	Joule	Volt-coulomb
Power	Watt	Joule/second
Force	Newton	Joule/metre
Electric charge	Coulomb	Ampere-second
Displacement density	Coulomb/square metre	
Electric current	Ampere	Coulomb/second
Current density	Ampere/square metre	
Electromotive force	Volt	Joule/coulomb
Electric intensity	Volt/metre	Newton/coulomb

TABLE I: THE M.K.S. SYSTEM OF UNITS (contd.)

Quantity	Unit	Dimensional Equivalent
Impedance	Ohm	Volt/ampere
Admittance	Mho	Ampere/volt
Inductance	Henry	Ohm-second
Permeability	Henry/metre	
Capacitance	Farad	
Dielectric constant	Farad/metre	
Conductivity	Mho/metre	
Magnetomotive force	Ampere	
Magnetic intensity	Ampere/metre	
Magnetic flux	Weber	Volt-second
Magnetic charge	Weber	Volt-second
Magnetic flux density	Weber/square metre	
Magnetic current	Volt	
Magnetic current density	Volt/square metre	

TABLE II: RELATIONSHIP OF UNITS

Quantity	Practical Unit	Size in M.K.S. Units	Size in e.m.u.	Size in c.s.u.
Energy	Joule	1	10^7 ergs	10^7 ergs
Power	Watt	1	10^7 ergs/sec	10^7 ergs/sec
Electric charge	Coulomb	1	10^{-1}	3×10^9
Displacement density	Coulomb Square centimetre	10^4 coulombs 4π m ²	10^{-1}	3×10^9
Electromotive force.	Volt	1	10^8	$1/300$
Electric intensity	Volt/centimetre	10^3 V/m	10^8	$1/300$
Impedance	Ohm	1	10^9	$1/(9 \times 10^{11})$
Conductivity	Mho/centimetre	10^9 mhos/m	10^{-9}	9×10^{11}
Inductance	Henry	1	10^9	$1/(9 \times 10^{11})$
Capacitance	Farad	1	10^{-9}	9×10^{11}
Current	Ampere	1	10^{-1}	3×10^9
Magnetomotive force	Gilbert*	$\frac{10^4}{4\pi}$ amp	1	3×10^{10}
Magnetic intensity	Oersted†	$\frac{10^3}{4\pi}$ amp/m	1	3×10^{10}
Magnetic flux	Maxwell	10^{-8} webers	1	$1/(3 \times 10^{10})$

* Although the gilbert has the same dimensions as current, it is numerically equal to $1/4\pi$ times the electromagnetic unit of current due to the relationship $\int H \cdot ds = 4\pi I$. In the rationalized M.K.S. system the unit of magnetomotive force is the ampere both dimensionally and numerically. On account of the presence of the 4π factor in unrationalized versions, it is safer to refer to the unit of magnetomotive force as the ampere-turn or abampere-turn. The addition of the word "turn" has no effect on the dimensions but serves to distinguish the unit from the unit of current. The main point to remember in converting from rationalized to unrationalized units is that the *rationalized units* of H and D (displacement) are 4π times larger.

† Formerly called the "gauss." In the c.g.s. system the name "gauss" is now reserved for use as the unit of magnetic induction (magnetic flux density). This change was made at the I.E.C. Convention held at Oslo in 1930.

APPENDIX III

NOTES ON THE MECHANICAL DESIGN OF ANTENNA STRUCTURES

THE following notes deal with some of the considerations involved in designing antennae whose size is such as to require masts of appreciable height. By far the most common heights are those between 15 and 50 m (50 and 150 ft), since these heights are suitable for long- and medium-wave antennae of low heights, and also for short-wave antennae such as rhombics, inverted-V's, horizontal dipoles, etc. Masts of such size are usually made of wood or tubular steel. In general, the taller the masts the more specialized is their construction. Therefore it becomes impossible to give any useful data in the space of a few pages on really tall masts of the type that are used, for instance, for broadcast purposes.

In view of the fact that most British and American mechanical engineering firms use tons, feet, etc., and that wire tables are in such units, the metric system has not been adhered to in the following pages.

Classification of Masts. The masts employed for radio antennae fall into two distinct classes. One of these consists of masts which are used to support radiating wires; the other class comprises masts which are in themselves the radiating elements.

Typical examples of the first-mentioned class as applied to long- and medium-wave antennae are the following—

(a) Guyed tubular steel masts, supporting a T or inverted-L antenna. In view of the relatively low heights of such masts they are not normally constructed with insulation from the ground.

(b) Guyed lattice steel masts, between two of which is supported a T or inverted-L antenna. The masts may be either grounded or insulated.

(c) Self-supporting lattice steel towers, performing the same function as those in group (a). These may also be either grounded or insulated.

(d) Guyed wooden masts performing the same function as those in group (a).

(e) Self-supporting wooden towers, down the centres of

which are suspended radiating wires. This type is often fitted with a top capacitor.

(*f*) Self-supporting wooden towers in which the upper portion contains a vertical dipole. In most cases the dipole is loaded at both ends by a capacitor to make a half-wavelength mode of oscillation possible.

The self-radiating type of antenna mast or tower occurs in the following forms—

(*g*) Self-supporting lattice steel towers.

(*h*) Lattice steel masts of uniform cross-section, guyed at several heights. These may be with or without a capacitor at the top.

(*i*) As above, but fitted with outriggers and vertical wires suspended from a crown at the top to attain a more uniform characteristic impedance.

(*j*) A “cigar-shaped” lattice steel mast, guyed at the centre only. Such masts usually contain an extra extendable piece on top, commonly called a “flag-pole.”

(*k*) Telescopic masts (unguyed). These are of low heights only, say 12 m (40 ft), but have the advantage of being transportable and speedily erected.

Fig. III.1 shows sketches of nine different types of antennae and mentions the typical heights of the masts in each case.

Axial and Bending Stresses

The loading on a guyed mast can be split into two components, namely the axial loading and the bending stresses. The axial loading is the downward thrust due to the weight of the superstructure plus the vertical components of the tensions of the mast stays, back stay, halyard, etc. The other component of the loading is given by the bending stresses produced by wind pressure on the mast, the tensions of windward and leeward guys (which in wind are unbalanced), and by the extent of the horizontal movements of the mast at the guy points (such movements depend on the initial tensions of the guys and back stay). Horizontal movements at the guy points are equivalent to the settlement of supports in a horizontal continuous beam—in the case of larger masts this stress calls for careful adjustments of the initial tension of the guys.

Since these bending stresses are accompanied by deflections of the mast, additional bending stresses will be produced by the effect of the axial load on such deflections.

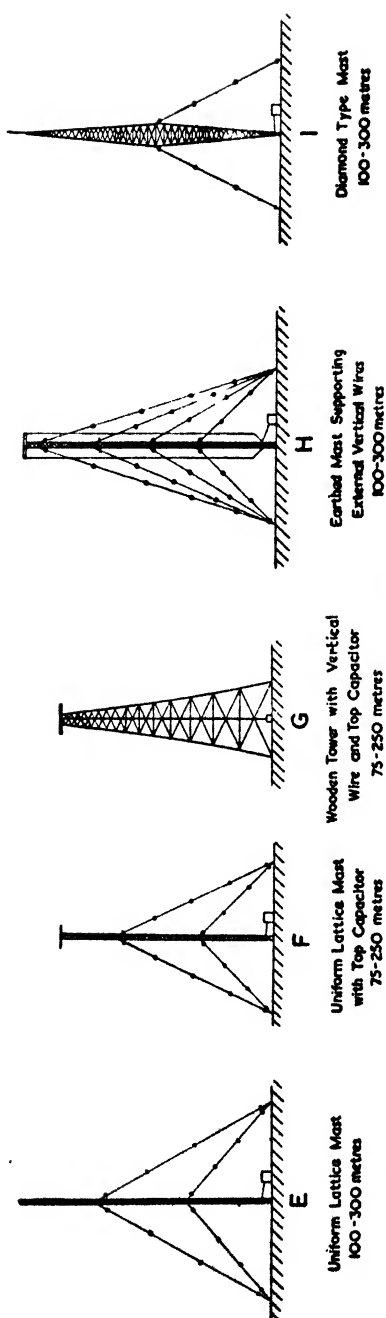
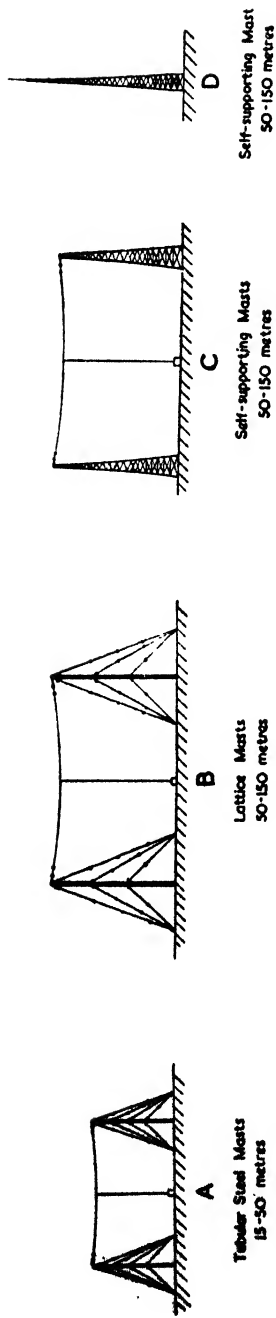


FIG. III.1. NINE TYPES OF TRANSMITTING ANTENNAE

In some of the larger masts the steelwork provided for the attachment of the guys to the mast is designed so that the loading due to the guy tensions is balanced about the central axis; in this way the bending stresses are minimized. The bending stresses produced by the wind pressure on the mast, however, cannot be avoided, and if (l/k) , the ratio of length to radius of gyration of the mast section, is high, the effect of the axial load on the deflected mast section will cause an appreciable increase in the bending stresses. It is the aim of most designers to keep the projected area of the mast as small as possible with a view to reducing the wind stresses.

The ratio of l/k is not unduly high in the case of a guyed lattice steel mast, probably varying between 30 and 60, and therefore the effect of the axial load on the lateral deflections is likely to be very small. In the case of guyed tubular steel masts l/k will be much higher, somewhere between 130 and 180 in fact (or even higher if the mast is a portable one). In such circumstances the applied bending moments may easily be increased by 40 or 50 per cent due to the axial loading.

An approximate estimate of this increase for steel masts is given by $\sec \{[0.25(l/k)\sqrt{f_c}] \text{ degrees}\}$, where f_c is the axial load in tons per square inch and the length l is measured between the points of inflection. The exact mathematical treatment for calculating the stresses in compression members subjected to simultaneous action of axial and lateral loads is given in ref. 1. A more general treatment of the design of a light guy-supported steel mast will be found in ref. 2.

Since the bending moments will vary throughout the section of a mast, the important value from a design point of view is the maximum value, i.e. the bending stress at the extreme fibres (sometimes known as the skin stress).

The loading on a self-supporting tower is more easily calculated than that on a guyed mast; moreover this type of structure may be treated as a cantilever and designed in accordance with the conventional methods of structural analysis.

Calculation of Wind Pressure

Whatever type of mast is used it is clear that a very large proportion of the loads and stresses will be due to wind pressure, and hence it is important to be able to estimate the pressure

due to various wind velocities. The formula most generally used for estimating this pressure is

$$P = kV^2 \quad . \quad . \quad . \quad (III.1)$$

where P = pressure of wind in pounds per square foot,

k = a coefficient depending on the aspect ratio of the structure or component,

V = velocity of wind in m.p.h.

When designing masts of medium height it is generally considered sufficient if a wind pressure of from about 25 to 30 lb/ft² is assumed, while the coefficient k is taken as 0.003. By equation (III.1) this would represent a wind velocity of from 90 to 100 m.p.h. (the velocity of a hurricane).

It is known that the wind velocity is actually a function of height (see, for example, ref. 3, p. 43). The velocity at 1 000 ft is, in fact, about one and a half times as great as that at 100 ft; consequently for heights of this order the assumed wind pressure would be increased to about 40 lb/ft². Furthermore in the case of a lattice structure the wind pressure is usually assumed to be acting on about one and a half times the projected area of the structure.

To find the total wind pressure on sections which are not flat, we must multiply the coefficient of k by another coefficient " c ." In the case of a cylindrical body, the value of c is usually taken to lie between 0.6 and 0.75. The latter value is approximately equal to the theoretical value, but the former is more frequently used.

Equation (III.1) then becomes

$$P = ckV^2 \quad . \quad . \quad . \quad (III.2)$$

The value of 0.003 for k applies only in the case of a flat surface of low aspect ratio, i.e. surfaces for which the ratio of height to breadth is approximately unity. When the aspect ratio is high the value of k should be increased to about 0.004. Thus equation (III.2) may be stated as follows—

For mast sections (i.e. flat surfaces of high aspect ratio)

$$P = 0.004V^2 \quad . \quad . \quad . \quad (III.3)$$

For mast guys (i.e. cylindrical surfaces of high aspect ratio)

$$P = 0.003V^2 \quad . \quad . \quad . \quad (III.4)$$

The variation of wind pressure with height may be allowed for by taking the following arbitrary rule—

$$P = 25 \text{ lb/ft}^2 \text{ at ground level, plus } 5 \text{ lb/ft}^2 \text{ for each } 100 \text{ ft increase in height}$$

These wind loadings may be reduced by 25 per cent for the mast guys on account of their circular cross-section. In addition, the loading on the guys should be multiplied by a factor equal to $\sin^2 \theta$, where θ = the angle between the guy and the direction of the wind (ref. 5, p. 94).

General Features of Mast Construction

For non-lattice masts a circular cross-section offers the advantage of a high weight-to-strength ratio because the material is then most favourably disposed for the resisting of extreme fibre stresses. Another advantage is that tubes can generally be obtained in high tensile steel which allows higher bending stresses and greater deflections without risk of permanent injury to the mast. Both these points are important in view of the high l/k ratios usually found necessary when designing a mast of this type. A high l/k ratio has the merit of avoiding an excessive number of guys with the corresponding increase in the axial loading.

In the case of lattice steel masts, angles, channels or other structural sections are generally used in preference to tubes, since such sections lead to more easily designed joints and connections. The advantage can also be claimed with these sections that all surfaces are visible for inspection. With a lattice steel mast a high weight-to-strength ratio can be obtained by the appropriate spacing of the corner legs and as a result the l/k ratio can be kept very much lower than in the case of a tubular mast, with the result that a much higher axial loading is permissible. At the same time it is important to ensure that the strength of the individual mast sections between panel points approximates to that of the mast section between guy points, otherwise failure might occur by local flexure.

In view of the foregoing mechanical design features it is common practice to construct the smaller masts (up to about 150 ft in height) of single tubular sections guyed at each joint, and to use high tensile steel tube of about 35 to 40 tons/in.² tensile strength. Larger masts, or masts designed for heavy aerial loads, are of lattice steel construction and employ ordinary mild steel of 28 to 33 tons/in.² tensile strength.

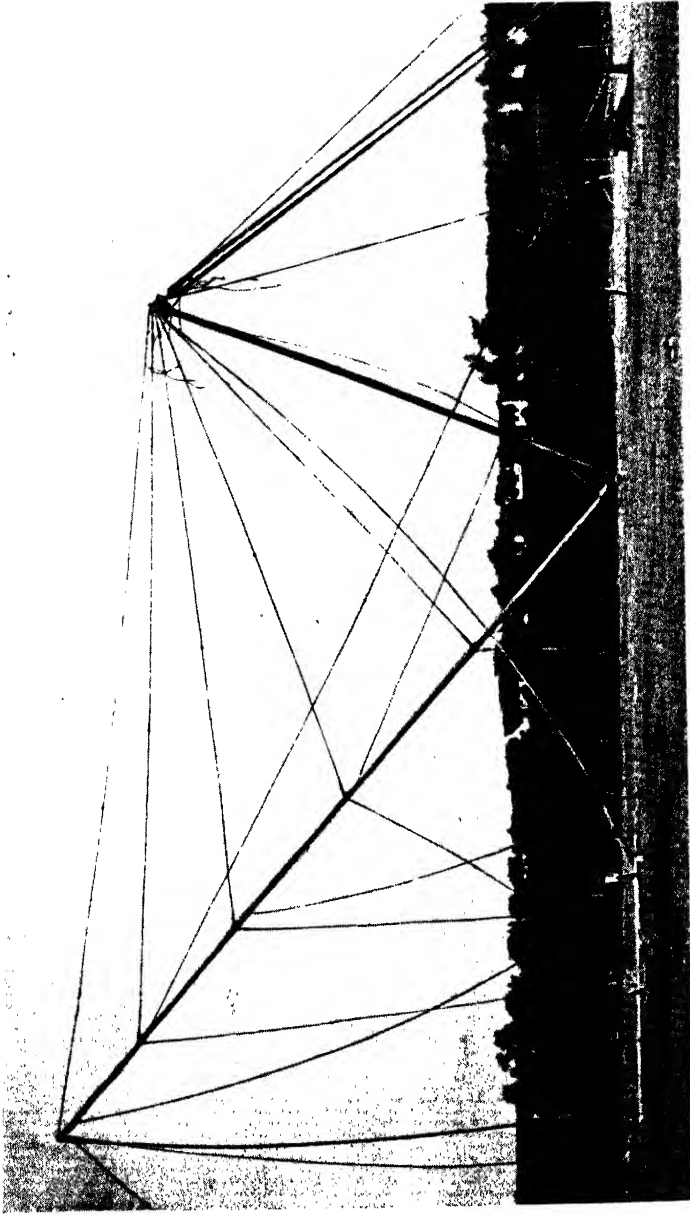


PLATE XVI. THE ERECTION OF A 95 FT TUBULAR MAST BY MEANS OF
THE "FALLING DERRICK" METHOD
(Courtesy of Coabro & Scrutton, Ltd.)

When designing a mast the optimum size of section must be found by trial and error. If the stresses in a trial design of a guy-supported mast are found to be satisfactory this does not necessarily imply that if the mast were constructed with a smaller overall breadth then the stresses would no longer be satisfactory. The reason for this is that both the dead load and the wind loading are decreased by the reduction in breadth. It is therefore a good policy to prepare several trial designs before deciding on the general dimensions of the mast and guys.

The individual sections of a guyed tubular mast are usually about 20 ft in length for practical reasons, such as ease of manufacture, handling, etc., while the overall diameter of the tube is generally between 5 and 7 in. If the base of the mast is fitted with a simple form of hinge pin this will greatly facilitate erection by means of the "falling-derrick" method. Plate XVI shows this method in operation, while Fig. III.2 gives a fairly detailed drawing of a 95 ft transportable mast capable of taking an antenna pull of 1 ton. Such a mast is suitable for T and inverted-L antennae and also for short-wave dipoles or rhombic antennae operating on wavelengths between 60 and 120 m.

As an example of lattice sections of a guyed mast, one may take the Rugby masts (ref. 6), which have a triangular "K" braced section whose sides are 10 ft, and are guyed at intervals of 162 ft (the sections themselves being built in lengths of 27 ft). It will again be noticed that the component lengths are limited to less than about 30 ft owing to manufacturing considerations and for easier transport and erection.

The corner legs of these masts are built up of channel sections placed so that the ratio of the greatest to least radius of gyration is near to unity. In the case of smaller lattice steel masts, it is generally found more economical to use single angle legs. Although in this case the value of the radius of gyration will vary by approximately 2 to 1 for different axes, the extra weight of material involved to maintain the ratio I/k will be offset by the greater ease in fabrication and erection.

To avoid bending stresses at the bottom of a big mast, a large steel pivot may be used, consisting of a ball and socket joint; obviously a joint of this kind is only possible on guyed masts. This pivot is normally mounted above the base insulator.

It is important that the mast structure should be protected against corrosion. Opinions differ as to the best method of

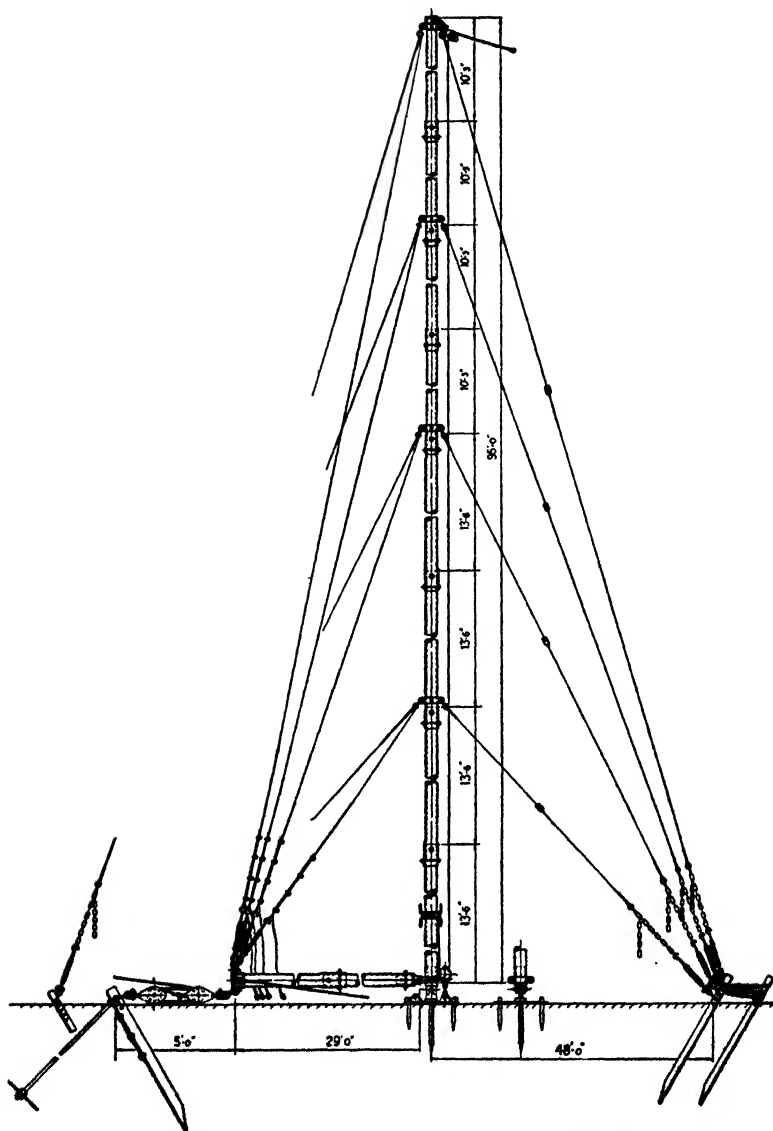


FIG. III.2. EXAMPLE OF A 95 FT PORTABLE MAST

protection; some prefer galvanizing the individual sections before they are erected, others prefer to have the steelwork coated with a good quality priming of red lead, followed by an undercoat, the finishing coat being applied on the site, after first touching up and making good any damage due to handling and transporting. The final coat should be applied after the mast has been erected.

Painting is generally preferred in the case of lattice steel masts, and galvanizing in the case of the smaller tubular masts.

Mast Stays. The choice of a suitable wire rope for the mast stays is important. A rope with a wire centre core should be used in preference to one with a fibre core, since flexibility is not required. A fibre core would tend to hold moisture and to increase the amount by which the rope would stretch under load; furthermore, a rope with a wire centre core has a higher breaking load than one with a fibre core.

To obtain the maximum strength for the minimum projected area, a high-tensile steel wire rope should be used, say 100–110 tons/in.² galvanized “Best Plough Steel.”

The properties of 100–110 tons/in.², 7 × 7 construction, galvanized wire ropes are given in Table 1, on page 488.

The elastic stretch of a rope must not be confused with the constructional stretch. In the case of large masts, where the cost of setting up the stays is a point to be considered, it would be desirable to pre-stretch the stays to about one-third of their breaking load before the mast is erected.

In the case of the small tubular masts, the cost of setting up the stays is not excessive, neither is this work carried out by highly skilled personnel, for these reasons pre-stretching is seldom thought necessary with small masts.

It is usual to provide adjustments at the lower ends of the mast stays in the form of removable link plates as a means of compensating for slight irregularities in the ground levels. Turnbuckles or rigging screws are used for controlling the initial tensions of the stays.

The dimensions of the concrete anchorages for the mast stays and of the concrete foundation for the mast both depend on the site and on the purpose for which the mast is required. Allowable bearing pressures on different types of soil are specified in most Civil Engineers' Handbooks (see also ref. 10, p. 39).

Elaborate calculations are often necessary for estimating the appropriate initial tensions and the maximum tensions of mast

stays. Descriptions of such methods are given in refs. 6 and 7, which deal with the design of the 800 ft Rugby masts. Simpler methods are described in refs. 2 and 8, the latter reference giving a simple graphical method.

TABLE I: PROPERTIES OF 7/7 CONSTRUCTION STAY WIRE (WITH WIRE CENTRE CORE), 100-110 TONS/IN.², BEST PLOUGH STEEL

Circ. of Rope	Approximate Diameter of Rope	Actual Breaking Load	Approximate Weight per 100 ft	Metallic Area of Rope
in.	in.	tons	lb	in. ²
$\frac{1}{8}$	$\frac{1}{16}$	1.0	4.5	0.0114
$\frac{1}{4}$	$\frac{1}{8}$	1.5	7	0.0186
$\frac{3}{8}$	$\frac{3}{16}$	2.3	10	0.0260
$\frac{1}{2}$	$\frac{1}{4}$	3.1	13	0.0370
1	$\frac{5}{16}$	4.8	21	0.0499
$1\frac{1}{8}$	$\frac{3}{8}$	5.8	27	0.0616
$1\frac{1}{4}$	$\frac{7}{16}$	7.1	30	0.0745
$1\frac{3}{8}$	$\frac{1}{2}$	8.8	38	0.0924
$1\frac{1}{2}$	$\frac{11}{16}$	10.3	44	0.1081
$1\frac{5}{8}$	$\frac{3}{4}$	12.0	52	0.1250
$1\frac{3}{4}$	$\frac{13}{16}$	14.1	60	0.1479
$1\frac{7}{8}$	$\frac{7}{8}$	16.0	67	0.1676
2	$\frac{15}{16}$	18.5	80	0.1940
$2\frac{1}{8}$	$\frac{1}{2}$	20.6	89	0.2165
$2\frac{1}{4}$	$\frac{11}{8}$	22.9	97	0.2402
$2\frac{3}{8}$	$\frac{3}{4}$	25.8	108	0.2716
$2\frac{1}{2}$	$\frac{13}{8}$	28.3	119	0.2980
$2\frac{5}{8}$	$\frac{7}{8}$	31.7	133	0.3328
$2\frac{3}{4}$	$\frac{15}{8}$	35.1	147	0.3696
$2\frac{7}{8}$	$\frac{1}{2}$	37.4	156	0.3926
3	$\frac{17}{8}$	41.1	171	0.4324
$3\frac{1}{8}$	$1\frac{1}{8}$	48.3	204	0.5090
$3\frac{1}{4}$	$1\frac{1}{4}$	56.3	241	0.5917
$3\frac{3}{8}$	$1\frac{3}{8}$	64.8	274	0.6808
4	$1\frac{5}{8}$	72.8	306	0.7651
$4\frac{1}{8}$	$1\frac{7}{8}$	82.4	342	0.8659
$4\frac{1}{4}$	$1\frac{7}{8}$	92.6	389	0.9729

Notes. The specified breaking loads (in tons of 2 240 lb) have been obtained by adding 1/7 to the breaking load of 6/7 construction rope with a fibre core.

The specified weight is 1/9 greater than that of 6/7 construction rope with a fibre core.

When estimating the elastic stretch of a 7/7 construction rope with a wire centre core, the value of the stress-extension ratio may be taken as $E = 20\ 000\ 000$ lb/in.²

The information in this table applies to wire ropes of British manufacture.

In the case of the small tubular masts, which are generally erected by semi-skilled labour, it is satisfactory if the stays are set up to initial dips of about $\frac{3}{4}$ to 1 per cent of their span. Little is to be gained by initial dips of less than $\frac{3}{4}$ per cent.

Earth Systems

Earth systems are of two distinct types, one employing buried wires, the other wires elevated above the ground.

The depth of the wire below the ground in the buried wire system is of the order of 1 ft. In order to facilitate the laying of such wires, special wire-laying ploughs have been devised (ref. 6)—these are pulled by tractors and lay the copper wire directly. As has been pointed out in § 2.5, when the antenna is relatively low an efficient earth system is particularly useful. Unfortunately low antennae are usually used on account of simplicity and cheapness, so that an elaborate earth system would defeat this purpose.

Elevated earth systems, i.e. counterpoise earths, are suspended from poles at a sufficient height to permit the passage of personnel and vehicles underneath them. To minimize cross-currents the pattern in which the wires are joined resembles that of a genealogical tree in which the head of the tree is at the base of the antenna.

Antenna Pull

Estimates of the pull exerted by an antenna slung between two masts vary quite considerably. The pull depends on many factors such as the number of wires, their modulus of elasticity, the initial dip, the movement of the masts, the stretching of the halyard and—to a very high degree—on the wind pressure. The figures usually assumed range from about $\frac{1}{2}$ to 1 ton in the case of the small tubular steel masts, and from about 5 to 10 tons for the large lattice steel masts.

The corresponding figures for the *total axial loading* would be of the order of 3 to 6 tons for small tubular masts of heights from about 80 to 120 ft, whilst in the case of the 800 ft Rugby masts with an antenna pull of 10 tons, the estimated total axial loading is 400 tons. Therefore the antenna pull represents about one-sixth to one-fortieth of the axial loading, according to the height and type of mast.

Under severe icing conditions the antenna pull may be

greatly increased. It is therefore good practice to terminate the halyard with a counterpoise weight so that the sag in the span can automatically increase under heavy loading conditions. In this way excessive antenna tensions are avoided.

Insulators

It is common practice to arrange for the insulators to be under compression. Furthermore, in the case of guy insulators, the design of the insulator mounting should be such as to keep the

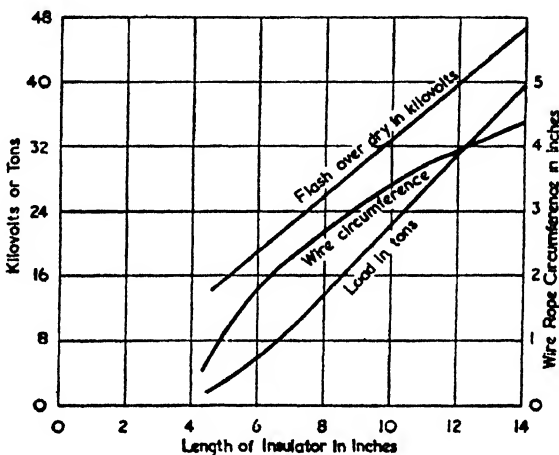


FIG. III.3. TYPICAL CHARACTERISTICS OF EGG INSULATORS

wires from falling apart if the insulator failed. The simple type of egg insulator fulfils both these requirements, although for large structures elaborate insulator mountings are often used.

Porcelain is by far the most common insulator material. An interesting exception is provided by the Rugby masts, which are mounted on large granite blocks as well as on porcelain insulators. These blocks were dried on site by radio-frequency currents and then coated to prevent subsequent moisture absorption. Preliminary tests for these masts showed that the Scandinavian granite was capable of standing 6 000 V/in. (ref. 6).

It is important that porcelain insulators should not be too thick, otherwise the vitrification during firing will not be even. Consequently large insulators are made with holes through the middle. The subsequent glazing also has an effect on

both the mechanical and electrical properties. A well-made cylindrical porcelain insulator will stand loads as high as 10 tons/in.² and R.F. voltages of 10 000 V/in.

The dielectric strength of porcelain does not vary appreciably with loads up to 30 per cent of the ultimate compressive strength. Actually the dielectric strength increases by about 10 per cent with the maximum occurring at 10 to 15 per cent of the ultimate mechanical strength (ref. 9).

When using egg insulators it is most important to use an insulator which has grooves large enough to take the wire rope in order to avoid any wedge action. Such a wedge action on the groove of an insulator will completely ruin its ability to take a load. A graph of the mechanical and electrical loads of typical egg insulators is given in Fig. III.3, together with appropriate rope diameters.

REFERENCES TO APPENDIX III

1. CASE, J. *The Strength of Materials*, Chap. XVI. Arnold (London, 3rd Edit., 1938).
2. MORRIS, C. T. and CARPENTER, S. T. *Structural Frameworks*, Chap. IX. J. Wiley & Sons (New York, 1944).
3. *The Meteorological Observer's Handbook*, p. 43. H.M. Stationery Office (London, 1939).
4. FIELD, J. Radio antenna suspended from 1 000 ft towers. *Journal of the Franklin Institute* (May, 1945).
5. RELF, E. F. Aerodynamics. *Handbook of Aeronautics*, Vol. I, p. 94. Pitman & Sons, Ltd. (London, 1937).
6. ANGIN, A. S. and WALMSLEY, T. The Rugby Radio Station. *Proc. Inst. Civil Eng.* Vol. 221 (1925-26), Part I, p. 201.
7. WALMSLEY, T. Length, tension and sag of stay ropes. Selected Engineering Paper No. 19., *Inst. Civil Eng.* (1924).
8. TOOLEY, H. Notes on determining the stresses in the guys of guy-supported masts. *Journal Inst. Civil Eng.* Vol. 15, No. 3, p. 220 (1941).
9. PARMELEE, C. W. and KRAEHNBUHL, J. O. Mechanical-electrical Stress Studies of Porcelain Insulator Bodies. *University of Illinois Engineering Experimental Station Bulletin* No. 273 (1935).
10. The use of structural steel in building, Section J: Pressures on subsoil, p. 39. British Standard Specification No. 449 (1937).

APPENDIX IV

LIST OF SYMBOLS

THE following list gives the symbols which occur most frequently in the text. As far as possible a consistent set of symbols has been used, but where exceptions occur these are indicated in the text.

A difficulty occurs in the case of multiples and submultiples of units. They may be indicated by suffixes (e.g. E_{mV} for field strength in millivolts/metre) but this system can easily lead to formulae containing an excessive number of suffixes. For this reason the frequently occurring dimensions of kilometres and kilowatts have been denoted by the symbols D and P respectively.

- A** = magnetic vector potential in webers/metre.
a = radius of circular or cylindrical bodies in metres.
B = magnetic flux density in webers/square metre.
B = susceptance in mhos.
C(x) = $\log_e x + j - Ci(x)$.
Ci(x) = $\int_{\infty}^x \frac{\cos z}{z} dz$
C = capacitance in farads—also capacitance/unit length of transmission line.
c = velocity of light *in vacuo* in metres/second
 = 3×10^8 m/sec.
D = displacement density in coulombs/square metre.
D = distance in kilometres.
d = distance in metres.
E = electric field strength in volts/metre.
Ei(x) = $Ci(x) + jSi(x)$.
e = electromotive force in volts.
F(θ) = standardized polar coefficient.
f = frequency in cycles/second, unless otherwise stated.
G = conductance in mhos—also conductance/unit length of transmission line.

- G_H = power gain over half-wave dipole.
 G_o = power gain over hypothetical omnidirectional source.
 g = conductivity in mhos/metre.
 H = magnetic field strength in amperes/metre.
 H = height of centre of antenna system above the ground.
 h = height of vertical radiator above the ground or half-length of a dipole.
 I_i = loop current, i.e. r.m.s. current at current antinode, sometimes it is the peak current.
 i = instantaneous current in amperes.
 J = current density in amperes/square metre.
 j = $\sqrt{-1}$.
 K = form factor.
 k = factor converting actual radius of the earth into "effective radius for radio propagation."
 k = Boltzmann's constant = 1.37×10^{-23} joules/degree.
 L = inductance in henrys—also inductance/unit length of transmission line.
 M = moment of magnetic doublet.
 o = the suffix "o" is used with $G, \mu, \alpha, \beta, \lambda, f, \omega$ and z_o to denote free-space values where such a distinction is necessary.
 $P(\theta)$ = polar coefficient.
 P = power in kilowatts.
 P = propagation constant of a transmission line
 $= \alpha + j\beta$.
 p = intrinsic propagation constant of a medium
 $= \alpha + j\beta$.
 R = resistance in ohms—also resistance per unit length of a transmission line.
 R_b = resistance at the base of an antenna.
 $R_{b,d}$ = base dead-loss resistance.
 $R_{b,r}$ = base radiation resistance.
 R_i = loop resistance, i.e. resistance at a current antinode.
 $R_{i,d}$ = loop dead-loss resistance.
 $R_{i,r}$ = loop radiation resistance.
 R_o = real part of characteristic impedance in ohms.

- r = distance to field point in metres.
 \mathbf{S} = energy flow in watts/square metre (Poynting's Vector).
 $S(x) = Si(x)$.
 $Si(x) = \int_0^x \frac{\sin z}{z} dz$
 T = temperature in degrees Kelvin.
 U = magnetic potential in amperes.
 V = electrical potential in volts.
 W = power in watts.
 X = reactance in ohms.
 Y = admittance in mhos.
 Z = impedance in ohms.
 Z_0 = characteristic impedance in ohms.
 z_0 = intrinsic impedance of a medium in ohms.
 α = attenuation constant in nepers/metre.
 β = phase constant in radians/metre.
 γ = 0.5772 (Euler's constant).
 Δ = angle of elevation (complement of the zenith angle).
 ϵ = dielectric constant in farads/metre.
 ϵ_r = dielectric constant relative to that of free space.
 ϵ' = complex dielectric constant
 $= \epsilon_r - j60\lambda g$.
 η = power efficiency.
 θ = zenith angle (complement of angle of elevation)—also angle between field point and direction of current element.
 λ = wavelength in metres.
 μ = permeability in henrys/metre.
 π = 3.14159.
 σ = surface charge density in coulombs/square metre.
 ρ = charge density in coulombs/cubic metre—also Sommerfeld's numerical distance—also standing wave ratio.

BIBLIOGRAPHY

REFERENCE in the text to various books and papers is by means of superior numbers, corresponding to the numbers given here.

BOOKS

1. ABRAHAM, M. and BECKER, R. *The Classical Theory of Electricity and Magnetism*. Blackie & Son, Ltd.
2. AHARONI, J. *Antennae—an Introduction to their Theory*. Oxford University Press (1946).
3. *A.R.R.L. Antenna Book*. American Radio Relay League Inc. (1942).
4. BAKER, B. B. and COPSON, C. T. *The Mathematical Theory of Huygens' Principle*. Oxford University Press (1939).
5. BERGMANN, L. and LASSEN, H. *Ausstrahlung, Ausbreitung und Aufnahme Elektromagnetischer Wellen*. Julius Springer (Berlin, 1940). (Also lithoprinted by Edwards Brothers, Inc., Michigan, 1944.)
6. BOND, D. S. *Radio Direction Finders*. McGraw-Hill Book Co. Inc. (1944).
7. BRÜCKMANN, H. *Antennen, ihre Theorie und Technik*. S. Hirzel (Leipzig, 1939).
8. HARPER, A. E. *Rhombic Antenna Design*. D. Van Nostrand Co., Inc. (New York, 1941).
9. JACKSON, W. *High Frequency Transmission Lines*. Methuen & Co., Ltd. (London, 1945).
10. JAHNKE, E. and EMDE, F. *Tables of Functions*. Teubner (Leipzig).
11. KEEN, R. *Wireless Direction Finding*. Iliffe & Sons, Ltd. (London, 4th Edition, 1947).
12. KING, R. W. P., MIMNO, H. R. and WING, A. H. *Transmission Lines, Antennas and Wave Guides*. McGraw-Hill Book Co. Inc. (1945).
13. LADNER, A. W. and STONER, C. R. *Short Wave Wireless Communication, including Ultra-short Waves*. Chapman and Hall (1942).
14. LAMONT, H. R. L. *Wave Guides*. Methuen & Co., Ltd. (London, 1942).
15. PEDERSEN, P. O. *The Propagation of Radio Waves along the Surface of the Earth and in the Atmosphere*. Copenhagen (1927). (On commission from G.E.C.—Gad, Copenhagen, K.)
16. PERONI, B. *Antenne e propagazione delle onde Elettromagnetiche*. Michele Dell'Alra—Loitore (Rome, 1945).
17. PIERCE, G. W. *Electric Oscillations and Electric Waves*. McGraw-Hill Book Co. Inc. (1920).
18. RAMO, S. and WHINNERY, J. R. *Fields and Waves in Modern Radio*. John Wiley & Sons, Inc. (New York, 1944).
19. SANDRETTO, P. C. *Principles of Aeronautical Radio Engineering*. McGraw-Hill Book Co. Inc. (1942).
20. SCHELKUNOFF, S. A. *Electromagnetic Waves*. D. Van Nostrand Co. Inc. (New York, 1943).

21. SLATER, J. C. *Microwave Transmission*. McGraw-Hill Book Co. Inc. (1942).
22. STRATTON, J. A. *Electromagnetic Theory*. McGraw-Hill Book Co. Inc. (1941).
23. TERMAN, F. E. *Radio Engineers' Handbook*. McGraw-Hill Book Co. Inc. (1943).
24. WATSON, W. H. *The Physical Principles of Wave Guide Transmission and Antenna Systems*. Oxford University Press (1947).
25. WEATHERBURN, C. E. *Advanced Vector Analysis*. G. Bell & Sons, Ltd. (1928).

PAPERS

Antenna Theory

26. ABRAHAM, M. Die elektrischen Schwingungen um einen stabförmigen Leiter, behandelt nach der Maxwellschen Theorie. *Ann. der Phys.* V. 66, p. 435 (Oct., 1898).
27. ALFORD, A. A discussion of methods employed in calculations of electromagnetic fields of radiating conductors. *Elec. Comm.* V. 15, p. 70 (July, 1936).
28. ALFORD, A. Coupled networks in radio frequency circuits. *Proc. I.R.E.* V. 29, p. 55 (Feb., 1941).
29. BALLANTINE, S. On the radiation resistance of a simple vertical antenna at wavelengths below the fundamental. *Proc. I.R.E.* V. 12, p. 823 (Dec., 1924).
30. BALLANTINE, S. On the optimum transmitting wavelength for a vertical antenna over perfect earth. *Proc. I.R.E.* V. 12, p. 833 (Dec., 1924).
31. BARROW, W. L. On the impedance of a vertical half-wave antenna above an earth of finite conductivity. *Proc. I.R.E.* V. 23, p. 150 (Feb., 1935).
32. BAUDOUX, P. Current distribution and radiation properties of a shunt-excited antenna. *Proc. I.R.E.* V. 28, p. 271 (June, 1940).
33. BECHMANN, R. On the calculation of radiation resistance of antennas and antenna combinations. *Proc. I.R.E.* V. 19, p. 1471 (Aug., 1931).
34. BERGMANN, L. Messungen im Strahlungsfelde einer in Grund und Oberschwingungen erregten stabförmigen Antenne. *Ann. der Phys.* V. 82, p. 504 (1927).
35. BOUWKAMP, C. J. and DE BRUIGN, N. G. The problem of optimum antenna current distribution. *Phil. Res. Rep. V.I.*, p. 135 (Jan., 1946).
36. BRILLOUIN, L. Sur l'origine de la résistance de rayonnement. *Radio-électricité*. V. 3, p. 147 (April, 1922).
37. BRILLOUIN, L. Antennae for ultra-high frequencies—wide-band antennae. *Elec. Comm.* V. 22, p. 11 (1944); V. 21, p. 257 (1944).
38. BROWN, G. H. The phase and magnitude of earth currents near radio transmitting antennas. *Proc. I.R.E.* V. 23, p. 168 (Feb., 1935).
39. BROWN, G. H. A critical study of the characteristics of broadcast antennas as affected by antenna current distribution. *Proc. I.R.E.* V. 24, p. 48 (Jan., 1936).

40. BROWN, G. H. Directional antennas. *Proc. I.R.E.* V. 25, p. 78 (Jan., 1937).
41. BROWN, G. H., with WOODWARD, O. M. (Jun.). Experimentally determined impedance characteristics of cylindrical antennas. *Proc. I.R.E.* V. 33, p. 257 (April, 1945).
42. BURGESS, R. E. Aerial characteristics—Relation between transmission and reception. *Wir. Eng.* V. 21, p. 154 (April, 1944).
43. CARTER, P. S. Circuit relations in radiating systems and applications to antenna problems. *Proc. I.R.E.* V. 20, p. 1004 (June, 1932).
44. CARTER, P. S. Antenna arrays around cylinders. *Proc. I.R.E.* V. 31, p. 671 (Dec., 1943).
45. COLEBROOK, F. M. The application of transmission line theory to closed aeriels. *Jour. I.E.E.* V. 83, p. 403 (Sept., 1938).
46. COLEBROOK, F. M. The electric and magnetic fields of a linear radiator carrying a progressive wave. *Jour. I.E.E.* V. 86, p. 169 (Feb., 1940).
47. GLINSKI, G. Note on impedance matching of shunt-fed half-wave dipole. *Proc. I.R.E.* V. 33, p. 408 (June, 1945).
48. HALLÉN, E. Theoretical investigations into the transmitting and receiving qualities of antennas. *Nova Acta Reg. Soc. Sci. Upsaliensia.* V. 11, p. 3 (Nov., 1938).
49. HANSEN, W. W. and BECKERLEY, J. G. Concerning new methods of calculating radiation resistance either with or without ground. *Proc. I.R.E.* V. 24, p. 1594 (Dec., 1936).
50. HOERSCHELMANN, H. VON. Über die Wirkungsweise des geknickten Marconischen Senders in der drahtlosen Telegraphie. *Jahr. d. Drahtl. Tel. u. Tel.* V. 5, p. 14 (Sept., 1911); V. 5, p. 188 (Nov., 1911).
51. HOWE, G. W. O. On the capacity of radio-telegraphic antennae. *Wir. World.* V. 2, pp. 546, 612, 680. *Electrician.* V. 73, pp. 829, 859, 906 (28th Aug., 1914).
52. HOWE, G. W. O. The capacity of aeriels of the umbrella type. *Electrician.* V. 75, p. 870 (1915).
53. HOWE, G. W. O. The calculation of the capacity of radiotelegraph antennae, including the effects of masts and buildings. *Electrician.* V. 77, p. 761 (Sept., 1916).
54. HOWE, G. W. O. The inductance, capacity and natural frequency of aeriels. *Year-book of Wireless Telegraphy and Telephony*, p. 694 (1917).
55. HOWE, G. W. O. The application of Helmholtz's Theorems to aerial characteristics. *Wir. Eng.* V. 21, p. 153 (April, 1944).
56. KING, L. G. On the radiation field of a perfectly conducting base-insulated cylindrical antenna over a perfectly conducting plane earth, and the calculation of radiation resistance and reactance on them. *Phil. Trans. Roy. Soc.* V. 236, p. 381 (Nov., 1937).
57. KING, R. Coupled antennas and transmission lines. *Proc. I.R.E.* V. 31, p. 626 (Nov., 1943).
58. KING, R., with BLAKE, F. G. The self-impedance of a symmetrical antenna. *Proc. I.R.E.* V. 30, p. 335 (July, 1942).

59. KING, R., with HARRISON, C. W., Jun. The distribution of current along a symmetrical center-driven antenna. *Proc. I.R.E.* V. 31, p. 548 (Oct., 1943).
60. KING, R. and HARRISON, C. W. (Jun.). The receiving antenna. *Proc. I.R.E.* V. 32, p. 18 (Jan., 1944).
61. KORSHENEWSKY, N. VON. Über die Schwingungen eines Oszillators im Strahlungsfelde. *Zeit. für Techn. Phys.* V. 10, p. 604 (1929).
62. LABUS, J. Rechnerische Ermittlung der Impedanz von Antennen. *Hoch. u. Elektro.* V. 41, p. 17 (Jan., 1933).
63. MIDDLETON, D. and KING, R. The thin cylindrical antenna: a comparison of theories. *Jour. of Appl. Phys.* V. 17, p. 273 (April, 1946).
64. MOULLIN, E. B. The radiation resistance of aerials whose length is comparable with the wavelength. *Jour. I.E.E.* V. 78, p. 540 (May, 1936).
65. MOULLIN, E. B. Radiation from large circular loops. *Jour. I.E.E.* V. 93, Pt. III, p. 345 (Sept., 1946).
66. NEIMAN, M. S. The principle of reciprocity in antenna theory. *Proc. I.R.E.* V. 31, p. 666 (Dec., 1943).
67. PAGE, LEIGH. The magnetic antenna. *Phys. Rev.* V. 69, p. 645 (June, 1946).
68. PAGE, L. and ADAMS, N. I. The electrical oscillations of a prolate spheroid. Paper 1, *Phys. Rev.* V. 53, p. 819 (May, 1938).
69. PAZ, L. LA and MILLER, G. A. Optimum current distributions on vertical antennas. *Proc. I.R.E.* V. 31, p. 214 (May, 1943).
70. PEDERSEN, P. O. Radiation from a vertical antenna over flat perfectly conducting earth. *Ingenirvidenskabelige Skrifter A* No. 38 (1935). (On commission by G.E.C.—Gad., Copenhagen.)
71. PIPPARD, A. B., BURRELL, O. J. and CROMIE, E. E. The influence of re-radiation on measurements of the power gain of an aerial. *Jour. I.E.E.* V. 93, Pt. IIIA, No. 4, p. 720 (March–May, 1946).
72. PISTOLKORS, A. A. The radiation resistance of beam antennas. *Proc. I.R.E.* V. 17, p. 562 (March, 1929).
73. VAN DER POL, B. Über die Wellenlängen und Strahlung mit Kapazität und Selbstinduktion beschwerter Antennen. *Jahr. d. Drahtl. Tel. u. Tel.* V. 13, p. 217 (1919).
74. RATCLIFFE, J. A., VEDY, L. G. and WILKINS, A. F. The spreading of electromagnetic waves from a Hertzian Dipole. *Jour. I.E.E.* V. 70, p. 522 (May, 1932).
75. RICE, S. O. Series for the wave function of a radiating dipole at the earth's surface. *B.S.T.J.* V. 16, p. 101 (Jan., 1937).
76. RYDER, R. M. The electrical oscillation of a perfectly conducting prolate spheroid. *Jour. of Appl. Phys.* V. 13, p. 327 (May, 1942).
77. SCHELKUNOFF, S. A. Some equivalence theorems of electromagnetics and their application to radiation problems. *B.S.T.J.* V. 15, p. 92 (Jan., 1936).

78. SCHELKUNOFF, S. A. A general radiation formula. *Proc. I.R.E.* V. 27, p. 660 (Oct., 1939).
79. SCHELKUNOFF, S. A. Theory of antennas of arbitrary shape and size. *Proc. I.R.E.* V. 29, p. 493 (Sept., 1941).
80. SCHELKUNOFF, S. A. A mathematical theory of linear arrays. *B.S.T.J.* V. 22, p. 80 (Jan., 1943).
81. SCHELKUNOFF, S. A. Concerning Hallén's integral equation for cylindrical antennas. *Proc. I.R.E.* V. 33, p. 872 (Dec., 1945).
82. SCHELKUNOFF, S. A. Principal and complementary waves in antennas. *Proc. I.R.E.* V. 34, p. 23 (Jan., 1946).
83. SCHELKUNOFF, S. A., with FELDMAN, C. B. On radiation from antennas. *Proc. I.R.E.* V. 30, p. 511 (Nov., 1942).
84. SIEGEL, E. Scheinwiderstand von beschwerten Antennen. *Hoch. u. Elektro.* V. 43, p. 172 (May, 1934).
85. SIEGEL, E., with LABUS, J. Scheinwiderstand von Antennen. *Hoch. u. Elektro.* V. 43, p. 166 (May, 1934).
86. SOMMERFELD, A. and RENNER, F. Radiation energy and earth absorption for dipole antennae. *Wir. Eng.* V. 29 (1942), p. 351 (Aug.), p. 409 (Sept.), p. 457 (Oct.).
87. STRATTON, J. A. and CHU, L. J. Steady state solutions of electromagnetic field problems. *Jour. Appl. Phys.* P. 230 (March, 1941).
88. WILMOTTE, R. M. The distribution of current in a transmitting antenna. *Jour. I.E.E.* V. 66, p. 617 (June, 1928).
89. WILMOTTE, R. M. General formulae for the radiation distribution of antenna systems. *Jour. I.E.E.* V. 68, p. 1174 (Sept., 1930).

Long- and Medium-wave Antennae

90. ALEXANDERSON, E. F. W. Transoceanic radio communication. *Trans. Amer. I.E.E.* V. 38, p. 1269 (Oct., 1919).
91. BAUER, F. Simplified shunt feeding. *Comm.* V. 19, p. 8 (Sept., 1939).
92. BROWN, G. H. A consideration of the radio-frequency voltages encountered by the insulating material of broadcast tower antennas. *Proc. I.R.E.* V. 27, p. 566 (Sept., 1939).
93. BROWN, G. H., with LEITCH, J. G. The fading characteristics of the top-loaded WCAU antenna. *Proc. I.R.E.* V. 25, p. 583 (May, 1937).
94. BROWN, G. H., with LEWIS, R. F. and EPSTEIN, J. Ground systems as a factor in antenna efficiency. *Proc. I.R.E.* V. 25, p. 753 (June, 1937).
95. CHAMBERLAIN, A. B. and LODGE, W. B. The broadcast antenna. *Proc. I.R.E.* V. 24, p. 11 (Jan., 1936).
96. ECKERSLEY, P. P., with ECKERSLEY, T. L. and KIRKE, H. L. The design of transmitting aerials for broadcast stations. *Jour. I.E.E.* V. 67, p. 507 (April, 1929).
97. ESPENSCHIED, L., ANDERSON, C. N. and BAILEY, A. Transatlantic radio telephone transmission. *Proc. I.R.E.* V. 14, p. 7 (Feb., 1926).
98. GHIRING, H. E. and BROWN, G. H. General considerations of tower antennas for broadcast use. *Proc. I.R.E.* V. 23, p. 311 (April, 1935).

99. GUY, R. F. Notes on broadcast antenna developments. *R.C.A. Rev.* V. 1, p. 39 (April, 1937).
100. HOLLAND, F., STRONG, C. E. and MCLEAN, F. C. The Budapest anti-fading antenna. *Elec. Comm.* V. 12, p. 289 (April, 1934).
101. McPHERSON, W. L. Electrical properties of aerials for medium and long wave broadcasting. *Elec. Comm.* V. 16, p. 306 (April, 1938); v. 17, p. 44 (July, 1938).
102. MORRISON, J. F. and SMITH, P. H. The shunt-excited antenna. *Proc. I.R.E.* V. 25, p. 673 (June, 1937).
103. SHAUGHNESSY, E. H. The Rugby Radio Station of the British Post Office. *Jour. I.E.E.* V. 64, p. 683 (June, 1926).
104. WELLS, N. Aerial characteristics. *Jour. I.E.E.* V. 89, Pt. III, p. 76 (June, 1942).
105. WILLIAMS, H. P. The broadcast antenna. *Jour. Brit. I.R.E.* V. 7, p. 140 (July-Aug., 1947).

Short- and Ultra-short-wave Antennae

106. ALFORD, A. and KANDOIAN, A. G. Ultra-high frequency loop antennas. *Elec. Comm.* V. XVIII, p. 255 (April, 1940).
107. BANWELL, C. J. The use of a common aerial for radar transmission and reception on 200 Mc/s. *Jour. I.E.E.* V. 93, Pt. IIIA, No. 3, p. 545 (March-May, 1946).
108. BROWN, G. H. and EPSTEIN, J. An ultra-high frequency antenna of simple construction. *Comm.* V. 20, p. 3 (July, 1940).
109. CARLSON, W. L. Television reception with built-in antennas for horizontally and vertically polarized waves. *R.C.A. Rev.* V. VI, p. 443 (April, 1942).
110. CARTER, P. S. Simple television antennas. *R.C.A. Rev.* V. IV, p. 168 (Oct., 1939).
111. ENGLUND, C. R. The natural period of linear conductors. *B.S.T.j.* V. 7, p. 404 (July, 1928).
112. HASENBECK, H. W. Design data for ground plane antennae. *Electronics.* V. 16, p. 98 (Aug., 1943).
113. KRAUS, J. D. Antenna arrays with closely spaced elements. *Proc. I.R.E.* V. 28, p. 76 (Feb., 1940).
114. LEVIN, S. A. and YOUNG, C. J. Field distribution and radiation resistance of a straight vertical unloaded antenna radiator at one of its harmonics. *Proc. I.R.E.* V. 14, p. 675 (Oct., 1926).
115. LINDENBLAD, N. E. Television transmitting antenna for Empire State Building. *R.C.A. Rev.* V. III, p. 387 (April, 1939).
116. LUTKIN, F. E., CARY, R. H. J. and HARDING, G. H. Wide-band aerials and transmission lines for 20-85 Mc/s. *Jour. I.E.E.* V. 93, Pt. IIIA, No. 3, p. 552 (March-May, 1946).
117. MASTERS, R. W. The super turnstile. *Broadcast News*, No. 42, p. 42 (Jan., 1946).
118. McPETRIE, J. S., FORD, L. H. and SAKTON, J. A. Polar diagrams

- experiments with a half-wavelength receiving aerial and a V-type wire netting reflector. *Wir. Eng.* V. 22, p. 263 (June, 1945).
119. MCPETRIE, J. S., with SAXTON, J. A. Some experiments with linear aeriels. *Wir. Eng.* V. 23, p. 107 (April, 1946).
120. NAGY, A. W. An experimental study of parasitic wire reflectors on 2.5 meters. *Proc. I.R.E.* V. 24, p. 233 (Feb. 1936).
121. ROBERTS, W. VAN B. Input impedance of a folded dipole. *R.C.A. Rev.* V. 8, p. 289 (June, 1947).
122. WELLS, N. Notes on short-wave dipole aeriels. *Wir. Eng.* V. 20, p. 219 (May, 1943).
123. WELLS, N. The quadrant aerial; an omnidirectional wide-band horizontal aerial for short waves. *Jour. I.E.E.* V. 91, Pt. III, p. 182 (Dec., 1944).

Microwave Antennae

124. BAILEY, C. E. G. Slot feeders and slot aeriels. *Jour. I.E.E.* V. 93, Pt. IIIA, No. 4, p. 615 (March–May, 1946).
125. BARROW, W. L., with CHU, L. J. Theory of the electromagnetic horn. *Proc. I.R.E.* V. 27, p. 51 (Jan., 1939).
126. BARROW, W. L., with CHU, L. J. and JANSEN, J. J. Biconical electromagnetic horns. *Proc. I.R.E.* V. 27, p. 769 (Dec., 1939).
127. BARROW, W. L., with LEWIS, F. D. The sectoral electromagnetic horn. *Proc. I.R.E.* V. 27, p. 41 (Jan., 1939).
128. BARROW, W. L., with SCHULMAN, C. Multiunit electromagnetic horns. *Proc. I.R.E.* V. 28, p. 130 (March, 1940).
129. BÖHM, O. Cheese aeriels. *Jour. I.E.E.* V. 93, Pt. IIIA, No. 1, p. 45 (March–May, 1946).
130. BOOKER, H. G. Slot aeriels and their relation to complementary wire aeriels (Babinet's principle). *Jour. I.E.E.* V. 93, Pt. IIIA, No. 4, p. 620 (March–May, 1946).
131. BRENDL, R. Beitrag zur Berechnung von Reflektoren für elektrische Wellen. *Hoch. u. Elektro.* V. 47, p. 14 (Jan., 1936).
132. BREWITT-TAYLOR, E. G. A detailed experimental study of the factors influencing the polar diagram of a dipole in a parabolic mirror. *Jour. I.E.E.* V. 93, Pt. IIIA, No. 4, p. 679 (March–May, 1946).
133. CHU, L. J. and BARROW, W. L. Electromagnetic horn design. *Trans. A.I.E.E.* V. 58, p. 333 (July, 1939).
134. CULLEN, A. L. and GOWARD, F. K. The design of a wave-guide-fed array of slots to give a specified radiation pattern. *Jour. I.E.E.* V. 93, Pt. IIIA, No. 4, p. 683 (March–May, 1946).
135. DARBORD, R. Réflecteurs et lignes de transmission pour ondes ultra-courtes. *L'Onde El.* V. 11, p. 54 (Feb., 1932).
136. DAWSON, L. H. and RUST, N. M. A wide-band linear-array aerial. *Jour. I.E.E.* V. 93, Pt. IIIA, No. 4, p. 693 (March–May, 1946).
137. ESSEN, L. and OLIVER, M. H. Aerial impedance measurements. *Wir. Eng.* V. 22, p. 587 (Dec., 1945).

138. GRESKY, G. Die Wirkungsweise von Reflektoren bei kurzen elektrischen Wellen. *Zeit. für Hochfr.* V. 32, p. 149 (Nov., 1928).
139. KANDOIAN, A. G. Three new antenna types and their applications. *Waves and El.* V. 1, p. 70 (Feb., 1946).
140. KOCK, W. E. Metal-lens antennas. *Proc. I.R.E.* V. 34, p. 828 (Nov., 1946).
141. KOHLER, W. Die Wirkungsweise von Vollmetall- und Gitterreflektoren bei ultrakurzen Wellen. *Hoch. u. Elektro.* V. 39, p. 207 (June, 1932).
142. KRAUS, J. D. The corner-reflector antenna. *Proc. I.R.E.* V. 28, p. 513 (Nov., 1940).
143. MALLACH, P. and ZINKE, O. Les antennes diélectriques. *L'Onde El.* V. 26, p. 387 (Oct., 1946).
144. MOULLIN, E. B. Theory and performance of corner reflectors for aerials. *Jour. I.E.E.* V. 92, Pt. III, p. 58 (June, 1945).
145. RUST, N. M. The phase correction of horn radiators. *Jour. I.E.E.* V. 93, Pt. IIIA, No. 1, p. 50 (March-May, 1946).
146. SOUTHWORTH, G. C., with KING, A. P. Metal horns as directive receivers of ultra-short waves. *Proc. I.R.E.* V. 27, p. 95 (Feb., 1939).
147. STAAL, C. I. H. A. Full parabolic reflectors for microwaves. *Phil. Trans. News.* V. 3, p. 14 (1937).
148. WATSON, W. H. Resonant slots. *Jour. I.E.E.* V. 93, Pt. IIIA, No. 4, p. 747 (March-May, 1946).

Receiving Antennae

149. AMOS, S. W. Receiver aerial couplings for medium wavelength. *Jour. Brit. I.R.E.* V. VI, p. 144 (July-Aug., 1946).
150. BEVERAGE, H. H., RICE, C. W. and KELLOGG, E. W. The wave antenna—a new type of highly directive antenna. *Trans. A.I.E.E.* V. 42, p. 215 (Feb., 1923).
151. BEVERAGE, H. H., with PETERSON, H. O. Diversity receiving system of R.C.A. Communications Inc. for radiotelegraphy. *Proc. I.R.E.* V. 19, p. 531 (April, 1931).
152. BURGESS, R. E. Receiver input circuits—design considerations for optimum signal/noise ratio. *Wir. Eng.* V. 20, p. 66 (Feb., 1943).
153. COLEBROOK, F. M. An experimental and analytical investigation of earthed receiving aerials. *Jour. I.E.E.* V. 71, p. 235 (July, 1932).
154. FRIIS, H. T. and FELDMAN, C. B. A multiple unit steerable antenna for short-wave reception. *Proc. I.R.E.* V. 25, p. 841 (July, 1937).
155. HARRISON, C. W. (Jun.), with KING, R. The receiving antenna in a plane-polarized field of arbitrary orientation. *Proc. I.R.E.* V. 32, p. 35 (Jan., 1944).
156. LONDON, V. D. and REID, J. D. A new antenna system for noise reduction. *Proc. I.R.E.* V. 27, p. 188 (March, 1939).
157. MOULLIN, E. B. On the current induced in a wireless telegraph receiving antenna. *Proc. Cam. Phil. Soc.* V. 22, p. 567 (1925).

158. STURLEY, K. R. Receiver aerial coupling circuits. *Wir. Eng.* V. 18, p. 317 (April, 1941); V. 18, p. 190 (May, 1941).
159. SWINYARD, W. O. Measurement of loop-antenna receivers. *Proc. I.R.E.* V. 29, p. 382 (July, 1941).
160. WHEELER, H. A. and WHITMAN, V. E. The design of doublet antenna systems. *Proc. I.R.E.* V. 24, p. 1257 (Oct., 1936).

Directive Antennae and Arrays

161. BRUCE, E. Developments in short-wave directive antennas. *Proc. I.R.E.* V. 19, p. 1406 (Aug., 1931).
162. BRUCE, E., BECK, A. C. and LOWRY, L. R. Horizontal rhombic antennas. *Proc. I.R.E.* V. 23, p. 24 (Jan., 1935).
163. CAFFERATA, H. A generalized radiation formula for horizontal rhombic aeriels. *Mar. Rev.* V. 9, p. 24 (Jan.-March, 1946).
164. CARTER, P. S., HANSELL, C. W. and LINDENBLAD, N. E. Development of directive transmitting antennas by R.C.A. Communications Inc. *Proc. I.R.E.* V. 19, p. 1773 (Oct., 1931).
165. CHIREIX, M. Un système français d'émission à ondes courtes projectées. *L'Onde El.* V. 7, p. 169 (1928).
166. FOSTER, D. Radiation from rhombic antennas. *Proc. I.R.E.* V. 25, p. 1327 (Oct., 1937).
167. HANSEN, W. W. and HOLLINGSWORTH, L. M. Design of "flat-shooting" antenna arrays. *Proc. I.R.E.* V. 27, p. 137 (Feb., 1939).
168. HANSEN, W. W. and WOODYARD, J. R. A new principle in directional antenna design. *Proc. I.R.E.* V. 26, p. 333 (March, 1938).
169. HARRISON, C. W. Radiation from Vee-antennas. *Proc. I.R.E.* V. 31, p. 362 (July, 1943).
170. HAYES, L. W. and MACLARTY, B. The Empire Service Broadcasting Station at Daventry. *Jour. I.E.E.* V. 85, p. 321 (Sept., 1939).
171. LADNER, A. W. The series phase array. *Mar. Rev.* No. 67, p. 1 (Sept.-Dec., 1937).
172. LEWIN, L. Rhombic transmitting aerial—increasing the power efficiency. *Wir. Eng.* V. 18, p. 180 (May, 1941).
173. MOULLIN, E. B. On estimating the total output of a curtain array of aeriels and the current distribution among its members. *Jour. I.E.E.* V. 91, Pt. III, p. 23 (March, 1944).
174. PAGE, H. The measured performance of horizontal dipole transmitting arrays. *Jour. I.E.E.* V. 92, Pt. III, p. 68 (June, 1945).
175. REID, D. G. The gain of an idealized Yagi array. *Jour. I.E.E.* V. 93, Pt. IIIA, No. 3, p. 564 (March-May, 1946).
176. SOUTHWORTH, G. C. Certain factors affecting the gain of directive antennas. *Proc. I.R.E.* V. 18, p. 1502 (Sept., 1930).
177. STERBA, E. J. Theoretical and practical aspects of directional transmitting systems. *Proc. I.R.E.* V. 19, p. 1184 (July, 1931).
178. WALKINSHAW, M. A. Theoretical treatment of short Yagi aeriels. *Jour. I.E.E.* V. 93, Pt. IIIA, No. 3, p. 598 (March-May, 1946).
179. WALMSLEY, T. An investigation into the factors controlling the

- economic design of beam arrays. *Jour. I.E.E.* V. 74, p. 543 (June, 1934).
180. YAGI, H. Beam transmission of ultra-short waves. *Proc. I.R.E.* V. 16, p. 715 (June, 1928).
- D.F. Antennae*
181. BARFIELD, R. H. Some principles underlying the design of spaced-aerial direction-finders. *Jour. I.E.E.* V. 76, p. 423 (April, 1935).
182. BARFIELD, R. H. The performance and limitations of the compensated loop direction-finder. *Jour. I.E.E.* V. 86, p. 396 (April, 1940).
183. BARFIELD, R. H. and FEREDAY, R. A. An improved medium-wave Adcock direction-finder. *Jour. I.E.E.* V. 81, p. 676 (Nov., 1937).
184. BARFIELD, R. H. and ROSS, W. A short-wave Adcock direction-finder. *Jour. I.E.E.* V. 81, p. 682 (Nov., 1937).
185. BARFIELD, R. H. and ROSS, W. The measurement of the lateral deviation of radio waves by means of a spaced-loop direction-finder. *Jour. I.E.E.* V. 83, p. 98 (July, 1938).
186. BURGESS, R. E. The screened loop aerial—a theoretical and experimental investigation. *Wir. Eng.* V. 16, p. 492 (Oct., 1939).
187. BURGESS, R. E. Reactance and effective height of screened loop aerials. *Wir. Eng.* V. 21, p. 210 (May, 1944).
188. BUSIGNIES, H. The automatic radio compass and its applications to aerial navigation. *Elec. Comm.* V. XV, p. 157 (Oct., 1936).
189. BUSIGNIES, H. La réduction de l'erreur nocturne par le collecteur d'ondes Adcock. *L'Onde El.* V. 17, p. 105 (March, 1938).
190. FEREDAY, R. A. A sense-finding device for use with spaced-aerial direction-finders. *Jour. I.E.E.* V. 84, p. 96 (Jan., 1939).
191. FOSTER, D. Loop antennas with uniform current. *Proc. I.R.E.* V. 32, p. 603 (Oct., 1934).
192. FOSTER, D. E. and FINNIGAN, C. W. A method of measuring the effectiveness of electrostatic loop shielding. *Proc. I.R.E.* V. 31, p. 253 (June, 1943).
193. MUNRO, G. H. and HUXLEY, L. G. H. Shipboard observations with a cathode-ray direction-finder between England and Australia. *Jour. I.E.E.* V. 71, p. 488 (Sept., 1932).
194. PEARCE, R. R. Some experiments on conducting screens for a U-type spaced-aerial radio direction-finder in the frequency range 600-1 200 Mc/s. *Jour. I.E.E.* Vol. 94, Pt. III, p. 115 (Mar., 1947).
195. ROSS, W. The calibration of four-aerial Adcock direction-finders. *Jour. I.E.E.* V. 85, p. 192 (Aug., 1939).
196. ROSS, W. The development and study of a practical spaced-loop radio direction-finder for high frequencies. *Jour. I.E.E.* V. 44, Pt. III, p. 99 (Mar., 1947).
197. ROSS, W. Site and path errors in short-wave direction-finding. *Jour. I.E.E.* V. 94, Pt. III, p. 108 (Mar., 1947).
198. SMITH, R. A. and SMITH, C. H. Elimination of errors from crossed-dipole direction-finding systems. *Jour. I.E.E.* V. 93, Pt. IIIA, No. 3, p. 575 (March-May, 1946).

199. SMITH-ROSE, R. L. Symposium on radio direction-finding. *Jour. I.E.E.* V. 85, p. 203 (Aug., 1939).
200. SMITH-ROSE, R. L. and HOPKINS, H. G. Radio direction-finding on wavelengths between 6 and 10 metres. *Jour. I.E.E.* V. 83, p. 87 (July, 1938).
201. SMITH-ROSE, R. L. and HOPKINS, H. G. Radio direction-finding on wavelengths between 2 and 3 metres (100 to 150 Mc/s). *Jour. I.E.E.* V. 87, p. 154 (Aug, 1940)
202. SMITH-ROSE, R. L. and ROSS, W. The use of earth mats to reduce the polarization error of U-type Adcock direction-finders. *Jour. I.E.E.* V. 94, Pt. III, p. 91 (Mar., 1947).
203. TERMAN, F. E. and PETTIT, J. M. The compensated-loop direction finder. *Proc. I.R.E.* V. 33, p. 307 (May, 1945).

Antennae for Ships, Aircraft and Automobiles

204. BENNETT, F. D., COLEMAN, P. D. and MEIER, A. S. Design of broadband aircraft antenna systems. *Proc. I.R.E.* V. 33, p. 671 (Oct., 1945).
205. BOVILL, C. B. Aerials for use on aircraft; a comparison between fixed and trailing types on the 900-metre waveband. *Jour. I.E.E.* V. 92, Pt. III, p. 105 (June, 1945).
206. BUSIGNIES, H. The automatic radio compass and its applications to aerial navigation. *Elec. Comm.* V. XV, No. 2, p. 157 (Oct., 1936).
207. DEWITT, J. H. and OMBERG, A. C. The relation of the carrying car to the accuracy of portable field-intensity measuring equipment. *Proc. I.R.E.* V. 27, p. 1 (Jan., 1939).
208. FOSTER, D. E. and MOUNTJOY, G. Measurement of effective height of automobile antennas. *R.C.A. Rev.* V. III, p. 369 (Jan., 1939).
209. HALL, G. G. Design problems in automobile radio receivers. *A.W.A. Tech. Rev.* V. 4, No. 3, p. 105 (1939).
210. HALLER, G. L. Constants of fixed antennas on aircraft. *Proc. I.R.E.* V. 26, p. 415 (April, 1938).
211. HALLER, G. L. Aircraft antennas. *Proc. I.R.E.* V. 30, p. 357 (Aug., 1942).
212. HOLMES, P. J. Aircraft antenna characteristics. *Electronics.* V. 15, p. 40 (Dec., 1942).
213. HYLAND, L. A. The constants of aircraft trailing antennas. *Proc. I.R.E.* V. 17, p. 2230 (Dec., 1929).
214. KEES, H. and GEHRES, F. Cavity aircraft antenna. *Electronics.* V. 20, p. 78 (Jan., 1947).
215. LEVY, G. F. Loop antennas for aircraft. *Proc. I.R.E.* V. 31, p. 56 (Feb., 1943).
216. LORING, F. G., MCPHERSON, W. L. and McALLISTER, W. H. A survey of marine radio progress, with special reference to R.M.S. *Queen Mary.* *Jour. I.E.E.* V. 81, p. 183 (Sept., 1937).
217. MARIQUE, J. Radiation of ship stations on 500 kc/s. *Wir. Eng.* V. 23, p. 146 (May, 1946).

218. RUSSELL, B. The design and positioning of aircraft radar aerials for metric wavelengths. *Jour. I.E.E.* V. 93, Pt. IIIA, No. 3, p. 567 (March-May, 1946).
219. SOLT, C. T. The development and application of marine radio direction finding equipment by the United States Coast Guard. *Proc. I.R.E.* V. 20, p. 228 (Feb., 1932).
220. STEWART, C. A proposed standard dummy antenna for testing aircraft-radio transmitters. *Proc. I.R.E.* V. 33, p. 772 (Nov., 1945).

Propagation of Radio Waves

221. APPLETON, E. V. Radio exploration of upper-atmospheric ionization. *Rep. of Prog. in Phys.* V. 2, p. 129 (1936).
222. APPLETON, E. V. and BARNETT, M. A. F. On some direct evidence for downward atmospheric reflection of electric rays. *Proc. Roy. Soc. A.* V. 109, p. 621 (Dec., 1925).
223. APPLETON, E. V. and BEYNON, W. J. G. The application of ionospheric data to radio-communication problems. Part I. *Proc. Phys. Soc.* V. 52, p. 518 (July, 1940).
224. AUSTIN, L. W. Preliminary note on proposed changes in the constants of the Austin-Cohen transmission formula. *Proc. I.R.E.* V. 14, p. 377 (June, 1926).
225. Australian Radio Propagation Committee. *Radio Propagation Bulletin* (Issued Monthly). Radio Research Board, University of Sydney, N.S.W., Australia.
226. BENNINGTON, T. W. The validity of ionospheric forecasts. *B.B.C. Quart.* V. 1, p. 130 (Oct., 1946).
227. BOOKER, H. G. Elements of radio meteorology: how weather and climate cause unorthodox radar vision beyond the geometrical horizon. *Jour. I.E.E.* V. 93, Pt. IIIA, No. 1, p. 69 (March-May, 1946).
228. BOOKER, H. G. The elements of wave propagation using the impedance concept. *Jour. I.E.E.* V. 94, Pt. III, p. 171 (May, 1947).
229. BREIT, G. and TUVE, M. A. A test of the existence of the conducting layer. *Phys. Rev.* V. 28, p. 555 (Sept., 1926).
230. BURROWS, C. R. The surface wave in radio propagation over plane earth. *Proc. I.R.E.* V. 25, p. 219 (Feb., 1937).
231. BURROWS, C. R. Existence of a surface wave in radio propagation. *Nature.* V. 138, p. 284 (Aug., 1936).
232. BURROWS, C. R. Radio propagation over plane earth—field strength curves. *B.S.T.J.* V. 16, p. 45 (Jan., 1937).
233. BURROWS, C. R., with DECINO, A. and HUNT, L. E. Ultra-short wave propagation over land. *Proc. I.R.E.* V. 23, p. 1507 (Dec., 1935).
234. BURROWS, C. R. and GRAY, M. C. The effect of the earth's curvature on ground-wave propagation. *Proc. I.R.E.* V. 29, p. 16 (Jan., 1941).
235. DEWITT, J. H. and RING, A. D. Significant radiation from directional antennas of broadcast stations for determining sky-wave

- interference at short distances. *Proc. I.R.E.* V. 32, p. 668 (Nov., 1934).
236. DOMB, C. and PRYCE, M. H. L. The calculation of field strengths over a spherical earth. *Jour. I.E.E.* V. 94, Pt. III, p. 325 (Sept., 1947).
237. ECKERSLEY, T. L. Studies in radio transmission. *Jour. I.E.E.* V. 71, p. 405 (Sept., 1932).
238. ECKERSLEY, T. L. Ultra-short-wave refraction and diffraction. *Jour. I.E.E.* V. 80, p. 286 (March, 1937).
239. ECKERSLEY, T. L. Analysis of the effect of scattering in radio transmission. *Jour. I.E.E.* V. 86, p. 548 (June, 1940).
240. ECKERSLEY, T. L. and FARMER, F. T. Short period fluctuations in the characteristics of wireless echoes from the ionosphere. *Proc. Roy. Soc.* V. 184, p. 196 (Aug., 1945).
241. ECKERSLEY, T. L., with MILLINGTON, G. Application of the phase integral method to the analysis of the diffraction and refraction of wireless waves round the earth. *Phil. Trans.* V. 237, p. 273 (June, 1938).
242. ECKERSLEY, T. L., with MILLINGTON, G. The experimental verification of the diffraction analysis of the relation between height and gain for radio waves of medium lengths. *Proc. Phys. Soc.* V. 51, p. 805 (Sept., 1939).
243. ENGLUND, C. R., CRAWFORD, A. B. and MUMFORD, W. W. Some results of a study of ultra-short-wave transmission phenomena. *Proc. I.R.E.* V. 21, p. 464 (March, 1933).
244. ENGLUND, C. R., CRAWFORD, A. B. and MUMFORD, W. W. Ultra-short-wave transmission and atmospheric irregularities. *B.S.T.J.* V. 17, p. 489 (Oct., 1938).
245. ENGLUND, C. R., CRAWFORD, A. B. and MUMFORD, W. W. Ultra-short-wave transmission over a 39 mile "optical" path. *Proc. I.R.E.* V. 28, p. 360 (Aug., 1940).
246. FELDMAN, C. B. The optical behaviour of the ground for short radio waves. *Proc. I.R.E.* V. 21, p. 764 (June, 1933).
247. FELDMAN, C. B. Deviations of short radio waves from the London-New York great-circle path. *Proc. I.R.E.* V. 27, p. 635 (Oct., 1939).
248. FINK, D. G. The radar equation. *Electronics.* P. 92 (April, 1945).
249. FORD, L. H. and OLIVER, R. An experimental investigation of the reflection and absorption of radiation of 9 cm wavelength. *Proc. Phys. Soc.* V. 58, p. 265 (May, 1946).
250. FRIIS, H. T., FELDMAN, C. B. and SHARPLESS, W. M. The determination of the direction of arrival of short radio waves. *Proc. I.R.E.* V. 22, p. 47 (Jan., 1934).
251. GODDARD, D. R. Transatlantic reception of London television signals. *Proc. I.R.E.* V. 27, p. 692 (Nov., 1939).
252. GRAY, M. C. Horizontally-polarised electromagnetic waves over a spherical earth. *Phil. Mag.* V. 27, p. 421 (April, 1939).

253. HOLLINGWORTH, J. The propagation of radio waves. *Jour. I.E.E.* V. 64, p. 579 (May, 1926).
254. HOWE, G. W. O. Wireless waves at the earth's surface. *Wir. Eng.* V. 17, p. 385 (Sept., 1940).
255. KIRKE, H. L. Frequency modulation: B.B.C. field trials. *B.B.C. Quart.* V. 1, p. 62 (July, 1946).
256. KNOX, J. B. and BRERETON, C. H. A multi-channel V.H.F. radio communication system. *R.C.A. Rev.* V. VII, p. 179 (June, 1946).
257. MCPETRIE, J. S. The reflection coefficient of the earth's surface for radio waves. *Jour. I.E.E.* V. 82, p. 214 (Feb., 1938).
258. MCPETRIE, J. S., with SAXTON, J. A. An experimental investigation of the propagation of radiation having wavelengths of 2 and 3 metres. *Jour. I.E.E.* V. 87, p. 146 (Aug., 1940).
259. MCPETRIE, J. S. and STICKLAND, A. C. Reflection curves and propagation characteristics of radio waves along the earth's surface. *Jour. I.E.E.* V. 87, p. 135 (Aug., 1940).
260. MCPETRIE, J. S. and FORD, L. H. An experimental investigation on the propagation of radio waves over bare ridges in the wavelength range 10 cm to 10 m. *Jour. I.E.E.* V. 93, Pt. IIIA, No. 3, p. 527 (March-May, 1946).
261. MCPETRIE, J. S. and FORD, L. H. Some experiments on the propagation over land of radiation of 9.2 cm wavelength, especially on the effect of obstacles. *Jour. I.E.E.* V. 93, Pt. IIIA, No. 3, p. 531 (March-May, 1946).
262. MCPHERSON, W. L. and ULLRICH, E. H. Micro-ray communication. *Jour. I.E.E.* V. 78, p. 629 (June, 1936).
263. MEGAW, E. C. S. Experimental studies of the propagation of very short radio waves. *Jour. I.E.E.* V. 93, Pt. IIIA, No. 1, p. 79 (March-May, 1946).
264. MILLINGTON, G. The relation between ionospheric transmission phenomena at oblique incidence and those at vertical incidence. *Proc. Phys. Soc.* V. 50, p. 801 (Sept., 1938).
265. MILLINGTON, G. The diffraction of wireless waves round the earth. (A summary of the diffraction analysis, with a comparison between the various methods.) *Phil. Mag.* V. 27, p. 517 (May, 1939).
266. MUELLER, G. E. Propagation of 6 millimeter waves. *Proc. I.R.E.* V. 34, p. 181 (April, 1946).
267. National Bureau of Standards, Washington, D.C. Monthly reports on the ionosphere in the *Proc. I.R.E.* from Sept., 1937, to Dec., 1941.
268. National Physical Laboratory. *The Prediction of Optimum Frequencies.* Monthly bulletin from the Radio Research Station, Slough, England.
269. NORTON, K. A. The propagation of radio waves over the surface of the earth and in the upper atmosphere. Part 1, *Proc. I.R.E.* V. 24, p. 1367 (Oct., 1936). Part 2, *Proc. I.R.E.* V. 25, p. 1203 (Sept., 1937).
270. NORTON, K. A. The physical reality of space and surface waves in

- the radiation field of radio antennas. *Proc. I.R.E.* V. 25, p. 1192 (Sept., 1937).
271. NORTON, K. A. The calculation of ground-wave field intensity over a finitely conducting spherical earth. *Proc. I.R.E.* V. 29, p. 623 (Dec., 1941).
272. NORTON, K. A. and ALLEN, E. W. (Jun.). FM and television signal propagation. *FM and Tel.* V. 6, p. 44 (April, 1946).
273. NORTON, K. A., KIRBY, S. S. and LESTER, G. H. An analysis of continuous records of field intensity at broadcast frequencies. *Proc. I.R.E.* V. 23, p. 1183 (Oct., 1935).
274. VAN DER POL, B., with BREMMER, H. The diffraction of electromagnetic waves from an electrical point source round a finitely conducting sphere, with applications to radio telegraphy and the theory of the rainbow. Part 1, *Phil. Mag.* V. 24, p. 141 (July, 1937). Part 2, *Phil. Mag.* V. 24, p. 825 (Nov., 1937 (supplement)).
275. VAN DER POL, B. and BREMMER, H. The propagation of radio waves over a finitely conducting spherical earth. *Phil. Mag.* V. 25, p. 817 (June, 1938).
276. VAN DER POL, B., with BREMMER, H. Ergebnisse einer Theorie über die Fortpflanzung elektromagnetischer Wellen über eine Kugel endlicher Leitfähigkeit. *Hoch. u. Elektro.* V. 51, p. 181 (June, 1938).
277. VAN DER POL, B., with BREMMER, H. Further note on the propagation of radio waves over a finitely conducting spherical earth. *Phil. Mag.* V. 27, p. 261 (March, 1939).
278. POTTER, R. K. and FRIIS, H. T. Some effects of topography and ground on short-wave reception. *Proc. I.R.E.* V. 20, p. 699 (April, 1932).
279. RATCLIFFE, J. A. The magneto-ionic theory. *Wir. Eng. and Elec. W.* V. 10, p. 354 (July, 1933).
280. ROBERTSON, S. D. and KING, A. P. The effect of rain upon the propagation of waves in the 1 and 3 centimeter regions. *Proc. I.R.E.* V. 34, p. 178 (April, 1946).
281. SCHELKUNOFF, S. A. The impedance concept and its application to problems of reflection, refraction, shielding and power absorption. *B.S.T.J.* V. 17, p. 17 (Jan., 1938).
282. SCHELLENG, J. C., BURROWS, C. R. and FERRELL, E. B. Ultra-short-wave propagation. *Proc. I.R.E.* V. 21, p. 427 (March, 1933).
283. SELVIDGE, H. Diffraction measurements at ultra-high frequencies. *Proc. I.R.E.* V. 29, p. 10 (Jan., 1941).
284. SMITH, N. The relation of radio sky-wave transmission to ionosphere measurements. *Proc. I.R.E.* V. 27, p. 332 (May, 1939).
285. SOMMERFELD, A. Über die Ausbreitung der Wellen in der drahtlosen Telegraphie. *Ann. der Phys.* V. 28, p. 665 (March, 1909). V. 81, p. 1135 (Dec., 1926).
286. STARNECKI, B. J. A study of some of the factors influencing microwave propagation. *Jour. I.E.E.* V. 93, Pt. IIIA, No. 1, p. 106 (March-May, 1946).

287. TREVOR, B. and GEORGE, R. W. Notes on propagation at a wavelength of seventy-three centimeters. *Proc. I.R.E.* V. 23, p. 461 (May, 1935).
288. WATSON, G. N. The transmission of electric waves around the earth. *Proc. Roy. Soc. A.* V. 95, p. 546 (July, 1919).
289. WEYL, H. Ausbreitung elektromagnetischer Wellen über einen ebenen Leiter. *Ann. der Phys.* V. 60, p. 481 (Nov., 1919).
290. WILKINS, A. F. Measurement of the angle of incidence at the ground of downcoming short waves from the ionosphere. *Jour. I.E.E.* V. 74, p. 582 (June, 1934).
291. WISE, W. H. The physical reality of Zenneck's surface wave. *B.S.T.J.* V. 16, p. 35 (Jan., 1937).
292. WVEDENSKY, B. The diffraction propagation of radio waves. *Tech. Phys. U.S.S.R.* V. 2, p. 624 (Nov., 1935); V. 3, p. 915 (Nov., 1936).
293. ZENNECK, J. Über die Fortpflanzung ebener elektromagnetischer Wellen längs einer ebenen Leiterfläche und ihre Beziehung zur drahtlosen Telegraphie. *Ann. der Phys.* V. 23, p. 846 (Sept., 1907).

Noise

294. APPLETON, SIR EDWARD. Extra-tropospheric influences on ultra-short-wave radar operation. *Jour. I.E.E.* V. 93, Pt. IIIA, No. 1, p. 110 (March-May, 1946).
295. Army-Navy Precipitation-Static Project. A series of six articles commencing in *Proc. I.R.E.* V. 34, p. 156 (April, 1946).
296. BENNINGTON, T. W. Tropical Broadcasting. *Wir. World.* V. LI, No. 6, p. 165 (June, 1945).
297. BURGESS, R. E. Noise in receiving aerial systems. *Proc. Phys. Soc.* V. 53, p. 293 (May, 1941).
298. BURRILL, C. M. Progress in the development of instruments for measuring radio noise. *Proc. I.R.E.* V. 29, p. 433 (Aug., 1941).
299. BURRILL, C. M. An evaluation of radio-noise-meter performance in terms of listening experience. *Proc. I.R.E.* V. 30, p. 473 (Oct., 1942).
300. GEORGE, R. W. Field strength of motor-car ignition between 40 and 450 Mc/s. *Proc. I.R.E.* V. 28, p. 409 (Sept., 1940).
301. GILL, A. J. and WHITEHEAD, S. Electrical interference with radio reception. *Jour. I.E.E.* V. 83, p. 345 (Sept., 1938).
302. FRÄNZ, K. Messung der Empfängerempfindlichkeit bei kurzen der elektrischen Wellen. *Hoch. u. Elek.* V. 59, p. 143 (1942).
303. FRIIS, H. T. Noise figures of radio receivers. *Proc. I.R.E.* V. 32, p. 419 (July, 1944).
304. HARRIS, W. A. Fluctuations in vacuum tube amplifiers and input systems. *R.C.A. Rev.* V. V, p. 505 (April, 1941), V. VI, p. 114 (July, 1941).
305. HUCKE, H. M. Precipitation-static interference on aircraft and at ground stations. *Proc. I.R.E.* V. 27, p. 301 (May, 1939).

306. JANSKY, K. G. Directional studies of atmospherics at high frequencies. *Proc. I.R.E.* V. 20, p. 1920 (Dec., 1932).
307. JANSKY, K. G. A note on the source of interstellar interference. *Proc. I.R.E.* V. 23, p. 1158 (Oct., 1935).
308. JARVIS, R. F. J. and SEAMEN, E. C. H. The effect of noise and interfering signals on television transmission. *P.O. Elec. Eng. Jour.* V. 32, Pt. 3, p. 193 (Oct., 1939).
309. JOHNSON, J. B. Thermal agitation of electricity in conductors. *Phys. Rev.* V. 32, p. 97 (July, 1928).
310. KOMPFFNER, R., HATTON, J., SCHNEIDER, E. F. and DRESEL, L. A. G. The transmission-line diode as noise source at centimetre wavelengths. *Jour. I.E.E.* V. 93, Pt. IIIA, No. 9, p. 1436 (March-May, 1946).
311. MOFFATT, J. A diode noise generator. *Jour. I.E.E.* V. 93, Pt. IIIA, No. 8, p. 1335 (March-May, 1946).
312. MOXON, L. A. The noise characteristics of radar receivers. *Jour. I.E.E.* V. 93, Pt. IIIA, No. 6, p. 1130 (March-May, 1946).
313. NORTH, D. O. The absolute sensitivity of radio receivers. *R.C.A. Rev.* V. VI, p. 332 (Jan., 1942).
314. NYQUIST, H. Thermal agitation of electric charge in conductors. *Phys. Rev.* V. 32, p. 110 (July, 1928).
315. POTTER, R. K. High-frequency atmospheric noise. *Proc. I.R.E.* V. 19, p. 1731 (Oct., 1931).
316. SASHOFF, S. P. and ROBERTS, W. K. Directional characteristics of tropical storm static. *Proc. I.R.E.* V. 30, p. 131 (March, 1942).
317. THOMAS, H. A. and BURGESS, R. E. Survey of existing information and data on atmospheric noise level over the frequency range 1-30 Mc/s. *Department of Scientific and Industrial Research, Radio Research Board Paper, R.R.B./C.90.*
318. ULLRICH, E. H. and ROGERS, D. C. An absolute method of measurement of receiver noise factor. *Jour. I.E.E.* V. 93, Pt. IIIA, No. 8, p. 1347 (March-May, 1946).

Transmission Lines and Waveguides

319. ALFORD, A. High-frequency transmission line networks. *Elec. Comm.* V. 17, p. 301 (Jan., 1939).
320. ALLANSON, J. T., COOPER, R. and COWLING, T. G. The theory and experimental behaviour of right-angled junctions in rectangular-section wave guides. *Jour. I.E.E.* V. 93, Pt. III, p. 177 (May, 1946).
321. BURROWS, C. R. The exponential transmission line. *B.S.T.J.* V. 17, p. 555 (Oct., 1938).
322. CARSON, J. R. Radiation from transmission lines. *Jour. A.I.E.E.* P. 789 (Oct., 1921).
323. CARSON, J. R. The guided and radiated energy in wire transmission. *Jour. A.I.E.E.* P. 906 (Oct., 1924).
324. CORK, E. C. and PAWSEY, J. L. Long feeders for transmitting wide

- side-bands, with reference to the Alexandra Palace aerial-feeder system. *Jour. I.E.E.* V. 84, p. 448 (April, 1939).
325. COX, C. R. Transmission lines for FM stations. *FM and Tel.* (June and July, 1946).
326. DINGLEY, E. N. (Jun.). The theory of transmission lines. *Proc. I.R.E.* V. 33, p. 118 (Feb., 1945).
327. EARLY, H. C. A wide-band wattmeter for wave guide. *Proc. I.R.E.* V. 34, p. 803 (Oct., 1946).
328. FRANKEL, S. Characteristic impedance of parallel wires in rectangular troughs. *Proc. I.R.E.* V. 30, p. 182 (April, 1942).
329. GENT, A. W. and WALLIS, P. J. Impedance matching by tapered transmission lines. *Jour. I.E.E.* V. 93, Pt. IIIA, No. 3, p. 559 (March-May, 1946).
330. HARRISON, C. W. (Jun.). On the pick-up of balanced four-wire lines. *Proc. I.R.E.* V. 30, p. 517 (Nov., 1942).
331. JACKSON, W. and HUXLEY, L. G. H. The solution of transmission line problems by use of the circle diagram of impedance. *Jour. I.E.E.* V. 91, Pt. III, p. 105 (Sept., 1944).
332. KUHN, S. Calculation of attenuation in wave guides. *Jour. I.E.E.* V. 93, Pt. IIIA, No. 4, p. 663 (March-May, 1946).
333. MACFARLANE, G. G. Quasi-stationary field theory and its application to diaphragms and junctions in transmission lines and wave guides. *Jour. I.E.E.* V. 93, Pt. IIIA, No. 4, p. 703 (March-May, 1946).
334. MACLESE, A. and ASHMEAD, J. The rhumbatron wave-guide switch. *Jour. I.E.E.* V. 93, Pt. IIIA, No. 4, p. 700 (March-May, 1946).
335. MCLEAN, F. C. and BOLT, F. D. The design and use of radio frequency open-wire transmission lines and switchgear for broadcasting systems. *Jour. I.E.E.* V. 93, Pt. III, p. 191 (May, 1946).
336. NERGAARD, L. S. and SALZBERG, B. Resonant impedance of transmission lines. *Proc. I.R.E.* V. 27, p. 579 (Sept., 1939).
337. PAINE, R. C. Graphical solution of voltage and current distribution and impedance of transmission lines. *Proc. I.R.E.* V. 32, p. 686 (Nov., 1944).
338. SALINGER, H. The quarter-wave step-up transformer. *Proc. I.R.E.* V. 32, p. 553 (Sept., 1944).
339. SMITH, P. H. A transmission line calculator. *Electronics.* V. 12, p. 29 (Jan., 1939).
340. SOUTHWORTH, G. C. Some fundamental experiments with wave guides. *Proc. I.R.E.* V. 25, p. 807 (July, 1937).
341. SURDIN, M. Directive couplers in wave guides. *Jour. I.E.E.* V. 93, Pt. IIIA, No. 4, p. 725 (March-May, 1946).
342. STARR, A. T. The non-uniform transmission line. *Proc. I.R.E.* V. 20, p. 1052 (June, 1932).
343. STERBA, E. J. and FELDMAN, C. B. Transmission lines for short-wave radio systems. *Proc. I.R.E.* V. 20, p. 1163 (July, 1932).
344. WATSON, W. H. Matrix methods in transmission-line and impedance

- calculations. *Jour. I.E.E.* V. 93, Pt. IIIA, No. 4, p. 737 (March-May, 1946).
345. WHINNERY, J. R., JAMIESON, H. W. and ROBBINS, T. E. Coaxial-line discontinuities. *Proc. I.R.E.* V. 32, p. 695 (Nov., 1944).
346. WHINNERY, J. R. and JAMIESON, H. W. Equivalent circuits for discontinuities in transmission lines. *Proc. I.R.E.* V. 32, p. 98 (Feb., 1944).
347. WILLOUGHBY, E. O. Some applications of field plotting. *Jour. I.E.E.* V. 93, Pt. III, p. 275 (July, 1946).
348. WILLOUGHBY, E. O. and WILLIAMS, E. M. Attenuation curves for 2 : 1 rectangular, square and circular wave guides. *Jour. I.E.E.* V. 93, Pt. IIIA, No. 4, p. 723 (March-May, 1946).

Miscellaneous

349. BARNES, C. C. The current rating of paper insulated power cables. *Elec. Comm.* V. 21, p. 27 (1942-44).
350. BROWN, G. H. and MORRISON, W. C. The R.C.A. antenna analyzer—an instrument useful in the design of directional antenna systems. *Proc. I.R.E.* V. 34, p. 992 (Dec., 1946).
351. BYRNES, I. F. Merchant marine radar. *R.C.A. Rev.* V. VII, p. 54 (March, 1946).
352. COLEBROOK, F. M. and GORDON-SMITH, A. C. A method of calibrating a field-strength measuring set. *Jour. I.E.E.* V. 88, Pt. III, p. 15 (March, 1941).
353. COLEBROOK, F. M. and GORDON-SMITH, A. C. The design of ultra-short-wave field-strength measuring equipment. *Jour. I.E.E.* V. 90, Pt. III, p. 28 (March, 1943).
354. *Electronic Engineering Data Sheets*, 51 to 62. Aug., 1943, to Feb., 1944.
355. GIORGI, G. Unita razionali di elettromagnetismo. *Atti Dell'Associazione Elettrotecnica Italiana*, V. 5, p. 6 (1901). Rational electromagnetic units. *El. World and Eng.* V. 40, p. 368 (1902).
356. GROVER, F. W. Methods, formulas and tables for the calculation of antenna capacity. *Bureau of Standards Paper No. 568* (Washington, 1928).
357. JORDON, E. C. and EVERITT, W. L. Acoustic models of radio antennas. *Proc. I.R.E.* V. 29, p. 186 (April, 1941).
358. LEWIS, W. B. Radar receivers. *Jour. I.E.E.* V. 93, Pt. IIIA, No. 1, p. 272 (March-May, 1946).
359. MACNAMARA, T. C. and BIRKINSHAW, D. C. The London Television Service. *Jour. I.E.E.* V. 83, p. 729 (Dec., 1938).
360. MCPETRIE, J. S. and PRESSEY, B. G. A method of using horizontally polarized waves for the calibration of short-wave field-strength measuring sets by radiation. *Jour. I.E.E.* V. 83, p. 210 (Aug., 1938).
361. MCPETRIE, J. S., with SAXTON, J. A. Theory and experimental confirmation of calibration of field-strength measuring sets by radiation. *Jour. I.E.E.* V. 88, Pt. III, p. 11 (March, 1941).

362. RATCLIFFE, J. A. Aerials for radar equipment. *Jour. I.E.E.* V. 93, Pt. IIIA, No. 1, p. 22 (March–May, 1946).
363. SALINGER, H. A dummy dipole network. *Proc. I.R.E.* V. 32, p. 115 (Feb., 1944).
364. SCHNEIDER, E. G. Radar. *Proc. I.R.E.* V. 34, p. 528 (Aug., 1946).
365. SMITH, R. A. Radar navigation. *Jour. I.E.E.* V. 93, Pt. IIIA, No. 1, p. 331 (March–May, 1946).
366. WILLIAMS, H. P. A machine for calculating the polar diagram of an antenna system. *Elec. Comm.* V. 21, p. 103 (1942–44).
367. WILLIAMS, H. P. Electrical units and the M.K.S. system. *Elec. Comm.* V. 23, p. 96 (March, 1946).
368. WOLFF, I. Determination of the radiating system which will produce a specified directional characteristic. *Proc. I.R.E.* V. 25, p. 630 (May, 1937).

Additional References (Unclassified)

369. ALRED, R. V. Experiments with Yagi aerials at 600 Mc/s. *Jour. I.E.E.* V. 93, Pt. IIIA, p. 1490 (March–May, 1946).
370. APPLETON, E. V. and BEYNON, W. J. G. The application of ionospheric data to radio-communication problems. Pt. II, *Proc. Phys. Soc.* V. 59, p. 58 (Jan., 1947).
371. BARKER, R. H. Rhombic aerial design chart. *Wir. Eng.* V. 25, p. 353 (Nov., 1948).
372. BARLOW, H. M. *Micro-waves and wave guides*. Constable and Co., Ltd. (1947).
373. BARZILAI, G. Mutual impedance of parallel aerials. *Wir. Eng.* V. 25, p. 343 (Nov., 1948).
374. BROWN, A. H. and STANIER, H. M. Recent developments in V.H.F. ground-communication aerials for short distances. *Jour. I.E.E.* V. 94, Pt. IIIA, p. 637 (1947).
375. BURGESS, R. E. Iron-cored loop receiving aerial. *Wir. Eng.* V. 23, p. 172 (June, 1946).
376. CHU, L. J. Physical limitations of omni-directional antennas. *Jour. of Appl. Phys.* V. 19, p. 1163 (Dec., 1948).
377. CLEAVER, R. F. The development of single-receiver automatic Adcock direction-finders for use in the frequency band 100–150 Mc/s. *Jour. I.E.E.* V. 94, Pt. IIIA, p. 783 (1947).
378. COHN, S. B. Design of simple broad-band wave-guide-to-coaxial-line junctions. *Proc. I.R.E.* V. 35, p. 920 (Sept., 1947).
379. COX, C. R. Mutual impedance between vertical antennas of unequal heights. *Proc. I.R.E.* V. 35, p. 1367 (Nov., 1947).
380. CUTLER, C. C. Parabolic-antenna design for microwaves. *Proc. I.R.E.* V. 35, p. 1285 (Nov., 1947).
381. CUTLER, C. C., KING, A. P. and KOCK, W. E. Microwave antenna measurements. *Proc. I.R.E.* V. 35, p. 1462 (Dec., 1947).
382. EARP, C. W. and GODFREY, R. M. Radio direction-finding by the

- cyclical differential measurement of phase. *Jour. I.E.E.* V. 94, Pt. IIIA, p. 705 (1947).
383. FISHENDEN, R. M. and WIBLIN, E. R. Design of Yagi aeriels. *Jour. I.E.E.* V. 96, Pt. III, p. 5 (Jan., 1949).
384. FRY, D. W. Some recent developments in the design of centimetric aerial systems. *Jour. I.E.E.* V. 93, Pt. IIIA, p. 1497 (March-May, 1946).
385. HALLÉN, E. Properties of a long antenna. *Jour. of Appl. Phys.* V. 19, p. 1140 (Dec., 1948).
386. HALLIDAY, D. F. and KEELY, D. G. Dielectric-rod aeriels. *Jour. I.E.E.* V. 94, Pt. IIIA, p. 610 (1947).
387. JOHNSON, W. A. Recent developments of aircraft communication aeriels. *Jour. I.E.E.* V. 94, Pt. IIIA, p. 452 (1947).
388. KIRKE, H. L. Calculation of ground-wave field strength over a composite land and sea path. *Proc. I.R.E.* V. 37, p. 489 (May, 1949).
389. KRAUS, J. D. Helical beam antennas for wide-band applications. *Proc. I.R.E.* V. 36, p. 1236 (Oct., 1948).
390. LAWSON, J. D. The practical aspects of paraboloid aerial design. *Jour. I.E.E.* V. 93, Pt. IIIA, p. 1511 (March-May, 1946).
391. LINDENBLAD, N. E. Slot antennas. *Proc. I.R.E.* V. 35, p. 1472 (Dec., 1947).
392. MACFARLANE, G. G. Surface impedance of an infinite parallel-wire grid at oblique angle of incidence. *Jour. I.E.E.* V. 93, Pt. IIIA, p. 1523 (March-May, 1946).
393. MILLINGTON, G. Ground wave propagation over an inhomogeneous smooth earth. *Jour. I.E.E.* V. 96, Pt. III, p. 53 (Jan., 1949).
394. OWEN, A. R. G. and REYNOLDS, L. G. The effect of flanges on the radiation patterns of small horns. *Jour. I.E.E.* V. 93, Pt. IIIA, p. 1528 (March-May, 1946).
395. *Meteorological factors in radio-wave propagation.* Report of a conference held on 8th April, 1946. (Published by The Physical Society, London).
396. PIPPARD, A. B. The hoghorn—an electromagnetic horn radiator of medium-sized aperture. *Jour. I.E.E.* V. 93, Pt. IIIA, p. 1536 (March-May, 1946).
397. PIPPARD, A. B. and ELSON, N. The elimination of standing waves in aeriels employing paraboloidal reflectors. *Jour. I.E.E.* V. 93, Pt. IIIA, p. 1531 (March-May, 1946).
398. PUTMAN, J. L. Input impedances of centre-fed slot aeriels near half-wave resonance. *Jour. I.E.E.* V. 95, Pt. III, p. 290 (July, 1948).
399. PUTMAN, J. L. and MACRO, W. B. Experiments with slot aeriels in corner reflectors. *Jour. I.E.E.* V. 93, Pt. IIIA, p. 1539 (March-May, 1946).
400. PUTMAN, J. L., RUSSELL, B. and WALKINSHAW, W. Field distributions near a centre-fed half-wave radiating slot. *Jour. I.E.E.* V. 95, Pt. III, p. 282 (July, 1948).

401. REBER, G. Antenna focal devices for parabolic mirrors. *Proc. I.R.E.* V. 35, p. 920 (Sept., 1947).
402. RIBLET, H. J. Note on the maximum directivity of an antenna. *Proc. I.R.E.* V. 36, p. 620 (May, 1948).
403. SEELY, S. Microwave antenna analysis. *Proc. I.R.E.* V. 35, p. 1092 (Oct., 1947).
404. SICHAK, W. and MILAZZO, S. Antennas for circular polarization. *Proc. I.R.E.* V. 36, p. 907 (Aug., 1948).
405. SILVER, S. (edited by). *Microwave antenna theory and design*. Vol. 12, M.I.T. Radiation Laboratory Series. (McGraw-Hill Book Co., 1949).
406. SINCLAIR, G., JORDAN, E. C. and VAUGHAN, E. W. Measurement of aircraft-antenna patterns using models. *Proc. I.R.E.* V. 35, p. 1451 (Dec., 1947).
407. SMITH, C. E. and JOHNSON, E. M. Performance of short antennas. *Proc. I.R.E.* V. 35, p. 1026 (Oct., 1947).
408. SMITH, P. H. Cloverleaf antenna for F.M. broadcasting. *Proc. I.R.E.* V. 35, p. 1556 (Dec., 1947).
409. SMITH-ROSE, R. L. Radio field-strength measurement. *Jour. I.E.E.* V. 96, Pt. III, p. 31 (Jan., 1949).
410. STRUTT, M. J. O. *Ultra- and extreme-short wave reception* (D. Van Nostrand Inc., 1947).
411. TAI, C. T. On the theory of biconical antennas. *Jour. of Appl. Phys.* V. 19, p. 1155 (Dec., 1948).
412. WESTCOTT, C. H. and GOWARD, F. K. The design of wide-band aerial elements for 500-600 Mc/s ground radar. *Jour. I.E.E.* V. 96, Pt. III, p. 41 (Jan., 1949).
413. WHEELER, H. A. Fundamental limitations of small antennas. *Proc. I.R.E.* V. 25, p. 1479 (Dec., 1947).
414. WHEELER, H. A. A helical antenna for circular polarization. *Proc. I.R.E.* V. 35, p. 1484 (Dec., 1947).
415. WHEELER, H. A. The radiation resistance of an antenna in an infinite array or waveguides. *Proc. I.R.E.* V. 36, p. 478 (April, 1948).
416. WICKIZER, G. S. and BRAATEN, A. M. Propagation studies on 45.1, 474 and 2 800 Megacycles within and beyond the horizon. *Proc. I.R.E.* V. 35, p. 670 (July, 1947).
417. WILKES, G. Wavelength lenses. *Proc. I.R.E.* V. 36, p. 206 (Feb., 1948).
418. WOODWARD, P. M. and LAWSON, J. D. The theoretical precision with which an arbitrary radiation-pattern may be obtained from a source of finite size. *Jour. I.E.E.* V. 95, Pt. III, p. 363 (Sept., 1948).

AUTHOR INDEX

- ABRAHAM, M., 139
 Adams, N. I., 139
 Alford, A., 121, 124, 266
 Allen, E. W., 203, 213
 Anderson, C. N., 376
 Appleton, E. V., 22, 27, 233, 396, 400
 Austin, L. W., 373
- BAILEY, A., 376
 Baker, B. B., 171
 Ballantine, S., 71
 Barfield, R. H., 324, 335
 Barnes, C. C., 470
 Barnett, M. A. F., 22, 233
 Barrow, W. L., 102, 174, 178, 180
 Beck, A. C., 293
 Beckerley, J. G., 102
 Bennett, F. D., 361
 Bergmann, L., 267, 423
 Beverage, H. H., 228, 231
 Beynon, W. J. G., 27, 396, 400
 Bolt, F. D., 464
 Booker, H. G., 184, 429, 326
 Bouwkamp, C. J., 77, 266
 Bovill, C. B., 353
 Breit, G., 23
 Bremmer, H., 423
 Brendel, R., 150
 Brewitt-Taylor, E. G., 154, 160
 Brillouin, L., 140
 Brown, G. H., 64, 66, 68, 70, 75, 77,
 91, 106, 119, 141, 241, 273
 Bruce, E., 293
 Brückman, H., 70, 78
 de Bruign, N. G., 77, 266
 Burgess, R. E., 202, 203, 206
 Burrell, O. J., 257
 Burrill, C. M., 208
 Burrows, C. R., 15, 366, 378, 381, 416,
 468
 Busignics, H., 348
 Byrnes, I. F., 432
- CARLSON, W. L., 227
 Carter, P. S., 104, 271, 280
 Cary, R. H. J., 127
 Chamberlain, A. B., 54
 Chu, L. J., 92, 136, 174, 178, 180
 Colebrook, F. M., 196, 218
 Coleman, P. D., 361
 Copson, C. T., 171
 Cork, E., 464
 Crawford, A. B., 422
 Cromie, E. E., 257
- DARBORD, R., 150
 De Witt, J. H., 362
 Domb, C., 424, 426
- ECKERSLEY, T. L., 28, 423
 Englund, C. R., 422
 Epstein, J., 68, 119
 Espenschied, L., 376
 Essen, L., 140
 Everitt, W. L., 134
- FELDMAN, C. B., 93, 102, 398, 464, 467
 Ferrell, E. B., 416
 Fink, D. G., 430
 Ford, L. H., 166, 425
 Franz, K., 204
 Friis, H. T., 93, 102
- GEORGE, R. W., 206
 Gray, M. C., 366, 378, 381
 Gresky, G., 150
 Grover, F. W., 35, 36, 40
 Guy, R. F., 78
- HALLÉN, E., 91, 139
 Haller, G. L., 358
 Hansell, C. W., 280
 Hansen, W. W., 102
 Harding, G. H., 127
 Harper, A. E., 235, 298
 Harrison, C. W., 91
 Hasenbeck, H. W., 119
 Hayes, L. W., 307
 Hertz, H., 8
 Hollingworth, J., 374
 Howe, G. W. O., 35, 36, 40
 Hucke, H. M., 205
 Huxley, L. G. H., 457
 Hyland, L. A., 353
- JACKSON, W., 457
 Jansen, J. J., 180
 Jansky, K. G., 203
 Johnson, J. B., 201
 Johnson, W. A., 358
- KANDOIAN, A. G., 145, 147
 Keen, R., 343, 347
 Kellogg, E. W., 228, 231
 King, A. P., 179
 King, R., 2, 91, 139, 179, 200
 Köhler, W., 167
 Korshenewsky, N. von, 196
 Krauss, J. D., 161, 165

- LADNER, A. W., 312, 314
 Landon, V., 219
 Lassen, H., 423
 Lewis, F. D., 174
 Lewis, R. F., 68
 Lindenblad, N. E., 127, 280
 Lodge, W. B., 54
 Lowry, L. R., 293
 Lutkin, F. E., 127
- MACLARTY, B., 307
 McLean, F. C., 464
 McPetric, J. S., 166, 267, 416, 425
 MacPherson, W. L., 40, 54, 74
 Mallach, P., 190, 192
 Marconi, G., 9, 22
 Meier, A. S., 361
 Morrison, J. F., 51, 52, 60
 Morrison, W. C., 241
 Moullin, E. B., 165, 265
 Moxon, L. A., 203, 213
 Mumford, W. W., 422
- NAGY, A. W., 150
 Norton, K. A., 203, 213, 366, 378,
 382
 Nyquist, H., 200
- OLIVER, M. H., 140
 Omberg, A. C., 362
- PAGE, H., 304
 Page, L., 139, 146
 Pawsey, J. L., 464
 Pippard, A. B., 257
 Pistolkors, A. A., 104
 van der Pol, B., 75
 Price, M. H. L., 424, 426
 Purcell, E. M., 257
- RATCLIFFE, J. A., 188
 Reid, D. G., 115
 Reid, J. D., 219
 Rice, C. W., 228, 231
 Roberts, W. van B., 118
 Ross, W., 339
- Rust, W. M., 179
 Ryder, R. M., 139
- SANDRETTO, P. C., 349, 356, 359
 Saxton, J. A., 166, 267, 416
 Schelkunoff, S. A., 31, 53, 91, 140, 266,
 440
 Schellung, J. C., 416
 Scott, 203
 Selvidge, H., 422
 Sharpless, W. M., 93, 102
 Slater, J. C., 458, 463
 Smith, P. H., 51, 52, 60
 Smith, P. S., 457
 Solt, C. T., 342
 Sommerfeld, A., 15
 Southworth, G. C., 179
 Staal, C. I. H. A., 154
 Sterba, E. J., 262, 464, 467
 Stickland, A. C., 416
 Stoner, C. R., 312
 Stratton, J. A., 92, 136, 200
- TERMAN, F. E., 134, 235, 439
 Thomas, H. A., 203, 206
 Tuve, M. A., 23
- VAN DER POL, B., 17, 423
- WALKINSHAW, M. A., 115
 Walmsley, T., 310
 Watson, G. N., 373
 Watson, W. H., 189
 Wells, N., 222
 Weyl, H., 15
 Wheeler, H. A., 221
 Whitman, V. E., 221
 Williams, H. P., 78, 241, 477
 Willoughby, E. O., 446
 Wolff, I., 253
 Woodward, O. M., 91, 141
 Wwedensky, B., 370
- YAGI, H., 114
- ZINKE, O., 192

SUBJECT INDEX

- ABSORPTION limit, 401
 Adcock antenna, 334
 Admittance diagrams, 472
 Admittance to impedance conversion, 459
 Aeroplane effect, 324, 354
 Aircraft, television from, 20
 Alford loop antenna, 121, 145
 All-wave antenna, 220
 Altimeter antenna, 349
 Angle—
 of arrival, 397
 of fire, 396
 Antenna—
 Adcock, 334
 Alford loop, 121, 145
 all-wave, 220
 anti-fade, 72, 77, 377
 automobile, 361
 Bellini-Tosi, 223, 322, 343
 Beverage, 7, 228, 236
 biconical, 142
 broadcasting, 52, 55
 cage type, 127
 "capacity," 227
 cartwheel, 120
 cheese, 161
 clover-leaf, 123
 coaxial loop, 145, 223
 conical horn, 179
 corner reflector, 161
 crossed-loop, 322
 dielectric, 189
 discone, 143
 echelon, 278
 electromagnetic dipole, 147
 fan, 360
 folded-top, 74
 ground-plane, 119
 half-wave dipole, 89, 135, 199
 Hertz, 8
 horn, 168
 inverted-L, 32, 38, 41, 44, 48, 57, 61, 71, 74, 217, 219
 inverted-V, 278, 283
 loop, 233, 315, 340, 346
 low-velocity, 77
 magnetic dipole, 144, 146
 Marconi, 9
 non-resonant wire, 274
 parabolic, 147
 polyrod, (*see* Dielectric)
 pylon type, (*see* Slotted cylinder)
 Antenna—(*contd.*)
 pyramid horn, 179
 reactance loaded, 32, 43, 55, 74, 77
 receiving, 217
 resonant long-wire, 266
 resonant-V, 281
 rhombic, 235, 285
 rocket, (*see* Slotted cylinder)
 sectionalized, 76
 sectoral horn, 172
 shielded loop, 320
 slot, 182
 slotted cylinder, 123
 spaced-loop, 337
 spherical, 136
 T-type, 32, 34, 38, 41, 44, 48, 57, 61, 71, 75, 83, 219
 tail-fin, 360
 trailing wire, 351
 unipole, 226
 wave, (*see* Beverage)
 whip, 359, 471
 wing, 357
 Antenna arrays—
 broadside, 264
 end-fire, 264
 fishbone, 236
 flat-top, 112
 Franklin, 10, 77, 272, 311
 Kooman, 262, 301
 M.U.S.A., 234
 series phase, 312
 Sterba, 309
 Walmsley, 310
 Yagi, 114, 168
 "Antenna effect," 319, 342
 Anti-fade antenna, 72, 77, 377
 Apparent radius of earth, 371, 405
 Appleton layer, (*see* F layer)
 Atmospheric refraction, 416
 Attenuation constant of line, 441
 Attenuation—
 of 4-wire lines, 465
 of dissipative lines, 468
 Austin-Cohen formula, 373, 376
 Automatic direction finding, 347
 Automobile antennae, 361
 Available noise power, 201, 210
 Axial stresses, 480
 BABINET's principle, 184
 B.A.B.S. antennae, 351
 Bandwidth, 127

- Bellini-Tosi antenna, 223, 322, 343
 Bending stresses, 480
 Beverage antenna, 7, 228, 236
 Biconical antenna, 142
 method, 51
 Boltzmann's constant, 201
 Broadcasting antenna, 52, 55
 Broadside array, 264
 Brewster angle, 241

 CAGE-TYPE antenna, 127
 Capacitance,
 of circular disk, 43
 of horizontal wire, 36
 of parallel wires, 37
 of short antenna, 33
 of single wire, 37
 of transmission line, 435, 437
 of vertical wire, 35
 of wire cages, 40
 static, 33
 "Capacity" antenna, 227
 Cartwheel antenna, 120
 Characteristic impedance—
 of transmission lines, 437, 445
 of vertical radiator, 41, 42
 Cheese antenna, 161
 Clover-leaf antenna, 123
 Coaxial—
 fed dipole, 131
 line, 434
 loop antenna, 145, 223
 Compensating loop or wire, 342
 Conductance of transmission line, 435,
 440
 Conductivity tables, 475
 Conical horn, 179
 Cophasal linear arrays, 252
 Corner reflector, 161
 Corona, 465
 Coupling circuits, 80, 87
 Critical frequency, 24
 Crossed-loop antenna, 322
 Current distributions, 6

 D LAYER, 28
 Dielectric—
 antenna, 189
 constant—
 complex form, 21
 tables, 475
 Diffraction, 423
 Discone antenna, 143
 Dissipative transmission line, 458
 Diverity reception, 234
 Dominant mode, (*see* Principal mode)
 Doublet, 2, 198, 254
 Duct effect, (*see* Super-refraction)
 Dummy antenna, 210

 E LAYER, 23, 371, 388, 392, 397
 Earth conductivity—
 effect on input resistance, 102
 effect on polar diagrams, 100
 Earth—
 currents, 62, 85
 curvature, 416
 resistance, 66
 systems, 68, 218, 489
 Echelon antenna, 278
 Effective area—
 of absorption, 198
 of target, 430
 Effective noise temperature, 203, 212
 Electrical volume of D.F. loop, 326
 Electromagnetic dipole, 147
 End-fire array, 264
 Energy bandwidth, 201
 Equivalent—
 noise resistance, 207
 transmission line, 5, 218
 Exponential line, 468
 Extraordinary ray, 404

 F LAYER, 23, 371, 396
 Fade-free radius, 386
 Fairlead, 352
 Falling-derrick method of erection, 485
 Fan antenna, 360
 Field—
 electrostatic, 2
 induction, 2
 plotting, 446
 radiation, 2
 Figure of merit, 12, 70, 78, 101
 Fishbone array, 236
 Fixed-wire aircraft antennae, 355
 Folded-top antenna, 74
 Flat-top array, 112
 Form factor, 73
 Franklin array, 10, 77, 272, 311
 Frequency modulation, 207
 Fresnel's formula, 369

 GAIN—
 of directive antenna, 254
 of linear arrays, 262, 265
 Goniometer, 322, 328
 Ground-plane antenna, 119
 Gyro-frequency, 24, 404

 HALF-WAVE dipole, 89, 135, 199
 folded type, 116
 for television, 223
 methods of feeding, 129
 power gain, 256
 terminated type, 118
 with parasitic dipole, 106
 with reflecting sheet, 111

- Heaviside layer, (*see* E layer)
 Height factor, (*see* Images)
 Hertz antenna, 8
 Homing, 347
 Horn antenna, 168
 Huygens' principle, 171
 "IDEAL" amplifier, 211
 Images, 14, 241
 negative, 97, 99
 positive, 96, 98
 Impedance chart—
 circular form, 457
 rectangular form, 455
 Impedance to admittance conversion, 459
 Impedance of terminated line, 452
 Inductance of transmission line, 435, 439
 Insulators, 465, 490
 power factors of, 476
 Interference suppression, 206, 215, 365
 Intrinsic impedance, 57
 Inverted-L antenna, 32, 38, 41, 44, 48, 57, 61, 71, 74, 217, 219
 Inverted-V antenna, 278, 283
 Ionosphere, 18, 22, 366, 394
 Iron-cored loop, 318
 Isotropic radiator, 199, 254
 "J"-FED dipole, 133
 KENNELLY-HEAVISIDE layer (*see* E layer)
 Kooman array, 262, 301
 LAMBERT's projection, 395
 Latitude correction factors, 404
 Linear radiator, 5
 Logarithmic scale, 97
 Loop—
 antenna, 233, 315, 340, 346
 dead-loss resistance, 45
 radiation resistance, 45
 Losses—
 conductor, 57
 dielectric, 58
 ground, 61
 joulean (or heat), 3
 Low-velocity antenna, 77
 MAGNETIC dipole antenna, 144, 146
 Magneto-ionic theory, 24
 Marconi antenna, 9
 Marker beacon antenna, 350
 Mast design, 479, 484
 Matching—
 of impedances, 460
 sections, 460
 Maximum usable frequency, 25, 398
 Maxwell's equations for transmission line, 435
 Milky Way, 202, 203
 M.K.S. system, 477
 Modes of oscillation, 136
 M.U.S.A. array, 234
 Mutual impedance, 106
 correlation with gain, 258
 of collinear dipoles, 104
 of parallel dipoles, 103
 of staggered dipoles, 105
 NEPERS, 436
 Night effect, 324
 Night-time field strengths, 393
 Noise, 197, 200
 atmospheric, 204, 223
 cosmic, 203
 fluctuation, 208
 from power line, 219
 impulse, 208
 man-made, 205, 215
 thermal, 200
 valve, 206
 variation with frequency, 215
 Noise figure, 207, 209
 of diode mixer, 213
 of goniometer, 328
 of stages in cascade, 212
 of transmission line, 331
 of valves, 213
 Noise-reducing antennae, 219
 Non-resonant wire antenna, 274
 OCTANTAL error, 323
 Optical horizon, 418, 423
 Ordinary ray, 404
 PARABOLIC antenna, 147
 Parallel-wire line, 434
 Parasitic dipoles, 106
 Phase constant—
 of transmission line, 436, 445
 of a medium, 442
 Phase slip, 176
 Pick-up factor, 318
 Polar coefficient, 73, 75, 78
 Polar-diagram principles, 238, 247
 Polarization errors, 324
 Polyrod antenna (*see* Dielectric antenna)
 Power handling capacity of lines, 464
 Poynting's vector, 199, 430
 Precipitation static, 205
 Principal mode, 434
 Propagation constant of line, 436, 445
 Pylon type antenna (*see* Slotted cylinder antenna)
 Pyramid horn antenna, 179

- Q-FACTOR**, 128
Quadrantal error, 341
RADAR equation, 430
Radiation losses of lines, 466
Radiation resistance, 3, 45
 base, 46, 48, 50
 loop, 46, 47
Radiator—
 grounded, 9
 standing-wave, 7
 travelling-wave, 7
 tuning of, 11
 ungrounded, 8
Radio duct, 428
Ray theory, 406
Reactance-loaded antenna, 32, 43, 55,
 74, 77
Reactance transformer, 82
Receiving antennae, 217
 equivalent circuit, 196
 properties identical with transmis-
 sion, 196
Reciprocity, 196, 202
Reflecting sheets, 111
Reflection coefficients, 406, 451
Resistance of transmission line, 436, 440
Resonant long-wire antenna, 266
Resonant-V antenna, 281
Rhombic antenna, 235, 285
Rocket antenna (*see* Slotted cylinder
 antenna)

SECTIONALIZED antenna, 76
Sectoral horn, 172
Semicircular error, 341
Sensitivity of D.F. loop, 325
Series phase array, 312
Shadow factor, 381
Shielded loop antenna, 320
Shunt feed, 80
Signal-to-noise ratio, 195, 207, 326
 minimum values, 208
Skin depth, 57, 64, 65, 440
Skip distance, 27
Sky wave, 19, 367, 371, 386, 391
Slewing of beam, 158
Slot antenna, 182
Slotted cylinder antenna, 123
Snell's law, 26
Sommerfeld's attenuation constant, 378
Sommerfeld's numerical distance, 378

Spherical antenna, 136
Space—
 phasing, 238
 wave, 15, 367, 369, 404, 406
Spaced-loop antenna, 337
Spherical surface divergence factor,
 417
Spherical trigonometry formulae, 395
Standard wave error, 324
Standing wave, 443
 ratio, 454, 458, 468
Stay wire table, 488
Stays, 487
Sterba array, 309
Stub for wide-band antenna, 470
Sun-spot cycle, 24
Super-refraction, 22, 428
Surface wave, 15, 16, 366, 405
S.W.G., radii in mm., 470

T-TYPE antenna, 32, 34, 38, 41, 44, 48,
 57, 61, 71, 75, 83, 219
Tail-fin antenna, 360
Temperature rise in lines, 470
Thunderstorms, 205
Tilt of surface wave, 368
Top pull on masts, 489
Trailing wire antenna, 351
Tuning stubs, 462

UNIPOLE antenna, 226
Units, 477

VAN DER POL's formula, 378
Vector diagrams, 247
"Vertical," (*see* "Antenna effect")

WALMSLEY array, 310
Water vapour reflections, 372
Wave antenna (*see* Beverage antenna)
Waveguides, 168
Wavelength—
 classification of, 1
 free-space value, 2
Whip antenna, 359, 471
Wind pressure, 482
"Windom" fed dipole, 134
Wing antenna, 357

YAGI array, 114, 168

"ZEPP" feed, 94

